Towards a Small Molecule Analogue of MoCu-CODH with an Unsupported Single-Chalcogen Bridge

AN ABSTRACT

SUBMITTED ON THE TENTH DAY OF AUGUST 2023

TO THE DEPARTMENT OF CHEMISTRY

IN PARTIAL FULFILLMENT OF THE REQUIREMENT

OF THE SCHOOL OF SCIENCE AND ENGINEERING

OF TULANE UNIVERSITY

FOR THE DEGREE

OF

DOCTOR OF PHILOSOPHY

Jared Taylor

APPROVED BY:

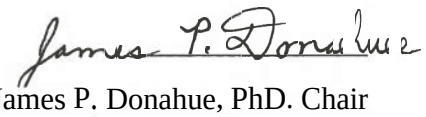

James P. Donahue, PhD. Chair

Alex MeSkimming, PhD.

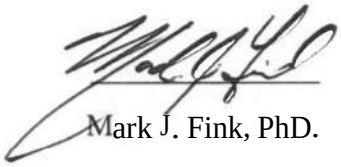

Mark J. Fink, PhD.

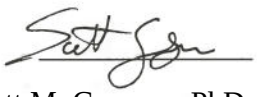

Scott M. Grayson, PhD.

Abstract:

The enzyme known as MoCu-CODH has a unique active site that has captured the interest of bioinorganic chemists since the elucidation of its structure in 2001. Thus, a high-fidelity small molecule analogue of the MoCu CODH active site has been a long-pursued target of synthetic bioinorganic chemistry. While there have been several published attempts at this target, none of the entrants has preserved both the single bridging sulfido moiety between the metal centers and the active equatorial molybdenum-bound oxo ligand. Both of these structural features are thought to be critical to the catalytic activity of this enzyme. Pursuant to this goal, a synthetic strategy has been designed that was based on a result that has resisted reproduction. This strategy includes the synthesis of a sterically hindered silylated mixed oxythiomolybdate and sterically crowded coordinatively unsaturated Cu(I) center with the aim that the steric bulk on both metal centers will prevent the molybdate chalcogen ligands from binding the Cu(I) in bidentate arrangement.

In Chapter 2 the synthesis of mixed oxythiomolybdates is explored. This synthesis has a long history going back to Berzelius nearly 200 years ago. Despite this long history of active investigation, no significant changes to the reagents or processes employed have resulted. The synthesis presented here is being undertaken utilizing a new chalcogen exchange reagent, hexamethyldisilathiane, $(Me_3Si)_2S$, whose mechanism and reaction thermodynamics toward the entire set of mixed oxythiomolybdates ($MoO_xS_{4-x}^{-2}$) are explored through synthetic and computational approaches. This synthetic exploration includes consideration of some observed byproducts.

Chapter 3 presents the copper center that is called for in the synthetic strategy. While this copper center has precedent in literature of structurally similar Cu(I) complexes, many of these

precedents show luminescent or photocatalytic properties. To explore the chemistry of the proposed copper complex, its coordination chemistry with a variety of hard and soft sulfur donors, halides, and pseudo-halides is investigated. Computational investigation of the frontier orbitals, coupled with some of the observed reactivity, reveals that this complex displays a metal-to-ligand charge transfer (MLCT) in its absorption spectrum that complicates the synthesis of the desired complex.

Towards a Small Molecule Analogue of MoCu-CODH with an Unsupported Single-Chalcogen Bridge

A DISSERTATION

SUBMITTED ON THE TENTH DAY OF AUGUST 2023

TO THE DEPARTMENT OF CHEMISTRY

IN PARTIAL FULFILLMENT OF THE REQUIREMENT

OF THE SCHOOL OF SCIENCE AND ENGINEERING

OF TULANE UNIVERSITY

FOR THE DEGREE

OF

DOCTOR OF PHILOSOPHY

Jared Taylor

APPROVED BY:

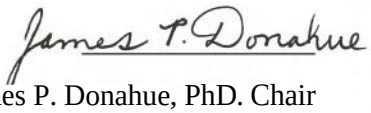

James P. Donahue, PhD. Chair

Alex McSKimming, PhD.

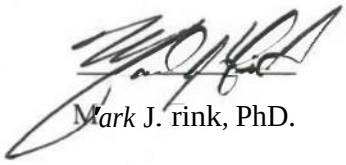

Mark J. rink, PhD.

Scott M. Grayson, PhD.

Dedicated to:

To Ava, for your future.

My loving wife Carmen, your inspiration, support, and unwavering faith in my abilities buoyed me and made this possible.

To my parents Stephen and Zona, for encouraging my curiosity, supporting my growth, and being role-models for the person I hope to become.

Acknowledgements:

No work, great or small, is an individual undertaking. To that end, there is no shortage of people who have encouraged me along the way to this culmination. Chief amongst those that deserve credit is Dr. James Donahue, my research advisor and mentor, his steadfast faith in this project and my abilities motivated me greatly when the road was rough. His courses provided the theoretical and practical insights I required to understand the obstacles I was facing, and his counsel and advice helped me find the way when the path was lost.

Further, the students of the Donahue Group have been an enormous help both in the lab and personally. I was lucky to start my time at Tulane while Antony Obanda, and Patricia Fontenot were senior graduate students. Their presence, advice, and expertise made the transition into research possible. Justin Barnes played a large role in my joining the Donahue Group and toiled alongside me in the mines of Cu(I) chemistry, his camaraderie and support will never be forgotten. Che Wu and I both joined the Donahue Lab in our first year; Che is talented chemist that is skilled in many fields. His technical and personal support and advice buoyed me; plus, he was always down for chatting about gaming as an escape from the burdens of graduate school. Titir Das Gupta has been a caring and helpful accomplice; she is always willing to go above and beyond to render whatever aid she can. Titir's assistance was particularly valuable toward the end as the pressure grew.

Other professors and faculty within the Department also stand out for their advice and assistance. Dr. Heiko Jacobsen played a huge role in the development of my computational chemistry skills and spared time constantly to answer questions and help investigate when he didn't know the answers. Dr Joel Mague is an expert crystallographer and the department will

sorely miss him; however, Dr. Xiaodong Zhang is doing an excellent job filling his shoes on top of his many other tasks. I eventually stopped being surprised when I got ESI-MS data from Dr. Zhang well outside of normal working hours.

Lastly, those who kept me tethered throughout graduate school. These include my wife, Carmen, and my Mother-in-Law, Claudia Zelaya; my roommate Mike Brady, and my church family at St. Lukes; all of whom played a vital role in providing their unending support in making sure I am eating, sleeping, and taking time for myself and others. I might have gotten the science done without them, but I would have lost my mind.

Table of Contents:

List of Figures

Chapter 1:

Chapter 2:

Chapter 3:

List of Tables:

Chapter 2

Chapter 3:

List of Equations:

Chapter 1:

Chapter2

Chapter 1: Synthesis of a Small Molecule Analogue of Molybdenum-Copper Carbon Monoxide Dehydrogenase

Introduction

Molybdenum has been known to play a vital role in enzymatic active sites since the mid-1950s, with several of those enzymes being well characterized both structurally and mechanistically through the synthesis of small molecule analogues by the mid-1990s.[1] Most molybdoenzymes catalyze some form of oxygen atom transfer reaction either to or from the metal center. These enzymes are categorized into several families, illustrated in **Figure 1** below, based on their active site structure, modifications to the pterin cofactor, and the substrate they activate.[2,3]

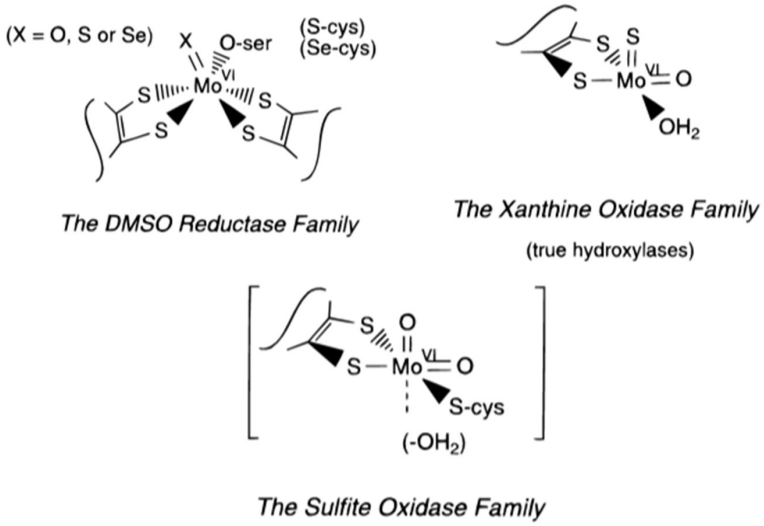

Figure 1: The general structure of the families of Molybdoenzymes reprinted with permission from Hille, R.; Hall, J.; Basu, P.; "The Mononuclear Molybdoenzymes" Chem. Rev.***2014.*** *114.7 3963-4038. Used with permission.*

Nearly all known molybdoenzymes contain the molybdopterin, or pyranopterin, cofactor which, while it supports some structural variation, always coordinates the metal center through a redox-active enedithiolate moiety.[4] The enzyme that enables the aerobic carboxidotrophic bacteria

Oligotropha carboxidivorans to employ carbon monoxide as its only source of carbon and reducing equivalents is a molybdoenzyme that belongs to the xanthine oxidase family.[5] This enzyme formally catalyzes the transfer of an oxygen atom from Mo(VI) to carbon monoxide and bears the name molybdenum-copper carbon monoxide dehydrogenase, or MoCu-CODH due to its unique active site which is illustrated in **Figure 2**, below. First elucidated in 2001, this enzyme has a unique heterobimetallic structure which contains the familiar Mo(VI) coordination environment, with mixed oxo/sulfido ligation in its first coordination sphere, arranged in a square pyramidal geometry, including a single molybdopterin cofactor.[6] Unusually, this molybdenum center is bound only through a single sulfido bridge to another metal, Cu(I). This copper ion resides in a linear coordination environment in which it is bound to only the bridging sulfido and a deprotonated cysteine residue. The enzyme also contains several Fe_2S_2 clusters for the purpose of electron transport and a FAD cofactor as the terminal electron acceptor.

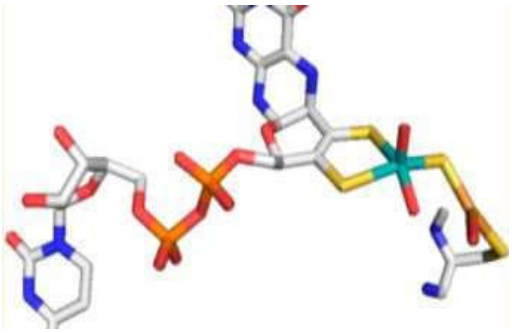

Figure 2: The active site of MoCu-CODH. Carbon=Grey, Nitrogen=Blue, Oxygen=Red, Sulfur=Yellow, Molybdenum=Teal, Phosphorous =Orange, Reprinted with permission from Shanmugam et al. "13C and 63,65Cu ENDOR studies of CO dehydrogenase from Oligotropha Carboxidivorans. Experimental Evidence in support of a Copper-carbonyl Intermediate." J. Am. Chem. Soc. 2013. 135 17775-17782. Copyright 2013 American Chemical Society.

Thus far, despite significant efforts, limited success has been reported for the synthesis of a structurally faithful or functional small molecule MoCu-CODH active site analogue. The challenge is attributable to several factors, among them the difficulty of avoiding the thermodynamic sink represented by molybdenum coordinating irreversibly to Cu(I) in a bidentate manner and failing to maintain the unsupported linear copper geometry.[7] Recently there has been some computational evidence that the natural enzyme may be best characterized as a frustrated Lewis-

pair (FLP), kept from forming a stable Lewis adduct by the steric bulk of the protein, which may provide an important strategy to synthetically interrogate this long-sought structure.[8]

Early Research and Structural Characterization:

Ortwin Meyer is primarily credited with much of the early research on *Oligotropha carboxidivorans* and has, in fact, dedicated much of his career to the research of carboxidotrophic bacteria and molybdoenzymes. His research is responsible for the isolation and reclassification of this microbe from the Pseudomonas family into the Oligotropha family.[9,10] Meyer's Group is also responsible for the isolation and purification of the MoCu-CODH protein and the identification of its substrate and products in the late 1970s and early 1980s.[11,12] Through this work, CODH was initially proposed to be just a molybdenum containing flavoprotein. Later, his group collected EPR and other spectral data,[13,14,15] identified the presence of molybdopterin,[16] determined the location of the protein within the cell,[17] identified selenium as promoting the reaction,[18] as well as identified and sequenced the genetic code that contains the instructions for biosynthesis.[19]

In 1999, Meyer and his coworkers reported the X-ray crystal structure of MoCu-CODH at a 2.2 Å resolution, seen in **Figure 3A** below. The results of their past experiments, coupled with this data, led them to declare that the CODH enzyme found in *O. carboxidivorans* was a molybdenum flavoprotein in which the molybdenum was bound to the molybdopterin and to a selenocysteinate residue, similar to the already known formate dehydrogenases at the time. They also proposed a catalytic cycle, seen in **Figure 3B** below, which was supported by previously known synthetic organic chemistry. In this mechanistic proposal carbon monoxide is coordinated between the selenocysteinate and a molybdenum bound hydroxide ligand. Following attack by Se^0, a selenocarbonate intermediate was proposed, which then leads to carbon dioxide after attachment of the deprotonated equatorial molybdenum oxido- ligand.[20,21]

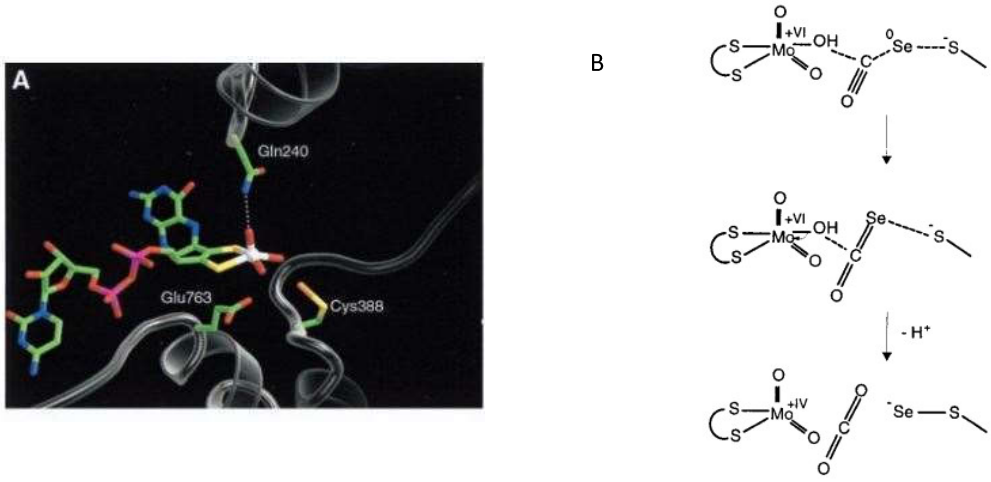

Figure 3: The 1999 Dobbek and Meyer structure and mechanism proposal, in the structure Green=carbon, blue=nitrogen, white =molybdenum, red=oxygen, orange=selenium, yellow=sulfur, purple=phosphorus. Reprinted with permission from Dobbbek et al. "Crystal structure and Mechanism of CO dehydrogenase, a molybdo iron-sulfur flavoprotein containing S-selenocysteine" Proc. Natl. Acad. Sci. USA. 96. 1999. 8884-8889 Copywrite 1999 National Academy of Sciences.

However, not all newly emerging data were consistent with Dobbek and Meyer's structural or mechanistic proposal. The next year, the group edited the initial structure to include an equatorial sulfido- ligand in the place of the previously identified hydroxy ligand on the molybdenum center. Even in this paper, they cite several pieces of evidence which challenge their proposed structure, namely: elemental analysis of the purified protein and electron paramagnetic resonance spectroscopy. The elemental analysis showed an insufficient amount of selenium to populate the active site and provide the activity levels which had been observed in purified samples. Furthermore, the EPR spectra of the spin-active reduced active site displayed hyperfine splitting patterns.[22] This hyperfine splitting had previously been assigned to the organic radicals in the electron receptor chain but was now shown to be a much better fit for a proximal copper(I) center in the place of the proposed selenocysteine. In 2002, the group reported several new XRD structures with an improved resolution of 1.1 Å. In this report, the selenocysteine was replaced with a hitherto unprecedented, unsupported linear copper (I) bound by a cysteinate residue and the

Mo=S ligand. They also reported structures of a n-butylisocyanide trapped intermediate in addition to the oxidized and reduced forms of the enzyme. These results also contained a new proposed catalytic cycle which was informed by the new data, illustrated in **Figure 4** to the right,.[23]

The Meyer group continued work on what was now being referred to as MoCu-CODH, including their report of its ability to split hydrogen in 2006 and a further investigation of the biosynthesis of the active site before moving on to other areas of interest.[24,25]

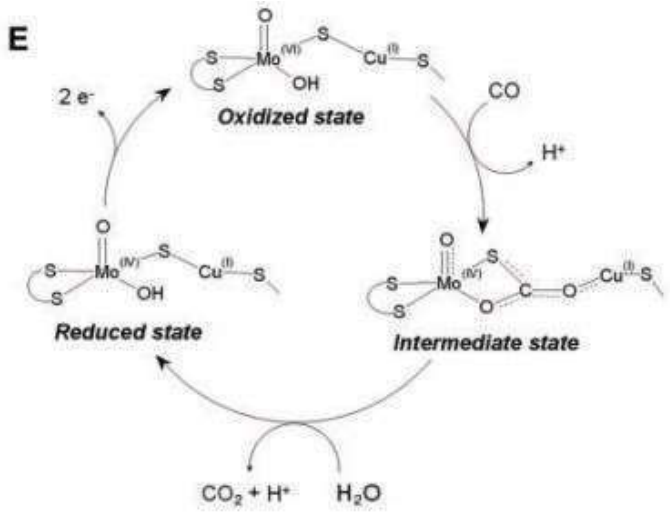

Figure 4: The Meyer and Dobbek proposed reaction mechanism, reprinted with permission from Dobbbek et al. "Catalysis at a dinuclear [CuSMo=O)OH] cluster in CO dehydrogenase resolved at 1.1-Å resolution." Proc. Natl. Acad. Sci. USA. 99, 25. 2001. 15971-15976. Copywrite 1999 National Academy of Sciences

Interest and the Water-Gas Shift Reaction:

The attention of synthetic chemists was almost immediately captured by this unique enzymatic active site. In addition to having an unusual active-site geometry, the reaction catalyzed by CODH is analogous to the water-gas shift reaction (WGS) that is employed industrially for the production of syngas. Syngas is vital for the synthesis of ammonia, hydrocarbons, methanol, and other products through a variety of industrial processes. The Fischer-Tropsch reaction, for which the feedstock is carbon monoxide and hydrogen, also uses Syngas mixtures as do other applications seen in **Figure 5** below.[26]

$$CO + H_2O \rightleftarrows CO_2 + H_2$$

$$CO + H_2O \xrightarrow[MoCu\ CODH]{} CO_2 + 2H^+ + 2e^-$$

Equation 1: The water-gas shift and the MoCu-CODH and other CODH enzymes' catalytic reactions

The water-gas shift reaction is also gaining more interest as a green fuel source for hydrogen-based power storage. For different applications, the exact composition of the syngas mixture varies, thus the conditions at which the WGS reaction is performed vary accordingly. However, in general, elevated temperatures are employed to shorten the amount of time that is required to reach the reaction's equilibrium state. Current low temperature water-gas shift reaction catalysts employ heavy and/or precious metals such as gold, platinum, palladium, or rhodium or expensive materials like multi-walled carbon nanotubes.[27,28]

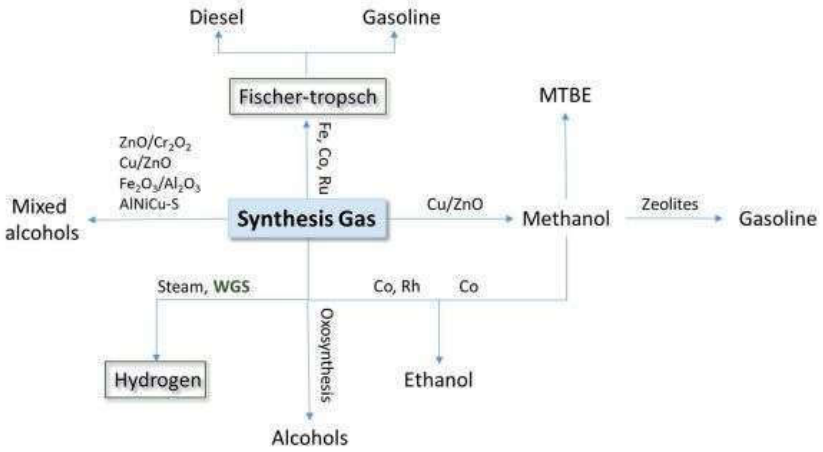

Figure 5: The Uses of Syngas and some of the catalysts involved, reprinted with permission from Alfano and Cavazza "TheBiologically mediated water-gas shift reaction: storage, function and biosynthesis of monofunctional [NiFe] Carbon monoxide dehydrogenases." Sus. Energ. Fuels. 2018. 2. 1653. Reprinted with permission from RSC.

The similarity between the WGS and the reaction catalyzed by MoCu-CODH can be seen in **equation 1** above. It is clear that a MoCu-CODH inspired catalytic system, which could be synthesized from relatively earth abundant elements and able to operate at near room temperature

would be a significant development. To this end, efforts to generate a small molecule analogue for structural and mechanistic studies began almost immediately.

Synthetic Efforts:

The first effort at synthesizing a small-molecule analogue of MoCu-CODH was by the group of Kazuyuki Tatsumi. Tatsumi had long had interests in research on transition metal chalcogenide and dithiolene compounds, particularly those of molybdenum and tungsten.[29,30,31] In 2005, Tatsumi reported the synthesis of the dinuclear molybdenum-copper compound, $[O_2MoS_2Cu(CN)]^{2-}$ and several derivatives including dithiolene bound compounds like the one illustrated in **Figure 6**.[32] These complexes appear as square pyramidal molybdenum, as found in the enzymatic active site, and were synthesized by the reaction of $[Et_4N]_2MoO_2S_2$ with an appropriate copper salt. Derivatization of the copper ligand was then performed by ligand exchange reactions utilizing a potassium salt of the desired ligand which resulted in the removal of KCN. The dithiolene was installed as the dithiol with the elimination of two equivalents of H_2O.

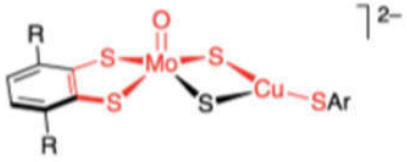

Figure 6 Tatsumi 2005 synthetic effort highlighting the similarity to the MoCu-CODHactive site in red. Reprinted with permission from Gourlay et al "Models for aerobic carbon monoxide dehydrogenase: synthesis, characterization and reactivity of Paramagnetic $Mo^{V}O(\mu\text{-}S)Cu^{I}$ complexes. Chem. Sci 2018. 9 876.

This effort was notable because the product was exclusively dinuclear with no trinuclear product of the form $[O_2MoS_2(CuCN)_2]^{2-}$, as is common in the analogous reaction with MoS_4^{2-}. These compounds were also the first dithiolene bearing sulfido-bridged Mo-Cu complexes. However, in these complexes the molybdate sulfido ligands chelate Cu(I), rather than form the single μ-S bridge as is found in the enzyme. This bridging occurs despite efforts to introduce steric bulk at the copper center to discourage the formation of the double sulfido bridge. Further, all

attempts to detect an interaction between this complex and carbon monoxide or t-butylisocyanate, as seen in the native enzyme, were unsuccessful despite the authors noting a color change under 10 atm of CO. Despite this setback recent investigations of this complex by Fontecave and Mougel showed that it is capable of the electrocatalytic reduction of CO_2 to formate at an overpotential of 800 mV.[33] Additionally, the Sarkar group was able to isolate a stable copper bound thiyl radical when the complex was reacted with a second equivalent of benzene dithiolene.[34]

Later in 2005, the group of Charles Young reported another MoCu-CODH active site analogue that took a different approach. The Young model system is illustrated in **Figure 7**, to the left, and is a [{Tp^{ipr}}MoO(OAr)(μ-S)(Cu(Me$_3$tcn))] complex in which the molybdenum center, in this case Mo(V), is bearing a *fac*-tris(pyrazolyl)borate ligand and its equatorial oxo ligand is protected as a 3,5-di-tertbutylphenolate ligand.[35] This molybdenum center is bound through a single bridging sulfido ligand to a copper ion whose remaining coordination sites are occupied by N,N',N''-trimethyl-1,4,7-triazacyclononane. This assembly was synthesized by a reaction of [{Tp^{ipr}}MoOS(OAr)]$^{1-}$ and [(MeCN)Cu(Me$_3$tcn)][BF$_4$] in acetonitrile. The anionic molybdenum complex had been prepared prior to mixing by the reduction of [{Tp^{ipr}}MoOS(OAr)] by cobaltocene, however, the coupling was also facile if the reductant was added to a solution with both species present. This modular approach reduced the difficulty of generating derivatives and many were later reported by the authors. These later reports of derivatives focused on varying the identity of the phenolate ligand and the effect this had on key structural parameters, EPR features, and the redox properties of the resulting complexes as gauged by cyclic voltammetry.[36] However,

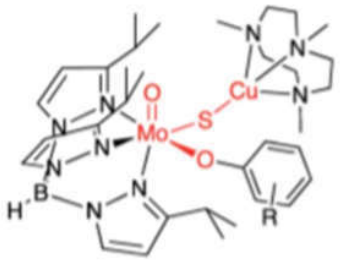

Figure 7 Young et al. synthetic effort, Reprinted with permission from Gourlay et al "Models for aerobic carbon monoxide dehydrogenase: synthesis, characterization and reactivity of Paramagnetic Mo^{V}O(μ-S)Cu^I complexes. Chem. Sci 2018. 9 876.

the supporting ligands in the Young system are decidedly abiological, the molybdenum ion is not in the starting oxidation state and lacks the dithiolene moiety, and the terminal oxo ligand is rendered unreactive by the arene ring. Furthermore, the copper center is coordinatively saturated rather than occurring with the linear, two-coordinate geometry found in the enzyme. Despite these perceived shortcomings, the Young system did provide valuable insights into the nature of the enzymatic system. Foremost, the reduced Mo(V) center has an unpaired electron which allows the collection of EPR spectra. Interestingly, these spectra closely match that of the native enzyme. The EPR spectral data collected allowed for the quantification of the delocalization of the SOMO containing the unpaired Mo(V) electron as 44% Mo d_{xy} character, 25% S_p character, and 21% Cu d_{z2}/d_{xy}. This assignment was further reinforced by DFT calculations of the electronic structure, which showed significant delocalization of the unpaired molybdenum electron across the Mo-S-Cu bridge. The involvement of the copper s- and d-orbitals in the delocalization of this unpaired electron led Young to surmise that only in a linear or pseudo-C_{3v} coordination environment can the appropriate orbital mixing take place for this orbital-stabilized radical to delocalize in this way. This conclusion led to a rethinking of the enzymatic mechanism that will be discussed later. Additionally, several key geometric parameters matched the native system quite well, including the Mo–S length (2.2844 Å in Young's model vs 2.27 Å in the native system), Cu–S length (2.1348 Å vs 2.21 Å), and the Mo–S–Cu angle (118.905 ° vs 113 °). Finally, the action of the cyanide anion on this system was similar to its action on native CODH, namely extraction of the bridging sulfide ligand, which leads to loss of the copper center.

Following on their work with other oxo-transferases,[37] the group of R. H. Holm reported synthesis efforts aimed at CODH active site models in 2010. The results reported by the Holm Group were not fundamentally different in the structures of their reported products from those of the Tatsumi effort noted above. Though the model compounds prepared by the Holm Lab employed tungsten dithiolene rather than the molybdenum dithiolene complexes and the synthetic route to these products was quite different.[38] The choice to use tungsten over molybdenum was made to simplify synthetic efforts by avoiding the self-reduction to which thiomolybdates are prone. The authors of this effort tried many different sterically bulky 2-coordinate copper starting materials in an effort to avoid the $(\mu\text{-S})_2$ binding motif including a 2,5-di-(1,3,5-tri-isopropyl) benzenethiolate complex, a di-isopropylcarbene complex, and a bis(triphenylsilanethiolate) complex. These sterically hindered copper complexes were reacted with benzene dithiolate tungsten compounds with the WO_2S, WOS_2, $WO_2(OSiMe_3)$, and $WS_2(OSiMe_3)$ cores. Interestingly, regardless of the first coordination sphere of the tungsten starting material only complexes with the $(\mu_2\text{-S})_2$ core were isolated, as seen in all the complexes in **Figure 8** above. This bridging arrangement is so stable that it was isolated even in the reactions in which the

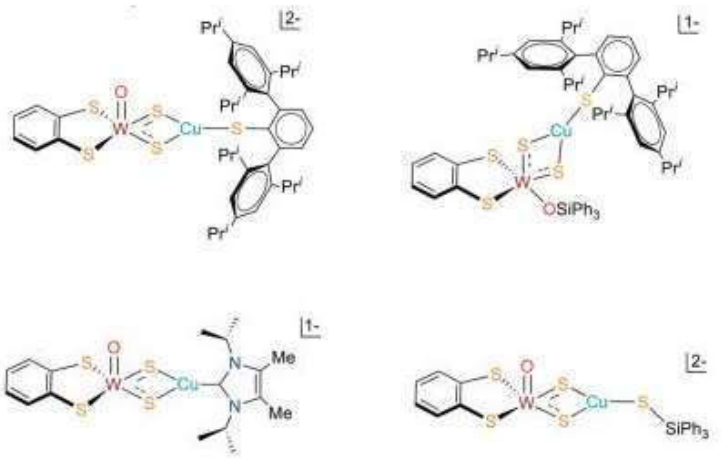

Figure 8: The products reported by the Holm Group. Adapted) with permission from Groysman et al." Reaction of monodithiolenetungsten (VI) sulfido complexes with copper(I) in relation to the structure of the active site of carbon monoxide dehydrogenase" Inorg Chem.2010. 49 1082-1089 Copyright 2010 American Chemical Society.

tungsten reactant bears only equatorial oxygen atoms, hypothetically from the disproportionation of the tungsten complex.

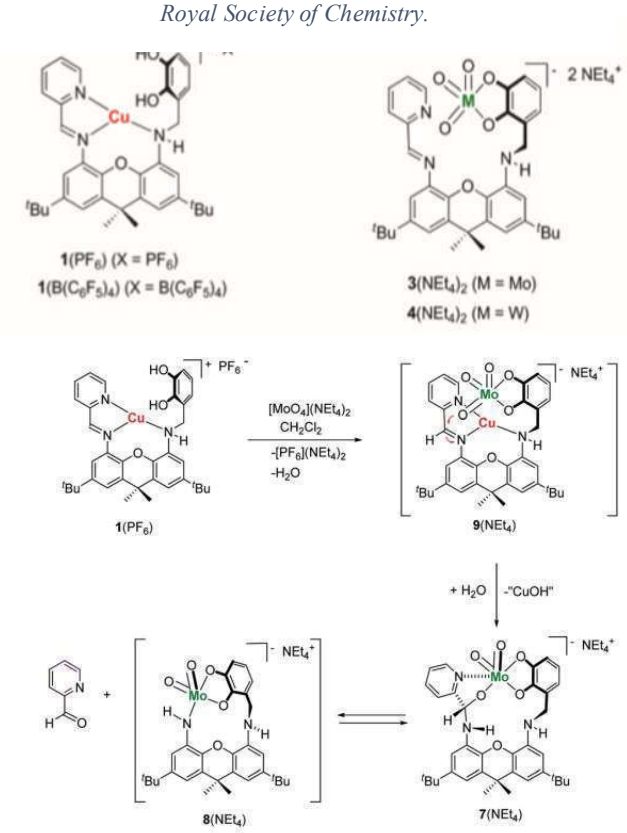

Figure 9: The Groysman monometallic complexes and the heterobimetallic reaction cascade. Reprinted with permission from T. S. Hollingsworth, R. L. Hollingsworth, R. L. Lord and S. Groysman, Dalton Trans.*, 2018, 47, 10017. Copywrite 2018 Royal Society of Chemistry.*

The next major synthetic effort was published in 2018 and was led by former Holm group member Stanislav Groysman. This report employed a third unique approach in the effort to emulate this elusive enzymatic active site.[39] The Groysman group postulated that the sulfido-bridge serves a merely structural role. Thus, rather than focusing on the construction of a single sulfido bridge, they instead hoped to place a coordinatively unsaturated copper center in close proximity to a molybdenum center which had several multiply bonded chalcogenide ligands. To accomplish this goal, they targeted a single organic backbone with a hard dianionic catechol site to bind the molybdenum, and a soft iminopyridine site to host the Cu(I). This design was built on a 2,7-di-*tert*butyl-9,9-dimethyl-4,5-diaminoxanthene backbone. While this host molecule could host either metal center in the desired location individually as seen at the top of **Figure 9**. Any attempt to place both metal centers resulted in the loss of copper and the isolation of pyridine-2-carbaldehyde and the O,O,N bound molybdenum center shown at the bottom of **Figure 9**. This result was postulated to be a cooperative bimetallic reactive cascade that resulted

from an intramolecular nucleophilic attack by the equatorial molybdenum oxo- ligand on the electrophilic copper-bound imine. This reaction is reminiscent of the mechanism of another molybdoenzyme, xanthine oxidoreductase, in that a molybdenum catalyzed oxygen atom transfer to a conjugation stabilized sp^2 carbon located between two imines is observed.

Figure 10: Groysman Dimerized Heterobimetallic product reprinted with permission from Kaluarachchige D. et al "Studies Relevant to the Functional Model of Mo-Cu CODH: In Situ Reactions of Cu(I)-L Complexes with Mo(VI) and Synthesis of Stable Structurally Characterized Heterotetranuclear $Mo^{VI}_2Cu^{I}_2$ Complex." Molecules *2023, 28, 3644.*

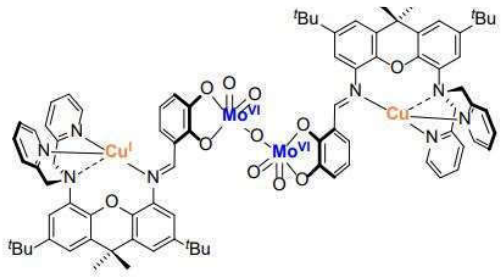

To avoid the problematic bimetallic reactivity they had observed, the Groysman group modified the copper binding site from an iminopyridine to an amino-dipyridine coordination site. Doing so deprived the nucleophilic molybdenum oxo ligand of an electrophilic target and allowed for the isolation of a heterobimetallic product as a dimer with a Mo-O-Mo linkage (**Figure 10**).[40] This approach has gleaned hopeful results, as they have demonstrated that the Cu(I) is coordinatively unsaturated by isolating phosphine-bound, cyanide-bound, and halide-bound products. Furthermore, exposure to an atmosphere of carbon monoxide produced a color change and a change in the ^{1}H NMR spectrum that suggested a new product was being formed. However, this product was not isolable, and the spectral changes simply revert back to the starting material in the absence of carbon monoxide.

The most recent entry into this field is the work of the group of Neal Mankad published in 2020.[41] Taking inspiration from their predecessors, the Mankad Group designed their synthetic strategy to include a tungsten dithiolene core with benzene dithiolate simulating the pyranopterin moiety and rendering the tungstate square pyramidal. To prevent the chelate coordination mode that is thermodynamically favored, they deactivated the equatorial oxo ligand using a cleavable tri-isopropylsilyloxy protecting group. The 2-coordinate geometry of the Cu(I) was enforced by employing a bulky carbene ligand with 2,5-diisopropylphenyl substituents. When the respective monometallic compounds were combined in dichloromethane at -40°C, the primary product was the desired singly-bridged W/Cu heterobimetallic complex. In the isolated complex the copper was by the carbene, the μ-S ligand, and a dative interaction with one of the dithiolene sulfur atoms, shown on the left side of **Figure 11**, below. When the silyl protecting group was cleaved with a fluoride source, the copper center rearranged to be reminiscent the Holm and Tatsumi efforts. However, this complex shows a mixed bridging system composed of a μ-O and μ-S, that had not previously been observed. The authors characterized the Cu-O interaction as a short dative bond with a length of 2.377(8) Å, which is much longer than an average Cu(I)-oxygen bond. Mankad further concludes that this "closed" conformation is the relaxed conformation of the CODH active

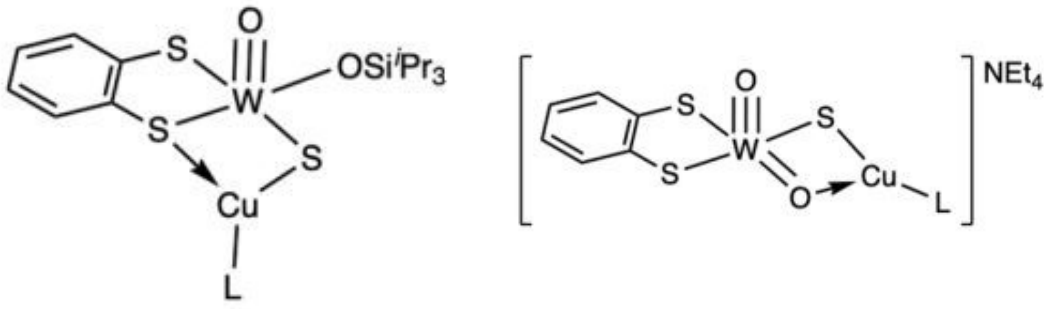

Figure 11: The initial and final product of the Mankad synthesis, reprinted with permission from Reprinted (adapted) with permission from Ghosh, D. et al. A W/Cu Synthetic Model for the Mo/Cu Cofactor of Aerobic CODH Indicates That Biochemical CO Oxidation Requires a Frustrated Lewis Acid/Base Pair Journal of the American Chemical Society 2020 142 (29), 12635-12642.Copywrite 2020 American Chemical Society.

site and that the enzymatically active native site is therefore the "open" conformation. The strain energy required to maintain the "open" conformation is compensated for by the protein environment. They take this observation to mean that native enzyme must represent a frustrated Lewis acid-base pair (FLP), that is a Lewis acid/base pair that cannot form a stable adduct due to steric or electronic effects.[42] Mankad postulates that this frustration is steric and enforced by the protein bulk and supports this by pointing out stabilizing interactions amongst conserved residues and water molecules found near the active site. By this conclusion, the current models show no enzyme-like activity due either to their ligated equatorial oxo-ligand, which is a much weaker Lewis base, or by the quenching of frustration through the formation of Lewis acid/base adducts in the form of the bidentate molybdate/tungstate coordination mode seen in numerous examples above.

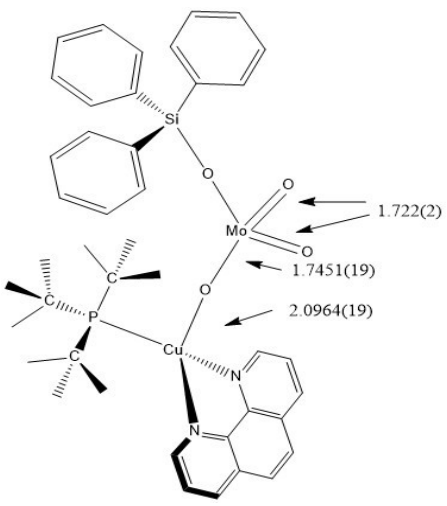

Figure 12: Unpublished Donahue Group structure

The Donahue group has an unpublished result from 2012 which has resisted replication thus far. This compound, seen in **Figure 12** to the left is [(Me$_4$phen)Cu(^{t}Bu$_3$P)(μ-O)MoO$_2$(OSiPh$_3$)]. This complex was synthesized by the reaction of [(^{t}Bu$_3$P)Cu(SSiPh$_3$)] and [(Me$_4$phen)MoO$_2$(OSiPh$_3$)$_2$] with XRD quality crystals forming upon standing in diethyl ether. The intended reaction was a coupling of the metal centers across a single sulfido bridge by silylative dioxygenation of the molybdenum silyloxy ligand to form hexaphenyldisiloxane, (Ph$_3$Si)$_2$O, similar to the approach by the Holm Group in 2010. However, the species lost in this reaction is the far less stable hexaphenyldisilathiane, (Ph$_3$Si)$_2$S, which likely

degraded through side reactions. Another unusual feature is the migration of the phenanthroline ligand from the molybdenum center, where it started, to the copper center, where it resides in the crystal structure. Phenanthroline ligands, by their bidentate nature, aren't generally considered particularly labile making this a surprising result. Regardless of the unusual reaction pathway, the product is quite similar to the native enzyme with its single, unsupported, chalcogen bridge, as well as its free equatorial molybdenum oxo- ligands, and d^{10} Cu(I). As none of the existing analogue candidates show all of these features this structure provides a tempting target for further synthetic efforts.

The Mechanism of Action of MoCu-CODH:

The mechanism by which MoCu-CODH catalyzes the oxidation of carbon monoxide to carbon dioxide is still the subject of some debate and has been since the initial selenocysteine structure and accompanying mechanism of action was proposed by Dobbek and Meyer. The mechanism suggested along with the original structure proposed that the carbon monoxide binds to the uncharged selenium moiety of the selenocysteine, which polarized the C-O bond. The polarized carbon was then attacked by the nearby equatorial molybdenum hydroxy ligand, forming a bridging selenocarbonate, from which CO_2 is freed through proton transfer (cf. **Figure 3** above).[20] This mechanistic proposal was reasonable for the proposed structure and has analogues in the synthetic chemistry literature for the synthesis of selenocarbamates.[21] Of course, this mechanism was discarded when the structure was corrected and the selenium removed from the active site.

A short time later, Dobbek and Meyer again proposed a mechanism for the activity of MoCu-CODH under the new structure. This proposal involved the insertion of CO into the Mo-S-Cu bond with immediate attack by the equatorial oxo-ligand to form a bridging thiocarbonate (cf.

Figure 4, above). This mechanistic proposal was based largely on the crystal structure of the n-butylisocyanide trapped intermediate the group had obtained of the enzyme as isocyanide is isostructural and isoelectronic to carbon monoxide.

Computational Investigation:

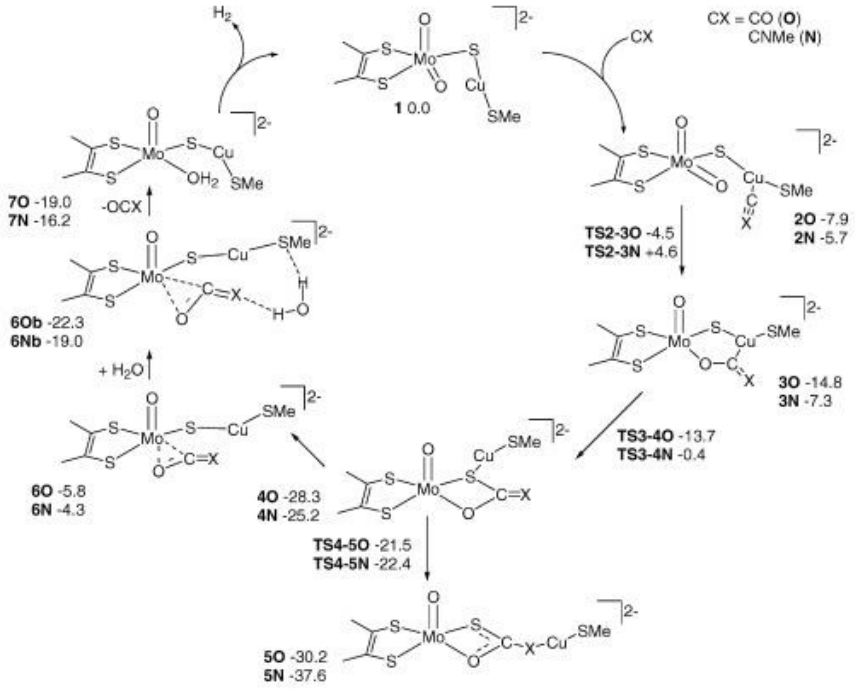

Figure 13: The Mechanistic Proposal by Hofmann and Graf. Reprinted with permission

The first two significant computational investigations of this mechanism were submitted a week apart in January of 2005 and reached similar conclusions. The first was undertaken by Hofmann and Graf, who calculated several steps of a mechanistic cycle at the B3LYP/LANL2dz level of theory, with the basis set supplemented by d-type polarization functions. Hofmann and Graf examined both the catalytic oxidation of carbon monoxide and the interaction of the enzyme with the n-butylisocyanide inhibitor.[43] The mechanism they proposed, show in **Figure 13** above, began with the coordination of carbon monoxide to the Cu(I) center followed by nucleophilic

attack by the nearby molybdenum bound oxo-ligand. This produces a five-membered Mo-O-C-Cu-S ring, which undergoes ring contraction by extrusion of the copper from the ring and formation of a C-S bond to form a four-membered ring. It was thought by the authors that, from this four-membered ring, the trapped intermediate described by Dobbek and Meyers is formed by the migration of the copper center to generate the thiocarbamate analogue of a bridging thiocarbonate. Their computations showed that the bridging thiocarbonate proposed by Dobbek and Meyers lays at the bottom of thermodynamic well, nearly 24 kcal/mol below the next step in the catalytic cycle. Such a thermodynamic barrier is insurmountable in a practical sense, making the formation of a thiocarbonate a dead end and thus ruling it out as a part of the mechanism. This point seems to be a reasonable conclusion when considering that the crystal structure that prompted the consideration of thiocarbonate as a part of the catalytic cycle is, in fact, catalytically inert.

The other paper that was submitted that week was by Siegbahn and Shestakov. This paper followed a similar approach of evaluating the relevant structures of the catalytic cycle by DFT. But Siegbahn and Shestakov employed a B3LYP/lacvp basis set, then followed geometric optimization with energy evaluation under a lacv3p* basis set that included effective Core potentials for the Mo, Cu, and S atoms. The positions of some atoms were frozen to

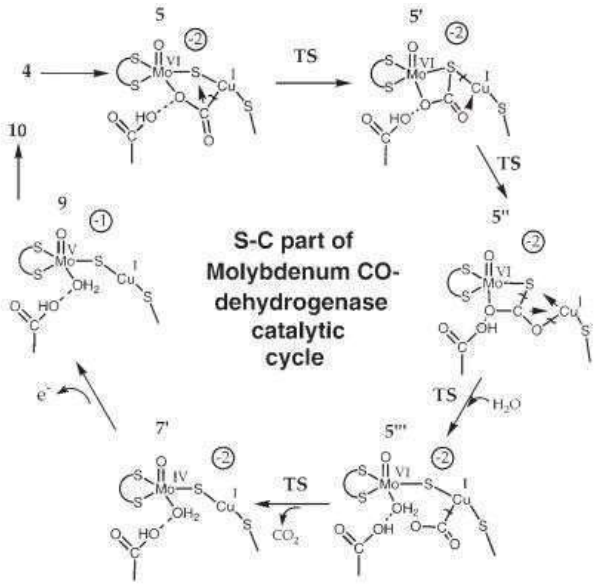

Figure 14: Siegbahn and Shestakov Mechanism steps showing the insertion of water in the Mo-CO_2 bond. Reprinted with permission from Shestakov, A. et a "Quantum chemical modelling of CO oxidation by the active site of molybdenum CO dehydrogenase" J. Comput. Chem. 2005 26.9. 888-898. Copyright 2005 Wiley Periodical Inc.

ensure active site geometry remains close to the native enzyme.[44] These authors were also quite troubled by the formation of the thiocarbonate intermediate and the resulting energy well. As such, they searched for pathways that might avoid its formation including altering the time of the oxidation event as well as interrogating various spin states and protonation states for the active site constituents. This investigation led them to a structure in which an incoming water molecule is located between the Mo center and CO_2 oxygen, shown in the starred structure of **Figure 14**, above. The association of this water molecule avoids the thermodynamic sink of thiocarbonate formation. As such, the carbon dioxide, or n-butylisocyanate, is released by the severing of the C–S bond followed by the association of the incoming water. These steps reduced the energy barrier for the release of CO_2 to only 17.9 kcal/mol. Later, EPR experiments have concluded that neither the Mo(V) nor the Mo(IV) centers are protonated due to the lack of change in these spectra in D_2O, which serves to deepen this mystery. Citing the inherent error in the calculations and the lack of clarity for the rate limiting step, Siegbahn and Shestakov were unwilling to propose a full alternative catalytic cycle at the and could not rule out thiocarbonate formation to their satisfaction. Biochemical work to measure the K_{cat} has since determined that the rate limiting step is after the formation of an enzyme-CO complex and before oxidation of the molybdenum. Further work by Hille *et al* suggests that the rate limiting step is the reductive half-reaction, i.e., the two step reduction the electron acceptor by the Molybdenum center, which results in the oxidation of Mo(IV) to Mo(VI) and the regeneration of the active site.[45] However, the question of the depth and very existence of the thiocarbonate energy well has persisted in spite of these revelations.

In 2013, the group of Russ Hille published the results of their ENDOR experiments on the partially reduced native enzyme using ^{12}CO and ^{13}CO as the reducing agents.[46] The aim of this experiment was elucidation of the structure of the enzyme containing the EPR active Mo(V). In these spectra, they observed hyperfine coupling between the Cu(I) and Mo(V) species which is affected by covalent interactions of the species to their immediate surroundings. Through comparison with similar molybdoenzyme intermediates and computational modelling, they believed that the signal did not arise from species containing a Mo–C bond or from a thiocarbonate intermediate. The authors also note that the data collected by these experiments does not match the computational model for the five membered intermediate that had been postulated.

Figure 15: The Hille Mechanism in 2015 highlighting the SOMO-CO2 resonance structure in red, reprinted with permission from Hille. R. et al. "^{13}C and $^{63,65}Cu$ ENDOR studies of CO Dehydrogenase from Oligotropha carboxidovorans. Experimental Evidence in Support of a Copper–Carbonyl Intermediate" J. Am. Chem. Soc. 2013. 135.47.17775-17782. Copywrite 2013 American Chemical society

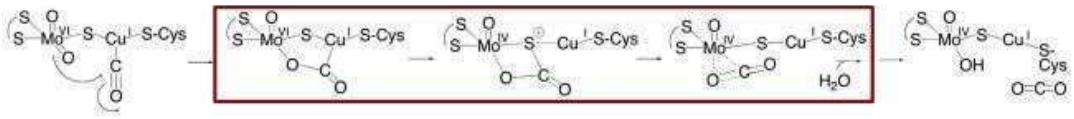

With these points in mind, the Hille Group concluded that the signal must be arising from an accumulated partially inactivated active site in which the carbon monoxide is coordinated to Cu(I) and that catalysis cannot proceed from there due to the molybdenum center being in a reduced state. They further concluded that the Mo(V) center does possess a protonated hydroxy rather than an oxo ligand. They followed this analysis with a lengthier review of the progress of the field to that point in 2015, in which they considered the thiocarbonate intermediate not as a true intermediate but as a complex resonance structure with the delocalized SOMO, seen above in **Figure 15**.[4] This mechanism includes the highlights of the previous computational studies.

The previously discussed mechanistic interrogations involved only small sets of atoms present in the enzymatic active site, with Hoffman and Graff only explicitly considering the first coordination sphere and Siegbahn and Shestakov including several nearby residues for a total of about 70 atoms but at a low level of theory. Neither group of researchers gave significant consideration to second sphere residues or the active participation of the several other water molecules which hydrate the active site found in the XRD structure. In 2014, Stein and Kirk postulated that one of these coordinating water molecules, located 2.4 Å from the Cu(I) center and additionally activated by a nearby glutamate residue, could be sufficiently activated to attack the carbon in the five-membered ring configuration shown in **Figure 16** above. Such an attack would yield a protonated carbonate intermediate that is coordinated only to the molybdenum. The reduction of the molybdenum center occurs simultaneously making this product a Mo(IV)-carbonate and thus avoiding C-S bond formation and the thiocarbonate sink. The thermodynamic effects of this theory are significant as the activation energy of this process is only 12.8 kcal/mol. The authors based this proposal on an orbital analysis of the intermediate, which shows significant CO_2 character in both the HOMO and LUMO of the examined complex. The result of this orbital character is a bent CO_2 molecule that is prone to nucleophilic attack at the

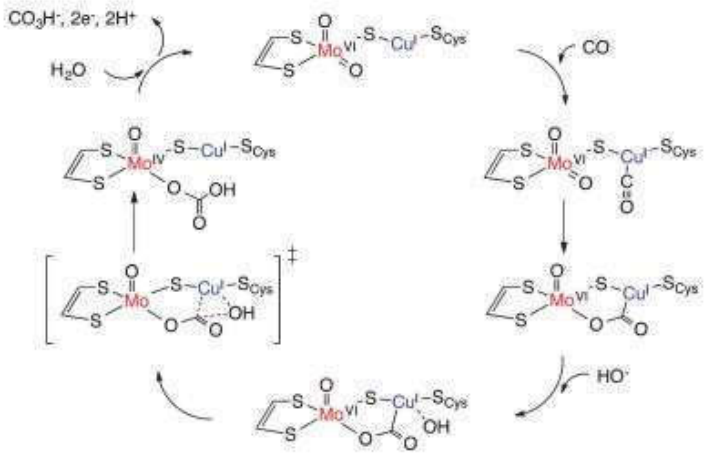

Figure 16: Stein and Kirk proposal suggesting an activated water molecule attack on coordinated CO_2, Reprinted with permission from Kirk, M. et al. "Electronic structure contributions to reactivity in xanthine oxidase family enzymes." J. Biol. Inorg. Chem. 2015. 20. 183-194. Copywrite 2015 Springer

carbon atom. This mechanism also shows parallels with other, better studied members of the xanthine oxidase family of molybdoenzymes.[48,49]

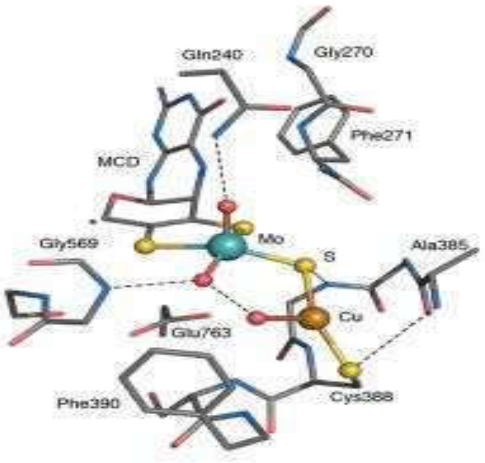

Figure 17: The Rakhsana computations "necessary" residues. Unlabeled atoms grey=carbon, blue=nitrogen, red=oxygen. Reprinted with permission from Rokhsana, D. et al "A realistic in silico model for structure/function studies of molybdenum–copper CO dehydrogenase" J. Biol. Inorg. Chem. 2016 21 491-499. Copywrite 2016 Springer

As the apparent importance of the second and outer sphere residues and hydrating waters grew, the necessity for a more comprehensive investigation became clear. The group of Dalia Rokhsana stepped in to complete this daunting task in 2016.[50] They ran the most comprehensive computational investigation to date that included all of the structurally essential features of the second and outer sphere. As well as including all the reasonable variations of the metals' ligand environments and all reasonable oxidation states. The determination of essentiality for a given residue was evaluated by deleting the residue in question and observing the effect upon the active site structure. This method led to a set of models that included nearly 180 atoms and is partially illustrated in **Figure 17** to the left. These models were optimized in ORCA under BP86/TZVP for all atoms except carbon and hydrogen, which were considered under the lower basis set def2-SVP. The resulting geometries and their computed spectra were then compared to all of the available experimental spectroscopic data for the native enzyme active site.

The structures that resulted from the endeavor led by Rokhsana compared well with the geometry obtained from XRD and EXAFS studies. Furthermore, the computed geometries were able to nearly reproduce the delocalization of the electron density across the sulfido bridge found

in the reduced Mo(V) native enzyme and the model compound from the Young Group. Rokhsana's computational model was also able to provide an acceptable estimate of the reduction potential, which was calculated to me -467 mV versus -558 mV for the experimental value, and Mo-O vibrational frequencies that were within 11 cm^{-1} of the experimental values. The vibrational simulation is particularly notable, as what had been assigned to an asymmetric Mo-O stretch in previous experiments was reassigned to N-H and O-H rocking motions of the residues that are hydrogen bonded to the equatorial Mo-O. Lastly, they found that many of the second- and outer sphere residues were important structurally. For example, the close loop comprised of Val^{384}-Arg^{387} has a significant impact on the S–Cu–S and Mo–S–Cu bond angles. The removal of Glu^{763} also had a major effect on these same bond angles, resulting in a contraction of 29° upon its removal. Based on this observation and the proximity of Glu^{763} to the vital equatorial oxygen it seems that this residue is likely involved in the catalytic process. While the removal of Ser^{570} had little impact on the structure of the complex, it is also located close to the molybdenum bound equatorial oxygen and might have a significant impact on its donor/acceptor properties.

Further investigation of the thiocarbonate intermediate was undertaken by Xu and Hirao in 2018, using a QM:MM hybrid investigation of the entire enzyme structure.[51] Their calculations determined that the thiocarbonate intermediate was in fact not as deep of a thermodynamic well as was previously thought, with an energetic barrier to CO_2 release of only 12.8-12.9 kcal/mol and depended on the protonation state of the active site and the location of a nearby promoter water molecule. The end fate of this water molecule is the reoxidation of the Mo (IV) center leading to the reset of the catalytic cycle. This water molecule also serves as the source of the 2 H^+ ions formed as part of the catalytic product.

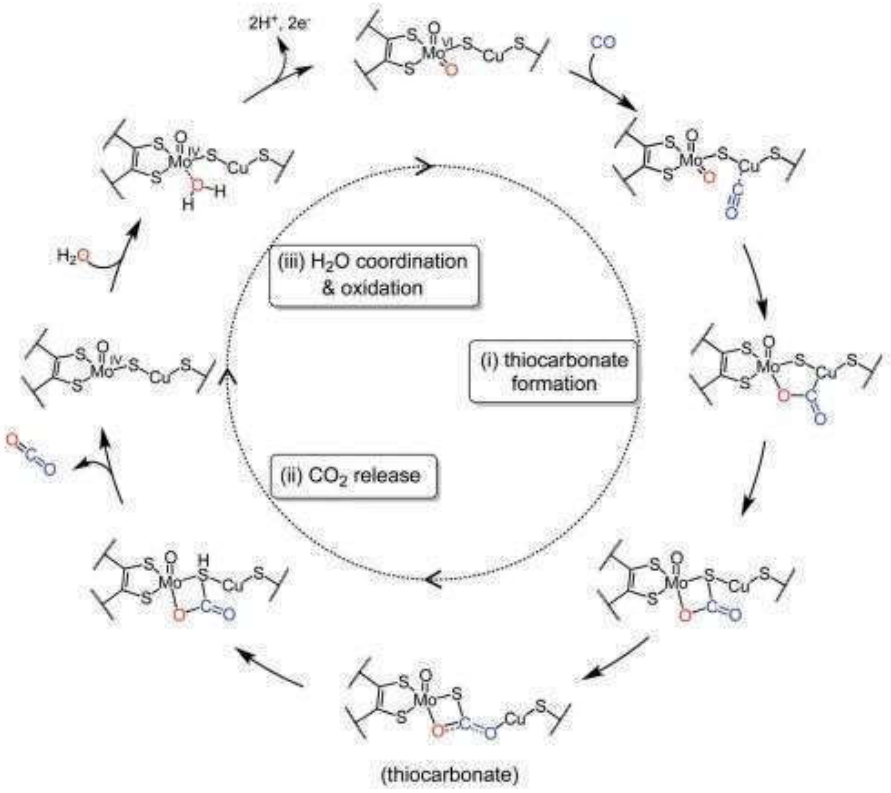

Figure 18: The Hirao catalytic cycle reprinted with permission from Xu, K et al. "Revisiting the catalytic mechanism of Mo-Cu carbon monoxide dehydrogenase using QM/MM and DFT calculations." Phys. Chem. Chem. Phys.2018, 20, 28, 18938 – 18948. Copywrite 2018 Royal Society of Chemistry.

Xu and Hirao produced the currently accepted model of the MoCu-CODH catalytic cycle. The catalytic cycle begins with the coordination of carbon monoxide to the Cu(I) center. This coordination of carbonyl to copper shifts a greater positive charge onto the carbon and promotes the attack by the nucleophilic molybdenum-bound equatorial oxo ligand forming the five-membered ring described above. This five-membered ring appears in many of the mechanistic proposals and pictured on the right side of **Figure 18** above. This five-membered ring then collapses to a four-membered ring as the CO_2 bond is partially formed. The release of CO_2 is prompted by the protonation of the bridging sulfido ligand, leading the reduction of the Mo (VI) to Mo(IV). The two electrons gained through this reduction are shuttled out through the electron

acceptor chain, one at a time as the Mo (IV) is oxidized by an incoming water molecule. The protons on the incoming water molecule are harvested as part of the catalytic cycle, thereby regenerating the Mo (VI)-S-Cu active site. The thiocarbonate-like trapped t-butylisocyanate intermediate is too stable to undergo release in the same manner, resulting in the trapped structure that has been characterized.[51]

However, consensus has still not been reached. The group of Russ Hille proposed in 2015 that perhaps an activated water molecule is the nucleophile in this enzyme, rather than the equatorial molybdenum oxo- ligand.[47] This idea was investigated computationally by Greco et al. in 2022, and found to be thermodynamically favorable.[52] A second, new camp of thought surrounding this mechanism, also proposed by Greco *et al.* in 2019, has recently developed which considers the active site not in a classical stepwise sense but as a frustrated Lewis pair, or FLP.[8] In the FLP scenario the copper d-orbitals form the Lewis acid and the molybdenum oxo-ligand is the Lewis base.[8] This proposal is consistent with a report that MoCu-CODH can split H_2, a type or reactivity that is a hallmark of FLP chemistry.[42] While FLP's can be formed by energy and symmetry mismatches between the donor and acceptor orbitals, in the case of MoCu-CODH it is thought that the FLP is prevented from quenching by the protein bulk and that carbon monoxide bridges this physical gap, is oxidized, and then the FLP is regenerated.[41] This conceptualization of the enzyme's working has been supported by synthetic efforts from Mankad et al. in 2020, detailed above, and is both a convenient explanation for the lack of high-fidelity small molecule analogues and an elegant description of the enzyme's reactivity. The FLP mechanistic theory implies that any small molecule analogue that hopes to be a high-fidelity model must either have a significant energetic mismatch between the Mo=O and Cu d-orbitals to prevent Lewis adduct formation or have a profound amount of steric hinderance sufficient to prevent attack by the former upon the

latter and the subsequent quenching of the frustrated Lewis pair. Overall, the amount of discussion around the mechanism is significant and seems unlikely to be swayed to consensus without the development of a functional small molecule analogue.

Synthetic Strategy:

Pursuant to the replication of the Donahue Group result shown above in **Figure 12**, a rational synthetic strategy was developed, shown below in **Figure 19**, to bypass the irreproducible original synthesis. A rational retrosynthetic analysis divides the heterobimetallic complex at the Cu-O bond, producing a three-coordinate $[(phen)Cu(P^tBu_3)]^+$ complex, which would be a monocation. The remainder would be best described as a silylated molybdate (VI) oxoanion, which would be monoanionic. Similar Cu(I) complexes exist in the literature and are detailed in Chapter 3 of this work. Molybdates of this type can easily be synthesized from the base oxometallate, which is a dianion, by reaction with the corresponding chlorosilane. Further, oxomolybdate has a long synthetic history detailed in chapter 2 of this work, including studies of its ability to exchange chalcogen ligands to form mixed oxythiomolybdates. Therefore, while the current complex has an oxo bridge it should be possible to synthesize a version in which the chalcogen bridge is the desired sulfido bridge. This is the target of this study.

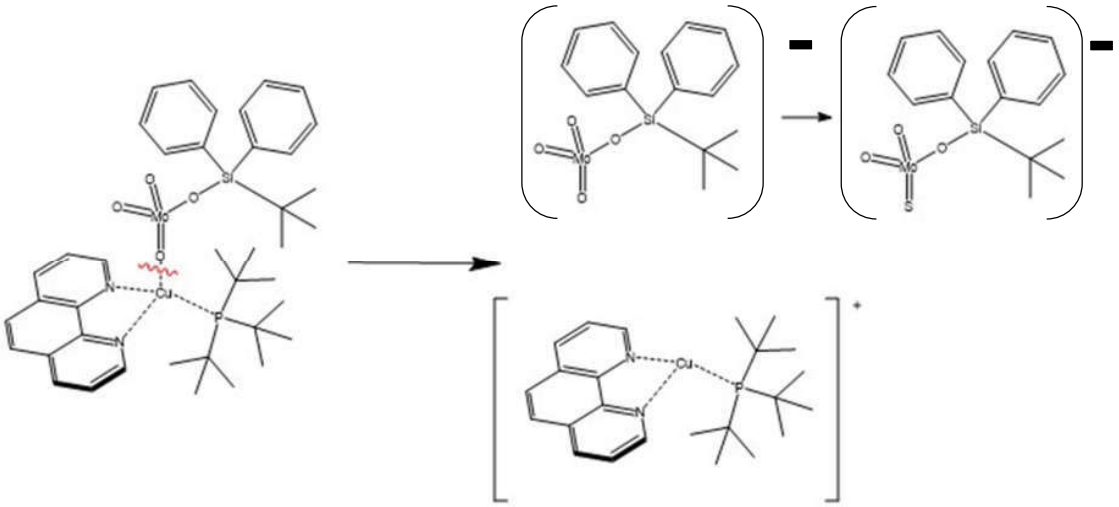

Figure 19: Retrosynthetic analysis for the rational synthesis of the unreported Donahue heterobimetallic complex

References

(1) Hille, R.; Nishino, T.; Bittner, F. "Molybdoenzymes in Higher Organisms" Coord Chem Rev. May 2011; 255(9-10): 1179–1205. doi:10.1016/j.ccr.2010.11.034

(2) Silke Leimkühler , Chantal Iobbi-Nivol, "Bacterial molybdoenzymes: old enzymes for new purposes" FEMS Microbiology Reviews. 40(1) January 2016, 1-18 DOI: 10.1093/femsre/fuv043

(3) Berg, J.M., Holm, R.H.; "A Model for the Active Sites of Oxo-transfer Molybdoenzymes: Reactivity, Kinetics, and Catalysis" J. Am. Chem. Soc. 107(4). 1985. 925-932.DOI: 10.1021/ja00290a030

(4) Hille, Russ. "The Mononuclear Molybdenum Enzymes" Chem. Rev. 96. 1996. 2757-2816. DOI: 10.1021/cr950061t

(5) Majumdar, A. "Bioinorganic modeling chemistry of carbon monoxide dehydrogenases: description of model complexes, current status and possible future scopes" Dalton Trans. 43. 2014. 12135. DOI: 10.1039/c4dt00729h.

(6) Dobbek, H.; Gremer, L., Kiefersauer, R. Huber, R., Meyer, O. "Catalysis at a dinuclear [CuSMo(AO)OH] cluster in a CO dehydrogenase resolved at 1.1-Å resolution" Proc. Natl. Acad. Sci. U.S.A. Dec. 10. 2002. 99(25). 15971-15976. DOI: 10.1073/pnas.212640899

(7) Dou, J.; Zhang, D.; Zhu, Y.; Li, D.; Wang, D. " Synthesis and characterization of two types of skeleton heterobimetallic trinuclear Mo(W)–Cu–S clusters containing 1,2-bis(diphenylphosphino)-1,2-dicarba-closo-dodecaborane" Polyhedron. 26 2007. 4216-4222. DOI: 10.1016/j.poly.2007.05.030.

(8) Rovaletti, A.; Bruschi, M.; Moro, G.; Cosentino, U.; Greco, C.; Ryde, U. "Theoretical Insights into the Aerobic Hydrogenase Activity of Molybdenum–Copper CO Dehydrogenase" Inorganics. 7(11). 2019. 135. 5; doi.org/10.3390/inorganics7110135

(9) Meyer, O.; Guenter, S. "Reisolation of the carbon monoxide utilizing hydrogen bacterium Pseudomonas carboxidivorans (Kistner) comb. Nov" Arch. Microbiol. 118(1) 1978. 35-43. DOI: 10.1007/bf00406071

(10) Meyer,O.; Stackebrandt, E.; Georg,A. "Reclassification of ubiquinone Q-10 containing carboxidotrophic bacteria: transfer of "[Pseudomonas] carboxydovorans" OM5T to Oligotropha, gen. nov., as Oligotropha carboxidovorans, comb. nov., transfer of "[Alcaligenes] carboxydus" DSM 1086T to Carbophilus, gen. nov., as Carbophilus carboxidus, comb. nov., transfer of "[Pseudomonas] compransoris" DSM 1231T to Zavarzinia, gen. nov., as Zavarzinia compransoris, comb. nov., and amended descriptions of the new genera" Syst. Appl. Microbiol. 16(3). 1993. 390-395. DOI: 10.1016/s0723-2020(11)80271-7

(11) Meyer, O.; Schlegel, H.G. "Oxidation of carbon monoxide in cell extracts of Pseudomonas carboxydovorans" J. Bacteriol. 137(2). 1979. 811-817. DOI: 10.1128/jb.137.2.811-817.1979

(12) Futo, S.; Meyer, O. "Carbon dioxide is the first species formed upon carbon monoxide oxidation by CO dehydrogenase from Pseudomonas carboxydovorans" Arch. Microbiol. 145(4). 1986. 358-360. DOI: 10.1007/bf00470871

(13) Meyer, O. “Chemical and spectral properties of carbon monoxide: methylene blue oxidoreductase. The molybdenum-containing iron-sulfur flavoprotein from Pseudomonas carboxydovorans” J. Biol. Chem. 257(3). 1982. 1333-1341. DOI: 10.1016/S0021-9258(19)68196-2.
(14) Meyer, O.; Schlegel, H.G. “Carbon monoxide: methylene blue oxidoreductase from Pseudomonas carboxydovorans” J. Bacteriol. 141(1). 1980. 74-80. DOI: 10.1128/jb.141.1.74-80.1980
(15) Bray, R.C.; George, G.N.; Reinhard, L.; Meyer, O. “ Studies by EPR spectroscopy of carbon monoxide oxidases from Pseudomonas carboxydovorans and Pseudomonas carboxydohydrogena” Biochem. J. 211(3). 1983. 687-694. DOI: 10.1042/bj2110687
(16) Meyer, O.; Rajagoapalan, K.V. “Molybdopterin in carbon monoxide oxidase from carboxidotrophic bacteria” J. Bacteriol. 157(2). 1984. 643-648. DOI: 10.1128/jb.157.2.643-648.1984
(17) Spreitler, F.; Brock, C.; Pelzmann, A.; Meyer, O; Koehler, J. “Interaction of CO dehydrogenase with the cytoplasmic membrane monitored by fluorescence correlation spectroscopy.” ChemBioChem. 11(17). 2010. 2419-2423. DOI: 10.1002/cbic.201000431
(18) Meyer, O.; Rajagopalan, K. V. “Selenite binding to carbon monoxide oxidase from Pseudomonas carboxydovorans. Selenium binds covalently to the protein and activates specifically the carbon monoxide → methylene blue reaction.” J. Biol. Chem. 259(9). 1984. 5612-5617. DOI: 10.1016/S0021-9258(18)91058-6
(19) Hugendieck, I.; Meyer, O. “The structural genes encoding carbon monoxide dehydrogenase subunits (cox L, M and S) in Pseudomonas carboxydovorans OM5 reside on plasmid pHCG3 and are, with the exception of Streptomyces thermoautotrophicus, conserved in carboxidotrophic bacteria.” Arch. Microbiol. 157(3). 1992. 301-304. DOI: 10.1007/bf00245166
(20) Dobbek, H.; Gremer, L.; Meyer, O.; Huber, R. “Crystal structure and mechanism of CO dehydrogenase, a molybdo iron-sulfur flavoprotein containing S-selenylcysteine” Proc. Natl. Acad. Sci. USA. 96(16). 1999. 8884-8889. DOI: 10.1073/pnas.96.16.8884
(21) Sonoda, N.; “Selenium Assisted carbonylation with carbon monoxide” *Pure & Appl. Chem.* **1993**. 65(4) 699-706. DOI: 10.1351/pac199365040699.
(22) Meyer, O.; Gremer, L; Ferner, R.; Ferner, M.; Dobbek, H; Gnida, M. Meyer-Klaucke, W.; Huber, R. “The Role of Se, Mo and Fe in the Structure and Function of Carbon Monoxide Dehydrogenase.” Biol. Chem. 381(9/10). 2000. 865-876. DOI: 10.1515/bc.2000.108.
(23) Gnida, M.; Ferner, R.; Gremer, L; Meyer, O.; Meyer-Klaucke, W. “A Novel Binuclear [CuSMo] Cluster at the Active Site of Carbon Monoxide Dehydrogenase: Characterization by X-ray Absorption Spectroscopy.” Biochem. 42(1). 2003. 222-230. DOI: 10.1021/bi026514n.
(24) Pelzmann, A.M.; Mickoleit, F.; Meyer, O. “Insights into the posttranslational assembly of the Mo-, S- and Cu-containing cluster in the active site of CO dehydrogenase of Oligotropha carboxidivorans.” J. Biol. Inorg. Chem. 19(8). 2014. 1399-1414. DOI: 10.1007/s00775-014-1201-y

(25) Santiago, B.; Meyer, O. "Characterization of hydrogenase activities associated with the molybdenum CO dehydrogenase from Oligotropha carboxidivorans" FEMS Microbiol. Lett. 136(2). 1996. 157-162. DOI: 10.1111/j.1574-6968.1996.tb08042.x

(26) Alfano, M.; Cavazza, C. "The biologically mediated water–gas shift reaction: structure, function and biosynthesis of monofunctional [NiFe]-carbon monoxide dehydrogenases." Sustain. Energy Fuels. 2018. 2. 1653-1670. DOI: 10.1039/c8se00085a

(27) Baraj, E.; Ciahotny, K.; Hlincik, T. "The water gas shift reaction: Catalysts and reaction mechanism." Fuel. 288. 2021. 119817. DOI: 10.1016/j.fuel.2020.119817

(28) Ebrahimi, P.; Kumar, A.; Khraisheh, M. "A Review of recent advances in water-gas shift catalysis for hydrogen production." Emerg. Mater. 3. 2020. 881-917. DOI: 10.1007/s42247-020-00116-y

(29) Komuro, T.; Matsuo, T.; Kawaguchi, H.; Tatsumi, K. "Unusual Coordination Modes of Arylthiolates in Mo{η^5-SC_6H_3-2,6-$SiMe_3)_2$}{η^7-SC_6H_3-2,6-$SiMe_3)_2$}." *J. Am. Chem. Soc.* **2003**. 125(8)/ 2070-2071. https://doi.org/10.1021/ja029541+

(30) Lang, J.; Ji, S.; XU, Q.; Shen, Q.; Tatsumi, K. "Structural Aspects of copper(I) and silver sulfide clusters of pentamethylcyclopentadienyl; trisulfido tungsten(VI) and molybdenum(VI)." *Coord. Chem. Rev.* **2003**. 241(1-2). 47-60. https://doi.org/10.1016/S0010-8545(02)00309-0

(31) Ohki, Y.; Marumoto, T.; Kawaguchi, H.; Tatsumi, K. "Heterolytic Cleavage of Dihydrogen Promoted by Sulfido-Bridged Tungsten-Ruthenium Dinuclear Complexes." *J. Am. Chem. Soc.* **2003**. 125(26) 7978-7988. https://doi.org/10.1021/ja029941x

(32) Takuma, M.; Ohki, Y.; Tatsumi, K. "Sulfido-Bridged Dinuclear Molybdenum−Copper Complexes Related to the Active Site of CO Dehydrogenase: $[(dithiolate)Mo(O)S_2Cu(SAr)]^{2-}$ (dithiolate = 1,2-$S_2C_6H_4$, 1,2-$S_2C_6H_2$-3,6-Cl_2, 1,2-$S_2C_2H_4$)." Inorg. Chem. 44(17) 2005. 6034–6043 DOI: 10.1021/ic050294v

(33) Mouchfiq, A.; Todorova, T.; Dey, S.; Fontecave, M.; Mougel, V. "A bioinspired molybdenum–copper molecular catalyst for CO2 electroreduction." Chem. Sci. 11. 2020. 5503-5510. DOI: 10.1039/d0sc01045f

(34) Bose, M.; Moula, G.; Begum, A.; Sarkar, S. "Dangling Thiyl Radical: Stabilized in [PPh4]2[(bdt)WVI(O)(μ-S)2CuI(SC6H4S•)]." Inorg. Chem. 50. 2011. 3852-3854. DOI: 10.1021/ic200258u

(35) Gourlay, C. Nielsen, D.J.; White, J.M.; Kottenbelt, S.Z.; Kirk, M.L.; Young, C.G. "Paramagnetic Active Site Models for the Molybdenum−Copper Carbon Monoxide Dehydrogenase." J. Am. Chem. Soc. 128(7). 2006. 2164-2165. DOI: 10.1021/ja056500f

(36) Gourlay, C.; Nielsen, D.J.; Evans, D. J.; White, J.M.; Young, C.G. "Models for aerobic carbon monoxide dehydrogenase: synthesis, characterization and reactivity of paramagnetic MoVO(μ-S)CuI complexes." Chem. Sci. 9. 2018. 876-888. DOI: 10.1039/c7sc04239f

(37) Groysman, S.; Wang, J.; Tagore, R.; Lee, S.C.; Holm, R.H. "A Biomimetic Approach to Oxidized Sites in the Xanthine Oxidoreductase Family: Synthesis and Stereochemistry

of Tungsten(VI) Analogue Complexes." J. Am. Chem. Soc. 130(38). 2008. 12794-12807. DOI: 10.1021/ja804000k
(38) Groysman, S.; Majumdar, A.; Zheng, S.; Holm, R.H. "Reactions of Monodithiolene Tungsten(VI) Sulfido Complexes with Copper(I) in Relation to the Structure of the Active Site of Carbon Monoxide Dehydrogenase." Inorg. Chem. 49(3). 2010. 1082-1089. DOI: 10.1021/ic902066m
(39) Hollingsworth, T.; Hollingsworth, R.L.; Lord, R.L.; Groysman, S. "Cooperative bimetallic reactivity of a heterodinuclear molybdenum–copper model of Mo–Cu CODH." Dalton Trans. 47. 2018. 10017-10024. DOI: 10.1039/c8dt02323a
(40) Don, U.; Almaat, A.; Ward, C.L.; Groysman, S. "Studies Relevant to the Functional Model of Mo-Cu CODH: In Situ Reactions of Cu(I)-L Complexes with Mo(VI) and Synthesis of Stable Structurally Characterized Heterotetranuclear MoVI2CuI2 Complex." Molecules. 28. 2023. 3644. DOI:10.3390/molecules28083644.
(41) Ghosh, D.; Sinhababu, S.; Santarsiero, B.D.; Mankad, N.P. "A W/Cu Synthetic Model for the Mo/Cu Cofactor of Aerobic CODH Indicates That Biochemical CO Oxidation Requires a Frustrated Lewis Acid/Base Pair." J. Am. Chem. Soc. 142. 2020. 12635-12642. DOI: 10.1021/jacs.0c03343.
(42) Stephan, D.W.; Erker, G." Frustrated Lewis Pair Chemistry: Development and Perspectives." Angew. Chem. Int. Ed. 54. 2015. 6400-6441. DOI: 10.1002/anie.201409800.
(43) Hofmann, M.; Kassube, J.K.; Graf, T. "The mechanism of Mo-/Cu-dependent CO dehydrogenase." J. Biol. Inorg. Chem. 10. 2005. 490-495. DOI 10.1007/s00775-005-0661-5.
(44) Siegbahn, P.E.M.; Shestakov, A.F. "Quantum Chemical Modeling of CO Oxidation by the Active Site of Molybdenum CO Dehydrogenase." J. Comput. Chem. 26(9). 2005. 888-898. DOI 10.1002/jcc.20230.
(45) Zhang, B.; Hemann, C.F.; Hille, R. "Kinetic and Spectroscopic Studies of the Molybdenum-Copper CO Dehydrogenase from Oligotropha carboxidivorans." J. Biol. Chem. 285(17). 2010. 12571-12578. DOI 10.1074/jbc.M109.076851
(46) Shanmugam, M.; Wilcoxen, J.; Habel-Rodriguez, D.; Cutsail, G.E. III; Kirk, M.L.; Hoffman, B.M.; Hille, Russ. " 13C and 63,65Cu ENDOR studies of CO Dehydrogenase from Oligotropha carboxidovorans. Experimental Evidence in Support of Copper−Carbonyl Intermediate." J. Am. Chem. Soc. 135. 2013. 17775-17782. DOI: 10.1021/ja406136f
(47) Hille, R.; Dingwall, S.; Wilcoxen, J. "The aerobic CO dehydrogenase from Oligotropha carboxidivorans." J. Biol. Inorg. Chem. 20. 2015. 243-251. DOI 10.1007/s00775-014-1188-4
(48) Stein, B.W.; Kirk, M.L. "Electronic structure contributions to reactivity in xanthine oxidase family enzymes." J. Biol. Inorg. Chem. 20. 2015. 183-194. DOI 10.1007/s00775-014-1212-8
(49) Stein, B.W.; Kirk, M.L." Orbital contributions to CO oxidation in Mo–Cu carbon monoxide dehydrogenase." Chem. Commun. 50. 2014. 1104-1106. DOI: 10.1039/c3cc47705c

(50) Rokhsana, D.; Large, T.A.G; Dienst, M.C.; Retegan, M.; Neese, F. “A realistic in silico model for structure/function studies of molybdenum–copper CO dehydrogenase.” J. Biol. Inorg. Chem. 21. 2016. 491-499. DOI 10.1007/s00775-016-1359-6
(51) Xu, K.; Hirao, H. “Revisiting the catalytic mechanism of Mo–Cu carbon monoxide dehydrogenase using QM/MM and DFT calculations.” Phys. Chem. Chem. Phys. 20. 2018. 18938-18948. DOI: 10.1039/c8cp00858b.
(52) Rovaletti, A.; Moro, G.; Cosentino, U.; Ryde, U.; Greco, C. “Can Water Act as a Nucleophile in CO oxidation catalyzed by Mo/Cu CO-dehydrogenase? Answers from Theory.” *Chem. Phys. Chem.* **2022**. 23(8) https://doi.org/10.1002/cphc.202200053

Chapter 2: Oxo- for Sulfido- Exchange in Molybdate and Tungstate Oxyanions and the Synthesis of Sterically Hindered Derivatives

Introduction:

Molybdenum is the 54th most abundant element in the Earth's crust where it is found in a variety of minerals as either Mo(VI), such as in the anion MoO_4^{2-}, or as Mo(IV), such as in MoS_2. The molybdate oxyanion is quite water-soluble, depending on the cation with which it is paired, and thus molybdenum is significantly more abundant in the oceans where it is the 25th most abundant element. [1] Aqueous molybdate is known to undergo ligand exchange reactions in the presence of aqueous sulfide in nature, which, depending on the conditions can lead to the accumulation of MoS_4^{2-} and small amounts of other mixed oxythiomolybdates $MoO_xS_{4-x}^{2-}$.[2,3] This chemistry is remarkably similar to that of the molybdenum's cousin, tungsten. [4] Perhaps it is due to this abundance, molybdenum's ready ability to exchange chalcogen atoms, and its rich redox chemistry that these species have been employed in several enzymes occurring in a wide range of organisms. Together these metallated enzymes number nearly 60 characterized members falling into four families.[5,6] With the notable exception of the nitrogen fixation enzyme, nitrogenase, nearly all of these enzymes catalyze oxygen-atom transfer reactions either from the metal to a substrate or the reverse reaction. Additionally, nearly all molybdoenzymes have a first coordination sphere that is a mixed oxygen/sulfur environment [7].

Beyond their biological applications mixed oxythiomolybdates and oxythiotungstates have found a wide variety of applications in other areas such as industrial lubricants and as corrosion control agents, as well as finding applications in nonlinear optics, as catalysts for hydrogen evolution reactions and ammonia evolution reactions, hydrodesulfurization catalysts in the oil industry, colorants and additives in the rubber industry, as reagents and catalysts in synthetic

organic chemistry for reactions such as alkene and alkyne metathesis like the famous Schrock catalyst, and as chromophores and ligands in inorganic chemistry. [8-19]

Original Synthesis:

The synthetic chemistry of mixed oxythiomolybdates and -tungstates predates their discovery in enzymatic active sites, with the original observation of their synthesis being credited to Berzelius in 1826.[20-24] Though his description of the reaction makes it difficult to know what was actually performed and the only characterization offered is a brief description of some of the physical properties of the product, Berzelius describe the synthesis:

> *In one of my experiment's, I received this salt crystallized: A somewhat dilute solution of potash molybdenum containing much double salt was decomposed by hydrogen sulfide gas and the solution concentrated by distillation. When the liquid no longer flowed with ease due to the amount of precipitate formed, it was cooled. Small runic red, heavy crystal grains appeared in the precipitate, which had the following properties when sloughed off: they were very small, showed up under the microscope as rectangular, transparent, ruby red scales, densely striped across the long side. At the usual air temperature, they were caustic potash. When boiled in water, they dissolved into an already red liquid, from which the super-sulfurous molybdenum was precipitated by hydrochloric acid. While*

it was gently glowing, with some crackling, they added water and a small trace of sulfur and hydrogen sulfide gas, and the salt became brilliantly grainy. Water only sucked sulfur-potassium from it, the undissolved was gray sulfur-molybdenum, which had retained the form of crystal flakes.

Reading between the lines of the archaic description produces the first report of the appearance of tetrathiomolybdate which was produced by the reaction:

$$H_2MoO_4 + KOH + xs\ H_2S(g) \underset{\Delta}{\rightarrow} K_2MoS_4$$

Equation 2: Berzelius' tetrathiomolybdate synthesis

The next chemist to approach this family of materials was Gerhard Krüss. In 1863, Krüss collated the works of Berzelius, and other early works by Debray, Bodenstab, and Braun, when he reported the first purposeful synthesis of the some of the mixed oxythiomolybdates in a manner more familiar to modern chemistry. He also included some rudimentary elemental analysis of the corresponding products and is credited with coining the name "mixed oxythiomolybdate."[22,23,24]

Krüss:

$$H_2MoO_4(s) + Na_2CO_3(s) \xrightarrow[\Delta(melt)]{} CO_2(g)\uparrow + Na_2Mo_3O_{10} + Na_2S \xrightarrow[EtOH]{} Red\ Oil + Yellow\ soln\ (Na_2MoO_3S)$$

$$H_2MoO_4(aq) + NH_4OH + H_2S \xrightarrow[\substack{6°C \\ 15-20}]{} (NH_4)_2MoO_2S_2\ (s)\downarrow$$

Equation 3: Krüss Mixed Oxythiomolybdate Synthesis

Using these methods, or adapted versions thereof, this report contained the synthesis and elemental analysis of $Na_2[MoO_3S]$, $(NH_4)_2[MoO_2S_2]$, $K_2[MoO_2S_2]$, $(NH_4)_2[MoS_4]$, $K_2[MoS_4]$ as well as

several other oxysulfido-molybdate compounds of higher nuclearity. Krüss also noted the hygroscopic nature of the isolated products and their propensity to discolor in air.

Ehrenfried Corleis credited the work of a different set of chemists in the field of the synthesis of sulfur compounds, specifically O.B. Kuhn, R. Schneider, and L.F. Nilson before noting the accomplishments of Krüss above.[25] Through noting the similarity between the reactivity of tungstates and molybdates, he was able to extend the above synthesis in 1886 with his reports of the syntheses of $Na_2[WS_4]$, $K_2[WS_4]$, $K_2[WOS_3]$, $K_2[WO_2S_2]$, and $K_2[WO_3S]$. This was accomplished through the employment of an adapted method, since higher nuclearity tungstate is insoluble in water. Corleis also found that the degree of chalcogen exchange could be controlled through adjustment of the pH of the tungstate solution.[26]

Modern Confirmation and Improvement

Another study of the synthesis of these species was not undertaken until 1961, when Bernard and Tredot published their replication of the previously performed syntheses as well as adaptations that allowed them to synthesize some of the sodium, potassium, and ammonium salts of the mixed oxythiotungstates and the ammonium salts of dithio- and tetrathiomolybdate. Most importantly the Bernard and Tredot report included the UV-vis spectra of their reported products.[26] Several things are notable about the first synthesis report of the modern era. Firstly, they do not report the synthesis or characterization of the monosulfido- species of either metal center, instead implying in their discussion that the dithiometallate is made directly from the oxyanion by the reaction of two equivalents of H_2S (*g*). Secondly, they note the difficulty in preparing any of the reported complexes in a pure form and present the observation that the oxo-for-sulfido reverse reaction is so facile that in a short time all the mixed oxo- sulfido species are present in a solution that initially contained only a single species.

A particularly notable improvement came in 1966, when Leroy and Kauffman prepared the first tetraalkylammonium salts (Me_4N^+ and Et_4N^+) of tri- and tetrathiomolybdate by the reaction of the tetraalkylammonium hydroxide with H_2MoO_4 or H_2WO_4 in a solution saturated with H_2S.[27]

$$NR_4OH + H2MO_4 + H_2S \xrightarrow[-5°C]{} [NR_4]_2MOS_3 \; or \; [NR_4]_2MS_4$$

$$[NH_4]_2MO_4 + 2\,P(Ph)_4Cl \; or \; 2\,As(Ph)_4Cl + H_2S \xrightarrow[\substack{Dilute\ NH_3 \\ water}]{} [P(Ph)_4]_2MS_4 \; or \; [As(Ph)_4]_2MS_4$$

$$R{=}Me, Et \qquad M{=}W, Mo$$

Equation 4: Leroy and Kauffman Mixed Oxythiomolybdate Synthesis wit organic cations

They also reported the synthesis of the tetraphenylphosphonium and arsonium salts by the reaction of $[NH_4]_2[MoO_4]$ or $[NH_4]_2[WO_4]$ with $(Ph_4P)Cl$ or $(Ph_4As)Cl$ in dilute aqueous ammonia. Finally, this report included a synthesis for trithiotungstate, $[WOS_3]^{2-}$, and the previously elusive trithiomolybdate, $[MoOS_3]^{2-}$ as their cesium salts by the acidification of a solution containing the dithiometallate, $[MO_2S_2]^{2-}$ (M=W, Mo), and 2 equivalents of cesium chloride over the course of a few hours at -5 °C. Their products were found by X-ray diffraction to be isomorphic with the lighter alkaline salts synthesized by previous methods. Lastly, this group also performed thermogravimetric analysis of the tetraethylammonium salt and found that it decomposes above 200 °C to MoS_3, triethylamine, and diethyl sulfide.

Müller and Diemann entered the field in 1968, having previously done vibrational analysis of the tetrathiomolybdate and tetrathiotungstate anions with a variety of cations.[28] Their first entry into the synthesis of mixed oxythiomolybdates was in confirming the synthesis and vibrational spectra of the cesium salt of trithiomolybdate and trithiotungstate which were previously reported by Leroy *et al.*[27] They also added a brief section on the reactivity of mixed oxythiomolybdates with the metal ammonium complexes of nickel and cobalt. This is the first available report of

mixed oxythiomolybdates in heterobimetallic complexes. [29] The employment of thiomolybdates as ligands and chromophores would be of great interest in the near future. Müller's work on the synthesis and characterization of this family of complexes continued, including a report in 1969 that showed evidence of the existence of $[MoO_3S]^{2-}$ and $[WO_3S]^{2-}$ through the examination of isosbestic points in the UV-vis spectrum of a reaction mixture taken throughout the course of the reaction of each respective oxyanion with hydrogen sulfide .[30] It wasn't until 1980 the Müller group reported a synthesis of the elusive monothiomolybdate by the vigorous shaking of a molybdate solution in an H_2S atmosphere for a short time followed by immediate precipitation. [31]

By 1954 mixed oxythiomolybdates had been discovered in the active sites of several biologically significant and chemically interesting enzymes, with the discovery of tungstates following in 1983.[32-36] Over the next decade this led to widened interest in the development of a simple and facile synthesis as well as the full characterization of these species. This discovery also strengthened the interest in the synthesis of derivatives and applications of the mixed oxythiomolybdates and oxythiotungstates. In 1983, the research group of John McDonald published their synthesis of mixed oxythiometallates.[37] While the syntheses of the tetrathiometallates and dithiometallates were essentially the same as those in the previous reports, the work of McDonald introduced several improvements and important observations. McDonald notes that tetrathiotungstate is sometimes contaminated by trithiotungstate, despite employing elevated temperatures. due to the much slower rate of chalcogen exchange to form the most substituted tungstate. This is not a problem for the molybdate, as the $[MoS_4]^{2-}$ species forms quite readily. The opposite problem is found for the trithiometallates with trithiotungstate being easily isolated in a pure form, while trithiomolybdate is often contaminated with tetrathiomolybdate. While the synthesis of Leroy and Muller's cesium salt of $[MoOS_3]^{2-}$ is simple and affords a

reasonably pure product, this cation imparts poor solubility. The McDonald synthesis modified the preparation of $[Et_4N]_2[MoOS_3]$ by flowing H_2S gas *over* a solution of ammonium molybdate at 0 °C, rather than bubbling the gas *through* the solution. McDonald followed this step with the immediate quenching of the reaction by precipitation and subsequent cation exchange. Also noted in this procedure is a key solubility difference; $[Et_4N]_2[MoOS_3]$ is soluble in isopropanol, whereas $[Et_4N]_2MoS_4$ is not. This work is considered a seminal paper in this field as it includes the UV-vis spectra of these products, including the molar extinction coefficients at their respective absorbance maxima. The inclusion of these values was particularly important as the absorption bands of the various products overlap extensively and good alternative characterization methods were lacking at the time.

McDonald's work represents the most significant improvement in the synthesis of these products since their original publication, but it glaringly omits any mention of the synthesis of the $[MO_3S]^{2-}$ anion for either metal. In fact, the 1980 Müller preparation remains the only published method for the synthesis of pure monothiomolybdate. However, in 1985, the group of R.H. Holm published a study on the reaction of $[^nBu_4N]_2[Mo_2O_7]$ with 0.5-7 equivalents of hexamethyldisilathiane, $Me_3Si\text{-}S\text{-}SiMe_3$, as seen in the reaction below.[38] The Holm group determined one of the early products of this reaction to be the silylated monosulfidomolybdate, $[MoO_2S(OSiMe_3)]^{1-}$. This monosulfido species was a minor product whose presence was primarily confirmed by ^{95}Mo, ^{17}O, and ^1H NMR measurements. The reactions described in this report produced solutions which were complex mixtures and were unstable under the experimental conditions. Due to these factors, this method was of limited usefulness until 7 equivalents of $(Me_3Si)_2S$ were added, at which point the multitude of contaminant NMR signals produced by the

mixtures of products shown in **Figure 20**, below, disappeared and a 31% yield of the triply exchanged trithotrimethylsilyloxymolybdate, [^{n}Bu$_4$N][MoS$_3$(OSiMe$_3$)], resulted.

$$(^nBu_4N)_2Mo_2O_7 + n(Me_3Si)_2S \xrightarrow{MeCN} (^nBu_4N)[MoO_{3-x}S_x(OSiMe_3)]$$

Equation5: The Holms Group chalcogen exchange reaction with hexamethyldisilathiane on Mo_2O_7

Figure 20: The Products and their proportions reported from the reaction of 1-7 equivalents of Hexamethyldisilathiane with Mo2O7 by Holms et al. Reprinted with permission from Do, Y. et al. "Oxo/Sulfido Ligand Substitution in $[Mo_2O_7]^{2-}$: Reaction Sequence and Characterization of the final product, $[MoS_3(OSiMe_3]^-$" Inorg Chem. 1985 24 1831-1838. Copywrite 1985 Amercian Chemical Society

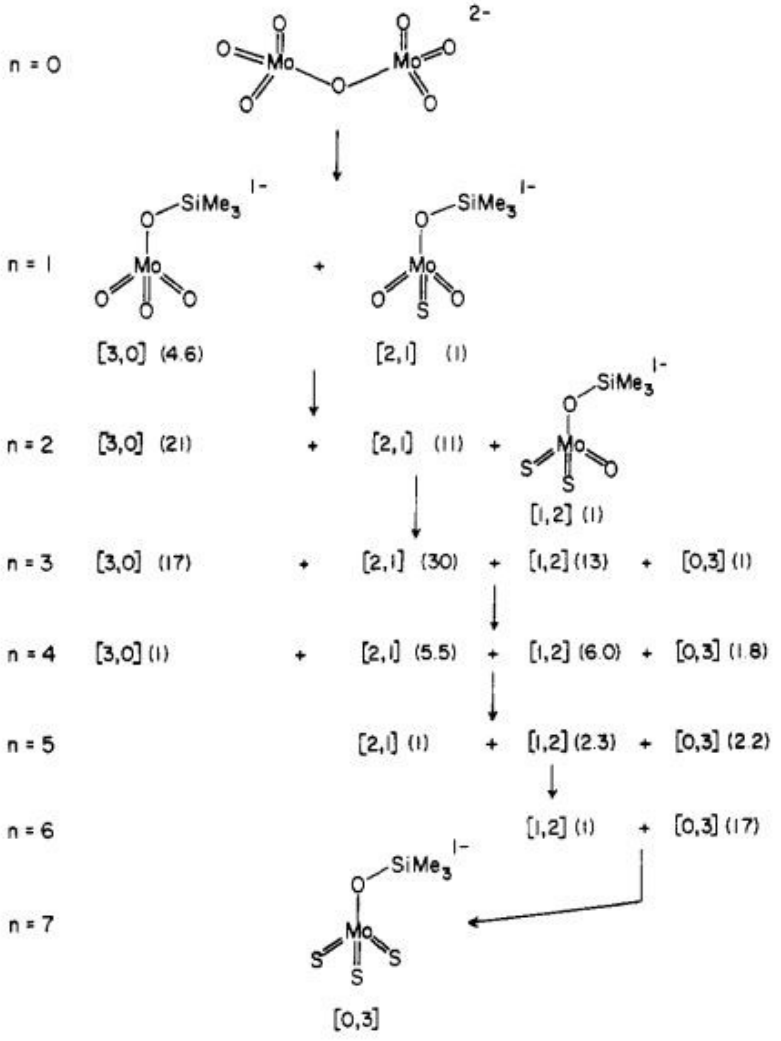

Much of the loss that resulted in the low yield of this reaction was thought to be due to the formation of NMR silent multinuclear clusters composed of reduced metal centers though none were reported. Similar work by the Holm group also found some other creative ways of generating the singly exchanged version of these metal oxyanions. In 2004 they reported the that the reaction of monosilylated molybdate with $(Et_4N)(SH)$ in dry acetonitrile at -20 °C in the presence of the 2,6-lutidine or $(Ph_3C)(PF_6)$ produced the monothiometallates in good yields and in high purity.[39] The same reagents carried out the desilylative chalcogen exchange on a monosilylated molybdate, $[MoO_3(OSiR_3)]^-$[40] as well as a later report of a chalcogen exchange procedure using Ph_3SiSH that was able to leave an existing silyl group in place.[41] Finally, they reported the chalcogen exchange reactions of triazacyclononane capped trioxometallates with Lawesson's reagent and B_2S_3.[41]

The employment of increasingly long chain tetraalkylammonium counter cations for the purpose of imparting solubility in organic solvents continued, first lead by the Holm Group, as noted above, then championed by Alonso *et al,* who reported the synthesis and characterization of the entire set of tetraalkylammonium (C=1-10) tetrathiomolybdates and -tungstates between 1998 and 2001.[42-44] The most recent advancement of this synthetic procedure was devised by Cruz-Reyes *et al* in 2017, when they reported that, in the synthesis of tetrathiotungstate, hydrogen sulfide gas can be replaced with a 40-48% solution of aqueous ammonium sulfide, $(NH_4)_2S$, which has the advantage of being more easily stored and measured than its gaseous predecessor though, it arguable that this is the reagent actually present in the earlier syntheses.[45] Most of the recent synthetic work has focused only on the synthesis of tetrathiomolybdate and none of the partially thiolated products have been reported from the use of this reagent.

Characterization:

The earliest characterization method for mixed oxythiometallates, employed by Krüss and Corleis was elemental analysis of crystalline samples.[22,25] While elemental analysis is still the gold standard by which much inorganic and organometallic chemistry is judged, it is insufficient to claim a positive identification based on this single data point. For example, for this family of compounds an equimolar mixture of $[Et_4N]_2[MoO_4]$, $[Et_4N]_2[MoO_3S]$, and $[Et_4N]_2[MoO_2S_2]$ would be indistinguishable from $[Et_4N]_2[MoO_3S]$.

The next step in the historical characterization of these products was the introduction of spectrophotometry, first UV-vis followed by vibrational spectroscopic methods.[26,27] As demonstrated by Müller and Leroy, all of the mixed oxythiometallates have clear and easily distinguishable IR transitions for both the M=O and the M=S bonds, illustrated as vertical lines on the chart in **Figure 21**, below. Many of these vibrations are also Raman active, a field in which Müller showed great interest and productivity.[46-50]

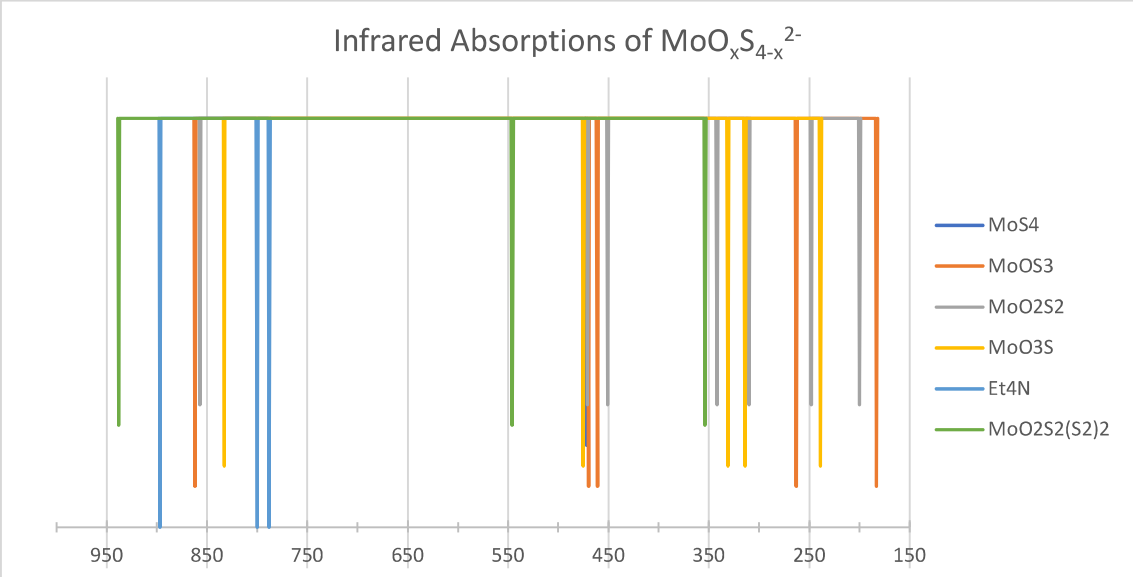

Figure 21: A line diagram of the infrared spectra maxima reported in Muller et al. 1973 and the reported absorption for the byproduct Mo2O2S2(S2)22-. Line lengths are only for discernment of maxima and not representative of extinction coefficient.

This makes IR and Raman spectrophotometry attractive characterization methods for any molybdate salt in which these regions aren't obscured by signals arising from the cation. Furthermore, the measurement of vibrational spectra allowed for the calculation of atomic force constants for the metal-chalcogen bonds in all of these species. The derivation of atomic force constant data from vibrational spectra was particularly important in light of the scant SC-XRD data on these species which is difficult to collect and model due to extensive disordering. This disorder arises from the tetrahedral shape of the molecule and the similarity in size of the oxo and sulfido ligands and is further exacerbated by the difficulty in synthesizing and crystallizing pure samples. The examination of the calculated force constants, shown in table 1 below, also helps to rationalize the kinetic data for the chalcogen exchange reaction examined in the next section. The force constant data shows that the strength of Mo-O bond increases as the number of bound oxygen atoms decreases. But there is no such linear relationship between the degree of sulfidation and the Mo-S bond strength, with the Mo-S bond strength initially decreasing as sulfur is substituted for oxygen until a marked increase when only one sulfido ligand remains.

	MoO_4^{2-}	MoO_3S^{2-}	$MoO_2S_2^{2-}$	$MoOS_3^{2-}$	MoS_4^{2-}
M=O	5.81	5.83	5.87	5.95	--
M=S	--	3.12	2.93	3.08	3.11

Table 1: The Mo-O and Mo-S force constant by the degree of chalcogen exchange on Molybdate. Data from Muller et al 1973

Vibrational spectroscopy, while useful, is not a standalone method. As can be seen in **Figure 21** above, the IR absorptions are not sufficiently resolved from those of other members of the mixed oxythiometallate family to be used as a measure of purity for any given sample. Instead, one is forced to rely on the number and position of these signals which overlap for the different species in question. Furthermore, the Mo=S vibrations for the mononuclear mixed

oxythiomolybdates occur below 500 cm^{-1} which is outside the measurement range of most modern IR instrumentation. Nearly all of the IR active vibrational modes are also Raman active for these species. The narrow linewidth of Raman scattering, coupled with the ability to measure lower energy transitions, allows the collection of the complete vibrational spectrum for any species. Thus, Raman can provide more clarity than IR when used on samples with more than one constituent.

The UV-vis spectra of these salts were discussed briefly above. The mixed oxythiometallates are highly colored, while the tetraoxomolybdate and tetraoxotungstate are both colorless. The molybdate progresses through yellow to orange, then red, and finally crimson as the chalcogen exchange is carried out, while tungstate progresses through increasing intense yellow hues.

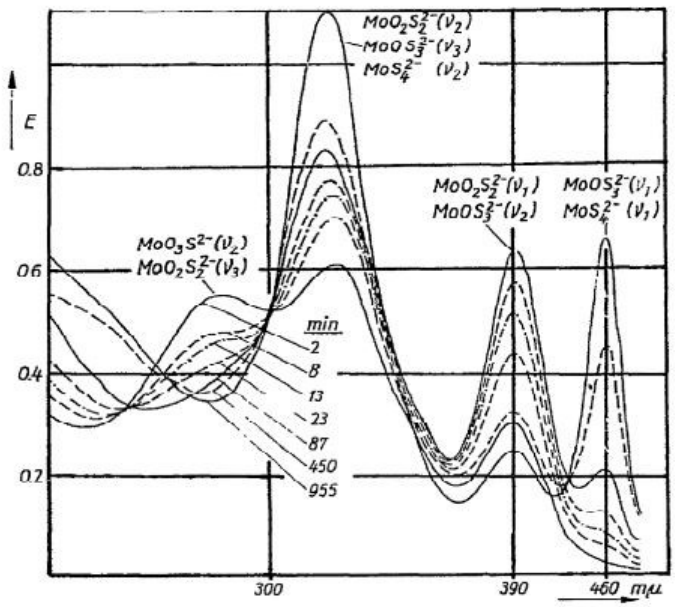

Figure 22: UV-Vis from Muller et al 1973 Showing the change in absorbance over time of a MoO42-/H2S reaction with absorbance maxima for each species labelled. Reproduced with permission from Müller, A. et al." Thiomolybdates and Thiotungstates: Their Properties and Role as Ligands in Coordination Chemistry." In: Müller, A., Newton, W.E. (eds) Nitrogen Fixation. (1983) Springer, Boston, MA. Copywrite 1973 Springer

UV-vis spectroscopy was first used to confirm the purity of synthesized samples by McDonald and coworkers but the spectra themselves were first published by Bernard and Tredot.[26,37] These spectra were the subject of intense discussion in the early mixed oxythiomolybdate and oxythiotungstate world, as the data they provided were used in sample systems for calculating transition energies and labelling electronic transitions. This scientific conversation included the synthetic chemists Bernard and Tredot[26], Müller[29,30,3146,6,50-54], and Leroy[27], but it also included such other participants such as Bartacki and Dembicka[19,55], and Clark[56] amongst them. The limitations of UV-vis as an analytical method began to be exposed by McDonald when he calculated that the absorption spectra could not confirm the presence of a $[MoOS_3]^{2-}$ impurity if it was less than 10% of the sample by mass.[37] This constraint is a direct result of the highly overlapping spectra, seen in **Figure 22** above, and is complicated by the difficulty in isolating a single pure species with which the spectra can be benchmarked. The problem of the lack of high-quality UV-vis data for these species is significant enough that consideration of it has extended to other facets of the study of these oxysulfido anion families including kinetics and reactivity studies.[57] The benchmarking problem may have been recently settled when Quagraine and Reid undertook a multivariate curve fitting study of the chalcogen exchange reaction using computationally deduced absorptivity values, though there have been throughout history several reported maxima and absorption coefficients for each constituent of the mixed oxythiometallate families.[57]

^{95}Mo is a spin active nucleus with a spin of 5/2 with a natural abundance of 15.92%. Lutz and Nolle were beginning to explore the applicability of NMR measurements in molybdenum structural determination when they first observed the ^{95}Mo NMR signals related to K_2MoO_4 in 1976.[58] The next year they created considerable impact in the mixed oxythiomolybdate field when

they demonstrated that each mixed of the oxythiomolybdates has a characteristic and well resolved ^{95}Mo signal. These signals are detectible at attainable concentrations and spread across a range of 2000ppm, the positions of the NMR signals can be seen in **Figure 23** below.[59]

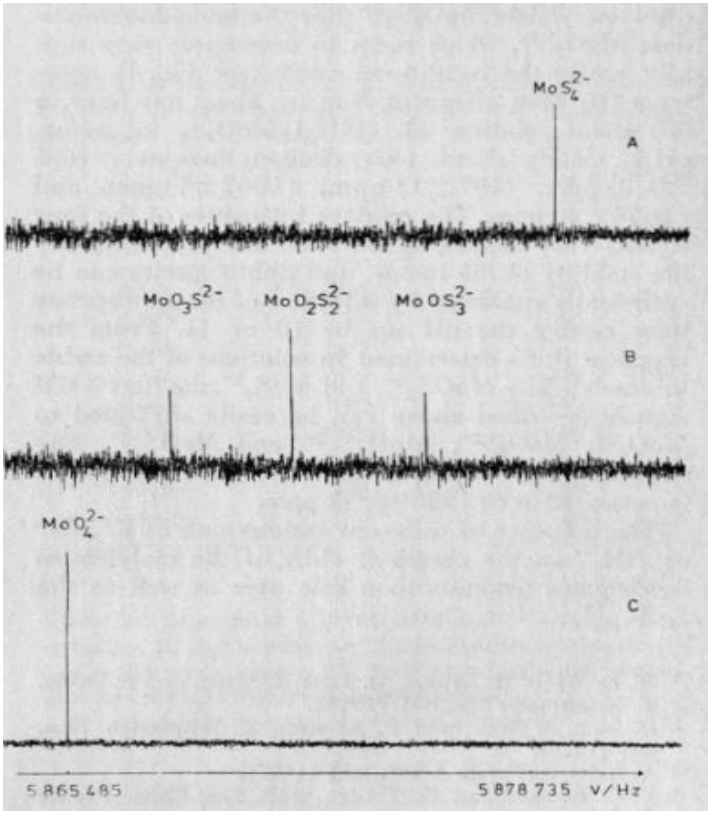

*Figure 23: ^{95}Mo NMR of the $[MoO_xS_{4-x}]^{2-}$ Reprinted from Lutz, O.; Nolle, A; Kroneck, P. "Use of ^{95}Mo NMR for Identification of Molybdenum(VI) Chalcogenide Anions in Aqueous Solution." Z. Naturforsch. **1977**. 31a 505-506. Copywrite DeGruyter 1977. Used with permission.*

While ^{95}Mo NMR may seem like a straightforward and unequivocal technique in this field, it has several drawbacks. Specifically, ^{95}Mo NMR is best collected in D_2O, at concentrations of 1 - 2 M, additionally, with its fast relaxation time, many replicate measurements are required causing long collection times. Under these conditions the less stable, i.e., less substituted, mixed oxythiomolybdates have enough time to decompose through ligand exchange and hydrolysis. Lutz and Knolle themselves showed that after 1 h at pH 7, a sample of $[NH_4]_2[MoO_2S_2]$ showed NMR

signals for $[MoO_4]^{2-}$, $[MoO_3S]^{2-}$, $[MoO_2S_2]^{2-}$, and $[MoOS_3]^{2-}$ which was the strongest evidence yet produced of molybdenum's facile ligand exchange processes.[59]

Ligand exchange and Nucleation Kinetics

Noticed early on in the modern examination of the mixed oxythiomolybdates and -tungstates was the ability of these species to undergo facile chalcogen exchange reactions. In other words, in solution, a pure sample of a single species will soon speciate into all of the members of the $[MO_xS_{4-x}]^{2-}$ (M = Mo or W) family quite quickly and for molybdenum can result in higher nuclearity complexes. While this behavior is one of the more interesting facets of the chemistry of these metalates and is of particular importance when utilized by the cell in metallated enzymatic active sites, it does have a confounding effect on efforts to synthesize and utilize these materials. Thus, this nucleation and ligand exchange phenomenon has undergone extensive investigation and quantification throughout the years, particularly for molybdenum, as it is of environmental and geochemical significance. This history of research has provided some clarity on the factors that control this ligand exchange.

The nature of H_2S, and of gaseous reagents in general, made kinetic and mechanistic studies challenging. The first study of any kinetics involving H_2S and inorganic salts appeared in the late 1970s, when the engineering adaptations arose that enabled them.[60] Harmer and Sykes followed not long after with a study of the mechanism, kinetics, and equilibria of the chalcogen exchange of $[MoO_xS_{4-x}]^{2-}$. This study was carried out using saturated aqueous solutions of H_2S, or 1.1 M solutions of ammonia and hydrogen sulfide for the more substituted members of the family. These reactions were buffered to pH ranges 3.6-5.6 or 8.2-10.2.[61] Harmer and Sykes explicitly considered several reactions including the oxygen-for-sulfur exchange of $[MoO_4]^{2-}$, the sulfur-for-oxygen exchange of $[MoS_4]^{2-}$, and both of these reactions of $[MoOS_3]^{2-}$. This set of reactions

allowed them to calculate an array of rate constants K_{01}, K_{10}, K_{23}, K_{32}, K_{34}, and K_{43}. In their notation, the first subscript is the degree of sulfidation of the starting species and the second subscript is the degree of sulfidation of the product species, so K_{23} is the rate at which $[MoO_2S_2]^{2-}$ becomes $[MoOS_3]^{2-}$. In the first exchange reaction, represented by the formula:

$$MoO_4^{2-} + H^+ + HS^- \rightleftarrows MoO_3S^{2-} + H_2O$$

the corresponding rate law expression resulted:

$$\frac{1}{\varepsilon_{obs}} = \frac{1}{K_{01}[H^+]\varepsilon_1}\frac{1}{[MoO_4^{2-}]} + \frac{1}{\varepsilon_1}$$

Equation 6: Harmer and Sykes' Rate Law

in which ε_{obs} and ε_1 are the molar absorptivity coefficients for $[MoO_3S]^{2-}$ and $[MoO_4]^{2-}$ respectively, and K_{01} is the rate of the forward reaction. Plotting the measured absorption vs $1/[MoO_4^{2-}]$ resulted in a linear plot the slope of which was $K_{01}[H^+]$, which is the proton concentration dependent rate of the first chalcogen exchange reaction. A value of $K_{01} = (5.8 \pm 0.3) \times 10^{11}$ was found for the forward reaction under the conditions studied by examining the equilibrium position over a range of pH values, similarly, K_{10} was determined to be $(6.5 \pm .05) \times 10^{-3}$ under the conditions studied. Both of these rates were also found to be dependent on the pH of the solution. Though the pH dependance of further exchange reactions was questioned, all the forward reactions were observed to be considerably more rapid than the reverse reactions. Furthermore, they calculated that subsequent oxo-for-sulfido exchanges took place at increasingly slow rates, with the trithiomolybdate to tetrathiomolybdate reaction requiring more forcing conditions than the other reactions for a rate constant to be measured at all.

Harmer and Sykes reached several conclusions from the analysis of their rate study. Mechanistically they concluded that the chalcogen exchange in either the forward or reverse

direction must take place by an associative addition mechanism, the H_2S (*aq*) or H_2O associates with a protonated tetrahedral molybdate anion, or perhaps a protonated octahedral molybdate with two coordinating water molecules, as the first step of the reaction. They rationalized that increasing sulfido-for-oxo substitution leads to a reduced rate of further substitution due to increased steric crowding by the larger sulfido- ligands. Further, this steric crowding may have the subsequent effect of reducing the amount of octahedral complex present in solution. While this point has not been the subject of much further investigation in relation to the reaction in question, Lu and Liu found in 2013 that the solution structure of molybdate in aqueous solution is most likely the doubly protonated, doubly hydrated octahedral form and that this hydration and protonation weakens the Mo=O bonds.[63] Lastly, Harmer and Sykes extended their speculation to the analogous reactions of the tungstate family of mixed oxythiometallates.

This work was followed by that of Laurie *et al.* in 1987, which did support the Harmer and Sykes data in some areas, notably their mechanistic proposals.[63] However, the Laurie study differed significantly in some of its findings and interpretations from its predecessor. Amongst the primary differences were that this study was limited to a pH range of 6-7 using phosphate buffers, a profoundly different scenario as the work of Harmer and Sykes had established the pH dependance of the forward and reverse reactions. Further, Laurie explicitly studied the monothio- to dithiomolybdate and dithio- to trithiomolybdate reactions whereas Harmer and Sykes had neglected the former and inferred the latter from other data. Finally, the Laurie work considered the possibility of several exchanges happening in near-simultaneous rapid succession, rather than as a single stepwise exchange that then stops. This idea harkens back to the thought of a double oxygen-for-sulfur exchange proposed by Leroy before the existence of $[MoO_3S]^{2-}$ was confirmed. While treating the chalcogen exchange as discrete events does simplify the data treatment, the

former is in much better agreement with observations. This concept of rapid successive reactions is particularly pertinent for the aqueous reverse reaction in which there is a large concentration of reactive species, H_2O, present in solution. Laurie also refutes the pH independence of the $[MoOS_3]^{2-}$ to $[MoO_2S_2]^{2-}$ transformation, arguing that they could isolate no product species and that the reaction must rapidly proceed all the way to $[MoO_4]^{2-}$ at pH 3-7 at a rate that matches the measurement by Harmer and Sykes for the single step reaction.

In 2000, Erikson and Helz reported their treatment of the equilibrium, stability, and lability of the mixed oxythiomolybdates in relation to their geochemical significance.[2] They employed carefully set-up, long reaction time experiments which they evaluated by UV-vis within time regimes where it was expected that only two mixed oxythiomolybdates were in solution. The concentrations of the two mixed oxythiomolybdates present were calculated from the measured absorbance values of the solutions and the reported extinction coefficients for the species present. The resulting calculated concentrations were used to calculate reaction quotients until the concentrations became stable. Thus, equilibrium constants for the forward and reverse reaction for each member of the mixed oxythiomolybdate family were obtained. This experimental design allowed them to test a wide regime of different reaction conditions and confirm that the reaction is indeed first order in both molybdate and H_2S (*aq*), and also that the reaction is subject to acid catalysis. They did postulate that there is perhaps an alternative reaction pathway for the trithiomolybdate to tetrathiomolybdate reaction that exists at very high buffer concentrations, but otherwise confirmed the reaction mechanism proposed by Harmer and Sykes. However, the accuracy of these results depends on only the two members of each stepwise pair being present in solution, an assumption that seems dubious given the apparent extent of the ability of these metals

to readily exchange sulfido- and oxo- ligands in light of the Lutz and Knolle NMR result, and the Laurie kinetics work detailed above.

Novel Work:

The work of Harmer and Sykes and those that came after them have shown a strong dependance on the protonation of an oxo or sulfido ligand to promote the reaction that causes chalcogen exchange in either direction. Despite nearly 200 years of innovation in this field, water and hydrogen sulfide are still the reagents most employed in the synthesis of mixed oxythiometallates, ignoring that they possess Brønstead acid/base behavior and thus give rise to facile ligand exchange. Since the problem of ligand exchange, and thus the difficulty of forming a single pure product, requires protonation as postulated in the kinetics work above. The ligand exchange problem might be eliminated by doing away with water as the reaction medium and instead performing the chalcogen exchange in an anhydrous organic solvent. By exchanging the cation of a molybdate or tungstate anion for a quaternary ammonium cation, or other organic cation, sufficient solubility in an organic medium is attained that enables this idea to be explored. To further this aim, rather than using hydrogen sulfide gas, the hydrosulfide anion, or ammonium sulfide as the chalcogen exchange reagent, an analogous disilylsulfide, such as hexamethyldisilathiane, can be employed to avoid another source of protons in solution. This reaction will be driven to completion by the formation of the more thermodynamically stable Si-O bonds from the less stable Si-S bonds in the starting material.

$$[Et_4N]_2MoO_4 + x(CH_3Si)_2S \xrightarrow[MeCN]{} [Et_4N]_2MoO_{4-x}S_x + x(CH_3Si)_2O$$

Equation 7: Synthesis of Mixed Oxythiomolybdates using hexamethyldisilathiane.

To investigate the feasibility of this hypothesis, an extensive computational investigation of the thermodynamics of each oxygen for sulfur exchange was undertaken for both the molybdate and tungstate anion, as well as a computation investigation of the proposed reaction pathway in an effort to elucidate the reaction mechanism.

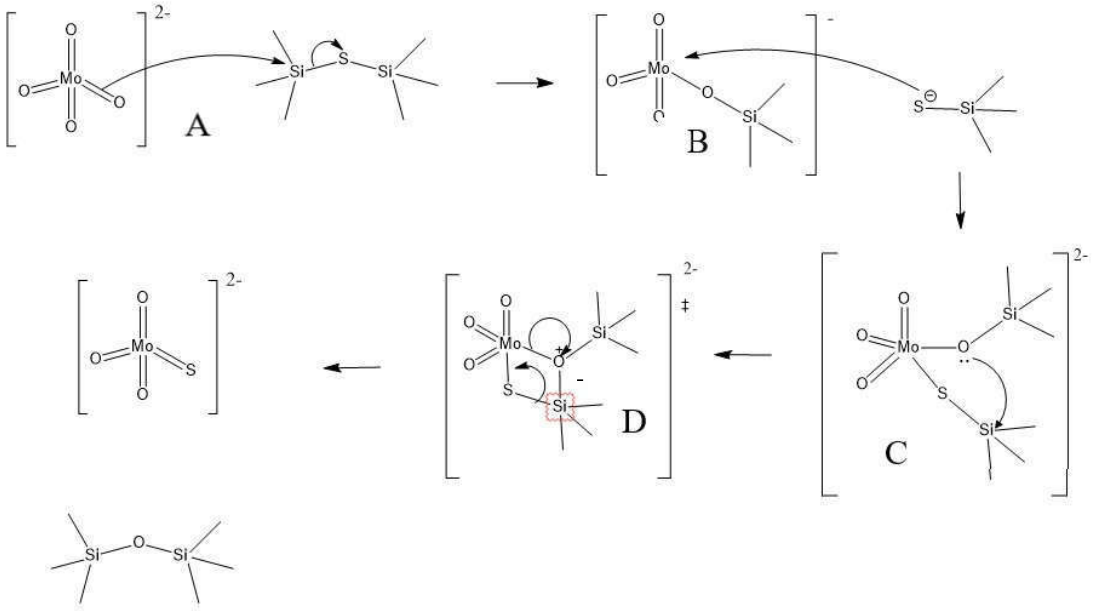

Figure 24: The reaction mechanism proposal for the chalcogen exchange of the molybdenum oxyanion with hexamethyldisilathiane

The proposed mechanism proceeds in a similar manner to that proposed for the aqueous reaction by Harmer and Sykes, above. The reaction begins when one of the trimethylsilyl groups of hexamethyldisilathiane is attacked by the nucleophilic molybdate oxo-ligand with the trimethylsilanethiolate anion acting as a leaving group as illustrated in **Figure 25** step A, above. This produces a metal bound silyloxy ligand which is shown to have notably longer metal-oxygen bond, labelled B above. The electropositive metal is then attacked by the trimethylsilanethiolate anion in a position adjacent to the silylated oxygen, thereby generating intermediate C above, in which the molybdate is in a distorted square planar geometry. As the new bond forms with the

incoming trimethylsilanethiolate, the bond to the leaving trimethylsilyloxide ligand lengthens, increasing the charge density on the oxygen and attracting the electropositive trimethylsilyl group from the incoming trimethylsilanethiolate ligand. This produces a four membered transition state, D in the scheme above, in which the metal center is forming a bond with the silanethiolate sulfur while the metal-oxygen bond, which was previously weakened by the first trimethylsilyl attack, is a forming a strong interaction with the thiolate silane group. The Si–O bond being much stronger than the Si–S bond, the four-membered ring intermediate collapses, breaking the Si–S bond and leaving the sulfur atom as a fully reduced terminal sulfido ligand (S^{2-}). This produces the stable hexamethyldisiloxane, which exits the coordination sphere of the metal center and completes the chalcogen exchange reaction.

While the four-membered ring intermediate, labelled D in figure 24 above, has been shown to form with the less sterically encumbered H_3Si- group its formation with the Me_3Si- has been shown to be much higher in energy. This may result in a different reaction pathway which deviates from the above pathway after the formation of intermediate C. Rather than forming the four-membered ring intermediate, the rearrangement of the distorted square planar transition state to tetrahedral causes the dissociation of the siloxide ligand. The siloxide then attacks the silicon atom of the associated silanethiolate in a manner analogous to an S_N2 reaction. This attack forms the Si-O bond, breaking the Si-S bond with the oxythiometallate acting as the leaving group, generating the products above.

Computational Investigation:

Theoretical calculations were carried out utilizing both the Supercomputing Facility at Tulane University New Orleans and through WebMO. The GAUSSIAN-09 package[64] was used to perform all calculations. Geometry optimizations were conducted using the Becke, 3- Parameter,

Lee-Yang-Parr (B3LYP) level of theory,[65] the pure functional of Perdew, Burke, Ernzerhof (PBE0),[66] and the Moller-Plesset expansion truncated at the second order (MP2) [67] for the purpose of comparison with the typical basis sets. Optimizations were carried out starting from the anion in T_d symmetry to the "verytight" tolerance level, with force constants recalculated at every step of the optimization, and with no symmetry restriction placed on the structure. Frequency calculations were used to confirm the validity of optimized structures and thermochemical quantities were calculated from these outputs in the standard way at 298.15 K.[68] For molybdenum, and silicon a double-ζ (DZ) basis set with an effective electron core potential (LANL2DZ ECP) was implemented.[69] For all lighter atoms (hydrogen, carbon, nitrogen, potassium, oxygen and sulfur) the Pople-style augmented basis set including diffuse functionals, 6-311++G (2d,2p), was chosen.[69,70] Implicitly solvated model systems were calculated using the polarizable continuum model employing on-the-fly selection of either acetonitrile or methanol as applicable.[71] The entire series of mixed oxythiomolybdates with the general formula, $[MoO_xS_{4-X}]^{2-}$ were optimized as the isolated anion and as the potassium or tetramethylammonium salts for the purpose of examining both tightly associated and loosely associated ion interactions. The set was also optimized in the gas phase, as well as solvated in either methanol or acetonitrile to investigate the effects of external polarity on the system energetics. ΔH_f^0 and ΔG_f^0 were calculated as detailed in the white paper from Ochterski,[68] which is from the ε_0+H_{Corr} and ε_0+G_{corr} of the products and reactants respectively, and follows the form of Hess' Law:

$$\Delta_{rxn}H^0(298.15\,K) = \sum(\varepsilon_0 + H_{corr})_{Prod} - \sum(\varepsilon_0 + H_{corr})_{react}$$

Equation 8: The calculation of $\Delta_{rxn}H^0(298.15\,K)$ from the white paper by Ochterski.

The ΔG_f^0 is calculated similarly. As the elements on both sides of this equation are the same, and thus cancel out, only the molecular information is left which is what is required to compute this value. The same thermodynamic parameters were also calculated from ΔH_f^0 and ΔG_f^0 to control for errors that arise from the effective core potential and misidentified anharmonic vibrations and internal rotations. This is a slightly more involved calculation which requires the calculation of the ΔH_f^0 (0 K) from the ΔH_f^0 of the constituent atoms and the atomization energy of the molecule:

$$\Delta H_f^0(M, 0K) = \sum_{atoms} x\Delta H_f^0(X, 0K) - C\left(\sum_{atoms} x\,\varepsilon_0(X) - \varepsilon_0(M) - \varepsilon_{ZPE}(M)\right)$$

Equation 9: The Second method for the calculation of $\Delta H_f^0(M, 0K)$ from the white paper by Ochterski

in which x is the number of each element present, the ΔH_f^0 is the literature value for the standard enthalpy of formation for that atom, taken from NIST or Argonne National Lab Active Thermochemical database,[72,73] C is the conversion factor from Hartree/particle to Kcal/mol which is 627.5095, ε_0(X) is the sum of the electronic and zero point energy for each atom from the frequency calculation, and $\varepsilon_0(M) - \varepsilon_{ZPE}(M)$ is the sum of the electronic energy and the zero point energy from the frequency output for the molecule. This is scaled to 298.15 K by:

$$\Delta H_f^0(M, 298.15\ K) = \Delta H_f^0(M, 0K) + C\left(H_{corr}(M) + \varepsilon_{zpe}(M)\right) - x\Delta H_f^0(T)X$$

Equation 10: The equation for the calculation of $\Delta H_f^0(M, 298.15\ K)$ from the white paper by Ochterski

where H_{corr}(M) and ε_{ZPE}(M) are from the frequency output for the molecule, and $x\Delta H_f^0(T)X$ is the difference between the ΔH_f^0 of the constituent elements at the different temperatures, 0 K and 298.15 K. With the corresponding ΔH_f^0 now in hand, ΔG_f^0 can be calculated in the usual way

employing literature values for the ΔS^0 of the constituent elements. With ΔH_f^0 and ΔG_f^0obtained through either method the entropic contribution to the Gibb's Free energy can be obtained by:

$$\Delta G_f^0 = \Delta H_f^0 - T\Delta S_f^0$$

$$\Delta G_f^0 - \Delta H_f^0 = -T\Delta S_f^0$$

Equation 11: That equation for Gibb's Free Energy Solved to isolate the entropy term.

In which ΔG_f^0 is the Gibb's free energy obtained by either method above in the standard state, $\Delta H_f^0$is the enthalpy of formation obtained by either method above in the standard state, ΔS_f^0 is the corresponding standard entropy of formation, and T is the temperature in kelvin.

The first step toward evaluating the quality of any DFT calculation is structural comparison of the computed geometries to those available in the literature. The computed structures are solvated or in gas phase while available measurements for Mo-O and Mo-S bond lengths are from SC-XRD crystal structures. Direct comparison, if not exact, are nonetheless useful. The three different levels of theory produced similar results for the bond lengths, seen in **Table 2** below, with the PBE0 level of theory consistently predicting the shortest bond lengths and MP2 consistently predicting the longest, though the two never differ by more than 0.06 Å with an average difference of 0.045 Å.

Table 2: Bond lengths for the structure computed under three levels of theory and their comparison to literature values.

	MoO4			K2MoO4			Literature
	B3LYP	MP2	PBE0	B3LYP	MP2	PBE0	
Mo-O	1.80	1.84	1.79	1.79	1.83	1.78	1.82[1]
	MoO3S			K2MoO3S			
	B3LYP	MP2	PBE0	B3LYP	MP2	PBE0	
Mo-O	1.78	1.82	1.76	1.78	1.81	1.76, 1.77	1.753[2]
Mo-S	2.32	2.35	2.30	2.25	2.29	2.23	2.2222[2]

	MoO2SS2			K2MoO2S2			
	B3LYP	MP2	PBE0	B3LYP	MP2	PBE0	
Mo-O	1.76	1.80	1.74	1.77	1.81	1.75	1.724[2]
Mo-S	2.28	2.30	2.26	2.24	2.27	2.22	2.141[2]
	MoOS3			K2MoOS3			
	B3LYP	MP2	PBE0	B3LYP	MP2	PBE0	
Mo-O	1.75	1.80	1.75	1.76	1.80	1.75	1.720[3]
Mo-S	2.25	2.28	2.25	2.22	2.24, 2.32	2.22	2.187[3]
	MoS4			K2MoS4			
	B3LYP	MP2	PBE0	B3LYP	MP2	PBE0	
Mo-S	2.22	2.22	2.20	2.21	2.25	2.19	2.179[3]

1: *Data retrieved from the Materials Project for MoO4 (mp-1221467) from database version v2022.10.28.*
2. Data retrieved from ref 47,48
3.Data retrieves from ref 49, 50

The evaluation of calculated vibrational frequencies also provides a simple method for determining the quality of any given calculation, and vibrational data for these species is readily available. As can be seen in **Table 3** below, there is no one level theory that outperforms the other two for every species in this series. Although for each set the PBE0 level of theory has the smallest average error, it is outperformed by B3LYP when average of the absolute value of the error is the metric of quality. For $[MoO_4]^{2-}$ both B3LYP and PBE0 do a reasonably good job approximating the experimental vibrational frequencies with PBE0 attaining an error of less than 2% on both vibrations, while B3LYP was slightly worse with an average error above 2.5%. PBE0 also performs the best for the monothiomolybdate anion when considering the whole set, though B3LYP has lower absolute error when considering the higher energy characteristic vibrations for this ion. For the prediction of the vibrational frequencies of the dithiomolybdate, again, B3LYP and PBE0 do an equally good job, though B3LYP has the lower average error when compared to the literature values. PBE0 also performs the best for the trithiomolybdate anion when both the average error and the average absolute value error are considered with the average error across all

of the trithiomolybdate vibrations being less than 1%. The tetrathiomolybdate is the only member of the set in which MP2 is the top performer, with its exact calculation for the frequency of the reported vibrational mode. Although PBE0 is a close second in this case with both of these levels of theory drastically outperforming the B3LYP level of theory. With the structural and vibrational comparison considered, it is evident that that PBE0 and B3LYP are the best performers when it comes to predicting the structures and vibrational frequencies of the mixed oxythiomolybdates. While the quality of MP2 calculations is not profoundly wrong, and indeed sometimes even the closest of the three, taken as a whole it seems to overestimate bond lengths which led to the calculation of lower vibrational frequencies sometimes by as much as 20%.

Table 3: The computed vibrational frequencies compared to literature values.

MoO_4				
Literature	901	857		
B3LYP	887	827	316	299
MP2	791	757	284	275
PBE0	892	846	320	304

MoO_3S								
Literature	882	833	475	331	314	239		
B3LYP	879	858	412	314	291	210		
MP2	827	781	408	287	266	192	191	144
PBE0	906	881	429	321	305			

MoO_2S_2									
Literature	857	471	451	342	310	248	200		
B3LYP	886	442	431	252	174	157	228	208	154
MP2	840	801	442	420	284	239	213	144	
PBE0	912	900	447	442	317	266	233	210	156

$MoOS_3$						
Literature	862	470	461	263	183	
B3LYP	886	442	431	252	174	157
MP2	818	461	419	231	163	148
PBE0	913	462	450	257	175	159

MoS_4					
Literature	472				
B3LYP	453	452	438	141	156
MP2	472	416	161	147	
PBE0	474	458	173	159	

Isolated Anion:

For the molybdate anion in the gas phase, all three employed levels of theory display a similar picture of the energetics for chalcogen exchange reaction with both hexamethyldisilathiane and H_2S, as can be seen in **Table 4** below. Under all three levels of theory employed, the ΔG_f^0 is more negative for the hexamethyldisilathiane/hexamethyldisiloxane reaction than for the hydrogen

Table 4: ΔHrxn and ΔGrxn of the modeled systems as the isolated anion in the gas pahse under the three levels of theory employed (B3LYP, MP2, and PBE0)

Gas Phase Anion Method 1	ΔH_{rxn} HMDS/HMDO (Kcal/mol)	ΔG_{rxn} HMDS/HMDO (Kcal/mol)	ΔH_{rxn} H2S/H2O (Kcal/mol)	ΔG_{rxn} H_2S/H_2O (Kcal/mol)
$MoO_4 \rightarrow MoO_3S$	-36.6258 (B3LYP)	-37.2885 (B3LYP)	-22.6261 (B3LYP)	-22.4435 (B3LYP)
	-37.1843(MP2)	-37.9894 (MP2)	-24.4900 (MP2)	-24.2991 (MP2)
	-32.5050 (PBE0)	-33.2825 (PBE0)	-25.9387 (PBE0)	-26.3253 (PBE0)
$MoO_3S \rightarrow MoO_2S_2$	-31.1420 (B3LYP)	-31.7143 (B3LYP)	-17.1423 (B3LYP)	-16.8694 (B3LYP)
	-30.2278 (MP2)	-30.9168 (MP2)	-17.5332 (MP2)	-17.2264 (MP2)
	-26.6748 (PBE0)	-27.3676 (PBE0)	-20.7015 (PBE0)	-20.4104 (PBE0)
$MoO_2S_2 \rightarrow MoOS_3$	-28.2216(B3LYP)	-28.7493 (B3LYP)	-14.2219 (B3LYP)	-13.9044 (B3LYP)
	-27.0664 (MP2)	-27.7045 (MP2)	-14.3719 (MP2)	-14.01416966 (MP2)
	-23.5630 (PBE0)	-24.1993(PBE0)	-17.5897 (PBE0)	-16.3762 (PBE0)
$MoOS_3 \rightarrow MoS_4$	-26.3723(B3LYP)	-26.8499 (B3LYP)	-12.3720 (B3LYP)	-12.0049 (B3LYP)
	-26.5656 (MP2)	-27.1605 (MP2)	-13.8711 (MP2)	-13.4702 (MP2)
	-21.6121 (PBE0)	-22.2226 (PBE0)	-15.6388(PBE0)	-15.2654 (PBE0)

sulfide/water reaction with an average difference of 4.5 kcal/mol between the largest ΔG_f^0 and the smallest ΔG_f^0 among the different levels of theory for each reaction step. The entropic contribution to ΔG_f^0, calculated by subtracting the enthalpy term from the Gibb's free energy term as shown in **Equation 11** above, is generally small and positive for the H_2S/H_2O reaction and larger and negative for the HMDS/HMDO reaction as shown on **Table 5**, below, the values for all entropic terms are plotted at the end of this section in **Figure 25**. Interestingly the energetic spacing of the

products, that is the $\Delta\Delta G_{rxn}$, for the formation of the same products under any given level of theory, employing either set of reagents, is equal. For example, the $\Delta\Delta G_{rxn}$ for the reaction to form $[MoOS_3]^{2-}$ from $[MoO_2S_2]^{2-}$ under B3LYP is 2.96 kcal/mol regardless of which reagent is used to carry out this transformation. Also of note is that the MP2 level of theory has the largest curvature, when calculated by its deviation from the best fit line. The curvature is also evident by noting that the largest and smallest $\Delta\Delta G_{rxn}$ belong to this set of calculations.

The ΔH_f^0 and ΔG_f^0 can be calculated from the ΔH_f and ΔG_f values that can also be extracted from the frequency calculation output file as shown above in **Equation 9** and **Equation 10**. Since the values calculated by method 1 employ values extracted from the partition function for the molecule, they might factor in errors from the incorrect assignment of vibrational modes. The values from method 2 employ only the sum of the electronic and zero-point energy and literature values for the ΔH_f^0 and ΔS_f^0 for their constituent atoms. Thus, they are not as exposed to errors

Table 5: ΔG_{rxn} and ΔH_{rxn} calculated by Method 2.

Gas Phase Anion Method 2	ΔH_{rxn} HMDS/HMDO (Kcal/mol)	ΔG_{rxn} HMDS/HMDO (Kcal/mol)	ΔH_{rxn} H2S/H2O (Kcal/mol)	ΔG_{rxn} H_2S/H_2O(Kcal/mol)
$MoO_4 \rightarrow MoO_3S$	-36.4062 (B3LYP)	-35.7429 (B3LYP)	-22.6075 (B3LYP)	-18.0970 (B3LYP)
	-37.1881 (MP2)	-38.6621 (MP2)	-24.4942 (MP2)	-24.7760 (MP2)
	-32.5042 (PBE0)	-31.7267 (PBE0)	-26.5305 (PBE0)	-26.7363 (PBE0)
$MoO_3S \rightarrow MoO_2S_2$	-30.9243 (B3LYP)	-30.3514 (B3LYP)	-17.1256 (B3LYP)	-12.7054 (B3LYP)
	-30.2102 (MP2)	-31.7545 (MP2)	-17.5163 (MP2)	-17.8683 (MP2)
	-26.6754 (PBE0)	-25.9825 (PBE0)	-20.7015 (PBE0)	-20.9921 (PBE0)
$MoO_2S_2 \rightarrow MoOS_3$	-28.0032 (B3LYP)	-27.4749 (B3LYP)	-14.2045 (B3LYP)	-9.8289 (B3LYP)
	-27.0463 (MP2)	-28.6370 (MP2)	-14.3524 (MP2)	-14.7509 (MP2)
	-23.5627 (PBE0)	-22.9271 (PBE0)	-17.5891 (PBE0)	-17.9367 (PBE0)
$MoOS_3 \rightarrow MoS_4$	-26.1540 (B3LYP)	--25.6764 (B3LYP)	-12.3553 (B3LYP)	- 8.0305 (B3LYP)
	-26.5324 (MP2)	-28.6370 (MP2)	-14.3523 (MP2)	-14.7509 (MP2)
	-21.6119 (PBE0)	-21.0007 (PBE0)	-15.6381 (PBE0)	-16.0103 (PBE0)

stemming from the incorrect assignment of vibrations in the same manner. Because of this

Figure 25: Graphs of the thermodynamic parameters for the chalcogen exchange of the isolated molybdate anion in the gas phase

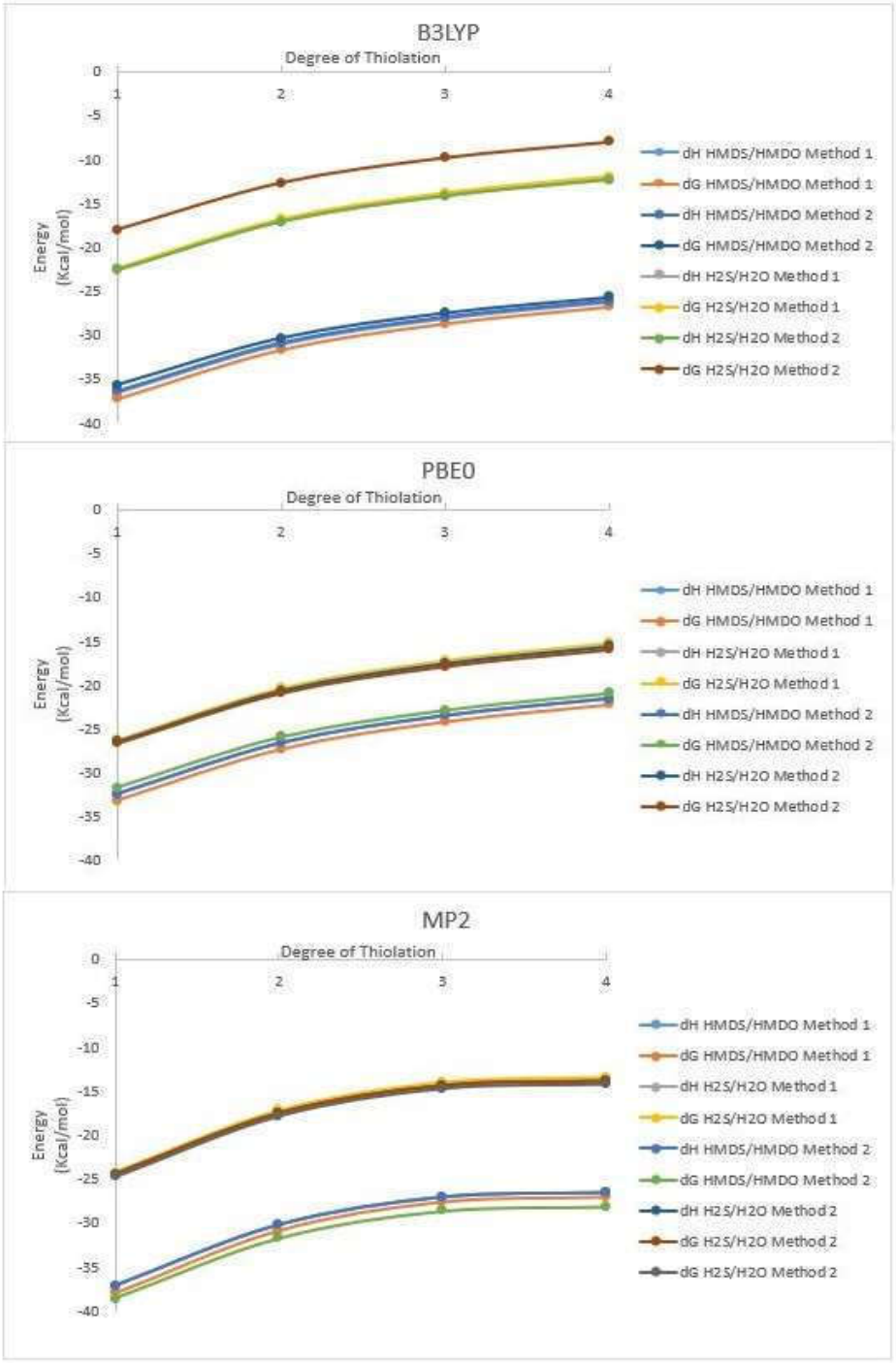

difference the values calculated in this way differ slightly as can be seen in **table 5** below.

While the values for the thermodynamic parameters are similar in magnitude and have comparable $\Delta\Delta G_{rxn}$ values when calculated from the ΔH_f^0, the most notable difference is the entropic contribution to the reported ΔG_f^0 values. The $\Delta\Delta G$ values and entropy term values can be see below in **Table 6**. Under the B3LYP level of theory the entropic term is negative and nearly equal to the above reported values for the HMDS/HMDO system; however, for the H_2S/H_2O system the entropic term calculated by this method is positive and much larger in magnitude than that calculated above, resulting in ΔG_f^0 values that are smaller by an average of more than 4 Kcal/mol. This example provides a stark contrast to those calculated under the MP2 level of theory

Table 6: The entropy term and the ΔG of the isolated anion in the gas phase under all three levels of theory.

Gas Phase Isolated Anion	Method 1				Method 2			
	HMDS/HMDO		H_2S/H_2O		HMDS/HMDO		H_2S/H_2O	
B3LYP	ΔS	ΔΔG	ΔS	ΔΔG	ΔS	ΔΔG	ΔS	ΔΔG
O4->S1	-0.6627		0.1826		-0.6633		4.5105	
		5.5742		5.5742		5.3916		5.3916
S1->S2	-0.5723		0.2730		-0.5729		4.4202	
		2.9650		2.9650		2.8765		2.8765
S2->S3	-0.5277		0.3175		-0.5284		4.3756	
		1.8995		1.8995		1.7984		1.7984
S3->S4	-0.4775		0.3677		-0.4775		4.3248	
PBE0	ΔS	ΔΔG	ΔS	ΔΔG	ΔS	ΔΔG	ΔS	ΔΔG
O4->S1	-0.7775		0.2065		0.7775		-0.2058	
		5.9149		5.9149		5.7442		5.7442
S1->S2	-0.6928		0.2912		0.6928		-0.2905	
		3.1683		3.1683		3.0553		3.0553
S2->S3	-0.6363		0.3476		0.6357		-0.3476	
		1.9767		1.9767		1.9265		1.9265
S3->S4	-0.6106		0.3734		0.6112		-0.3721	
MP2	ΔS	ΔΔG	ΔS	ΔΔG	ΔS	ΔΔG	ΔS	ΔΔG
O4->S1	-0.8051		0.1908		-1.4740		-0.2818	
		7.0727		7.0727		-6.9076		6.9076
S1->S2	-0.6890		0.3069		-1.5443		-0.3520	
		3.2122		3.2122		-3.1175		3.1175
S2->S3	-0.6382		0.3577		-1.5907		-0.3985	
		0.5441		0.5441		-0.4844		0.4844
S3->S4	-0.5949		0.4010		-1.6202		-0.4280	

in which the entropic term for HMDS/HMDO system is negative but larger in magnitude by an average of 0.88 Kcal/mol. For the H_2S/H_2O system, the entropic term is opposite in sign but nearly equal in magnitude to the value calculated through method 1. For the entropy term calculated under PBE0, yet a different relationship is seen, with the HMDS/HMDO and H_2S/H_2O systems having an entropic term that is opposite in sign but roughly equal in magnitude to their counterparts. Despite these differences, the contribution of the entropic term is small in comparison to the enthalpic term and the general relationship between the reported ΔG_f^0 and ΔH_f^0 are similar.

With the calculated ΔG_f^0 values from the equations above, the equilibrium coefficient for each reaction can be calculated by the standard relationship:

$$\ln K = -\frac{\Delta G_f^0}{RT} \; therefore: K = e^{\frac{-\Delta G_f^0}{RT}}$$

Equation 12: The calculation of the equilibrium constant from ΔG_f^0

As all of the ΔG_f^0 values are large and negative, it follows that the calculated *K* values will heavily favor the product. It is clear that under all levels of theory in the gas phase for the isolated anion, the reaction with HMDS more heavily favors the products that does the H_2S reaction, with the HMDS being more favorable than the current reaction system by ~11 orders of magnitude under B3LYP when calculated in the standard way and ~13 order of magnitued when calculated using method 2 as seen below in **Table 7**. Under MP2, the HMDS reaction favors the product by roughly 10 order of magnitude in both cases, while, by contrast, under PBE0 the products are only favored more when formed through the reaction with HMDS by ~5 orders of magnitude. However, the comparison of the calculated equilibrium constants for the H_2S/H_2O reaction with those reported by Harmer and Sykes show significant differences for all but the lowest calculated values, those being the equilibrium constants calculated by method 2from the ΔH_f under B3LYP. As this

system is examining only the unsolvated, isolated anions this is not surprising and begs further investigations of ion paired salts under solvation conditions.

Table 7: The Calculate equilibrium constants for the isolated anion in the gas phase under all levels of theory and both computational methods

	B3LYP			
T=293	From H_{corr} and Gc_{orr}		from ΔH_f and ΔG_f	
	HMDS/HMDO	H_2O/H_2S	HMDS/HMDO	H_2S/H_2O
O4->S1	2.2204E+27	2.8806E+16	1.6329E+26	1.8700E+13
S1->S2	1.8133E+23	2.3525E+12	1.8152E+22	2.08E+09
S2->S3	1.2135E+21	1.5743E+10	1.4105E+20	1.62E+07
S3->S4	4.9092E+19	6.3690E+08	6.7676E+18	7.75E+05
	MP2			
	From H_{corr} and Gc_{orr}		from ΔH_f and ΔG_f	
	HMDS/HMDO	H_2O/H_2S	HMDS/HMDO	H_2O/H_2S
O4->S1	7.2522E+27	6.6115E+17	2.2584E+28	1.4793E+18
S1->S2	4.7159E+22	4.2992E+12	1.9406E+23	1.2711E+13
S2->S3	2.0787E+20	1.8951E+10	1.0038E+21	6.5752E+10
S3->S4	8.2948E+19	7.5620E+09	4.4298E+20	2.9016E+10
	PBE			
	From H_{corr} and Gc_{orr}		from ΔH_f and ΔG_f	
	HMDS/HMDO	H_2O/H_2S	HMDS/HMDO	H_2O/H_2S
O4->S1	2.5616E+24	2.0243E+19	1.8516E+23	4.0524E+19
S1->S2	1.1767E+20	9.2992E+14	1.1347E+19	2.4834E+15
S2->S3	5.5863E+17	4.4147E+12	6.5188E+16	1.4267E+13
S3->S4	1.9838E+16	1.5677E+11	2.5197E+15	5.5148E+11

The Potassium Salts:

As the potassium salts of molybdates have a long history in the literature, it makes this alkali metal a fitting choice for this computational examination. In general terms, the computed thermodynamic values are very different for these salts than for the isolated anion. For the potassium salts in gas phase, the *ΔH* and *ΔG* values are negative when calculated using either method under any level of theory as seen in **Table 7** below.

Figure 26: Plots of the thermodynamic parameters for the chalcogen exchange of potassium molybdate in the gas phase

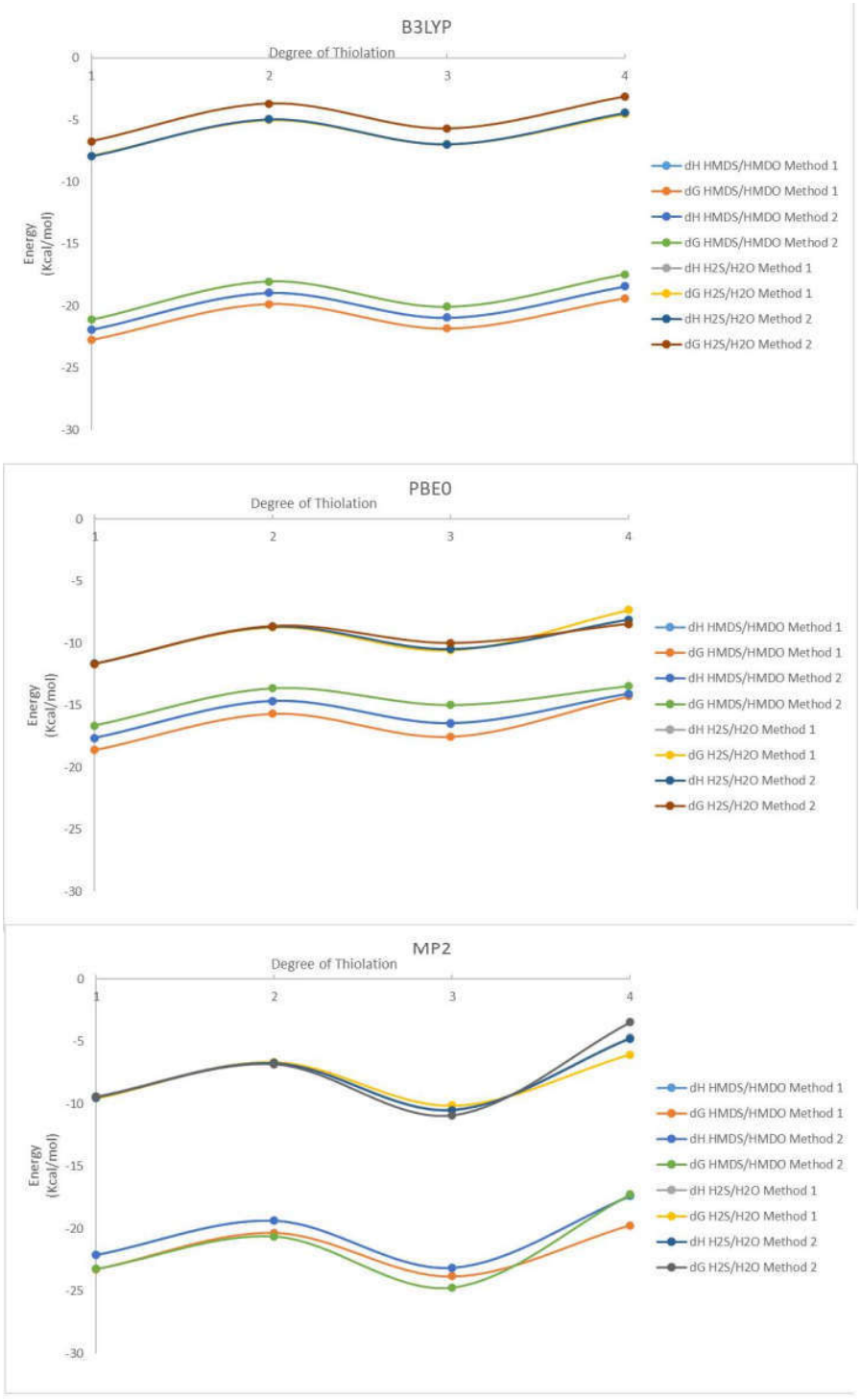

However, the shape of the plot of these values is no longer a smooth concave downward

curve toward less negative values. As seen in the **Figure 26** above, the *ΔΔG* and *ΔΔH* of the S2→S3 reaction is now a negative value under all three levels of theory resulting in a plot with local maxima and minima. A curve of this shape serves to divide the products into the even-numbered, higher energy and therefore less stable set, and the lower energy, and therefore more stable, odd-numbered set, though these energy differences are only around 2-4 Kcal/mol in this example, which is a quite small gap. When computed using method number 2, this overall picture remains the same, though the energy well for K_2MoOS_3 under the MP2 level of theory grows to more than 6 Kcal/mol, as seen in **Table 8** below.

The shape of the plot formed from the thermodynamic parameters for the chalcogen exchange on potassium trithiomolybdate under all three levels of theory show that similar energy is required to move in either direction. The *ΔΔG* values to move in either the forward direction, toward K_2MoS_4, or the reverse direction, toward $K_2MoO_2S_2$ are nearly equal under PBE0 and B3LYP, while the MP2 level of theory shows a wider range of *ΔH* and *ΔG* values for the reaction.

Table 8: The calculated thermodynamic parameters for the chalcogen exchange of potassium moybdate in the gas phase

Gas Phase Potassium Salt Method 1	ΔH_{rxn} HMDS/HMDO (Kcal/mol)	ΔG_{rxn} HMDS/HMDO (Kcal/mol)	ΔH_{rxn} H2S/H2O (Kcal/mol)	ΔG_{rxn} H_2S/H_2O (Kcal/mol)
$MoO_4 \rightarrow MoO_3S$	-21.9283 (B3LYP)	-22.7472 (B3LYP)	-7.9286 (B3LYP)	-7.9022 (B3LYP)
	-22.1134 (MP2)	-23.2455 (MP2)	-9.4189 (MP2)	-9.5551 (MP2)
	-17.6186 (PBE0)	-18.5931 (PBE0)	-11.6453 (PBE0)	-11.6359 (PBE0)
$MoO_3S \rightarrow MoO_2S_2$	-18.9495 (B3LYP)	-19.8626 (B3LYP)	-4.9498 (B3LYP)	-5.0176 (B3LYP)
	-19.3618 (MP2)	-20.3539 (MP2)	-6.6673 (MP2)	-6.6635 (MP2)
	-14.6592 (PBE0)	-15.6702 (PBE0)	-8.6860 (PBE0)	-8.7130 (PBE0)
$MoO_2S_2 \rightarrow MoOS_3$	-20.9475 (B3LYP)	-21.8254 (B3LYP)	-6.9478 (B3LYP)	-6.9804 (B3LYP)
	-23.1482 (MP2)	-23.8215 (MP2)	-10.4536 (MP2)	-10.1311 (MP2)
	-16.4244 (PBE0)	-17.5169 (PBE0)	-10.4512 (PBE0)	-10.5597(PBE0)
$MoOS_3 \rightarrow MoS_4$	-18.4256 (B3LYP)	-19.3888 (B3LYP)	-4.4258 (B3LYP)	-4.5438 (B3LYP)
	-17.3770 (MP2)	-19.7471 (MP2)	-4.6825 (MP2)	-6.0567 (MP2)
	-14.0612 (PBE0)	-14.2733 (PBE0)	-8.0880 (PBE0)	-7.3161 (PBE0)

This brings the complicated solution behavior of these species, which were described in the kinetics studies above into focus. Considering that under this energetic profile the likelihood of the reaction proceeding forward or backward is similar.

The consideration of the potassium molybdate ion pair greatly improved the accuracy of the calculation. This is best exemplified by the calculated equilibrium constants for the chalcogen exchange reaction on potassium molybdate for the H_2S/H_2O system, which can be seen below on **table 9**. These reported values compare much better than those of the isolated anion in the section above to the equilibrium constants calculated by Helz *et al*.[2] This comparison is particularly good for the calculations under the B3LYP level of theory for both computational methods. Under the MP2 and PBE0 levels of theory the reaction energies are overestimated, resulting in K_{eq} values that are larger than those calculated determined Helz. However, these data are for the gas phase, which might be the cause of the discrepancies between these computations and the available data.

Table 9: The equilibrium values computed for potassium molybdate in the gas phase under both computational methods and all three levels of theory.

T=293	Method 1		Method 2	
	HMDS/HMDO	H2O/H2S	HMDS/HMDO	H2S/H2O
O4->S1	4.719E+16	6.200E+05	2.964E+15	8.928E+04
S1->S2	3.625E+14	4.763E+03	1.661E+13	5.003E+02
S2->S3	9.957E+15	1.308E+05	5.142E+14	1.549E+04
S3->S4	1.630E+14	2.141E+03	6.283E+12	1.892E+02
	MP2			
	From Hcorr and Gcorr		from dHf and dGf	
	HMDS/HMDO	H2O/H2S	HMDS/HMDO	H2S/H2O
O4->S1	1.0941E+17	1.0091E+07	1.0599E+17	8.1219E+06
S1->S2	8.3084E+14	7.6630E+04	1.2894E+15	9.8813E+04
S2->S3	2.8927E+17	2.6680E+07	1.3196E+18	1.0112E+08
S3->S4	2.9835E+14	2.7518E+04	4.4155E+12	3.3837E+02
	PBE			
	From Hcorr and Gcorr		from dHf and dGf	
	HMDS/HMDO	H2O/H2S	HMDS/HMDO	H2S/H2O
O4->S1	4.2545E+13	3.3821E+08	1.5884E+12	3.4913E+08
S1->S2	3.0642E+11	2.4359E+06	9.3550E+09	2.0562E+06
S2->S3	6.9183E+12	5.4997E+07	9.5042E+10	2.0889E+07
S3->S4	2.9002E+10	2.3055E+05	6.9617E+09	1.5301E+06

Values Reported by Helz *et al*: $K_{01}=1.54 \times 10^5$ $K_{12}=6.31 \times 10^4$ $K_{23}=1.0 \times 10^5$ $K_{34}=7.59 \times 10^4$

$K_{01}=5.75 \times 10^4$ $K_{12}=5.89 \times 10^4$ $K_{23}=6.03 \times 10^4$ $K_{34}=8.13 \times 10^4$

Table 10: The thermodynamic parameters for the chalcogen of exchange of potassium molybdate calculated by the second method

Gas Phase Potassium Salt Method 2	ΔH_{rxn} HMDS/HMDO (Kcal/mol)	ΔG_{rxn} HMDS/HMDO (Kcal/mol)	ΔH_{rxn} H2S/H2O (Kcal/mol)	ΔG_{rxn} H_2S/H_2O (Kcal/mol)
$MoO_4 \rightarrow MoO_3S$	-21.9277 (B3LYP)	-21.1075 (B3LYP)	-7.9394 (B3LYP)	-6.7540 (B3LYP)
	-22.1128 (MP2)	-23.2266 (MP2)	-9.5049 (MP2)	-9.4265 (MP2)
	-17.6190 (PBE0)	-16.6451 (PBE0)	-11.6453 (PBE0)	-11.6547 (PBE0)
$MoO_3S \rightarrow MoO_2S_2$	-18.9489 (B3LYP)	-18.0359 (B3LYP)	-4.9606 (B3LYP)	-3.6824 (B3LYP)
	-19.3612 (MP2)	-20.6143 (MP2)	-6.7533 (MP2)	-6.8142 (MP2)
	-14.6365 (PBE0)	-13.6030 (PBE0)	-8.6628 (PBE0)	-8.6126 (PBE0)
$MoO_2S_2 \rightarrow MoOS_3$	-20.9475 (B3LYP)	-20.0696 (B3LYP)	-6.9592 (B3LYP)	-5.7161 (B3LYP)
	-23.1482 (MP2)	-24.7207 (MP2)	-10.5403 (MP2)	-10.9206 (MP2)
	-16.4475 (PBE0)	-14.9766 (PBE0)	-10.4738 (PBE0)	-9.9862 (PBE0)
$MoOS_3 \rightarrow MoS_4$	-18.4243 (B3LYP)	-17.4600 (B3LYP)	-4.4360(B3LYP)	-3.1063 (B3LYP)
	-17.3757 (MP2)	-17.2509 (MP2)	-4.7678 (MP2)	-3.4507 (MP2)
	-14.0598 (PBE0)	-13.4279 (PBE0)	-8.0861 (PBE0)	-8.4375 (PBE0)

Tetramethylammonium salts:

There are no reports of the chalcogen exchange reaction being performed on molybdates with tetraalkylammonium cations. In all of the reported syntheses, including those performed by MacDonald, Alonso, and others, the cation exchange is performed after the chalcogen exchange is carried out as the NH_4^+ salt. The proposed synthesis would require these reactions to occur in the opposite order for the reactants to possess the necessary solubility in anhydrous solvents and eliminate the acidic proton which catalyzes the ligand exchange and nucleation reactions. Thus, a computational examination of the chalcogen exchange thermodynamics was carried out using a tetraalkylammonium cation. The use of tetraalkylammonium cations for calculations such as these can rapidly make them much more computationally demanding, as the memory and time demands of the calculations are proportional to at best N^3 where N is the number of atoms and the number of functionals included in a basis set. Furthermore, the saturated and unbranched sidechains that

are employed in these reactions must undergo conformational analysis to ensure that any minimum energy point found is the true global minimum not a local minimum for a given conformation. To eliminate these complications the simplest tetraalkylammonium salt possible,

Table 11: The ΔΔG and values for the entropic term of the chalcogen exchange reaction on tetramethylammonium molybdate.

Gas Phase Tetramethylammonium	Method 1				Method 2			
	HMDS/HMDO		H_2S/H_2O		HMDS/HMDO		H_2S/H_2O	
B3LYP	ΔS	ΔΔG	ΔS	ΔΔG	ΔS	ΔΔG	ΔS	ΔΔG
O4->S1	-1.6397		-0.7944		1.6397		2.0224	
		1.4765		1.4765		-0.4531		-0.4531
S1->S2	-0.6156		0.2297		0.6162		0.9990	
		3.8378		3.8378		-3.5643		-3.5643
S2->S3	-0.3414		0.5039		0.3426		0.7254	
		0.8754		0.8754		-0.8647		-0.8647
S3->S4	-0.3313		0.5139		0.3320		0.7147	

tetramethylammonium, was chosen for the purpose of these calculations despite that it was not employed synthetically. Additionally, the computations for this cation were run only under B3LYP due to the computational demands.

This cation had a surprising effect on the thermodynamic parameters calculated for the studied reactions, the ΔG_f^0 and ΔH_f^0values can be found on **Table 12** below while the ΔΔG and entropic contributions can be found on **Table 11** above. These reactions have similar contributions

Table 12: The calculated thermodynamic parameters for the chalcogen exchange on tetramethylammonium molybdate in the gas phase

Tetramethylammonium Molybdate Gas Phase Method 1	ΔH_{rxn} HMDS/HMDO (Kcal/mol)	ΔG_{rxn} HMDS/HMDO (Kcal/mol)	ΔH_{rxn} H2S/H2O (Kcal/mol)	ΔG_{rxn} H_2S/H_2O (Kcal/mol)
$MoO_4 \rightarrow MoO_3S$	-23.9351	-25.5748	-9.9354	-10.7298
$MoO_3S \rightarrow MoO_2S_2$	-23.4827	-24.0982	-9.4829	-9.2533
$MoO_2S_2 \rightarrow MoOS_3$	-19.9190	-20.2604	-5.9193	-5.4154
$MoOS_3 \rightarrow MoS_4$	-19.0537	-19.3850	-5.0540	-4.5400
Method 2	ΔH_{rxn} HMDS/HMDO (Kcal/mol)	ΔG_{rxn} HMDS/HMDO (Kcal/mol)	ΔH_{rxn} H2S/H2O (Kcal/mol)	ΔG_{rxn} H_2S/H_2O (Kcal/mol)
$MoO_4 \rightarrow MoO_3S$	-23.9351	-22.2954	-9.9196	-7.8971
$MoO_3S \rightarrow MoO_2S_2$	-23.4820	-22.8658	-9.4665	-8.4675
$MoO_2S_2 \rightarrow MoOS_3$	-19.9178	-19.5752	-5.9022	-5.1769
$MoOS_3 \rightarrow MoS_4$	-19.0531	-18.7211	-5.0375	-4.3228

from the entropic term as those discussed above, with the HMDS reaction in the gas phase, calculated in the usual way, having entirely negative entropic contributions. However, the analogous H_2S reaction has a negative entropic term for the first substitution but positive entropic terms for all remaining reactions. Again, this relationship is reversed when the other computational method is employed, with the HMDS reaction entropic contribution being nearly equal in magnitude but opposite in sign, while the entropic term for the H_2S reaction has a larger positive value in all reactions. Furthermore, the reactions are grouped into lower energy and higher energy pairs by the thermodynamic parameters calculated by both methods in the gas phase as seen above in **Table 12** and **Figure 27** below, respectively.

The reactions that form the mono- and disubstituted products form a pair that are separated by a small energy gap, having ΔH values that are only separated by roughly 0.45 kcal/mol when reacted with H_2S and calculated by method 2. Meanwhile, the reaction to form the tri- and tetrasubstituted members form the other pair with a change in enthalpy for these reactions of roughly 0.86 Kcal/mol under the same conditions. While the later set of reactions is separated by a much larger energetic difference than the former pair, the difference seems meager when compared to the energy difference between the reactions that form the di- and trisubstituted products, which is more than 4 Kcal/mol for the standard method compared with 3.576 Kcal/mol when computed under method 2. These values are roughly eight times larger than the previous step and more than four times larger than the next step in the set. These computed thermodynamic values separate these products into the more substituted, more reactive, higher energy pair and less substituted, less reactive, lower energy pair as opposed to the even/odd comparison that was seen in the potassium salts as seen in the plot of the thermodynamic values below in **Figure 27**.

In most cases, these levels of theory produce similar thermodynamic parameters for reactions examined in the gas phase. When the molybdate is paired with different cations, computational examinations predict a variation in the relative energies of the various products and thus the shape of the reaction profile for this series of chalcogen exchange reactions changes. In spite of these variations between ion pairing effects seen under different levels of theory, examination of the predicted Gibb's free energy of reaction and the equilibrium constants that are calculated from it show a clear picture: Hexamethyldisilathiane undergoes a more thermodynamically favorable reaction with molybdate to form tetrathiomolybdate and the mixed oxythiomolybdates by between 4 and 12 orders of magnitude in this series of reactions in the gas phase than do the same reactions employing hydrogen sulfide as the chalcogen exchange reagent.

Solvation Models:

The calculations were also run implicitly solvated using the polarizable continuum model with acetonitrile, the solvent in which the synthesis was performed for this study, and in methanol for comparison. The results are tabulated in **Table 13** below.[76]. While acetonitrile and methanol have similar ε values, solvation had a significant effect on both the computed energies and the shape of the reaction energy profile. Interestingly there is much larger disagreement between the two computational methods and among the different levels of theory employed under the solvation model than was seen in the gas phase calculations. For example, for the isolated molybdate anion under the B3LYP level of theory, the shape of the curves plotting the ΔG and ΔH of this series of reactions were generally similar to those of the gas phase calculation under both solvation conditions examined when these values were computed under method 1. However, under method 2, the calculated ΔG value is roughly the same, but the ΔH values shows a "hockey stick" like

shape with the ΔΔH between the reactions that form $[MoO_3S]^{2-}$ and $[MoO_2S_2]^{2-}$ being quite large and the remaining reactions being nearly equal.

The chalcogen exchange reactions under the B3LYP level of theory were calculated to be overall less exergonic while solvated than they were in the gas phase, with this difference being more pronounced for the earlier reactions, to form the less substituted products, than for the formation of the more substituted products. The thermodynamic parameters for the solvated reactions are also generally higher energy when calculated under the acetonitrile conditions than when calculated under the methanol conditions. This is not to say the shape of these curves are identical, only that there are no significant changes to the general relationship between the produced values as can be seen in the plots in **Figure 28**, below.

Figure 28: The plots of the thermodynamic parameters of the chalcogen exchange reaction on the isolated anion under the tested solvation conditions.

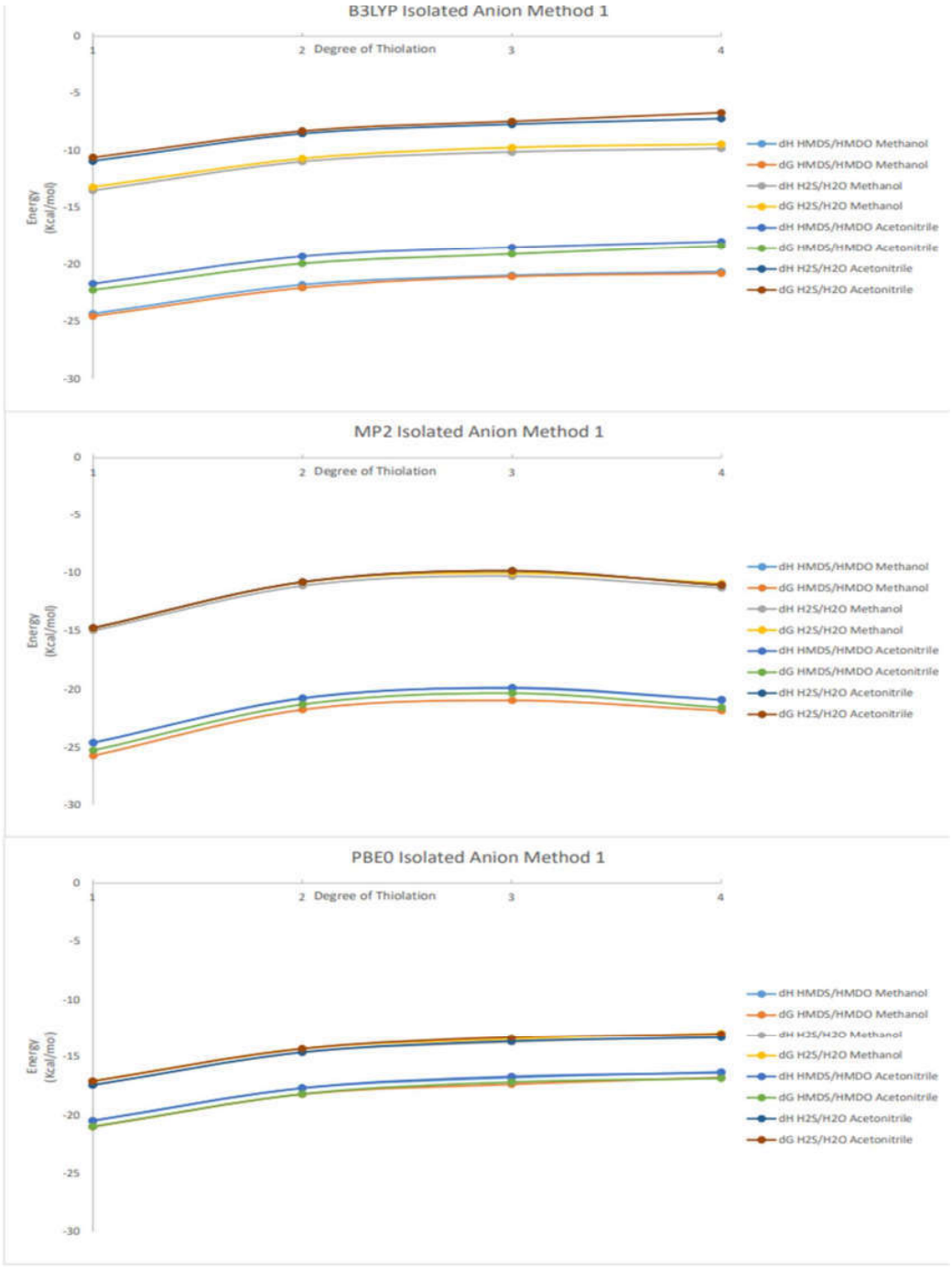

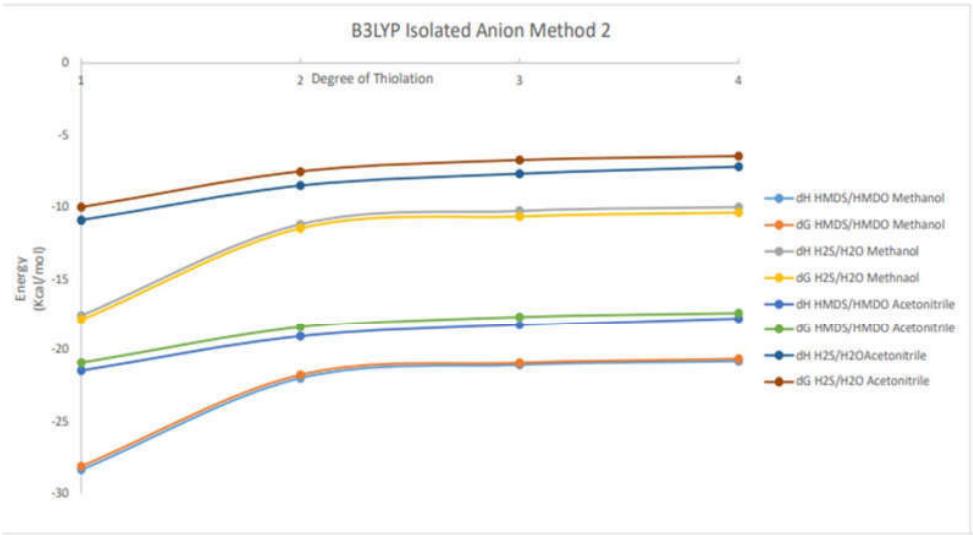
B3LYP Isolated Anion Method 2
Degree of Thiolation
Energy (Kcal/mol)
dH HMDS/HMDO Methanol
dG HMDS/HMDO Methanol
dH H2S/H2O Methanol
dG H2S/H2O Methnaol
dH HMDS/HMDO Acetonitrile
dG HMDS/HMDO Acetonitrile
dH H2S/H2OAcetonitrile
dG H2S/H2O Acetonitrile

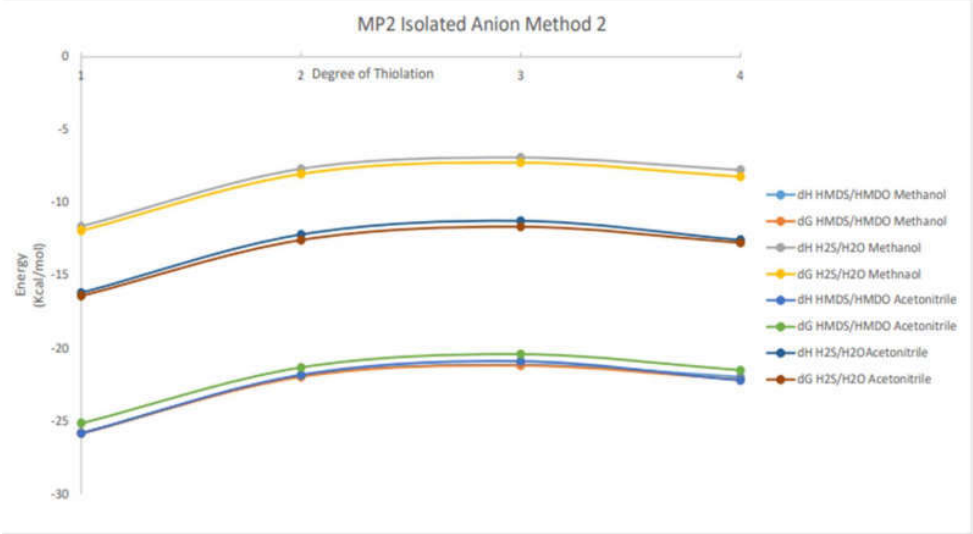
MP2 Isolated Anion Method 2
Degree of Thiolation
Energy (Kcal/mol)
dH HMDS/HMDO Methanol
dG HMDS/HMDO Methanol
dH H2S/H2O Methanol
dG H2S/H2O Methnaol
dH HMDS/HMDO Acetonitrile
dG HMDS/HMDO Acetonitrile
dH H2S/H2OAcetonitrile
dG H2S/H2O Acetonitrile

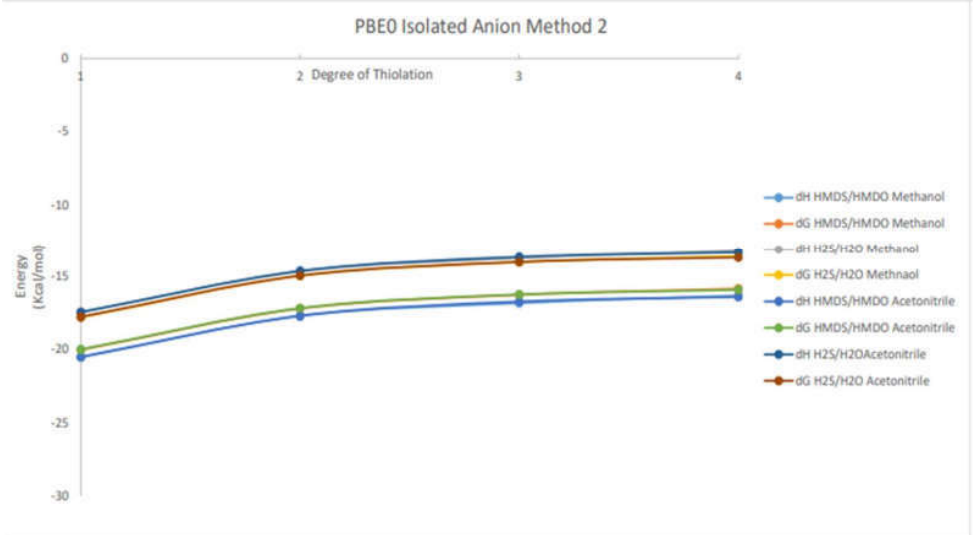
PBE0 Isolated Anion Method 2
Degree of Thiolation
Energy (Kcal/mol)
dH HMDS/HMDO Methanol
dG HMDS/HMDO Methanol
dG H2S/H2O Methnaol
dH HMDS/HMDO Acetonitrile
dG HMDS/HMDO Acetonitrile
dH H2S/H2OAcetonitrile
dG H2S/H2O Acetonitrile

Amongst the specific differences that are important to note under the B3LYP level of theory for the isolated anion is that, when calculated in the usual way, the solvation condition decreases the magnitude of both the change in enthalpy and Gibb's free energy for each reaction when compared to the gas phase condition, as well as the relative change in these values between reactions. The only notable deviation to the trends is the series of chalcogen exchange reactions under the methanol solvation condition when calculated by method 2, this set has both the largest and smallest $\Delta\Delta G$ values seen, and the smallest unsigned entropy values seen amongst the set of isolated anions under solvation conditions. While the smallest $\Delta\Delta G$ value is not an outlier in these data, the largest $\Delta\Delta G$ value seen is above 6 Kcal/mol, nearly eight times the size of the next $\Delta\Delta G$ in this set. This very large $\Delta\Delta G$ does not fit the trend established under the other conditions for the isolated anion examined under B3LYP.

For the isolated anion under solvation conditions using the PBE0 level of theory, the increase in energy due to solvation is comparable to that seen under the B3LYP, even though the difference in energy between the acetonitrile and methanol conditions is less pronounced. Additionally, the shape of the curve of the plotted thermodynamic parameters stays relatively consistent between the gas phase reaction, the reaction in methanol, and the reaction in acetonitrile, so much so that the $\Delta\Delta G$ for the S0 to S1 reaction, when calculated using method one, is identical under both solvation conditions. PBE0 also shows the smallest thermodynamic difference between the two reagents than any other level of theory and shows a high level of agreement between all conditions examined when calculated using either method.

When calculated under method 1 the MP2 level of theory also shows a high level of similarity between the two solvation conditions, though shows the reaction with HMDS to be much more thermodynamically favorable than does PBE0. Under MP2, the thermodynamic preference

for HMDS is roughly equal to the thermodynamic preference that is seen under the B3LYP level of theory. The same parameters under the MP2 level of theory change very little for the HMDS reaction when calculated using method 2. Though, the hydrogen sulfide reaction is found to be nearly 5 kcal/mol less favorable when calculated under the alternative method for the methanol condition without any significant change in the trends observed for each reaction.

The more complex shape of the graphs for the potassium salts makes it more difficult to make broad comments about the effects of the solvation conditions on the thermodynamic parameters of the reactions examined. However, some general statements can be made before an examination of the specific effects under each condition are discussed. Firstly, for the potassium salts, regardless of the level of theory or solvation condition employed, the effect of the solvation conditions on the calculated parameters, as compared to the gas phase values, are minor when computed under method 1. However, the impact is more pronounced when calculated by method 2. This is illustrated well by the series of potassium salts calculated under the B3LYP level of theory under both solvation conditions and calculated by both methods as can be seen tabulated on **Table 13** and plotted in **Figure 29**, below.

The reaction with hexamethyldisilathiane has very similar thermodynamic parameters across all three solvation conditions, regardless of which method was used to calculate these values, and while the reaction with hydrogen sulfide shows more variability when calculated by method 2, the general trends and shape of the plot do not deviate from the reminder of the set. Interestingly for these salts, solvation resulted in a slight loss of exothermicity and spontaneity for the reactions with hexamethyldisilathiane but an increase in these parameters with the hydrogen sulfide. The scale of these changes was more pronounced for the hydrogen sulfide system by an impressive amount with the calculated ΔG_{rxn} nearly doubling under methanol solvation.

Table 13: The thermodynamic parameters for the chalcogen exchange of reaction for the isolated anion (left) and potassium molybdate (right) in acetonitrile and methanol, calculated by both methods, under all three levels of theory.

Isolated anion Methanol Method 1	ΔH_{rxn} HMDS\HMDO (Kcal/mol)	ΔG_{rxn} HMDS\HMDO (Kcal/mol)	ΔH_{rxn} H2S\H2O (Kcal/mol)	ΔG_{rxn} H_2S/H_2O (Kcal/mol)	Isolated anion Methanol Method 2	ΔH_{rxn} HMDS\HMDO (Kcal/mol)	ΔG_{rxn} HMDS\HMDO (Kcal/mol)	ΔH_{rxn} H2S\H2O (Kcal/mol)	ΔG_{rxn} H_2S/H_2O (Kcal/mol)
$MoO_4 \rightarrow MoO_3S$	-24.3110 (B3LYP)	-24.5349 (B3LYP)	-13.4758 (B3LYP)	-13.1859 (B3LYP)	$MoO_4 \rightarrow MoO_3S$	-28.3490 (B3LYP)	-28.1250 (B3LYP)	-17.5299 (B3LYP)	-17.8185 (B3LYP)
	-32.5050 (MP2)	-33.2825 (MP2)	-26.5317 (MP2)	-26.3253 (MP2)		-25.8239 (MP2)	-25.8157 (MP2)	-11.6560 (MP2)	-11.9296 (MP2)
	-24.5714 (PBE0)	-25.6538 (PBE0)	-14.9542 (PBE0)	-14.7408 (PBE0)		-20.5226982	-20.01755305	-17.4516667	-17.78361923
$MoO_3S \rightarrow MoO_2S_2$	-21.7903 (B3LYP)	-22.0457 (B3LYP)	-10.9551 (B3LYP)	-10.6965 (B3LYP)	$MoO_3S \rightarrow MoO_2S_2$	-22.0059 (B3LYP)	-21.7712 (B3LYP)	-11.1868 (B3LYP)	-11.4647 (B3LYP)
	-26.6748 (MP2)	-27.3678 (MP2)	-20.7015 (MP2)	-20.4104 (MP2)		-21.8819 (MP2)	-21.9528 (MP2)	-7.7140 (MP2)	-8.0666 (MP2)
	-20.7248 (PBE0)	-21.72811(PBE0)	-11.1075 (PBE0)	-10.8151 (PBE0)		-17.71961326	-17.20003539	-14.64858177	-14.96610157
$MoO_2S_2 \rightarrow MoOS_3$	-20.9588 (B3LYP)	-21.0686 (B3LYP)	-10.1236 (B3LYP)	-9.7195 (B3LYP)	$MoO_2S_2 \rightarrow MoOS_3$	-21.0748 (B3LYP)	-20.9461(B3LYP)	-10.2556 (B3LYP	-10.6396 (B3LYP)
	-23.5630 (MP2)	-24.1993 (MP2)	-17.5897 (MP2)	-17.2421(MP2)		-21.1163 (MP2)	-21.1672 (MP2)	-6.9484 (MP2)	-7.2810 (MP2)
	-19.3115 (PBE0)	-20.9350 (PBE0)	-10.2943 (PBE0)	-10.0220 (PBE0)		-16.82039215	-16.26190869	-13.74936065	-14.02797487
$MoOS_3 \rightarrow MoS_4$	-20.6476 (B3LYP)	-20.7925 (B3LYP)	-9.8124 (B3LYP)	-9.4434 (B3LYP)	$MoOS_3 \rightarrow MoS_4$	-20.8174 (B3LYP)	-20.6725 (B3LYP)	-9.9983 (B3LYP)	-10.3660 (B3LYP)
	-21.6121(MP2)	-22.2226 (MP2)	-15.6388 (MP2)	-15.2654 (MP2)		-21.9515 (MP2)	-22.1304 (MP2)	-7.7836 (MP2)	-8.2442 (MP2)
	-20.9161(PBE0)	-21.8116 (PBE0)	-11.2989 (PBE0)	-10.8986 (PBE0)		-16.31650202	-15.84837993	-13.24547053	-13.61444611
Isolated anion Acetonitrile Method 1	ΔH_{rxn} HMDS\HMDO (Kcal/mol)	ΔG_{rxn} HMDS\HMDO (Kcal/mol)	ΔH_{rxn} H2S\H2O (Kcal/mol)	ΔG_{rxn} H_2S/H_2O (Kcal/mol)	Isolated anion Acetonitrile Method 2	ΔH_{rxn} HMDS\HMDO (Kcal/mol)	ΔG_{rxn} HMDS\HMDO (Kcal/mol)	ΔH_{rxn} H2S\H2O (Kcal/mol)	ΔG_{rxn} H_2S/H_2O (Kcal/mol)
$MoO_4 \rightarrow MoO_3S$	-21.6961(B3LYP)	-22.2458 (B3LYP)	-10.9143 (B3LYP)	-10.5905 (B3LYP)	$MoO_4 \rightarrow MoO_3S$	-21.4721(B3LYP)	-20.9212 (B3LYP)	-10.9012 (B3LYP)	-10.0081(B3LYP)
	-24.5394 (MP2)	-25.2083 (MP2)	-14.9366 (MP2)	-14.7245 (MP2)		-25.7938 (MP2)	-25.1243 (MP2)	-16.1916 (MP2)	-16.4037 (MP2)
	-20.4951 (PBE0)	-20.3946 (PBE0)	-17.4372 (PBE0)	-17.1065 (PBE0)		-20.49446027	-19.9943352	-17.43848901	-17.76981402
$MoO_3S \rightarrow MoO_2S_2$	-19.2991(B3LYP)	-19.9310 (B3LYP)	-8.5172 (B3LYP)	-8.2756 (B3LYP)	$MoO_3S \rightarrow MoO_2S_2$	-19.0750 (B3LYP)	-18.4431(B3LYP)	-8.5041(B3LYP)	-7.5301(B3LYP)
	-20.7712 (MP2)	-21.2763 (MP2)	-11.1684 (MP2)	-10.7925 (MP2)		-21.8167 (MP2)	-21.313 (MP2)	-12.2145 (MP2)	-12.5922 (MP2)
	-17.6914 (PBE0)	-18.2060 (PBE0)	-14.6335 (PBE0)	-14.3179 (PBE0)		-17.69012031	-17.17556252	-14.63414905	-14.95104135
$MoO_2S_2 \rightarrow MoOS_3$	-18.4820 (B3LYP)	-19.0920 (B3LYP)	-7.7002 (B3LYP)	-7.4366 (B3LYP)	$MoO_2S_2 \rightarrow MoOS_3$	-18.2580 (B3LYP)	-17.6475 (B3LYP)	-7.6871(B3LYP)	-6.7344 (B3LYP)
	-19.8463 (MP2)	-20.3257 (MP2)	-10.2441(MP2)	-9.8419 (MP2)		-20.8766 (MP2)	-20.3378 (MP2)	-11.2745 (MP2)	-11.6767 (MP2)
	-16.7219 (PBE0)	-17.1906 (PBE0)	-13.6640 (PBE0)	-13.3026 (PBE0)		-16.71936312	-16.2493585	-13.66339185	-14.02483732
$MoOS_3 \rightarrow MoS_4$	-17.9738 (B3LYP)	-18.3509 (B3LYP)	-7.19189 (B3LYP)	-6.8955 (B3LYP)	$MoOS_3 \rightarrow MoS_4$	-17.7437 (B3LYP)	-17.3720 (B3LYP)	-7.1788 (B3LYP)	-6.4589 (B3LYP)
	-20.8703 (MP2)	-21.5562 (MP2)	-11.2676 (MP2)	-11.0724 (MP2)		-22.1618 (MP2)	-21.496 (MP2)	-12.5797 (MP2)	-12.775 (MP2)
	-16.3924 (PBE0)	-16.8637 (PBE0)	-13.3346 (PBE0)	-12.9756 (PBE0)		-16.3918 (MP2)	-15.9205 (MP2)	-13.3358 (MP2)	-13.6960 (MP2)

Potassium Molybdate Methanol Method 1	ΔH_{rxn} HMDS/HMDO (Kcal/mol)	ΔG_{rxn} HMDS/HMDO (Kcal/mol)	ΔH_{rxn} H2S/H2O (Kcal/mol)	ΔG_{rxn} H_2S/H_2O (Kcal/mol)	Potassium Molybdate Methanol Method 2	ΔH_{rxn} HMDS/HMDO (Kcal/mol)	ΔG_{rxn} HMDS/HMDO (Kcal/mol)	ΔH_{rxn} H2S/H2O (Kcal/mol)	ΔG_{rxn} H_2S/H_2O (Kcal/mol)
$MoO_4 \rightarrow MoO_3S$	-23.0691 (B3LYP)	-22.2703 (B3LYP)	-12.2691 (B3LYP)	-10.9212 (B3LYP)	$MoO_4 \rightarrow MoO_3S$	-22.4285 (B3LYP)	-22.4791 (B3LYP)	-12.2404 (B3LYP)	-12.2363 (B3LYP)
	-21.6497 (MP2)	-22.8163 (MP2)	-12.0325 (MP2)	-11.9039 (MP2)		-21.6503 (MP2)	-20.4838 (MP2)	-12.2823 (MP2)	-12.4115 (MP2)
	-17.2164 (PBE0)	-17.8232 (PBE0)	-14.1447 (PBE0)	-13.9150 (PBE0)		-17.2176 (PBE0)	-16.6108 (PBE0)	-14.1466 (PBE0)	-14.3763 (PBE0)
$MoO_3S \rightarrow MoO_2S_2$	-18.5253 (B3LYP)	-19.2325 (B3LYP)	-7.7253 (B3LYP)	-7.8834 (B3LYP)	$MoO_3S \rightarrow MoO_2S_2$	-17.8841 (B3LYP)	-17.9393 (B3LYP)	-7.696 (B3LYP)	-7.6966 (B3LYP)
	-18.2913 (MP2)	-19.7797 (MP2)	-8.6747 (MP2)	-8.8667 (MP2)		-18.2919 (MP2)	-16.8041 (MP2)	-8.9238 (MP2)	-8.7318 (MP2)
	-14.5174 (PBE0)	-15.4832 (PBE0)	-11.4458 (PBE0)	-11.575 (PBE0)		-16.3393 (PBE0)	-15.4323 (PBE0)	-13.3283 (PBE0)	-13.1984 (PBE0)
$MoO_2S_2 \rightarrow MoOS_3$	-19.5582 (B3LYP)	-19.7302 (B3LYP)	-8.7582 (B3LYP)	-8.3810 (B3LYP)	$MoO_2S_2 \rightarrow MoOS_3$	-18.9176 (B3LYP)	-18.9712 (B3LYP)	-8.7295 (B3LYP)	-8.7284 (B3LYP)
	-19.3311 (MP2)	-19.2896 (MP2)	-9.7138 (MP2)	-8.3766 (MP2)		-19.3311 (MP2)	-19.3725 (MP2)	-9.9630 (MP2)	-11.3002 (MP2)
	-15.3037 (PBE0)	-16.0241 (PBE0)	-12.2320 (PBE0)	-12.1160 (PBE0)		-13.4205 (PBE0)	-12.6989 (PBE0)	-10.3495 (PBE0)	-10.4650 (PBE0)
$MoOS_3 \rightarrow MoS_4$	-18.1620 (B3LYP)	-18.0704 (B3LYP)	-7.3619 (B3LYP)	-6.7213 (B3LYP)	$MoOS_3 \rightarrow MoS_4$	-17.5214 (B3LYP)	-17.5742 (B3LYP)	-7.3333 (B3LYP)	-7.3314 (B3LYP)
	-18.8165 (MP2)	-20.8923 (MP2)	-9.1993 (MP2)	-9.3799 (MP2)		-18.4725 (MP2)	-16.3967 (MP2)	-9.1044 (MP2)	-8.3244 (MP2)
	-13.8855 (PBE0)	-14.2652 (PBE0)	-10.8139 (PBE0)	-10.3570 (PBE0)		-13.8862 (PBE0)	-13.5065 (PBE0)	-10.8151 (PBE0)	-11.2726 (PBE0)
Potassium Molybdate Acetonitrile Method 1	ΔH_{rxn} HMDS/HMDO (Kcal/mol)	ΔG_{rxn} HMDS/HMDO (Kcal/mol)	ΔH_{rxn} H2S/H2O (Kcal/mol)	ΔG_{rxn} H_2S/H_2O (Kcal/mol)	Potassium Molybdate Acetonitrile Method 2	ΔH_{rxn} HMDS/HMDO (Kcal/mol)	ΔG_{rxn} HMDS/HMDO (Kcal/mol)	ΔH_{rxn} H2S/H2O (Kcal/mol)	ΔG_{rxn} H_2S/H_2O (Kcal/mol)
$MoO_4 \rightarrow MoO_3S$	-21.0900 (B3LYP)	-22.1109 (B3LYP)	-10.2491 (B3LYP)	-10.7524 (B3LYP)	$MoO_4 \rightarrow MoO_3S$	-21.0893 (B3LYP)	-21.7774 (B3LYP)	-10.2576 (B3LYP)	-10.2592 (B3LYP)
	-21.6566 (MP2)	-22.5496 (MP2)	-12.0538 (MP2)	-12.0658 (MP2)		-21.6572 (MP2)	-20.1387 (MP2)	-12.1411 (MP2)	-9.7415 (MP2)
	-17.2138 (PBE0)	-17.9273 (PBE0)	-14.1560 (PBE0)	-14.0393 (PBE0)		-17.2126 (PBE0)	-16.4979 (PBE0)	-14.1566 (PBE0)	-14.2733 (PBE0)
$MoO_3S \rightarrow MoO_2S_2$	-18.5536 (B3LYP)	-18.8535 (B3LYP)	-7.7127 (B3LYP)	-7.4950 (B3LYP)	$MoO_3S \rightarrow MoO_2S_2$	-18.5529 (B3LYP)	-19.2388 (B3LYP)	-7.7212 (B3LYP)	-7.7205 (B3LYP)
	-18.3390 (MP2)	-19.1817 (MP2)	-8.7362 (MP2)	-8.6379 (MP2)		-18.3383 (MP2)	-16.8693 (MP2)	-8.8222 (MP2)	-6.4722 (MP2)
	-14.4264 (PBE0)	-15.2579 (PBE0)	-11.3696 (PBE0)	-11.3698 (PBE0)		-14.4258 (PBE0)	-13.5944 (PBE0)	-11.3698 (PBE0)	-11.3698 (PBE0)
$MoO_2S_2 \rightarrow MoOS_3$	-19.7239 (B3LYP)	-20.1556 (B3LYP)	-8.8830 (B3LYP)	-8.7971 (B3LYP)	$MoO_2S_2 \rightarrow MoOS_3$	-19.7226 (B3LYP)	-20.4089 (B3LYP)	-8.8909 (B3LYP)	-8.8906 (B3LYP)
	-19.2275 (MP2)	-18.8799 (MP2)	-9.6247 (MP2)	-8.3961 (MP2)		-19.2275 (MP2)	-18.9508 (MP2)	-9.7114 (MP2)	-8.5536 (MP2)
	-15.3420 (PBE0)	-16.4583 (PBE0)	-12.2841 (PBE0)	-12.5703 (PBE0)		-15.3401 (PBE0)	-14.2225 (PBE0)	-12.2841 (PBE0)	-11.9980 (PBE0)
$MoOS_3 \rightarrow MoS_4$	-18.2599 (B3LYP)	-18.3283 (B3LYP)	-7.4190 (B3LYP)	-6.9697 (B3LYP)	$MoOS_3 \rightarrow MoS_4$	-18.2599 (B3LYP)	-18.9450 (B3LYP)	-7.4282 (B3LYP)	-7.4268 (B3LYP)
	-18.8265 (MP2)	-20.1092 (MP2)	-9.2238 (MP2)	-9.6254 (MP2)		-18.8265 (MP2)	-16.9177 (MP2)	-9.3104 (MP2)	-6.5205 (MP2)
	-13.9910 (PBE0)	-14.0524 (PBE0)	-10.9331 (PBE0)	-10.1644 (PBE0)		-13.9897 (PBE0)	-13.9276 (PBE0)	-10.9337 (PBE0)	-11.7031 (PBE0)

values nearly doubling under methanol solvation when compared to the gas phase computations.

This set of effects, taken together, has the impact that the hexamethyldisilathiane reaction is calculated to be favored by only roughly 10 orders of magnitude under the solvation conditions as compared to the nearly 15 orders of magnitude in the gas phase.

When calculated by the first method under B3LYP, a similar trend is seen for the thermodynamic parameters under the solvation condition as were seen in the gas phase calculations. However, when calculated by the second method, the shape of the plots produced from graphing the calculated thermodynamic values show less resilience for the potassium salts computed under the PBE0 level of theory than has been seen in the above cases. When calculated using the first method for the gas phase and both solvation conditions, the shape of the plots of the calculated thermodynamic values were similar to those seen under all conditions when calculated by B3LYP. However, when calculated using the second method the relative changes in energy are altered enough that the shape of the curve is distorted. Furthermore, these impacts are different under the two solvation conditions.

Figure 29: The plots of the thermodynamic values for the chalcogen exchange reaction on potassium molybdate under both solvation conditions

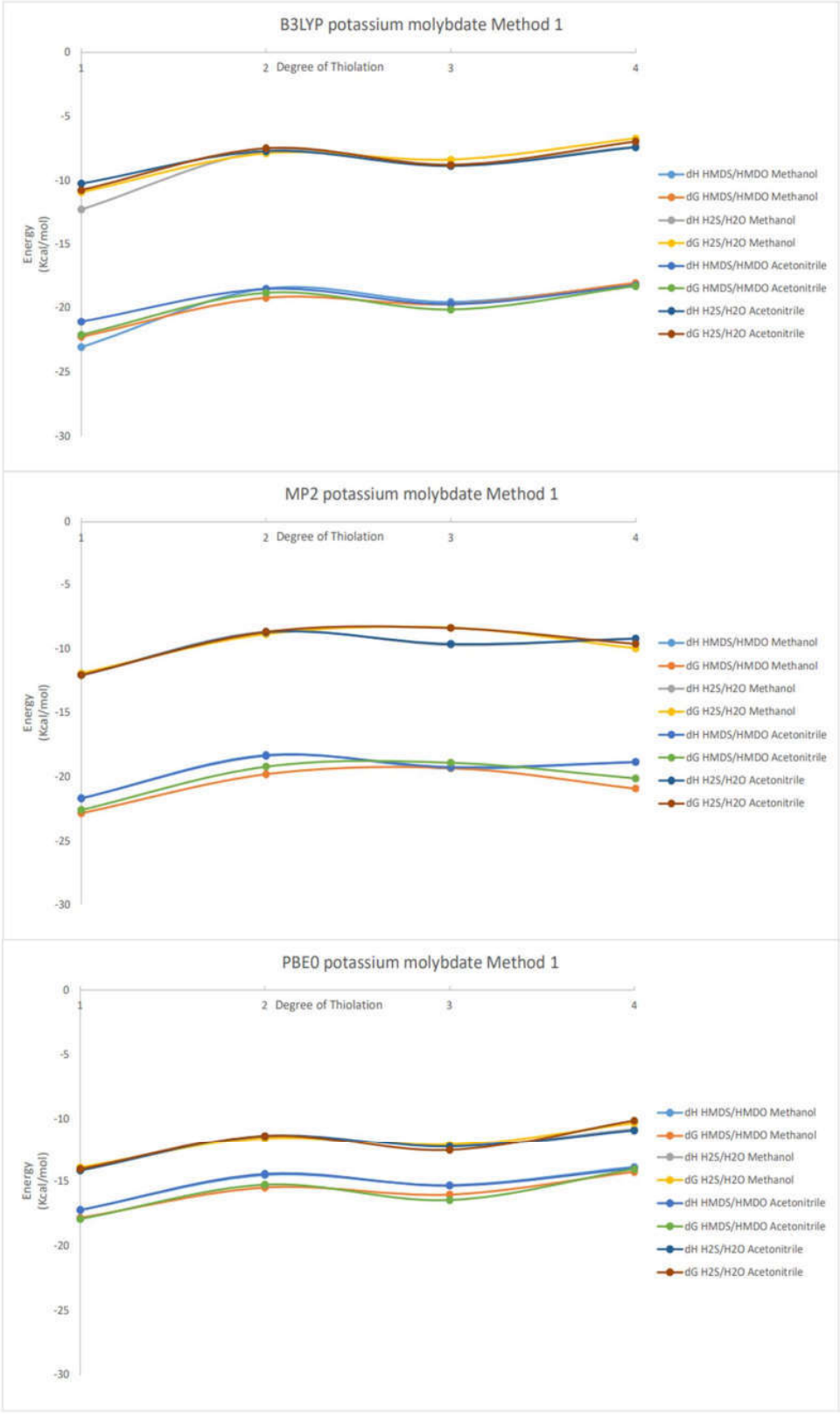

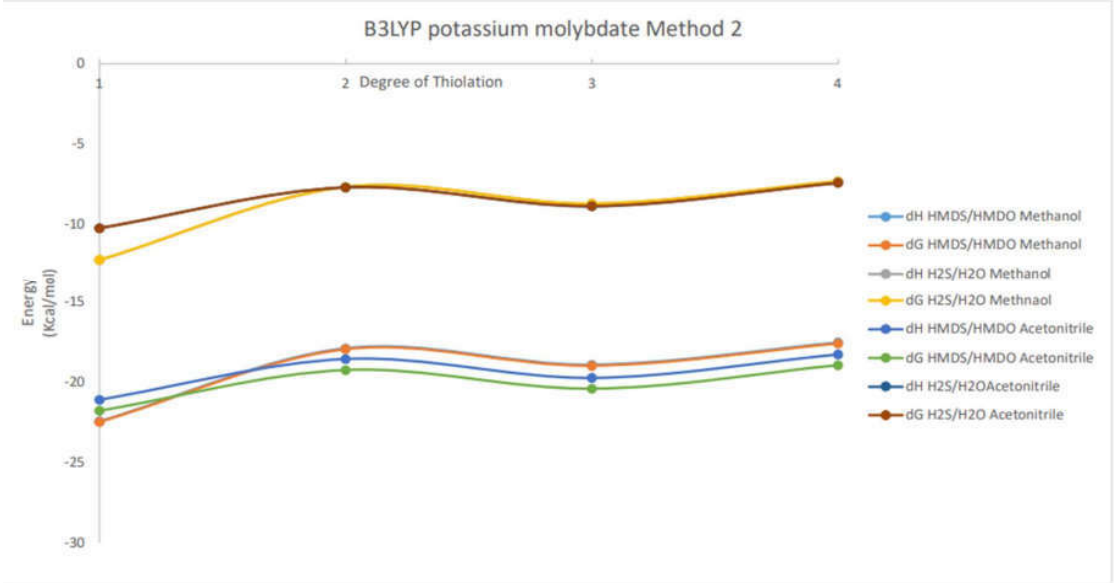
B3LYP potassium molybdate Method 2
Degree of Thiolation
Energy (Kcal/mol)
dH HMDS/HMDO Methanol
dG HMDS/HMDO Methanol
dH H2S/H2O Methanol
dG H2S/H2O Methnaol
dH HMDS/HMDO Acetonitrile
dG HMDS/HMDO Acetonitrile
dH H2S/H2OAcetonitrile
dG H2S/H2O Acetonitrile

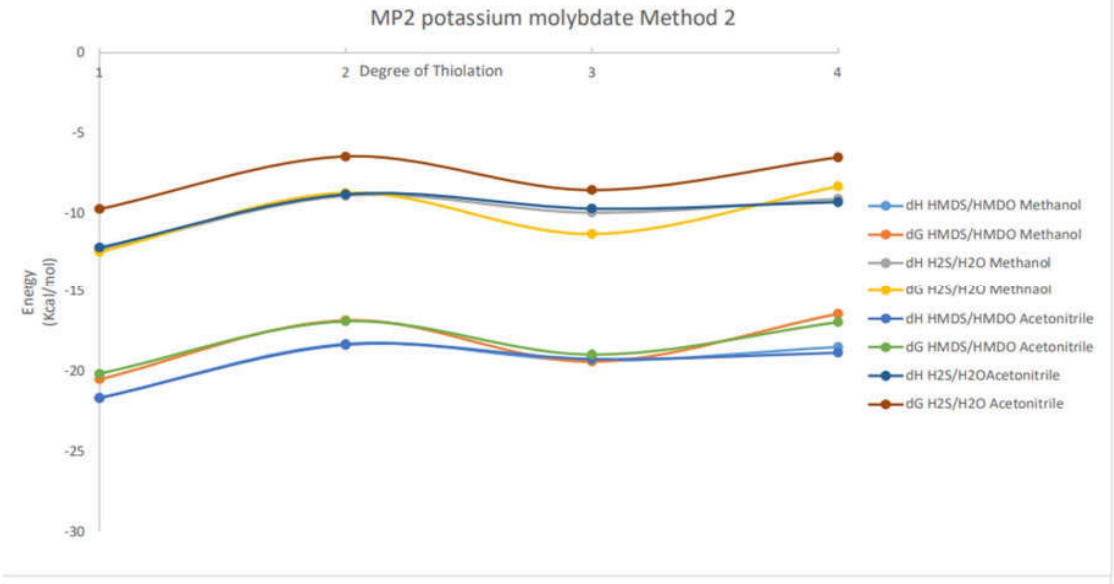
MP2 potassium molybdate Method 2
Degree of Thiolation
Energy (Kcal/mol)
dH HMDS/HMDO Methanol
dG HMDS/HMDO Methanol
dH H2S/H2O Methanol
dG H2S/H2O Methnaol
dH HMDS/HMDO Acetonitrile
dG HMDS/HMDO Acetonitrile
dH H2S/H2OAcetonitrile
dG H2S/H2O Acetonitrile

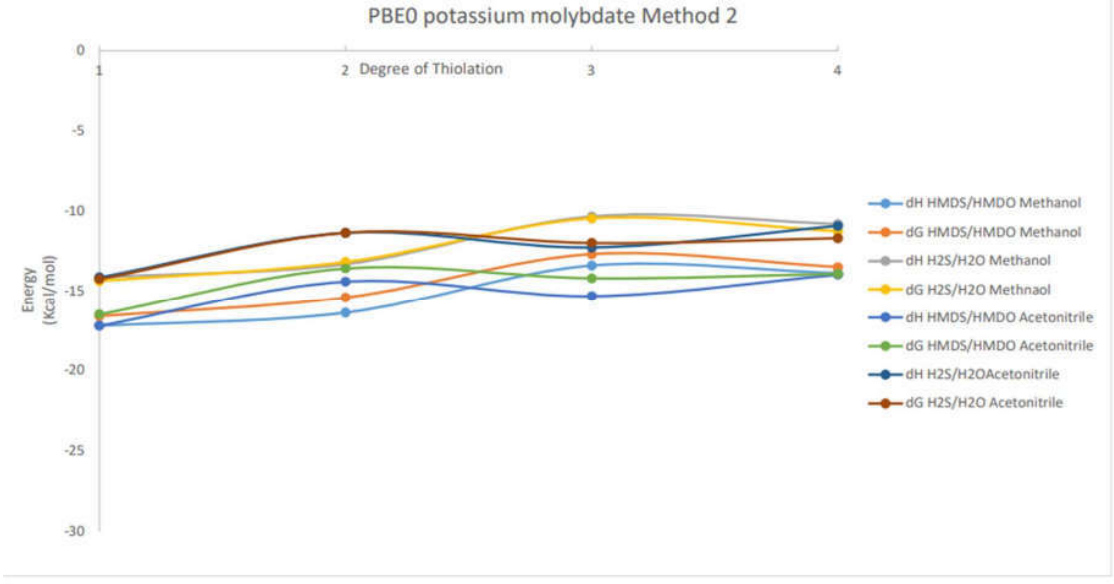
PBE0 potassium molybdate Method 2
Degree of Thiolation
Energy (Kcal/mol)
dH HMDS/HMDO Methanol
dG HMDS/HMDO Methanol
dH H2S/H2O Methanol
dG H2S/H2O Methnaol
dH HMDS/HMDO Acetonitrile
dG HMDS/HMDO Acetonitrile
dH H2S/H2OAcetonitrile
dG H2S/H2O Acetonitrile

The most interesting effect of the solvation condition is the impact it has on the entropic contribution of all the reactions examined. While the entropic term is reasonably linear for the gas phase reactions, with R^2 values for a linear regression greater than 0.94. The behavior is decidedly more complex when the dielectric constant is considered within the calculations, as in the polarizable continuum model, and even more so when the ion pair is included as seen below in **Figure 30**.

Figure 30: The value of the entropic term for all reaction conditions and levels of theory examined for the isolated anion.

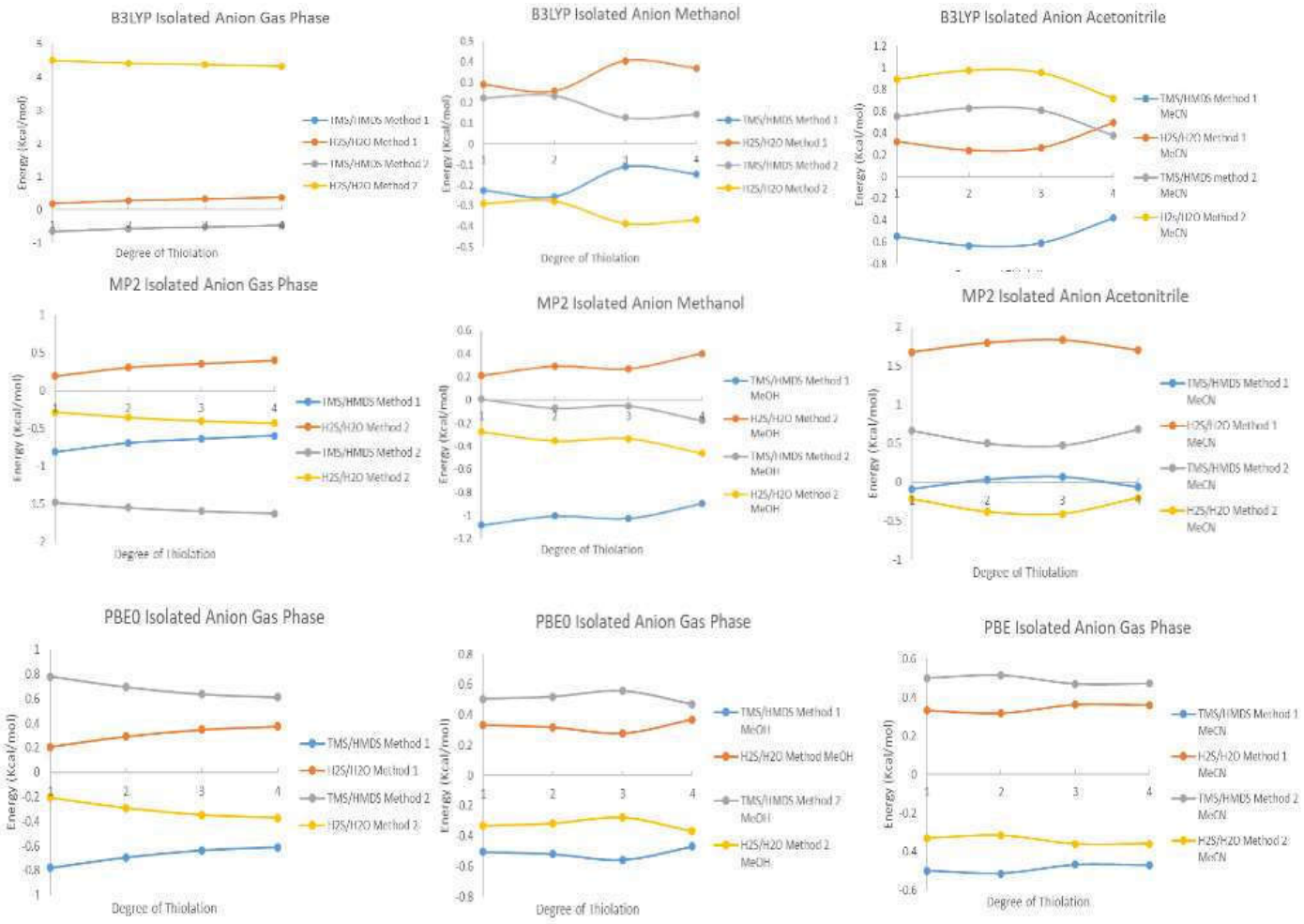

Figure 31: The plots of the entropic term for chalcogen exchange reaction on potassium molybdate under all conditions and levels of theory investigated.

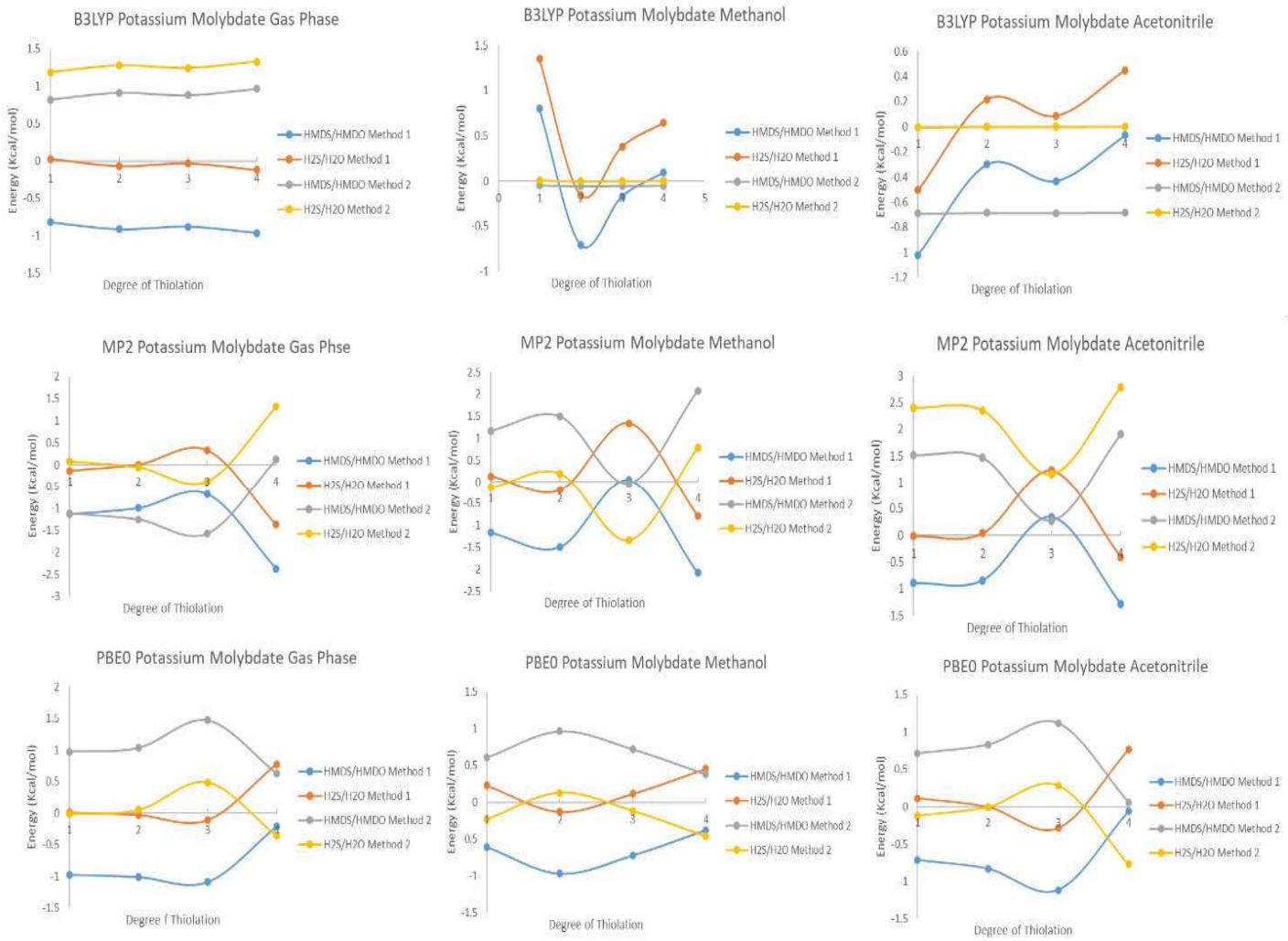

Since the chalcogen exchange reaction performed on the molybdate oxyanion involves the same number of molecules on the product and reactant side of the equation, and over the course of all four exchanges there is only minimal change in the symmetry of the molecules, both the magnitude and variation in the entropy term are surprising. One would expect the entropy change for these reactions to be low and roughly equal throughout the course of all four exchanges. While

that is the case for many of the reactions, seen in Figure 30 above. For the gas phase chalcogen exchange, only small variations in the entropy term and reasonably linear relationships can be seen even for the solvated reactions, which in practice would also have some solvation contribution to the entropy term. The exception to this gas phase trend is the reaction with H_2S calculated using method two under the B3LYP level of theory, which is the largest entropy term in any of the examined calculations by a large margin.

The entropy contribution for the ion paired potassium molybdate is a very different story than that of the isolate anion. In this set, linear or even nearly linear entropic terms for the Gibb's free energy equation are the exception rather than rule and are seen in only four of the 36 combinations of computational methods and levels of theory, as seen in **Figure 31** above. In general, the entropy term is small in comparison to the calculated Gibb's free energy, and the averages compare well across sets and even somewhat between sets. Though none reach the size of the largest entropy value seen in the isolated anion set.

While the tetramethylammonium cation chosen was intended to be a loosely interacting cation, and certainly is less interacting than the potassium ion. The computed structures here, and other work by Chang *et al* show that each of the chalcogen atoms bound to the metal are hydrogen bound to at least two alkyl C-H hydrogen bond donors. In the XRD structures reported by Chang the hydrogen bond donor ability of the cation had a significant effect on the Mo-S length with the tetraphenylphosphonium salt producing a larger number of hydrogen bonds to the sulfido ligand than does $[Et_4N]^+$ or $[NH_4]^+$ and also displaying the longest Mo-S bond length by 0.02Å though this is small and the effect on reactivity has not been explored further.[75]

Syntheses

All reactions and manipulations were performed under a pure dinitrogen or argon atmosphere using either modified Schlenk techniques or an inert atmosphere glovebox. Solvents used for syntheses and crystallizations were dried with a system of drying columns from the Glass Contour Company (Et_2O and THF), freshly distilled according to standard procedures (MeOH and CH_3CN) or purchased in an anhydrous form suitable for immediate use (CH_3CN). All NMR spectra were recorded at 25 °C with a Bruker DSX 300 operating at 300 MHz for ^1H and were referenced to the partially labeled solvent residual. Ultraviolet−visible (UV−vis) spectra were recorded at ambient temperature with a Hewlett-Packard 8455A diode array spectrometer, while IR spectra were recorded as KBr pellets using a Thermo Nicolet Nexus 670 Fourier transform infrared instrument in transmission mode, or as the neat solid by ATR on a Thermo Nicolet iS10. Mass spectra (ESI-) were recorded with a Bruker microTOF II mass spectrometer, Elemental analyses were performed by Kolbe Microanalytical Laboratory in Oberhausen, Germany. Procedural details regarding crystal growth, X-ray diffraction data collection, data processing, and structure solution and refinement are available in Appendix A. Unit cell data and selected refinement statistics for the compounds that have been structurally identified are listed in **Table 14**; more complete crystallographic data are presented in Appendix A.

$[Et_4N]_2MoO_4$.

This method in analogous to that reported by McDonald for the synthesis of $[Et_4N]_2MoO_xS_{4-x}$ ($x \neq 4$).[33] 0.300 g (1.53 mmol) of ammonium molybdate, $(NH_4)_2MoO_4$, is suspended in 30 mL of acetonitrile. To this suspension is added 2.15 mL of tetraethylammonium hydroxide, $[(C_2H_5)_4N]OH$, (25% in methanol, 3.1 mmol). The solution clarifies upon addition and is allowed to stir for ~30 min. A vacuum is applied to remove the ammonia formed in the reaction and is maintained until all that remains is white solid. The solid residue is taken up in minimal

volume of dry acetonitrile, and the product is precipitated with diethyl ether and separated by cannula filtration. The solid is rinsed with diethyl ether and tetrahydrofuran (2x10 mL) and dried *in vacuo*. Yield: 0.520 g, 81%. ^{1}H NMR (δ, in CD_3CN): 1.07 ppm tt (J = 7.3 Hz, 1.9 Hz, 12H), 3.07 ppm (q, *J* = 7.3Hz, 8H); IR (cm^{-1}): 3006, 2976, 2945, 2281, 1485, 1475, 1455, 1436, 1393, 1315, 1185, 1172, 1080, 1077, 1053, 1039, 1001, 802, 794(sh), 780(sh), 617. This procedure works with any quaternary ammonium hydroxide, and has been performed with $[Me_4N]OH$, $[(^nPr)_4N]OH$, $[(^nBu)_4N]OH$, $[Et_2Me_2N]OH$, and choline hydroxide.

Alternatively, 0.300 g (0.8 mmol) of silver molybdate, Ag_2MoO_4, is suspended in 30 mL of acetonitrile and protected from light by completely wrapping the vessel in aluminum foil. To this suspension is added a solution of 0.260 g (1.5 mmol) of tetraethylammonium chloride, $[(C_2H_5)_4N]Cl$, in 10 mL of acetonitrile. This mixture is heated to reflux and stirred for 48 h. The solution is allowed to cool, then separated by filtration from the AgCl that forms. The solution is then concentrated *in vacuo* to ~10% the original volume. The $[Et_4N]_2[MoO_4]$ is precipitated as a white powder by the addition of diethyl ether, separated by cannula filtration and dried *in vacuo*. Yield: 0.285 g (85%). Characterization is identical to the above method.

$[Et_4N]_2WO_4$.

0.300 g (1.2 mmol) of tungstic acid, H_2WO_4, is suspended in ~30 mL of acetonitrile. To this suspension is added 1.7 mL (2.4 mmol) of tetraethylammonium hydroxide 25% in methanol. This solution is allowed to stir until clear (~ 1 h) and then is taken to dryness *in vacuo*. The resulting white powder is taken up in minimal volume of dry acetonitrile and precipitated with diethyl ether. The liquid is removed by cannula filtration and the solid dried *in vacuo*. Yield: 0.730 g (85%) ^{1}H NMR (δ, in CD_3CN): 1.07 ppm tt (J = 7.3 Hz, 1.9 Hz, 12H), 3.07 ppm q (*J* = 7.3Hz, 8H); IR (cm^{-1}): 3012, 2977, 1491, 1458, 1419, 1240, 1203, 1029(sh), 1020, 971, 923, 798.

$[Et_4N]_2MoS_4$.

0.45 mL (2.25 mmol) of hexamethyldisilathiane, $(CH_3Si)_2S$, is diluted with 30 mL of dry acetonitrile and cooled to 0 °C. This solution is added dropwise over the course of 1 h to a vigorously stirred solution of 0.200 g (0.5 mmol) of $[Me_2Et_2N]_2MoO_4$ and 0.050 g of freshly resublimed DABCO in 50 mL of dry acetonitrile. The reaction solution changes color as addition proceeds of the reaction, first to yellow, then to orange, and finally to a deep red color. The reaction is then allowed to warm slowly to room temperature, and stirring is continued for a total of 24 h. The volatiles are removed *in vacuo*. The resulting red solid residue is taken up in 10 mL dry MeCN and precipitated as a red powder by the addition of dry Et_2O. This powder is washed with dry diethyl ether (2 x 20 mL) and dried *in vacuo*. Crystalline material can be grown by the diffusion of diethyl ether into a MeCN solution containing 5% DABCO. Yield: 80% (0.185 g) Analysis Calcd for $C_{16}H_{40}N_2MoS_4$: C, 39.65%; H, 8.32%; N, 5.78%. Found: C, 39.94%; H, 8.37%; N, 5.82%. ^{1}H NMR (δ, in CD_3CN): 1.07 ppm tt (J = 7.3 Hz, 1.9 Hz, 12H), 3.07 ppm (q *J* = 7.3Hz, 8H); IR (cm^{-1}): 3005(sh), 3003, 2971, 1489, 1472, 1453(sh), 1447, 1436, 1423, 1394, 1330, 1234, 1201, 1160, 1136, 1090, 1076, 1020(sh), 1016, 967, 919, 863, 815, 794. UV-vis:

$[Et_4N]_2WS_4$.

Hexamethyldisilathiane (0.45 mL, 2.25 mmol) is diluted with 30 mL of dry acetonitrile. This solution is added dropwise over the course of 1 h to a solution of 0.200 g (0.5 mmol) of tetraethylammonium tungstate, $[Et_4N]_2WO_4$ in 40 mL of dry acetonitrile. This reaction mixture assumes an increasingly intense yellow color over the course of the addition. Once addition is complete, the solution is allowed to stir for 24 h, then the volatiles are removed *in vacuo*. The resulting yellow solid is then taken up in 15 mL of dry acetonitrile and precipitated by the addition of 50 mL dry diethyl ether this step is repeated three times. The resulting yellow powder is dried

in vacuo. Yield: 70% (0.158 g). ^{1}H NMR (δ, in CD_3CN): 1.07 ppm (tt, J = 7.3 Hz, 1.9 Hz, 12H), 3.07 ppm (q, *J* = 7.3Hz, 8H); IR (cm^{-1}): 2976, 2940, 1647, 1452, 1396, 1306, 1248, 1181, 1118, 1078, 1011, 1007, 880, 849, 790, 697.

$[Et_4N]_2[(S_2)Mo(O)(\mu\text{-}S)_2Mo(O)(S_2)]$.

Tetraethylammonium molybdate (0.250 g, 0.6 mmol) is solvated in 30 mL of acetonitrile and warmed to 50°C. To this solution hexamethyldisilathiane (0.56 mL, 2.6 mmol) in 10 mL of acetonitrile is added dropwise over the course of 10 minutes. After 2 hours the volume of the reaction is reduced 50% *in vacuo*, the stopper is removed, and the reaction mixture is allowed to stir overnight. The volume is then reduced *in vacuo* to 10% of the original volume. The product is precipitated by the addition of diethyl ether (70 mL). The liquid is removed by cannula filtration, and the resulting red/orange powder is dried *in vacuo*. Xray quality crystals can be grown by the vapor diffusion of diethyl ether into a solution of the product in acetonitrile. Yield 60% ^{1}H NMR (300MHz, CD_3CN) 1.08 (tt, J=7.3 Hz, 1.9Hz, 12H), 3.07 (q, J=7.3 Hz 8H).

$(^{i}Bu_2NCS_2)MoO(\mu\text{-}S)_2MoO(S_2CNiBu_2)$

To a solution of 0.100 g (0.15 mmol) of $[Et_4N]_2[(S_2)Mo(O)(\mu\text{-}S)_2Mo(O)(S_2)]$ in 10 mL of acetonitrile is added 1.5 equivalents (0.092g, .23 mmol) of tetra-*iso*butylthiuram disulfide in 5 mL of methylene chloride. The reaction is allowed to stir, open to the air, for 24 hours producing a red solution with a large amount of black solid suspended in a red solution. This mixture is filtered through celite, and volatiles are removed *in vacuo*. The resulting red oil is taken up in 2 mL of tetrahydrofuran and precipitated with 20 mL pentane, then washed with pentane 2x10 mL. XRD quality crystals can be grown by the layered diffusion of 10% THF in pentane into a concentrated

methylene chloride solution in the freezer Yield: 20% ^{1}H NMR (δ, in CD_3CN): 5.32 (s, 3H), 3.81 (d J=7.2 Hz, 6H); 3.51 (d J=7.6 Hz), 2.39 (m 4H); 2.21 (m 4H).

$[Ph_3P{=}N{=}PPh_3][MoO_3(OSiPh_2{}^tBu)]$.

Silver molybdate, Ag_2MoO_4 (0.300 g, 0.8 mmol), is suspended in 30 mL of dry acetonitrile and completely wrapped in aluminum foil. To this suspension is added a solution of chloro-*tert*-butyldiphenylsilane, $^tBuPh_2SiCl$ (0.219 g, 0.8 mmol) in 10 mL of dry acetonitrile. The mixture is allowed to stir for 72 h, whereupon a solution 0.458 g of $[Ph_3P{=}N{=}PPh_3]Cl$ in dry acetonitrile (10 mL) is added by cannula transfer, and the mixture is allowed to stir for an additional 24 h. The reaction is then cannula filtered through 2 cm of packed celite under inert atmosphere into a flame dried Schlenk flask. The reaction vessel is rinsed with CH_2Cl_2 (2 x 10mL), and the rinses are passed through the celite filter. The resulting clear colorless filtrate is brought to dryness *in vacuo*, resulting in a white foamy product. X-ray diffraction quality crystals can be grown by the layered diffusion of diethyl ether onto a dichloromethane solution of the product. Yield: 0.376 g (40%) ^{1}H NMR (δ, in CD_2Cl_2): 7.57 (m, 40H), 2.20 (s, 9H) ESI-M/S: m/z=400.99 IR (KBr, cm^{-1}): 2200, 1500, 1440, 1400, 1100, 1050. 975, 955, 900.

Structures:

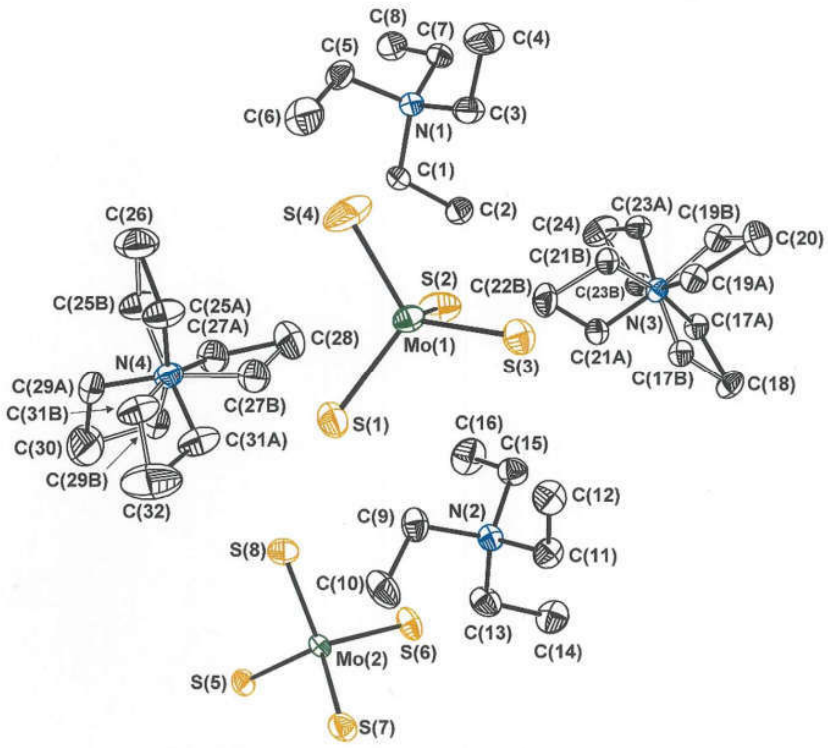

Figure 32. Thermal ellipsoid plot of [Et4N]2[MoS4] at the 50% probability level. Two equivalents of [Et4N]2[MoS4] occur in the asymmetric unit of the unit cell. All H atoms are omitted for clarity. The methylene groups of two of the independent [Et4N]+ cations are disordered and refined as best fit distributions between the two sites.

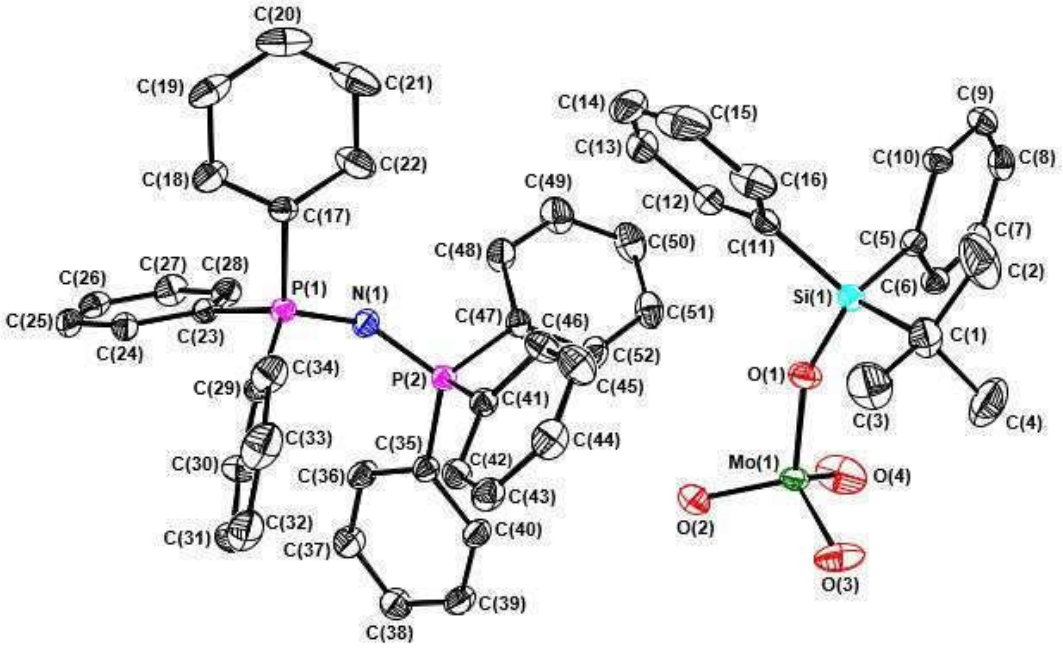

Figure 33: Thermal ellipsoid plot of [Ph3P=N=PPh3][MoO3(OSiPh2tBu)] at the 50% probability level. All H atoms omitted for clarity

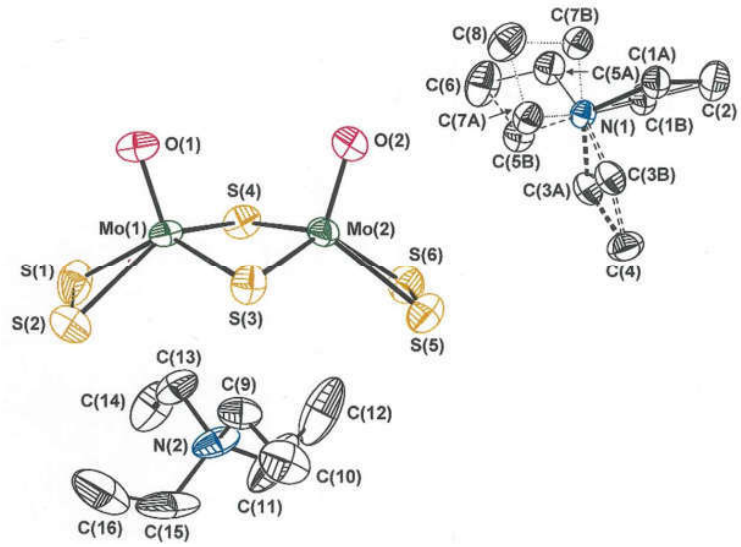

Figure 34: Thermal ellipsoid plot of [Et4N]2[(S2)Mo(O)(μ-S)2Mo(O)(S2)] at the 50% probability level. All H atoms are omitted for clarity. The methylene groups of one of the [Et4N]+ cations are disordered and refined as best fit distributions between the two sites.

Figure 35: Thermal ellipsoid plot of (iBu2NCS2)MoO(μ-S)2MoO(S2CNiBu2) at the 50% probability level. All H atoms omitted for clarity.

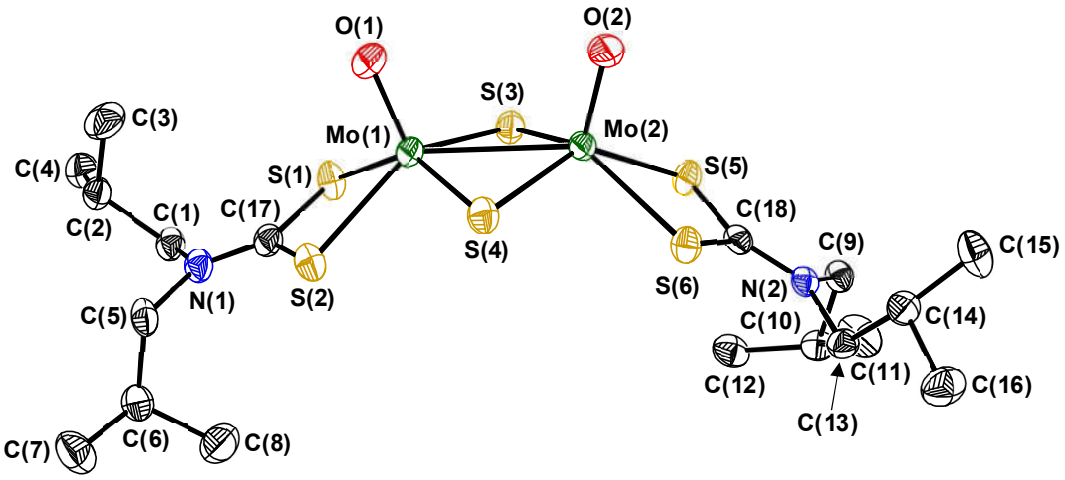

Table 12. Crystal and refinement data for [Et4N]2[MoS4],[Et4N]2[(S2)Mo(O)(μ-S)2Mo(O)(S2)], [PPN][MoO3(OSiPh2tBu)], (iBu2NCS2)MoO(μ-S)2MoO(S2CNiBu2)

compound #	$[Et_4N]_2[MoS_4]$	$[Et_4N]_2[(S_2)Mo(O)(\mu\text{-}S)_2Mo(O)(S_2)]$	$[PPN][MoO_3(OSiPh_2{}^tBu)]$	$(^iBu_2NCS_2)MoO(\mu\text{-}S)_2MoO(S_2CNiBu_2)$
structure code	JPD911_0m	JPD901_0m_a	JPD1290_0m_4_a	JPD1399_0m_M_a
Formula	$C_{16}H_{40}N_2MoS_4$	$C_{16}H_{40}N_2O_2S_2$	$C_{52}H_{49}MoNO_4P_2Si$	$C_{18}H_{36}Mo_2N_2O_2S_6$
Fw	484.68	676.74	937.89	696.73
temperature, K	150	150	150	150(2)
wavelength, Å	0.71073	0.71073	0.71073	1.54178 Å
2θ range, deg.	3.018 - 60.354	4.254 – 43.628	2.203 – 32.8875	2.54-72.31
crystal system	triclinic	monoclinic	Monoclinic	Monoclinic
space group	*P*-1	$P2_1/n$	$P2_1$	$P2_1/c$
a, Å	12.9317(18)	9.8786(11)	9.8005(5)	18.7186(5)
b, Å	13.6008(19)	27.947(3)	18.4905(10)	9.6217(2)
c, Å	15.903(2)	10.2875(11)	12.9652(7)	16.9453(4)
α, deg.	110.9156(18)	90	90	90
β, deg.	112.603(2)	97.7611(15)	103.327(2)	11.6280(10)
γ, deg.	91.066(2)	90	90	90
volume, $Å^3$	2372.4(6)	2814.1(5)	2286.2(2)	2837.06(12)
Z	4	4	2	4
density, g/cm^3	1.357	1.597	1.362	1.631
μ, mm^{-1}	0.906	1.351	0.429	
F(000)	1024	1384	972	1416
crystal size	0.260 x 0.294 x 0.423	0.039 x 0.117 x 0.336	0.516 x 0.286 x 0.111	.0178 x .0145 x .071
color, habit	red-orange block	orange needle	Colorless block	Red Block
limiting indices, *h*	$-18 \le h \le 18$	$-10 \le h \le 10$	$-14 \le h \le 14$	$-23 \le h \le 23$
limiting indices, *k*	$-18 \le k \le 18$	$-29 \le k \le 29$	$0 \le k \le 27$	$-11 \le k \le 11$
limiting indices, *l*	$-22 \le l \le 21$	$-10 \le l \le 10$	$0 \le l \le 19$	$20 \le l \le 20$
reflections collected	46625	30730	17263	67808
independent data	13042	3369	8303	5576
Restraints	0	0	1	0
parameters refined	463	269	554	279
GooF[a]	1.056	1.064	1.055	1.053
R1,[b,c] wR2[d,c]	0.0312, 0.0910	0.0503, 0.1324	0.0260, 0.0656	.0190,.0478
R1,[b,e] wR2[d,e]	0.0371, 0.0941	0.0565, 0.1363	0.0286, 0.0674	.0199, .0485
largest diff. peak, $e·Å^{-3}$	1.450	2.138	0.358	0.391
largest diff. hole, $e·Å^{-3}$	–0.729	–0.556	-0.755	-0.658

[a]GooF = $\{\Sigma[w(F_o^2 - F_c^2)^2]/(n-p)\}^{½}$, where n= number of reflections and p is the total number of parameters refined; [b]R1 = $\Sigma||F_o| - |F_c||/\Sigma|F_o|$; [c]R indices for data cut off at I > 2σ(I); [d]wR2 = $\{\Sigma[w(F_o^2 - F_c^2)^2]/\Sigma w(F_o^2)^2\}^{1/2}$; $w = 1/[\sigma^2(F_o^2) + (xP)^2 + yP]$, where $P = (F_o^2 + 2F_c^2)/3$; [e]R indices for all data.

Discussion:

The cation exchange is easily undertaken by the reaction of the ammonium salt of the metalate with two equivalents of the corresponding tetraalkylammonium hydroxide. The product is isolated by removing under vacuum the $NH_3(g)$ byproduct and water followed by solvation in acetonitrile and precipitation with diethyl ether producing a white solid in good yield for the molybdate (81%). The reaction is less effective for the tungstate, with a yield of 54% due to the formation of an insoluble white solid which is ascribed to the formation of a higher nuclearity polyoxotungstate.

The cation exchange can also be executed by refluxing the silver salt of the metalate with the corresponding tetraalkylammonium halide in acetonitrile for 48 hours, removing the silver halide precipitate by filtration, and finally concentrating the solution and precipitating with diethyl ether. While this approach is comparable to the $[R_4N][OH]$ method in its yield for the molybdate anion (85%), this method results in higher yields for the synthesis of tetraethylammonium tungstate (~80%) by avoiding the intractable solid that forms from the ammonium tungstate salt under basic conditions. The reaction of tungstic acid with a quaternary ammonium salt of $[OH]^-$ is faster, less costly, and proceeds with comparable yield, making it the preferred synthetic method for the organic soluble tungstate salt.

Once the tetraalkylammonium oxometallate is purified and thoroughly dried, it is solvated in enough 1% DABCO in very dry acetonitrile to form a solution with a metalate concentration between 7.5 mM and 10.0 mM. To this solution is added four equivalents of hexamethyldisilathiane (HMDS) which has been diluted to 2.0-3.0 mM in very dry acetonitrile.

For the molybdate, both solutions are cooled to 0 °C in an ice bath. The HMDS solution is then added dropwise at a rate of approximately 0.5 mL/min. The low concentration, low temperature, addition of an organic base, exclusion of air, and slow addition rate are necessary to reduce the formation of the $[Et_4N]_2[(S_2)Mo(O)(\mu\text{-}S)_2Mo(O)(S_2)]$ side product, which while interesting in its own right, is not the targeted compound. The addition of the base is successful in managing the product distribution and suppressing formation $[Et_4N]_2[(S_2)Mo(O)(\mu\text{-}S)_2Mo(O)(S_2)]$ in the synthesis of $[Et_4N][MoS_4]$, as evidence by elemental analysis and the reactions monitored UV-Vis presented in **Figure 36,** below. Despite this improvement, a single pure product has not been isolated for any mixed oxythiomolybdates by this method to date. The reaction time varies for the formation of each of the molybdate species with the less substituted molybdates forming faster than their more substituted counter parts. For the $[MoS_4]^{2-}$, after addition of the hexamethyldisilathiane the solution is stirred for at least an additional 12 hours, while $[MoO_3S]^{2-}$ can be seen almost instantaneously by UV-vis spectroscopy. Crystalline material can be grown from the vapor diffusion of diethyl ether into a concentrated solution of the tetraalkylammonium metalate in acetonitrile, though these crystals suffer from extensive disorder due to the similar ligand size and interaction strength with the cation. Because of this disorder only $[Et_4N]_2[MoS_4]$ has been fully characterized using this method.

Figure 36: The UV-vis spectra taken over the course of the reaction of [Et4N]2MoO4 with 4 equivalents of (Me3Si)2S without the addition of base (top) and with the addition of 1% by volume DABCO (bottom).

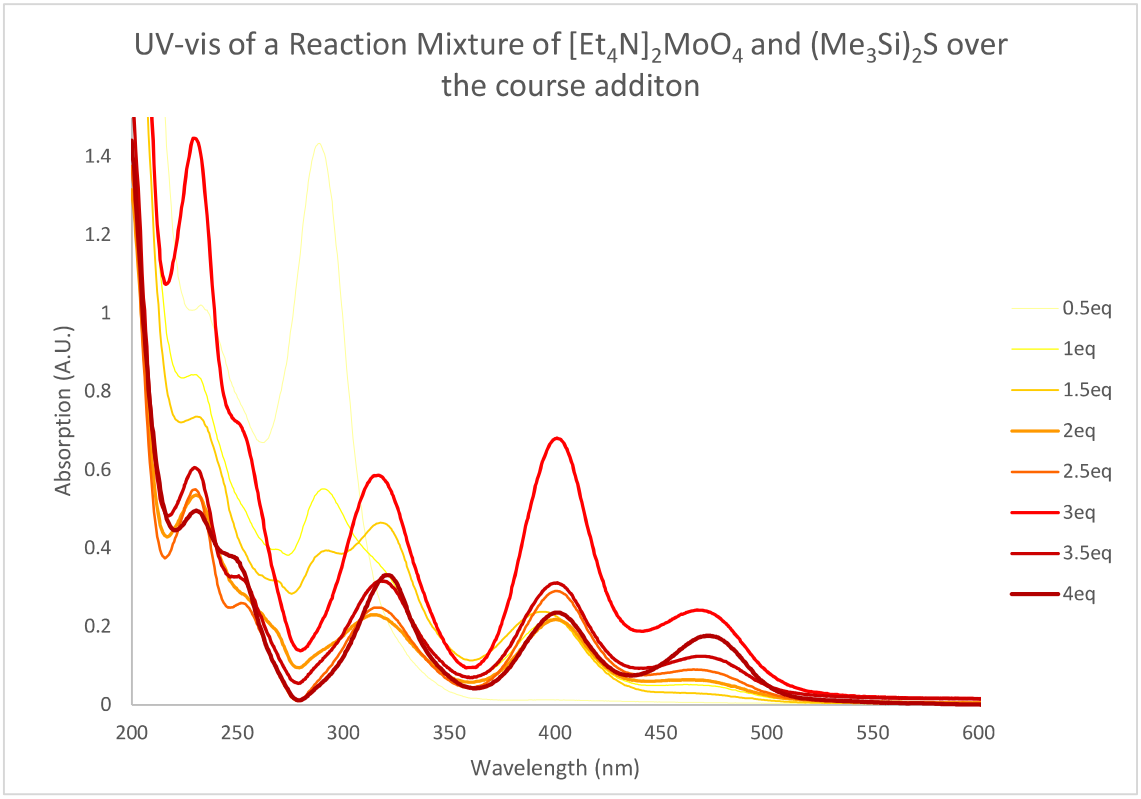

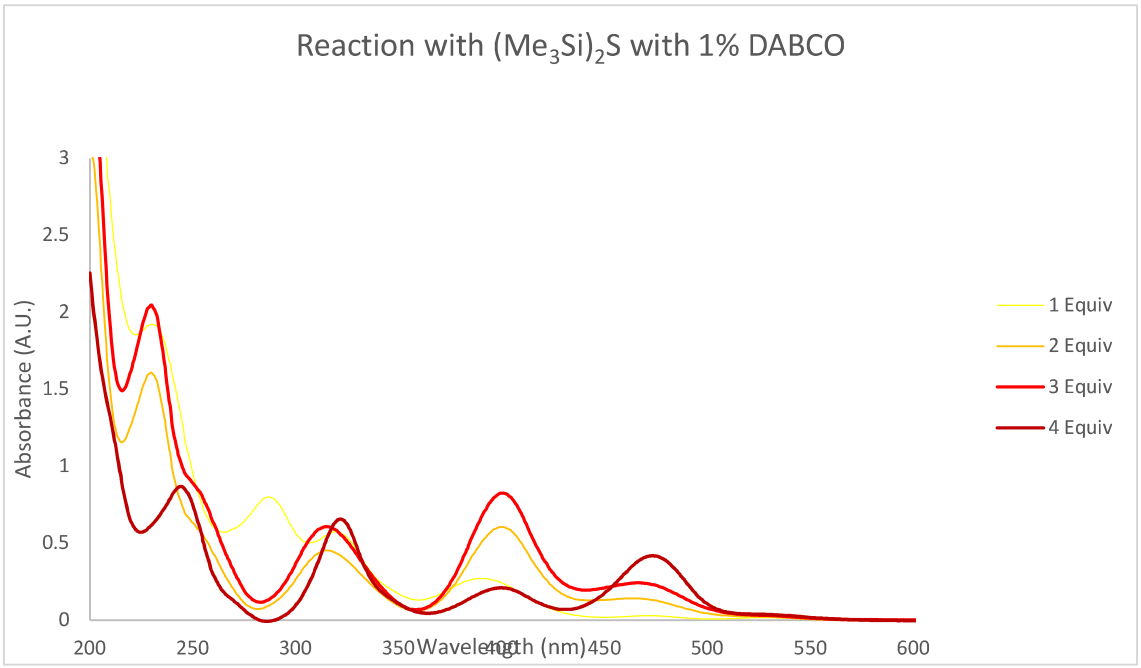

The silylation of the molybdate oxo-ligand is carried out in a similar manner as that reported by both DeKock and Holms with adaptations to account to for the difference is solubility caused by the more sterically bulky organosilane employed in this report and the new cation choice, which was selected due to its comparatively less hydroscopic character than the tetraethylammonium chloride employed in the previous reports. [39,77] The molybdate-bound silyloxy ligand generated by this procedure is profoundly water sensitive, with only a small amount of atmospheric water or oxygen leading to the widespread degradation of a sample. With water this is accomplished by the hydrolysis of the silyloxy ligand which is lost as the silanol. This formed silanol is acidic and is capable of causing the further hydrolysis of other metal bound silyloxy ligands, the ultimate product of this unfortunate cascade is the formation of higher nuclearity polyoxomolybdates. Products a nuclearity between 2 and 8 having been isolated as a result of this process including molybdenum blue, of which the first description is ascribed to Scheele in 1778 and further investigated by Berzelius in 1826.[78,79]

Characterization:

As purity has always been the primary problem plaguing the aqueous synthesis of these salts, it was also the main focus of our characterization priorities. While others have had success with ^{95}Mo NMR, we found that the extraordinarily wide chemical shift range, long collection time, and high concentrations necessary to produce a usable signal-to-noise ratio to be overly cumbersome. This concern was magnified by the desire to avoid water wherever possible, including D_2O, which is the preferred solvent for ^{95}Mo NMR experiments. We found that ESI-MS shows good signal intensity and that the products are easily identified by *m/z* and isotopic distribution as the protonated monoanion as seen below in **Figure 36**. It is clear from the total ion count that a variety of impurities are present in the recrystallized sample, including higher

nuclearity products with *m/z* of up to 460 mass units. However, a significant majority of the product is represented by the $HMoO_xS_{4-x}^{1-}$ species with *m/z* ratios as follows: $HMoO_4^{1-}$ = 156-169 mass units, $HMoO_3S^{1-}$ = 172-185 mass units, $HMoO_2S_2^{1-}$ = 188-203, $HMoOS_3^{1-}$ = 204-219, and $HMoS_4^{1-}$ = 220-237.

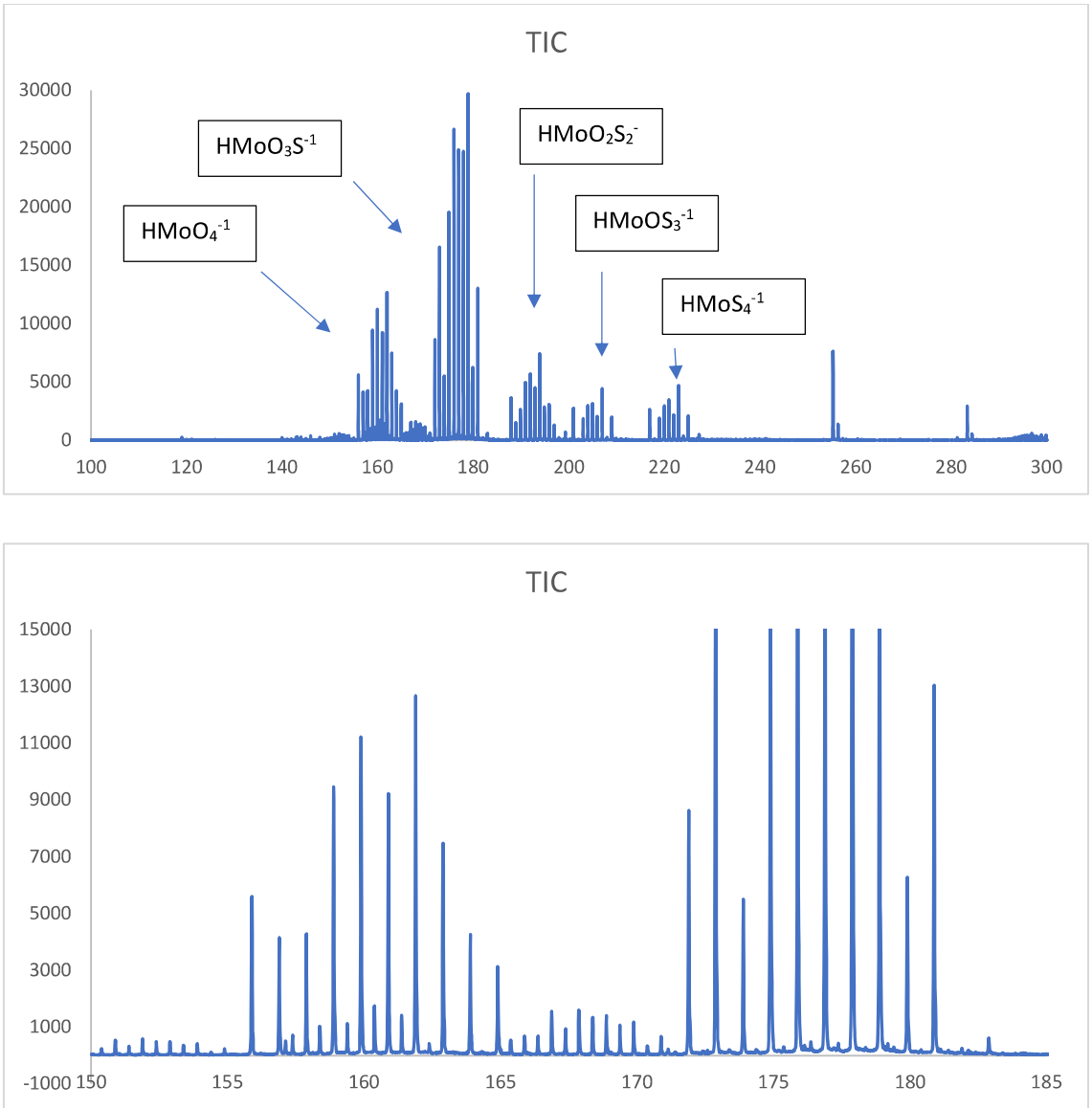

Figure 37: The TIC from m/z=100 to m/z=300 (above) for a reaction of $[Et_4N]_2MoO_4$ with 1 equivalent of $(Me_3Si)_2S$ and closer view of m/z=150 to m/z=185 (below)

The ESI-MS experiment suggests that the reaction conditions do not produce a single product even under the constraining conditions used. However, these indications may be deceiving, as there is evidence from the work of Quagraine that the ESI-MS method results in a significant amount of ligand scrambling. The result of this ligand scrambling is a drastic lowering the apparent purity of any given product.[80] This suggestion was rationalized as the ESI process liberating "free" sulfide from the complex, which then reacts with other molecules throughout the nucleation and evaporation process and produces a wide array of byproducts as evidenced by the 0.5 *m*/*z* spacing seen in the $HMoO_4^{-1}$ and $HMoO_3S^{-1}$ mass spectra in **Figure 36** which are attributed to an unknown contaminant that possesses a 2^- charge. In their work, the purity of synthesized mixed oxythiometallates was established by both aqueous ^{95}Mo NMR measurements and through UV-vis spectrometry. As noted earlier, however, both of these methods also have their shortcomings. However, the purity established by both methods deviates significantly from the apparent purity from ESI-MS experiments as can be seen in **Figure 37** below., further the deviation observed by Quagraine is similar to that in the ESI-MS sample produced through the method presented here. Quagraine observed that the ligand scrambling is reduced for the more intrinsically

stable $[MoOS_3]^{2-}$ and $[MoS_4]^{2-}$ complexes and was ultimately led to reject ESI-MS as a reliable measurement of purity for mixed oxythiometallates.[80]

Figure 38: An example of the curve fitting analysis results

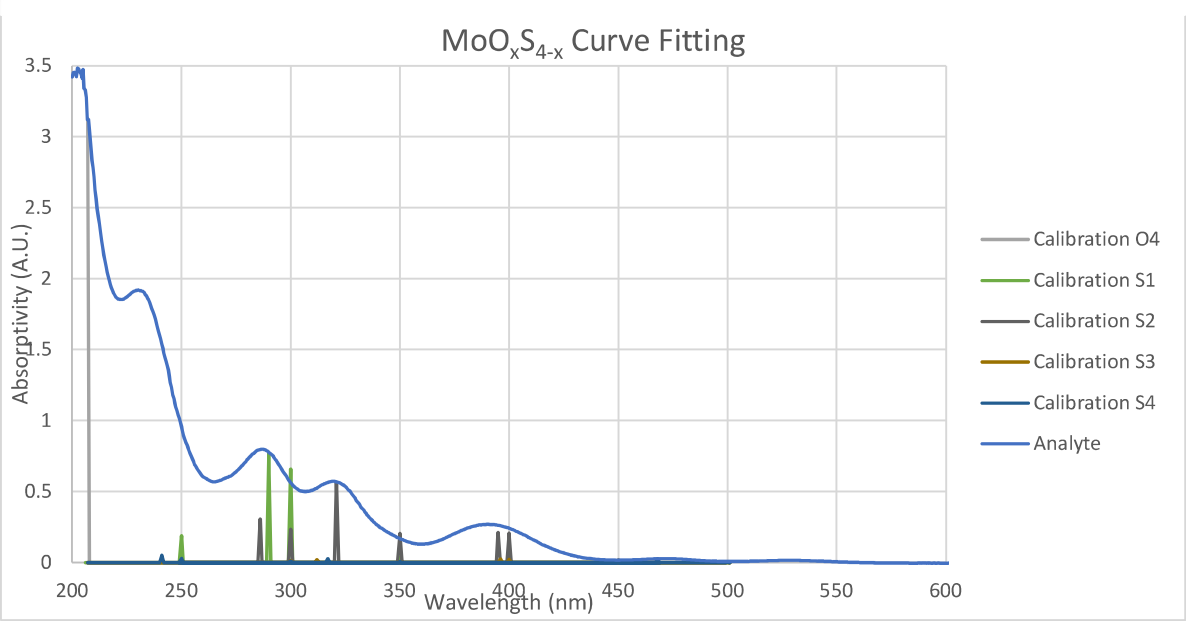

Figure 39: The compositions of the Quagraine samples by two methods and samples from this study by two methods, UV-vis and ESI-MS

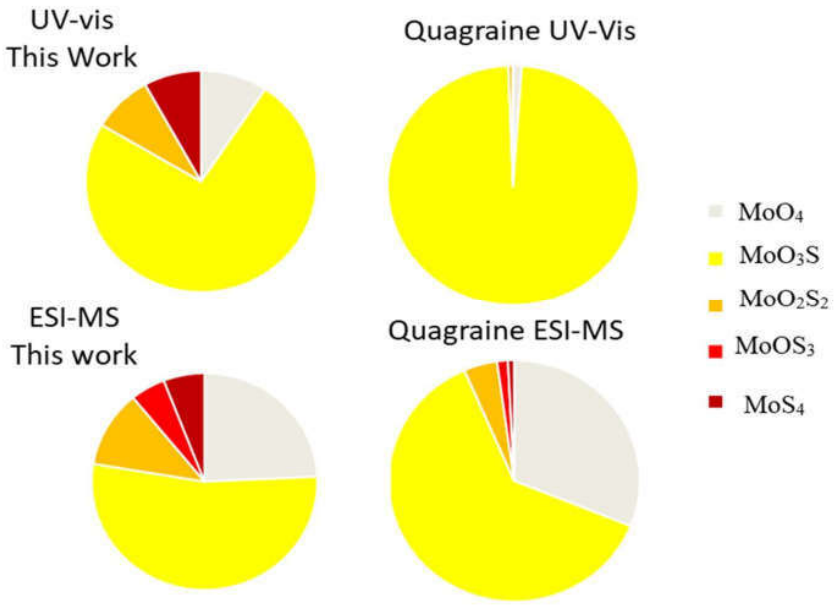

Thus, we are relegated to relying on a combination of the oldest methods to determine the degree of success of these reactions: a combination of multivariate analysis of the UV-vis spectra, vibrational spectroscopy, and elemental analysis. The UV-vis curve fitting analysis was undertaken in the same manner similar to that by Quagraine and Reid, with a wavelength cut off of 285 nm.[80] The molar extinction coefficients for the absorption maxima of each product were taken from literature and an absorbance value at each of eight points was calculated from these values. An initial guess was then made as to the concentration of each product in a reaction mixture from the known concentration of the analyte solution and compared to the calculated values for each mixed oxythiomolybdate species as seen in **Figure 38**. The sum of the absolute value of the error was minimized mathematically by the use of an evolutionary algorithm, finally the root mean squared error was minimized in the same manner. This procedure produces a value for each mixed oxythiomolybdate in solution with the results of one such analysis seen in **Figures 39** above.

One of the byproducts of this reaction is the previously known$[(S_2)MoO(\mu\text{-}S)_2Mo(O)(S_2)]^{2-}$ anion, whose structure is shown above in **Figure 35** above. This doubly sulfido bridged di-Mo(V) complex is somewhat common in the history of the chemistry of mixed oxythiomolybdates and forms more readily at higher levels of thiolation.[81] The hazard the formation of this complex presents in monitoring reaction progress and purity is difficult to overstate. The vibrational absorptions for the dimolybdate complex differ only slightly from the mononuclear precursors with the dimetallic complex Mo=O and bridging Mo-S vibrations being found at only slightly higher wavenumbers than their monometallic counter parts. These minor differences leave only the S-S stretching frequency of the terminal disulfides as diagnostic in the IR spectrum. In the UV-vis spectrum, the dimolybdenum complex is characterized by absorptions at 460 nm and 390 nm, the latter of which is common to all of the mixed oxythiomolybdates and

the former of which is shared with $[MoOS_3]^{2-}$ effectively adding a sixth species to these already significantly overlapping spectra. The UV-vis spectra can be seen in the spectrum of the base free reaction presented above in **Figure 36** as the final product.

In the past, the formation of the dimolybdenum byproduct was thought to be the result of an internal redox process in which the metal center is reduced by 2 electrons through the oxidation of two of its sulfido ligands to form a coordinated disulfide.[81] This disulfide then attacks another metal ion in solution and a metal-metal electron transfer produces a pair of Mo(V) ions bound by two bridging sulfides. However, the reagent employed in this study may reach this product through another mechanism, shown below in **Figure 40**. The mechanism for the formation of the byproduct begins the same way as the that of the intended product, with the nucleophilic attack of the of the molybdenum bound oxo-ligand on the trimethylsilyl group of hexamethyldisilathiane with the trimethylsilylsulfide acting as the leaving group. In the formation of the byproduct however this is not followed by the subsequent nucleophilic attack of that silylsulfide on the same metal center but a different one, on that has already undergone three previous chalcogen exchanges, that is $[Et_4N]_2MoOS_3$. This produces an 18 e^- complex that undergoes a similar internal redox mechanism as proposed for the formation of the product in the classical synthesis.[81] The result of which is an oxidized coordinated disulfide and a two electron reduced Mo(IV) center coordinated to a trimethylsilylsulfide group and one oxo and one sulfido ligand. This silylsulfide ligand undergoes an intermolecular attack by the silylated oxo ligand formed in the first step, this attack is similar to the intramolecular attack seen in the mechanism of the intended product. The resulting dimetallic complex contains a single bridging sulfide between a reduced Mo(IV) and a Mo(VI) center. The sulfido ligand bound to the Mo(IV) center is well positioned for nucleophilic attack on the electrophilic Mo(VI), this causes the oxidation of the two terminal sulfido ligands bound to the

Mo(VI) atom to form another coordinated disulfide and prompt the reduction of the Mo(VI) to Mo(IV). One electron from each metal is then used to form a metal-metal bond, oxidizing the molybdenum centers to Mo(V).

Figure 40: Proposed mechanism for the formation of the major byproduct $[Et_4N]_2[(S_2)Mo(O)(\mu\text{-}S)_2Mo(O)(S_2)]$

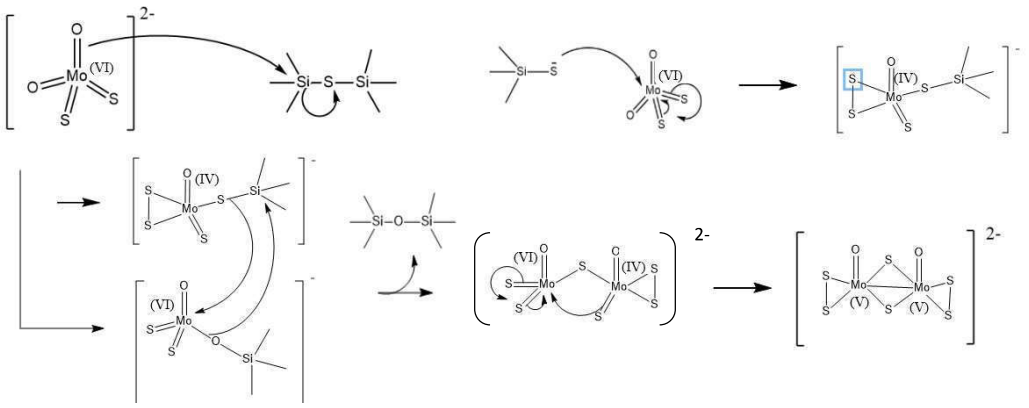

In pursuit of other projects of interest to the Donahue group, the optimization of the synthesis of dimolybdenum byproduct was carried out and investigations into its derivatization were undertaken. The dimolybdenum byproduct was first described by Müller and the chemistry of such complexes have been explored extensively in the past by Coucouvanis and others.[82,83,84] However, the hexamethyldisilathiane employed in this study provides a new synthetic route to this potentially useful material. While oxygen and moisture still play a role in the optimized synthesis of the dimolybdenum compound as detailed above, the byproduct still appears in the synthesis of the more substituted mixed oxythiomolybdates even when meticulous care is taken to ensure the exclusion of room air. At elevated temperatures and rapid addition rates, the bright colors of the mixed oxythiomolybdates aren't the only colors seen over the course of the reaction with each drop of added $(Me_3Si)_2S$ generating a deep blue color that rapidly fades, such colors are common to Mo(V) and Mo(IV) complexes such as those in the mechanism proposed above. However, this

suspected intermediate is short-lived and has not been isolated thus the mechanism in **Figure 40** is not confirmed. The derivatization of the dimolybdenum byproduct by the substitution of the terminal disulfide groups with di-*iso*butyldithiocarbamate was explored pursuant to hydrogen evolution reaction applications, an application in which this complex has shown to be a decomposition product of the Mo_3S_{13} cluster and has further been theorized to be active in its own right.[85,86] Scale up and HER activity evaluation are pending.

Future Work:

The thermodynamic calculations suggest that the hexamethyldisilathiane should be able to carry out the chalcogen exchange in a stepwise manner however, this has thus far been complicated by the ability of the mixed oxythiomolybdates to undergo ligand exchange even in the absences of catalytic water. The investigation of the analogous reaction with hydrogen sulfide in aqueous solution shows that raising the pH reduces the rate of ligand exchange, and the rate of the forward and reverse reaction are heavily dependent on the hydroxyl ion concentration. The addition of a Brønsted base to the ostensibly anhydrous organic system has been shown to decrease the rate of internal reduction and improve selectivity for the formation of $[MoS_4]^{2-}$. These improved reaction outcomes have come along with a modest reduction in the rate of reaction for the formation of the desired products. The effect of the addition of an appropriate base on the formation and selectivity of this reaction system for the less substituted mixed oxythiomolybdates may prove fruitful, additionally the effect of the choice of cation and solvent should be further explored as ion interactions and solvent effects could play a vital in the synthesis of the target compounds. Furthermore, the extension of this reactivity to other oxyanions, with the exception of tungsten, has not been investigated.

Further improvements could also be found by slowing the rate of reaction in other ways. For example, rather than employing hexamethyldisilathiane as the chalcogen exchange reagent, an a bulk silathiane, such as hexaphenyldisilathiane, or an asymmetric silathiane, such as trimethyl-tri-*iso*propyldisilathiane, could reduce the rate of reaction and raise the steric barrier to the formation of the byproduct. Additionally, a cyclic silathiane could also serve the same purpose and reduce the hazard posed ionized silanethiolate to this reaction's selectivity. Alternatively, to further slow the reaction down and increase selectivity, the reaction could be performed in two steps. The first step being the silylation of the oxo ligand with silyl halide followed by the chalcogen exchange with an appropriate silanethiolate. This would serve to reduce the possibility of more than one silylated oxo ligand on a single metal center, as well as reducing the chance of silanethiolate attack on an unsilylated metal center.

References:

(1) Haynes, W. M. *CRC Handbook of Chemistry and Physics*, 97th ed.; CRC Press, 2016.

(2) Erickson, B. E.; Helz, George R. "Molybdenum (VI) Speciation in Sulfidic Waters: Stability and Lability of Thiomolybdates." *Geochim. Cosmochim. Acta* **1999**, *64* (7), 1149–1158. https://doi.org/10.1016/S0016-7037(99)00423-8.

(3) Helz, G. R.; Miller, C. V.; Charnock, J. M.; Mosselmans, J. F. W.; Pattrick, R. A. D.; Garner, C. D.; Vaughan, D. J. Mechanism of Molybdenum Removal from the Sea and Its Concentration in Black Shales: EXAFS Evidence. *GeoChimica et Cosmochimica Acta* **1996**, *60* (19), 3631–3642. https://doi.org/10.1016/0016-7037(96)00195-0.

(4) Cui, M.; Mohajerin, T. J.; Adebayo, S.; Datta, S.; Johannesson, K. H. Investigation of Tungstate Thiolation Reaction Kinetics and Sedimentary Molybdenum/Tungsten Enrichments: Implication for Tungsten Speciation in Sulfidic Waters and Possible Applications for Paleoredox Studies. *GeoChimica et Cosmochimica Acta* **2020**, No. 287, 277–295. https://doi.org/10.1016/j.gca.2020.04.004.

(5) Leimkühler, S.; Iobbi-Nivol, C. Bacterial Molybdoenzymes: Old Enzymes for New Purposes. *FEMS Microbiol. Rev.* **2015**, *40* (1), 1–18. https://doi.org/10.1093/femsre/fuv043.

(6) Bevers, L. E.; Hagedoorn, P.-L.; Hagen, W. R. The Bioionorganic Chemistry of Tungsten. *Coord. Chem. Rev.* **2008**, No. 253, 269–290. https://doi.org/10.1016/j.ccr.2008.01.017.

(7) Majumdar, A.; Sarkar, S. Bioinorganic Chemistry of Molybdenum and Tungsten Enzymes: A Structural-Functional Modeling Approach. *Coord. Chem. Rev.* **2010**, No. 255, 1039–1054. https://doi.org/10.1016/j.ccr.2010.027.

(8) Robertson, W. D. Molybdate and Tungstate as Corrosion Inhibitors and the Mechanism of Inhibition. *J. Electrochem. Soc* **1951**, *98* (3), 94–100. https://doi.org/10.1149/1.2778118.

(9) Chinas-Castillo, F.; Lara-Romero, J.; Alonso-Núñez, G.; Barceinas-Sánchez, J. D. O.; Jiménez-Sandoval, S. Friction Reduction by Water-Soluble Ammonium Thiometallates. *Tribol* **2006**, *26* (2), 137–144. https://doi.org/10.1007/s11249-006-9179-4.

(10) Li, Y.; Lu, J.; Cui, X.-B.; Xu, J.-Q.; Li, K.-C.; Sun, H.-Y.; Li, G.-H.; Pan, L.; Yang, Q.-X. Syntheses, Structures and Third-Order Non-Liner Optical Properties of Homometal Clusters Containing Molybdenum. *J. Solid State Chem,* **2004**, No. 178, 363–369. https://doi.org/10.1016/j.jssc.2004.11.004.

(11) Mertis, C.; Kravaritoy, M.; Chorianopoulou, M.; Koinis, S.; Psaroudakis, N. Homogeneous Catalytic Hydrogen Formation Using Dinuclear Multiply Bonded Complexes of Molybdenum (III) and Tungsten (III) and Low-Valency Metal Ions, M=Cr(III), V(II), in Aqueous Acidic Solutions. *T. Molec. Org 11*, 321–329. https://doi.org/10.1007/978-94-011-0822-5_30.

(12) Li, Y.; Yamaguchi, A.; Yamamoto, M.; Takai, K.; Nakamura, R. Molybdenum Sulfide: A Bioinspired Electrocatalyst for Dissimilatory Ammonia Synthesis with Geoelectrical Current. *J. Phys. Chem. C* **2016**, No. 121, 2154–2164. https://doi.org/10.1021/acs.jpcc.6b08343.

(13) Howard, K. E.; Lockemeyer, J. R.; Massa, M. A.; Rauchfuss, T. B.; Wilson, S. R.; Yang, X. Thiometalate Complexes Containing Arene, Thiophene, and Cyclobutadiene

Coligands. Are Thiometalate Clusters Good Models for Desulfurization Catalysts? *Inorg. Chem.* **1990**, *29* (22), 4385–4390. https://doi.org/10.1021/ic00347a012.
(14) Gao, L.; Sun, Y.; Wu, M.; Wang, D.; Wei, J.; Wu, B,; Wang, G.; Wu, W.; Jin, X.; Wang, X.; He, P. "Physiological and Proteomic Analyses of Molybdenum- and Ethylene-Responsive Mechanisms in Rubber Latex." *Front. Plant. Sci.* **2018**, 9, 621. https://doi.org/10.3389/fpls.2018.00621
(15) Dhar, P.; Chandrasekaran, S. Novel Alkylation with Tetrathiotungstates and Tetrathiomolybdates: Facile Synthesis of Disulfide from Alkyl Halides. *J. Org. Chem* **1989**, *54* (13), 2998–3000. https://doi.org/10.1021/jo00274a002.
(16) Heppekausen, J.; Stade, R.; Goddard, R.; Fürstner, A. Practical New Silyloxy-Based Alkyne Metathesis Catalysts with Optimized Activity and Selectivity Profiles. *J. Am. Chem. Soc* **2010**, *132* (20), 11045–11057. https://doi.org/10.1021/ja104800w.
(17) Malcolmson, S.J.; Meek, S.J.; Sattely, E.S. Schrock, R.R.; Hoveyda, A.H. "Highly Efficient molybdenum-based catalysts for enantioselective alkene metathesis." *Nature*. **2008**. 456. 933-937. https://doi.org/10.1038/nature07594
(18) Abrantes, M.; Valente, A. A.; Pillinger, M.; Gonçalves, I. S.; Rocha, J.; Romão, C. C. Preparation and Characterization of Organotin-Oxomolybdate Coordination Polymers and Their Ys Ein Sulfoxidation Catalysis. *Chem. Eur. J* **2003**, *9* (12), 2685–2695. https://doi.org/10.1002/chem.200204399.
(19) Bartecki, A.; Dembicka, D. Tetrahedral Sulphur Containing Mo(VI) and W(VI) Chromophores. *Inorganica Chim. Acta* **1973**, *7* (4), 610–612. https://doi.org/10.1016/S0020-1693(00)94895-3.
(20) Müller, A.; Diemann, E. Thiomolybdates and Thiotungstates: Their Properties and Role as Ligands in Coordination Chemistry. *Nitrogen Fixation* **1983**, 183–201. https://doi.org/10.1007/978-1-4684-8523-3_8.
(21) Berzelius, J. J. About the Sulfurous Salts. *Poggendorf's Annalen der Physik* No. 1, 1826. https://doi.org/10.1002/andp.18260841102.
(22) Krüss, G. About the Sulfur Compounds of Molybdenum. *Justus Liebig's Ann. Chem.* **1884**, *225*, 1–57. (283)
(23) Debray, H. Studies on molybdenum. *Justus Liebig's Ann. Chem* **1858**, *108* (2), 129–256. https://doi.org/10.1002/jlac.18581080217.
(24) Bodenstab, H. On an oxysulfurate salt of molybdenum with sulfuric ammonium. *Justus Liebig's Ann. Chem. 185*
(25) Corleis, E. Sulfur Compounds of Tungsten. *Justus Liebig's Ann. Chem* **1886**, No. 232, 244–270.
(26) Bernard, J.-C.; Tridot, G. Contribution to the study of alkaline thiotungstates and thiomolybdates: identification and filiation of their ions in aqueous solution. *Bull. Soc. Chim. Fr.* **1961**, 810–822.
(27) Leroy, M.; Kaufmann, G.; Charlionet, R.; Rohmer, R. A few sulfur salts of a new type: M2MoOS3; study of the ion by infrared and ultraviolet spectrography. *C. R. Acad. Sc. Paris* **1966**, No. 263, 601–604. https://doi.org/12148/bpt6k6237425w.
(28) Gattow, G.; Franke, A.; Müller, A. Infrared spectrum of tetrathiomolybdate and tetrathiotungstate. *Sci. Nat.* **1965**, *52* (14), 428–429. https://doi.org/10.1007/BF00589682.

(29) Müller, A.; Diemann, E. Preparation of some di- tri- and tetrathiomolybdates and tungstates. *Z. Naturforschg* **1968**, *23* (b), 1607–1608. https://doi.org/10.1515/znb-1968-1211.
(30) Müller, A.; Diemann, E.; Ranade, A. C.; Aymonino, P. J. Electronic Spectra of MoO3S 2- and WO3S 2- and Their Comparison with the Spectra of the Ions $MoO_xS_{4-x}^{2-}$ and $WO_xS_{4-x}^{2-}$. *Z. Naturforschg* **1969**, *24* (10), 1247–1249. https://doi.org/10.1515/znb-1969-1007.
(31) Müller, A.; Dornfeld, H.; Schulze, H.; Sharma, R. C. On K2MoO3S, Preparation of a pure monothiomolybdate. *Z. Anorg. Alleg. Chem* **1980**, *468* (1), 193–196. https://doi.org/10.1002/zaac.19804680124.
(32) Yamamoto, I.; Saiki, T.; Liu, S.; Ljungdahl, L.G. "Purification and Properties of NADP-dependent formate dehydrogenase from *Clostridium thermoaceticum*, a tungsten-selenium-iron protein." *J. Biol. Chem.* **1983,** 258 1826-1832. https://doi.org/10.1016/S0021-9258(18)33062-X
(33) De Renzo EC, Heytler PG. *Arch Biochem Biophys*. **1954**;49:242–244
(34) Mahler HR, Mackler B, Green DE, Bock RM. *J Biol Chem*. **1954**;210:465–480.
(35) Nicholas DJD, Nason A, McElroy WD. *J Biol Chem*. **1954**;207:341–352.
(36) Hille, R.; Nishino, T.; Bittner, F. Molybdenum Enzymes in Higher Organisms. *Coord. Chem. Rev.* **2012**, *255* (9–10), 1179–1205. https://doi.org/10.1016/j.ccr.2010.11.034.
(37) McDonald, J. W.; Friesen, G. D.; Rosenhein, L. D.; Newton, W. E. Synthesis and Characterization of Ammonium and Tetraalkylammonium Thiomolybdates and Thiotungstates. *Inorganica Chim. Acta* **1982**, *72*, 205–210. https://doi.org/10.1016/S0020-1693(00)81720-X.
(38) Do, Y.; Simhon, E. D.; Holm, R. H. Oxo/Sulfido Ligand Substitution in [Mo2O7]2-: Reaction Sequence and Characterization of the Final Product [MoS3(OSiMe3)]-. *Inorg. Chem* **1984**, *24*, 1831–1838. https://doi.org/10.1021/ic00206a028.
(39) Partyka, D. V.; Holm, R. H. Oxygen/Sulfur Substitution Reactions of Tetraoxometalates Effected by Electrophilic Carbon and Silicon Reagents. *Inorg. Chem* **2004**, *43* (26), 8609–8616. https://doi.org/10.1021/ic040097g.
(40) Wang, J.; Holm, R.H. Silylation, Sulfidation, and Benzene-1,2-dithiolate Complexation Reactions of Oxo- and Oxosulfidomolybdates(VI) and -tungstates(VI). *Inorg. Chem.* **2007**, 46, 11156-11164. DOI: 10.1021/ic701294y
(41) Partyka, D. V.; Staples, R. J.; Holm, R. H. Nucleophilic Reactivity of Oxo/Sulfido Substitution Reactions of M(VI)O3 Groups (M=Mo,W). *Inorg. Chem* **2003**, *42* (24), 7877–7886. https://doi.org/10.1021/ic030185I.
(42) Alonso, G.; Aguirre, G.; Rivero, I. A.; Fuentes, S. Synthesis and Characterization of Tetraalkylammonium Thiomolybdates and Thiotungstates in Aqueous Solution. *Inorganica Chim. Acta* **1997**, *274*. https://doi.org/10.1016/S0020-1693(97)05901-X.
(43) Alonso, G.; Berhault, G.; Chianelli, R. R. Synthesis and Characterization of Tetraalkylammonium Thiomolybdates and Thiotungstates in Aqueous Solution. *Inorganica Chim. Acta* **2000**, *316*. https://doi.org/10.1016/S0020-1693(01)00648-X.
(44) Alonso, G.; Yang, J.; Siadati, M. H.; Chianelli, R. R. Synthesis of Tetraalkylammonium Thiometallates in Aqueous Solution. *Inorganica Chim. Acta* **2001**, *325*, 193–197. https://doi.org/10.1016/S0020-1693(01)00648-X.
(45) Vega-Granados, K.; Del Valle, M.; Licea-Claverie, A.; Alonso-Núñez, G.; Romero-Rivera, R.; López-Sosa, L.; Avalos-Borja, M.; Cruz-Reyes, J. A New Route for the

Synthesis of Ammonium Thiotungstate, a Catalyst Precursor. *Catal.Lett* **2017**, No. 147, 1339–1346. https://doi.org/10.1007/s10562-017-2041-5.
(46) Muller, A.; Mohan, N.; Dornsfeld, H.; Tellez, C. Raman Spectrum (in Aqueous Solution) and Force Constants of MoO3S 2-. *Spectrochim 34a* (5), 561–562. https://doi.org/10.1016/0584-8539(78)80054-3.
(47) Leroy, M.; Kaufmann, G. Infrared spectrum and Raman and normal coordinate analysis of the ions MoO2S2 2- and WO2S2 2-. *Bull. Soc. Chim. Fr.* **1967**, No. 9, 3586–3591.
(48) Leroy, M.; Kaufmann, G. Raman Spectra of the ions MoOS3 2-, WOS32- and MoS4 2- in the solid. *Bull. Soc. Chim. Fr.* **1968**, No. 10, 4028–4031.
(49) Leroy, M.; Burgard, M.; Müller, A. Infrared and Raman spectra of the MoO3S 2- and WO3S 2- ions in the solids. *Bull. Soc. Chim. Fr.* **1970**, No. 4, 1183–1186.
(50) Müller, A.; Weinstock, N.; Schulze, H. Laser-Raman spectra of the MoS4 2- WS4 2- MoOS3 2- and WOS3 2- ions in aqueous solution and their crystalline alkali salts. *Spectrochim* **1971**, *28* (6), 1075–1082.
(51) Müller, A.; Diemann, E. Depiction of some di-, tri- and tetrathiomolybdates and tungsten. Z. Naturforschg **1968**, 23b (12), 1607–1608. https://doi.org/10.1515/znb-1968-1211.
(52) Müller, A.; Diemann, E.; Krebs, B.; Leroy, M. J. F. About Trithiomolybdate. *Angew. Chem.* 1968, 80 (20), 846–847. https://doi.org/10.1002/ange.19680802012.
(53) Müller, A.; Rittner, W.; Nagarajan, G. Electron absorption spectra of thiomolybdate and thiotungstate ions. Comparative qualitative observation of binding ratios in the tetraoxo and tetrathioanions of molybdenum and tungsten. *Z. Phys. Chem. Neue. Fol* **1967**, 54 (5/6), 229–236. https://doi.org/10.1524/zpch.1967.54.5_6.229.
(54) Diemann, E.; Müller, A. Electronic Spectrum of VOS3 3-, MoOS3 2-, and WOS3 2- ions. *Spectrochim* **1970**, 26 (1), 215–219. https://doi.org/10.1016/0584-8539(70)80262-8.
(55) Bartecki, A.; Dembicka, D. Electronic Absorption Spectra of Tetrahedral Thioanions and Thiooxyanions of Molybdenum(VI) and Tungsten(VI). *Pol. J. Chem.* **1973**, *47* (3), 477–483.
(56) Clark, R. J. H.; Dines, T. J.; Proud, G. P. Studies of the Electronic Properties of the Tetrathiotungstate(VI) Ion, WS4 2- by Low Temperature Absorption and Resonance Raman Spectroscopy. *J. Chem. Soc., Dalton Trans.* **1983**, 2019–2024. https://doi.org/10.1039/DT9830002019.
(57) Reid, R. S.; Clark, R. J.; Quagraine, E. K. Accurate UV-Visible Spectral Analysis of Thiomolybdates. *Can. J. Chem*. **2007**, 85, 1083–1089. https://doi.org/10.1139/V07-122.
(58) Lutz, O.; Nolle, A.; Kroneck, P. Use of 95Mo NMR Spectroscopy as a New Approach to Structural Analysis of Diamagnetic Molybdenum Complexes. *Zeitschrift Für Naturforschung* **1976**, 31 (5), 454–456. https://doi.org/10.1515/zna-1976-0506.
(59) Lutz, O.; Nolle, A.; Kroneck, P. Use of 95Mo NMR for Identification of Molybdenum (VI) Chalcogenide Anions in Aqueous Solution. *Z. Naturforschg* **1977**, 32 (5), 505–506. https://doi.org/10.1515/zna-1977-0522.
(60) Kuehn, C. G.; Taube, H. Ammineruthenium Complexes of Hydrogen Sulfide and Related Sulfur Ligands. *J. Am. Chem. Soc* **1976**, 98 (3), 689–702. https://doi.org/10.1021/ja00419a010.

(61) Harmer, M. A.; Sykes, G. Kinetics of the Interconversion of Sulfido- and Oxomolybdate Species MoOxS4-x 2- in Aqueous Solutions. *Inorg. Chem* **1980**, 19 (10), 2881–2885. https://doi.org/10.1021/ic50212a006.
(62) Liu, X.; Cheng, J.; Sprik, M.; Lu, X. Solution Structures and Acidity Constants of Molybdic Acid. *J. Phys. Chem. Lett*. **2013**, 4 (17), 2926–230. https://doi.org/10.1021/jz401444m.
(63) Clarke, N. J.; Laurie, S. H.; Blandamer, M. J.; Burgess, J.; Hakin, A. Kinetics of the Formation and Hydrolysis Reactions of Some Thiomolybdate (VI) Anions in Aqueous Solution. *Inorganica Chim. Acta* **1987**, 130 (1), 79–83. https://doi.org/10.1016/S0020-1693(00)85933-2.
(64) Gaussian 09, Revision A. 02, Frisch, M. J.; Trucks, G. W.; Schlegel, H. B.; Scuseria, G. E.; Robb, M. A.; Cheeseman, J. R.; Scalmani, G.; Barone, V.; Mennucci, B.; Petersson, G. A.; Nakatsuji, H.; Caricato, M.; Li, X.; Hratchian, H. P.; Izmaylov, A. F.; Bloino, J.; Zheng, G.; Sonnenberg, J. L.; Hada, M.; Ehara, M.; Toyota, K.; Fukuda, R.; Hasegawa, J.; Ishida, M.; Nakajima, T.; Honda, Y.; Kitao, O.; Nakai, H.; Vreven, T.; Montgomery, J. A., Jr.; Peralta, J. E.; Ogliaro, F.; Bearpark, M.; Heyd, J. J.; Brothers, E.; Kudin, K. N.; Staroverov, V. N.; Kobayashi, -S11- R.; Normand, J.; Raghavachari, K.; Rendell, A.; Burant, J. C.; Iyengar, S. S.; Tomasi, J.; Cossi, M.; Rega, N.; Millam, J. M.; Klene, M.; Knox, J. E.; Cross, J. B.; Bakken, V.; Adamo, C.; Jaramillo, J.; Gomperts, R.; Stratmann, R. E.; Yazyev, O.; Austin, A. J.; Cammi, R.; Pomelli, C.; Ochterski, J. W.; Martin, R. L.; Morokuma, K.; Zakrzewski, V. G.; Voth, G. A.; Salvador, P.; Dannenberg, J. J.; Dapprich, S.; Daniels, A. D.; Farkas, Ö.; Foresman, J. B.; Ortiz, J. V.; Cioslowski, J.; Fox, D. J. Gaussian, Inc., Wallingford CT, 2009.
(65) (a) Becke, A. D. Density-Functional Thermochemistry. III. The Role of Exact Exchange. J. Chem. Phys. 1993, 98, 5648-5652. (b) Lee, C. T.; Yang, W. T.; Parr, R. G. Development of the Colle-Salvetti Correlation-Energy Formula into a Functional of the Electron Density Phys. Rev. B 1988, 37, 785-789.
(66) John P. Perdew, Matthias Ernzerhof, Kieron Burke; Rationale for mixing exact exchange with density functional approximations. *J. Chem. Phys.* 8 December 1996; 105 (22): 9982–9985. https://doi.org/10.1063/1.472933
(67) Head-Gordon, M.l; Pople, J.A.; Frisch, M.J. "MP2 energy evaluation by direct methods". Chemical Physics Letters. 153 (6). 1988. 503-506, https://doi.org/10.1016/0009-2614(88)85250-3.
(68) Ochterski, J.W. "Thermochemistry in Gaussian." Gaussian. 2000. https://gaussian.com/thermo/
(69) (a) P. J. Hay and W. R. Wadt, J. Chem. Phys. 82, 270 (1985). (b) P. J. Hay and W. R. Wadt, J. Chem. Phys. 82, 284 (1985). © P. J. Hay and W. R. Wadt, J. Chem. Phys. 82, 299 (1985).20.) A.D. McLean and G.S. Chandler J. Chem. Phys. 72, 5639, (1980).
(70) F. Weigend and R. Ahlrichs, Phys. Chem. Chem. Phys., Balanced basis sets of split valence, triple zeta valence and quadruple zeta valence quality for H to Rn: Design and assessment of accuracy 7, 3297 (2005).
(71) Mennucci, B. WIREs Comput Mol Sci. 2. 2012. 386–404 doi: 10.1002/wcms.1086
(72) Cox, J.D.; Wagman, D.D.; Medvedev, V.A., CODATA Key Values for Thermodynamics, Hemisphere Publishing Corp., New York, 1984, 1.

(73) Chase, M.W., Jr., NIST-JANAF Thermochemical Tables, Fourth Edition, J. Phys. Chem. Ref. Data, Monograph 9, 1998, 1-1951.
(74) Active Thermochemical TablesV1.124. Argonne National Laboratory, US Department of Energy, Office of Science, Office of Basic Energy Science, Division of Chemical Sciences, Geosciences and Biosciences https://atct.anl.gov/Thermochemical%20Data/version%201.124/index.php Accessed: 29 July 2023.
(75) Tomasi, J.; Mennucci, B.; Cammi, R. "Quantum Mechanical Continuum Solvation Models." *Chem. Rev.* **2005**. 105(8): 2999-3094.
(76) Chang, A.S.; Pintauer, T.; Basu, P.; Eckenhoff, W.T. "Structural and Electronic Investigation of Tetrachalcogenidomolybdate Dianions" *Chemistry Select* **2018**, 3, 5808. 10.1002/slct.201800506
(77) Huang, M.; DeKock, C. W. Triphenylsiloxy complexes. A Novel Compound Containing a Mo(VI)-P Bond: $MoO_2(OSiPh_3)_2(PPh_3)$. *Ino*rg. *Chem.* **1993**, 33, 2287-2291
(78) C. W. Scheele. Sumtliche Physische und Chemische Werke, Vol. I1 (Ed.: D. S. F. Hermbsthdt), 1793, reprint: Martin Siindig oHG, Niederwalluf/Wiesbaden, 1971, pp. 185-200
(79) J. J. Berzelius, PoggendorffS Ann. Phys Chem. 1826, 6, 385
(80) Quagraine, E. K. Competitive Interactions Between Copper(II) Ions, Thiomolybdates, and Some Biological Ligands. University of Saskatchewan, **2002**.
(81) Rittner, W.; Muller, A.; Neumann, A.; Bather, W.; Sharma, R. "Generation of the *triangulo*-Group Mo^{V}-η-S_2 in the "Condensation" of $[Mo^{VI}O_2S_2]^{2-}$ to $[Mo_2{}^{V}O_2S_2(S_2)_2]^{2-}$" *Angew. Chem. Int. Ed. Engl.* **1979**. 18(7). 530-531. https://doi.org/10.1002/anie.197905301
(82) Coucouvanis, D.; Toupadakis, A.; Koo, S.; Hadjikyriacou, A.; "An Inorganic Functional Group Approach to the Systematic Synthesis and Reactivity Studies of Binuclear Mo/S and Mo/S/O Complexes." *Polyhedron.* **1989.** 8(13/14). 1705-1716. https://doi.org/10.1016/S0277-5387(00)80621-X
(83) Coucouvanis, D.; "Synthesis, Structures, and Reactions of Binary and Tertiary Thiomolybdate Complexes Containing the (O)Mo(S_x) and (S)Mo(S_x) functional groups (S=1,2,4). *Advances in Inorganic Chemistry.* **1998.** Academic Press
(84) Müller, A.; Rittner,W.; Neumann, A.; Sharma, R.C. "Reaktionen von koordinierten S^{2-}Liganden I: Neuartige Redoxkondensationsreaktionen von $MoO_2S_2^{2-}$ in H_2O und tur Darstellung des bis-disulfido-Komplexes $[Mo_2O_2S_2(S_2)_2]^{2-}$. *Z. anorg. Allg. Chem.* **1981.** 470. 35-38. https://doi.org/10.1002/zaac.1980470010.
(85) Bertolini, S.; Jacob, T. "Elucidating active sites and decomposition mechanisms for oxythiomolybdate clusters (Mo2O2Sx, x = 6;8) as catalyzers for hydrogen evolution reactions." *Electrochem. Sci. Adv.* **2022**. 1-13 https://doi.org/10.1002/elsa.202100088.
(86) Baloglou, A.; Pritzi, M.; Pascher, T.F.; Hartmann, J.C.; Grutza, M.; Občák, M.; Kurz, P.; Meyer, M. "Proton transfer reactivity of molybdenum oxysulfide dianions $[Mo_2O_2S_6]^{2-}$ and $[Mo_2O_2S_5]^{2-}$ The role of Coulomb barriers." *Int. J. Mass. Spectrom.* **2021**. 464. 116558. https://doi.org/10.1016/j.ijms.2021.116558.

Schmidt, J.R.; Polik, W.F. WebMO Enterprise, version .0; WebMO LLC: Holland, MI, USA, 20; http://www.webmo.net (accessed March 20)

Chapter 3: The Structure and Reactivity of Three-Coordinate Copper(I) Complexes Bearing tri-*tert*-butylphosphine and Aromatic Diimine Ligands

Introduction:

Copper has been utilized from the very beginning of civilization as the earliest tools and ornaments and in the first alloys, such as bronze.[1,2] This is partly due to its occurrence in nature in its native metallic form as well as its various salts where it is found in the +1 or +2 oxidation state from which it can easily be reduced to the workable metal. As the lightest member of the group 11 transition metals above its cousin's silver and gold, copper exhibits desirable properties including good thermal and electrical conductivity in its elemental state.[3]

The most commonly occurring ionized forms of copper are Cu(I) and Cu(II), which form an easily accessible redox pair. There also exists a limited, but growing, number of isolated Cu(III) compounds. Though this higher oxidation state is most commonly invoked in the mechanisms of many copper catalyzed processes including the reductive elimination from Cu-centers to from C-C and C-heteroatom bonds in reactions like the Ullmann coupling.[4,5,6] Copper's three common oxidation states (0,1+,2+) are closely spaced with Cu^{+}/Cu^{0} redox pair having a standard reduction potential in aqueous solution of 0.52 V and the Cu^{2+}/Cu^{1+} redox pair having a standard reduction potential of 0.159 V under the same conditions. [7] This relatively small spacing provides copper with a rich redox chemistry.

As its two common ions, that is Cu^{1+} and Cu^{2+}, a large number of applications have been developed which include, but are not limited to, industrially important homogenous and heterogeneous catalysts for water oxidation and other processes, as well as important applications in C-C and C-heteroatom bond formation reactions and polymerizations.[8-12] Copper also has applications at the center of organometallic complexes that can act as photosensitizers and light emitting materials, medicines such as chemotherapy, and stoichiometric reagents for organic

transformations such as the click reaction.[13-18] In many of its potential and current applications copper can replace heavier, more expensive, and less environmentally benign metals like Ru, Re, Ir, or Pt.[19]

Copper is considered less hazardous than other metals in part because it has been adopted across prokaryotic and eukaryotic life to such a wide extent that it is considered an essential trace nutrient.[20] While copper deficiency is detrimental to cellular function, excess copper in the cell, caused by the failure of copper transport proteins or environmental excess, can also lead to significant diseases such as Wilson's disease for which one treatment is tetrathiomolybdate.[20,21] Furthermore, life has evolved several classes of enzymes specifically for the biological sequestration and transport of copper ions.[21] This versatile element also occupies the metallated active sites of proteins that perform actions such as defending the organism from pathogens, scavenging reactive oxygen species, transfer electrons, reducing molecular oxygen, and catalyzing the oxidation of substrates. Notably nearly all reactions catalyzed by copper are dependent on dioxygen as either substrate or electron acceptor.[21,22] Based on its many applications, low toxicity, relative abundance, and ease of processing, copper has been coined the "new green metal" for the role it will play in the economic and industrial transformation in response to climate change from the combustion of fossil fuels.[23]

Taking lessons from relevant natural systems provides an informative study of the structure-function relationships that give rise to the reactivity and other properties of Cu centered systems, such as its redox activity and ligand preferences. While most copper-based proteins are redox active electron transfer proteins or oxidoreductases, the copper atoms at the center of this reactivity are only found as Cu(I) or Cu(II) and are often permanently bound to the protein.[21] These active sites tend to undergo little conformational change throughout the catalytic cycle despite the

change in oxidation state, perhaps due to the distorted binding geometry and mixed ligating systems sometimes employed. Such coordination sites also serve to tune the reduction potential of the active metal site. This occurs by destabilizing the metal d-orbitals by bending them out of a preferred conformation to predispose the metal center to redox activity. Conversely by providing a strong and stable first coordination sphere, a copper center can be stabilized against redox events. This tunability leads to redox potentials for the metals in copper active that range from nearly 0.2 V to nearly 0.8V.[22]

As such, the nuclearity and coordination environments of copper containing enzymes vary widely and are broadly categorized into three categories type I, type II, and type III, with most copper active sites falling into one of these categories. Type I copper enzymes are generally coordinated in histidine, cysteine, histidine, and methionine ligand environment in a distorted trigonal bipyramidal or tetrahedral geometry. Type I copper proteins are characterized by intense absorption of visible light in the 600 nm range which is due to a ligand-to-metal charge transfer from the cysteine residues that coordinate the metal center. This first category of copper proteins also has a wide range of redox potentials that are high in comparison to the Cu(II)/Cu(I) redox couple in water with a range of 0.183V-0.68V; this serves the function of these sites which are often found electron transfer chains. The intense spectral features of the type I copper proteins are contrasted by the type II active sites which are essentially colorless. This second category of copper proteins are involved in the activation of dioxygen with Cu(II) and are found in a more diverse ligand environment that most commonly includes histidine, modified tyrosine, methionine, and cysteine in a square planar or tetrahedral geometry. The common structural feature that all type II proteins share is an empty coordination site for the binding of molecular oxygen. The remaining copper category is type III, which features a pair of anti-ferromagnetically coupled Cu(II) that

reside in a trigonal planar geometry coordinated exclusively by histidine residues, these proteins have a role in the transport of molecular oxygen. Other, higher nuclearity, copper proteins that aren't easily categorized into the above three types exist including trinuclear copper sites, the dinuclear Cu_A site, the heterodinuclear heme containing Cu_B site, and the tetranuclear Cu_Z.[21]

Aside from redox tuning, these variations in coordination have large impacts on the reactivity of the metal center. One notable feature of the above Cu categories is that enzymes responsible for copper sequestration or electron transfer have saturated first coordination spheres around the metal center, while the enzymes whose copper atoms require the activation of molecular oxygen or the direct binding of a substrate are bound in a coordination geometry that leaves a vacant or labile site.[21] Type 2 copper centers provide a good example these active sites are square pyramidal with an empty octahedral site, whereas type 3 copper sites contain a pair of trigonal planar copper sites that share a vacant binding site and are bound to the imidazole rings of three histidine residues for stability.[21]

MoCu-CODH, discussed in Chapter 1, is one of the few redox inactive copper containing enzymes, however the function of the copper center is complex despite its redox inactivity. The electron delocalization that has been observed across the bridging sulfido in MoCu-CODH requires a Cu(I) that is in either a linear or pseudo C_{3v} arrangement.[24] A low-coordinate geometry is also required for the bonding of the substrate to the copper center, as seen with other copper enzymes.[21] It is thought that the binding of CO to Cu in MoCu-CODH is only for the purpose of positioning and polarizing the carbon monoxide to be susceptible to nucleophilic attack by the equatorial molybdenum oxo-ligand.[25] This role is somewhat simplified in the frustrated Lewis pair description of the enzyme in which the Cu center only needs to be one part of an unquenched Lewis acid/base pair.[26] In both cases the polarization of the carbon monoxide resembles a metal-

ligand charge transfer state (MLCT), in which electron density has been transferred from a metal d- orbital to the carbon monoxide π* orbital, weaking the bond and placing a positive charge on the carbon monoxide carbon atom.[27]

Simple lessons as to what type of ligands bind strongly to copper and what coordination geometry promotes different kinds of reactivity have been gleaned from the study of copper proteins.[28] In synthetic systems stable monovalent copper complexes can be found as two-, three-, or four-coordinate varieties with linear, trigonal planar, and tetrahedral coordination environments, respectively, with tetrahedral being the most common coordination geometry. The tetrahedral geometry characterizes sterically saturated Cu(I), while Cu(II) can also adopt a five- or six-coordinate geometry. The properties of the resultant complexes vary significantly between the different coordination modes due to the arrangement, hybridization, and relative energy levels of the metal d-orbitals. Enzyme structures and hard-soft acid base theory show that Cu(I) prefers softer ligands than Cu(II) and that steric unsaturation and distorted coordination geometries can promote reactivity.[21,28] Thus, for a synthetic metal complex to carry out catalysis, either the complex must be isolable in a coordinatively unsaturated form without undue steric crowding or one of the four coordination sites must contain a moiety that is sufficiently labile to be replaced by an incoming substrate.

Biological coordination environments point to ligands like 2,2'-bipyridine or 1,10-phenanthroline which have histidine-like aromatic imine coordination sites that are linked with different degrees of flexibility and thus can take advantage of the chelation effect. These systems also call the enzyme coordination environment to mind in another manner: when the ligand environment does not interfere with the Cu d-orbital rearrangement upon reduction or oxidation these complexes are profoundly easier to reduce than when steric bulk prevents such

rearrangement. This is the synthetic analog to the tuning of redox potential in enzymatic active sites.[29]

It was noticed early on that homoleptic or heteroleptic systems containing either the bipyridine or 1,10-phenanthroline chromophore possess metal-to-ligand charge transfer (MLCT) bands in their electronic excitation spectra. These MLCT bands lead to these complexes being brightly colored and exhibiting photo-induced redox chemistry and luminescent properties. The earliest report available of Cu(I)-phenanthroline possessing MLCT transitions was by Day and Sanders in 1967, it was quickly adopted as a field of interest.[30,31]

Metal-to-Ligand Charge Transfer:

The metal-to-ligand charge transfer excitation has undergone significant investigation across a variety of ligand metal pairs. This has led to the elucidation of the mechanisms and characteristics of complexes that exhibit this phenomenon across a spectrum that contains luminescence and phosphorescence versus photosensitization and photocatalytic activity as competing phenomena.[32,33] This investigation for copper complexes in particular spans nearly 50 years from the Day and Sanders report and is still a very active field. To design a system that is optimized for one of these tasks, or if the desire is to avoid either of these competing chemistries, it is vital to understand the nature of the metal-to ligand charge transfer excitation.

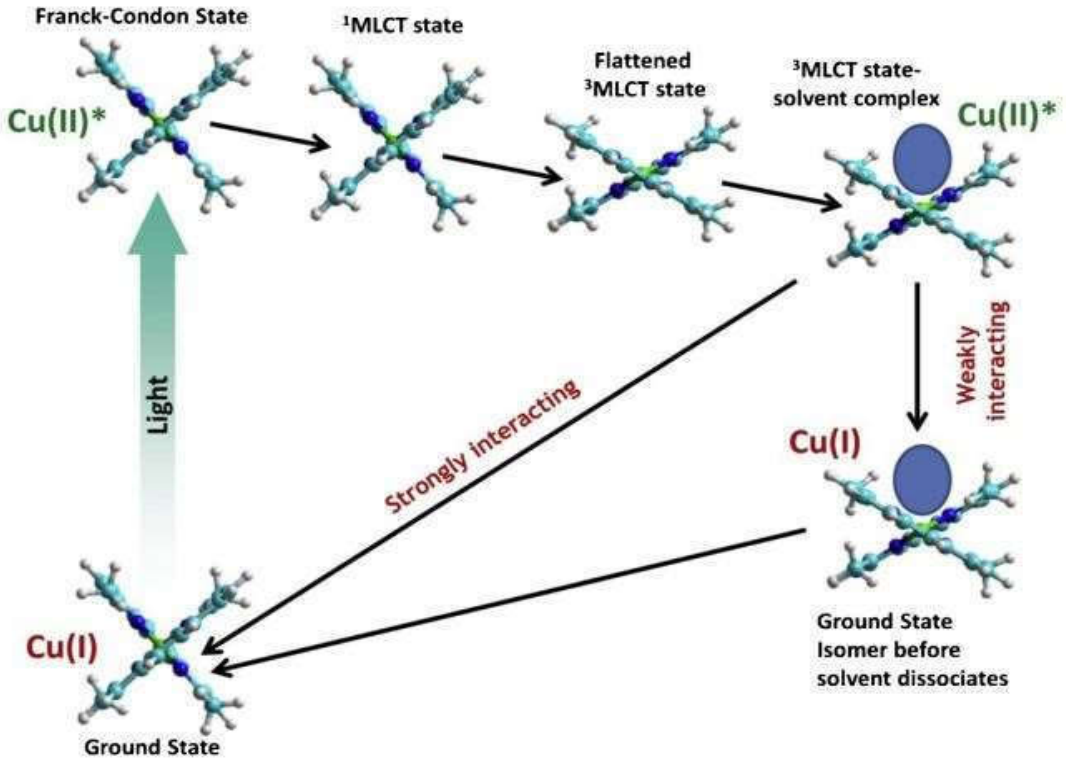

Figure 41: The dynamics of the MLCT excited state. Reprinted with permission from Mara, M.W. Fransted, K.A.; Chen, L. "Interplays of the Excited State dynamics in copper(I) diimine complexes: Implications and perspectives" Coord. Chem. Rev. ***282-283****.* (2015) 2-18. Copywrite 2015 Elsevier

The dynamics of photoexcitation of a Cu(I) bi(diimine) complex are illustrated above in **Figure 41**. Upon initial excitation of a homoleptic Cu(I) bis(diimine), an electron from a frontier orbital that is composed primarily of metal d orbital character is promoted into a low-lying unoccupied orbital that is generally of ligand π* character. This excitation results in the virtual oxidation of the metal by one electron, from Cu(I) to Cu(II), and the production of an excited-state ligand-based radical. This initial state is termed the Franck-Condon (FC) state, this state is characterized by the above described virtual one electron redox process which, while it can be accompanied by the weakening or strengthening of some bonding interactions depending on the origin of the promoted electron and its destination orbital. The FC state exists on a time scale that

places it before the change in atomic coordinates in response to the changes in its electronic characteristics. [32,33,34]

Sometimes this is where this story ends, through simple relaxation mechanisms such the quenching of the excited state by emission and the concomitant re-reduction of the metal or through charge transfer to an outside acceptor, often the solvent, which makes causes the reduction of the metal center. However, if the ligand based radical is sufficiently long lived (>10 fs) then the virtually oxidized Cu(II)* undergoes Jahn-Teller distortions to reach the minimum energy electron configuration for its newly oxidized orbitals, this manifests as changes in the coordination geometry of the ligands.[35] For the Cu(I) case, the virtual oxidation to Cu(II) changes the preferred coordination geometry from tetrahedral to square planar, which produces a flattening of the complex, that is the dihedral angle formed between the diimine ligand the other ligands moves away from the idealized 90° angle.[36] This geometry change opens a new apical coordination site for the solvent or some other external electron acceptor to quench the excited state externally. This path results in the nonradiative decay of the excited state and the oxidation of the metal center.

If the aim is to optimize a system for fluorescence, then ligand engineering that discourages such a rearrangement in four-coordinate systems can generate long-lived excited states and thus promote longer emissive lifetimes Examples of such ligand engineering includes the elaboration of the phenanthroline at carbons number two and nine of the ring system, or the six and six prime positions of bipyridine. Substituents in these positions project steric bulk near the metal center and hinder flattening. The result of such steric hinderance to rearrangement, and the extended excited lifetime caused by it, is the rise of triplet excited states from intersystem crossing, which results in phosphorescence from the slower relaxation of such states. Such sterically bulky diimine ligands are found in both homoleptic and heteroleptic systems.[37,38] When found in heteroleptic systems

they are often paired with xantphos, or POP, ligands due to their projection of steric bulk that complements that of the elaborated diimine and their inflexibility.[39]

The opposite ligand environment can also be engineered. While the simple exclusion of prohibitive steric bulk on the diimine is sufficient to tilt the energetic landscape away from luminescence and toward more reactive excitation behaviors, other coordination environments have been explored.[29] Such coordination environments promote d-orbital rearrangement upon excitation through ligand flexibility or coordinative unsaturation of the metal in which a vacant coordination site is built into a three-coordinate system or one is opened upon photoinduced ligand loss. An example of this is a heteroleptic system that contains a labile fourth ligand, such as solvent, or, alternatively, a three-coordinate system which is stabilized in the ground state by a sterically demanding third ligand. Complexes with such coordination spheres have many examples that include ligands such as bis- and tris(pyrazolyl)borates, NHC's, dipyridylamine, phosphaalkenes, and halides amongst others.[40-44] Such a ligand environment can lead to photosensitizing or

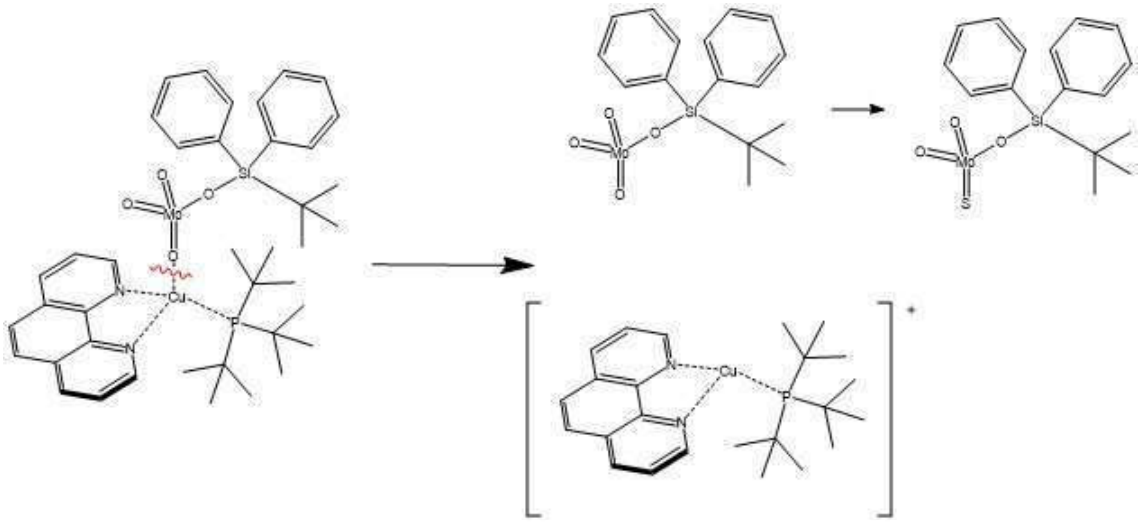

Figure 42: Retrosynthetic analysis of the Donahue unpublished result.

photocatalytic redox behavior from their complexes though the success of this aim competes with luminescent and phosphorescent behaviors.[32,33,34]

In this study, the copper scaffold arrived at by the retrosynthetic analysis of the unpublished Donahue MoCu-CODH analogue in Chapter 1 and reproduced above in **Figure 42**, contains an aromatic diimine that does not project any steric bulk toward the metal center and a very sterically bulky phosphine. This fits well with the structural motif of these photoactive complexes discussed above. While this specific complex has not been reported many similar to it are known which employ different sterically bulky phosphenes.[45,46,47]

Synthesis:

$Cu(MeCN)_4PF_6$ or $Cu(MeCN)_4BF_4$ were synthesized by published methods and recrystallized twice from acetonitrile and diethyl ether prior to use.[48,49] $[Et_4N]N_3$, $[Et_4N]CN$, and $[Et_4N]SCN$ were synthesized by salt metathesis between their sodium or potassium salt and $[Et_4N]_{Cl}$. Acetonitrile was dried over 3 Å molecular sieves followed by distillation from calcium hydride, methanol was dried over 3 Å molecular sieves followed by distillation from magnesium methoxide. Other solvents including THF, diethyl ether, pentane, hexane, and dichloromethane were dried on a glass contour solvent system. All other reagents were purchased commercially and used without further purification. Experiments were carried out under a nitrogen atmosphere using standard Schlenk line technique. NMR spectra were collected on a Bruker 300 MHz spectrometer, UV-Vis was collected on an Agilent Cary 60 UV-Vis, IR was collected on Thermoscientific Nicolet iS10. Single crystal X-ray diffraction data were collected using either a Bruker Smart APEX II CCD diffractometer equipped with a Mo fine-focus sealed tube providing radiation at λ = 0.71073 nm or a Bruker D8 Venture fitted with a Photon 100 detector and operating with Cu Kα radiation at λ = 1.54178 nm. Computational chemistry was performed on the Tulane Cypress computing core or through WebMO. Computational details are available in the appendix.

[Cu(MeCN)(^{t}Bu$_3$P)(3,4,7,8-tetramethyl-1,10-phenanthroline)]PF_6-Compound 1

To a solution of 0.100g (0.2 mmol) of $[Cu(MeCN)]_4PF_6$ in 10 mL of dry acetonitrile was added 0.80 mL of tri-*tert*-butylphosphine (10% in hexanes) which has been diluted with 2 mL of THF. The solution is allowed to stir for 30 minutes. The reaction was then brought to dryness *in vacuo* before being redissolved in 10 mL of dry acetonitrile. To this solution, 0.061 g of 3,4,7,8-tetramethyl-1,10-phenantholine is directly added. The solution immediately takes on a lemon-yellow color and is allowed to stir for 1 h. The solvent volume was reduced *in vacuo* until precipitation began. The product is then precipitated with 50 mL of cold diethyl ether, separated by cannula filtration, and washed with 30 mL each of cold diethyl ether and pentane before being dried *in vacuo*. X-ray quality crystals were grown by the vapor diffusion of diethyl ether in an acetonitrile solution of the product Yield: 0.200g (93%) of $[Cu(MeCN)(^tBu_3P)(Me_4phen)]PF_6$. The powder is air stable for a period of months under inert atmosphere. ^1H NMR: (δ, CD_3CN): 1.39 ppm (d, J = 12.0, 27 H), 2.22 ppm (s, 2H), 2.55 ppm (s, 6H), 2.68 ppm (s, 6H), 8.14 ppm (s, 2H), 8.85 ppm (s, 2H). ^{31}P NMR (δ, CD_3CN vs H_3PO_4): 63.00 ppm. UV-vis [MeCN, λ_{max}, nm (ε in $M^{-1}\cdot cm\text{-}1$)]: 204 (58100), 253 (40400), 273 (37200), 329 (sh, ~5640), 363 (3780).

[Cu(MeCN)(^{t}Bu$_3$P)(4,4'-dimethyl-2,2'-bipyridine)]PF$_6$-Compound 2

This product is prepared in the same manner as compound 1, with substitution of 4,4'-dimethyl-2,2'-bipyridine for 3,4,7,8-tetramethyl-1,10-phenanthroline. Yield: 0.165g (85%) ^1H NMR (δ, CD_3CN): 1.39 ppm (d, J=12.1 Hz, 27H); 2.52 ppm (s, 6H); 7.49 ppm (s, 2H); 8.24 ppm (s, 2H); 8.69 ppm (s, 2H). ^{31}P NMR (δ, CD_3CN vs H_3PO_4): 59.62 ppm. UV-vis [MeCN, λ_{max}, nm (ε in $M^{-1}\cdot cm\text{-}1$)]: 205 (29700), 225 (sh, ~12400), 250 (sh, ~11000), 290 (8200), 303 (sh, 6300), 358 (1380)

[Cu(MeCN)(^{i}Pr$_3$P)(3,4,7,8-tetramethylphenanthroline)]PF$_6$-Compound 3

This product is prepared in the same manner as compound 1, with the substitution of tri-propylphosphine in place of tri-*tert*-butylphosphine. This complex shows are significant reduction in benchtop stability and oxidizes in the air over a period of several hours. Yield: 0.139g (70%) ^{1}H NMR (δ, CD_3CN): 1.38 ppm (dd J=15.0, 7.3; 21H); 2.31 (m, 3H); 2.63 (s, 6H); 2.82 (s, 6H); 8.25 (s, 2H); 8.75 (s, 2H).

[Cu(MeCN)(^{i}Pr$_3$P)(4,4'-dimethyl-2,2'-bipyridine)]PF_6-Compound 4-

This product is prepared in the same manner as compound 1, with substitution of 4,4'-dimethyl-2,2'-bipyridine for 3,4,7,8-tetramethyl-1,10-phenanthroline and the substitution of tri-isopropylphosphine in place of tri-tert-butylphosphine. Yield: 0.114 g(70%)

[Cu(R$_3$P)(NN)]PF_6-

Compounds **1-4** can be converted into the corresponding three-coordinate complex through the loss of the coordinating acetonitrile by solvation in minimal dry dichloromethane followed by precipitation with excess dry pentane and separation by filtration. This process is repeated three times resulting in a red solid. This ligand loss is reversible, and the yield is quantitative.

[Cu(Me$_4$phen)(^{t}Bu$_3$P)]PF_6-Compound 1a-

^{1}H NMR (δ, CD_2Cl_2): 1.6 ppm (d J=12.8 Hz, 27H); 2.64 ppm (2, 6H); 2.83 ppm)(s, 6H); 8.27 ppm (s, 2H); 8.80 ppm (s, 2H). ^{31}P NMR (δ, CD_2Cl_2 vs PF_6^{1-}): 69.23 ppm. UV-vis [CH_2Cl_2, λ_{max}, nm (ε in $M^{-1}\cdot$cm-1)]: 205 (58000), 234 (34000), 279 (38000), 305 (sh, 13200), 332 (sh, 3700), 438 (1300).

[Cu(Me$_2$bpy)(^{t}Bu$_3$P)]PF_6-Compound2a-

^{1}H NMR (δ, CD_2Cl_2): 1.54 ppm (d, J=12.8 Hz, 27H); 2.60 ppm (s, 6H); 7.50 ppm (d, J=5.4 Hz, 2H); 8.21 (s, 2H); 8.60 (d, J=5.4 Hz, 2H). UV-vis [CH_2Cl_2, λ_{max}, nm (ε in $M^{-1}\cdot cm\text{-}1$)]: 205 (31700), 225 (sh, ~12500), 250 (12700), 292 (9100), 302 (sh, 7900), 358 (1500).

[Cu(X)(R_3P)(NN)] (X=Cl^-, Br^-, I^-, CN^-, SCN^-, $SeCN^-$, N_3^-)

The three-coordinate complexes are able to bind a variety of X type ligands by reaction with the appropriate (R_4N)X salts in CH_2Cl_2 or methanol. These complexes can also be made in a manner analogous to that of complex 1, with the substitution of the appropriate Cu(I)X salt for [Cu(MeCN)$_4$]PF_6. The first method works best for thiocyanate, selenocyanate, azide, and chloride salts. While the second method is preferred for the formation of the bromide and iodide salts perhaps due to steric bulk. The azide bound complex has only been isolated as the μ-$\eta^{1,3}$-azide dimer.

[Cu(Me$_4$phen)(^{t}Bu$_3$P)]CN-Compound 5-

^{1}H NMR (δ, CD_2Cl_2): 1.41ppm (d, J=11.8Hz, 27H), 2.51ppm (s, 6H), 2.65ppm (s, 6H), 8.05ppm (s, 2H), 8.87 ppm (s, 2H). ^{31}P (300MHz CD_2Cl_2 vs H_3PO_4): 65.97 ppm. UV-vis [CH_2Cl_2, λ_{max}, nm (ε in $M^{-1}\cdot cm\text{-}1$)]: 207 (15180), 237 (sh, 10750), 275 (9700), 330 (sh, 1250), 363 (825).

[Cu(Me$_2$bpy)(^{t}Bu$_3$P)]CN-Compound 6-

^{1}H NMR (δ, CD_2Cl_2): 1.32 ppm (d =11.5 Hz, 27H), 2.43 (s, 6H), 7.19 (s, 2H), 8.17 (s, 2H), 8.58 (s, 2H). ^{31}P (300 MHz, CD_2Cl_2 vs H_3PO_4): 65.48 Hz. UV-vis [Ch_2Cl_2, λ_{max}, nm (ε in $M^{-1}\cdot cm\text{-}1$)]: 219 (sh, 14000), 250 (sh, 5600), 289 (4000), 330 (sh, 1250), 358 (600).

[Cu(Me$_4$phen)(^{t}Bu$_3$P)]Cl-Compound 1Cl-

^{1}H NMR (δ, CD_2Cl_2): 1.62ppm (d J=12.7 Hz) 27H; 2.66 ppm (s, 6H); 2.84 ppm (s,6H); 8.29ppm (s, 2H); 8.83 ppm (s, 2H). ^{31}P (300 MHz, CD_2Cl_2 vs H_3PO_4): 72.15 ppm. UV-vis [CH_2Cl_2, λ_{max}, nm (ε in M^{-1}·cm-1)]: 203 (150000), 246 (sh, 43000), 274 (42000), 328 (sh, ~7600), 341(sh, ~7000), 419 (5600)

[Cu(Me$_4$phen)(^{t}Bu$_3$P)]Br-Compound 1Br-

^{1}H NMR (δ, CD_2Cl_2): 1.56 27H (d J=12.6), 2.51 (s, 6H), 2.67 (s, 6H), 8.09 (s, 2H), 8.88 (s 2H). ^{31}P (300 MHz, CD_2Cl_2 vs H_3PO_4): 69.23 Hz UV-vis [CH_2Cl_2, λ_{max}, nm (ε in M^{-1}·cm-1)]: 207 (34600), 238 (26800), 274 (22000), 326 (sh, 3400), 368 (1900).

[Cu(Me$_4$phen)(^{t}Bu$_3$P)]I-Compound 1I-

^{1}H NMR (δ, CD_2Cl_2): 1.59 ppm (d, J=12.8 Hz, 27H); 2.62ppm (s,6H); 2.81 ppm (s,6H); 8.26 ppm (s 2H); 8.78 ppm (s, 2H). ^{31}P (300 MHz, CD_2Cl_2 vs H_3PO_4): 72.33 ppm UV-vis [CH_2Cl_2, λ_{max}, nm (ε in M^{-1}·cm-1)]: 207 (51000), 242 (sh, ~15600), 275 (12900), 326 (sh, ~2400), 341 (sh, 2100), 400 (1800)

[Cu(Me$_2$bpy)(^{t}Bu$_3$P)]Br-Compound 2Br-

^{1}H NMR (δ, CD_2Cl_2): 1.43 ppm 27H (d, J=12.2 Hz), 2.48 ppm 6H, 7.31 ppm 2H, 8.01 ppm 2H, 8.73 ppm 2H. ^{31}P NMR (300Mhz, CD_2Cl_2 vs H_3PO_4) 60.05 ppm UV-vis [CH_2Cl_2, λ_{max}, nm (ε in M^{-1}·cm-1)]: 204 (18700), 227 (sh, ~7400), 241 (sh, 6600). (sh, 5800), 281 (5500), 364 (380)

[Cu(Me$_4$phen)(^{t}Bu$_3$P)NCS]-Compound 7-

^{1}H NMR (δ, CD_2Cl_2): 1.37ppm (d, J=12.3 Hz, 27H), 2.51ppm 6H, 2.65ppm 6H, 8.05ppm 2H, 8.87 ppm 2H. ^{31}P (300MHz CD_2Cl_2 vs PF_6^-) 59.88 ppm UV-vis [CH_2Cl_2, λ_{max}, nm (ε in M^{-1}·cm-1)]: 208 (9200), 236 (7900), 273 (7300), 300 (sh, 2300), 362 (600).

[[Cu(Me$_4$phen)(^{t}Bu3P)]$_2$N$_3$]BF$_4$-Compound 8-

^{1}H NMR (δ, CD_2Cl_2): 1.48ppm (d, J=12.2Hz, 54H), 2.51ppm (s, 6H), 2.65ppm (s, 6H), 8.05ppm (s, 2H), 8.87 ppm (s, 2H). ^{31}P (300MHz CD_2Cl_2 vs H_3PO_4): 66.20 ppm UV-vis [CH_2Cl_2, λ_{max}, nm (ε in M^{-1}·cm-1)]: 210 (26900), 236 (20200), 275, (16400), 330 (sh, 2700), 370 (sh, 1500)

[Cu(L)(R$_3$P)(NN)]PF$_6$ (L=thiourea, dimethylsulfide, thiophene)

The three-coordinate copper complex can bind a variety of L-type sulfur donating ligands through the solvation of the three-coordinate complexes in a concentrated solution containing excess of the desired ligand, followed by crystallization by layered diffusion with pentane or diethyl ether.

[Cu(Me$_2$bpy)(^{t}Bu$_3$P)(thiourea)]BF$_4$-Compound 9-

^{1}H NMR (δ, CD_2Cl_2): 1.34 ppm (d, J=12.0 Hz, 27H); 2.54 ppm, (s, 6H); 5.61 ppm (Broad s, 2H); 6.46 ppm (Broad s, 2H); 7.41ppm (d, J=5.3Hz 2H); 8.07 (s, 2H); 8.69 (d, J=5.3Hz, 2H). ^{31}P (300MHz CD_2Cl_2 vs PF_6^-): 60.05 ppm.

[Cu(Me$_4$phen)(^{t}Bu$_3$P)(tetrahydrothiophene)]-Compound 10-

Discussion:

With the retrosynthetic analysis of the unpublished Donahue group MoCu-CODH analogue (**Figure 42,** above) in mind, a study of the reactivity of copper scaffold was undertaken

to evaluate the electronic and steric properties of the synthesized complex. As such, the bonding of the copper complex with a variety of hard and soft nucleophiles, as well as anionic and neutral sulfide donors was investigated. While the fluorescence of the above complexes were not investigated in this study, some of the reactivity observed, when considered in light of computational molecular orbital and excited state investigations by DFT, suggests that photoredox events may be occurring. The result of these redox events is oxidation of the copper center and a ligand-based reduction in some cases. These could complicate the study of the reactivity of these complexes depending on the orbital energy of the incoming fourth ligand as compared to the phenanthroline, or bipyridine ligand, and the phosphine. Aside from photo-induced redox events, the most common struggles of Cu(I) synthetic chemistry are the suppression of the tendency of Cu(I) systems to form cluster compounds through cuprophilic interactions, and the ability of Cu(I) to be chemically oxidized to Cu(II) by oxygen or other oxidizing agents.

The combination of an aromatic diimine and a bulky phosphine with a large cone angle is capable of producing a surprisingly stable, coordinatively unsaturated 16 e- Cu(I) center upon loss of the coordinating acetonitrile. Furthermore, this family of complexes is also resistant to cluster formation. It is thought that these desirable properties are imparted through both steric hindrance of the nucleophilic attack on the metal and the electronic stabilization of the copper d-electrons via push-pull interactions between the phosphine and the aromatic diimine ligands. Another factor affecting this stability is the reduction in energy of the metal d-electrons by orbital delocalization into the aromatic system and the phosphine bonding orbitals. This trend can be seen by varying both the basicity and steric bulk of the phosphine and by the difference in flexibility and the extent of the π network of the aromatic diimine. The system with the more Lewis basic phosphine and the more extended, less flexible aromatic diimine, that is $[Cu(Me_4phen)(^tBu_3P)]^+$, is significantly

more stable to oxidation in room air in both its 3-coorindate, trigonal planar, and 4-coordinate, tetrahedral configurations than its congener at the opposite end of the set, that is $[Cu(Me_2bpy)(^iPr_3P)]^+$. These same factors, of course, impact the reactivity of these complexes to both L-type and X-type nucleophiles, where it can be seen that the choice of aromatic diimine (Me_4phen vs Me_2bpy) has a more significant effect on the reactivity than does the steric bulk of the phosphine. This point is best illustrated by the thiourea complex $[Cu(R_3P)(Me_2bpy)(thiourea)]PF_6$, which forms readily with the Me_2bpy complex bearing both $^iPr_3P$ and $^tBu_3P$ but cannot be isolated with either phosphine when the copper center is bearing the Me_4phen ligand.

Computational investigation shows that this key reactivity difference between the two diimine ligand systems is due to partially to the flexibility of the bipyridine backbone, as an N-H of the thiourea ligand forms a hydrogen bond with one of the bipyridine imine nitrogen atoms and the planarity of the coordinating ligand is disrupted. Another example of the choice of diimine ligand impacting reactivity of the complex is the azide-bridged dicopper complex, $[[Cu(Me_4phen)(^tBu_3P)]_2N_3]BF_4$ which was isolable with the larger, more rigid phenanthroline ligand but rapidly decomposed when attempts were taken to synthesize it with the Me_2bpy ligand. The thiourea ligand also reveals the steric allowances of this system, as no tetramethylthiourea complex has been isolated with any of the synthesized systems despite repeated attempts. Other complexes that will form with both sets of ligands also show the superior flexibility of the Me_2bpy ligand over the Me_4phen ligand, as do computational structures that were used to examine the excited states and ligand bonding in these complexes. Based on these results, it is unsurprising that other complexes with bulky sulfur donor ligands have not been isolable, including triphenylphosphine sulfide, which instead forms an intractable oxidized product. The significant

delocalization of the Cu orbitals also results in this system's preference for very soft sulfur donors, such as tetrahydrothiophene and dimethylsulfide.

The binding of L-type ligands above stands in contrast to the type of X-type ligands that have been found to form adducts readily, especially chloride. Chloride is the second hardest halide below fluoride and seems to form preferentially over many of the other X-type complexes when more than one is present in solution. While all the halide complexes have been synthesized, the remaining X-type ligands for which complexes have been isolated all have some π-accepting behavior. This is contrasted by the lack of reaction with benzenethiolate or phenolate, which are a hard sulfur-donor and oxide-donor respectively, no reaction with either of these was observed. It is also worth noting that no bidentate ligands have been isolated bound to this complex though o-isopropylxanthate and thioacetate were attempted. This is likely due to steric considerations and the small number of examples of pentacoordinate of Cu(I) complexes.[50,51,52] This leaves open the question of which molybdate bound chalcogen ligand will form the lower energy adduct with the copper center in the target complex as it seems this Cu(I) center will prefer the softer sulfido-ligand over another available, comparatively harder oxo-ligand, Though it does seem that this scaffold will have sufficient steric bulk to resist the formation of the thermodynamically more stable O,S-bidentate molybdenum binding geometry.

Structural Analysis:

All of the complexes synthesized presented here present in the expected four coordinate Cu(I) geometry, which is tetrahedral. While the loss of the labile acetonitrile ligand leads to a trigonal planar configuration. The amount that the copper is pulled out of the triangular plane can give clues as to the electronic structure of the complex, the strength of the metal ligand bonding, and the balance of the competing ligand forces. The tetrahedron is measured as shown in **Figure 43** to the right, by drawing a plane through the diimine ligand nitrogen atoms and the phosphorous atom of the phosphine ligand. A centroid is placed on top of the intersection of a set of lines, one drawn from each vertex which bisect the side opposite that vertex. The distance from the copper atom to the centroid and the orthogonal distance from the copper atom to the plane that makes the base of the tetrahedron are then measured as well as the angle from the first atom of L to the centroid with the copper at the vertex of this angle. These measurements provide both the distance the copper has been pulled out of the triangular plane of the ligands that are held constant as well the deviation of the copper from a vector normal to the base of the tetrahedron with the phosphorous and both diimine nitrogen atoms at the vertices. A second plane may be drawn through the bound atom of L, the copper atom, and the phosphine phosphorous to further evaluate dihedral distortions to the tetrahedral geometry. This plane is the

Figure 43: The placement of the plane and centroid used in this study to quantify the degree of tetrahedralization of the complex

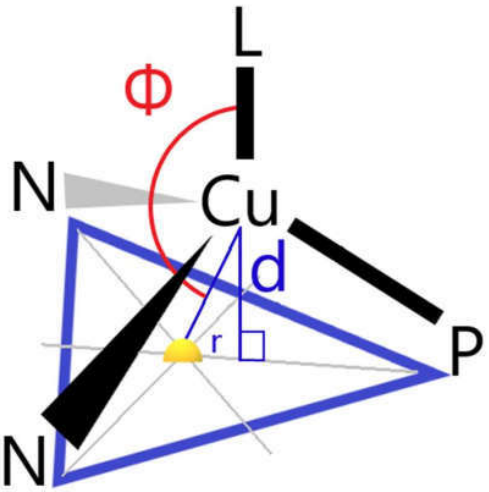

mirror plane of these complexes in an idealized symmetry. The measurements presented in **Figure 43** for each of the complexes are summarized below in **table 13**.

Table 13: The values of the measurements presented in figure 3 for each of the complexes discussed below.

	1a	2a	1	8	5(Cu1)	5(Cu2)	1Cl	1I	9	11
Phi	90	90	151.05	145.53	137.49	143.06	149.37	151.13	158.9	152.21
r	0.308	0.311	0.763	0.741	0.653	0.68	0.728	0.787	0.883	0.765
d	0	0	0.713	0.685	0.576	0.61	0.667	0.744	0.841	0.72

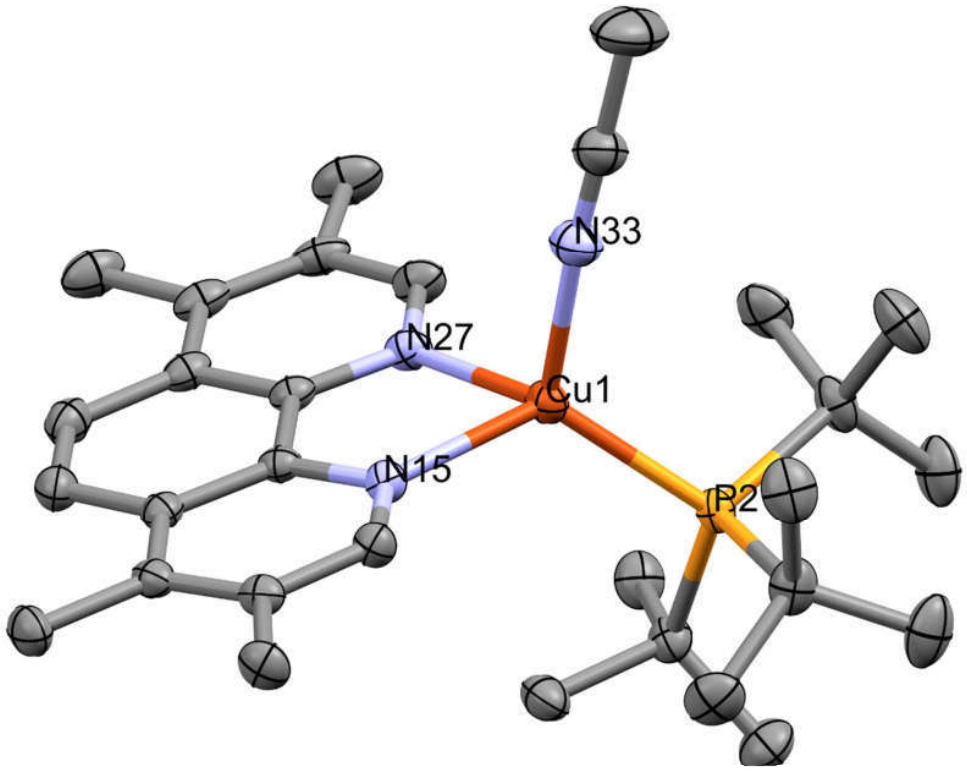

Figure 44: The structure of [Cu(Me$_4$phen)(^{t}Bu$_3$P)(MeCN)]BF$_4$. Thermal ellipsoids are drawn at 50% probability, carbons are unlabeled, hydrogens are omitted for clarity, as is a single acetonitrile solvate molecule and the BF4 anion

In the acetonitrile bound complex, [Cu(Me$_4$phen)(^{t}Bu$_3$P)(MeCN)]PF$_6$, the structure of which is presented in **Figure 44** below. The copper center is located 0.713 Å above a plane drawn through the 2,3,4,7-tetramethyl-1,10-phenanthroline nitrogen atoms and the tri-t-butylphosphine phosphorous atom, distances to calculated surfaces and centroids will not include error. A centroid placed in the middle of these three atoms is found to be located 0.763 Å away from the copper, on

the Me_4phen side forming an angle of 151.05 ° between the acetonitrile nitrogen, the copper, and the centroid. A plane drawn through the acetonitrile nitrogen, the copper and the phosphorous of $^tBu_3P$ intersects the base of the tetrahedron at an angle of 88.84 °. The acetonitrile is nearly linear with C-C-N angle of 179.1(2) ° but not bound colinear to the plane formed between its bound nitrogen atom, the copper center, and the phosphine, it is instead found leaning to the side by 3.08 °. The two Me_4phen are also not equidistant from this plane at distances of 1.286 and 1.393 Å respectively, indicating a slight twist to the tetrahedral structure of the complex. The presence of a solvent molecule in this structure allows for the easy comparison of the bound and unbound nitrile bond lengths, which are found to be \equal at 1.131(2) Å and 1.132(4) Å, this and the near linearity of the solvent ligand itself indicate that little to no metal-to-ligand back bonding is

Figure 45: The structure [Cu(Me_2bpy)($^tBu_3P$)]BF_4. Thermal ellipsoids are drawn at 50% probability level, carbon atoms are unlabeled, hydrogens and the anion have been omitted for clarity.

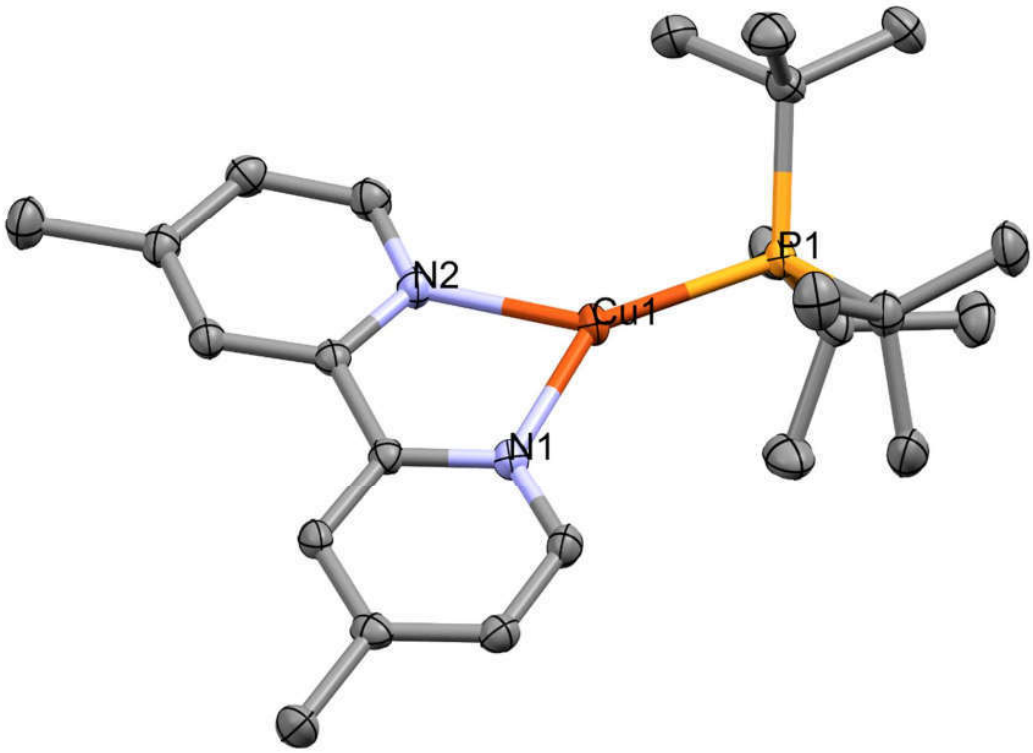

occurring, which further explains the lability of this moiety. The Cu-N (acetonitrile) distance is 2.013(2) Å which is equal to the average value for that of the compound $[Cu(MeCN)_4]PF_6$ which also clearly possesses acetonitrile ligands that are considerably labile. Cu-N bond length in its parent

The structural changes that accompany the loss of this labile solvent ligand are significant as can be seen in the structure of $[Cu(Me_2bpy)(^tBu_3P)]BF_4$, **Figure 45** above. Most notably the bond lengths to all remaining ligands, the Me_4phen and the $^tBu_3P$, contract significantly with the Cu-P distance shrinking to 2.1917(5) Å from 2.2218(4) Å and the Cu-N distances shrinking to 2.035(1) Å and 2.070(1) Å from 2.100(1) Å and 2.109(1) Å respectively. The only sign that molecule isn't completely planar is a slight tilt to the Me4phen orientation. This is isostructural to the $[Cu(Me_2bpy)(^tBu_3P)]PF_6$, at nearly every measurement with that notable exception that the Me_2bpy rings display a torsion angle of 5.0(2)° and is bound to the copper more symmetrically with Cu-N bond distance of 2.031(1) Å and 2.055(1)Å. It is also notable that the Me_4phen ligand seems to have a superior ability to stabilize the weakly bound acetonitrile ligand as this structure has been isolated several times from a variety of conditions, whereas the complementary complex $[Cu(Me_2bpy)(^tBu_3P)MeCN]PF_6$ is inferred solution from the UV-vis and NMR measurements, but

has not been directly observed by SC-XRD as all crystals that have been evaluated from attempts to crystallize this complex have proven to be the three-coordinate trigonal planar complex.

Figure 46: The Structure of [Cu(Me4phen)(tBu3P)(NCS)], thermal ellipsoids are drawn at the 50% probability range, grey=carbon, yellow=sulfur, hydrogen atoms are omitted for clarity.

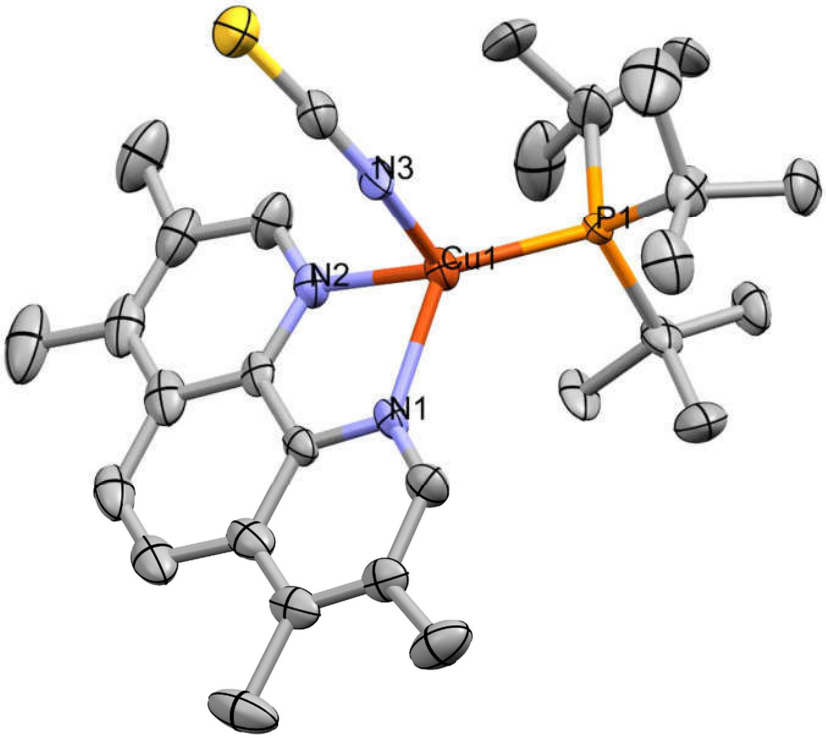

The acetonitrile bound complex can be compared to that which has been complexed with the thiocyanate anion, the structure of which can be seen in **Figure 46**, above. Surprisingly the thiocyanate anion is coordinated through the nitrogen terminus, as opposed to the comparably softer sulfide terminus. This complex, [Cu(Me$_4$phen)(^{t}Bu$_3$P)(NCS)], isostructural to the acetonitrile complex but electronically different, as the ligand is anionic and makes the complex overall neutral. Therefore, it must be electronic factors not steric factors which causes a more profound tilt to the base of the tetrahedron formed between the Cu(I), the two Me$_4$phen nitrogen atoms, the thiocyanate nitrogen atom, and the phosphorous atom at its vertices. The skewing of

the tetrahedral formed is evidenced by the distance and angle with the centroid, placed in the same manner as above, which are 0.741 Å and 145.53 ° respectively. The distance to the base of the tetrahedron is 0.685 Å, the shortest we have seen of the complexes examined. While the Cu-thiocyanate bond length is similar to the Cu-acetonitrile bond length at 2.041(9) Å, the Me_4phen ligand is significantly skewed with the distance from nitrogen atom to the idealized vertical mirror plane of the molecule, which is defined by the P-Cu-$N_{thiocyanate}$ atoms being 1.470 and 1.192 Å. However, the two Cu-N and the Cu-P distances are roughly equivalent to the previous example at 2.102(6), 2.125(6), 2.230(2) Å respectively. The complex reported here shows the scale of the effect of the sterically large $^tBu_3P$ by comparison to the complex reported by Sargentelli *et al.,* which is [Cu(phen)(Ph_3P)(NCS)] and the bipyridine ligated complexes reported by Pettinari *et al.*[44,53] The Sargentelli complex reports a Cu-thiocyanate bond length of 1.985(9) Å, with Cu-N_{phen} distances of 2.095(8) Å and 2.096(8) Å, and a Cu-P distance of 2.191(3) Å, further they report no skewing of the phenanthroline coordination.[44] While the thiocyanate complex reported here has the thermal ellipsoids for the N- and S- terminus that are quite large, it is clear that there is significant tilt in its coordination with a C-N-Cu angle of 151.6(7) °, the thiocyanate anion itself has also lost some linearity, with an S,C,N bond angle of 175.1(9) °. Compared to the bond angle in KSCN at (178.3 ± 1.2)°, this difference approaches statistical significance. The distances within the anionic ligand itself are also interesting, as the C-N bond length (1.18(1) Å) is very similar to the 1.149(14) Å reported in KSCN, while the C-S bond length in this complex is significantly shorter at 1.61(1) Å in this complex compared 1.689(13) Å in KSCN.[54]

The halo complexes also provide an axis for measuring electronic effects on the geometry of the complex while simultaneously providing a simple control for the steric effects from the fourth ligand. All the halo complexes were crystallized by the vapor diffusion of *n*-pentane into a

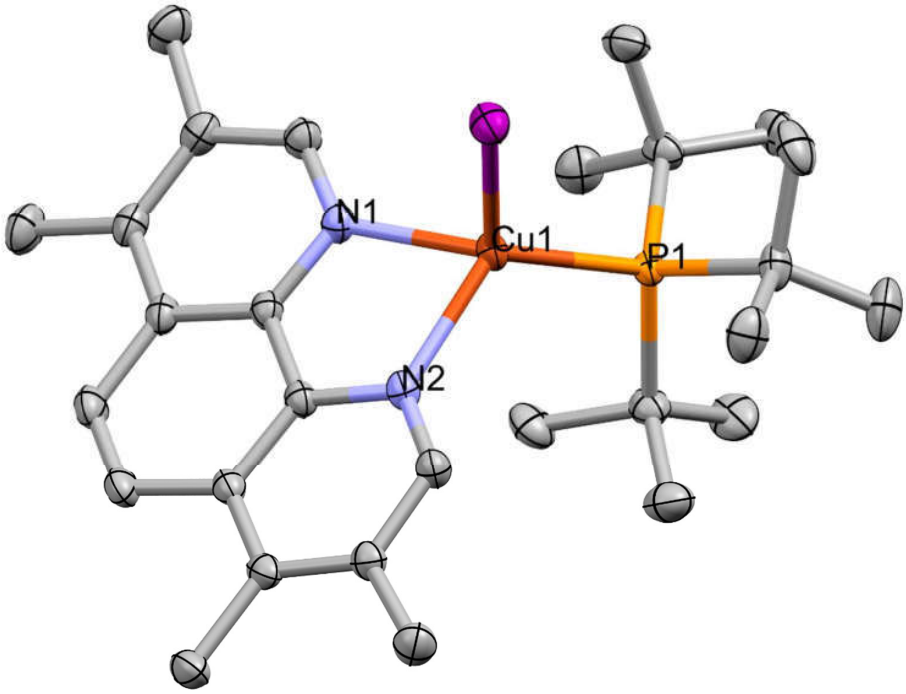

Figure 47: The Structure of [Cu(Me4phen)(tBu3P)]I. Thermal ellipsoids are drawn at 50% probability level, purple=iodine, grey=carbon, hydrogens and one solvent molecule are omitted for clarity

solution of the complex in CH_2Cl_2 and present in the expected tetrahedral geometry about the Cu(I) center. The iodo complex, the structure of which is presented above in **Figure 47,** is tetrahedral and similar to the acetonitrile complex with the N_2P centroid located 0.787 Å away from the copper center and nearer to the nitrogen atoms such that the I-Cu-$N_2P_{centroid}$ angle is 151.13 °. However, due to electronic and steric effects from the size of the iodine anion, the tetrahedron formed with the Cu(I), the phenanthroline nitrogen, and phosphorous atom is less symmetric than in the above example, with the perpendicular distance from copper to the N_2P base 0.744 Å. The source of this deformation is found in the Cu-N and Cu-P bond lengths. The Cu-N bond lengths of 2.111(1) and

2.088(1) Å are notably less symmetric than in either of the above examples. However, the distance from the nitrogen atoms to the vertical plane defined by I-Cu-P, at 1.285 and 1.390 Å are very similar to the values noted in the earlier examples. The Cu-P distance is 2.2258(5) Å, which is nominally longer than the acetonitrile complex. The Cu-I bond is quite long at 2.6450(4) Å, which is significantly longer than that of CuI which has a Cu-I bond length of 2.338 Å, and a [CuI(dppmS_2] complex reported by Nishioka, which has a reported Cu-I bond lengths of 2.4937(5) Å.[55,56] This Cu-I bond is more similar in length to those of reported $(\mu\text{-I})_2$ complexes such as that reported by Lobana and Noren which have Cu-I bond lengths of 2.6503(8) Å and 2.637(1) Å respectively.[57,58] Interestingly, the Me_4phen ligand has a significant distortion from planarity with C13 being located more than 0.5 Å above the plane of the central ring of the Me_4phen ligand.

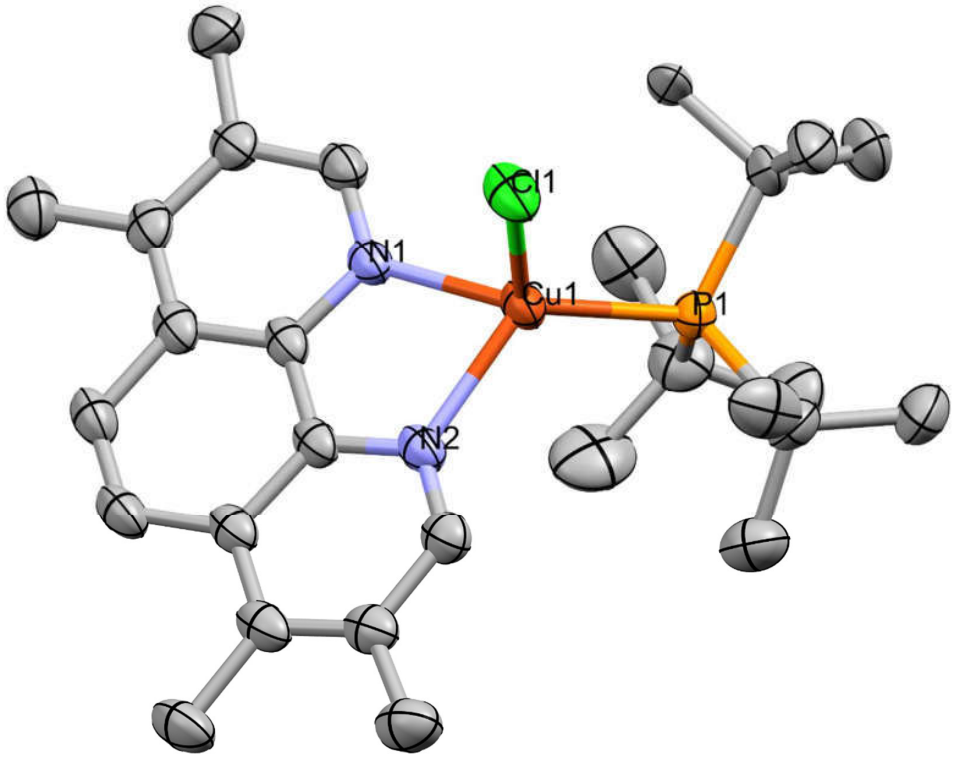

Figure 48: The structure of [Cu(Me_4phen)(^{t}Bu_3P)]Cl. Thermal ellipsoids are drawn at the 50% level, green=chlorine, grey=carbon, hydrogens are omitted for clarity, as is a disordered methylene chloride molecule

If we compare the above iodo complex to the nearly isostructural chloro complex, whose structure can see above in **Figure 48,** the most notable difference is that the chloro complex is less tetrahedral, with the centroid (defined as previously) only 0.728 Å below the Cu(I) center at an angle of 149.34° towards the diimine ligand. It follows that the copper is also closer to the base of the tetrahedron formed by a plane drawn through the diimine nitrogen atoms and the phosphine atom. This plane is located only 0.667 Å below the Cu(I) center. Due to the much smaller steric profile of the chloride ligand the coordination environment of this complex is less distorted than complex 1I. This reduced strain can be seen in the two Cu-N distances which are crystallographically indistinguishable with distances of 2.108(4) and 2.111(3) Å respectively. These two imine nitrogen atoms are also located similar distances, 1.351 Å and 1.329 Å, from the symmetry plane that bisects the molecule. The Cu-P distance (2.207(1) Å) is also much shorter in this complex than in its iodo bound cousin. Based on the set of measurement just mentioned and the significant difference in size of the two halogen atoms discussed, it shouldn't come as a surprise that the Cu-Cl distance is much shorter than the Cu-I distance at 2.340(1) Å, though this is quite long as compared to other Cu(I)-Cl bonds including CuCl, the five coordinate Cu(I) complex reported by Paul *et al.*, and the $(\mu\text{-Cl})_2$ complex reported by Noor which have Cu-Cl bond lengths of 2.0512 Å, 2.2352 Å, and 2.318(7) Å respectively.[50,59,60] This complex also shows a significant loss of planarity in its Me_4phen ring system with the largest displacement of the terminal methyl unit being 0.427 Å above the plane of the central ring.

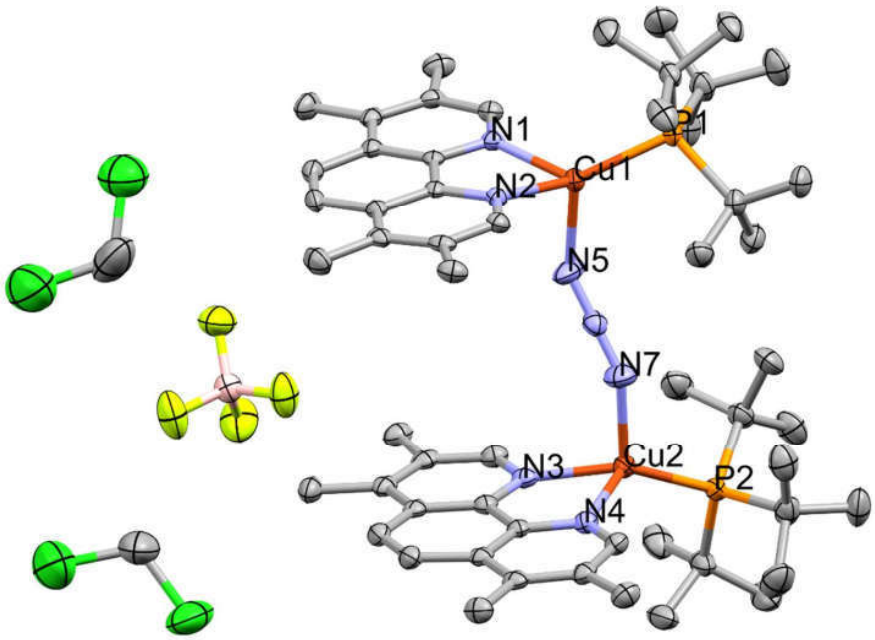

Figure 49: The Structure of [Cu(Me$_4$phen)(^{t}Bu$_3$P)]$_2$N$_3$]BF$_4$. Thermal ellipsoids are drawn at the 50% probability level, grey=carbon, green=chlorine, yellow=fluorine, pink=boron, hydrogens are omitted for clarity

The azide bound complex, whose structure is presented above in **Figure 49**, is unique amongst those being presented here as the only dimetallic complex. In fact, it is only the second example of a discrete singly bridged μ_2-$\eta^{1,3}$-azide Cu(I) complex available in the literature.[60,61,62] There are several interesting things to note about this structure. Firstly, the two halves are not generated by crystallographic symmetry. Instead, the whole molecule is contained within the asymmetric unit, including a structurally important BF_4^- anion and two structurally important solvent molecules, which support the structure by hydrogen bonding interactions. The two copper centers are tetrahedral to different extents, which can be examined using the same methods discussed previously by examining the relationship of the Cu(I) center to a centroid placed between the Me$_4$phen nitrogen atoms and the ^{t}Bu$_3$P phosphorous atom. Keeping in mind that these computational distances do not have crystallographic uncertainty the centroid between N1, N2, and P1 is located 0.653 Å from Cu1 at an angle of 137.49°, while the centroid of N3, N4, and P2

is located 0.680 Å at angle 143.06°. The azide ligand is bound to Cu1 at an angle of 143.5(4)° and to copper Cu2 at an angle of 147.4(3)° with the azide itself being nearly linear with and N-N-N angle of 178.8(5)°. The Cu1-Cu2 distance is 6.2013(8) Å. The Me4phen ligand of both copper metals is bound with a different orientation than seen in previous examples as the copper does not lie within the plane of the ligand in either case.

While the coordination environments are similar for both copper centers, they are not identical. The coordination environment of Cu1 has two equal Cu-N distances of 2.111(3) Å, while Cu2 has two dissimilar Cu-N distances of 2.127(4) and 2.099(3) Å. The Cu-P distances also differ with Cu1 having a Cu1-P bond length of 2.203(1), while the same bond length in Cu2 is 2.214(1) Å. The entire ligand environment of Cu2 is offset from that of Cu1 due to steric interactions from

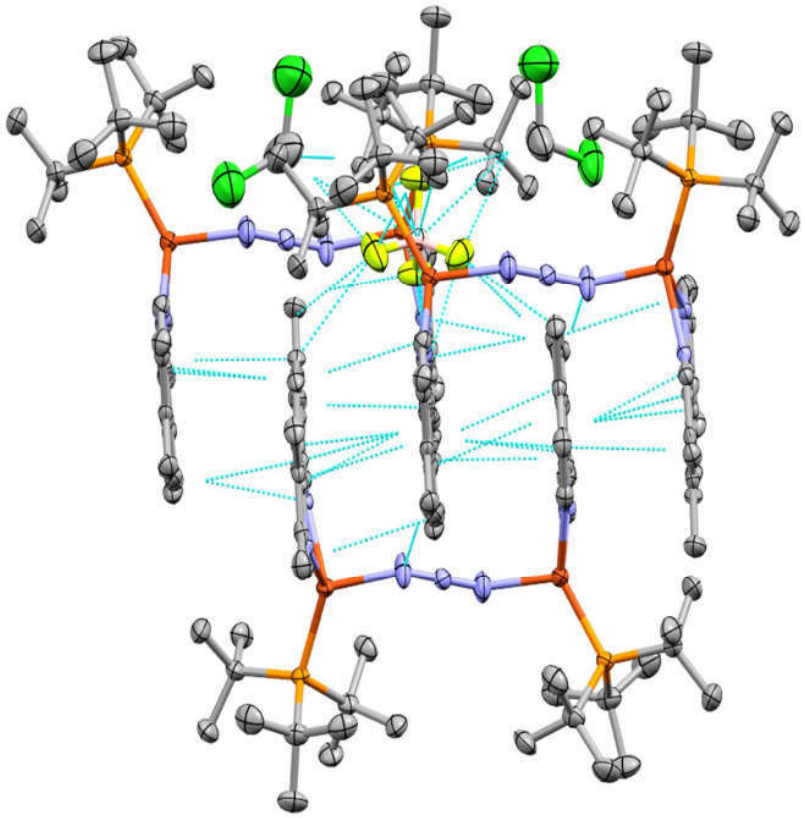

Figure 50: Showing the packing and close contact interaction of the azide bridge dicopper compound.

the $^{t}Bu_3P$ ligands as seen by the P1-Cu1-Cu2-P2 torsion angle which is 30.05°. The anion forms several hydrogen bonds both with the co-crystallized solvent molecules and the Me_4phen methylene C-H hydrogens, the Me_4phen methylene groups also act as intermolecular hydrogen bond donors to Me_4phen ring system of neighboring molecules and to N5, the azide nitrogen bound to Cu1, as seen above in **Figure 50**. This B-F---C-H hydrogen bonding, C-H---Ar hydrogen bonding, and C-H---N hydrogen bonding promotes a very tight packing between neighboring molecules in the solid state that is not attributable to π-stacking of the Me_4phen moieties as the steric hinderance prevents significant interaction of the ring systems, this extensive system of hydrogen bonding also promotes the syn-confirmation of the sterically demanding $^{t}Bu_3P$ ligands which one would expect to be anti.

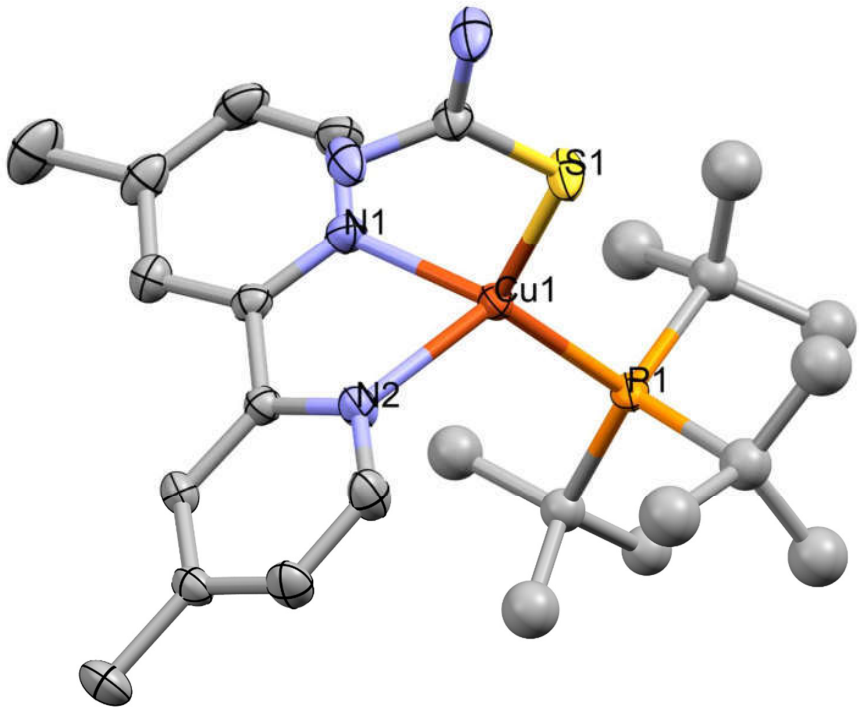

Figure 51: The structure of [Cu(Me2bpy)(tBu3P)thiourea]BF4. Thermal ellipsoids are drawn at the 50% probability level, the $^{t}Bu_3P$ ligand is disordered over two positions and has been modeled isotropically with distance constraints. Grey=carbon, Hydrogens and the anion are omitted for clarity.

Due to increased flexibility imparted by the Me_2bpy ring system, the complexes bearing this moiety and a fourth ligand show increased tetrahedral distortions and a superior ability to accept ligands that the complexes bearing the Me_4phen ligand system cannot. This includes soft sulfur donors such as thiourea and tetrahydrothiophene. This greater flexibility also increases the crystallographic disordering seen in these complexes. The complex containing thiourea as a fourth ligand, [Cu(Me_2bpy)(^{t}Bu$_3$P)(thiourea)]BF_4, whose structure can seen above in **Figure 51** is significantly more tetrahedral than any of the complexes containing Me_4phen discussed above, as evidenced by the Cu---N_2P distance of 0.883 Å and the S-Cu-N_2P angle of 158.9°. These values are the largest discussed; consequently, the centroid distance is quite close to the shortest distance measurement from the copper center to the horizontal plane which is 0.841 Å. The Cu-P distance is among the longer bonds discussed here with a length of 2.2411(9) Å. Furthermore, the phosphine ligand is disordered over two positions that are separated by roughly 13.5°. The Me_2bpy is more asymmetrically bound than that seen in the three-coordinate trigonal planar geometry, with this complex exhibiting Cu-N bond distances of 2.153(2) and 2.098(2) Å. This difference is accentuated by the significant distortion to the planarity of the Me_2bpy ring system, which in this case exhibits a dihedral twist of 8.9(3)°. Furthermore, the ring system of the Me_2bpy lies significantly out of the plane of the N-Cu-N bonds which can be illustrated by the distance between the bipyridine methylene groups and this plane which are 1.601 Å and 0.666 Å.

One explanation for this notable loss of planarity is seen in the minimized computational model and hinted by the orientation of thiourea complex in the SC-XRD structure, which is offset such that the plane of the S-Cu-P bonds and that of the C-S-Cu bonds differ by roughly 3.6°. The remainder of the thiourea ligand is also tilted such that the nitrogen bound hydrogen atoms favor one of the Me_2bpy imine nitrogen atoms, as such the thiourea N-C-N plane is twisted by almost

9.14° compared to the plane of the P-Cu-S bond. Further suggestions of this interaction can be seen in the shape of the thermal ellipsoids for the thiourea and Me_2bpy nitrogen atoms. DFT computations suggest an intramolecular hydrogen bonding interaction between the urea N-H bond and the Me_2bpy nitrogen atoms, which pulls one nitrogen out of plane resulting in the dihedral torsion. The thiourea ligands themselves are certainly linked by hydrogen bonding interactions with their crystallographically generated counterpart and the anion, with the top thiourea N-H acting as a hydrogen bond donor to the sulfur of another, and the other N-H protons donating hydrogen bonds to anion illustrated above in **Figure 52**.

Figure 53: The structure of [Cu(me2bpy)(tBu3P)Tetrahydrothiophene]BF4 Thermal ellipsoids are drawn at 30% probability, the THT ligand is disordered over two positions, only one is shown here with the carbons modeled isotropically. Grey = Carbon. Hydrogens omitted for clarity

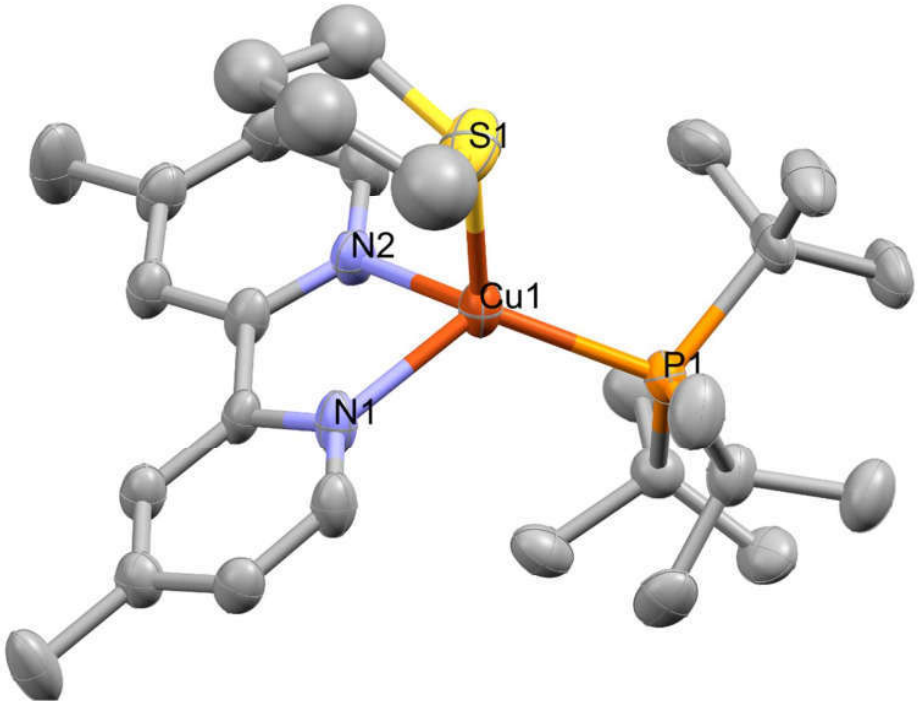

The other Me_2bpy complex that does not have a Me_4phen counterpart is the [Cu(Me_2bpy)($^tBu_3$P)(tetrahydrothiophene)]PF_6 complex, whose structure can be seen above in

Figure 53. This complex is less distorted than its thiourea cousin due to the smaller steric profile of the ligand that is projected at the Me_2bpy ligand and the reduction in intra- and intermolecular forces from the lack of good hydrogen bond donors in the ligand. This difference manifests as a shorter Cu---$N_2P_{centroid}$ distance, which is 0.765 Å and roughly equivalent to that found in the acetonitrile bound complex. This is coupled with a less steep S-Cu-$N_2P_{centroid}$ angle which is also similar to the acetonitrile complex at 151.21°. These two values are related to the Cu-P at 2.231(2) Å and an indistinguishable pair of Cu-N distances which are reported at 2.092(5) and 2.095(6) Å. The THT ligand itself is bound at a distance of 2.373(3) Å and its saturated ring is disordered by a rotation of approximately 23° around the Cu-S axis.

^{31}P and ^{1}H NMR:

Both of the trialkylphosphine ligands employed, tri-*iso*propylphosphine ($^{i}Pr_3P$) and tri-*tert*-butylphosphine ($_{t}Bu_3P$) in the above syntheses have the desirable electronic properties of high σ Lewis basicity and low π acidity as well as significant steric bulk with cone angles of 160-181.4° and 182°-196.3° respectively.[63] All of the complexes discussed here will contain the $^{t}Bu_3P$ ligand, as it was quickly discovered that the steric bulk and σ basicity of the larger phosphine imparted more desirable properties than did the $^{i}Pr_3P$ ligand, based on the stability of the acetonitrile bound four-coordinate complex in air and in solution. Another attractive facet of these ligands is that the phosphorous atom of the $^{t}Bu_3P$ phosphine ligand provides a useful NMR handle for the characterization of the products and monitoring of reactions. The chemical shift in both ^{31}P and ^{1}H NMR and the three-bond *J*-coupling between the chemically equivalent hydrogen atoms and the phosphorous center that is observable in proton NMR are very sensitive to the ligand environment

Figure 54: The ^{1}H NMR spectrum of the Acetonitrile-bound and trigonal planar complexes with tri-tertbutyl phosphine and each diimine ligands.

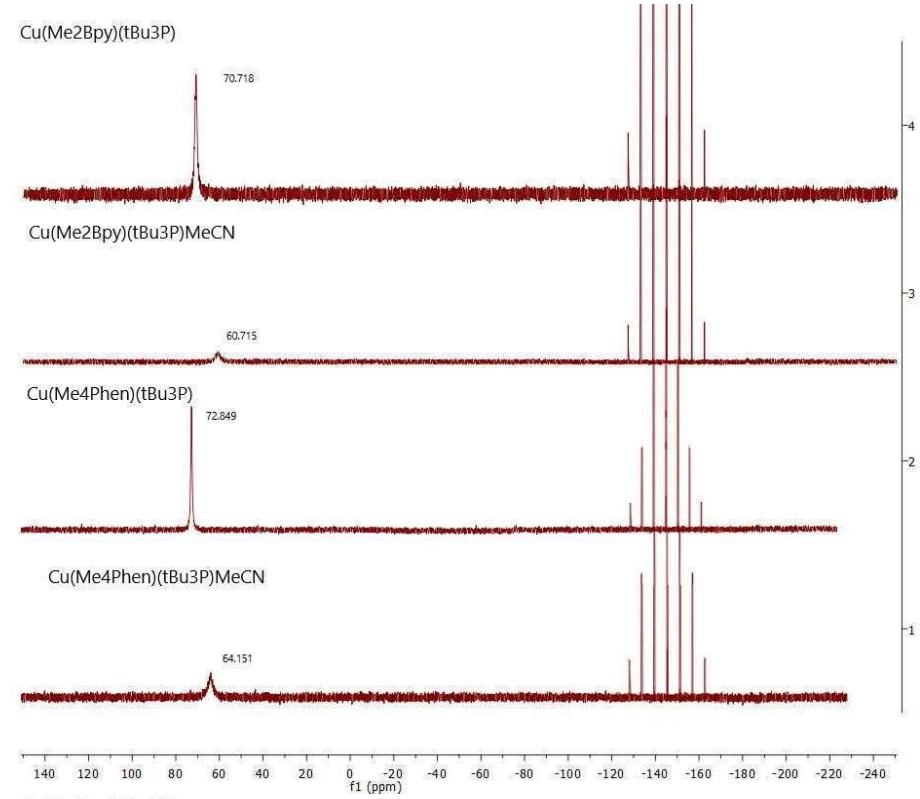

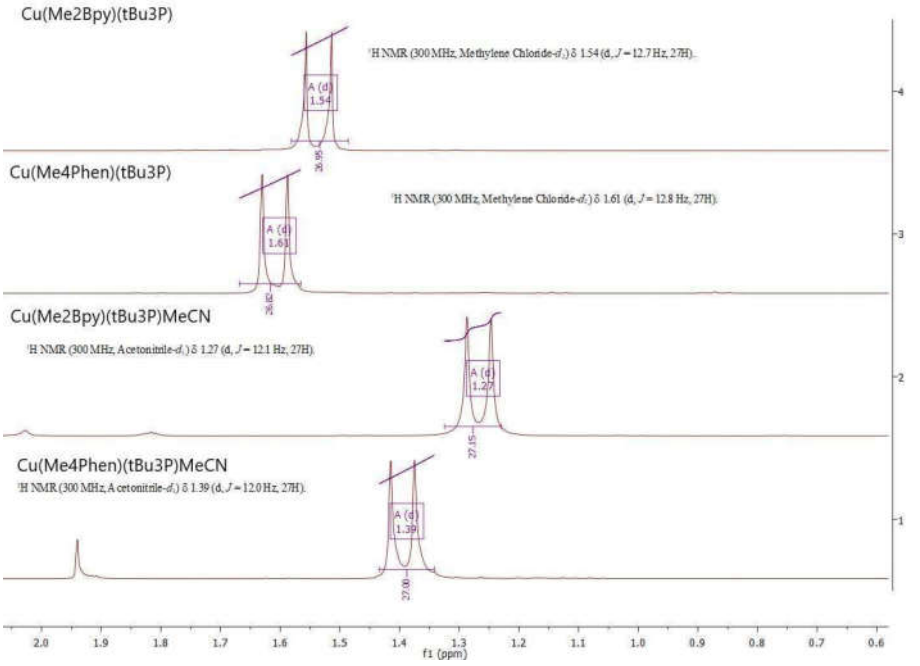

Figure 55: The ^{31}P NMR spectra of the acetonitrile bound complexes and their trigonal planar counter parts

of the copper system as seen in the spectra presented in **Figure 54** and **55**. One notable feature of the sensitivity of the ^{31}P NMR peak position to the structure of the complex is seen in the NMR of the acetonitrile bound complex for both diimine ligands, these spectra display a broadened peak that is nearly 10ppm in width at the base. While variable temperature experiments have not been performed that could elucidate the source of this broadening it is thought to be either from the slow exchange of the acetonitrile ligand with the solvent or the sampling of a wide range of low frequency butterfly and wagging motions that affect the local geometry on the NMR timescale. The sensitivity of the phosphine to the local environment also extends to the proton NMR in terms of both the position of the peaks for the phosphine hydrogens and the magnitude of the $^{3}J_{P\text{-}H}$ coupling that can be observed in these NMR spectra.

Electronic structure and UV-Vis Spectra:

The removal of the labile acetonitrile ligand is accompanied by a color change of the solution from a pleasant lemon yellow to a red/orange color. UV-vis measurements of the resulting complexes, seen below in **Figure 56**, show that this color change is not the result of a new absorbance maxima. Instead, what is observed is a general increase in the absorptivity prompted by improved orbital overlap of the donor orbitals with the aromatic diimine based π^* LUMO and a minor rearranging of the orbital energy levels due to the loss of the ligand. This also serves to explain the intermediate yellow and orange hues of the other complexes examined here, as the degree of tetrahedralization and the amount the various ligands perturb the orbital energies varies. Computational examination of the excited states can assist in understanding the excitation dynamics. The orbitals of these structures were calculated at the B3LYP level of theory using the 6-311++G(2d,2p) basis set for all main group elements (H, C, N, P, S, Cl, Br, I) and LANL2DZ with ECP for the metals (Cu, Mo). The geometry was converged in the gas phase with no symmetry

restraints to tight convergence criteria. The starting geometry was either from the XRD derived structure or generated *de novo* from similar structures for molecules for which XRD data was not obtained. Molecular orbitals were calculated based on this minimized geometry in the standard way. Excited states were calculated by TD-DFT methods. The first ten excited states of the four coordinate $[Cu(Me_4phen)(^tBu_3P)(MeCN)]^+$ cation are formed by excitation of electrons out of the HOMO through HOMO-6 molecular orbitals which are primarily Cu based with mixed amounts

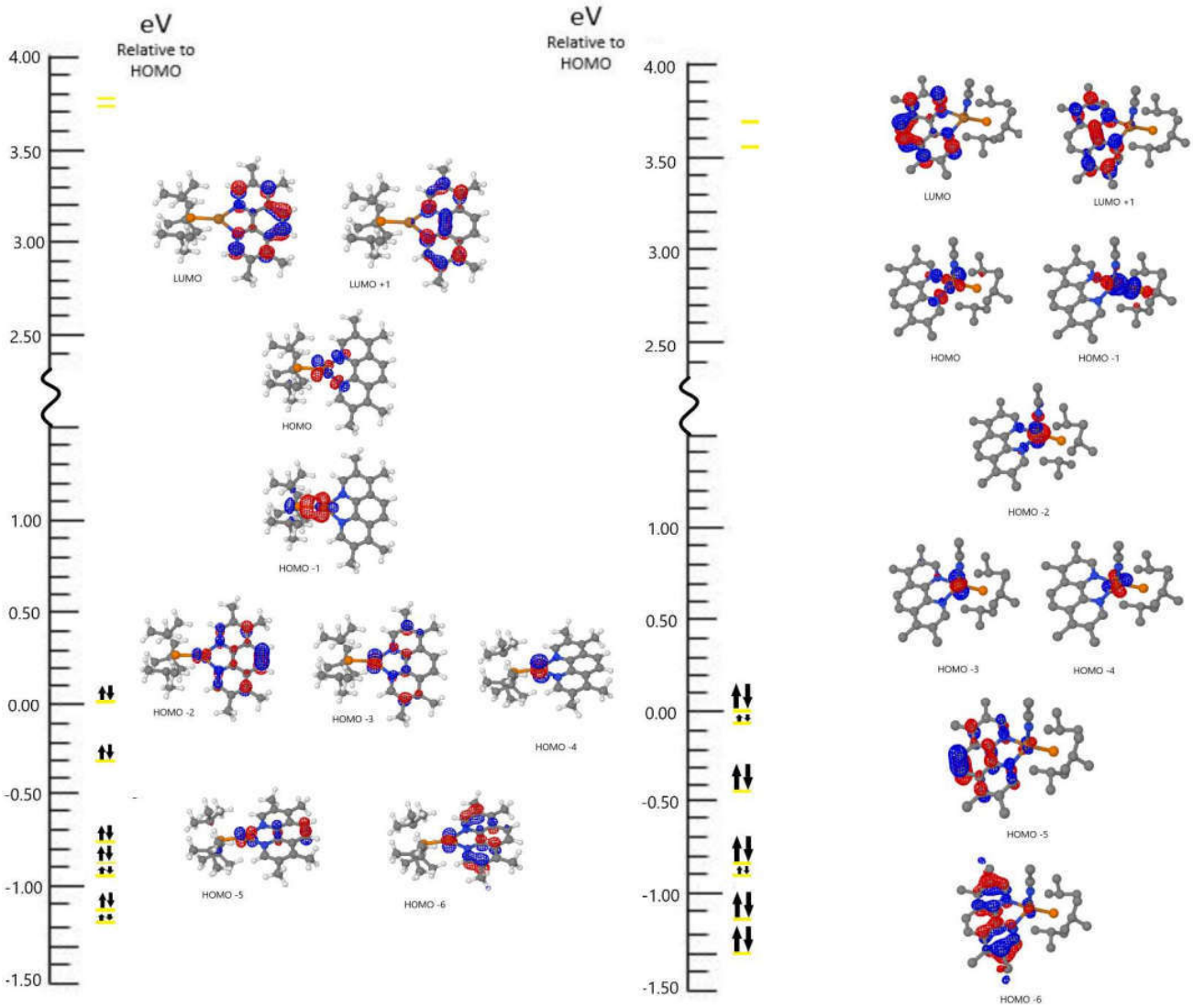

Figure 55: The molecular orbitals involved in the first ten excited states of $[Cu(Me_4phen)(^tBu_3P)MeCN]^+$ (right) and $[Cu(Me_4phen)(^tBu_3P)]^+$ (left)

of ligand character from all the surrounding ligands as seen on the right side of **Figure 55** below. The electrons occupying these orbitals are excited into the LUMO or LUMO+1 orbital which are almost entirely located on the Me_4phen ligand and can be characterized as π-antibonding orbitals. Thus, these excitations are metal-to-ligand excitations which are consistent with the MLCT state observed in similar structure types.[64,65,66]

Figure 56: The UV-Vis spectra of the acetonitrile and trigonal planar copper complex.

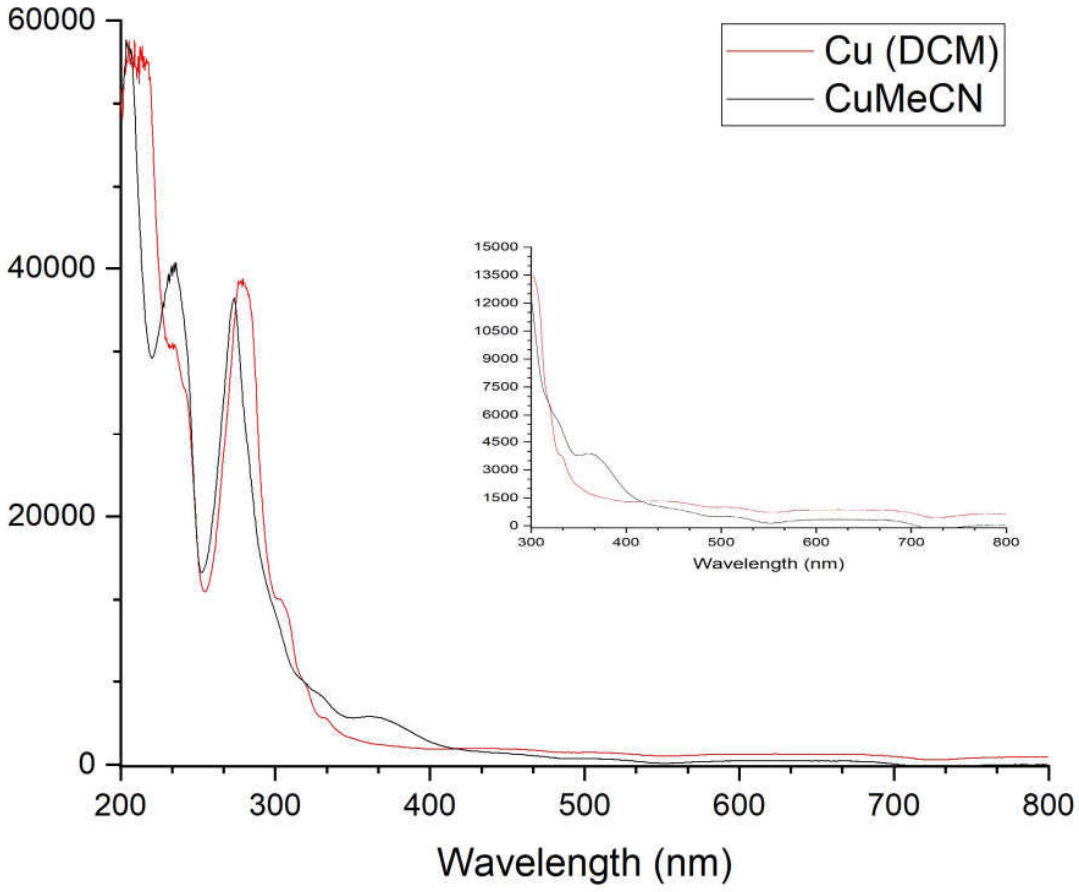

Of the seven occupied orbitals that make up the first ten excited states of the acetonitrile bound complex, only one involves the Cu-P bonding orbitals or the Cu-N (acetonitrile) bonding orbitals. Those that involve these two ligands are HOMO-1 and HOMO-2 respectively and, in fact the HOMO-2 orbital is anti-bonding with respect to the Cu-N(acetonitrile) interaction. Photoexcitation serves to depopulate this orbital, thus strengthening the metal-acetonitrile bond.

The molecular orbitals involved in the first ten excited states of the corresponding trigonal planar complex can be seen above on the left side of **Figure 55**. These orbitals are quite similar to those of its solvent ligated counterpart, with the obvious exception of the orbital that corresponds the Cu-N (acetonitrile) antibonding orbital of the solvent ligated complex (HOMO-2 on the right of **Figure 55)**. The loss of the acetonitrile ligand changes the energy of the frontier orbitals significantly, which manifests as the loss of degeneracy of the HOMO and HOMO-1, the latter of which now occupies the energy level of the formerly solvent bound orbital.

The orbital that once formed the Cu-N (acetonitrile) antibonding interaction has fallen in energy and is now part of a closely spaced set of three orbitals that are comprised of extensive Cu d/Me_4phen antibonding interactions, seen on the left side of **Figure 55** above. Even a cursory inspection of these orbitals shows that planarity of the complex allows for the reorientation of the Cu d-orbitals to align with those of the ligands. This adjustment increases the Cu-P bonding interaction as well as the ease of donation of electron density into the acceptor orbitals upon excitation. Interestingly, the identity of the excitation with the strongest oscillator strength changes upon the change in the geometry of the complex. In the tetrahedral arrangement, the transition with the strongest oscillator strength included the orbitals which were part of metal/Me_4phen bonding, as well as the Cu-P bonding, and Cu-N (acetonitrile) anti-bonding orbitals. Upon the loss of the fourth ligand and accompanying geometry change, the orbitals that make up the excited state with the strongest oscillator strength are now entirely comprised of Cu d-orbitals and the π^*-system of the Me_4phen ligand. The improved orbital interaction in the trigonal planar complex makes for a more strongly allowed Cu-d to Me_4phen MLCT excitation. This can be seen in the UV-Vis spectrum of these two complexes, seen in **Figure 56** above, as the slight broadening, increase in intensity, and shift to lower wavelengths of the absorption band located around 270 nm in the

trigonal planar complex as well as the decrease in absorption in the 230 nm range and the growth of a new shoulder above 300 nm. Since the tetrahedral shape is consistent for all examined complexes, the UV-vis data provides a controlled method to measure electronic effects on the frontier orbitals and correlate the ligand strength with observed structural changes. These effects are quite notable in the comparison of the halide bound copper complexes and the copper-acetonitrile complex absorbance spectra despite relatively minor structural differences, which can be easily observed in the structural overlay shown in **Figure 57** above and whose effects can be seen in the absorbance spectra in **Figure 58** below.

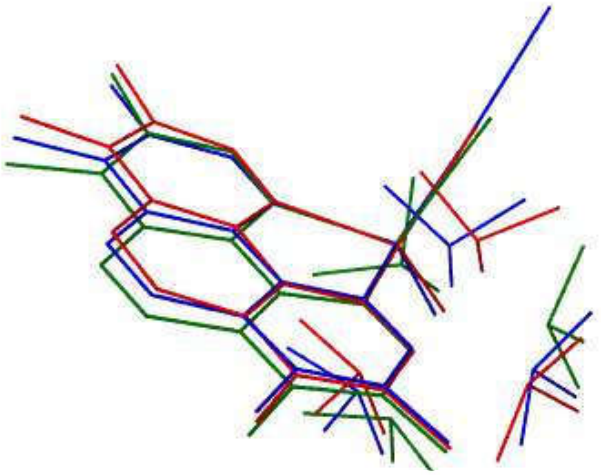

Figure 57: Wireframe structural overlay of [Cu(Me$_4$phen)(^{t}Bu$_3$P)(MeCN)]PF$_6$ in blue, [Cu(Me$_4$phen)(^{t}Bu$_3$P)]Cl in red, and [Cu(Me$_4$phen)(^{t}Bu$_3$P)]I in green

Despite the fact that these structures are nearly isostructural, the substitution of a halide ligand for the acetonitrile has a profound impact on the shapes and energies of the frontier orbitals. As compared to the acetonitrile ligated complex, the halide atoms' orbitals are heavily involved in the frontier orbitals of their complexes that are involved in the first ten excited states, with the involvement of the halide orbitals decreasing as the size of the halide increases. In the chloride

complex, the chlorine atom is involved in all of the occupied orbitals that take part of the examined transitions, the bromine is involved in all the occupied orbitals but one for its complex, and in the iodide complex, only four of the seven occupied orbitals have any iodide character.

These orbital interactions serve to reduce the copper character in the frontier orbitals for the complexes with extensive Cu-halide orbital interactions. While chloride interacts extensively with the copper center to which it is bound and contributes, along with copper, to the MOs primarily involved in the electronic excitations, the larger halides show weaker interactions with the copper center and have a more negliable impact on the energy of its orbitals as seen in **Figures**

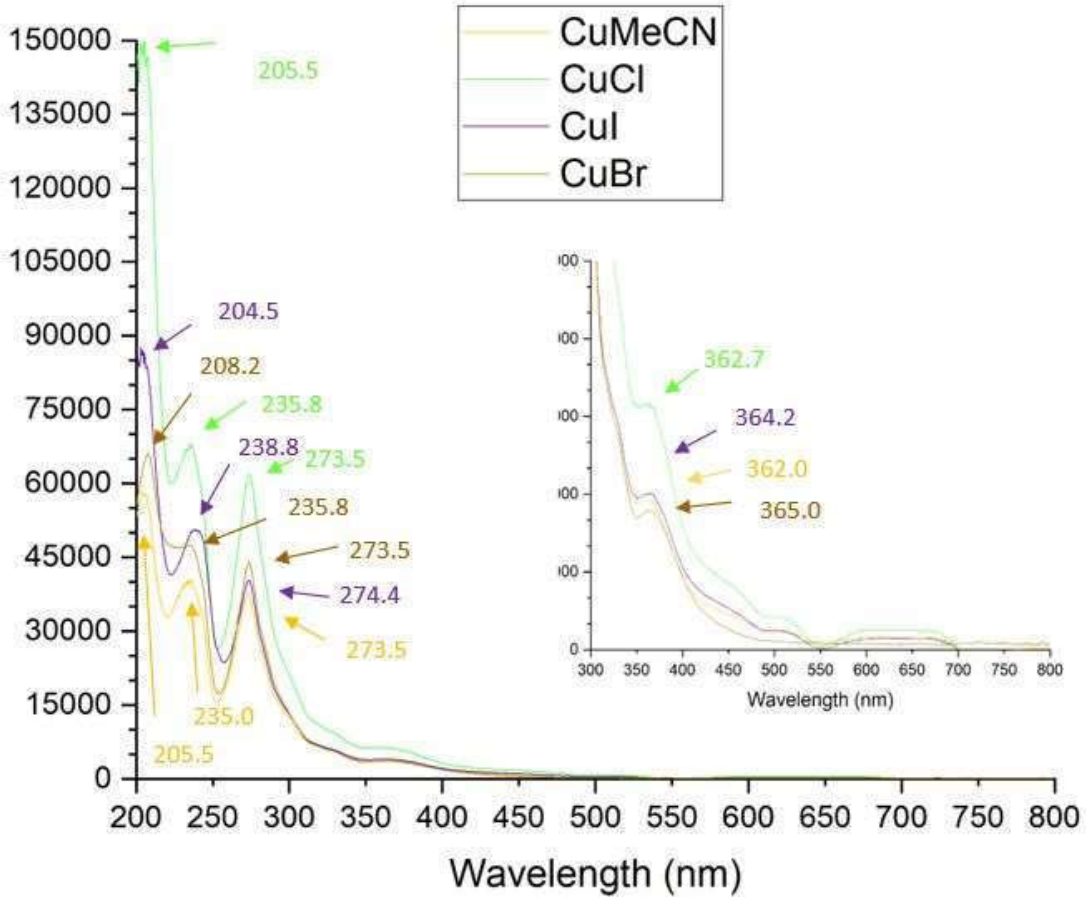

Figure 58: The UV-vis spectra of 1, 1Cl, 1Br, 1I.

59, **60**, and **61** below. The unoccupied orbitals, on the other hand, are almost completely unaffected by the halide atom in terms of identity or relative energy.

Thus, while the steric effects discussed above have a minor impact on the degree of tetrahedralization of the copper center, the electronic effects have a profound impact on energy and the copper character of the donor orbitals to the excited states. These effects taken together result in only minor differences in the positions and shapes of the peaks in the absorption spectra of these complexes but result in profound differences in the absorptivity of these species with the molar extinction coefficients of the chloride complex being nearly twice that of the next most absorbative species at the lowest wavelengths and remaining more than 20% higher at the lowest energy absorption.

Figure 59: The orbitals involved in the first ten excited states of 1Cl

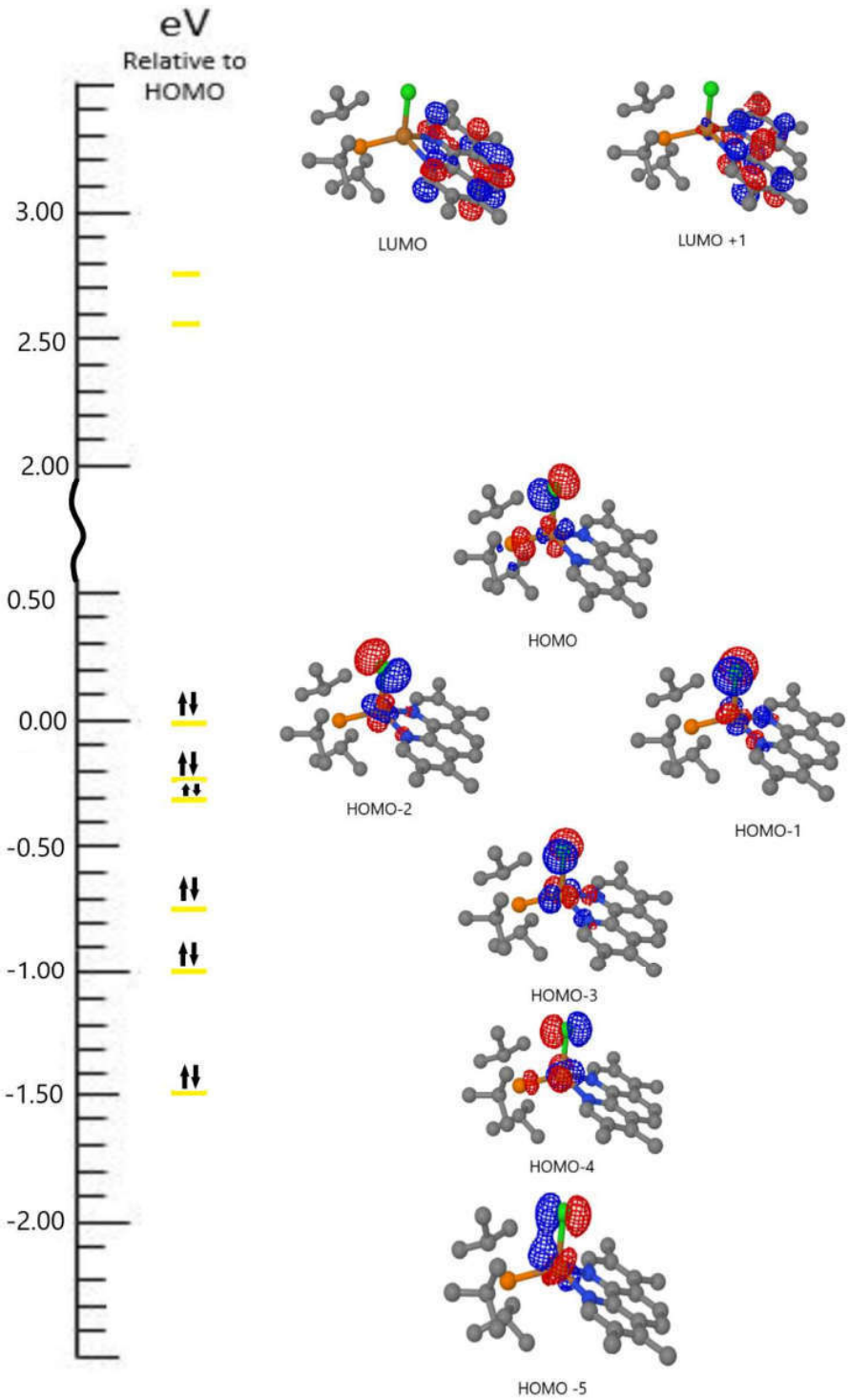

Figure 60: The orbitals involved in the first ten excited states of complex 1Br

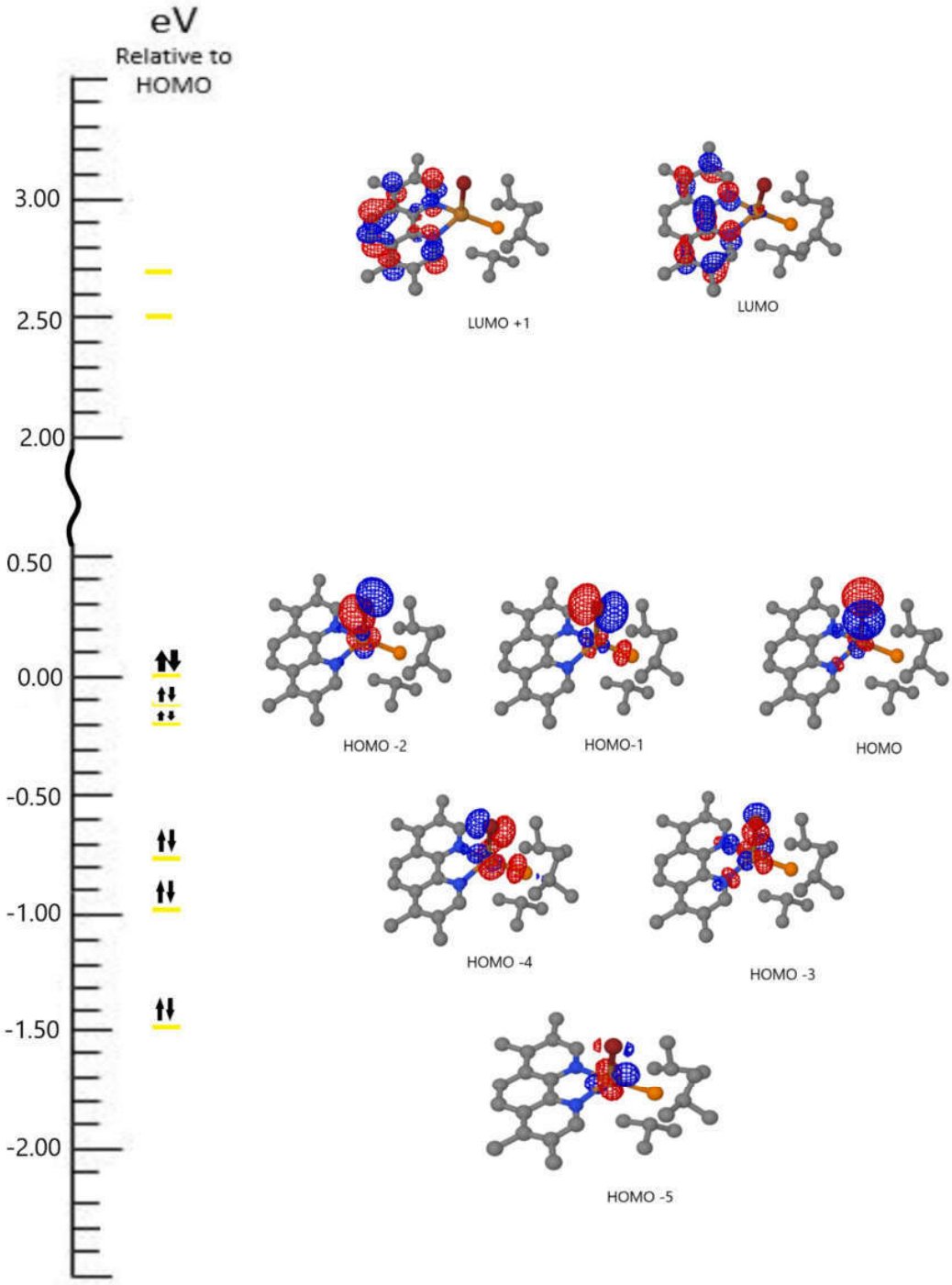

Figure 9: The orbitals involved in the first ten excited states of complex 1I

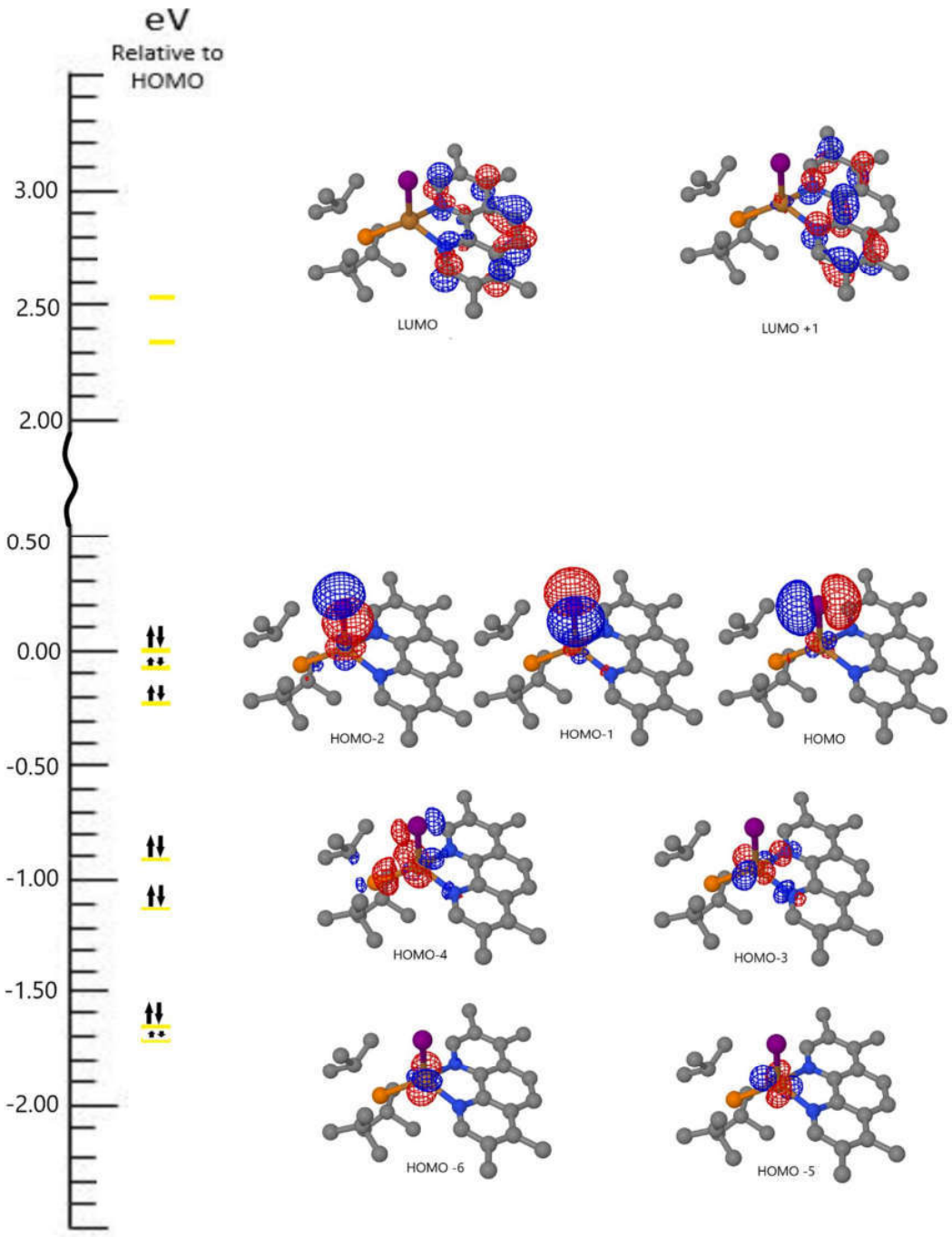

Figure 62: The Orbitals involved in the first ten excited states of [Cu(Me$_2$bpy)(^{t}Bu$_3$P)thiourea]$^+$

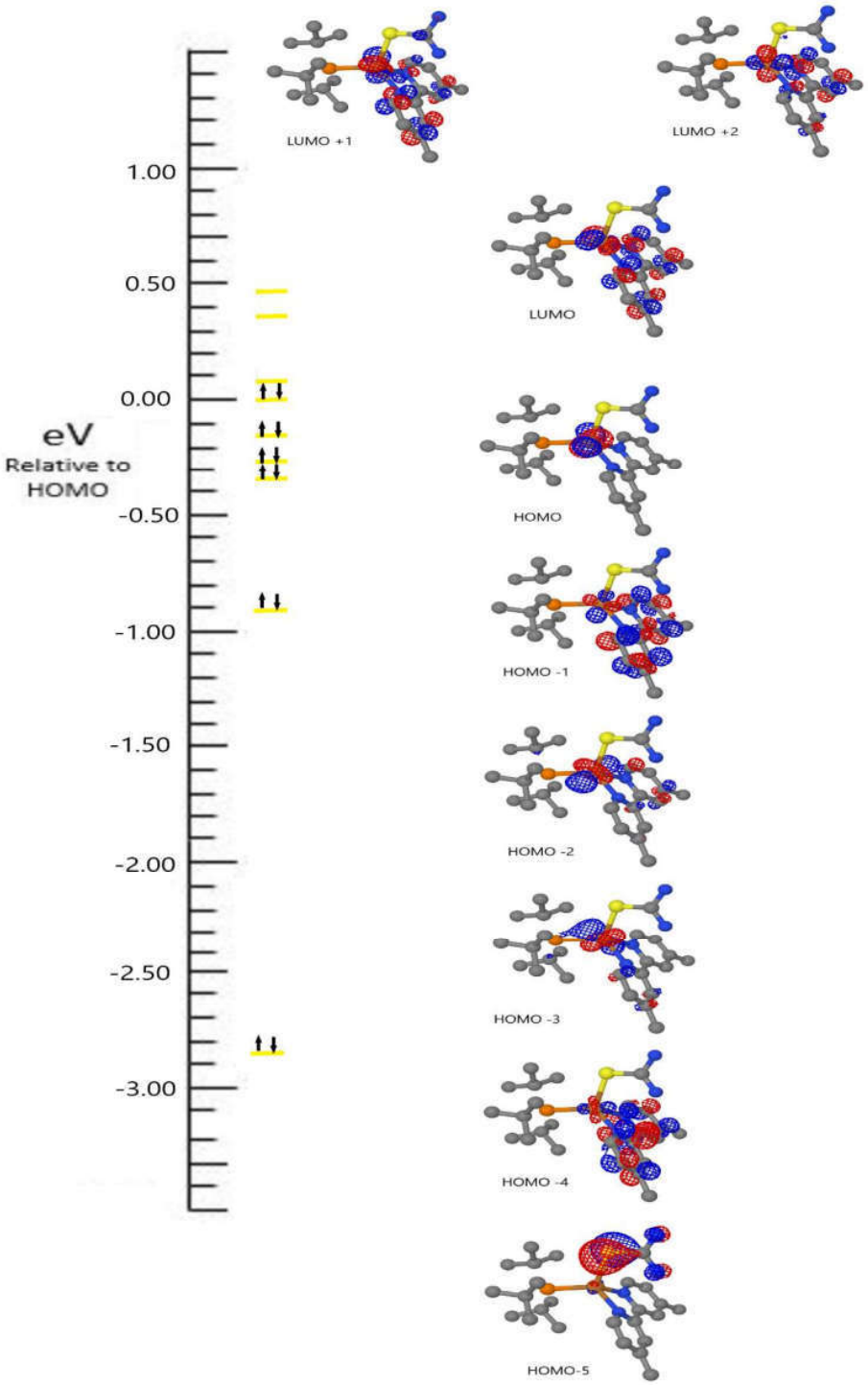

The L-type ligands show some surprising differences to the anionic ligands already examined. Amongst the obvious differences as compared to the anionic ligands is that of the significant steric bulk of the L-type ligands for which complexes with a neutral fourth ligand have been isolated. These neutral ligands include tetrahydrothiophene, dimethylsulfide, thiourea, and the acetonitrile ligand which has already been discussed at length. The tetrahydrothiophene, dimethylsulfide, and thiourea ligands are the only examples so far of this copper center binding to any sulfur donor atom as none of the anionic sulfur donors, which included benzenethiolate and adamantylthiolate, yielded any isolated complexes. The lack of complexation with the anionic sulfur donors is even more surprising given the significant impact the neutral sulfur donor ligands had on the geometry and electronic properties of the copper center.

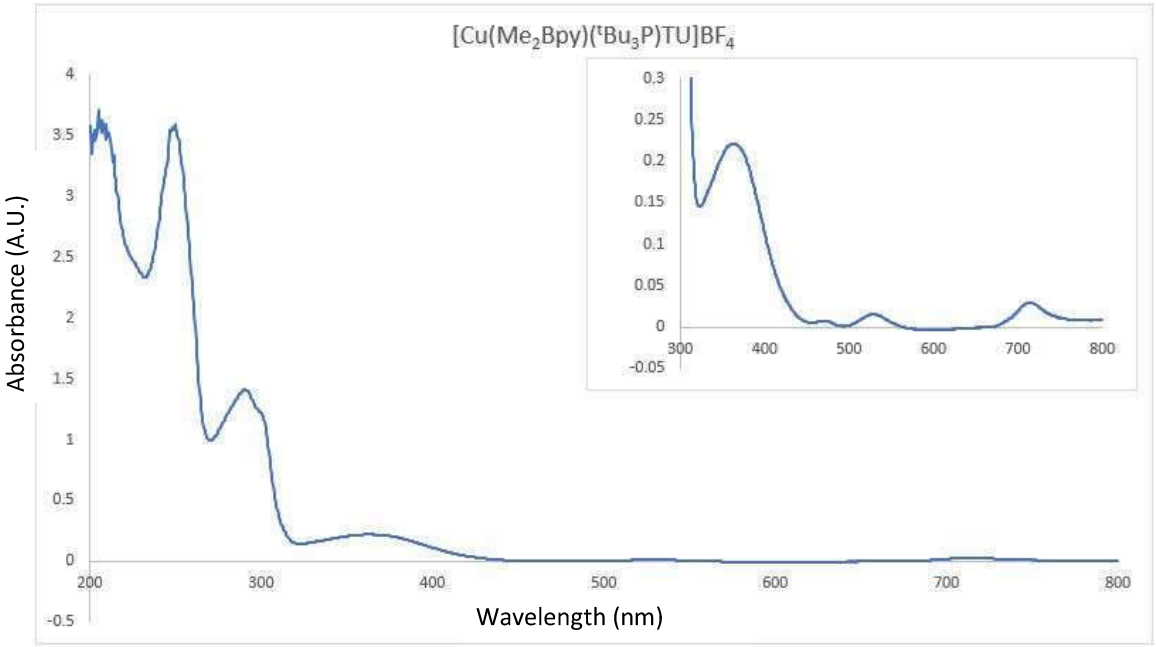

Figure 63: The UV-vis spectrum of [Cu(Me$_2$bpy)(^{t}Bu$_3$P)(thiourea)]BF$_4$

An examination of the lowest energy absorptions for the complexes that have been successfully isolated supports the calculated frontier molecular orbitals indication of a

photoinduced charge transfer. The lowest energy absorptions for these complexes occur between 300-500 nm, which is consistent with the MLCT absorptions reported by other groups.[64,65,66]

The complex with thiourea, [Cu(Me_2bpy)(^{t}Bu_3P)thiourea]BF_4 has a very interesting electronic structure that provides insight into some of the complexes that were not isolated. The absorption spectrum of the thiourea complex is seen above in **Figure 61**. Most notably the orbitals involved in the first ten excited states, seen above in **Figure 60**, are unique when compared to the examples detailed above. Amongst the differences are that the phosphine ligand orbitals are not involved in any of the occupied orbitals that participate in the examined excitations and the thiourea ligand itself is only involved in the lowest energy orbital involved, that being the HOMO-5 orbital. All of the higher energy occupied orbitals are Cu-Me_2bpys orbitals, as seen in other examples, or simply nonbonding Cu d-orbitals which characterize the HOMO of this complex. All the unoccupied orbitals involved in the first ten excited states, these being the LUMO, LUMO +1 and LUMO +2, have significant Cu character as compared with the excited states of the complexes examined above. These excitations also reach higher levels of unoccupied orbitals due to the very small energetic difference between the HOMO and the LUMO of this complex, which has a HOMO-LUMO gap of only 0.09 eV according to DFT. This very small band gap, as well as the structural distortions of the complex may explain why the complex is yellow in color as opposed to the red/orange shades seen in the halide complexes and the planar complex. The red bands are indicative of the MLCT transition, and this transition is considerably weaker in the thiourea complex due to the significant metal character of the unoccupied orbitals and the significant ligand character of the occupied orbitals involved in the relevant excited states.

Figure 64: The orbitals involved in the first ten excited states of the [Cu(Me$_4$phen)(^{t}Bu$_3$P)Ph$_3$PS]$^+$

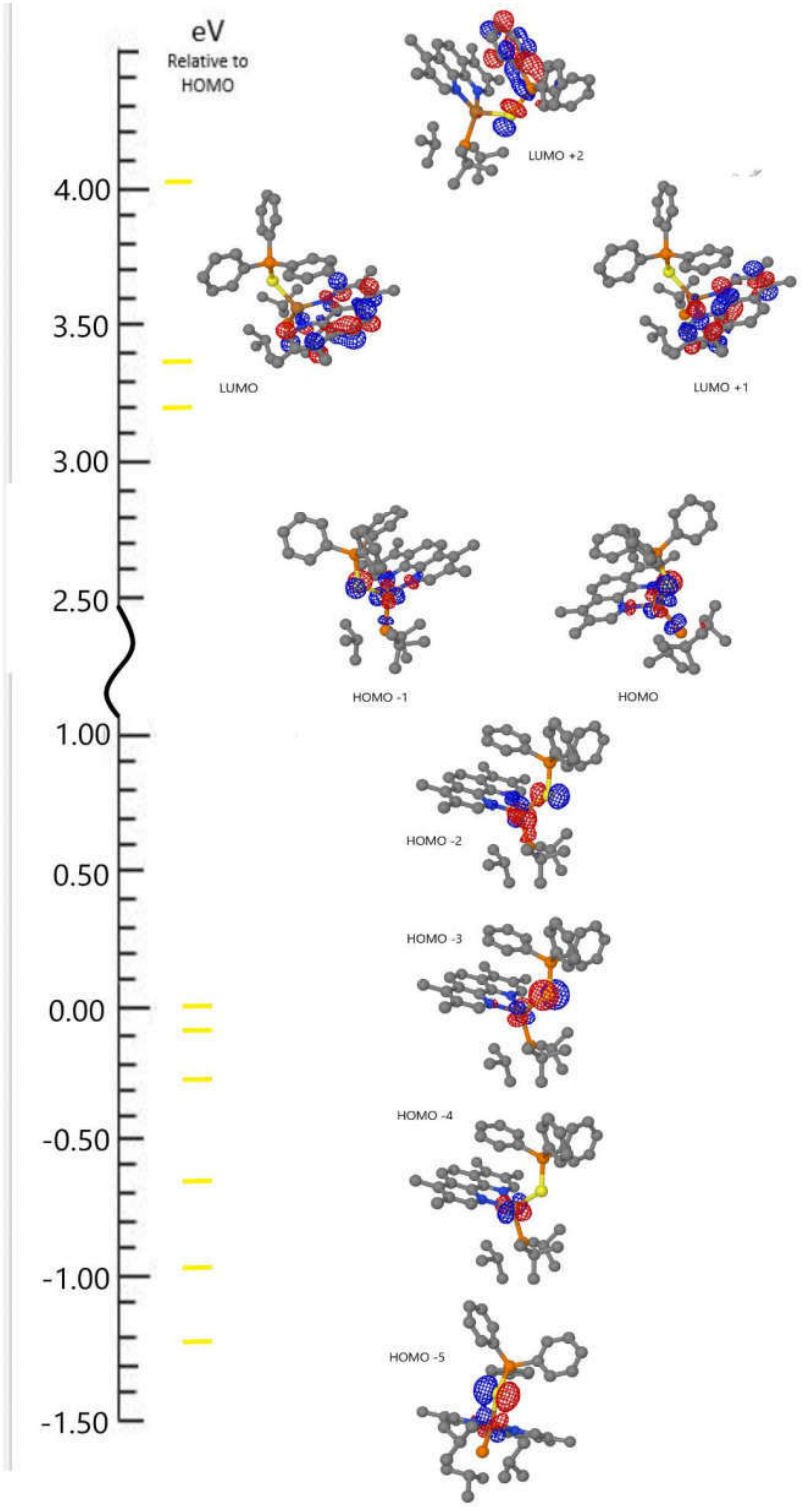

The complexation with thiourea led to the investigation of other potential neutral sulfide donor ligands as it was thought that these types of sulfides are chemically similar to the desired metal bound sulfido ligand of the target complex. One of these was triphenylphosphine sulfide for which complexes with d^{10} metals have been reported.[67,68,69] The reaction of the trigonal planar complex with triphenylphosphine sulfide led to the formation of intractable blue and white solids despite repeated attempts at its crystallization. However, DFT investigation might render an explanation as to why this complex failed to form. The DFT minimized structure, show in **Figure 63** below, indicates a π-stacking interaction between the diimine π-system and one phosphine bound phenyl ring. It further suggests a Cu-S bond length of 2.51 Å, which is a longer bond length than that found in the trigonal planar homoleptic complex of this ligand with copper, which was reported by Wu et al. as 2.2559 Å and 2.2600 Å for two inequivalent bonds. The P-S-Cu bond angle of the minimized DFT structure is 121.1 ° which is comparable to those reported by Wu which average 119.767 °. [69]

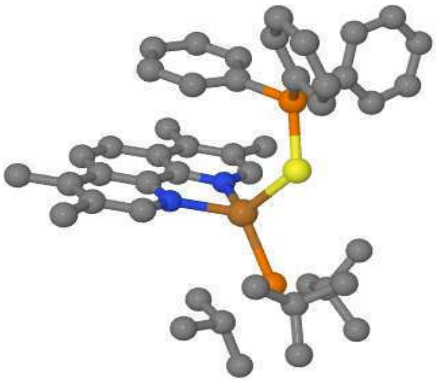

Figure 65: The DFT minimized geometry of the complex [Cu(Me4phen)(tBu3P)Ph3PS)]⁺. Grey=carbon, blue=nitrogen, brown =copper, yellow=sulfur, orange=phosphorous.

The DFT produced molecular orbitals for this structure and the examination of the first ten excited states reveals a number of intriguing interactions, seen in **Figure 62** above. One observation is that the diimine ligand is not involved in the occupied orbitals that take part in these excited states to any significant degree, with only weak Cu-N nonbonding interactions having any reported electron density. Rather the orbitals involved in the electronic excitations are largely Cu-S in character and include some P character from the $^{t}Bu_3P$ ligand in the HOMO-2. The LUMO and LUMO+1 are comparable to what has been seen in the prior example, mostly having Me_4phen π^* character. However the LUMO+2 resides entirely on the Ph_3PS ligand and is antibonding between the phosphorus and sulfur atoms. This represents a type of MLCT transition not seen in the above examples in which the charge is transferred from the copper center to the incoming fourth ligand rather than onto the diimine ring system as it was in every previously isolated complex. With reports of the chemistry of the triphenylphosphine sulfide complex being rare no speculation will be made as to the fate of the species involved in this reaction.

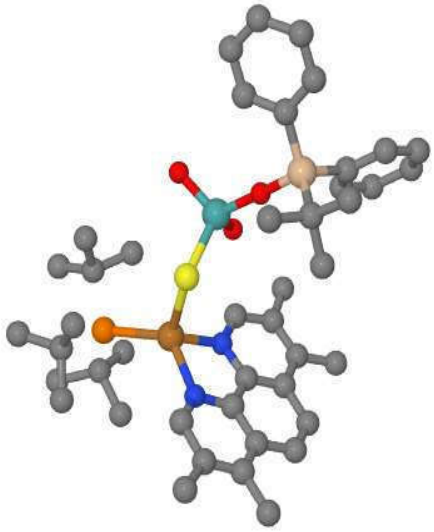

Figure 66: The DFT minimized structure of the target complex [Cu(Me$_4$phen)(^{t}Bu$_3$P)](μ-s)[MoO$_2$(OSiPh$_2$^{t}Bu)]. Grey = carbon, blue = nitrogen, red = oxygen, yellow = sulfur, tan = silicon, orange = phosphorous, brown = copper.

The structure and electronics of the triphenylphosphine sulfide complex are quite similar to that of the target complex, [Cu(Me_4phen)($^{t}Bu_3P$)](μ-S)[MoO_2(OSiPh$_2$^{t}Bu)], which has also undergone DFT investigation. The DFT minimized structure of the target complex suggests a Cu-S bond length of 2.51 Å, which is identical to the triphenylphosphine sulfide complex above but

with a slightly smaller Cu-S-Mo angle of 113.3 °. The organization of the molecular orbitals is also quite similar to the Ph_3PS complex, though differ energetically. The occupied orbitals that take part in the first ten excited states all have significant Cu-S character, and while the first two unoccupied orbitals are diimine π* orbitals the LUMO+2 sits entirely of the monothiomolybdate center. This excitation represents a similar kind of MLCT as that seen for the triphenylphosphine complex in that the copper electron is being transferred to a fully oxidized ligand. Given that the calculated band gap for the triphenylphosphine sulfide complex and the target complex are 3.2 eV and 2.95 eV respectively, while the triphenylphosphine sulfide may be more capable of delocalizing this excited electron through its phenyl ligands, the thiomolybdate orbitals in the excited state of the target complex are highly localized and could yield the reduction of the Mo(VI) to Mo(V) and the fracturing of the complex.

Heterobimetallic Coupling Reactions:

While the target complex has not been isolated in the solid state there is evidence from the reaction samples in ^{1}H and ^{31}P NMR that some interaction is occurring between the copper cation and the silylmolybdate anion based on the coupling constant and peak positions discussed above. The ^{31}P NMR shows the broad peak for the acetonitrile complex in its usual position as well as a new peak located at 65.89 ppm vs the PPN cation at 21.80 ppm, this peak is comparable to the shift observed for the azide complex. The proton NMR data shows two sets of peaks for the phosphine protons which is also consistent with the two phosphine peaks in the ^{31}P spectrum. The phosphine proton peaks are found at 1.26 and 1.32 ppm with coupling constants of 12.1 Hz and 12.3 Hz respectively. These peak positions and coupling constants are comparable to those of the azide and thiocyanate bound complexes and are accompanied by significant broadening and unusual splitting for the Me_4phen aromatic and methylene protons. Such splitting would be

Figure 67: NMR spectra of the reaction of [Cu(Me$_4$phen)(^{t}Bu$_3$P)]PF$_6$ with PPN[MoO$_3$(OSiPh$_2$^{t}Bu)] showing unidentified ^{31}P peaks and a previously unseen ^{3}JP-H coupling constant

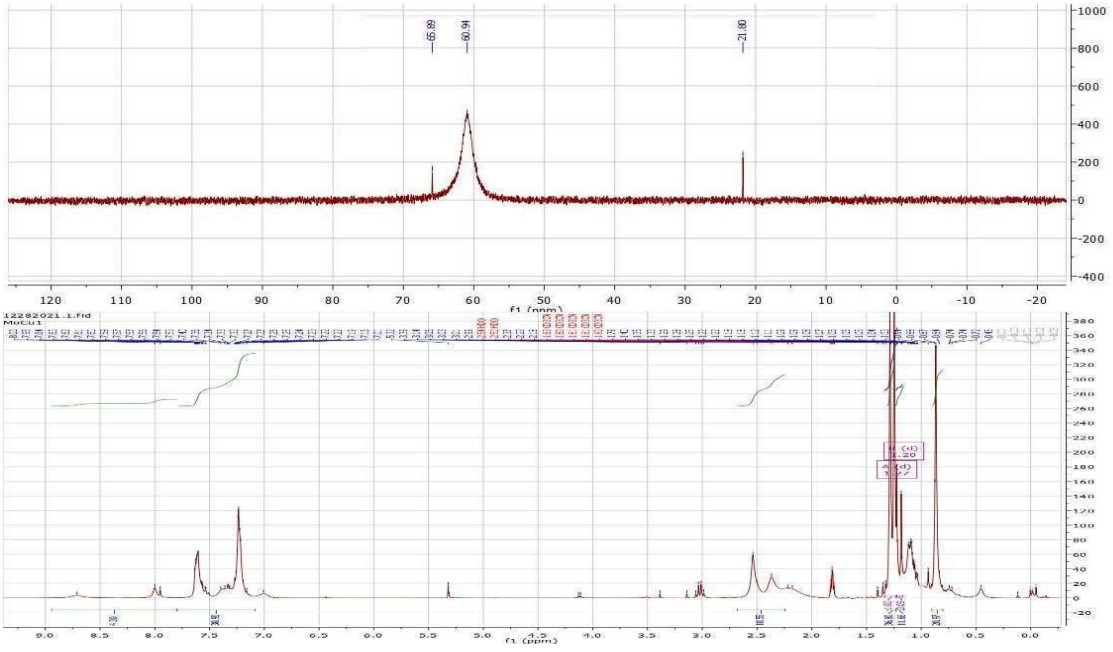

expected in the heterobimetallic complex, which would be asymmetric. Unfortunately, this solution, nor any other from similar reactions, did not produced crystals consistent with this NMR spectrum as they have shown to be quite air, moisture, and light sensitive and rapidly degrade into an intractable oxidized blue solid. Reaction mixtures stored in the freezer have produced crystals of charge neutral, cubane type clusters including the previously known $Cu_4(^tBu_3P)_4Cl_4$ and the unreported $[(O{=}Mo)Cu_3S_4(^tBu_3P)_3]$, whose structure is shown below.

Figure 68: Product Isolated from the reaction of [Cu(Me4phen)(tBu3P)]PF6 and PPN[MoO3(OSiPh2tBu)]. Grey = carbon, red = oxygen, yellow = sulfur, orange = phosphorous, Dark Orange = copper

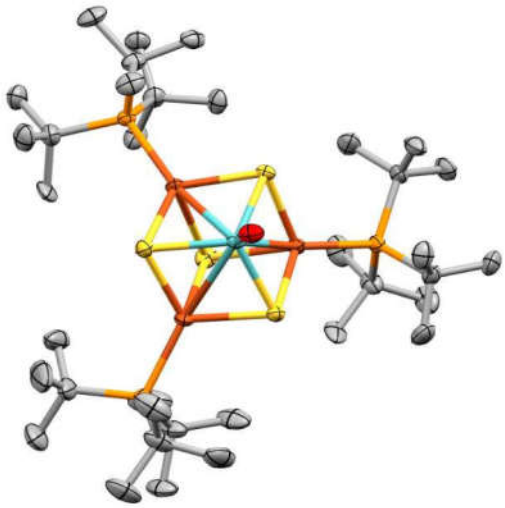

Figure 69: The orbitals involved in the first ten excited states of the target complex

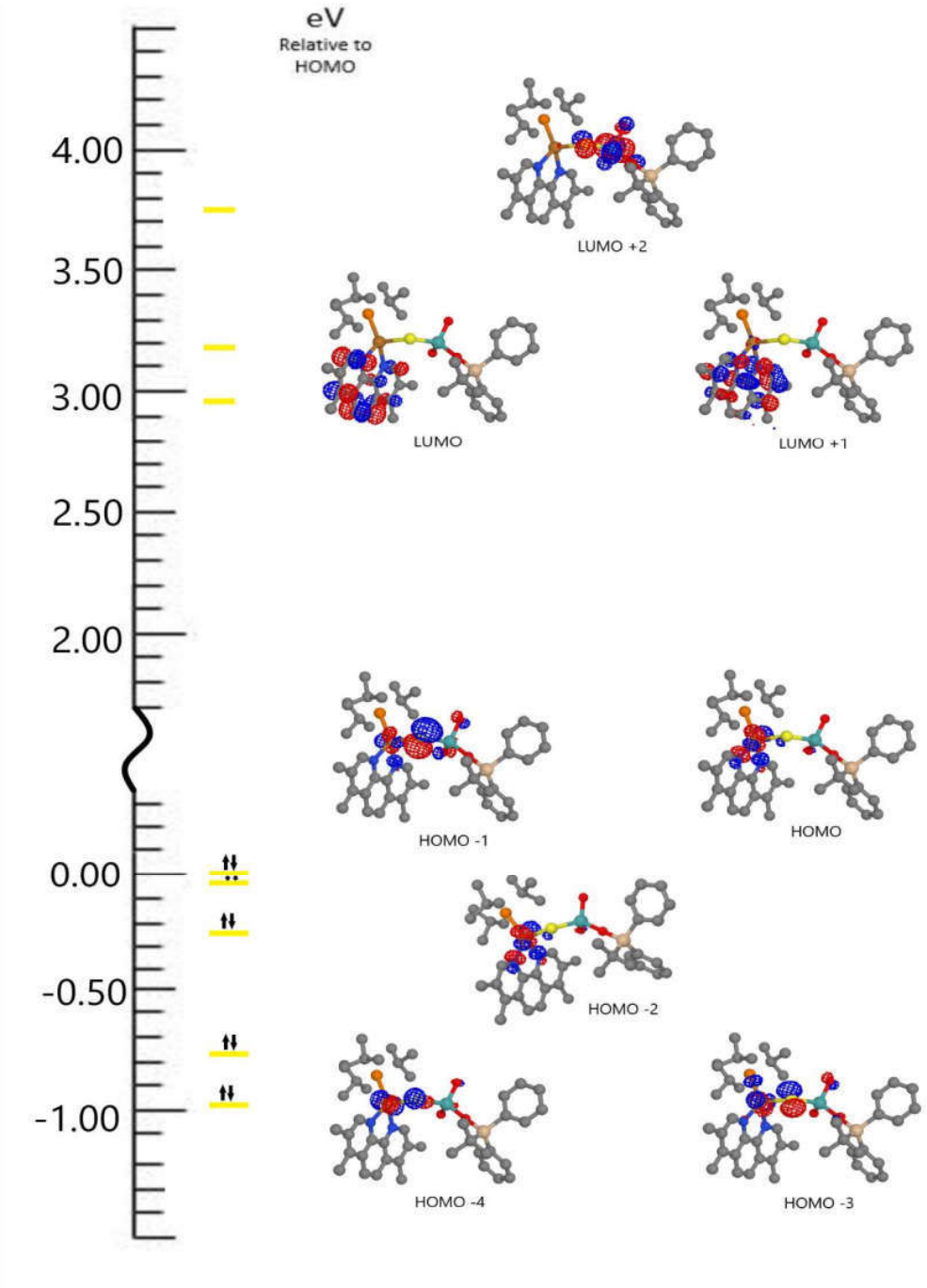

References:

(1) Britannica, The Editors of the Encyclopedia. "Copper" Encyclopedia Britannica. July 2023. https://www.britannica.com/science/copper.

(2) Pearce, M. "The Copper Age-A History of the Concept." *J. World Prehist*. **2019**. 32. 229-250. https://doi.org/10.1007/s10963-019-09134-z

(3) Emsley, J. "Natures Building Blocks: An A-Z Guide to the Elements" Oxford University Press. 2011.

(4) DiMucci, I. M.; Lukens, J.T.; Chatterjee, S.; Carsch, K.M.; Titus, C.J.; Lee, S.J.; Nordlund, D.; Betley, T.A.; MacMillan, S.N.; Lancaster, K.M. "The Myth of d8 copper(III)." *J. Am. Chem. Soc*. **2019**. 141. 18508-18520. https://doi.org/10.1021/jacs.9b09016

(5) Lie, H.; Shen, Q. "Well-defined organometallic Cu(III) complexes: Preparation, Characterization and reactivity." *Coord. Chem. Rev*. **2011**. 439. 213923. https://doi.org/10.1016/j.ccr.2021.213923

(6) Bera, M.; Kaur, S.; Keshari, K.; Santra, A.; Moonshiram, D.; Paria, S. "Structural and Spectroscopic Characterization of Copper(III) Complexes and Subsequent One-Electron Oxidation Reaction and Reactivity Studies." *Inorg. Chem*. **2023**. 62(14) 5387-5399. https://doi.org/10.1021/acs.inorgchem.2c04168

(7) Bard, A.J.; Parsons, R.; Jordan, J. "Standard Potentials in Aqueous Solutions." CRC Press. **1985**.

(8) Lee, H.; Wu, X.; Sun, L. "Copper-based homogeneous and heterogeneous catalysts for electrochemical water oxidation." *Nanoscale*. **2020**. 12(7). 4187-4218. https://doi.org/10.1039/c9nr10437b

(9) Barnett, S.M.; Goldberg, K.I.; Mayer, J.M. "A soluble copper–bipyridine water-oxidation electrocatalyst." *Nat. Chem*. **2012**. 4. 498-502. https://doi.org/10.1038/NCHEM.1350

(10) Najafpour, M.M.; Mehrabani, S.; Mousazade, Y.; Holynska, M. "Water oxidation by a copper(II) complex: new findings, questions, challenges and a new hypothesis." *Dalton Trans*. **2018**. 47. 9021-9029. https://doi.org/10.1039/c8dt01876f

(11) Zhang, R.; Chen, Y.; Ding, M.; Zhao, J. "Heterogeneous Cu catalyst in organic transformations." *Nano Res*. **2022**. 15(4). 2810-2833. https://doi.org/10.1007/s12274-021-3935-5

(12) Dinka Mulugeta. "A Review on Recent Trends in Copper-Catalyzed Organic Synthesis. *Journal of Chemical, Environmental and Biological Engineering*." **2022**. 6(1). 24-33. https://doi:.org/10.11648/j.jcebe.20220601.14

(13) Wang, J.; Li, Z.; Luo, Z.; Huang, Y.; Ma, F.; Kupfer, S.; Ouyang, G. "Boosting CO2 photoreduction by π–π-induced preassembly between a Cu(I) sensitizer and a pyrene-appended Co(II) catalyst." *PNAS*. **2023**. 120(13). https://doi.org/10.1073/pnas.2221219120

(14) Dumer, F.; "Recent advances in organic light-emitting devices comprising copper complexes: A realistic approach for low-cost and highly emissive devices?" *Org. Electron.* **2015**. 21. 27-39. http://dx.doi.org/10.1016/j.orgel.2015.02.026

(15) Oladipo, S.D.; Omondi, B. "Pseudo-Tetrahedral Copper(I) Symmetrical Formamidine Dithiocarbamate-Phosphine Complexes: Antibacterial, Antioxidant and Pharmacokinetics Studies" *Inorganics*. **2022**. 10(79). https://doi.org/10.3390/inorganics10060079.

(16) Normant, J.F. “Stoichiometric Versus Catalytic Use of Copper(I) Salts in the Synthetic Use of Main Group Organometallics.” *Pure and Appl. Chem*. **1978**. 50. 709-715. https://doi.org/10.1016/B978-0-08-022035-2.50015-3
(17) Thirumurugan, P.; Matosiuk, D.; Jozwiak, K. “Click Chemistry for Drug Development and Diverse Chemical−Biology Applications.” *Chem. Rev*. **2013**. 113. 4905-4979. dx.doi.org/10.1021/cr200409f
(18) Sheokand, S.; Mohite, M.A.; Mondal, D.; Rangarajan, S.; Balakrishna, M. S. “ 1,2,3-Triazolyl bisphosphine with pyridyl functionality: synthesis, copper(I) chemistry and application in click catalysis” *New J. Chem*. **2023**. 47. 13538-13546. https://doi.ord/10.1039/d3nj01445b.
(19) Lu, C.; Zeng, A.; Wang, Y.; Wang, A. “Copper-Based Catalysts for Selective Hydrogenation of Acetylene Derived from Cu(OH)2” *ACS Omega*. **2021**. 6. 3363−3371. https://dx.doi.org/10.1021/acsomega.0c05759
(20) Olivares, M.; Uauy, R. “Copper as an essential neutriant” *Am. J. Clin. Nutr*. **1996**. 63(5). 791S-796S. https://doi.org/10.1093/ajcn/63.5.791
(21) Messerschmidt, A. “Copper Metalloenzymes” *Comprehensive Natural Products II* **2010**. 489-545. https://doi.org/10.1016/B978-008045382-8.00180-5.
(22) Randall, D.W; Gamelin, D.R.; LaCroix, L.B.; Solomon, E.I. “Electronic structure contributions to electron transfer in blue Cu and CuA” *J. Biol. Inorg. Chem*. **2000**. 5. 16-19. https://doi.org/10.1007/s007750050003
(23) Snowdon, N.; Sharp, D.; Currie, J. “Green metals: Copper is the New Oil” Goldman Sachs Commodities Research. (**2021**). https://www.goldmansachs.com/intelligence/pages/gs-research/copper-is-the-new-oil/report.pdf. Accessed 19 July 2023.
(24) Gourlay, C. Nielsen, D.J.; White, J.M.; Kottenbelt, S.Z.; Kirk, M.L.; Young, C.G. “Paramagnetic Active Site Models for the Molybdenum−Copper Carbon Monoxide Dehydrogenase.” *J. Am. Chem. Soc*. **2006**. 128(7). 2164-2165. DOI: 10.1021/ja056500f
(25) Xu, K.; Hirao, H. “Revisiting the catalytic mechanism of Mo–Cu carbon monoxide dehydrogenase using QM/MM and DFT calculations.” *Phys. Chem. Chem. Phys.* **2018**. 20. 18938-18948. DOI: 10.1039/c8cp00858b
(26) Rovaletti, A.; Bruschi, M.; Moro, G.; Cosentino, U.; Greco, C.; Ryde, U. “Theoretical Insights into the Aerobic Hydrogenase Activity of Molybdenum–Copper CO Dehydrogenase” *Inorganics*. **2019**. 7(11). 135. doi.org/10.3390/inorganics7110135
(27) Rovaletti, A.; Moro, G.; Consentino, U.; Ryde, U.; Greco, C. “Can Water Act as a Nucleophile in CO Oxidation Catalysed by Mo/Cu CO-Dehydrogenase? Answers from Theory*” Chem. Phys. Chem*. **2022**. 23. https://doi.org/10.1002/cphc.202200053
(28) Rubino, J.T.; Franz, K.J. “Coordination chemistry of copper proteins: How nature handles a toxic cargo for essential function” *J. Inorg. Biochem*. **2012**. 107. 129-143. https://doi.org/10.1016/j.jinorgbio.2011.11.024
(29) Cope, J.D.; Valle, H.U.; Hall, R.S.; Riley, K.M.; Goel, E.; Biswas, S.; Hendrich, M.P.; Wipf, D.O.; Stokes, S.L.; Emerson, J.P. “Tuning the Copper(II)/Copper(I) Redox Potential for More Robust Copper-Catalyzed C–N Bond Forming Reactions” *Eur, J. Inorg. Chem*. **2020** 1278-1285. https://doi.org/10.1002/ejic.201901269

(30) McMillin, D.R.; Buckner, M.T.; Ahn, B.T. "A Light-induced redox reaction of bis(2,9-dimethyl-1,10-phenantroline) copper(I)" *Inorg. Chem*. **1977**. 16(4). 943-945. https://doi.org/10.1021/j100655a006
(31) Day, P.; Sanders, N. "The Spectra of Complexes of Conjugate Ligands. Part I: Charge-transfer in phenanthroline complexes: energy shifts on substitution" J. Chem. Soc. A. **1967**. 1530-1536. https://doi.org/10.1039/J19670001530
(32) Vlcek, A Jr. "Mechanistic roles of metal-to-ligand charge-transfer excited states in organometallic photochemistry." *Coord. Chem. Rev*. **1998**. 177. 219-256. https://doi.org/10.1016/S0010-8545(98)00187-8
(33) Vogler, A.; Kunkely, H. "Photoreactivity of metal-to-ligand charge transfer excited states" *Coord. Chem. Rev*. **1998**. 177. 81-96. https://doi.org/10.1016/S0010-8545(98)00131-3
(34) Ruthkosky, M.; Kelly, C.A.; Castellano, F.N.; Meyer, G.J. "Electron and energy transfer from Cu I MLCT excited states" *Coord. Chem. Rev*. **1998**. 177. 309-322. https://doi.org/10.1016/S0010-8545(98)90045-5
(35) Grupe, M.; Bäppler, F.; Thieß, M.; Busch, J.M.; Dietrich, F.; Volz, D.; Gerhards, M.; Bräse, S.; Diller, R. "Real-time observation of molecular flattening and intersystem crossing in [(DPEPhos)Cu(I)(PyrTet)] via ultrafast UV/Vis- and mid-IR spectroscopy on solution and solid samples." *Phys. Chem. Chem. Phys*. **2020**. 22. 14187-14200. https://doi.org/10.1039/c9cp05749h
(36) Garakyaraghi, S.; Koutnik, P.; Castellano, F.N. "Photoinduced structural distortions and singlet–triplet intersystem crossing in Cu(I) MLCT excited states monitored by optically gated fluorescence spectroscopy" *Phys. Chem. Chem. Phys.* **2017**. 19. 16662-16668. https://doi.org/10.1039/C7CP03343E
(37) Paderina, A.; Melnikov, A.; Slavova, S.; Sizov, V.; Gurzhiy,; Petrovskii, S.; Luginin, M.; Levin, O.; Koshevoy, I.; Grachova, Elena. "The Tail Wags the Dog: The Far Periphery of the Coordination Environment Manipulates the Photophysical Properties of Heteroleptic Cu(I) Complexes." *Molecules*. **2022**. 27. 2250. https://doi.org/10.3390/ molecules27072250
(38) Cortés, P.A.F.; Marx, M.; Trose, M.; Beller, M. "Heteroleptic copper complexes with nitrogen and phosphorus ligands in photocatalysis: Overview and perspectives." *Chem. Catal*. **2021**. 1. 298-338. https://doi.org/10.1016/j.checat.2021.05.005
(39) Hamze, R.; Jazzar, R.; Soleilhavoup, M.; Djurovich, P.; Bertrand, G.; Thompson, M.E. "Phosphorescent 2-, 3- and 4-coordinate cyclic (alkyl)(amino)carbene (CAAC) Cu(I) complexes" *Chem. Comm*. **2017**. 53. 9008-9011. https://doi.org/10.1039/c7cc02638b
(40) Bissember, A.C.; Lundgren, R.L.; Creutz, S.E.; Peters, J.C.; Fu, G.C. "Transition-Metal-Catalyzed Alkylations of Amines with Alkyl Halides:Photoinduced, Copper-Catalyzed Couplings of Carbazoles.' *Angew. Chem. Int. Ed.* **2013**. 52. 5129-5133. https://doi.org/10.1002/anie.201301202
(41) Clausing, S.T.; Salazar, D.M.; Orthaber, A. "Preparation, photo- and electrochemical studies of a homoleptic iminephosphaalkene Cu(I) complex" *Inorganica. Chim. Acta*. **2020**. 513. 119958 https://doi.org/10.1016/j.ica.2020.119958
(42) Marion, R.; Sguerra, F.; Meo, F.D.; Sauvageot, E.; Lohier, J.; Daniellou, R.; Renaud, J.; Linares, M.; Hamel, M.; Gaillard, S. "NHC Copper(I) Complexes Bearing Dipyridylamine Ligands:Synthesis, Structural, and Photoluminescent Studies" *Inorg. Chem*. **2014**. 53. 9181-9191. dx.doi.org/10.1021/ic501230miie

(43) Elie, M.; Sguerra, F.; Meo, F.D.; Weber, M.D.; Marion, R.; Grimault, A.; Lohier, J.; Stallivieri, A.; Brosseau, A.; Pansu, R.B.; Renaud, J.; Linares, M.; Hamel, M.; Costa, R.D.; Gaillard,S. "Designing NHC–Copper(I) Dipyridylamine Complexes for Blue Light Emitting Electrochemical Cells" *ACS. Appl. Mater. Interfaces*. **2016**. 8. 14678-14691. https://doi.org/10.1021/acsami.6b04647.

(44) Mauro, A.E.; Porta, C.C.; Ananias, S.P.; Sargentelli, V.; Santos, R.H.; Gambardella, T. "Synthesis and Structural Studies of (1, 10-phenanthroline)(thiocyanate-N)-(triphenylphosphine) Copper(I)." *J. Coord. Chem.* **1999**. 49. 9-15. https://doi.org/10.1080/00958979908024370

(45) Hu, L.; Shen, C.; Chu, W.; Xiang, J.; Yu, F.; Xiang, G.; Nie, Y.; Kwok, C.; Leung, C.; Ko, C. "Synthesis, structures and photophysical properties of Cu(I) phosphine complexes with various diimine ligands." *Polyhedron*. **2017**. 127. 203-211. http://dx.doi.org/10.1016/j.poly.2017.01.046.

(46) Alvarez, N.; Noble, C.; Torre, M.H.; Kremer, E.; Ellena, J.; Araujo, M.P.; Costa-Filho, A.J.; Mendes, L.F; Kramer, M. G.; Facchin, G. "Synthesis, structural characterization and cytotoxic activity against tumor cells of heteroleptic copper (I) complexes with aromatic diimines and phosphines" *Inorg. Chim. Acta.* **2017**. 466. 559-564. http://dx.doi.org/10.1016/j.ica.2017.06.050

(47) Ziolo, R.F.; Guaghan, A.P.; Dori, Z.; Pierpont, C.G. Eisenberg, R. "The Crystal and Molecular Structure of μ-diazido-tatrakis(triphenylphosphine)dicopper(I)". Inorg. Chem. **1971**. 10(6). 1289-1296. https://doi.org/10.1021/ic50100a038

(48) Kubas, G.J.; Monzyk, B.; Crumblis, A.L. "Tetrakis(Acetonitrile) Copper(1+) Hexafluorophosphate (-1)" Inorganic Syntheses, **1990**. R.J. Angelici (Ed.). https://doi.org/10.1002/9780470132593.ch15

(49) Kritchenkov, I.S.;Shakirova, J.R.; Tunik, S.P. "Efficient one-pot Green synthesis of tetrakis(acetonitrile)copper (I) complex in aqueous media." *RSC Adv*. **2019**. 9. 15531-15535. https://doi.org/10.1039/C8RA10564B

(50) Paul, G.C.; Das, K.; Maity, S.; Begum, S.; Srivastava, H.K.; Mukherjee, C. "Geometry-Driven Iminosemiquinone Radical to Cu(II) Electron Transfer and Stabilization of an Elusive Five-Coordinate Cu(I) Complex: Synthesis, Characterization, and Reactivity with KO_2" *Inorg. Chem.* **2019**. 58(3). 1782-1793. DOI:10.1021/acs.inorgchem.8b01931

(51) Gagne, R.R.; Allison, J.L.; Gall, R.S.; Koval, C.A. "Models for Copper-Containing Proteins: Structure and Properties of Novel Five-Coordinate Copper(I) Complexes." *J. Am. Chem. Soc*. **1977**. 99(22). 7170-7178. DOI: 10.1021/ja00464a012.

(52) Sakuri, T.; Kimura, M.; Nakahara, A. "A Facile Reduction of Cu(II) leading to Formation of Stable Cu(I) Complexes. Redox Properties of Four- and Five-coordinate Copper Complexes." *Bull. Chem. Soc. Jpn.* **1981**. 54(10). 2976-2978. https://doi.org/10.1246/bcsj.54.2976.

(53) Pettinari, C.; Nicola, C.; Marchetti, F.; Pettinari, R.; Skelton, B.W.; Somers, N.; White, A.H.; Robinson, W.T.; Chierotti, M.R.; Gobetto, R.; Nervi, C. "Synthesis, Characterization, Spectroscopic and Photophysical Properties of New [Cu(NCS){(L-N)$_2$ or (L'-N^N)}(Ph_3P)] complexes (L-N, L'-N^N = Aromatic nitrogen base). *Eur. J. Inorg. Chem.* **2008.** 1974-1984. DOI: 10.1002/ejic.200701236

(54) Akers, C.; Peterson, S.W.; Willett, R.D. "A refinement of the crystal structure of KSCN." *Acta Cryst.* **1968**. . B24. 1125-1126. https://doi.org/10.1107/S0567740868003808
(55) Macintyre, J. *Dictionary of Inorganic Compounds*. Chapman and Hall, London. **1992**. 3. 3103.
(56) Lobana, T.A.; Singh, G.; Nishikoa, T. "Copper-Sulfur Interactions: Synthesis and Structure of a trigonal Planar Copper(I) Complex with Bis(diphenylthiophosphinyl)methane, [Cu(dppmS_2)]•MeCN" *J. Coord. Chem.* **2004**. 57(11). 955-960. DOI: 10.1080/00958970412331272368
(57) Lobana, T.S.; Mahajan, R.; Castineiras, A. "Metal-phosphine chalcogenide interactions. Crystal and molecular structure of [di-μ-iodo-bis{methyl cyanide-N}(triphenylthiophosphorane-S)copper(I)}] and [di-μ-chloro-bis[μ-1,2-ethylenebis(diphenylphosphine selenide- Se,Se,)}dicopper(I)]." *Transit. Met. Chem.* **2001**. 26. 440-444. https://doi.org/10.1023/A:1011081632766
(58) Noren, B.; Oskarsson, A. Bond length variations in Tetrahydrothiphene Solvates of the Coinage Metals. The Crystal Structure of Di-μ-iodo-bis[bis(tetrahydrothiophene)copper(I)]." *Acta. Chem. Scand.* **1987**. A41. 12-17. 10.3891/acta.chem.scand.41a-0012
(59) Lovas, F.J.; Tiemann, E.; Coursey, J.S.; Kotochigova, S.A.; Chang, J.; Olsen, K.; Dragoset, R.A. "Diatomic Spectral Database NIST Standard Reference Database 114." DOI: https://dx.doi.org/10.18434/T4T59X.
(60) Khan, S.A.; Khan, E.; Qayyum, S.; Noor, A. "Synthesis and Crystal structure of Chlorido-bridged binuclear Cu(I) complexes with carbodithioate-type ligands." *Crystals*. **2023**. 13(2). 322. https://doi.org/10.3390/cryst13020322
(61) Kuang, S.; Zhang, Z.; Wang, Q.; Mak, T.C.W. "Novel binuclear copper(I) complexes with unusual azide and thiocyanate bridges. Crystal structures of [Cu2(μ-Ph2Ppypz)2(μ-1,1-N3)]-[ClO4]•Et2O and [Cu2(μ-Ph2Ppypz)2(μ-1,1-SCN)][ClO4] [Ph2Ppypz=2-(diphenylphosphino)-6-(pyrazol-1-yl)pyridine]" *J. Chem. Soc., Dalton Trans*. **1997** 4477-4478. https://doi.org/10.1039/A706986C
(62) Fehlhammer, W.P.; Beck, W. "Azide Chemistry – An Inorganic Perspective, Part I Metal Azides:Overview, General Trends and Recent Developments" *Z. Anorg. Allg. Chem*. **2013**. 639(7). 1053-1082. https://doi.org/10.1002/zaac.201300162
(63) Tolman, C.A. "Phosphorus Ligand Exchange Equilibria on Zerovalent Nickel A Dominant Role for Steric Effects" *J. Am. Chem. Soc*. **1970**. 92(10). https://doi.org/10.1021/ja00713a007.
(64) Bergmann, L.; Braun, C.; Nieger, M.; Bräse, S. "The coordination- and photochemistry of copper(I) complexes: variation of N^N ligands from imidazole to tetrazole." *Dalton Trans*. **2018**. 47. 608-621. DOI:
(65) Zhang, Q.; Ding, J.; Cheng, Y.; Wang, L.; Xie, Z.; Jing,; Wang, F. "Novel Heteroleptic, CuI Complexes with Tunable Emission Color for Efficient Phosphorescent Light-Emitting Diodes." *Adv. Funct. Mater.* **2007**. 17. 2983-2990. DOI: 10.1002/adfm.200601053
(66) Zhao, Y.; Chai, W.; Song, L.; Zhang, Y.; Shi, H.; Tao, X.; Shu, K. "Facile preparation of a three-coordinate copper(I) complex: steric hinderance, supramolecular structure, optical property, and TD-DFT study." *Phosphorous Sulfur Silicon Relat. Elem.* **2016**. 191(8). 1123-128. https://doi.org/10.1080/10426507.2016.1146274.

(67) Ainscough, E.W.; Brodie, A.M.; Freeman, G.H.; Plieger, P.G. "Structural Studies of tribenzylphosphane sulfide complexes of copper(I) and silver(I)." *Polyhedron*. **2016**. 106. 40-43. http://dx.doi.org/10.1016/j.poly.2015.12.010
(68) Tiethof, J.A.; Hetey, A.T.; Meek, D.W. "Three-coordinate Copper(I) Complexes of Tertiary Phosphine Sulfide, Phosphine selenide and Arsine Sulfide Ligands." *Inorg. Chem*. **1974**. 13(10). 2505-2509 https://doi.org/10.1021/ic50140a039
(69) Wu,H.; Qu, Y.; Wang, C.; Wu, Y.; Zhao, K. "Mononuclear copper(I) and binuclear silver(I) complexes of SPPh3 ligand: synthesis, crystal structure, and properties." *Phosphorous Sulfur Silicon Relat. Elem*. **2019**. 195(2). 88-95. DOI: 10.1080/10426507.2019.1635597

Appendix A: Chapter 2 Supplementary Information

Computational Information:

The Computations were performed using Gaussian09 on the Tulane Cypress Central Computing Core or the WebMO service. The initial input geometries were generated *de novo* as the idealized tetrahedral anions then underwent geometry optimization under the B3LYP level of theory, using the LANL2dz basis set for the molybdenum center and 6-311++G(2d,2p) for the oxygen or sulfur atoms. The calculations were performed with no symmetry restrictions, first at the "loose" level of geometry optimization, then at the standard level of geometry optimization. The geometry that was output from this process was then used as the input for the PBE0 and MP2 input geometry, these were optimized with the Calcall keyword at the "tight" then "verytight" optimization level. After a "verytight" optimization was achieved a "freq" calculation was run and the thermodynamic outputs were taken from this output file. The results of the "verytight" calculations on the isolated anions had the cations added to them which were modeled *de novo*. The charge neutral ion pairs were then put through the same process as the isolated anions with the cations atoms, that is potassium or nitrogen, carbon, and hydrogen using the 6-31++G(2d,2p) basis set. The process was reported for hexamethyldisilathiane and hexamethyldisiloxane, as well as H_2S and H_2O. Each element also underwent the same process to obtain the values required for the calculations by method 2, described in chapter 2. The fully optimized outputs from the above calculations were then reoptimized under solvation conditions with SCRF=(PCM, solvent="solvent") with acetonitrile and methanol. After optimization the freq calculation was executed on these reoptimized structures. The optimized atomic coordinates are supplied below:

MoO_4 Gas Phase Isolated Anion B3LYP

Mo	2E-5	0	0
O	1.78132	-0.00203	0.15224
O	-0.65038	-1.55717	0.59031
O	-0.45125	0.22226	-1.71556
O	-0.67979	1.33694	0.97298

MoO_3S Gas Phase Isolated Anion B3LYP

Mo			
S	-2.0291	1E-5	1E-5
O	0.88166	1.63124	-0.26581
O	0.88161	-1.04582	-1.27979
O	0.88166	-0.58543	1.54559

MoO_2S_2 Gas Phase Isolated Anion B3LYP

Mo	0	0.2673	0
S	1.86754	-0.99732	1E-5

S	-1.86754	-0.99732	-1E-5
O	2E-5	1.29297	-1.41107
O	-2E-5	1.29298	1.41107

$MoOS_3$ Gas Phase Isolated Anion B3LYP

Mo	-3E-5	-3E-5	0.20356
S	1.58133	-1.39829	-0.50055
S	-2.00173	-0.67014	-0.50053
S	0.42045	2.06855	-0.50047
O	6E-5	-9E-5	1.93441

MoS_4 Gas Phase Isolated Anion B3LYP

Mo	0	0	0
S	-0.94042	1.92885	-0.49194
S	-0.01987	-0.29075	2.18218
S	2.07962	-0.00794	-0.72249
S	-1.11933	-1.63016	-0.96776

MoO_4 Isolated Anion B3LYP Acetonitrile

Mo	-0.00175	-0.0019	-6.3E-4
O	2.8E-4	0.00408	1.8277
O	1.72285	-0.00266	-0.60618
O	-0.86307	1.48758	-0.61644
O	-0.86172	-1.49546	-0.6083

MoO_3S Isolated Anion B3LYP Acetonitrile

Mo	-7E-5	0	0.00458
S	-3.3E-4	1E-5	2.34021
O	1.69243	0	-0.62364
O	-0.84602	1.46571	-0.62307
O	-0.846 -	1.46573	-0.62306

MoO_2S_2 Isolated Anion B3LYP Acetonitrile

Mo	0.00475	-0.00325	0.00483

S	-0.0072	0.0014	2.29511
S	2.13965	0.00414	-0.82323
O	-0.86572	1.44409	-0.59823
O	-0.85598	-1.45842	-0.59311

$MoOS_3$ Isolated Anion B3LYP Acetonitrile

Mo	0.07256	0	-0.0238
S	0.10245	0	2.24134
O	1.75763	1E-5	-0.62525
S	-0.96634	1.85433	-0.79614
S	-0.96631	-1.85434	-0.79615

MoS_4 Isolated Anion B3LYP Acetonitrile

Mo	-0.00223	-1E-5	-0.0017
S	0.00623	1E-5	2.24703
S	2.12045	1E-5	-0.74309
S	-1.06222	1.83346	-0.75111
S	-1.06222	-1.83348	-0.75112

MoO_4 Isolated Anion B3LYP Methanol

Mo	0.00116	-5.9E-4	-2.9E-4
O	-0.96227	0.00458	-1.51406
O	1.68638	-0.50191	-0.35779
O	-0.73475	-1.14775	1.16608
O	0.00455	1.64818	0.70728

MoO_3S Isolated Anion B3LYP Methanol

Mo	0.2708	1.3E-4	3.1E-4
S	-2.02012	0.00232	0.00136
O	0.86803	-0.42118	-1.61681
O	0.87139	-1.19176	1.16927
O	0.8791	1.60764	0.44321

MoO_2S_2 Isolated Anion B3LYP Methanol

Mo	0	0.26967	0
S	1.86808	-1.00103	0
S	-1.86809	-1.00103	0
O	1E-5	1.29418	-1.43108
O	0	1.29417	1.43109

$MoOS_3$ Isolated Anion B3LYP Methanol

Mo	-0.00806	-0.0013	0.01371
S	0.33246	0.35993	2.19816
S	1.939	-0.34593	-1.02493
S	-1.08151	1.73844	-0.89053
O	-1.00475	-1.42832	-0.1734

MoS_4 Isolated Anion B3LYP Methanol

Mo	0.14064	-0.15056	-0.03119
S	0.67325	-0.97648	0.03086
S	2.28024	0.75889	0.02175
S	-1.68245	0.29061	0.25725
S	-1.64021	0.32222	-0.22798

MoO_4 Isolated Anion MP2 Gas Phase

Mo	0	0	0
O	1.21856	0.78121	1.13419
O	-1.54071	-0.38543	0.92694
O	0.70799	-1.5528	-0.68492
O	-0.38583	1.15702	-1.37622

MoO_3S Isolated Anion MP2 Gas Phase

Mo	0.26706	0	0
S	-2.08638	0	0
O	0.92355	-0.63257	-1.56985
O	0.92356	-1.04324	1.33274
O	0.92357	1.67581	0.2371

MoO_2S_2 Isolated Anion MP2 Gas Phase

Mo	0	0.25839	0
S	1.92563	-1.00783	3E-5
S	-1.92564	-1.00782	-1E-5
O	7E-5	1.33734	-1.44411
O	-5E-5	1.33739	1.44407

$MoOS_3$ Isolated Anion MP2 Gas Phase

Mo	0	0	0.19898
S	1.0819	1.87446	-0.50679
S	1.08241	-1.87417	-0.50679
S	-2.16429	-3E-4	-0.50681
O	-2E-5	0	1.99615

MoS_4 Isolated Anion MP2 Gas Phase

Mo	1E-5	0	0
S	-1.23619	1.16149	1.49429
S	-0.06524	-2.1999	0.51604
S	2.13973	0.72625	0.06567
S	-0.83833	0.31216	-2.07601

MoO_4 Isolated Anion MP2 Acetonitrile

Mo	-0.00106	0	2.2E-4
O	0.00277	0	1.82852
O	1.7229	0	-0.60721
O	-0.86231	1.49143	-0.61076
O	-0.86231	-1.49143	-0.61076

MoO_3S Isolated Anion MP2 Acetonitrile

Mo	-0.00125	0.0021	-9E-5
S	0.00132	-0.00269	2.33551
O	1.69062	-9.6E-4	-0.62985
O	-0.84434	1.47078	-0.62437

O	-0.85113	-1.46072	-0.62918

MoO_2S_2 Isolated Anion MP2 Acetonitrile

Mo	0.03693	-0.06233	-0.05145
S	0.06027	-0.10739	2.23873
O	1.7229	-0.08621	-0.6636
S	-1.03363	1.78962	-0.86231
O	-0.78647	-1.53371	-0.66137

$MoOS_3$ Isolated Anion MP2 Acetonitrile

Mo	-0.00369	0.00165	-0.002
S	0.00888	-0.00215	2.25997
S	2.12341	0.00105	-0.77311
S	-1.12258	1.80301	-0.78954
O	-0.82655	-1.47954	-0.57443

MoS_4 Isolated Anion MP2 Acetonitrile

Mo	-0.00152	-2.6E-4	-0.00139
S	0.00577	5.8E-4	2.24742
S	2.12221	-5.9E-4	-0.73976
S	-1.06112	1.83229	-0.75366
S	-1.06113	-1.83373	-0.75112

MoO_4 Isolated Anion MP2 Methanol

Mo	-0.00175	-0.0019 -	6.3E-4
O	2.8E-4	0.00408	1.8277
O	1.72285	-0.00266	-0.60617
O	-0.86307	1.48758	-0.61644
O	-0.86172	-1.49546	-0.6083

MoO_3S Isolated Anion MP2 Methanol

Mo	-7E-5	0	0.00458
S	-3.3E-4	1E-5	2.34021
O	1.69243	0	-0.62364

O	-0.84602	1.46571	-0.62307
O	-0.846	-1.46573	-0.62306

MoO_2S_2 Isolated Anion MP2 Methanol

Mo	0.00475	-0.00325	0.00483
S	-0.0072	0.0014	2.29511
S	2.13965	0.00414	-0.82323
O	-0.86572	1.44409	-0.59823
O	-0.85598	-1.45842	-0.59311

$MoOS_3$ Isolated Anion MP2 Methanol

Mo	0.07256	0	-0.0238
S	0.10245	0	2.24134
O	1.75763	1E-5	-0.62525
S	-0.96634	1.85433	-0.79614
S	-0.96631	-1.85434	-0.79615

$MoOS_3$ Isolated Anion MP2 Methanol

Mo	-0.00223	-1E-5	-0.0017
S	0.00623	1E-5	2.24703
S	2.12045	1E-5	-0.74309
S	-1.06222	1.83346	-0.75111
S	-1.06222	-1.83348	-0.75112

MoO_4 Gas Phase Isolated Anion PBE0

Mo	1E-5	-2E-5	0
O	1.62711	-0.54811	-0.54492
O	0.18303	1.15151	1.37305
O	-0.96525	-1.42372	0.53489
O	-0.84492	0.8204	-1.36301

MoO_3S Gas Phase Isolated Anion PBE0

Mo	0.27247	0	0
S	-2.04535	2E-5	0

O	0.8867	-1 .48896	0.75021
O	0.88677	1.39418	0.91435
O	0.88674	0.09476	-1.66457

MoO_2S_2 Gas Phase Isolated Anion PBE0

Mo	0	0.27084	0
S	1.8827	-1.00671	3E-5
S	-1.88271	-1.0067	-2E-5
O	8E-5	1.30244	-1.42549
O	-6E-5	1.30249	1.42545

$MoOS_3$ Gas Phase Isolated Anion PBE0

Mo	0	0	0.20596
S	-1.31797	1.6733	-0.50562
S	2.1081	0.30474	-0.50563
S	-0.79014	-1.97803	-0.50563
O	-1E-5	-2E-5	1.95248

MoS_4 Gas Phase Isolated Anion PBE0

Mo	-0.54529	0.4102	0.16025
S	-0.85121	0.44098	2.33356
S	1.49166	-0.37249	-0.30588
S	-0.63209	2.48919	-0.64554
S	-2.06324	-0.83305	-0.82364

MoO_4 Isolated Anion Acetonitrile PBE0

Mo	-0.00125	0	5.5E-4
O	0.00101	-1E-5	1.78224
O	1.6779	-4E-5	-0.59378
O	-0.83879	1.45404	-0.59459
O	-0.83887	-1.45398	-0.59462

MoO_3S Isolated Anion Acetonitrile PBE0

Mo	-0.00104	-7.6E-4	-0.00128

S	-0.00195	0.00127	2.27395
O	1.65321	-3E-5	-0.6025
O	-0.82633	1.43421	-0.59902
O	-0.82411	-1.43785	-0.59681

MoO_2S_2 Isolated Anion Acetonitrile PBE0

Mo	-0.00987	-1E-5	-0.00673
S	0.02137	1E-5	2.23038
S	2.08056	2E-5	-0.80828
O	-0.84817	1.42229	-0.57371
O	-0.84813	-1.42233	-0.57369

$MoOS_3$ Isolated Anion Acetonitrile PBE0

Mo	-0.03998	-0.06611	-0.02851
S	-0.04821	-0.09029	2.18582
S	2.04628	-0.08752	-0.77024
S	-1.09733	1.72628	-0.78165
O	-0.85654	-1.48407	-0.60392

MoS_4 Isolated Anion Acetonitrile PBE0

Mo	0	0	0
S	0	0	2.19606
S	2.07108	0	-0.73114
S	-1.0405	1.78908	-0.73433
S	-1.03096	-1.7955	-0.73105

MoO_4 Isolated Anion Methanol PBE0

Mo	-0.00211	-3.4E-4	0.00129
O	0.00194	0.00263	1.78297
O	1.67639	-0.0017	-0.59484
O	-0.83979	1.45313	-0.59511
O	-0.84065	-1.45504	-0.59087

MoO_3S Isolated Anion Methanol PBE0

Mo	-0.00232	-1.3E-4	-7.6E-4
S	-6E-4	3.8E-4	2.27434
O	1.65126	2E-5	-0.6038
O	-0.82737	1.43571	-0.59671
O	-0.82687	-1.43647	-0.59615

MoO_2S_2 Isolated Anion Methanol PBE0

Mo	-0.00753	1E-5	-0.00528
S	0.02148	-3E-5	2.23177
S	2.08373	2E-5	-0.80465
O	-0.84535	1.42237	-0.57281
O	-0.84535	-1.42233	-0.57285

$MoOS_3$ Isolated Anion Methanol PBE0

Mo	0.01613	-0.01032	4.9E-4
S	-0.09384	0.03549	2.21091
S	2.07169	0.4679	-0.67792
S	-1.42785	1.42757	-0.8622
O	-0.39248	-1.60329	-0.55054

MoS_4 Isolated Anion Methanol PBE0

Mo	-5E-5	-0.00156	-3.9E-4
S	-0.1507	0.17643	2.18206
S	2.10597	-0.22943	-0.58001
S	-0.814	1.80898	-0.93642
S	-1.14129	-1.75461	-0.66521

K_2MoO_4 Gas Phase B3LYP

Mo	0	0	0
O	1.12218	-0.12487	-1.38977
K	3.2288	0	-1E-5
O	1.1222	0.12487	1.38976
O	-1.12218	-1.38977	0.12487

K	-3.2288	0	-1E-5
O	-1.12219	1.38976	-0.12486

K_2MoO_3S Gas Phase B3LYP

Mo	-0.11762	-0.16735	3E-5
S	1.10994	1.76698	1E-5
K	3.40045	-0.31515	-5E-5
O	1.04798	-1.55501	7E-5
O	-1.23855	-0.24016	-1.42341
K	-3.47336	0.05404	-6E-5
O	-1.23863	-0.2401	1.42342

$K_2MoO_2S_2$ Gas Phase B3LYP

Mo	0.24041	-1E-5	0
S	-1.03782	-1.83628	2E-5
K	-3.40575	1E-5	-2E-5
S	-1.0378	1.83628	2E-5
O	1.35242	-1E-5	-1.37622
K	3.48331	1E-5	-2E-5
O	1.35244	-1E-5	1.37621

K_2MoOS_3 Gas Phase B3LYP

Mo	-0.04171	-0.06837	-0.01006
S	0.10434	0.15944	2.19565
S	1.98873	-0.24568	-0.90027
S	-1.10476	1.67396	-0.8937
O	-0.96296	-1.55211	-0.256
K	1.51164	2.44215	-2.14211
K	-1.49591	-2.4187	2.01471

K_2MoS_4 Gas Phase B3LYP

Mo	0	2E-5	2E-5
S	-1.27784	0.21813	-1.79237

K	-3.66204	-6E-5	-5E-5
S	-1.27789	-0.21802	1.79237
S	1.27791	1.79236	0.21811
K	3.66204	-6E-5	-5E-5
S	1.27782	-1.79238	-0.21805

K_2MoO_4 Methanol B3LYP

Mo	-0.00851	0.30348	0.10847
O	0.1013	-0.68621	1.60136
K	2.79408	-0.43202	1.91684
O	1.68019	0.79344	-0.24171
O	-1.02512	1.74068	0.38677
K	-2.85953	-1.0452	-2.52647
O	-0.67948	-0.67103	-1.24906

K_2MoO_3S Methanol B3LYP

Mo	-0.03998	0	0.04189
S	-0.05464	6E-5	2.31403
K	3.22872	-3E-5	1.66281
O	1.66121	-3E-5	-0.48402
O	-0.8967	1.41525	-0.60502
K	-2.76094	1E-5	-2.05797
O	-0.89675	-1.41525	-0.60496

$K_2MoO_2S_2$ Methanol B3LYP

Mo	-0.02057	0	-0.03425
S	-0.03257	2E-5	2.21335
K	3.22534	-3E-5	2.25971
S	2.10475	-3E-5	-0.77176
O	-0.88838	1.40838	-0.64904
K	-2.89635	3E-5	-1.94874
O	-0.88841	-1.40836	-0.64902

K_2MoOS_3 Methanol B3LYP

Mo	0.02209	1.3E-4	-0.01344
S	-0.13134	6.7E-4	2.2083
K	3.23414	2.9E-4	1.8041
O	1.73582	2.7E-4	-0.40455
S	-0.94447	1.82916	-0.85078
K	-3.51095	-8.9E-4	-1.74837
S	-0.94389	-1.82961	-0.84993

K_2MoS_4 Methanol B3LYP

Mo	-0.02966	-0.1342	0.04916
S	0.12656	-0.12454	2.25772
K	3.34143	0.43204	2.10919
S	1.84443	0.69044	-0.79728
S	-1.75207	1.1043	-0.58249
K	-2.80621	-1.24657	-2.59458
S	-0.31951	-2.20844	-0.67623

K_2MoO_4 Acetonitrile B3LYP

Mo	-0.00381	0.00265	0.00338
O	-0.00928	0.13328	1.79193
K	2.69544	0.01344	2.10672
O	1.72609	-0.06595	-0.46154
O	-0.82885	1.4017	-0.75323
K	-2.68291	-0.04201	-2.12174
O	-0.89669	-1.44311	-0.56549

K_2MoO_3S Acetonitrile B3LYP

Mo	-0.12895	-0.05597	1E-5
S	1.12403	1.84213	0
K	3.49727	-0.54339	-1E-5
O	1.00243	-1.42936	3E-5

O	-1.20441	-0.13216	-1.41122
K	-3.5666	-0.17104	-1E-5
O	-1.20444	-0.13213	1.41122

$K_2MoO_2S_2$ Acetonitrile B3LYP

Mo	-0.02075	0	-0.0345
S	-0.03263	2E-5	2.21321
K	3.22685	-3E-5	2.26086
S	2.10479	-3E-5	-0.77157
O	-0.88832	1.40854	-0.64925
K	-2.89776	3E-5	-1.94927
O	-0.88836	-1.40852	-0.64923

K_2MoOS_3 Acetonitrile B3LYP

Mo	0.13696	0	-0.15746
S	1.1014	0	1.85289
K	3.82916	0	-0.18207
O	1.43516	0	-1.34343
S	-1.12513	1.81755	-0.42955
K	-3.76875	0	0.25893
S	-1.12512	-1.81755	-0.42955

K_2MoOS_3 Acetonitrile B3LYP

Mo	0.00259	-0.06694	0.07819
S	1.09698	1.64565	-0.80499
K	3.97501	0.13687	-0.4337
S	1.46761	-1.57854	0.76959
S	-1.33805	-0.96775	-1.43789
K	-3.97654	0.26986	0.05502
S	-1.21269	0.63353	1.79242

K_2MoO_4 Gas Phase MP2

Mo	0	0	-2E-5

O	1.12509	0.00446	-1.43785
K	3.34671	0	4E-5
O	1.12505	-0.00448	1.43784
O	-1.12507	-1.43784	-0.00449
K	-3.34672	0	4E-5
O	-1.12505	1.43785	0.00444

K_2MoO_3S Gas Phase MP2

Mo	-0.11762	-0.16735	3E-5
S	1.10994	1.76698	1E-5
K	3.40045	-0.31515	-5E-5
O	1.04798	-1.55501	7E-5
O	-1.23855	-0.24016	-1.42341
K	-3.47336	0.05404	-6E-5
O	-1.23863	-0.2401 1.42342	

$K_2MoO_2S_2$ Gas Phase MP2

Mo	-0.22742	-1E-5	2E-5
S	1.04073	-1.88039	4E-5
K	3.50517	1E-5	-6E-5
S	1.04071	1.88039	4E-5
O	-1.35223	-1E-5	1.41423
K	-3.61655	1E-5	-5E-5
O	-1.35217	-1E-5	-1.41424

K_2MoOS_3 Gas Phase MP2

Mo	0.06866	0.53261	0
S	0.51915	-1.74093	-2E-5
K	3.43	-0.61371	0
O	1.64352	1.40361	0
S	-1.1548	0.98589	1.81882
K	-2.76602	-1.34905	0

S	-1.15482	0.98591	-1.81881

K_2MoS_4 Gas Phase MP2

Mo	0	2E-5	0
S	-1.28039	1.84796	-0.00185
K	-3.77359	5E-5	0
S	-1.28046	-1.84795	0.00186
S	1.28043	0.00182	1.84795
K	3.77359	5E-5	0
S	1.28042	-0.0019	-1.84795

K_2MoO_4 Acetonitrile MP2

Mo	0.00755	9E-5	-0.01206
O	0.05192	-6.1E-4	1.81222
K	2.93853	-7.8E-4	2.0551
O	1.74418	1.2E-4	-0.57656
O	-0.88236	1.46523	-0.63664
K	-2.97747	6.2E-4	-2.00449
O	-0.88244	-1.46466	-0.63744

K_2MoO_3S Acetonitrile MP2

Mo	-0.0512	2.8E-4	0.06062
S	-0.05788	0.00252	2.38063
K	3.39443	-0.00148	1.7403
O	1.66049	-4.7E-4	-0.51928
O	-0.91298	1.44578	-0.59233
K	-3.10882	-5.9E-4	-1.91113
O	-0.91366	-1.44584	-0.59001

$K_2MoO_2S_2$ Acetonitrile MP2

Mo	-0.02008	0.19811	0.01188
S	-0.00265	0.40337	2.28634
K	3.32557	-0.68518	2.20643

S	2.07476	0.40853	-0.87238
O	-1.09812	1.4424	-0.7047
K	-2.9909	-0.35781	-2.10263
O	-0.72116	-1.3926	-0.44234

K_2MoOS_3 Acetonitrile MP2

Mo	-0.01295	-0.10127	0.05131
S	-0.02578	-0.23926	2.31927
K	3.4953	0.32867	1.74562
O	1.69072	-0.1442	-0.50382
K	-3.63636	0.17286	1.29482
S	-0.95884	1.83874	-0.61603
S	-1.13375	-1.8555	-0.81412

K_2MoS_4 Acetonitrile MP2

Mo	0.05499	0.25183	-0.02788
S	-0.01506	0.44785	2.21195
K	3.31977	-0.88175	2.39564
S	2.1852	0.42549	-0.72117
S	-1.16695	1.88271	-0.97791
K	-3.61231	-0.37053	-2.24804
S	-0.76573	-1.7556	-0.63246

K_2MoO_4 Methanol MP2

Mo	-0.00297	0.00371	0.00315
O	0.00327	0.02962	1.82832
K	2.87439	-0.0183	2.14413
O	1.74344	-0.00841	-0.52809
O	-0.87139	1.46526	-0.6597
K	-2.87685	0.00298	-2.14093
O	-0.88628	-1.46401	-0.6253

K_2MoO_3S Methanol MP2

Mo	0.01186	-0.05964	-0.01542
S	-0.01659	-0.09582	2.3051
K	3.42439	0.22275	1.70761
O	1.72743	-0.01845	-0.58293
O	-0.87298	1.37946	-0.652
K	-3.01943	-0.10184	-2.02463
O	-0.8193	-1.51062	-0.69579

$K_2MoO_2S_2$ Methanol MP2

Mo	0.03024	-5E-5	-0.07535
S	-0.04674	-3E-5	2.20935
K	3.42996	1.5E-4	2.41301
S	2.19111	-6E-5	-0.81816
O	-0.84228	1.43618	-0.70582
K	-3.19704	-5E-5	-1.83344
O	-0.84228	-1.43628	-0.7058

K_2MoOS_3 Methanol MP2

Mo	-0.00142	-0.01312	-0.14454
S	-0.25256	0.06822	2.1109
O	1.75135	-0.04336	-0.51476
K	3.36025	0.00309	1.88018
S	-0.93241	1.8181	-1.0831
S	-0.96952	-1.88646	-0.95229
K	-3.77011	0.03262	0.60309

K_2MoS_4 Methanol MP2

Mo	0.11508	0.26133	-0.0682
S	0.0066	0.49376	2.16862
S	2.2595	0.40477	-0.72353
S	-1.07714	1.8822	-1.06479
S	-0.71068	-1.7516	-0.65011

K	3.13079	-1.19097	2.37833
K	-3.53817	-0.39283	-2.28862

K_2MoO_4Gas Phase PBE0

Mo	0	6E-5	3E-5
O	1.11268	1.05548	-0.89843
K	3.20327	3.3E-4	9.2E-4
O	1.11235	-1.05516	0.89912
O	-1.11214	-0.89881	-1.0556
K	-3.20328	-2.1E-4	-8.7E-4
O	-1.1129	0.89874	1.05504

K_2MoO_3SGas Phase PBE0

Mo	-0.12296	-0.10336	0
S	1.16061	1.72509	0
K	3.24455	-0.43515	0
O	0.99386	-1.47321	0
O	-1.22908	-0.14016	-1.37432
K	-3.33355	-0.05075	0
O	-1.22909	-0.14015	1.37432

$K_2MoO_2S_2$ Gas Phase PBE0

Mo	0.11707	0	-0.14617
K	3.50993	0	-0.26999
K	-3.46686	-1E-5	0.16598
S	-0.02436	-0.88106	1.67403
S	0.0286	-0.15084	-1.89108
O	1.4764	1.716	0.36565
O	-1.47858	1.71929	0.33309

K_2MoOS_3Gas Phase PBE0

Mo	0.11707	0	-0.14617
S	1.26969	1E-5	1.73154

K	3.50993	0	-0.26999
O	1.31361	0	-1.41989
S	-1.14248	1.80586	-0.25719
K	-3.46686	-1E-5	0.16598
S	-1.14247	-1.80587	-0.25719

K_2MoS_4Gas Phase PBE0

Mo	0	0	-2E-5
S	-1.26283	-1.52074	-0.94605
K	-3.62348	1E-5	6E-5
S	-1.26278	1.52078	0.946
S	1.26283	0.94599	-1.52077
K	3.62348	1E-5	6E-5
S	1.26277	-0.94605	1.52075

K_2MoO_4 Acetonitrile PBE0

Mo	-0.01201	-0.00541	0.01338
O	-0.02913	-0.18517	1.78339
K	2.6396	0.00666	2.11965
O	1.7045	0.14947	-0.42945
O	-0.94572	1.41356	-0.51404
K	-2.5918	0.02024	-2.17909
O	-0.76548	-1.39948	-0.79378

K_2MoO_3S Acetonitrile PBE0

Mo	-0.12621	-0.06383	-0.01361
S	1.12275	1.81536	0.00559
K	3.45845	-0.52205	0.02249
O	0.98355	-1.43529	-0.05523
O	-1.21418	-0.1066	-1.39842
K	-3.53494	-0.15137	0.02498
O	-1.17062	-0.15438	1.40114

$K_2MoO_2S_2$ Acetonitrile PBE0

Mo	-0.25458	0	3E-5
S	1.01171	1.83792	5E-5
K	3.65047	0	-8E-5
S	1.01171	-1.83792	5E-5
O	-1.31634	0	-1.3888
K	-3.68311	0	-7E-5
O	-1.31643	0	1.38879

K_2MoOS_3 Acetonitrile PBE0

Mo	-0.13131	-1E-5	-0.17362
S	-1.0903	-1E-5	1.81828
K	-3.77891	1E-5	-0.13939
O	-1.4139	-1E-5	-1.35164
S	1.11633	-1.80481	-0.43912
K	3.70254	1E-5	0.30067
S	1.1163	1.80482	-0.43912

K_2MoS_4 Acetonitrile PBE0

Mo	9.8E-4	-0.05805	0.00685
S	-0.01541	-0.40038	2.17337
K	3.15633	0.1585	2.37328
S	2.07294	0.18853	-0.67152
S	-1.15326	1.74785	-0.46169
K	-3.26662	0.06481	-2.21372
S	-0.90795	-1.76955	-1.02053

K_2MoO_4 Methanol PBE0

Mo	-0.0048	-1E-5	0.00309
O	0.01361	-2E-4	1.78099
K	2.6978	9E-5	2.04544
O	1.70766	8E-5	-0.48198

O	-0.86911	1.41757	-0.63583
K	-2.67612	3E-5	-2.07572
O	-0.86899	-1.41756	-0.63608

K_2MoO_3S Methanol PBE0

Mo	-0.12627	-0.0644	-2.1E-4
S	1.12274	1.81497	9E-5
K	3.45797	-0.52079	3.5E-4
O	0.9851	-1.43533	-8.6E-4
O	-1.19356	-0.13141	-1.39956
K	-3.53428	-0.14991	3.8E-4
O	-1.19289	-0.13216	1.3996

$K_2MoO_2S_2$ Methanol PBE0

Mo	-0.25436	0	-2E-5
S	1.01172	-1.83798	-3E-5
K	3.64865	1E-5	6E-5
S	1.0117	1.83798	-3E-5
O	-1.31633	-1E-5	1.38866
K	-3.68179	1E-5	5E-5
O	-1.31639	-1E-5	-1.38866

K_2MoOS_3 Methanol PBE0

Mo	-0.02967	1.1E-4	0.08652
S	0.03367	4.5E-4	2.29188
K	3.2583	-2.5E-4	1.65356
O	1.62388	1E-5	-0.46113
S	-1.0576	1.80567	-0.66567
K	-3.30968	-2.2E-4	-2.09491
S	-1.05752	-1.80578	-0.66494

K_2MoS_4 Methanol PBE0

Mo	0	0	0

S	0	1.79216	1.266
K	0	0	3.94613
S	0	-1.79216	1.266
S	1.79216	0	-1.266
K	0	0	-3.94613
S	-1.79216	0	-1.266

Tetramethylammonium MoO_4 Gas Phase B3LYP

Mo	0	0	0
O	0	0	1.79171
O	1.69472	0	-0.58966
O	-0.81559	1.4844	-0.58476
O	-0.83983	-1.45628	-0.6282
N	2.26579	3.58102	1.40617
C	1.06156	4.02368	0.62074
H	0.52007	3.14869	0.26524
H	0.43054	4.62118	1.2718
H	1.40307	4.6242	-0.21691
C	1.82169	2.75785	2.58438
H	1.19187	3.37747	3.21546
H	1.26707	1.89041	2.23107
H	2.70431	2.44529	3.13405
C	3.01519	4.78651	1.89223
H	3.33337	5.36913	1.0336
H	2.35665	5.37664	2.52147
H	3.87876	4.45592	2.46051
C	3.1623	2.75327	0.52615
H	2.61722	1.87501	0.18218
H	3.47162	3.36464	-0.31633

H	4.03071	2.4575	1.10729
N	0.4988	-3.04946	-3.53735
C	-0.69189	-2.16776	-3.79762
H	-1.52682	-2.79632	-4.09226
H	-0.91716	-1.63958	-2.87424
H	-0.44219	-1.47952	-4.59921
C	0.18599	-3.96541	-2.38603
H	-0.06446	-3.34265	-1.53017
H	-0.65663	-4.59115	-2.66468
H	1.05826	-4.58128	-2.18994
C	1.68118	-2.19199	-3.17867
H	1.90148	-1.54373	-4.02133
H	1.44273	-1.59985	-2.29825
H	2.52772	-2.84252	-2.98047
C	0.81275	-3.8566	-4.76068
H	-0.04594	-4.47529	-5.00103
H	1.0267	-3.17927	-5.58157
H	1.67677	-4.48058	-4.55536

Tetramethylammonium MoO_3S Gas Phase B3LYP

Mo	-1.56277	-0.26638	-0.48786
O	-1.39295	-0.20639	1.26921
S	0.4743	-0.64546	-1.39689
O	-2.20941	1.26662	-1.1537
O	-2.5996	-1.66137	-0.84998
N	-0.59933	3.31914	-3.05858
C	-1.99398	3.794	-2.74741
H	-2.45094	3.03626	-2.10725
H	-1.92465	4.75344	-2.24072
H	-2.53558	3.90372	-3.68368

C	0.15896	3.16128	-1.76461
H	0.25041	4.14227	-1.30439
H	-0.41173	2.47737	-1.14148
H	1.13535	2.74061	-1.98287
C	0.0984	4.2996	-3.93919
H	-0.45568	4.40021	-4.86864
H	0.14959	5.25993	-3.43305
H	1.10148	3.93647	-4.14494
C	-0.68435	1.98023	-3.74847
H	-1.21232	1.30529	-3.07933
H	-1.21842	2.11733	-4.6858
H	0.32241	1.61544	-3.9238
N	-1.0408	-4.02734	1.2746
C	-0.1547	-2.97968	1.90472
H	0.87203	-3.17929	1.6127
H	-0.46818	-1.98654	1.5769
H	-0.26629	-3.05853	2.98358
C	-0.76014	-4.12577	-0.20475
H	-1.01885	-3.1807	-0.67662
H	0.29341	-4.35229	-0.33805
H	-1.3779	-4.92437	-0.60829
C	-2.48588	-3.64559	1.47872
H	-2.64429	-3.46695	2.53862
H	-2.69136	-2.7558	0.87988
H	-3.10409	-4.47248	1.13732
C	-0.76913	-5.34799	1.91597
H	0.28125	-5.59441	1.78613
H	-1.00528	-5.28325	2.97456
H	-1.38775	-6.1065	1.44433

Tetramethylammonium MoO_2S_2 Gas Phase B3LYP

Mo	1E-4	0.76842	0.15453
S	-0.02436	-0.88106	1.67403
S	0.0286	-0.15084	-1.89108
O	1.4764	1.716	0.36565
O	-1.47858	1.71929	0.33309
N	4.11868	-0.50428	-0.09713
C	3.94946	0.16093	1.24649
H	2.95508	0.60628	1.28256
H	4.08137	-0.59133	2.01885
H	4.70778	0.93484	1.33614
C	3.16396	-1.66455	-0.20357
H	3.43389	-2.39445	0.55501
H	2.14805	-1.31791	-0.03461
H	3.25304	-2.09185	-1.19809
C	5.51766	-1.00681	-0.23922
H	6.20416	-0.16751	-0.17171
H	5.72189	-1.71714	0.55723
H	5.62238	-1.49345	-1.2051
C	3.82948	0.49761	-1.1884
H	2.83489	0.90849	-1.02379
H	4.57554	1.28581	-1.12372
H	3.89416	-0.01178	-2.14516
N	-4.12003	-0.503	-0.10328
C	-3.81817	-0.02469	1.29612
H	-3.87498	-0.87618	1.96748
H	-2.82412	0.41885	1.3015
H	-4.56292	0.72171	1.56127
C	-3.16436	-1.60334	-0.48428

H	-2.15142	-1.21125	-0.51983
H	-3.23469	-2.39185	0.25922
H	-3.4493	-1.97274	-1.46587
C	-3.9657	0.648	-1.06644
H	-4.72591	1.38845	-0.83014
H	-2.97209	1.07523	-0.92836
H	-4.10463	0.26989	-2.07522
C	-5.51742	-1.02631	-0.1607
H	-5.61043	-1.86284	0.52654
H	-6.20425	-0.23469	0.12541
H	-5.73193	-1.35422	-1.17415

Tetramethylammonium $MoOS_3$ Gas Phase B3LYP

Mo	0.08527	-0.0552	0.16361
S	0.35451	-0.05065	2.35511
S	2.06866	0.09888	-0.84566
S	-1.13955	1.70315	-0.45496
O	-0.71727	-1.52144	-0.40718
N	2.12599	3.69084	1.50807
C	1.95672	3.71802	0.01097
H	1.46003	2.80471	-0.30834
H	1.35407	4.58477	-0.24598
H	2.94266	3.78839	-0.44007
C	0.77299	3.59778	2.16701
H	0.1901	4.46416	1.86708
H	0.28391	2.68059	1.84727
H	0.92061	3.58832	3.24336
C	2.80789	4.94336	1.95257
H	3.78143	5.00499	1.47409
H	2.19982	5.79747	1.66749

H	2.92675	4.91712	3.03218
C	2.96393	2.49998	1.89937
H	2.45959	1.59042	1.58161
H	3.92967	2.59013	1.40996
H	3.07885	2.50721	2.97971
N	-1.38983	-2.14254	-3.50326
C	-2.09057	-0.86496	-3.10853
H	-3.15966	-1.00958	-3.24182
H	-1.85041	-0.64812	-2.07114
H	-1.73296	-0.06514	-3.74993
C	-1.83336	-3.25001	-2.58521
H	-1.56573	-2.95373	-1.57107
H	-2.90837	-3.37245	-2.69028
H	-1.32195	-4.16344	-2.87805
C	0.10243	-1.95808	-3.36803
H	0.4051 -	1.13237	-4.00487
H	0.32831	-1.73123	-2.32955
H	0.58772	-2.87836	-3.683
C	-1.72745	-2.4844	-4.91634
H	-2.80263	-2.61521	-5.0036
H	-1.40051	-1.67487	-5.56292
H	-1.2189	-3.40454	-5.19108

Tetramethylammonium MoS_4 Gas Phase B3LYP

Mo	-0.54529	0.4102	0.16025
S	-0.85121	0.44098	2.33356
S	1.49166	-0.37249	-0.30588
S	-0.63209	2.48919	-0.64554
S	-2.06324	-0.83305	-0.82364
N	2.47779	2.91047	2.3662

C	1.09718	3.45958	2.62498
H	0.36767	2.84446	2.10287
H	0.91459	3.42706	3.69539
H	1.06718	4.48316	2.26209
C	2.56201	1.48566	2.85362
H	2.35745	1.47976	3.92053
H	1.82162	0.88695	2.32785
H	3.56496	1.11902	2.65374
C	3.48575	3.7422	3.09024
H	3.42154	4.76647	2.7335
H	3.2731	3.70716	4.15503
H	4.4779	3.34337	2.89765
C	2.76152	2.94997	0.88824
H	2.02189	2.34321	0.37072
H	2.70068	3.98345	0.55837
H	3.75921	2.55247	0.72325
N	-0.08893	0.21983	-4.31277
C	-1.43975	0.80073	-3.97743
H	-2.20164	0.16169	-4.41484
H	-1.55368	0.83143	-2.89616
H	-1.49113	1.80116	-4.39789
C	0.02607	-1.17181	-3.74286
H	-0.09808	-1.12399	-2.66334
H	-0.757	-1.78365	-4.18177
H	1.00675	-1.56217	-4.00009
C	0.98883	1.09072	-3.7242
H	0.89225	2.08536	-4.1508
H	0.86202	1.12796	-2.64455
H	1.95218	0.65644	-3.97708

C	0.07111	0.16212	-5.79702
H	-0.70999	-0.46862	-6.21209
H	-0.01097	1.16726	-6.20133
H	1.04684	-0.25415	-6.03198

Tetramethylammonium MoO_4 Acetonitrile B3LYP

Mo	0	0	0
O	0	0	1.79171
O	1.69472	0	-0.58966
O	-0.81559	1.4844	-0.58476
O	-0.83983	-1.45628	-0.6282
N	2.26579	3.58102	1.40617
C	1.06156	4.02368	0.62074
H	0.52007	3.14869	0.26524
H	0.43054	4.62118	1.2718
H	1.40307	4.6242	-0.21691
C	1.82169	2.75785	2.58438
H	1.19187	3.37747	3.21546
H	1.26707	1.89041	2.23107
H	2.70431	2.44529	3.13405
C	3.01519	4.78651	1.89223
H	3.33337	5.36913	1.0336
H	2.35665	5.37664	2.52147
H	3.87876	4.45592	2.46051
C	3.1623	2.75327	0.52615
H	2.61722	1.87501	0.18218
H	3.47162	3.36464	-0.31633
H	4.03071	2.4575	1.10729
N	0.4988	-3.04946	-3.53735
C	-0.69189	-2.16776	-3.79762

H	-1.52682	-2.79632	-4.09226
H	-0.91716	-1.63958	-2.87424
H	-0.44219	-1.47952	-4.59921
C	0.18599	-3.96541	-2.38603
H	-0.06446	-3.34265	-1.53017
H	-0.65663	-4.59115	-2.66468
H	1.05826	-4.58128	-2.18994
C	1.68118	-2.19199	-3.17867
H	1.90148	-1.54373	-4.02133
H	1.44273	-1.59985	-2.29825
H	2.52772	-2.84252	-2.98047
C	0.81275	-3.8566	-4.76068
H	-0.04594	-4.47529	-5.00103
H	1.0267	-3.17927	-5.58157
H	1.67677	-4.48058	-4.55536

Tetramethylammonium MoO_3S Acetonitrile B3LYP

Mo	0.00356	0.19819	0.24603
O	-0.02322	0.40725	2.00267
S	2.15922	0.11138	-0.49497
O	-0.83733	1.56525	-0.52314
O	-0.83516	-1.31518	-0.17159
N	-0.83577	3.5211	-3.38304
C	-1.33388	4.29669	-2.19465
H	-1.30286	3.63399	-1.33469
H	-0.68692	5.15601	-2.04813
H	-2.34892	4.62344	-2.39768
C	0.57242	3.06317	-3.11665
H	1.19541	3.93872	-2.9624
H	0.55992	2.43454	-2.23068

H	0.92053	2.50478	-3.97991
C	-0.86844	4.38565	-4.60702
H	-1.89115	4.70457	-4.78204
H	-0.23037	5.24807	-4.4429
H	-0.50699	3.80805	-5.45183
C	-1.7128	2.31645	-3.586
H	-1.66175	1.71706	-2.68163
H	-2.72733	2.65589	-3.77033
H	-1.34253	1.7616	-4.44246
N	-1.26913	-4.38938	1.38928
C	-1.51823	-3.28768	2.38297
H	-0.83451	-3.41518	3.21637
H	-1.3438	-2.34116	1.8796
H	-2.54497	-3.36145	2.72744
C	0.14721	-4.29166	0.8935
H	0.26682	-3.31691	0.43005
H	0.81812	-4.40323	1.73948
H	0.31628	-5.08702	0.17451
C	-2.20753	-4.22411	0.22536
H	-3.22696	-4.2871	0.59331
H	-2.01205	-3.25172	-0.21741
H	-2.01708	-5.02153	-0.48627
C	-1.49281	-5.72144	2.03926
H	-0.80802	-5.82219	2.87526
H	-2.51917	-5.77025	2.38881
H	-1.30859	-6.50249	1.30844

Tetramethylammonium MoO_2S_2 Acetonitrile B3LYP

Mo	-0.00278	-0.73982	0.01916
S	-0.68709	-2.21535	1.57359

S	0.44019	-1.77963	-1.9259
O	1.45651	0.07884	0.58755
O	-1.28077	0.45	-0.24353
N	4.7728	1.03086	0.07586
C	4.37837	1.25479	1.50982
H	3.34242	0.94872	1.61909
H	5.02753	0.65755	2.14235
H	4.49788	2.30871	1.74044
C	4.60773	-0.42678	-0.25683
H	5.25689	-1.00405	0.39399
H	3.56598	-0.68776	-0.09567
H	4.88797	-0.57723	-1.29452
C	6.20037	1.44072	-0.12923
H	6.29987	2.49464	0.11023
H	6.8301	0.8473	0.52585
H	6.46878	1.26534	-1.16612
C	3.87314	1.84257	-0.81496
H	2.85314	1.51212	-0.64325
H	3.98798	2.89134	-0.55967
H	4.16573	1.67426	-1.84653
N	-4.71136	1.08381	-0.0285
C	-4.02086	1.45087	1.25658
H	-4.46855	0.88027	2.06402
H	-2.96788	1.20819	1.14694
H	-4.15676	2.51387	1.42962
C	-4.51655	-0.38494	-0.28776
H	-3.44917	-0.57125	-0.35336
H	-4.9549	-0.94155	0.53445
H	-5.01205	-0.6416	-1.21881

C	-4.09966	1.86918	-1.15605
H	-4.24099	2.92657	-0.95538
H	-3.04342	1.62094	-1.19658
H	-4.59934	1.59451	-2.07974
C	-6.17482	1.39361	0.07241
H	-6.59812	0.81737	0.88886
H	-6.29466	2.45543	0.26211
H	-6.65372	1.12479	-0.86367

Tetramethylammonium $MoOS_3$ Acetonitrile B3LYP

Mo	0.29639	0.00889	-0.14398
S	-0.11887	0.01932	2.04919
S	2.49732	0.03115	-0.52323
S	-0.6663	1.76985	-1.12174
O	-0.38188	-1.44908	-0.84933
N	2.34155	4.21337	1.98465
C	1.42463	4.55901	0.84456
H	1.01316	3.64211	0.43121
H	0.62691	5.19077	1.22227
H	1.9972	5.08977	0.09055
C	1.56893	3.46813	3.03714
H	0.76337	4.10478	3.38928
H	1.16699	2.55742	2.60049
H	2.24119	3.22947	3.85529
C	2.90826	5.47272	2.57332
H	3.46338	5.998	1.80295
H	2.09011	6.08906	2.93149
H	3.56573	5.20859	3.39527
C	3.45992	3.34634	1.47723
H	3.03652	2.4468	1.03802

H	4.01483	3.90313	0.72868
H	4.10759	3.09292	2.3105
N	-1.66022	-2.67356	-3.89469
C	-1.5231	-1.17968	-4.00425
H	-2.49792	-0.76054	-4.2327
H	-1.15539	-0.80234	-3.05504
H	-0.823	-0.95593	-4.80301
C	-2.61488	-2.99915	-2.77929
H	-2.20582	-2.58972	-1.86089
H	-3.57663	-2.55031	-3.00685
H	-2.71231	-4.07806	-2.7107
C	-0.31518	-3.27114	-3.58491
H	0.36449	-3.02801	-4.39548
H	0.03138	-2.84395	-2.64878
H	-0.42696	-4.34754	-3.50069
C	-2.17815	-3.23219	-5.18648
H	-3.14904	-2.79325	-5.39248
H	-1.47962	-2.98365	-5.97895
H	-2.26672	-4.30951	-5.09007

Tetramethylammonium MoS_4 Acetonitrile B3LYP

Mo	4.5E-4	-0.06451	0.08905
S	0.02973	-0.23232	2.30033
S	2.08382	-0.00426	-0.6649
S	-1.04798	1.79663	-0.50531
S	-1.04881	-1.81251	-0.77268
N	2.59531	3.26218	3.14129
C	1.10918	3.46898	3.24127
H	0.61404	2.59516	2.82687
H	0.84689	3.58991	4.28753

H	0.84419	4.36055	2.68238
C	2.97217	2.01602	3.89298
H	2.70428	2.14679	4.93651
H	2.42469	1.18088	3.46558
H	4.04214	1.86267	3.7963
C	3.31269	4.44311	3.72818
H	3.03453	5.33175	3.17081
H	3.02257	4.54672	4.76869
H	4.3818	4.27325	3.65236
C	2.98135	3.10627	1.69656
H	2.46639	2.24328	1.28476
H	2.69516	4.0072	1.16341
H	4.05591	2.96404	1.64073
N	-0.35914	0.01583	-5.07216
C	-1.13699	1.1572	-4.47856
H	-2.16038	1.10123	-4.83545
H	-1.10739	1.07792	-3.39533
H	-0.67957	2.08832	-4.79749
C	-0.99724	-1.28549	-4.67289
H	-0.99259	-1.35933	-3.58844
H	-2.01533	-1.30028	-5.04892
H	-0.4258	-2.09833	-5.1097
C	1.05367	0.0587	-4.55996
H	1.49937	1.00281	-4.85677
H	1.03998	-0.025	-3.47699
H	1.60482	-0.76883	-4.9949
C	-0.35503	0.1331	-6.56902
H	-1.38044	0.10914	-6.92325
H	0.11481	1.0717	-6.84459

H	0.20349	-0.70094	-6.9815

Tetramethylammonium MoO_4 Methanol B3LYP

Mo	-0.17012	0.15943	-0.14995
O	-0.11627	-0.02735	1.63005
O	1.50502	0.15021	-0.79428
O	-0.93762	1.72957	-0.5468
O	-1.08985	-1.19111	-0.89258
N	2.28277	3.53999	1.42443
C	1.03647	4.07617	0.77436
H	0.45642	3.24955	0.36652
H	0.46214	4.6086	1.52656
H	1.33229	4.75798	-0.01731
C	1.90518	2.6061	2.54127
H	1.32992	3.16394	3.27389
H	1.31266	1.78625	2.14061
H	2.81722	2.22921	2.99405
C	3.08787	4.6792	1.97618
H	3.35412	5.34547	1.16186
H	2.48787	5.20723	2.71034
H	3.98394	4.28091	2.44127
C	3.09938	2.79394	0.40493
H	2.51709	1.95593	0.02343
H	3.35348	3.48076	-0.39676
H	4.00393	2.43771	0.88888
N	0.53241	-3.0542	-3.5112
C	-0.69581	-2.2832	-3.91097
H	-1.48838	-2.99219	-4.13091
H	-0.9733	-1.6478	-3.07286
H	-0.46236	-1.69855	-4.79552

C	0.23733	-3.82367	-2.25306
H	-0.08565	-3.11022	-1.49842
H	-0.55279	-4.53739	-2.46618
H	1.13906	-4.34601	-1.94867
C	1.65875	-2.09195	-3.25174
H	1.84422	-1.53118	-4.16299
H	1.38249	-1.42135	-2.44028
H	2.54175	-2.66443	-2.98369
C	0.91915	-4.00031	-4.60719
H	0.09671	-4.68667	-4.78182
H	1.12665	-3.42857	-5.50615
H	1.80426	-4.54838	-4.29999

Tetramethylammonium MoO_3S Methanol B3LYP

Mo	-0.22548	-0.18496	-0.29604
O	-0.33834	0.00678	1.46114
S	1.96468	-0.11268	-0.93323
O	-1.12573	1.12571	-1.09641
O	-0.94117	-1.75131	-0.73557
N	-0.81384	3.6715	-3.4348
C	-1.55708	4.14633	-2.21641
H	-1.61967	3.31051	-1.52564
H	-1.00752	4.97325	-1.77765
H	-2.54611	4.47409	-2.52091
C	0.55329	3.19672	-3.02174
H	1.08177	4.02691	-2.56342
H	0.42598	2.38077	-2.31601
H	1.08217	2.86159	-3.90842
C	-0.6868	4.78867	-4.42598
H	-1.68016	5.11757	-4.71451

H	-0.14276	5.60589	-3.96317
H	-0.14615	4.42506	-5.29419
C	-1.56555	2.52304	-4.04914
H	-1.63188	1.73741	-3.30184
H	-2.55343	2.87024	-4.336
H	-1.02045	2.18146	-4.92348
N	-1.22431	-4.42465	1.59658
C	-1.19949	-3.20669	2.47894
H	-0.37672	-3.30775	3.17984
H	-1.0609	2.32535	1.85974
H	-2.14087	-3.1538	3.01698
C	0.06054	-4.49677	0.81771
H	0.12535	-3.60263	0.20445
H	0.8873	-4.5509	1.51911
H	0.03779	-5.38744	0.19742
C	-2.3751	-4.31651	0.63405
H	-3.29591	-4.24626	1.20468
H	-2.21727	-3.42731	0.0294
H	-2.38798	-5.20735	0.01344
C	-1.37957	-5.65481	2.43958
H	-0.5408	-5.71639	3.12558
H	-2.31086	-5.58347	2.99251
H	-1.39576	-6.52429	1.79029

Tetramethylammonium MoO_2S_2 Methanol B3LYP

Mo	0.0022	-0.83003	0.02132
S	-0.68755	-2.30411	1.57465
S	0.44861	-1.87203	-1.92154
O	1.46169	-0.01389	0.59274
O	-1.27251	0.36253	-0.24574

N	4.71608	1.12622	0.07513
C	4.39578	1.10984	1.54467
H	3.37614	0.75407	1.65611
H	5.09415	0.44471	2.04279
H	4.49844	2.11851	1.93221
C	4.56912	-0.26644	-0.47464
H	5.26101	-0.91873	0.04875
H	3.54246	-0.5803	-0.31067
H	4.80298	-0.2457	-1.53433
C	6.11826	1.6137	-0.13693
H	6.20437	2.61767	0.26644
H	6.80254	0.94481	0.37522
H	6.32828	1.6196	-1.20174
C	3.74693	2.03544	-0.62914
H	2.74669	1.65071	-0.45429
H	3.85359	3.03637	-0.22281
H	3.98146	2.03486	-1.68884
N	-4.6643	1.17826	-0.03184
C	-3.92504	1.71667	1.16218
H	-4.36383	1.29203	2.05949
H	-2.8833	1.42578	1.065
H	-4.02538	2.79738	1.17226
C	-4.51455	-0.31804	-0.06789
H	-3.45398	-0.54377	-0.12177
H	-4.9517	-0.73069	0.83569
H	-5.03523	-0.69611	-0.9421
C	-4.06841	1.76155	-1.28347
H	-4.17693	2.8411	-1.2471
H	-3.02067	1.47822	-1.31367

H	-4.60274	1.36055	-2.13898
C	-6.11576	1.54301	0.06046
H	-6.52407	1.11973	0.97273
H	-6.20427	2.62461	0.07766
H	-6.6332	1.13907	-0.80379

Tetramethylammonium $MoOS_3$ Methanol B3LYP

Mo	-0.11863	8E-4	0.05561
S	-0.17135	0.22603	2.27579
S	1.99398	-0.12186	-0.6542
S	-1.16713	1.71275	-0.92022
O	-0.9432	-1.47987	-0.4014
N	2.54904	4.08992	1.66433
C	1.38532	4.42883	0.77487
H	0.87645	3.51119	0.49427
H	0.71137	5.08064	1.32173
H	1.76109	4.93534	-0.10844
C	2.04479	3.39266	2.89718
H	1.37508	4.0657	3.42327
H	1.51409	2.49163	2.59931
H	2.89389	3.14337	3.5256
C	3.2672	5.34878	2.05587
H	3.62413	5.84063	1.15672
H	2.57526	5.99437	2.58689
H	4.10304	5.0877	2.69687
C	3.49307	3.18237	0.92593
H	2.96081	2.28032	0.63487
H	3.85436	3.70457	0.04567
H	4.32268	2.93928	1.58225
N	-2.35602	-2.77139	-3.37298

C	-2.50591	-1.27583	-3.42944
H	-3.563	-1.03824	-3.49491
H	-2.07251	-0.8539	-2.52799
H	-1.98627	-0.91072	-4.30971
C	-3.07528	-3.29368	-2.15993
H	-2.62763	-2.83393	-1.28431
H	-4.12529	-3.03088	-2.24132
H	-2.96175	-4.37262	-2.12889
C	-0.89596	-3.11806	-3.26904
H	-0.38619	-2.73045	-4.14534
H	-0.50875	-2.66156	-2.36313
H	-0.79997	-4.19857	-3.22824
C	-2.93672	-3.38513	-4.61192
H	-3.98774	-3.12125	-4.67211
H	-2.40395	-2.99844	-5.47475
H	-2.82336	-4.46298	-4.55407

Tetramethylammonium MoS_4 Methanol B3LYP

Mo	-0.09458	0.27135	-0.3141
S	0.19887	0.49762	1.87537
S	1.83966	0.58358	-1.35019
S	-1.55241	1.77662	-1.02792
S	-0.85653	-1.76059	-0.75492
N	2.72689	3.33275	3.65529
C	1.30451	3.78928	3.82848
H	0.65276	3.05743	3.36073
H	1.09055	3.86716	4.88954
H	1.19072	4.75716	3.35095
C	2.90035	1.9862	4.30148
H	2.66377	2.07448	5.35686

H	2.22712	1.28576	3.81682
H	3.93075	1.67122	4.1729
C	3.65702	4.32156	4.29616
H	3.51452	5.2893	3.8266
H	3.42636	4.38049	5.35495
H	4.67824	3.98274	4.15436
C	3.03498	3.22162	2.18702
H	2.3481	2.50338	1.74827
H	2.9067	4.19841	1.73183
H	4.06057	2.88593	2.07272
N	-0.45955	-0.15361	-5.46723
C	-1.33505	0.96061	-4.96524
H	-2.36792	0.71737	-5.1932
H	-1.20034	1.05762	-3.89148
H	-1.04688	1.87926	-5.46639
C	-0.84029	-1.43462	-4.77837
H	-0.71136	-1.31114	-3.70665
H	-1.87806	-1.6542	-5.00806
H	-0.19956	-2.22913	-5.14731
C	0.97782	0.16791	-5.16634
H	1.2353	1.09679	-5.66527
H	1.09657	0.2713	-4.09077
H	1.59848	-0.64101	-5.53841
C	-0.64121	-0.30813	-6.94978
H	-1.68187	-0.54094	-7.15102
H	-0.36526	0.62257	-7.43474
H	-0.00301	-1.11453	-7.29616

WO_4 Isolated Anion Gas Phase B3LYP

W	-0.00139	0	3.6E-4

O	0.00272	-3E-5	1.79719
O	1.69291	8E-5	-0.59677
O	-0.84712	1.4653	-0.60031
O	-0.84702	-1.46534	-0.60041

WO_3S Isolated Anion Gas Phase B3LYP

W	-0.00106	-1E-5	-0.09611
S	-0.00187	1.3E-4	2.19826
O	1.66998	-4E-5	-0.70088
O	-0.83347	1.44859	-0.70067
O	-0.83348	-1.44866	-0.70052

WO_2S_2 Isolated Anion Gas Phase B3LYP

W	-0.08789	0	-0.06291
S	-0.10212	1E-5	2.19681
S	2.03867	1E-5	-0.82834
O	-0.92428	1.43605	-0.65275
O	-0.92427	-1.43607	-0.65273

WOS_3 Isolated Anion Gas Phase B3LYP

W	-0.04133	-0.06043	-0.02819
S	-0.04371	-0.09834	2.2097
S	2.06663	-0.09246	-0.7782
S	-1.11648	1.74504	-0.79439
O	-0.86502	-1.4938	-0.60886

WS_4 Isolated Anion Gas Phase B3LYP

W	-0.00173	-0.00212	-0.00178
S	-0.13443	0.13326	2.21077
S	2.13214	-0.03846	-0.61392
S	-1.00032	1.76695	-0.8947
S	-0.99557	-1.85962	-0.70031

WO_4 Isolated Anion Acetonitrile B3LYP

W	-0.00139	0	3.6E-4
O	0.00272	-3E-5	1.79719
O	1.69291	8E-5	-0.59677
O	-0.84712	1.4653	-0.60031
O	-0.84702	-1.46534	-0.60041

WO_3S Isolated Anion Acetonitrile B3LYP

W	-0.00106	-1E-5	-0.09611
S	-0.00187	1.3E-4	2.19826
O	1.66998	-4E-5	-0.70088
O	-0.83347	1.44859	-0.70067
O	-0.83348	-1.44866	-0.70052

WO_2S_2 Isolated Anion Acetonitrile B3LYP

W	-0.08789	0	-0.06291
S	-0.10212	1E-5	2.19681
S	2.03867	1E-5	-0.82834
O	-0.92428	1.43605	-0.65275
O	-0.92427	-1.43607	-0.65273

WOS_3 Isolated Anion Acetonitrile B3LYP

W	-0.04133	-0.06043	-0.02819
S	-0.04371	-0.09834	2.2097
S	2.06663	-0.09246	-0.7782
S	-1.11648	1.74504	-0.79439
O	-0.86502	-1.4938	-0.60886

WS_4 Isolated Anion Acetonitrile B3LYP

W	-0.00173	-0.00212	-0.00178
S	-0.13443	0.13326	2.21077
S	2.13214	-0.03846	-0.61392
S	-1.00032	1.76695	-0.8947
S	-0.99557	-1.85962	-0.70031

WO_4 Isolated Anion Methanol B3LYP

W	0	-1E-5	0
O	-0.25841	0.65487	1.65855
O	-0.11655	1.33948	-1.19944
O	-1.2579	-1.23901	-0.35921
O	1.63282	-0.75526	-0.09986

WO_3S Isolated Anion Methanol B3LYP

W	0.19539	0	0
S	-2.12067	6E-5	2E-5
O	0.81137	0.16967	1.65997
O	0.81142	1.35269	-0.97696
O	0.81117	-1.5225	-0.68301

WO_2S_2 Isolated Anion Methanol B3LYP

W	0	0.19854	0
S	1.88611	-1.0762 0	
S	-1.88609	-1.07621	0
O	0	1.23417	-1.42507
O	-1E-5	1.23417	1.42506

WOS_3 Isolated Anion Methanol B3LYP

W	0	-1E-5	0.15427
S	-1.84936	-1.06316	-0.55488
S	0.00387	2.13314	-0.55484
S	1.84545	-1.06989	-0.55493
O	6E-5	-8E-5	1.90229

WS_4 Isolated Anion Methanol B3LYP

W	0	1E-5	-1E-5
S	0.70072	-1.52411	-1.46242
S	-2.07943	0.61144	-0.50472
S	1.33669	1.77735	-0.08297

S	0.04201	-0.86473	2.05013

WO_4 Isolated Anion Gas Phase PBE0

W	0	0	0
O	-0.51928	-0.92625	-1.44099
O	1.52658	-0.68764	0.63304
O	-1.26678	-0.09833	1.26082
O	0.25943	1.7122	-0.45289

WO_3S Isolated Anion Gas Phase PBE0

W	0.19306	0	-1E-5
S	-2.10447	0	-4E-5
O	0.80777	1.43512	-0.82643
O	0.80777	-1.43333	-0.82954
O	0.80761	-0.0018	1.65612

WO_2S_2 Isolated Anion Gas Phase PBE0

W	0	0.19596	0
S	0	-1.0665	1.87225
S	0	-1.0665	-1.87225
O	1.41296	1.22669	0
O	-1.41296	1.22669	0

WOS_3 Isolated Anion Gas Phase PBE0

W	0	0	0.15229
S	-1.1036	1.80543	-0.54934
S	2.11535	0.05302	-0.54933
S	-1.01176	-1.85845	-0.54933
O	-1E-5	0	1.88727

WS_4 Isolated Anion Gas Phase PBE0

W	0	0	0
S	1.78513	0.60332	-1.14801
S	-1.72987	-0.16	-1.36035

S	-0.42185	1.51091	1.5517
S	0.36659	-1.95423	0.95666

WO_4 Isolated Anion Acetonitrile PBE0

W	-0.0015	0	4.3E-4
O	0.00162	0	1.78536
O	1.68104	0	-0.59407
O	-0.84052	1.45655	-0.59584
O	-0.84052	-1.45655	-0.59584

WO_3S Isolated Anion Acetonitrile PBE0

W	-0.00103	4E-5	-0.09415
S	-0.00327	-6.4E-4	2.18265
O	1.65712	2E-4	-0.69812
O	-0.82635	1.43923	-0.69477
O	-0.82635	-1.43884	-0.69555

WO_2S_2 Isolated Anion Acetonitrile PBE0

W	-0.08579	0	-0.0615
S	-0.10284	1E-5	2.18071
S	2.02354	1E-5	-0.82365
O	-0.91741	1.42428	-0.64775
O	-0.9174	-1.42429	-0.64774

WOS_3 Isolated Anion Acetonitrile PBE0

W	-0.03994	-0.06156	-0.02791
S	-0.0468	-0.09504	2.19174
S	2.04993	-0.09086	-0.7749
S	-1.1053	1.73128	-0.78469
O	-0.85777	-1.48383	-0.60419

WS_4 Isolated Anion Acetonitrile PBE0

W	-0.00132	0	-0.00104
S	0.00443	0	2.20046

S	2.0758	0	-0.72927
S	-1.03939	1.79563	-0.73505
S	-1.03939	-1.79563	-0.73505

WO_4 Isolated Anion Methanol PBE0

W	-0.00148	0	4.2E-4
O	0.00153	0	1.78535
O	1.68103	0	-0.59414
O	-0.84048	1.4566	-0.59579
O	-0.84048	-1.45661	-0.59579

WO_3S Isolated Anion Methanol PBE0

W	-9.9E-4	4E-5	-0.09415
S	-0.0034	-6.5E-4	2.18261
O	1.65712	2E-4	-0.69825
O	-0.82631	1.43929	-0.6947
O	-0.8263	-1.43888	-0.69546

WO_2S_2 Isolated Anion Methanol PBE0

W	-0.08574	-1E-5	-0.06151
S	-0.10296	2E-5	2.18062
S	2.02354	4E-5	-0.82378
O	-0.91739	1.4243	-0.64766
O	-0.91733	-1.42435	-0.64763

WOS_3 Isolated Anion Methanol PBE0

W	-0.03991	-0.0616	-0.02794
S	-0.04687	-0.09498	2.19169
S	2.04998	-0.09078	-0.77489
S	-1.10536	1.73124	-0.78465
O	-0.85773	-1.48389	-0.60416

WS_4 Isolated Anion Methanol PBE0

W	-0.00129	1E-5	-0.00102

S	0.00442	-1E-5	2.20053
S	2.07585	-1E-5	-0.72927
S	-1.03944	1.79556	-0.7351
S	-1.03942	-1.79555	-0.73508

Potassium WO_4 Gas Phase B3LYP

W	0	0	0
O	1.12241	-0.89399	-1.07372
O	1.12241	0.89399	1.07372
O	-1.12241	-1.07372	0.89399
O	-1.12241	1.07372	-0.89399
K	-3.23885	1E-5	0
K	3.23885	1E-5	0

Potassium WO_3S Gas Phase B3LYP

W	-0.09788	-0.07374	0
S	1.20332	1.76861	0
O	-1.21533	-0.11387	-1.38424
O	-1.21534	-0.11388	1.38424
O	1.02636	-1.45813	0
K	3.30407	-0.44419	0
K	-3.34489	-0.04811	0

Potassium WO_2S_2 Gas Phase B3LYP

W	0.18976	-1E-5	0
S	-1.08604	-1.84447	0
S	-1.08601	1.84447	0
O	1.30466	-1E-5	-1.37345
O	1.30466	0	1.37345
K	-3.45418	1E-5	0
K	3.44556	1E-5	0

Potassium WOS_3 Gas Phase B3LYP

W	0.09479	0	-0.10746
S	1.27673	1E-5	1.77921
S	-1.17838	1.82528	-0.22321
S	-1.17842	-1.82529	-0.22319
O	1.29926	-1E-5	-1.39456
K	3.52656	0	-0.27839
K	-3.53326	2E-5	0.16175

Potassium WS_4 Gas Phase B3LYP

W	0	0	0
S	-1.2808	0.13181	-1.80348
S	-1.28081	-0.1318	1.80348
S	1.28081	1.80348	0.13181
S	1.2808	-1.80349	-0.1318
K	-3.66611	0	-1E-5
K	3.66611	-1E-5	-1E-5

Potassium WO_4 Acetonitrile B3LYP

W	0	2E-5	0
O	-1.0897	0.85011	-1.1458
O	-1.08966	-0.85007	1.14584
O	1.08969	1.14584	0.85007
O	1.08966	-1.1458	-0.85011
K	3.43097	-5E-5	-1E-5
K	-3.43097	-5E-5	-1E-5

Potassium WO_3S Acetonitrile B3LYP

W	-0.10061	-0.03882	0.00924
S	1.15692	1.86259	-0.00807
O	-1.15491	-0.14703	-1.41777
O	-1.19979	-0.09528	1.40598
O	1.02466	-1.41947	0.05737

K	3.52528	-0.54897	-0.02319
K	-3.54768	-0.16862	-0.02518

Potassium WO_2S_2 Acetonitrile B3LYP

W	0.20271	0	0
S	-1.06525	-1.86837	0
S	-1.06525	1.86837	0
O	1.28019	0	-1.39742
O	1.2802	0	1.39742
K	-3.74477	0	-1E-5
K	3.67131	0	-1E-5

Potassium WOS_3 Acetonitrile B3LYP

W	0.10377	-2E-5	-0.14604
S	1.04921	-6E-5	1.85968
S	-1.14221	1.8103	-0.4307
S	-1.14232	-1.81027	-0.43073
O	1.40379	-4E-5	-1.31004
K	3.75986	6E-5	-0.08015
K	-3.71479	7E-5	0.35992

Potassium WS_4 Acetonitrile B3LYP

W	-0.0065	-0.03482	0.01247
S	-0.01444	-0.04695	2.20999
K	2.9459	0.1071	2.11576
S	2.06388	0.07617	-0.71579
S	-1.13051	1.70878	-0.71256
K	-2.96125	-0.17643	-2.08782
S	-0.94498	-1.8773	-0.73161

Potassium WO_4 Methanol B3LYP

W	-1E-5	0.00451	-3.3E-4
O	1.0763	-1.08797	0.93145

O	1.0913	1.09451	-0.91732
O	-1.09069	0.92993	1.08336
O	-1.07691	-0.91892	-1.09914
K	-3.42803	-0.01256	0.0012
K	3.42809	-0.01241	7.7E-4

Potassium WO_3S Methanol B3LYP

W	-0.10024	-0.03791	0.01152
S	1.15871	1.86237	-0.0106
O	-1.15023	-0.15274	-1.41805
O	-1.20329	-0.08704	1.40533
O	1.02159	-1.42055	0.07158
K	3.52495	-0.55131	-0.02914
K	-3.54949	-0.17025	-0.03156

Potassium WO_2S_2 Methanol B3LYP

W	0.20256	0	0
S	-1.06524	-1.86837	1E-5
S	-1.06524	1.86837	1E-5
O	1.28019	0	-1.3973
O	1.28021	0	1.3973
K	-3.74286	0	-1E-5
K	3.66998	0	-1E-5

Potassium WOS_3 Methanol B3LYP

W	0.1081	-3E-5	-0.13202
S	1.06188	-3E-5	1.88852
S	-1.15174	1.82207	-0.42073
S	-1.15187	-1.82205	-0.42073
O	1.42003	-6E-5	-1.30337
K	3.80806	6E-5	-0.12975
K	-3.78131	8E-5	0.31099

Potassium WS_4 Methanol B3LYP

W	-0.00275	0.08381	-0.00187
S	1.45541	1.62381	-0.6586
K	3.98996	-0.30251	0.0136
S	1.10369	-1.64852	0.83404
S	-1.21746	-0.57835	-1.73761
K	-3.97124	-0.30947	0.01329
S	-1.35113	0.94218	1.53889

Potassium WO_4 Gas Phase PBE0

W	-1E-5	-9.7E-4	1E-5
O	0.04517	-6.6E-4	1.78004
K	2.55748	0.00187	1.94583
O	1.72764	7E-4	-0.43114
O	-0.88793	1.38726	-0.6745
K	-2.55868	-0.00384	-1.94422
O	-0.88513	-1.39118	-0.67409

Potassium WO_3S Gas Phase PBE0

W	-0.09641	-0.07684	0
S	1.19411	1.75383	0
O	-1.20507	-0.11643	-1.37564
O	-1.20507	-0.11643	1.37564
O	1.01655	-1.45506	0
K	3.27507	-0.43031	0
K	-3.31836	-0.03662	0

Potassium WO_2S_2 Gas Phase PBE0

W	-0.10068	-0.59032	0.16057
S	-0.15512	1.61898	0.72364
S	1.61478	-0.95867	-1.2102
O	-1.65563	-0.89203	-0.60786

O	0.0517	-1.54315	1.58414
K	2.7529	1.54641	-0.08499
K	-2.91463	1.22202	-0.54171

Potassium WOS_3 Gas Phase PBE0

W	0.09313	0	-0.12491
S	1.22862	0	1.7702
S	-1.16598	1.81231	-0.25721
S	-1.16598	-1.81231	-0.25721
O	1.30884	0	-1.38295
K	3.49722	0	-0.21348
K	-3.48188	0	0.22476

Potassium WS_4 Gas Phase PBE0

W	-0.0065	-0.03482	0.01247
S	-0.01444	-0.04695	2.20999
K	2.9459	0.1071	2.11576
S	2.06388	0.07617	-0.71579
S	-1.13051	1.70878	-0.71256
K	-2.96125	-0.17643	-2.08782
S	-0.94498	-1.8773	-0.73161

Potassium WO_4 Acetonitrile PBE0

W	-8E-5	0.00118	4E-4
O	1.08276	1.32311	0.50751
O	1.07819	-1.3244	-0.50503
O	-1.07946	0.50892	-1.32333
O	-1.08276	-0.50409	1.32301
K	-3.39493	-0.00298	-0.00117
K	3.39577	-0.00312	-0.00129

Potassium WO_3S Acetonitrile PBE0

W	-0.09853	-0.04492	0.01324

S	1.15242	1.83958	-0.00944
O	-1.1392	-0.1494	-1.40826
O	-1.19666	-0.08759	1.39521
O	1.00941	-1.42322	0.07109
K	3.48805	-0.52643	-0.03252
K	-3.51625	-0.14869	-0.03554

Potassium WO_2S_2 Acetonitrile PBE0

W	-0.13863	-0.63894	0.14047
S	-0.07984	1.43743	1.00397
S	1.62522	-1.00785	-1.18706
O	-1.62671	-0.77427	-0.78195
O	-0.16599	-1.80513	1.43567
K	2.97434	1.68789	-0.11066
K	-2.98099	1.52494	-0.55749

Potassium WOS_3 Acetonitrile PBE0

W	0.10377	-2E-5	-0.14604
S	1.04921	-6E-5	1.85968
S	-1.14221	1.8103	-0.4307
S	-1.14232	-1.81027	-0.43073
O	1.40379	-4E-5	-1.31004
K	3.75986	6E-5	-0.08015
K	-3.71479	7E-5	0.35992

Potassium WS_4 Acetonitrile PBE0

W	-0.00335	-0.0975	0.01398
S	0.00205	-0.15402	2.21281
K	3.19539	0.33979	2.29786
S	2.07433	-0.0263	-0.7033
S	-1.08074	1.69112	-0.68039
K	-3.23272	-0.10446	-2.28004

S	-1.00285	-1.89207	-0.77048
Potassium WO_4 Methanol PBE0			
W	-9.8E-4	0.00535	-0.00324
O	1.07864	0.43794	-1.35438
O	1.0788	-0.43728	1.34449
O	-1.08818	-1.3389	-0.43873
O	-1.07311	1.35996	0.43657
K	-3.39726	0.02397	0.00609
K	3.39518	-0.02408	-0.01295
Potassium WO_3S Methanol PBE0			
W	-0.10024	-0.03791	0.01152
S	1.15871	1.86237	-0.0106
O	-1.15023	-0.15274	-1.41805
O	-1.20329	-0.08704	1.40533
O	1.02159	-1.42055	0.07158
K	3.52495	-0.55131	-0.02914
K	-3.54949	-0.17025	-0.03156
Potassium WO_2S_2 Methanol PBE0			
W	-0.15159	-0.69149	0.10664
S	-0.04684	1.24088	1.25298
S	1.71751	-1.00353	-1.0804
O	-1.53272	-0.55396	-0.97022
O	-0.4018	-2.0314	1.19313
K	2.8049	1.86122	-0.1045
K	-2.80683	1.72066	-0.55002
Potassium WOS_3 Methanol PBE0			
W	0.10381	-2E-5	-0.1462
S	1.04973	-2E-5	1.85923
S	-1.14243	1.81015	-0.43006

S	-1.14251	-1.81013	-0.43005
O	1.40359	-4E-5	-1.3105
K	3.7583	4E-5	-0.08007
K	-3.71344	6E-5	0.35991

Potassium WS_4 Methanol PBE0

W	-0.00298	-0.02402	-0.02278
S	1.27415	1.11201	-1.41023
K	3.95177	0.08579	0.07378
S	1.26552	-1.21294	1.32361
S	-1.33541	-1.37192	-1.13965
K	-3.92209	0.09377	0.06929
S	-1.22573	1.3707	1.16172

Hexamethyldisilathiane B3LYP Gas Phase

Si	-0.01346	0.00552	0.00662
S	1.7627	1.29717	-0.00185
Si	3.53886	0.00552	-0.01032
C	4.93999	1.16853	-0.51533
H	5.89238	0.63709	-0.50514
H	4.77523	1.56185	-1.5171
H	5.01167	2.00961	0.17287
C	3.87377	-0.6834	1.71898
H	4.81777	-1.23091	1.72444
H	3.94362	0.12722	2.44272
H	3.08606	-1.36045	2.04302
C	3.39798	-1.41241	-1.25519
H	4.35048	-1.94257	-1.30388
H	2.63166	-2.1315	-0.97109
H	3.16577	-1.03544	-2.24969
C	-1.41459	1.16853	0.51164

H	-1.48627	2.00961	-0.17656
H	-2.36698	0.63709	0.50144
H	-1.24983	1.56185	1.5134
C	-0.34837	-0.6834	-1.72267
H	0.43934	-1.36045	-2.04671
H	-1.29237	-1.23091	-1.72813
H	-0.41822	0.12722	-2.44641
C	0.12742	-1.41241	1.25149
H	0.89374	-2.1315	0.96739
H	0.35963	-1.03544	2.24599
H	-0.82508	-1.94257	1.30018

Hexamethyldisilathiane PBE0 Gas Phase

Si	1.74673	-0.02539	-0.001
S	0	1.28085	0
Si	-1.74673	-0.02539	0.001
C	-3.15858	1.11099	0.51815
H	-4.10407	0.56599	0.50553
H	-2.99199	1.497	1.52346
H	-3.23955	1.95658	-0.16498
C	-2.07362	-0.69967	-1.72991
H	-3.01178	-1.25854	-1.73819
H	-2.15366	0.1214	-2.44213
H	-1.27535	-1.36259	-2.0602
C	-1.5818	-1.44556	1.23264
H	-2.52885	-1.9872	1.27936
H	-0.80544	-2.15168	0.93979
H	-1.35159	-1.06685	2.22808
C	3.15858	1.11099	-0.51815
H	3.23955	1.95658	0.16498

H	4.10407	0.56599	-0.50553
H	2.99199	1.497	-1.52346
C	2.07362	-0.69967	1.72991
H	1.27535	-1.36259	2.0602
H	3.01178	-1.25854	1.73819
H	2.15366	0.1214	2.44213
C	1.5818	-1.44556	-1.23264
H	0.80544	-2.15168	-0.93979
H	1.35159	-1.06685	-2.22808
H	2.52885	-1.9872	-1.27936

Hexamethyldisilathiane MP2 Gas Phase

Si	1.73297	-0.02217	-2.2E-4
S	0	1.3112	0
Si	-1.73297	-0.02217	2.2E-4
C	-3.16192	1.07431	0.527
H	-4.09341	0.51298	0.51559
H	-3.00066	1.45828	1.52979
H	-3.26272	1.91953	-0.14786
C	-2.03995	-0.69642	-1.7262
H	-2.96666	-1.26696	-1.74105
H	-2.12831	0.11988	-2.43741
H	-1.23332	-1.34439	-2.05242
C	-1.52609	-1.44143	1.21596
H	-2.46058	-1.99687	1.2716
H	-0.74552	-2.13118	0.91051
H	-1.28997	-1.06917	2.20849
C	3.16192	1.07431	-0.527
H	3.26272	1.91953	0.14785
H	4.09341	0.51298	-0.5156

H	3.00066	1.45828	-1.52979
C	2.03995	-0.69642	1.7262
H	1.23333	-1.34439	2.05242
H	2.96667	-1.26696	1.74105
H	2.12831	0.11988	2.43741
C	1.52608	-1.44143	-1.21595
H	0.74552	-2.13118	-0.9105
H	1.28997	-1.06917	-2.20849
H	2.46058	-1.99687	-1.2716

Hexamethyldisiloxane B3LYP Gas Phase

Si	0	1.57897	0.06982
O	0	0	0.66625
Si	0	-1.57897	0.06982
C	0.6165	-2.66594	1.47651
H	0.62135	-3.71724	1.18747
H	1.62928	-2.38533	1.76392
H	-0.02462	-2.55457	2.3504
C	-1.75815	-2.06616	-0.41464
H	-1.79204	-3.10648	-0.74084
H	-2.43307	-1.95543	0.4338
H	-2.13241	-1.44605	-1.22863
C	1.14208	-1.73097	-1.42842
H	1.18168	-2.76771	-1.76529
H	0.79439	-1.12438	-2.2645
H	2.15632	-1.41978	-1.1795
C	-0.6165	2.66594	1.47651
H	0.02462	2.55457	2.3504
H	-0.62135	3.71724	1.18747
H	-1.62928	2.38533	1.76392

C	1.75815	2.06616	-0.41464
H	2.13241	1.44605	-1.22863
H	1.79204	3.10648	-0.74084
H	2.43307	1.95543	0.4338
C	-1.14208	1.73097	-1.42842
H	-0.79439	1.12438	-2.2645
H	-2.15632	1.41978	-1.1795
H	-1.18168	2.76771	-1.76529

Hexamethyldisiloxane PBE0 Gas Phase

Si	-1.55489	-0.00199	0.07759
O	0	-1E-5	0.73179
Si	1.55489	0.00199	0.07759
C	2.693	0.55546	1.46313
H	3.73364	0.56022	1.13562
H	2.43005	1.5602	1.79466
H	2.6023	-0.11845	2.3154
C	2.00529	-1.73725	-0.48622
H	3.03797	-1.76611	-0.83871
H	1.90714	-2.44171	0.34047
H	1.35953	-2.07076	-1.29896
C	1.6655	1.19193	-1.3807
H	2.69111	1.22756	-1.75279
H	1.02241	0.88045	-2.20494
H	1.37779	2.20033	-1.0814
C	-2.693	-0.55549	1.46311
H	-2.6023	0.1184	2.3154
H	-3.73364	-0.56025	1.13561
H	-2.43005	-1.56024	1.79463
C	-2.00529	1.73726	-0.48618

H	-1.35953	2.07079	-1.29892
H	-3.03797	1.76613	-0.83867
H	-1.90714	2.4417	0.34053
C	-1.6655	-1.19189	-1.38073
H	-1.02241	-0.8804	-2.20496
H	-1.3778	-2.20031	-1.08145
H	-2.69111	-1.22752	-1.75282

Hexamethyldisiloxane MP2 Gas Phase

Si	-1.54611	-0.00291	0.08566
O	0	-1E-5	0.76336
Si	1.54611	0.00291	0.08565
C	2.71022	0.5529	1.44281
H	3.73987	0.56469	1.0945
H	2.45064	1.55049	1.78508
H	2.6418	-0.123	2.29048
C	1.97829	-1.72956	-0.49729
H	2.99983	-1.76296	-0.86955
H	1.89257	-2.43851	0.32184
H	1.31575	-2.0518	-1.29554
C	1.61355	1.18957	-1.37249
H	2.6243	1.23263	-1.77257
H	0.95177	0.87326	-2.1748
H	1.32668	2.1932	-1.07027
C	-2.71021	-0.55293	1.4428
H	-2.6418	0.12295	2.29048
H	-3.73987	-0.56471	1.09449
H	-2.45064	-1.55052	1.78505
C	-1.97829	1.72957	-0.49725
H	-1.31575	2.05182	-1.2955

H	-2.99983	1.76298	-0.86951
H	-1.89257	2.4385	0.3219
C	-1.61356	-1.18954	-1.37251
H	-0.95177	-0.87321	-2.17482
H	-1.32668	-2.19318	-1.07032
H	-2.6243	-1.23259	-1.77259

Hexamethyldisilathiane B3LYP Acetonitrile

Si	-0.03179	-0.00561	0.01387
S	1.7627	1.28211	-0.00184
Si	3.55719	-0.00561	-0.01756
C	4.94584	1.17863	-0.50372
H	5.89911	0.64892	-0.49545
H	4.78307	1.58009	-1.50277
H	5.01032	2.00988	0.1972
C	3.87688	-0.70165	1.70934
H	4.81843	-1.25311	1.70851
H	3.95166	0.10477	2.43751
H	3.08471	-1.3779	2.02364
C	3.41305	-1.40175	-1.28125
H	4.36655	-1.93005	-1.3286
H	2.64403	-2.12192	-1.00846
H	3.18814	-1.00963	-2.27162
C	-1.42044	1.17863	0.50003
H	-1.48492	2.00988	-0.20089
H	-2.37371	0.64892	0.49175
H	-1.25767	1.58009	1.49908
C	-0.35148	-0.70165	-1.71303
H	0.44069	-1.3779	-2.02734
H	-1.29303	-1.25311	-1.7122

H	-0.42626	0.10477	-2.4412
C	0.11235	-1.40175	1.27755
H	0.88137	-2.12192	1.00477
H	0.33726	-1.00963	2.26793
H	-0.84115	-1.93005	1.32491

Hexamethyldisilathiane PBE0 Acetonitrile

Si	1.7627	-0.03079	-0.00185
S	0	1.27375	0
Si	-1.7627	-0.03079	0.00185
C	-3.16268	1.11598	0.52465
H	-4.10799	0.57074	0.50816
H	-2.9958	1.49358	1.53334
H	-3.24089	1.96324	-0.15698
C	-2.0819	-0.68813	-1.73477
H	-3.01201	-1.26026	-1.7381
H	-2.18097	0.13866	-2.43827
H	-1.27529	-1.33732	-2.07205
C	-1.58438	-1.44763	1.23037
H	-2.52986	-1.99261	1.26918
H	-0.80284	-2.14707	0.9359
H	-1.36151	-1.06923	2.22768
C	3.16268	1.11598	-0.52465
H	3.24089	1.96324	0.15698
H	4.10799	0.57074	-0.50816
H	2.9958	1.49358	-1.53334
C	2.0819	-0.68813	1.73477
H	1.27529	-1.33732	2.07205
H	3.01201	-1.26026	1.7381
H	2.18097	0.13866	2.43827

C	1.58438	-1.44763	-1.23037
H	0.80284	-2.14707	-0.9359
H	1.36151	-1.06923	-2.22768
H	2.52986	-1.99261	-1.26918

Hexamethyldisilathiane MP2 Acetonitrile

Si	0	1.74964	-0.02849
S	0	0	1.30273
Si	0	-1.74964	-0.02849
C	0.52429	-3.16656	1.08301
H	0.50861	-4.09913	0.52362
H	1.5294	-3.00566	1.46159
H	-0.15258	-3.26	1.92764
C	-1.73116	-2.04285	-0.69084
H	-1.74324	-2.96121	-1.27463
H	-2.43565	-2.1469	0.12962
H	-2.05902	-1.22625	-1.32537
C	1.21893	-1.53416	-1.4392
H	1.27263	-2.47035	-1.9919
H	0.91274	-0.7539	-2.12873
H	2.21024	-1.29957	-1.06265
C	-0.52429	3.16656	1.08301
H	0.15258	3.26	1.92764
H	-0.50861	4.09913	0.52362
H	-1.5294	3.00566	1.46159
C	1.73116	2.04285	-0.69084
H	2.05902	1.22625	-1.32537
H	1.74324	2.96121	-1.27463
H	2.43565	2.1469	0.12962
C	-1.21893	1.53416	-1.4392

H	-0.91274	0.7539	-2.12873
H	-2.21024	1.29957	-1.06265
H	-1.27263	2.47035	-1.9919

Hexamethyldisiloxane B3LYP Acetonitrile

Si	0	1.57652	0.06905
O	0	0	0.69629
Si	0	-1.57652	0.06905
C	0.53873	-2.68739	1.49023
H	0.5429	-3.73248	1.17957
H	1.54234	-2.42606	1.82526
H	-0.14205	-2.58488	2.3352
C	-1.74407	-2.02849	-0.49127
H	-1.77132	-3.06463	-0.83108
H	-2.45151	-1.92151	0.33105
H	-2.07398	-1.39316	-1.31247
C	1.20479	-1.72577	-1.37642
H	1.23904	-2.76138	-1.71743
H	0.90268	-1.10553	-2.21989
H	2.21112	-1.4337	-1.07732
C	-0.53873	2.68739	1.49023
H	0.14205	2.58488	2.3352
H	-0.5429	3.73248	1.17957
H	-1.54234	2.42606	1.82526
C	1.74407	2.02849	-0.49127
H	2.07398	1.39316	-1.31247
H	1.77132	3.06463	-0.83108
H	2.45151	1.92151	0.33105
C	-1.20479	1.72577	-1.37642
H	-0.90268	1.10553	-2.21989

H	-2.21112	1.4337	-1.07732
H	-1.23904	2.76138	-1.71743

Hexamethyldisiloxane PBE0 Acetonitrile

Si	-1.55367	-0.00189	0.07612
O	0	-1E-5	0.75542
Si	1.55367	0.00189	0.07612
C	2.70372	0.55559	1.45295
H	3.73796	0.56096	1.10547
H	2.44638	1.56141	1.78688
H	2.63006	-0.12151	2.30486
C	1.99505	-1.73938	-0.48471
H	3.02369	-1.76122	-0.84946
H	1.91092	-2.44088	0.34637
H	1.33938	-2.07426	-1.28881
C	1.64677	1.19305	-1.37913
H	2.67078	1.22169	-1.75651
H	0.99503	0.88289	-2.19676
H	1.36623	2.2018	-1.07408
C	-2.70372	-0.55563	1.45294
H	-2.63006	0.12146	2.30487
H	-3.73796	-0.56098	1.10546
H	-2.44638	-1.56145	1.78684
C	-1.99505	1.7394	-0.48467
H	-1.33938	2.07429	-1.28876
H	-3.02369	1.76124	-0.84942
H	-1.91091	2.44088	0.34642
C	-1.64678	-1.19302	-1.37916
H	-0.99503	-0.88284	-2.19678
H	-1.36623	-2.20178	-1.07413

H	-2.67078	-1.22165	-1.75653

Hexamethyldisiloxane MP2 Acetonitrile

Si	0	1.54582	0.08332
O	0	0	0.78285
Si	0	-1.54582	0.08332
C	0.55611	-2.71771	1.43236
H	0.56604	-3.74189	1.06806
H	1.55643	-2.46226	1.77082
H	-0.11912	-2.6616	2.28191
C	-1.73732	-1.9695	-0.48748
H	-1.76613	-2.98843	-0.86731
H	-2.43875	-1.8932	0.33928
H	-2.06379	-1.30005	-1.27809
C	1.18155	-1.59857	-1.37635
H	1.21812	-2.60945	-1.77695
H	0.86143	-0.93287	-2.17358
H	2.18594	-1.31533	-1.07321
C	-0.55611	2.71771	1.43236
H	0.11912	2.6616	2.28191
H	-0.56604	3.74189	1.06806
H	-1.55643	2.46226	1.77082
C	1.73732	1.9695	-0.48748
H	2.06379	1.30005	-1.27809
H	1.76613	2.98843	-0.86731
H	2.43875	1.8932	0.33928
C	-1.18155	1.59857	-1.37635
H	-0.86143	0.93287	-2.17358
H	-2.18594	1.31533	-1.07321
H	-1.21812	2.60945	-1.77695

Hexamethyldisilathiane B3LYP Methanol

Si	0	0	0
S	1.7627	1.30454	-0.00185
Si	3.5254	0	-0.00369
C	4.92537	1.14676	-0.5265
H	5.8707	0.60155	-0.50994
H	4.75853	1.52431	-1.53522
H	5.00354	1.99407	0.15508
C	3.8446	-0.65733	1.73292
H	4.7747	-1.22948	1.73625
H	3.9437	0.16946	2.43642
H	3.03799	-1.30651	2.07022
C	3.34708	-1.41684	-1.23221
H	4.29255	-1.96182	-1.27103
H	2.56553	-2.11628	-0.93775
H	3.1242	-1.03844	-2.22953
C	-1.39998	1.14676	0.52281
H	-1.47814	1.99407	-0.15878
H	-2.3453	0.60155	0.50625
H	-1.23314	1.52431	1.53153
C	-0.31921	-0.65733	-1.73662
H	0.48741	-1.30651	-2.07392
H	-1.2493	-1.22947	-1.73994
H	-0.4183	0.16946	-2.44011
C	0.17832	-1.41684	1.22852
H	0.95987	-2.11628	0.93405
H	0.4012	-1.03844	2.22583
H	-0.76715	-1.96183	1.26734

Hexamethyldisilathiane PBE0 Methanol

Si	1.76259	-0.03075	-0.00184
S	0	1.27381	0
Si	-1.76259	-0.03075	0.00184
C	-3.16267	1.11591	0.52463
H	-4.10798	0.57066	0.50815
H	-2.99579	1.49355	1.5333
H	-3.24091	1.96317	-0.157
C	-2.08185	-0.68818	-1.73474
H	-3.01194	-1.26033	-1.73807
H	-2.18092	0.13858	-2.43826
H	-1.27523	-1.33736	-2.07204
C	-1.58432	-1.44763	1.23036
H	-2.52978	-1.99263	1.26919
H	-0.80277	-2.14707	0.93592
H	-1.36145	-1.06923	2.22767
C	3.16267	1.11591	-0.52463
H	3.24091	1.96317	0.157
H	4.10798	0.57066	-0.50815
H	2.99579	1.49355	-1.5333
C	2.08185	-0.68818	1.73474
H	1.27523	-1.33736	2.07204
H	3.01194	-1.26033	1.73807
H	2.18092	0.13858	2.43826
C	1.58432	-1.44763	-1.23036
H	0.80277	-2.14707	-0.93592
H	1.36145	-1.06923	-2.22767
H	2.52978	-1.99263	-1.26919

Hexamethyldisilathiane MP2 Methanol

Si	0	1.74953	-0.02844

S	0	0	1.3028
Si	0	-1.74953	-0.02844
C	0.52425	-3.16656	1.08295
H	0.50858	-4.09911	0.52354
H	1.52935	-3.00568	1.46159
H	-0.15262	-3.26003	1.92757
C	-1.73111	-2.04282	-0.69093
H	-1.74316	-2.96121	-1.27469
H	-2.43567	-2.14682	0.12947
H	-2.05895	-1.22626	-1.32551
C	1.21893	-1.5341	-1.43918
H	1.27263	-2.47027	-1.99192
H	0.91277	-0.75381	-2.1287
H	2.21024	-1.29953	-1.06264
C	-0.52425	3.16656	1.08295
H	0.15262	3.26003	1.92757
H	-0.50858	4.09911	0.52354
H	-1.52935	3.00568	1.46159
C	1.73111	2.04282	-0.69093
H	2.05895	1.22626	-1.32551
H	1.74316	2.96121	-1.27469
H	2.43567	2.14682	0.12947
C	-1.21893	1.5341	-1.43918
H	-0.91277	0.75381	-2.1287
H	-2.21024	1.29953	-1.06264
H	-1.27263	2.47027	-1.99192

Hexamethyldisiloxane B3LYP Methanol

Si	0	1.57652	0.06906
O	0	0	0.69615

Si	0	-1.57652	0.06906
C	0.53919	-2.6873	1.49014
H	0.54332	-3.73242	1.17958
H	1.54287	-2.42588	1.82488
H	-0.14135	-2.58473	2.33529
C	-1.74416	-2.02868	-0.49084
H	-1.77147	-3.06483	-0.8306
H	-2.45141	-1.92168	0.33164
H	-2.07433	-1.3934	-1.31198
C	1.20444	-1.72577	-1.37672
H	1.23869	-2.76138	-1.71773
H	0.9021	-1.10558	-2.22015
H	2.21082	-1.43362	-1.07789
C	-0.53919	2.6873	1.49014
H	0.14135	2.58473	2.33529
H	-0.54332	3.73242	1.17958
H	-1.54287	2.42588	1.82488
C	1.74416	2.02868	-0.49084
H	2.07433	1.3934	-1.31198
H	1.77147	3.06483	-0.8306
H	2.45141	1.92168	0.33164
C	-1.20444	1.72577	-1.37672
H	-0.9021	1.10558	-2.22015
H	-2.21082	1.43362	-1.07789
H	-1.23869	2.76138	-1.71773

Hexamethyldisiloxane PBE0 Methanol

Si	-1.55367	-0.00189	0.07614
O	0	-1E-5	0.7553
Si	1.55367	0.00189	0.07614

C	2.70365	0.55584	1.45291
H	3.73793	0.56116	1.10554
H	2.44625	1.56169	1.78666
H	2.6299	-0.12111	2.30494
C	1.99518	-1.73943	-0.48449
H	3.02385	-1.76132	-0.84916
H	1.91098	-2.44082	0.34667
H	1.33958	-2.07443	-1.28858
C	1.64679	1.19285	-1.3793
H	2.67079	1.22151	-1.75669
H	0.99507	0.88257	-2.1969
H	1.36619	2.20163	-1.07439
C	-2.70365	-0.55587	1.4529
H	-2.62989	0.12106	2.30494
H	-3.73793	-0.56118	1.10553
H	-2.44625	-1.56173	1.78663
C	-1.99518	1.73944	-0.48445
H	-1.33958	2.07446	-1.28854
H	-3.02384	1.76134	-0.84912
H	-1.91097	2.44082	0.34672
C	-1.64679	-1.19282	-1.37933
H	-0.99507	-0.88253	-2.19692
H	-1.36619	-2.20161	-1.07444
H	-2.67079	-1.22147	-1.75672

Hexamethyldisiloxane MP2 Methanol

Si	-1.54579	-0.00289	0.08335
O	0	-1E-5	0.7828
Si	1.54579	0.00289	0.08335
C	2.71671	0.56093	1.43243

H	3.74089	0.57271	1.06818
H	2.45948	1.56074	1.77102
H	2.66175	-0.11449	2.2819
C	1.97265	-1.73357	-0.48775
H	2.99162	-1.76054	-0.86759
H	1.8976	-2.43525	0.33892
H	1.30378	-2.06115	-1.27838
C	1.5964	1.18474	-1.37619
H	2.60717	1.22327	-1.77685
H	0.93125	0.86354	-2.17345
H	1.3113	2.18856	-1.07289
C	-2.71671	-0.56097	1.43242
H	-2.66175	0.11443	2.28191
H	-3.74089	-0.57274	1.06817
H	-2.45948	-1.56078	1.77098
C	-1.97265	1.73358	-0.48771
H	-1.30378	2.06118	-1.27833
H	-2.99162	1.76056	-0.86755
H	-1.8976	2.43524	0.33897
C	-1.5964	-1.18471	-1.37621
H	-0.93125	-0.86349	-2.17347
H	-1.3113	-2.18854	-1.07294
H	-2.60717	-1.22323	-1.77687

Hydrogen Sulfide B3LYP Gas Phase

S	0	0	0.10311
H	0	0.96847	-0.82492
H	0	-0.96847	-0.82492

Hydrogen Sulfide PBE0 Gas Phase

S	0	0	0.1033

H	0	0.96595	-0.82643
H	0	-0.96595	-0.82643

Hydrogen Sulfide MP2 Gas Phase

S	0	0	0.10258
H	0	0.95842	-0.82066
H	0	-0.95842	-0.82066

Water B3LYP Gas Phase

O	0	0	0.11681
H	0	0.76299	-0.46723
H	0	-0.76299	-0.46723

Water PBE0 Gas Phase

O	0	0	0.11672
H	0	0.75928	-0.4669
H	0	-0.75928	-0.4669

Water MP2 Gas Phase

O	0	0	0.11762
H	0	0.75636	-0.47048
H	0	-0.75636	-0.47048

Hydrogen Sulfide B3LYP Acetonitrile

S	0	0	0.10268
H	0	0.97233	-0.82146
H	0	-0.97233	-0.82146

Hydrogen Sulfide PBE0 Acetonitrile

S	0	0	0.10288
H	0	0.97009	-0.82304
H	0	-0.97009	-0.82304

Hydrogen Sulfide MP2 Acetonitrile

S	0	0	0.10214
H	0	0.96263	-0.81716

H 0 -0.96263 -0.81716

Water B3LYP Acetonitrile

O 0 0 0.11765

H 0 0.76179 -0.47058

H 0 -0.76179 -0.47058

Water PBE0 Acetonitrile

O 0 0 0.11757

H 0 0.75811 -0.47026

H 0 -0.75811 -0.47026

Water MP2 Acetonitrile

O 0 0 0.11838

H 0 0.75563 -0.4735

H 0 -0.75563 -0.4735

Hydrogen Sulfide B3LYP Methanol

S 0 0 0.10268

H 0 0.97231 -0.82148

H 0 -0.97231 -0.82148

Hydrogen Sulfide PBE0 Methanol

S 0 0 0.10288

H 0 0.97007 -0.82305

H 0 -0.97007 -0.82305

Hydrogen Sulfide MP2 Methanol

S 0 0 0.10215

H 0 0.96261 -0.81717

H 0 -0.96261 -0.81717

Water B3LYP Methanol

O 0 0 0.11764

H 0 0.7618 -0.47057

H 0 -0.7618 -0.47057

Water PBE0 Methanol

O	0	0	0.11756
H	0	0.75812	-0.47025
H	0	-0.75812	-0.47025

Water MP2 Methanol

O	0	0	0.11837
H	0	0.75564	-0.47348
H	0	-0.75564	-0.47348

Characterization:

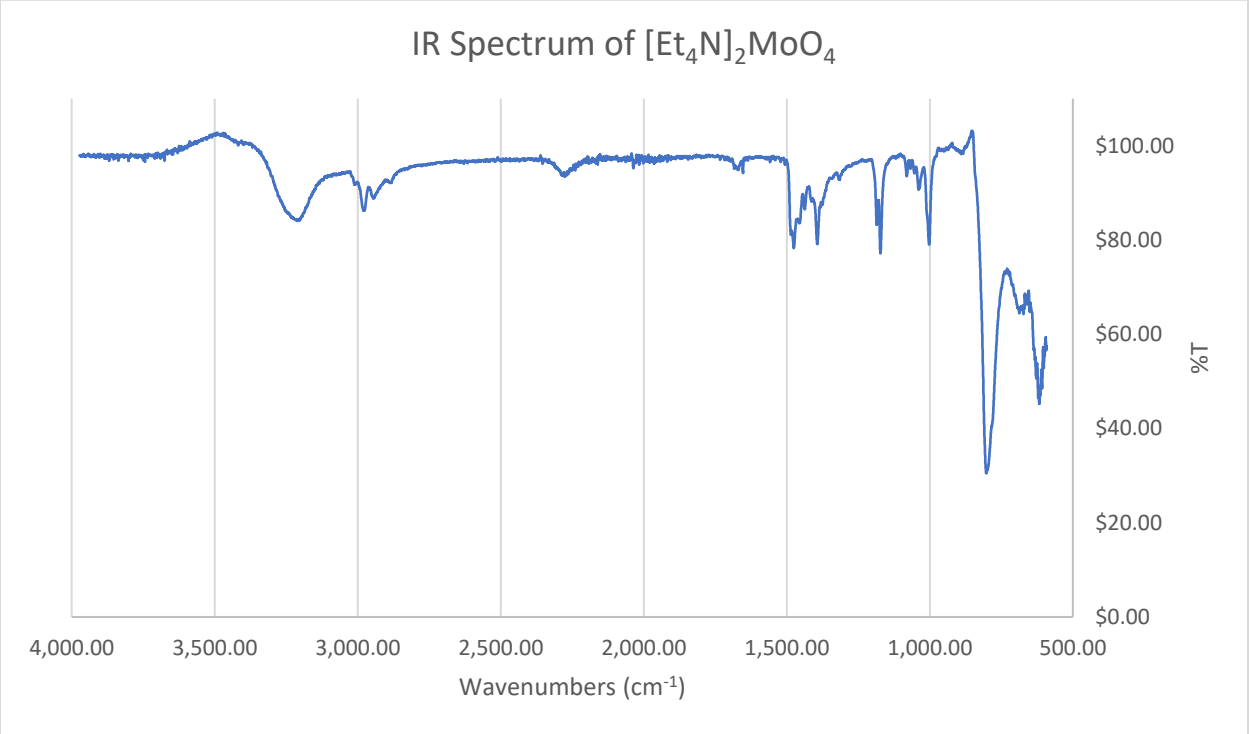

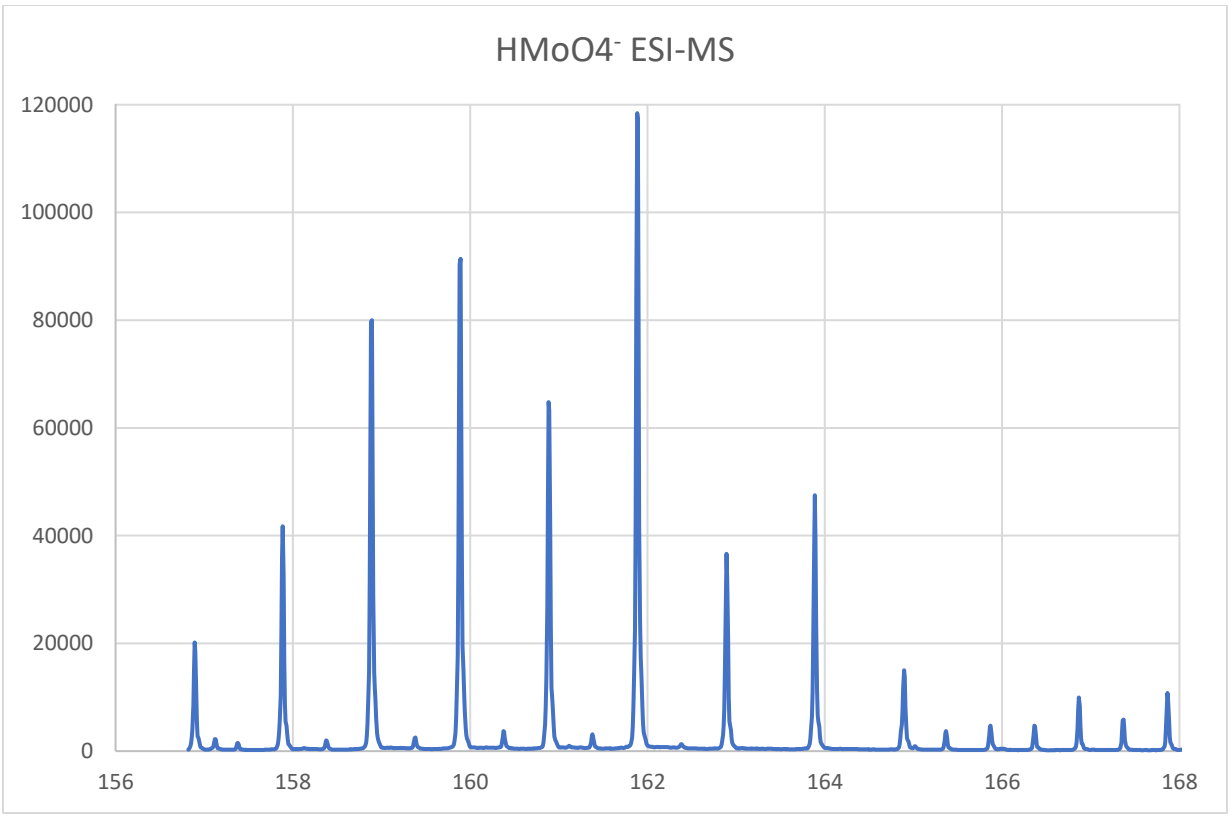
HMoO4- ESI-MS
120000
100000
80000
60000
40000
20000
0
156
158
160
162
164
166
168

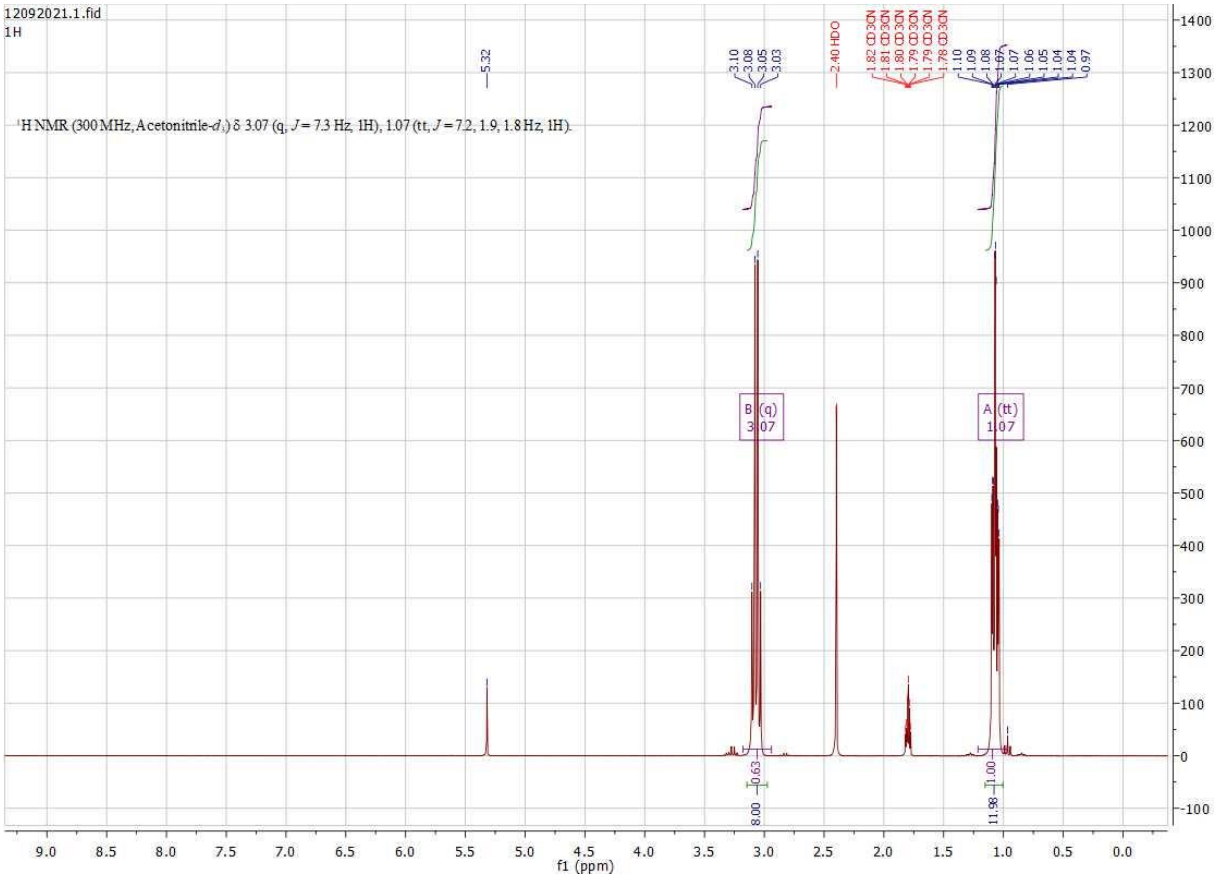
12092021.1.fid
1H
¹H NMR (300 MHz, Acetonitrile-d₃) δ 3.07 (q, J = 7.3 Hz, 1H), 1.07 (tt, J = 7.2, 1.9, 1.8 Hz, 1H).
5.32
2.40 HDO
B (q) 3.07
A (tt) 1.07
f1 (ppm)

^{1}H NMR (300 MHz, Acetonitrile-d_3) δ 3.07 (q, J = 7.3 Hz, 8H), 1.07 (tt, J = 7.2, 1.9, 1.8 Hz, 12H).

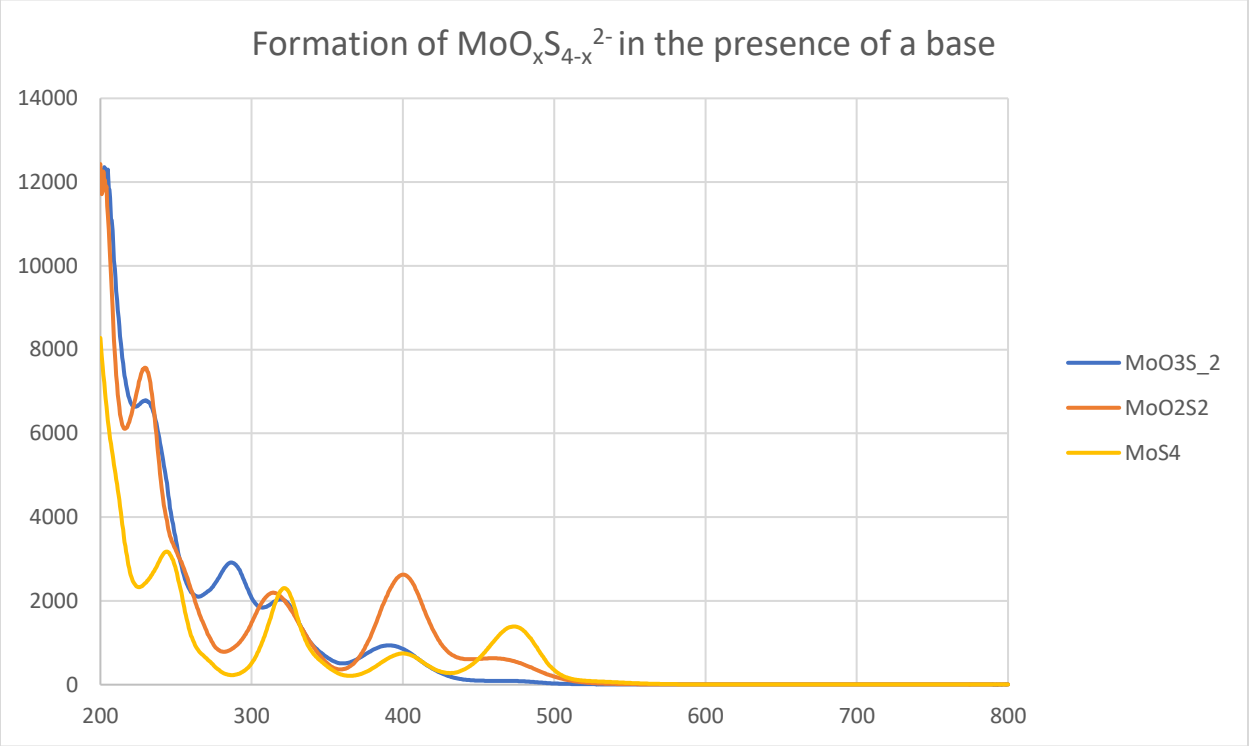

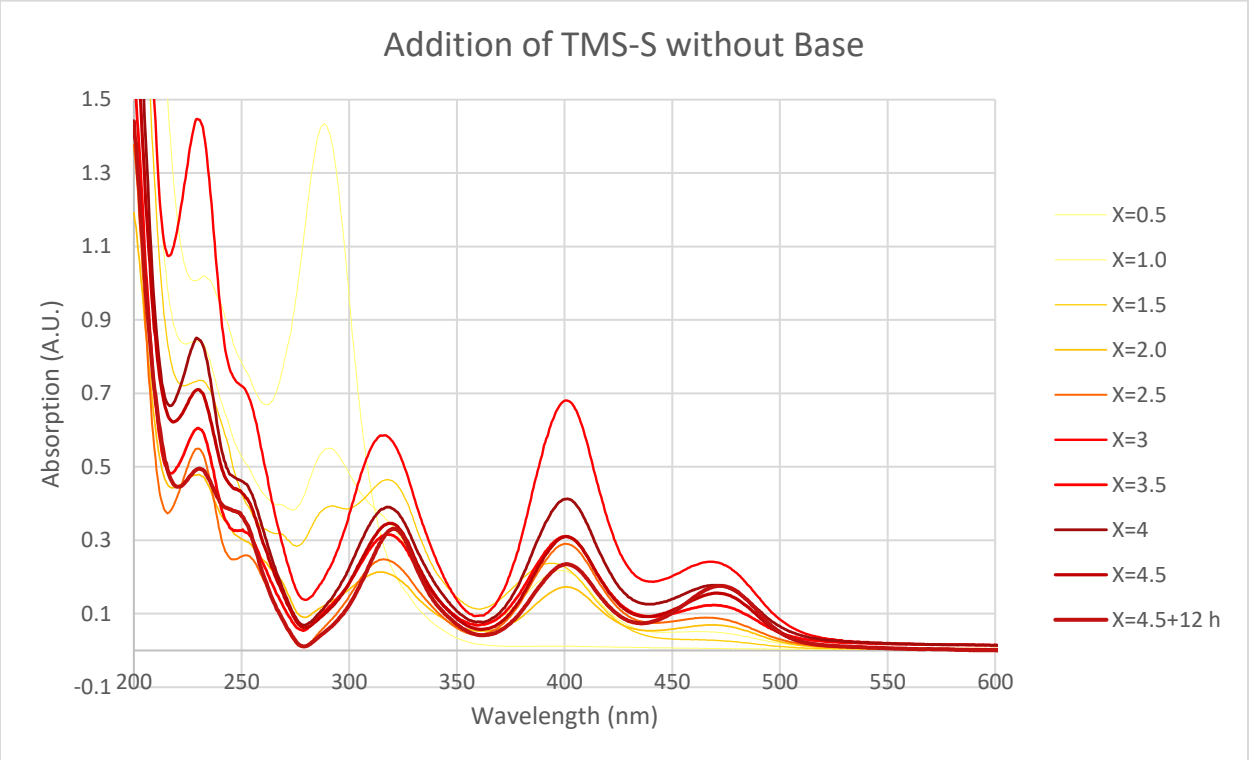

Structure Determination Summary

Crystal Data and Structure Refinement for $[Ph_3PNPPh_3][MoO_3(OPh_2{}^tBu)]$

Partial Atom Labeling for $[Ph_3PNPPh_3][MoO_3(OSiPh_2{}^tBu)]$

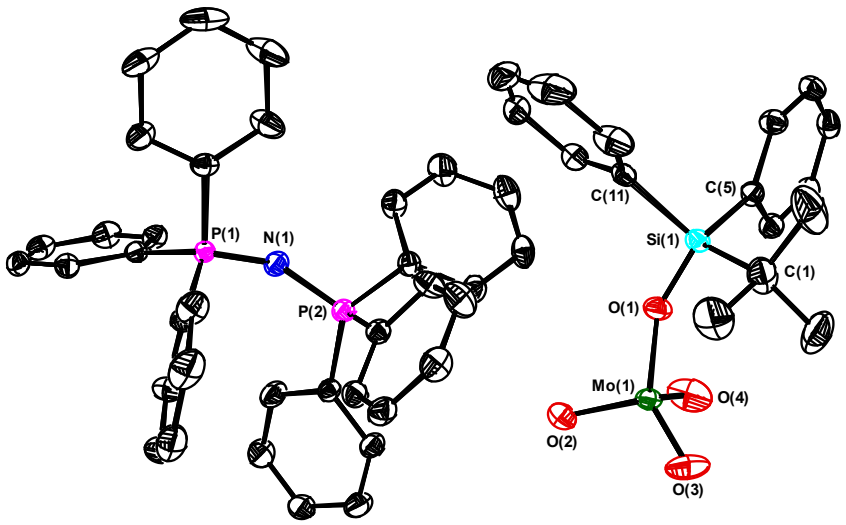

The thermal ellipsoid plot is drawn at the 50% level. All H atoms are omitted for clarity.

Identification code	JPD1290_0m_4_a	
Empirical formula	$C_{52}H_{49}MoNO_4P_2Si$	
Formula weight	937.89	
Temperature	150(2)K	
Wavelength	0.71073 Å	
Crystal system	Monoclinic	
Space group	$P2_1$	
Unit cell dimensions	a = 9.8005(5)Å	α = 90°
	b = 18.4905(10)Å	β = 103.327(2)°
	c = 12.9652(7)Å	γ = 90°
Volume	2286.2(2)Å^3	
Z	2	
Density (calculated)	1.362 g/cm^3	
Absorption coefficient	0.429 mm^{-1}	
F(000)	972	
Crystal size	0.516 x 0.286 x 0.111 mm^3	
θ range for data collection	2.203 to 33.037°	
Index ranges	$-14 \le h \le 14$, $0 \le k \le 27$, $0 \le l \le 19$	
Reflections collected	8303	
Independent reflections	8303 [R(int)= 0.4856]	

Completeness to θ = 25.242°	99.4 %
Absorption correction	Semi-empirical from equivalents
Refinement method	Full-matrix least-squares on F^2
Data / restraints / parameters	8303 / 1 / 554
Goodness-of-fit on F^2	1.055
Final R indices [I>2σ(I)]	R1 = 0.0260, wR2 = 0.0656
R indices (all data)	R1 = 0.0286, wR2 = 0.0674
Absolute structure parameter	0.49(4)
Extinction coefficient	n/a
Largest diff. peak and hole	0.358 and -0.755 e·Å^{-3}

Table S1. Atomic coordinates (x 10^4)and equivalent isotropic displacement parameters ($Å^2$ x 10^3) for $[Ph_3PNPPh_3][MoO_3(OPh_2{}^tBu)]$. U(eq)is defined as one third of the trace of the orthogonalized U^{ij} tensor.

Atom	x	y	z	U(eq)
Mo(1)	5190(1)	5543(1)	10315(1)	22(1)
P(1)	2138(1)	3214(1)	4210(1)	17(1)
P(2)	3813(1)	4082(1)	5974(1)	18(1)
Si(1)	1782(1)	6186(1)	9891(1)	19(1)
O(1)	3287(2)	5832(1)	9830(1)	28(1)
O(2)	5652(3)	4977(2)	9388(2)	62(1)
O(3)	5426(2)	5099(1)	11516(2)	46(1)
O(4)	6238(2)	6300(1)	10461(2)	52(1)
N(1)	3002(2)	3873(1)	4810(1)	23(1)
C(1)	1305(3)	5898(1)	11164(2)	33(1)
C(2)	-55(4)	6251(2)	11295(3)	54(1)
C(3)	1175(4)	5069(2)	11189(3)	47(1)
C(4)	2515(4)	6134(2)	12091(2)	56(1)
C(5)	1926(2)	7195(1)	9839(2)	20(1)
C(6)	3219(2)	7556(1)	10091(2)	22(1)
C(7)	3284(2)	8310(1)	10046(2)	25(1)
C(8)	2060(2)	8715(1)	9751(2)	26(1)
C(9)	768(2)	8367(1)	9504(2)	26(1)
C(10)	707(2)	7614(1)	9545(2)	22(1)
C(11)	464(2)	5902(1)	8661(2)	23(1)
C(12)	819(3)	6026(1)	7693(2)	32(1)
C(13)	-68(4)	5833(2)	6734(2)	54(1)
C(14)	-1338(4)	5519(2)	6705(3)	64(1)
C(15)	-1732(3)	5398(2)	7634(4)	62(1)
C(16)	-851(2)	5584(2)	8612(2)	37(1)
C(17)	319(2)	3466(1)	3787(2)	21(1)
C(18)	-647(2)	3008(1)	3147(2)	28(1)
C(19)	-2026(2)	3244(2)	2770(2)	35(1)
C(20)	-2434(3)	3927(2)	3029(2)	44(1)
C(21)	-1475(3)	4370(2)	3681(3)	47(1)
C(22)	-94(2)	4147(1)	4070(2)	36(1)
C(23)	2771(2)	3016(1)	3044(1)	18(1)
C(24)	2553(2)	2344(1)	2553(2)	22(1)
C(25)	3008(2)	2215(1)	1630(2)	24(1)
C(26)	3684(2)	2760(1)	1204(2)	27(1)
C(27)	3907(2)	3433(1)	1689(2)	28(1)
C(28)	3447(2)	3565(1)	2608(2)	24(1)
C(29)	2255(2)	2399(1)	4987(1)	21(1)
C(30)	3525(2)	2024(1)	5228(2)	29(1)

Table S1. Atomic coordinates (x 10^4)and equivalent isotropic displacement parameters ($Å^2$ x 10^3) for $[Ph_3PNPPh_3][MoO_3(OPh_2{}^tBu)]$. U(eq)is defined as one third of the trace of the orthogonalized U^{ij} tensor.

Atom	x	y	z	U(eq)
C(31)	3721(3)	1465(1)	5964(2)	38(1)
C(32)	2663(4)	1280(1)	6464(2)	43(1)
C(33)	1379(3)	1632(2)	6189(2)	41(1)
C(34)	1169(3)	2199(1)	5459(2)	30(1)
C(35)	5592(2)	3750(1)	6250(2)	21(1)
C(36)	6153(2)	3525(1)	5409(2)	27(1)
C(37)	7517(2)	3246(2)	5602(2)	32(1)
C(38)	8294(2)	3186(2)	6630(2)	31(1)
C(39)	7747(2)	3419(2)	7479(2)	31(1)
C(40)	6404(2)	3705(1)	7288(2)	25(1)
C(41)	3053(2)	3768(1)	7035(1)	20(1)
C(42)	3404(2)	3092(1)	7501(2)	23(1)
C(43)	2760(2)	2843(1)	8285(2)	26(1)
C(44)	1787(2)	3276(1)	8615(2)	30(1)
C(45)	1429(2)	3949(1)	8155(2)	34(1)
C(46)	2051(2)	4194(1)	7359(2)	28(1)
C(47)	3813(2)	5056(1)	6037(2)	21(1)
C(48)	3252(3)	5463(1)	5137(2)	30(1)
C(49)	3209(3)	6215(1)	5214(2)	38(1)
C(50)	3710(3)	6555(1)	6176(2)	36(1)
C(51)	4270(2)	6150(1)	7073(2)	32(1)
C(52)	4327(2)	5400(1)	7009(2)	26(1)

Table S2. Bond lengths (Å) for $[Ph_3PNPPh_3][MoO_3(OPh_2{}^tBu)]$. Symmetry transformations used to generate equivalent atoms.

Mo(1)-O(3)	1.7272(19)	C(13)-C(14)	1.367(6)
Mo(1)-O(2)	1.730(2)	C(13)-H(13)	0.9500
Mo(1)-O(4)	1.721(2)	C(14)-C(15)	1.365(6)
Mo(1)-O(1)	1.9029(15)	C(14)-H(14)	0.9500
P(1)-N(1)	1.5819(18)	C(15)-C(16)	1.403(4)
P(1)-C(23)	1.7990(18)	C(15)-H(15)	0.9500
P(1)-C(29)	1.8014(19)	C(16)-H(16)	0.9500
P(1)-C(17)	1.8014(19)	C(17)-C(18)	1.393(3)
P(2)-N(1)	1.5833(17)	C(17)-C(22)	1.398(3)
P(2)-C(41)	1.8038(19)	C(18)-C(19)	1.397(3)
P(2)-C(35)	1.8047(19)	C(18)-H(18)	0.9500
P(2)-C(47)	1.803(2)	C(19)-C(20)	1.389(5)
Si(1)-O(1)	1.6322(16)	C(19)-H(19)	0.9500
Si(1)-C(5)	1.8738(19)	C(20)-C(21)	1.379(5)
Si(1)-C(11)	1.881(2)	C(20)-H(20)	0.9500
Si(1)-C(1)	1.892(2)	C(21)-C(22)	1.393(3)
C(1)-C(2)	1.528(4)	C(21)-H(21)	0.9500
C(1)-C(3)	1.539(4)	C(22)-H(22)	0.9500
C(1)-C(4)	1.544(4)	C(23)-C(24)	1.391(3)
C(2)-H(2A)	0.9800	C(23)-C(28)	1.400(3)
C(2)-H(2B)	0.9800	C(24)-C(25)	1.391(3)
C(2)-H(2C)	0.9800	C(24)-H(24)	0.9500
C(3)-H(3A)	0.9800	C(25)-C(26)	1.388(3)
C(3)-H(3B)	0.9800	C(25)-H(25)	0.9500
C(3)-H(3C)	0.9800	C(26)-C(27)	1.390(3)
C(4)-H(4A)	0.9800	C(26)-H(26)	0.9500
C(4)-H(4B)	0.9800	C(27)-C(28)	1.390(3)
C(4)-H(4C)	0.9800	C(27)-H(27)	0.9500
C(5)-C(10)	1.401(3)	C(28)-H(28)	0.9500
C(5)-C(6)	1.403(3)	C(29)-C(34)	1.394(3)
C(6)-C(7)	1.398(3)	C(29)-C(30)	1.396(3)
C(6)-H(6)	0.9500	C(30)-C(31)	1.390(3)
C(7)-C(8)	1.390(3)	C(30)-H(30)	0.9500
C(7)-H(7)	0.9500	C(31)-C(32)	1.387(4)
C(8)-C(9)	1.390(3)	C(31)-H(31)	0.9500
C(8)-H(8)	0.9500	C(32)-C(33)	1.389(5)
C(9)-C(10)	1.395(3)	C(32)-H(32)	0.9500
C(9)-H(9)	0.9500	C(33)-C(34)	1.396(3)
C(10)-H(10)	0.9500	C(33)-H(33)	0.9500
C(11)-C(12)	1.396(3)	C(34)-H(34)	0.9500
C(11)-C(16)	1.404(3)	C(35)-C(36)	1.393(3)
C(12)-C(13)	1.390(4)	C(35)-C(40)	1.399(3)
C(12)-H(12)	0.9500	C(36)-C(37)	1.400(3)

Table S2. Bond lengths (Å) for $[Ph_3PNPPh_3][MoO_3(OPh_2{}^tBu)]$. Symmetry transformations used to generate equivalent atoms.

C(36)-H(36)	0.9500
C(37)-C(38)	1.378(3)
C(37)-H(37)	0.9500
C(38)-C(39)	1.399(3)
C(38)-H(38)	0.9500
C(39)-C(40)	1.387(3)
C(39)-H(39)	0.9500
C(40)-H(40)	0.9500
C(41)-C(42)	1.398(3)
C(41)-C(46)	1.398(3)
C(42)-C(43)	1.393(3)
C(42)-H(42)	0.9500
C(43)-C(44)	1.386(3)
C(43)-H(43)	0.9500
C(44)-C(45)	1.389(4)
C(44)-H(44)	0.9500
C(45)-C(46)	1.391(3)
C(45)-H(45)	0.9500
C(46)-H(46)	0.9500
C(47)-C(48)	1.391(3)
C(47)-C(52)	1.398(3)
C(48)-C(49)	1.396(3)
C(48)-H(48)	0.9500
C(49)-C(50)	1.382(4)
C(49)-H(49)	0.9500
C(50)-C(51)	1.386(4)
C(50)-H(50)	0.9500
C(51)-C(52)	1.390(3)
C(51)-H(51)	0.9500
C(52)-H(52)	0.9500

Table S3. Bond angles (deg.) for $[Ph_3PNPPh_3][MoO_3(OPh_2{}^tBu)]$. Symmetry transformations used to generate equivalent atoms.

O(3)-Mo(1)-O(2)	109.65(12)	H(3B)-C(3)-H(3C)	109.5
O(3)-Mo(1)-O(4)	109.60(12)	C(1)-C(4)-H(4A)	109.5
O(2)-Mo(1)-O(4)	108.81(15)	C(1)-C(4)-H(4B)	109.5
O(3)-Mo(1)-O(1)	110.44(9)	H(4A)-C(4)-H(4B)	109.5
O(2)-Mo(1)-O(1)	109.51(9)	C(1)-C(4)-H(4C)	109.5
O(4)-Mo(1)-O(1)	108.81(9)	H(4A)-C(4)-H(4C)	109.5
N(1)-P(1)-C(23)	108.70(9)	H(4B)-C(4)-H(4C)	109.5
N(1)-P(1)-C(29)	114.31(9)	C(10)-C(5)-C(6)	117.89(18)
C(23)-P(1)-C(29)	108.03(9)	C(10)-C(5)-Si(1)	119.61(14)
N(1)-P(1)-C(17)	109.31(10)	C(6)-C(5)-Si(1)	122.50(15)
C(23)-P(1)-C(17)	107.79(8)	C(7)-C(6)-C(5)	120.82(19)
C(29)-P(1)-C(17)	108.51(9)	C(7)-C(6)-H(6)	119.6
N(1)-P(2)-C(41)	116.32(9)	C(5)-C(6)-H(6)	119.6
N(1)-P(2)-C(35)	110.85(9)	C(8)-C(7)-C(6)	120.24(19)
C(41)-P(2)-C(35)	106.77(9)	C(8)-C(7)-H(7)	119.9
N(1)-P(2)-C(47)	106.36(9)	C(6)-C(7)-H(7)	119.9
C(41)-P(2)-C(47)	106.43(9)	C(9)-C(8)-C(7)	119.80(19)
C(35)-P(2)-C(47)	109.95(9)	C(9)-C(8)-H(8)	120.1
O(1)-Si(1)-C(5)	108.69(9)	C(7)-C(8)-H(8)	120.1
O(1)-Si(1)-C(11)	107.38(9)	C(8)-C(9)-C(10)	119.83(19)
C(5)-Si(1)-C(11)	106.88(9)	C(8)-C(9)-H(9)	120.1
O(1)-Si(1)-C(1)	109.71(11)	C(10)-C(9)-H(9)	120.1
C(5)-Si(1)-C(1)	110.34(10)	C(9)-C(10)-C(5)	121.41(19)
C(11)-Si(1)-C(1)	113.67(12)	C(9)-C(10)-H(10)	119.3
Si(1)-O(1)-Mo(1)	157.63(11)	C(5)-C(10)-H(10)	119.3
P(2)-N(1)-P(1)	138.66(12)	C(12)-C(11)-C(16)	116.4(2)
C(2)-C(1)-C(3)	110.2(3)	C(12)-C(11)-Si(1)	116.82(16)
C(2)-C(1)-C(4)	109.0(3)	C(16)-C(11)-Si(1)	126.81(18)
C(3)-C(1)-C(4)	108.5(3)	C(13)-C(12)-C(11)	121.9(3)
C(2)-C(1)-Si(1)	111.92(19)	C(13)-C(12)-H(12)	119.1
C(3)-C(1)-Si(1)	109.7(2)	C(11)-C(12)-H(12)	119.1
C(4)-C(1)-Si(1)	107.5(2)	C(14)-C(13)-C(12)	120.8(3)
C(1)-C(2)-H(2A)	109.5	C(14)-C(13)-H(13)	119.6
C(1)-C(2)-H(2B)	109.5	C(12)-C(13)-H(13)	119.6
H(2A)-C(2)-H(2B)	109.5	C(15)-C(14)-C(13)	119.1(2)
C(1)-C(2)-H(2C)	109.5	C(15)-C(14)-H(14)	120.4
H(2A)-C(2)-H(2C)	109.5	C(13)-C(14)-H(14)	120.4
H(2B)-C(2)-H(2C)	109.5	C(14)-C(15)-C(16)	121.1(3)
C(1)-C(3)-H(3A)	109.5	C(14)-C(15)-H(15)	119.4
C(1)-C(3)-H(3B)	109.5	C(16)-C(15)-H(15)	119.4
H(3A)-C(3)-H(3B)	109.5	C(15)-C(16)-C(11)	120.7(3)
C(1)-C(3)-H(3C)	109.5	C(15)-C(16)-H(16)	119.6
H(3A)-C(3)-H(3C)	109.5	C(11)-C(16)-H(16)	119.6

Table S3. Bond angles (deg.) for $[Ph_3PNPPh_3][MoO_3(OPh_2{}^tBu)]$. Symmetry transformations used to generate equivalent atoms.

C(18)-C(17)-C(22)	120.44(19)	C(32)-C(31)-H(31)	119.9
C(18)-C(17)-P(1)	120.88(16)	C(30)-C(31)-H(31)	119.9
C(22)-C(17)-P(1)	118.61(16)	C(31)-C(32)-C(33)	119.7(2)
C(17)-C(18)-C(19)	119.2(2)	C(31)-C(32)-H(32)	120.2
C(17)-C(18)-H(18)	120.4	C(33)-C(32)-H(32)	120.2
C(19)-C(18)-H(18)	120.4	C(32)-C(33)-C(34)	120.6(2)
C(20)-C(19)-C(18)	120.6(2)	C(32)-C(33)-H(33)	119.7
C(20)-C(19)-H(19)	119.7	C(34)-C(33)-H(33)	119.7
C(18)-C(19)-H(19)	119.7	C(29)-C(34)-C(33)	119.3(2)
C(21)-C(20)-C(19)	119.7(2)	C(29)-C(34)-H(34)	120.4
C(21)-C(20)-H(20)	120.2	C(33)-C(34)-H(34)	120.4
C(19)-C(20)-H(20)	120.2	C(36)-C(35)-C(40)	119.67(18)
C(20)-C(21)-C(22)	120.9(3)	C(36)-C(35)-P(2)	118.94(15)
C(20)-C(21)-H(21)	119.5	C(40)-C(35)-P(2)	121.38(15)
C(22)-C(21)-H(21)	119.5	C(35)-C(36)-C(37)	120.20(19)
C(21)-C(22)-C(17)	119.2(2)	C(35)-C(36)-H(36)	119.9
C(21)-C(22)-H(22)	120.4	C(37)-C(36)-H(36)	119.9
C(17)-C(22)-H(22)	120.4	C(38)-C(37)-C(36)	119.6(2)
C(24)-C(23)-C(28)	120.01(17)	C(38)-C(37)-H(37)	120.2
C(24)-C(23)-P(1)	121.34(14)	C(36)-C(37)-H(37)	120.2
C(28)-C(23)-P(1)	118.60(15)	C(37)-C(38)-C(39)	120.6(2)
C(25)-C(24)-C(23)	120.04(18)	C(37)-C(38)-H(38)	119.7
C(25)-C(24)-H(24)	120.0	C(39)-C(38)-H(38)	119.7
C(23)-C(24)-H(24)	120.0	C(40)-C(39)-C(38)	119.8(2)
C(26)-C(25)-C(24)	119.7(2)	C(40)-C(39)-H(39)	120.1
C(26)-C(25)-H(25)	120.1	C(38)-C(39)-H(39)	120.1
C(24)-C(25)-H(25)	120.1	C(39)-C(40)-C(35)	120.04(18)
C(27)-C(26)-C(25)	120.63(19)	C(39)-C(40)-H(40)	120.0
C(27)-C(26)-H(26)	119.7	C(35)-C(40)-H(40)	120.0
C(25)-C(26)-H(26)	119.7	C(42)-C(41)-C(46)	119.66(18)
C(26)-C(27)-C(28)	119.8(2)	C(42)-C(41)-P(2)	120.95(14)
C(26)-C(27)-H(27)	120.1	C(46)-C(41)-P(2)	119.32(15)
C(28)-C(27)-H(27)	120.1	C(43)-C(42)-C(41)	120.21(18)
C(27)-C(28)-C(23)	119.79(19)	C(43)-C(42)-H(42)	119.9
C(27)-C(28)-H(28)	120.1	C(41)-C(42)-H(42)	119.9
C(23)-C(28)-H(28)	120.1	C(44)-C(43)-C(42)	119.6(2)
C(34)-C(29)-C(30)	120.05(19)	C(44)-C(43)-H(43)	120.2
C(34)-C(29)-P(1)	120.70(16)	C(42)-C(43)-H(43)	120.2
C(30)-C(29)-P(1)	118.69(16)	C(43)-C(44)-C(45)	120.59(19)
C(31)-C(30)-C(29)	119.9(2)	C(43)-C(44)-H(44)	119.7
C(31)-C(30)-H(30)	120.0	C(45)-C(44)-H(44)	119.7
C(29)-C(30)-H(30)	120.0	C(44)-C(45)-C(46)	120.0(2)
C(32)-C(31)-C(30)	120.3(2)	C(44)-C(45)-H(45)	120.0

Table S3. Bond angles (deg.) for $[Ph_3PNPPh_3][MoO_3(OPh_2{}^tBu)]$. Symmetry transformations used to generate equivalent atoms.

C(46)-C(45)-H(45)	120.0
C(45)-C(46)-C(41)	119.9(2)
C(45)-C(46)-H(46)	120.1
C(41)-C(46)-H(46)	120.1
C(48)-C(47)-C(52)	120.08(19)
C(48)-C(47)-P(2)	120.42(16)
C(52)-C(47)-P(2)	119.45(15)
C(47)-C(48)-C(49)	119.4(2)
C(47)-C(48)-H(48)	120.3
C(49)-C(48)-H(48)	120.3
C(50)-C(49)-C(48)	120.5(2)
C(50)-C(49)-H(49)	119.8
C(48)-C(49)-H(49)	119.8
C(49)-C(50)-C(51)	120.1(2)
C(49)-C(50)-H(50)	120.0
C(51)-C(50)-H(50)	120.0
C(50)-C(51)-C(52)	120.2(2)
C(50)-C(51)-H(51)	119.9
C(52)-C(51)-H(51)	119.9
C(51)-C(52)-C(47)	119.7(2)
C(51)-C(52)-H(52)	120.1
C(47)-C(52)-H(52)	120.1

Table S4. Anisotropic displacement parameters (Å^2 x 10^3) for [Ph_3PNPPh_3][$MoO_3(OPh_2{}^tBu)$]. The anisotropic displacement factor exponent takes the form: $-2\pi^2[h^2a^{*2}U^{11} + ... + 2hka^*b^*U^{12}]$.

Atom	U^{11}	U^{22}	U^{33}	U^{23}	U^{13}	U^{12}
Mo(1)	21(1)	19(1)	24(1)	1(1)	0(1)	4(1)
P(1)	17(1)	18(1)	16(1)	1(1)	3(1)	1(1)
P(2)	19(1)	18(1)	16(1)	0(1)	4(1)	0(1)
Si(1)	21(1)	15(1)	21(1)	1(1)	4(1)	1(1)
O(1)	21(1)	27(1)	33(1)	0(1)	0(1)	6(1)
O(2)	66(1)	72(2)	39(1)	-15(1)	-4(1)	48(1)
O(3)	41(1)	50(1)	43(1)	25(1)	2(1)	9(1)
O(4)	31(1)	35(1)	87(2)	8(1)	5(1)	-8(1)
N(1)	27(1)	21(1)	19(1)	0(1)	2(1)	-1(1)
C(1)	53(2)	24(1)	26(1)	4(1)	16(1)	3(1)
C(2)	77(2)	46(2)	54(2)	5(1)	46(2)	12(2)
C(3)	72(2)	28(1)	45(2)	14(1)	24(1)	3(1)
C(4)	97(3)	45(2)	22(1)	0(1)	3(1)	2(2)
C(5)	23(1)	17(1)	20(1)	1(1)	4(1)	-1(1)
C(6)	21(1)	23(1)	22(1)	0(1)	5(1)	0(1)
C(7)	28(1)	24(1)	25(1)	-4(1)	10(1)	-7(1)
C(8)	38(1)	17(1)	26(1)	0(1)	12(1)	-1(1)
C(9)	30(1)	20(1)	27(1)	1(1)	6(1)	5(1)
C(10)	21(1)	20(1)	25(1)	1(1)	3(1)	0(1)
C(11)	19(1)	16(1)	31(1)	-4(1)	2(1)	3(1)
C(12)	35(1)	33(1)	27(1)	-4(1)	3(1)	12(1)
C(13)	71(2)	50(2)	30(1)	-11(1)	-9(1)	32(2)
C(14)	63(2)	43(1)	62(2)	-27(2)	-37(2)	20(2)
C(15)	32(1)	29(1)	106(3)	-13(2)	-23(2)	-1(1)
C(16)	22(1)	22(1)	64(2)	0(1)	4(1)	-3(1)
C(17)	18(1)	25(1)	20(1)	3(1)	4(1)	4(1)
C(18)	22(1)	40(1)	22(1)	-2(1)	4(1)	0(1)
C(19)	21(1)	61(2)	22(1)	3(1)	0(1)	-1(1)
C(20)	23(1)	60(2)	48(1)	24(1)	5(1)	11(1)
C(21)	34(1)	33(1)	74(2)	10(1)	14(1)	14(1)
C(22)	26(1)	26(1)	55(2)	0(1)	7(1)	6(1)
C(23)	18(1)	21(1)	17(1)	1(1)	4(1)	1(1)
C(24)	20(1)	22(1)	23(1)	-2(1)	6(1)	-1(1)
C(25)	22(1)	29(1)	22(1)	-6(1)	4(1)	3(1)
C(26)	22(1)	42(1)	19(1)	0(1)	6(1)	4(1)
C(27)	30(1)	34(1)	24(1)	6(1)	10(1)	-2(1)
C(28)	26(1)	23(1)	21(1)	3(1)	5(1)	-2(1)
C(29)	26(1)	20(1)	18(1)	1(1)	4(1)	1(1)
C(30)	31(1)	26(1)	28(1)	4(1)	3(1)	7(1)

Table S4. Anisotropic displacement parameters (Å^2 x 10^3) for [Ph_3PNPPh_3][$MoO_3(OPh_2{}^tBu)$].

The anisotropic displacement factor exponent takes the form: $-2\pi^2[h^2a^{*2}U^{11} + ... + 2hka^*b^*U^{12}]$.

Atom	U^{11}	U^{22}	U^{33}	U^{23}	U^{13}	U^{12}
C(31)	51(2)	26(1)	32(1)	5(1)	-3(1)	9(1)
C(32)	75(2)	25(1)	23(1)	7(1)	0(1)	-8(1)
C(33)	57(2)	40(1)	26(1)	8(1)	10(1)	-16(1)
C(34)	33(1)	32(1)	24(1)	4(1)	7(1)	-5(1)
C(35)	19(1)	24(1)	20(1)	0(1)	4(1)	0(1)
C(36)	25(1)	37(1)	19(1)	-1(1)	5(1)	2(1)
C(37)	25(1)	45(1)	29(1)	-4(1)	9(1)	4(1)
C(38)	23(1)	39(1)	31(1)	-3(1)	7(1)	6(1)
C(39)	24(1)	45(1)	21(1)	-1(1)	3(1)	7(1)
C(40)	24(1)	33(1)	18(1)	-1(1)	4(1)	2(1)
C(41)	20(1)	21(1)	18(1)	0(1)	5(1)	0(1)
C(42)	28(1)	23(1)	19(1)	1(1)	8(1)	3(1)
C(43)	32(1)	28(1)	20(1)	4(1)	6(1)	-1(1)
C(44)	30(1)	37(1)	26(1)	2(1)	13(1)	-4(1)
C(45)	30(1)	36(1)	43(1)	-1(1)	21(1)	4(1)
C(46)	25(1)	24(1)	36(1)	4(1)	12(1)	3(1)
C(47)	23(1)	19(1)	22(1)	-1(1)	7(1)	-2(1)
C(48)	44(1)	22(1)	22(1)	2(1)	8(1)	-1(1)
C(49)	58(2)	23(1)	35(1)	6(1)	15(1)	0(1)
C(50)	48(1)	20(1)	47(1)	-4(1)	22(1)	-8(1)
C(51)	31(1)	28(1)	38(1)	-11(1)	13(1)	-10(1)
C(52)	25(1)	26(1)	26(1)	-5(1)	5(1)	-4(1)

Table S5. Hydrogen coordinates (x 10^4) and isotropic displacement parameters (Å^2 x 10^3) for [Ph_3PNPPh_3][$MoO_3(OPh_2{}^tBu)$].

H atom	x	y	z	U(eq)
H(2A)	-303	6061	11933	81
H(2B)	-809	6143	10673	81
H(2C)	76	6776	11361	81
H(3A)	2054	4848	11111	70
H(3B)	407	4911	10607	70
H(3C)	981	4920	11867	70
H(4A)	2696	6651	12030	85
H(4B)	3362	5859	12068	85
H(4C)	2254	6040	12765	85
H(6)	4061	7285	10296	27
H(7)	4168	8547	10216	30
H(8)	2107	9227	9719	32
H(9)	-71	8642	9309	31
H(10)	-180	7381	9369	27
H(12)	1692	6249	7691	39
H(13)	213	5921	6091	65
H(14)	-1940	5387	6047	77
H(15)	-2618	5183	7617	75
H(16)	-1146	5493	9248	45
H(18)	-371	2540	2969	34
H(19)	-2691	2935	2333	42
H(20)	-3369	4088	2759	53
H(21)	-1760	4834	3866	57
H(22)	559	4454	4522	43
H(24)	2092	1972	2849	26
H(25)	2857	1757	1293	29
H(26)	3997	2671	574	33
H(27)	4372	3803	1393	34
H(28)	3591	4026	2940	28
H(30)	4255	2151	4890	35
H(31)	4584	1208	6125	46
H(32)	2815	913	6992	51
H(33)	636	1486	6501	49
H(34)	296	2446	5285	36
H(36)	5609	3562	4703	32
H(37)	7904	3099	5028	39
H(38)	9210	2985	6763	37
H(39)	8294	3382	8184	37
H(40)	6035	3871	7862	30
H(42)	4085	2800	7283	28

Table S5. Hydrogen coordinates (x 10^4) and isotropic displacement parameters (Å^2 x 10^3) for [Ph_3PNPPh_3][$MoO_3(OPh_2{}^tBu)$].

H atom	x	y	z	U(eq)
H(43)	2985	2379	8592	32
H(44)	1362	3111	9160	36
H(45)	759	4242	8385	41
H(46)	1795	4651	7036	33
H(48)	2901	5231	4475	36
H(49)	2832	6496	4600	45
H(50)	3671	7067	6222	44
H(51)	4616	6385	7733	38
H(52)	4715	5123	7624	31

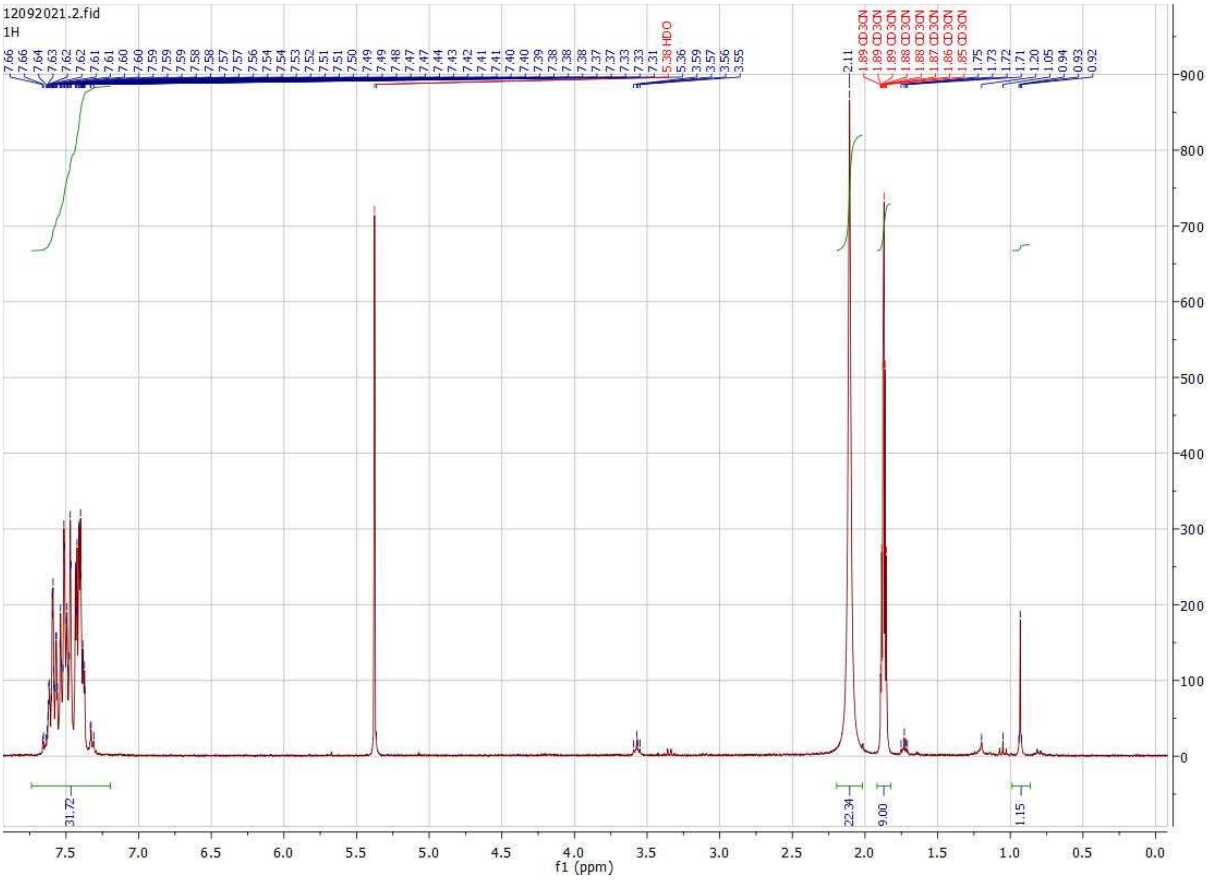

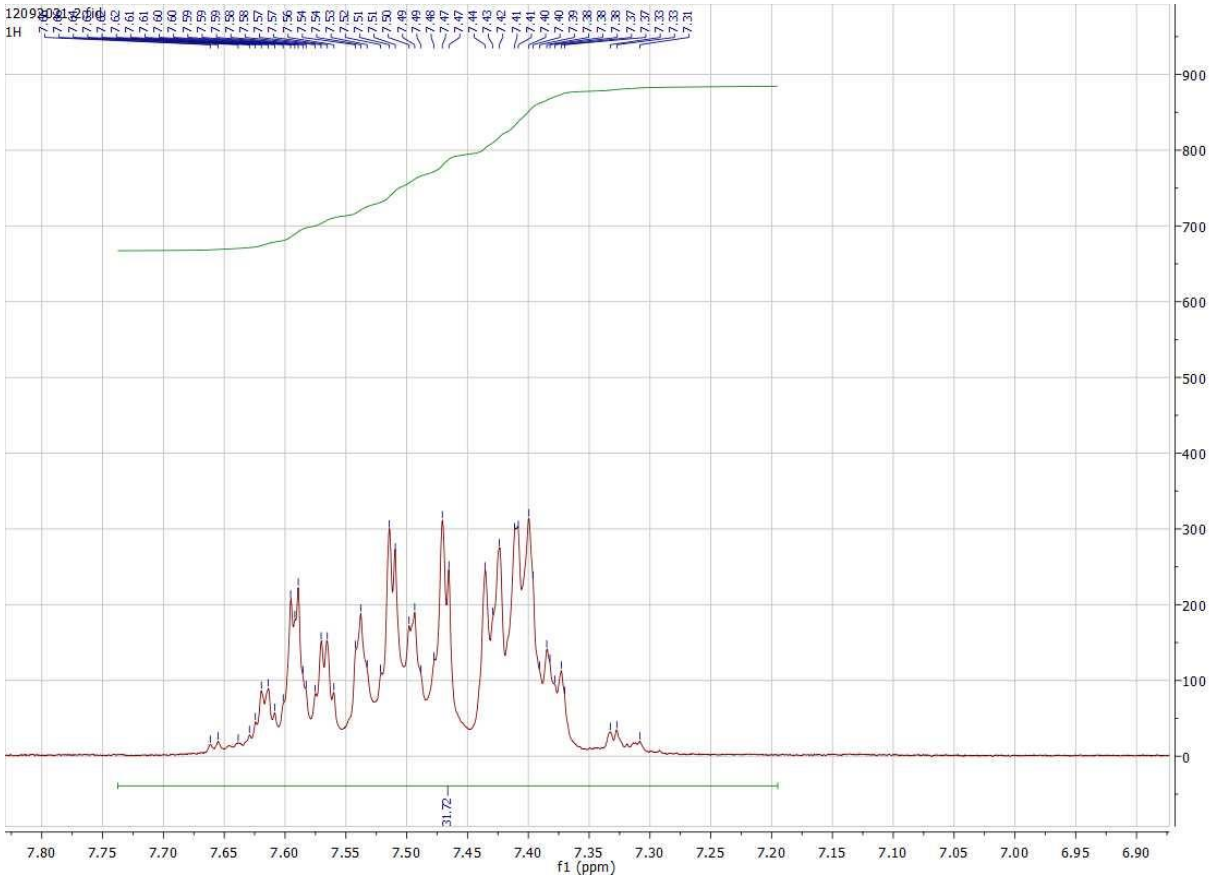
1H
31.72
f1 (ppm)

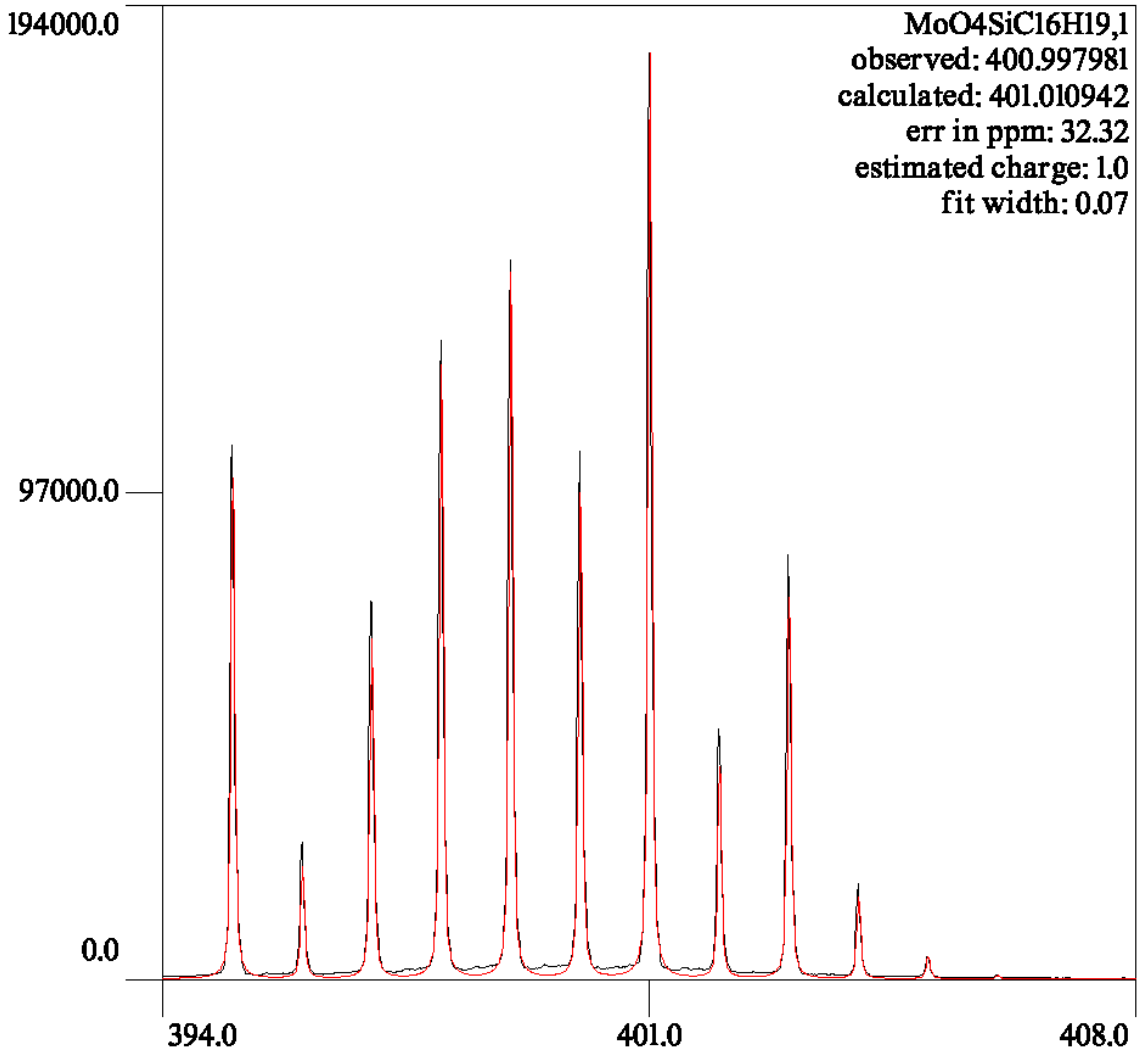
194000.0
97000.0
0.0
394.0
401.0
408.0
MoO4SiC16H19,1
observed: 400.997981
calculated: 401.010942
err in ppm: 32.32
estimated charge: 1.0
fit width: 0.07

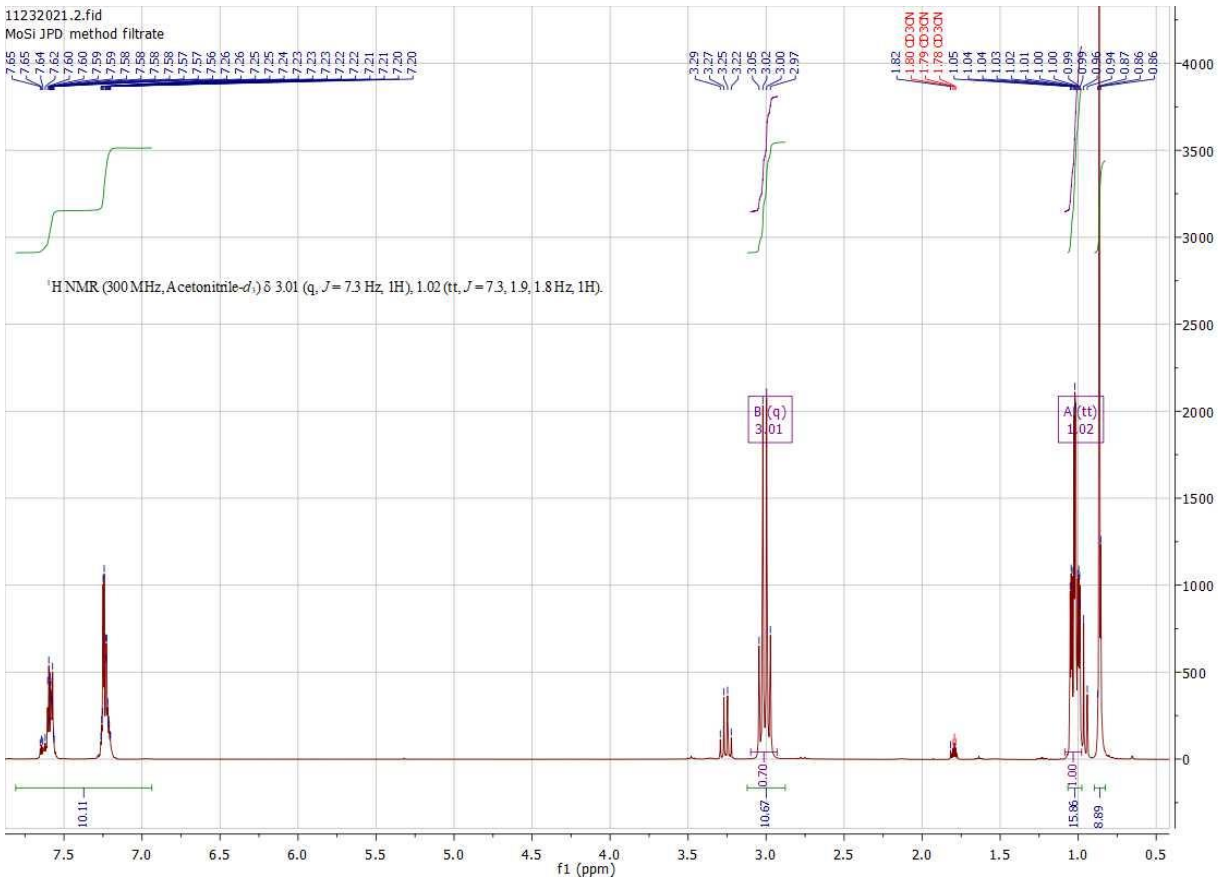
11232021.2.fid
MoSi JPD: method filtrate
^{1}H NMR (300 MHz, Acetonitrile-d_3) δ 3.01 (q, J = 7.3 Hz, 1H), 1.02 (tt, J = 7.3, 1.9, 1.8 Hz, 1H).
B (q) 3.01
A (tt) 1.02
10.11
0.70
10.67
15.86
1.00
8.89
f1 (ppm)

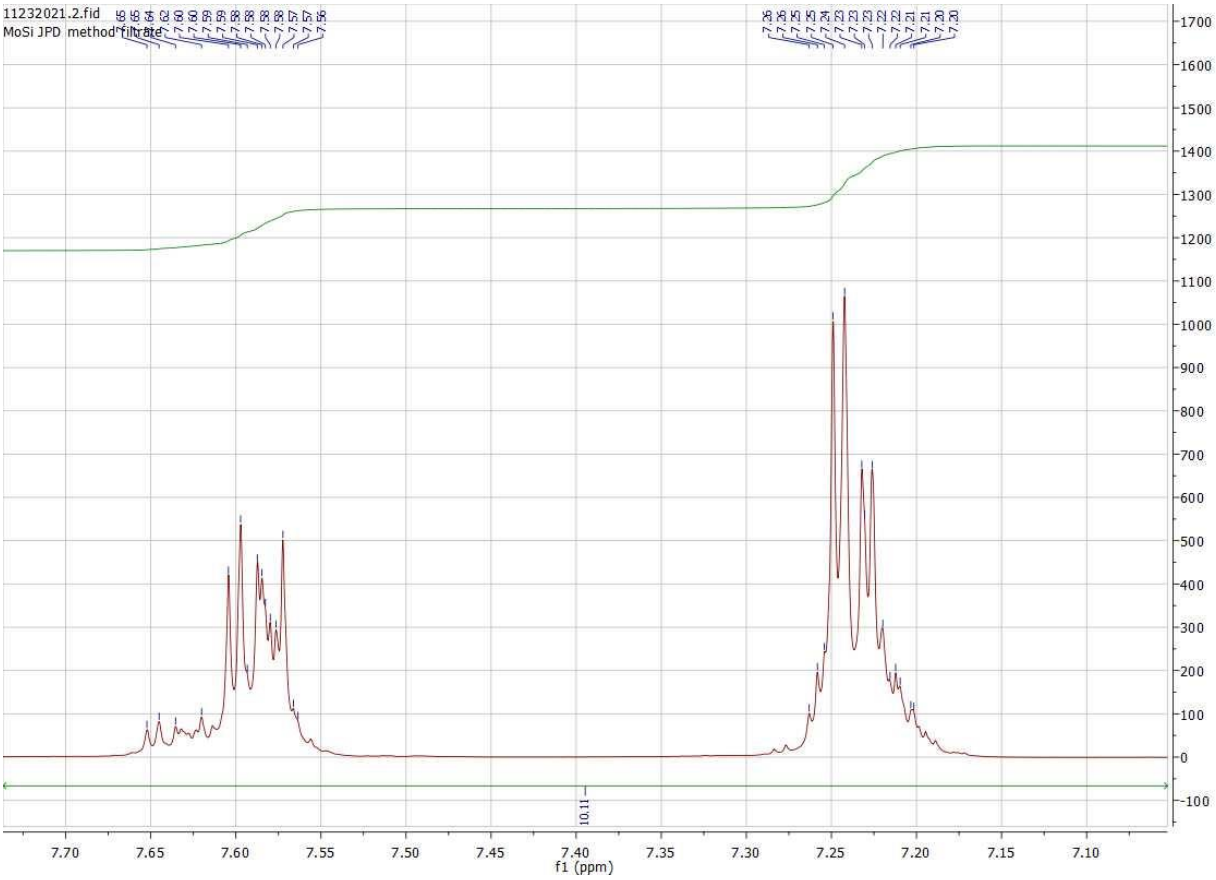

The NMR of [Et4N][MoO_3(OSiPh_2^{t}Bu)] is presented for comparison to the above newly reported PPN[MoO_3(OSiPh_2^{t}Bu)].

Structure Determination Summary

Crystal Data and Structure Refinement for $[Et_4N]_2[MoS_4]$

Tulane University

Atom Labeling for $[Et_4N]_2[MoS_4]$

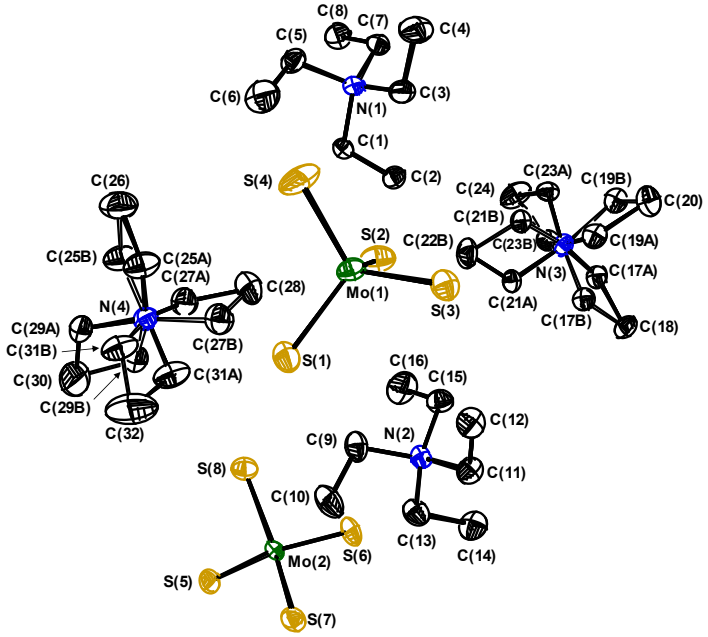

Thermal ellipsoids are presented at the 50% level. All H atoms are omitted for clarity. The methylene groups of two of the independent Et_4N^+ cations are disordered and refined as best fit distributions between the two sites.

Identification code	JPD911_0m	
Empirical formula	$C_{16}H_{40}MoN_2S_4$	
Formula weight	484.68	
Temperature	150(2) K	
Wavelength	0.71073 Å	
Crystal system	triclinic	
Space group	*P*-1	
Unit cell dimensions	a = 12.9317(18) Å	α = 110.9156(18)°
	b = 13.6008(19) Å	β = 112.603(2)°
	c = 15.903(2) Å	γ = 91.066(2)°
Volume	2372.4(6) Å^3	
Z	4	
Density (calculated)	1.357 g/cm^3	
Absorption coefficient	0.906 mm^{-1}	
F(000)	1024	
Crystal size	0.423 x 0.294 x 0.260 mm^3	
θ range for data collection	1.509 to 30.177°	
Index ranges	$-18 \le h \le 18$, $-18 \le k \le 18$, $-22 \le l \le 21$	
Reflections collected	46625	
Independent reflections	13042 [R(int) = 0.0233]	
Completeness to θ = 25.242°	99.7 %	

Absorption correction	None
Max. and min. transmission	0.80 and 0.71
Refinement method	Full-matrix least-squares on F^2
Data / restraints / parameters	13042 / 0 / 463
Goodness-of-fit on F^2	1.056
Final R indices [I>2σ(I)]	R1 = 0.0312, wR2 = 0.0910
R indices (all data)	R1 = 0.0371, wR2 = 0.0941
Extinction coefficient	n/a
Largest diff. peak and hole	1.450 and -0.729 e·Å^{-3}

Table S1. Atomic coordinates (x 10^4) and equivalent isotropic displacement parameters (Å^2 x 10^3) for $[Et_4N]_2[MoS_4]$. U(eq) is defined as one third of the trace of the orthogonalized U^{ij} tensor.

Atom	x	y	z	U(eq)
Mo(1)	9081(1)	6496(1)	2782(1)	25(1)
Mo(2)	13641(1)	11365(1)	2447(1)	20(1)
S(1)	10596(1)	6270(1)	2484(1)	34(1)
S(2)	8589(1)	8012(1)	2706(1)	39(1)
S(3)	9473(1)	6611(1)	4282(1)	31(1)
S(4)	7709(1)	5135(1)	1715(1)	55(1)
S(5)	14241(1)	11717(1)	1456(1)	27(1)
S(6)	13197(1)	12805(1)	3291(1)	34(1)
S(7)	14991(1)	10853(1)	3455(1)	31(1)
S(8)	12130(1)	10100(1)	1562(1)	33(1)
N(1)	5121(1)	8005(1)	921(1)	22(1)
N(2)	12014(1)	10212(1)	4402(1)	22(1)
N(3)	7190(1)	14233(1)	4372(1)	22(1)
N(4)	9536(1)	7125(1)	-432(1)	29(1)
C(1)	6158(2)	8680(2)	1033(1)	23(1)
C(2)	6527(2)	9796(2)	1838(2)	30(1)
C(3)	5434(2)	7789(2)	1856(2)	32(1)
C(4)	4539(2)	7021(2)	1820(2)	44(1)
C(5)	4804(2)	6979(2)	7(2)	31(1)
C(6)	5686(2)	6270(2)	46(2)	50(1)
C(7)	4117(2)	8585(2)	797(1)	26(1)
C(8)	3700(2)	8866(2)	-104(2)	33(1)
C(9)	11869(2)	9223(2)	3497(2)	31(1)
C(10)	12919(2)	8709(2)	3602(2)	41(1)
C(11)	12310(2)	9966(2)	5314(2)	29(1)
C(12)	11561(2)	8985(2)	5160(2)	34(1)
C(13)	12968(2)	11038(2)	4590(2)	33(1)
C(14)	13165(2)	12112(2)	5429(2)	37(1)
C(15)	10896(2)	10632(2)	4197(2)	31(1)
C(16)	10545(2)	11050(2)	3380(2)	44(1)
C(17A)	7685(2)	15411(2)	5041(2)	26(1)
C(17B)	8358(10)	14463(8)	5142(9)	26(1)
C(18)	8801(2)	15610(2)	5931(2)	34(1)
C(19A)	7195(2)	13569(2)	4954(2)	30(1)
C(19B)	6309(12)	14292(10)	4914(10)	30(1)
C(20)	6497(2)	13868(2)	5557(2)	46(1)
C(21A)	7959(2)	13838(2)	3827(2)	30(1)
C(21B)	6849(11)	13078(10)	3630(10)	30(1)
C(22)	7536(2)	12734(2)	3039(2)	41(1)
C(23A)	5991(2)	14146(2)	3650(2)	30(1)

Table S1. Atomic coordinates (x 10^4) and equivalent isotropic displacement parameters (Å^2 x 10^3) for $[Et_4N]_2[MoS_4]$. U(eq) is defined as one third of the trace of the orthogonalized U^{ij} tensor.

Atom	x	y	z	U(eq)
C(23B)	6870(10)	15007(10)	3907(9)	30(1)
C(24)	5838(2)	14714(2)	2969(2)	46(1)
C(25A)	8717(2)	6161(2)	-575(2)	41(1)
C(25B)	8392(9)	6765(8)	-1254(8)	41(1)
C(26)	7582(2)	5893(2)	-1382(2)	56(1)
C(27A)	9063(3)	8111(2)	-271(2)	39(1)
C(27B)	9514(9)	7831(7)	588(8)	39(1)
C(28)	8791(3)	8577(3)	602(2)	74(1)
C(29A)	9711(3)	6790(3)	-1383(2)	40(1)
C(29B)	10147(8)	8048(7)	-611(6)	40(1)
C(30)	10525(3)	7593(3)	-1381(2)	75(1)
C(31A)	10635(3)	7243(3)	451(2)	42(1)
C(31B)	10219(8)	6340(8)	-325(8)	42(1)
C(32)	11355(3)	6447(3)	332(3)	82(1)

Table S2. Bond lengths (Å) for $[Et_4N]_2[MoS_4]$. Symmetry transformations used to generate equivalent atoms:

Mo(1)-S(4)	2.1852(6)	C(4)-H(4C)	0.9800
Mo(1)-S(3)	2.1845(6)	C(5)-C(6)	1.504(3)
Mo(1)-S(1)	2.1894(6)	C(5)-H(5A)	0.9900
Mo(1)-S(2)	2.2002(6)	C(5)-H(5B)	0.9900
Mo(2)-S(6)	2.1738(5)	C(6)-H(6A)	0.9800
Mo(2)-S(5)	2.1880(5)	C(6)-H(6B)	0.9800
Mo(2)-S(7)	2.1891(5)	C(6)-H(6C)	0.9800
Mo(2)-S(8)	2.1892(6)	C(7)-C(8)	1.514(3)
N(1)-C(7)	1.516(2)	C(7)-H(7A)	0.9900
N(1)-C(5)	1.517(2)	C(7)-H(7B)	0.9900
N(1)-C(3)	1.521(2)	C(8)-H(8A)	0.9800
N(1)-C(1)	1.526(2)	C(8)-H(8B)	0.9800
N(2)-C(11)	1.512(2)	C(8)-H(8C)	0.9800
N(2)-C(13)	1.517(2)	C(9)-C(10)	1.518(3)
N(2)-C(9)	1.523(2)	C(9)-H(9A)	0.9900
N(2)-C(15)	1.523(2)	C(9)-H(9B)	0.9900
N(3)-C(23B)	1.470(13)	C(10)-H(10A)	0.9800
N(3)-C(17B)	1.471(12)	C(10)-H(10B)	0.9800
N(3)-C(19A)	1.506(3)	C(10)-H(10C)	0.9800
N(3)-C(23A)	1.504(3)	C(11)-C(12)	1.521(3)
N(3)-C(17A)	1.526(3)	C(11)-H(11A)	0.9900
N(3)-C(21B)	1.519(12)	C(11)-H(11B)	0.9900
N(3)-C(21A)	1.542(3)	C(12)-H(12A)	0.9800
N(3)-C(19B)	1.660(14)	C(12)-H(12B)	0.9800
N(4)-C(31B)	1.414(10)	C(12)-H(12C)	0.9800
N(4)-C(27A)	1.465(3)	C(13)-C(14)	1.520(3)
N(4)-C(25B)	1.472(10)	C(13)-H(13A)	0.9900
N(4)-C(29A)	1.523(3)	C(13)-H(13B)	0.9900
N(4)-C(31A)	1.521(3)	C(14)-H(14A)	0.9800
N(4)-C(27B)	1.574(10)	C(14)-H(14B)	0.9800
N(4)-C(25A)	1.563(3)	C(14)-H(14C)	0.9800
N(4)-C(29B)	1.635(10)	C(15)-C(16)	1.517(3)
C(1)-C(2)	1.512(3)	C(15)-H(15A)	0.9900
C(1)-H(1A)	0.9900	C(15)-H(15B)	0.9900
C(1)-H(1B)	0.9900	C(16)-H(16A)	0.9800
C(2)-H(2A)	0.9800	C(16)-H(16B)	0.9800
C(2)-H(2B)	0.9800	C(16)-H(16C)	0.9800
C(2)-H(2C)	0.9800	C(17A)-C(18)	1.517(3)
C(3)-C(4)	1.514(3)	C(17A)-H(17A)	0.9900
C(3)-H(3A)	0.9900	C(17A)-H(17B)	0.9900
C(3)-H(3B)	0.9900	C(17B)-C(18)	1.534(11)
C(4)-H(4A)	0.9800	C(17B)-H(17C)	0.9900
C(4)-H(4B)	0.9800	C(17B)-H(17D)	0.9900

Table S2. Bond lengths (Å) for $[Et_4N]_2[MoS_4]$. Symmetry transformations used to generate equivalent atoms:

C(18)-H(18A)	0.9800		
C(18)-H(18B)	0.9800	C(27B)-C(28)	1.393(10)
C(18)-H(18C)	0.9800	C(27B)-H(27C)	0.9900
C(19A)-C(20)	1.516(3)	C(27B)-H(27D)	0.9900
C(19A)-H(19A)	0.9900	C(28)-H(28A)	0.9800
C(19A)-H(19B)	0.9900	C(28)-H(28B)	0.9800
C(19B)-C(20)	1.293(13)	C(28)-H(28C)	0.9800
C(19B)-H(19C)	0.9900	C(29A)-C(30)	1.502(4)
C(19B)-H(19D)	0.9900	C(29A)-H(29A)	0.9900
C(20)-H(20A)	0.9800	C(29A)-H(29B)	0.9900
C(20)-H(20B)	0.9800	C(29B)-C(30)	1.433(9)
C(20)-H(20C)	0.9800	C(29B)-H(29C)	0.9900
C(21A)-C(22)	1.491(3)	C(29B)-H(29D)	0.9900
C(21A)-H(21A)	0.9900	C(30)-H(30A)	0.9800
C(21A)-H(21B)	0.9900	C(30)-H(30B)	0.9800
C(21B)-C(22)	1.495(13)	C(30)-H(30C)	0.9800
C(21B)-H(21C)	0.9900	C(31A)-C(32)	1.448(5)
C(21B)-H(21D)	0.9900	C(31A)-H(31A)	0.9900
C(22)-H(22A)	0.9800	C(31A)-H(31B)	0.9900
C(22)-H(22B)	0.9800	C(31B)-C(32)	1.404(9)
C(22)-H(22C)	0.9800	C(31B)-H(31C)	0.9900
C(23A)-C(24)	1.499(3)	C(31B)-H(31D)	0.9900
C(23A)-H(23A)	0.9900	C(32)-H(32A)	0.9800
C(23A)-H(23B)	0.9900	C(32)-H(32B)	0.9800
C(23B)-C(24)	1.481(12)	C(32)-H(32C)	0.9800
C(23B)-H(23C)	0.9900		
C(23B)-H(23D)	0.9900		
C(24)-H(24A)	0.9800		
C(24)-H(24B)	0.9800		
C(24)-H(24C)	0.9800		
C(25A)-C(26)	1.460(4)		
C(25A)-H(25A)	0.9900		
C(25A)-H(25B)	0.9900		
C(25B)-C(26)	1.471(10)		
C(25B)-H(25C)	0.9900		
C(25B)-H(25D)	0.9900		
C(26)-H(26A)	0.9800		
C(26)-H(26B)	0.9800		
C(26)-H(26C)	0.9800		
C(27A)-C(28)	1.485(4)		
C(27A)-H(27A)	0.9900		
C(27A)-H(27B)	0.9900		

Table S3. Bond angles (deg.) for $[Et_4N]_2[MoS_4]$. Symmetry transformations used to generate equivalent atoms:

S(4)-Mo(1)-S(3)	109.42(3)	C(29A)-N(4)-C(25A)	105.7(2)
S(4)-Mo(1)-S(1)	109.42(3)	C(31A)-N(4)-C(25A)	105.41(19)
S(3)-Mo(1)-S(1)	109.60(2)	C(31B)-N(4)-C(29B)	111.2(6)
S(4)-Mo(1)-S(2)	111.52(3)	C(25B)-N(4)-C(29B)	104.4(5)
S(3)-Mo(1)-S(2)	107.54(2)	C(27B)-N(4)-C(29B)	99.3(5)
S(1)-Mo(1)-S(2)	109.30(2)	C(2)-C(1)-N(1)	115.88(15)
S(6)-Mo(2)-S(5)	108.67(2)	C(2)-C(1)-H(1A)	108.3
S(6)-Mo(2)-S(7)	109.93(2)	N(1)-C(1)-H(1A)	108.3
S(5)-Mo(2)-S(7)	109.46(2)	C(2)-C(1)-H(1B)	108.3
S(6)-Mo(2)-S(8)	109.37(2)	N(1)-C(1)-H(1B)	108.3
S(5)-Mo(2)-S(8)	109.15(2)	H(1A)-C(1)-H(1B)	107.4
S(7)-Mo(2)-S(8)	110.22(2)	C(1)-C(2)-H(2A)	109.5
C(7)-N(1)-C(5)	109.15(14)	C(1)-C(2)-H(2B)	109.5
C(7)-N(1)-C(3)	108.49(15)	H(2A)-C(2)-H(2B)	109.5
C(5)-N(1)-C(3)	111.94(16)	C(1)-C(2)-H(2C)	109.5
C(7)-N(1)-C(1)	111.35(14)	H(2A)-C(2)-H(2C)	109.5
C(5)-N(1)-C(1)	107.71(14)	H(2B)-C(2)-H(2C)	109.5
C(3)-N(1)-C(1)	108.22(14)	C(4)-C(3)-N(1)	114.97(17)
C(11)-N(2)-C(13)	109.03(15)	C(4)-C(3)-H(3A)	108.5
C(11)-N(2)-C(9)	111.94(14)	N(1)-C(3)-H(3A)	108.5
C(13)-N(2)-C(9)	107.98(15)	C(4)-C(3)-H(3B)	108.5
C(11)-N(2)-C(15)	108.05(15)	N(1)-C(3)-H(3B)	108.5
C(13)-N(2)-C(15)	111.08(15)	H(3A)-C(3)-H(3B)	107.5
C(9)-N(2)-C(15)	108.79(15)	C(3)-C(4)-H(4A)	109.5
C(23B)-N(3)-C(17B)	117.0(7)	C(3)-C(4)-H(4B)	109.5
C(19A)-N(3)-C(23A)	109.78(17)	H(4A)-C(4)-H(4B)	109.5
C(19A)-N(3)-C(17A)	112.10(16)	C(3)-C(4)-H(4C)	109.5
C(23A)-N(3)-C(17A)	108.73(16)	H(4A)-C(4)-H(4C)	109.5
C(23B)-N(3)-C(21B)	113.5(7)	H(4B)-C(4)-H(4C)	109.5
C(17B)-N(3)-C(21B)	112.2(7)	C(6)-C(5)-N(1)	115.63(18)
C(19A)-N(3)-C(21A)	108.80(16)	C(6)-C(5)-H(5A)	108.4
C(23A)-N(3)-C(21A)	111.00(16)	N(1)-C(5)-H(5A)	108.4
C(17A)-N(3)-C(21A)	106.40(16)	C(6)-C(5)-H(5B)	108.4
C(23B)-N(3)-C(19B)	103.0(7)	N(1)-C(5)-H(5B)	108.4
C(17B)-N(3)-C(19B)	107.4(7)	H(5A)-C(5)-H(5B)	107.4
C(21B)-N(3)-C(19B)	102.0(7)	C(5)-C(6)-H(6A)	109.5
C(31B)-N(4)-C(25B)	117.3(6)	C(5)-C(6)-H(6B)	109.5
C(27A)-N(4)-C(29A)	109.9(2)	H(6A)-C(6)-H(6B)	109.5
C(27A)-N(4)-C(31A)	111.8(2)	C(5)-C(6)-H(6C)	109.5
C(29A)-N(4)-C(31A)	111.4(2)	H(6A)-C(6)-H(6C)	109.5
C(31B)-N(4)-C(27B)	110.6(6)	H(6B)-C(6)-H(6C)	109.5
C(25B)-N(4)-C(27B)	112.4(6)	C(8)-C(7)-N(1)	115.21(16)
C(27A)-N(4)-C(25A)	112.5(2)	C(8)-C(7)-H(7A)	108.5

Table S3. Bond angles (deg.) for $[Et_4N]_2[MoS_4]$. Symmetry transformations used to generate equivalent atoms:

N(1)-C(7)-H(7A)	108.5	C(13)-C(14)-H(14C)	109.5
C(8)-C(7)-H(7B)	108.5	H(14A)-C(14)-H(14C)	109.5
N(1)-C(7)-H(7B)	108.5	H(14B)-C(14)-H(14C)	109.5
H(7A)-C(7)-H(7B)	107.5	C(16)-C(15)-N(2)	115.05(18)
C(7)-C(8)-H(8A)	109.5	C(16)-C(15)-H(15A)	108.5
C(7)-C(8)-H(8B)	109.5	N(2)-C(15)-H(15A)	108.5
H(8A)-C(8)-H(8B)	109.5	C(16)-C(15)-H(15B)	108.5
C(7)-C(8)-H(8C)	109.5	N(2)-C(15)-H(15B)	108.5
H(8A)-C(8)-H(8C)	109.5	H(15A)-C(15)-H(15B)	107.5
H(8B)-C(8)-H(8C)	109.5	C(15)-C(16)-H(16A)	109.5
C(10)-C(9)-N(2)	114.60(18)	C(15)-C(16)-H(16B)	109.5
C(10)-C(9)-H(9A)	108.6	H(16A)-C(16)-H(16B)	109.5
N(2)-C(9)-H(9A)	108.6	C(15)-C(16)-H(16C)	109.5
C(10)-C(9)-H(9B)	108.6	H(16A)-C(16)-H(16C)	109.5
N(2)-C(9)-H(9B)	108.6	H(16B)-C(16)-H(16C)	109.5
H(9A)-C(9)-H(9B)	107.6	C(18)-C(17A)-N(3)	114.65(17)
C(9)-C(10)-H(10A)	109.5	C(18)-C(17A)-H(17A)	108.6
C(9)-C(10)-H(10B)	109.5	N(3)-C(17A)-H(17A)	108.6
H(10A)-C(10)-H(10B)	109.5	C(18)-C(17A)-H(17B)	108.6
C(9)-C(10)-H(10C)	109.5	N(3)-C(17A)-H(17B)	108.6
H(10A)-C(10)-H(10C)	109.5	H(17A)-C(17A)-H(17B)	107.6
H(10B)-C(10)-H(10C)	109.5	N(3)-C(17B)-C(18)	116.9(7)
N(2)-C(11)-C(12)	114.70(16)	N(3)-C(17B)-H(17C)	108.1
N(2)-C(11)-H(11A)	108.6	C(18)-C(17B)-H(17C)	108.1
C(12)-C(11)-H(11A)	108.6	N(3)-C(17B)-H(17D)	108.1
N(2)-C(11)-H(11B)	108.6	C(18)-C(17B)-H(17D)	108.1
C(12)-C(11)-H(11B)	108.6	H(17C)-C(17B)-H(17D)	107.3
H(11A)-C(11)-H(11B)	107.6	C(17A)-C(18)-H(18A)	109.5
C(11)-C(12)-H(12A)	109.5	C(17A)-C(18)-H(18B)	109.5
C(11)-C(12)-H(12B)	109.5	H(18A)-C(18)-H(18B)	109.5
H(12A)-C(12)-H(12B)	109.5	C(17A)-C(18)-H(18C)	109.5
C(11)-C(12)-H(12C)	109.5	H(18A)-C(18)-H(18C)	109.5
H(12A)-C(12)-H(12C)	109.5	H(18B)-C(18)-H(18C)	109.5
H(12B)-C(12)-H(12C)	109.5	N(3)-C(19A)-C(20)	115.80(19)
N(2)-C(13)-C(14)	114.65(17)	N(3)-C(19A)-H(19A)	108.3
N(2)-C(13)-H(13A)	108.6	C(20)-C(19A)-H(19A)	108.3
C(14)-C(13)-H(13A)	108.6	N(3)-C(19A)-H(19B)	108.3
N(2)-C(13)-H(13B)	108.6	C(20)-C(19A)-H(19B)	108.3
C(14)-C(13)-H(13B)	108.6	H(19A)-C(19A)-H(19B)	107.4
H(13A)-C(13)-H(13B)	107.6	C(20)-C(19B)-N(3)	119.7(9)
C(13)-C(14)-H(14A)	109.5	C(20)-C(19B)-H(19C)	107.4
C(13)-C(14)-H(14B)	109.5	N(3)-C(19B)-H(19C)	107.4
H(14A)-C(14)-H(14B)	109.5	C(20)-C(19B)-H(19D)	107.4

Table S3. Bond angles (deg.) for $[Et_4N]_2[MoS_4]$. Symmetry transformations used to generate equivalent atoms:

N(3)-C(19B)-H(19D)	107.4	H(24B)-C(24)-H(24C)	109.5
H(19C)-C(19B)-H(19D)	106.9	C(26)-C(25A)-N(4)	116.0(2)
C(19A)-C(20)-H(20A)	109.5	C(26)-C(25A)-H(25A)	108.3
C(19A)-C(20)-H(20B)	109.5	N(4)-C(25A)-H(25A)	108.3
H(20A)-C(20)-H(20B)	109.5	C(26)-C(25A)-H(25B)	108.3
C(19A)-C(20)-H(20C)	109.5	N(4)-C(25A)-H(25B)	108.3
H(20A)-C(20)-H(20C)	109.5	H(25A)-C(25A)-H(25B)	107.4
H(20B)-C(20)-H(20C)	109.5	C(26)-C(25B)-N(4)	121.3(7)
C(22)-C(21A)-N(3)	114.7(2)	C(26)-C(25B)-H(25C)	107.0
C(22)-C(21A)-H(21A)	108.6	N(4)-C(25B)-H(25C)	107.0
N(3)-C(21A)-H(21A)	108.6	C(26)-C(25B)-H(25D)	107.0
C(22)-C(21A)-H(21B)	108.6	N(4)-C(25B)-H(25D)	107.0
N(3)-C(21A)-H(21B)	108.6	H(25C)-C(25B)-H(25D)	106.7
H(21A)-C(21A)-H(21B)	107.6	C(25A)-C(26)-H(26A)	109.5
C(22)-C(21B)-N(3)	115.9(9)	C(25A)-C(26)-H(26B)	109.5
C(22)-C(21B)-H(21C)	108.3	H(26A)-C(26)-H(26B)	109.5
N(3)-C(21B)-H(21C)	108.3	C(25A)-C(26)-H(26C)	109.5
C(22)-C(21B)-H(21D)	108.3	H(26A)-C(26)-H(26C)	109.5
N(3)-C(21B)-H(21D)	108.3	H(26B)-C(26)-H(26C)	109.5
H(21C)-C(21B)-H(21D)	107.4	N(4)-C(27A)-C(28)	119.6(3)
C(21A)-C(22)-H(22A)	109.5	N(4)-C(27A)-H(27A)	107.4
C(21A)-C(22)-H(22B)	109.5	C(28)-C(27A)-H(27A)	107.4
H(22A)-C(22)-H(22B)	109.5	N(4)-C(27A)-H(27B)	107.4
C(21A)-C(22)-H(22C)	109.5	C(28)-C(27A)-H(27B)	107.4
H(22A)-C(22)-H(22C)	109.5	H(27A)-C(27A)-H(27B)	106.9
H(22B)-C(22)-H(22C)	109.5	C(28)-C(27B)-N(4)	118.4(7)
C(24)-C(23A)-N(3)	116.9(2)	C(28)-C(27B)-H(27C)	107.7
C(24)-C(23A)-H(23A)	108.1	N(4)-C(27B)-H(27C)	107.7
N(3)-C(23A)-H(23A)	108.1	C(28)-C(27B)-H(27D)	107.7
C(24)-C(23A)-H(23B)	108.1	N(4)-C(27B)-H(27D)	107.7
N(3)-C(23A)-H(23B)	108.1	H(27C)-C(27B)-H(27D)	107.1
H(23A)-C(23A)-H(23B)	107.3	C(27A)-C(28)-H(28A)	109.5
C(24)-C(23B)-N(3)	120.3(9)	C(27A)-C(28)-H(28B)	109.5
C(24)-C(23B)-H(23C)	107.3	H(28A)-C(28)-H(28B)	109.5
N(3)-C(23B)-H(23C)	107.3	C(27A)-C(28)-H(28C)	109.5
C(24)-C(23B)-H(23D)	107.3	H(28A)-C(28)-H(28C)	109.5
N(3)-C(23B)-H(23D)	107.3	H(28B)-C(28)-H(28C)	109.5
H(23C)-C(23B)-H(23D)	106.9	C(30)-C(29A)-N(4)	114.4(2)
C(23A)-C(24)-H(24A)	109.5	C(30)-C(29A)-H(29A)	108.7
C(23A)-C(24)-H(24B)	109.5	N(4)-C(29A)-H(29A)	108.7
H(24A)-C(24)-H(24B)	109.5	C(30)-C(29A)-H(29B)	108.7
C(23A)-C(24)-H(24C)	109.5	N(4)-C(29A)-H(29B)	108.7
H(24A)-C(24)-H(24C)	109.5	H(29A)-C(29A)-H(29B)	107.6

Table S3. Bond angles (deg.) for $[Et_4N]_2[MoS_4]$. Symmetry transformations used to generate equivalent atoms:

C(30)-C(29B)-N(4)	111.8(6)
C(30)-C(29B)-H(29C)	109.3
N(4)-C(29B)-H(29C)	109.3
C(30)-C(29B)-H(29D)	109.3
N(4)-C(29B)-H(29D)	109.3
H(29C)-C(29B)-H(29D)	107.9
C(29A)-C(30)-H(30A)	109.5
C(29A)-C(30)-H(30B)	109.5
H(30A)-C(30)-H(30B)	109.5
C(29A)-C(30)-H(30C)	109.5
H(30A)-C(30)-H(30C)	109.5
H(30B)-C(30)-H(30C)	109.5
C(32)-C(31A)-N(4)	118.9(3)
C(32)-C(31A)-H(31A)	107.6
N(4)-C(31A)-H(31A)	107.6
C(32)-C(31A)-H(31B)	107.6
N(4)-C(31A)-H(31B)	107.6
H(31A)-C(31A)-H(31B)	107.0
C(32)-C(31B)-N(4)	130.3(8)
C(32)-C(31B)-H(31C)	104.7
N(4)-C(31B)-H(31C)	104.7
C(32)-C(31B)-H(31D)	104.7
N(4)-C(31B)-H(31D)	104.7
H(31C)-C(31B)-H(31D)	105.7
C(31A)-C(32)-H(32A)	109.5
C(31A)-C(32)-H(32B)	109.5
H(32A)-C(32)-H(32B)	109.5
C(31A)-C(32)-H(32C)	109.5
H(32A)-C(32)-H(32C)	109.5
H(32B)-C(32)-H(32C)	109.5

Table S4. Anisotropic displacement parameters ($Å^2$ x 10^3) for $[Et_4N]_2[MoS_4]$. The anisotropic displacement factor exponent takes the form: $-2\pi^2[h^2a^{*2}U^{11} + ... + 2hka^*b^*U^{12}]$.

Atom	U^{11}	U^{22}	U^{33}	U^{23}	U^{13}	U^{12}
Mo(1)	23(1)	23(1)	27(1)	10(1)	7(1)	0(1)
Mo(2)	20(1)	21(1)	23(1)	9(1)	13(1)	6(1)
S(1)	39(1)	31(1)	36(1)	10(1)	22(1)	7(1)
S(2)	28(1)	36(1)	52(1)	26(1)	8(1)	9(1)
S(3)	38(1)	30(1)	33(1)	15(1)	19(1)	7(1)
S(4)	47(1)	45(1)	47(1)	11(1)	-1(1)	-21(1)
S(5)	29(1)	32(1)	25(1)	12(1)	16(1)	3(1)
S(6)	46(1)	26(1)	42(1)	12(1)	31(1)	15(1)
S(7)	29(1)	42(1)	31(1)	20(1)	15(1)	16(1)
S(8)	28(1)	32(1)	37(1)	11(1)	14(1)	-3(1)
N(1)	19(1)	24(1)	21(1)	7(1)	8(1)	3(1)
N(2)	24(1)	20(1)	24(1)	9(1)	12(1)	4(1)
N(3)	25(1)	17(1)	22(1)	6(1)	9(1)	4(1)
N(4)	24(1)	33(1)	25(1)	10(1)	6(1)	1(1)
C(1)	21(1)	26(1)	23(1)	8(1)	11(1)	2(1)
C(2)	30(1)	26(1)	29(1)	7(1)	12(1)	0(1)
C(3)	25(1)	44(1)	27(1)	19(1)	8(1)	0(1)
C(4)	39(1)	55(1)	42(1)	29(1)	12(1)	-4(1)
C(5)	31(1)	24(1)	28(1)	4(1)	9(1)	2(1)
C(6)	46(1)	29(1)	60(2)	5(1)	19(1)	14(1)
C(7)	20(1)	31(1)	26(1)	10(1)	10(1)	7(1)
C(8)	29(1)	39(1)	31(1)	17(1)	9(1)	10(1)
C(9)	41(1)	23(1)	31(1)	9(1)	20(1)	7(1)
C(10)	49(1)	28(1)	58(2)	12(1)	37(1)	13(1)
C(11)	31(1)	28(1)	27(1)	13(1)	10(1)	4(1)
C(12)	41(1)	32(1)	35(1)	19(1)	17(1)	2(1)
C(13)	33(1)	28(1)	42(1)	14(1)	21(1)	2(1)
C(14)	43(1)	24(1)	39(1)	10(1)	15(1)	-3(1)
C(15)	28(1)	29(1)	35(1)	13(1)	13(1)	9(1)
C(16)	48(1)	44(1)	38(1)	23(1)	11(1)	19(1)
C(17A)	31(1)	16(1)	28(1)	6(1)	13(1)	4(1)
C(17B)	31(1)	16(1)	28(1)	6(1)	13(1)	4(1)
C(18)	36(1)	26(1)	28(1)	3(1)	7(1)	3(1)
C(19A)	36(1)	22(1)	32(1)	12(1)	13(1)	3(1)
C(19B)	36(1)	22(1)	32(1)	12(1)	13(1)	3(1)
C(20)	51(2)	56(2)	40(1)	22(1)	25(1)	8(1)
C(21A)	30(1)	28(1)	27(1)	5(1)	14(1)	6(1)
C(21B)	30(1)	28(1)	27(1)	5(1)	14(1)	6(1)
C(22)	50(1)	36(1)	32(1)	3(1)	21(1)	10(1)
C(23A)	23(1)	33(1)	30(1)	11(1)	9(1)	5(1)

Table S4. Anisotropic displacement parameters ($Å^2$ x 10^3) for $[Et_4N]_2[MoS_4]$. The anisotropic displacement factor exponent takes the form: $-2\pi^2[h^2a^{*2}U^{11} + ... + 2hka^*b^*U^{12}]$.

Atom	U^{11}	U^{22}	U^{33}	U^{23}	U^{13}	U^{12}
C(23B)	23(1)	33(1)	30(1)	11(1)	9(1)	5(1)
C(24)	43(1)	44(1)	41(1)	24(1)	1(1)	6(1)
C(25A)	31(1)	38(1)	47(2)	22(1)	6(1)	-4(1)
C(25B)	31(1)	38(1)	47(2)	22(1)	6(1)	-4(1)
C(26)	36(1)	52(2)	69(2)	18(1)	18(1)	-6(1)
C(27A)	41(2)	29(1)	45(2)	10(1)	20(1)	9(1)
C(27B)	41(2)	29(1)	45(2)	10(1)	20(1)	9(1)
C(28)	50(2)	100(3)	53(2)	1(2)	30(1)	19(2)
C(29A)	40(2)	42(2)	27(1)	1(1)	15(1)	-1(1)
C(29B)	40(2)	42(2)	27(1)	1(1)	15(1)	-1(1)
C(30)	73(2)	95(3)	51(2)	13(2)	37(2)	-17(2)
C(31A)	30(1)	43(2)	42(2)	22(1)	0(1)	-2(1)
C(31B)	30(1)	43(2)	42(2)	22(1)	0(1)	-2(1)
C(32)	38(2)	94(3)	99(3)	52(2)	2(2)	18(2)

Table S5. Hydrogen coordinates (x 10^4) and isotropic displacement parameters (Å^2 x 10^3) for $[Et_4N]_2[MoS_4]$.

H atom	x	y	z	U(eq)
H(1A)	6805	8294	1165	28
H(1B)	5991	8741	393	28
H(2A)	5904	10197	1709	45
H(2B)	7193	10162	1846	45
H(2C)	6725	9751	2482	45
H(3A)	6149	7498	1987	38
H(3B)	5585	8478	2421	38
H(4A)	3854	7338	1769	66
H(4B)	4836	6880	2425	66
H(4C)	4348	6348	1241	66
H(5A)	4092	6564	-107	37
H(5B)	4642	7170	-571	37
H(6A)	6381	6654	114	75
H(6B)	5393	5621	-566	75
H(6C)	5857	6074	615	75
H(7A)	3478	8132	757	31
H(7B)	4334	9254	1396	31
H(8A)	4348	9214	-134	50
H(8B)	3158	9355	-56	50
H(8C)	3323	8212	-704	50
H(9A)	11232	8687	3356	37
H(9B)	11654	9424	2920	37
H(10A)	13488	9152	3560	62
H(10B)	12709	7995	3069	62
H(10C)	13237	8646	4244	62
H(11A)	12255	10594	5845	35
H(11B)	13111	9861	5548	35
H(12A)	10759	9016	4814	51
H(12B)	11695	8971	5805	51
H(12C)	11747	8338	4763	51
H(13A)	12796	11156	3975	39
H(13B)	13682	10746	4743	39
H(14A)	12460	12405	5293	55
H(14B)	13768	12607	5481	55
H(14C)	13393	12015	6053	55
H(15A)	10284	10048	4018	37
H(15B)	10961	11215	4815	37
H(16A)	11152	11617	3538	65
H(16B)	9844	11338	3324	65
H(16C)	10413	10465	2750	65

Table S5. Hydrogen coordinates (x 10^4) and isotropic displacement parameters ($Å^2$ x 10^3) for $[Et_4N]_2[MoS_4]$.

H atom	x	y	z	U(eq)
H(17A)	7803	15780	4641	31
H(17B)	7119	15736	5280	31
H(17C)	8879	14289	4810	31
H(17D)	8402	13973	5484	31
H(18A)	8683	15290	6357	51
H(18B)	9074	16383	6305	51
H(18C)	9367	15287	5705	51
H(19A)	7993	13623	5410	36
H(19B)	6907	12811	4486	36
H(19C)	6289	15056	5244	36
H(19D)	5537	13952	4382	36
H(20A)	6759	14622	6015	69
H(20B)	6589	13418	5935	69
H(20C)	5692	13758	5110	69
H(21A)	8042	14339	3523	35
H(21B)	8725	13863	4320	35
H(21C)	6901	12609	3993	35
H(21D)	6041	12960	3164	35
H(22A)	7455	12229	3331	62
H(22B)	8079	12541	2742	62
H(22C)	6795	12707	2527	62
H(23A)	5668	13378	3238	36
H(23B)	5536	14424	4033	36
H(23C)	6786	15655	4401	36
H(23D)	7523	15218	3790	36
H(24A)	6145	15479	3362	69
H(24B)	5025	14616	2548	69
H(24C)	6243	14419	2552	69
H(25A)	9081	5522	-691	49
H(25B)	8632	6321	51	49
H(25C)	8016	7398	-1200	49
H(25D)	8496	6551	-1876	49
H(26A)	7214	6523	-1289	84
H(26B)	7124	5310	-1382	84
H(26C)	7645	5667	-2016	84
H(27A)	8354	7978	-870	47
H(27B)	9607	8666	-231	47
H(27C)	9310	7342	857	47
H(27D)	10298	8221	1051	47
H(28A)	8012	8261	429	111

Table S5. Hydrogen coordinates (x 10^4) and isotropic displacement parameters (Å^2 x 10^3) for $[Et_4N]_2[MoS_4]$.

H atom	x	y	z	U(eq)
H(28B)	8853	9353	798	111
H(28C)	9326	8425	1153	111
H(29A)	9997	6106	-1494	48
H(29B)	8965	6660	-1945	48
H(29C)	9600	8517	-791	48
H(29D)	10806	8494	12	48
H(30A)	10223	8258	-1321	112
H(30B)	10620	7307	-2002	112
H(30C)	11264	7739	-820	112
H(31A)	11099	7948	672	50
H(31B)	10433	7262	997	50
H(31C)	9780	5830	-217	50
H(31D)	10196	5952	-992	50
H(32A)	10925	5741	134	123
H(32B)	12022	6625	961	123
H(32C)	11603	6437	-180	123

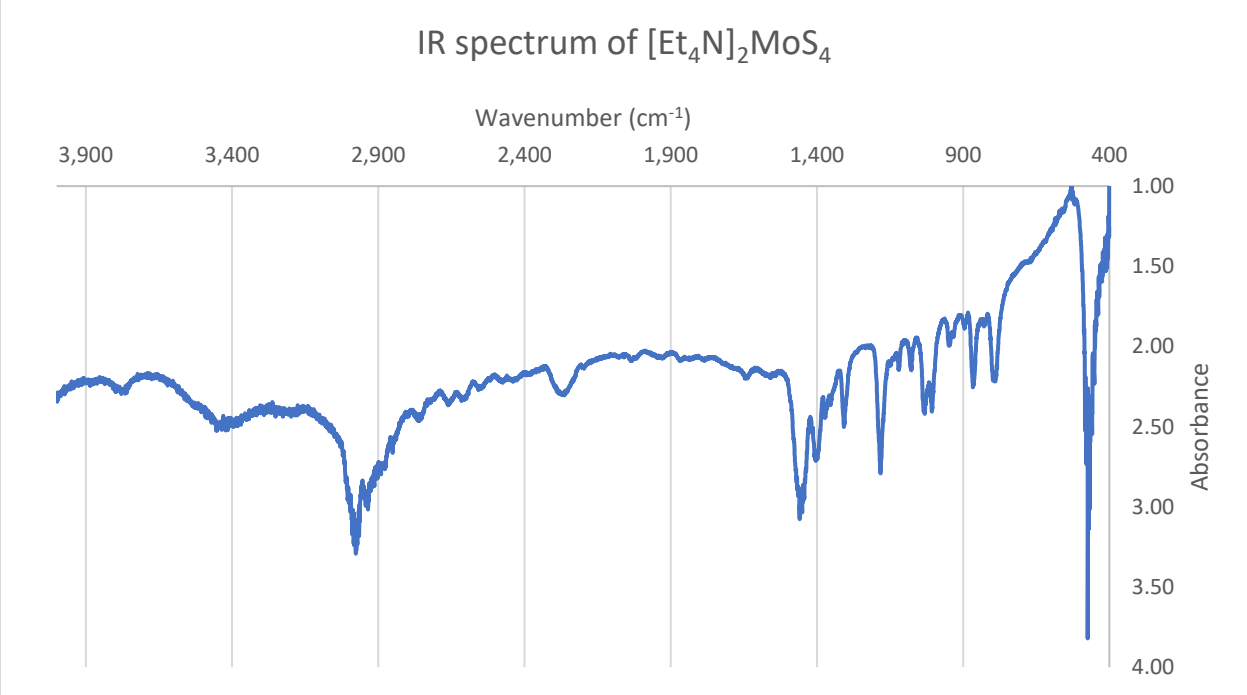

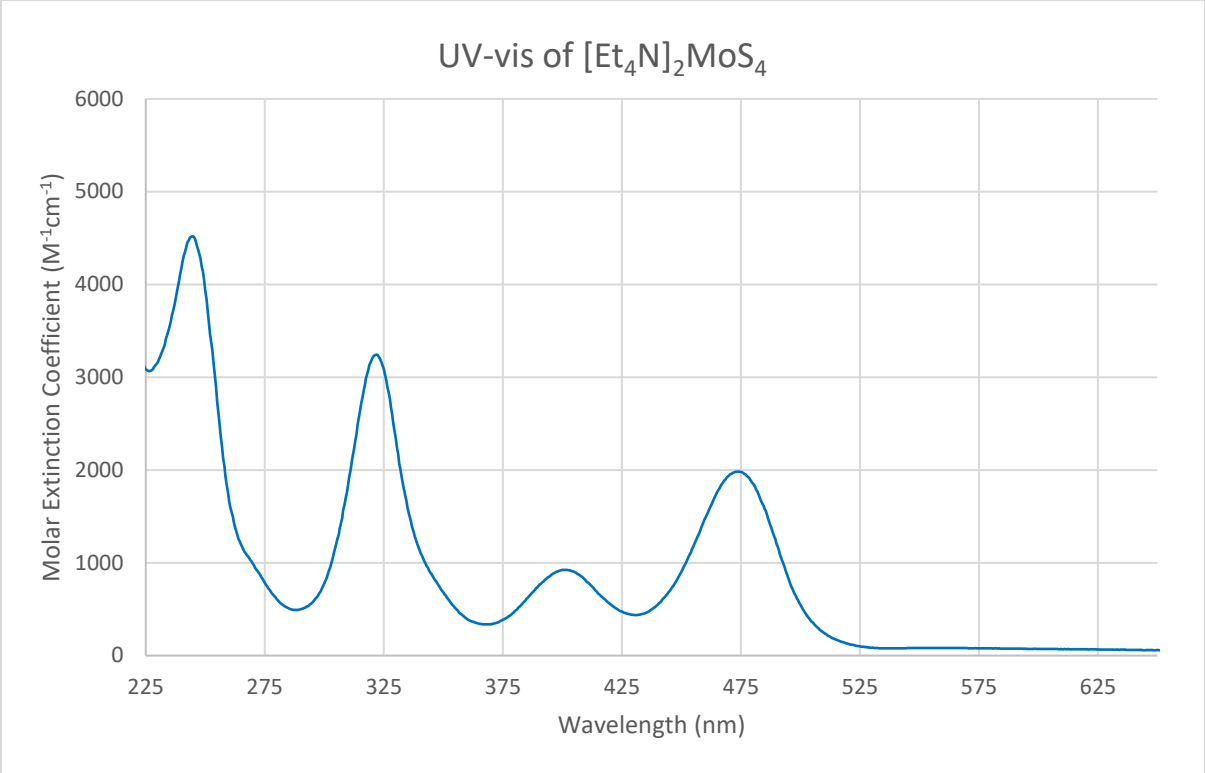

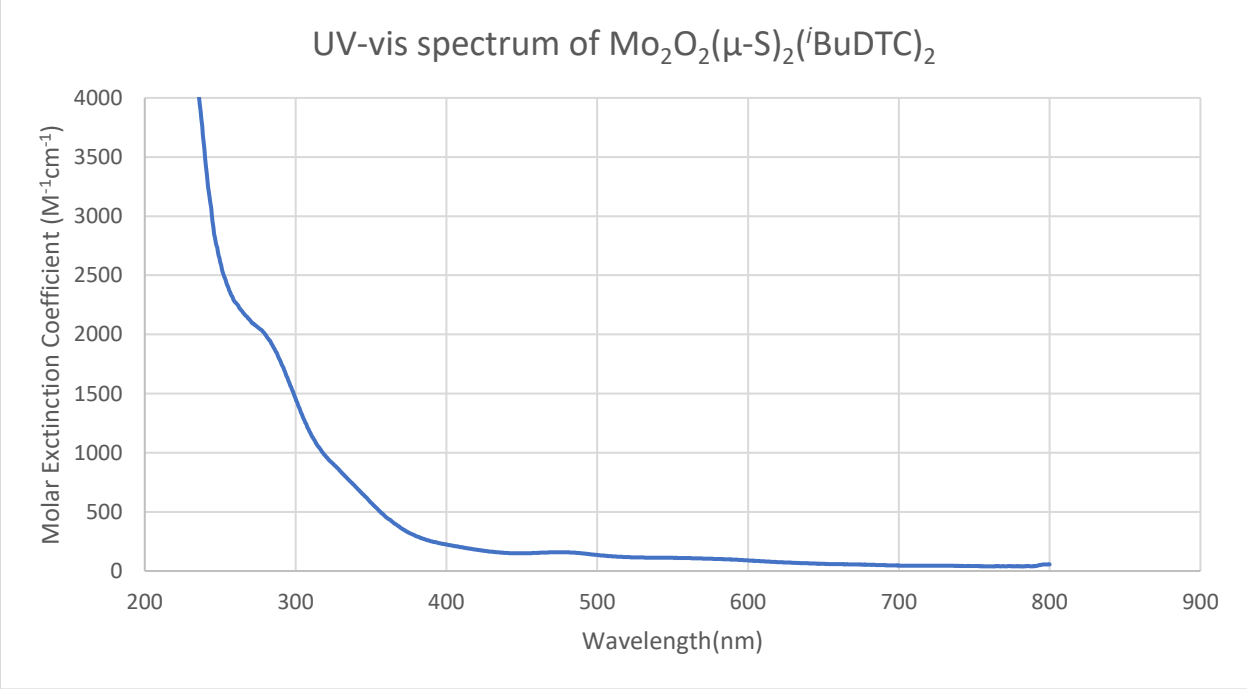

Structure Determination Summary

Atom Labeling for $[Et_4N]_2[(S_2)Mo(O)(\mu\text{-}S)_2Mo(O)(S_2)]$

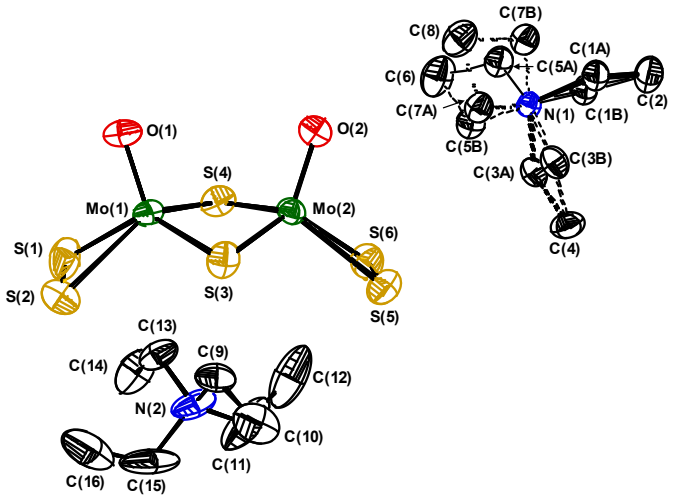

Thermal ellipsoid plot is drawn at the 50% level. All H atoms are omitted for clarity. The methylene carbon atoms of the N(1) Et_4N^+ cation are disordered over two positions and refined as a best fit distribution between them.

Crystal Data and Structure Refinement for $[Et_4N]_2[(S_2)Mo(O)(\mu\text{-}S)_2Mo(O)(S_2)]$

Identification code	JPD901_0m	
Empirical formula	$C_{16}H_{40}Mo_2N_2O_2S_6$	
Formula weight	676.74	
Temperature	150(2) K	
Wavelength	0.71073 Å	
Crystal system	monoclinic	
Space group	$P2_1/n$	
Unit cell dimensions	a = 9.8786(11) Å	α = 90°
	b = 27.947(3) Å	β = 97.7611(15)°
	c = 10.2875(11) Å	γ = 90°
Volume	2814.1(5) Å^3	
Z	4	
Density (calculated)	1.597 g/cm^3	
Absorption coefficient	1.351 mm^{-1}	
F(000)	1384	
Crystal size	0.336 x 0.117 x 0.039 mm^3	
θ range for data collection	2.127 to 21.814°	
Index ranges	$-10 \le h \le 10$, $-29 \le k \le 29$, $-10 \le l \le 10$	
Reflections collected	30730	
Independent reflections	3369 [R(int) = 0.0428]	

Completeness to $\theta = 21.814°$	99.9 %
Absorption correction	Semi-empirical from equivalents
Max. and min. transmission	0.95 and 0.80
Refinement method	Full-matrix least-squares on F^2
Data / restraints / parameters	3369 / 0 / 269
Goodness-of-fit on F^2	1.064
Final R indices [I>2σ(I)]	R1 = 0.0503, wR2 = 0.1324
R indices (all data)	R1 = 0.0565, wR2 = 0.1363
Extinction coefficient	n/a
Largest diff. peak and hole	2.138 and -0.556 $e \cdot Å^{-3}$

Table S1. Atomic coordinates (x 10^4) and equivalent isotropic displacement parameters (Å^2 x 10^3) for $[Et_4N]_2[(S_2)Mo(O)(\mu\text{-}S)_2Mo(O)(S_2)]$. U(eq) is defined as one third of the trace of the orthogonalized U^{ij} tensor.

Atom	x	y	z	U(eq)
Mo(1)	3233(1)	1266(1)	1057(1)	29(1)
Mo(2)	2282(1)	1533(1)	3415(1)	33(1)
S(1)	4165(3)	560(1)	200(2)	60(1)
S(2)	2303(2)	806(1)	-811(2)	57(1)
S(3)	1024(2)	1496(1)	1345(2)	38(1)
S(4)	4188(2)	1065(1)	3167(2)	40(1)
S(5)	241(2)	1428(1)	4420(2)	48(1)
S(6)	1982(2)	1113(1)	5385(2)	49(1)
O(1)	4027(5)	1752(2)	558(5)	43(1)
O(2)	2861(6)	2095(2)	3746(5)	53(2)
N(1)	2080(5)	2556(2)	7665(5)	24(1)
N(2)	2289(7)	-434(2)	2865(8)	56(2)
C(1A)	1503(12)	2966(4)	8317(11)	32(2)
C(1B)	2370(19)	2611(7)	9182(17)	32(2)
C(3A)	1531(11)	2080(4)	8018(11)	33(2)
C(3B)	539(19)	2454(7)	7318(19)	33(2)
C(5A)	3631(11)	2540(4)	7997(11)	36(2)
C(5B)	2867(18)	2169(7)	7250(19)	36(2)
C(7A)	1723(11)	2613(4)	6152(10)	31(2)
C(7B)	2348(18)	3045(7)	7102(17)	31(2)
C(2)	1648(8)	2955(3)	9803(8)	48(2)
C(4)	11(7)	2028(3)	7851(8)	41(2)
C(6)	4409(8)	2202(4)	7398(9)	58(2)
C(8)	2313(8)	3040(3)	5591(7)	43(2)
C(9)	1730(8)	64(3)	2689(9)	52(2)
C(10)	245(9)	118(4)	2801(11)	71(3)
C(11)	2067(13)	-634(5)	4155(15)	105(5)
C(12)	2698(13)	-367(6)	5341(14)	118(6)
C(13)	3822(8)	-405(4)	2745(9)	60(3)
C(14)	4582(10)	-874(4)	2904(11)	82(3)
C(15)	1580(10)	-762(3)	1762(16)	94(4)
C(16)	1756(13)	-616(5)	397(14)	106(5)

Table S2. Bond lengths (Å) for $[Et_4N]_2[(S_2)Mo(O)(\mu\text{-}S)_2Mo(O)(S_2)]$. Symmetry transformations used to generate equivalent atoms:

Mo(1)-O(1)	1.684(5)
Mo(1)-S(4)	2.316(2)
Mo(1)-S(3)	2.3326(19)
Mo(1)-S(2)	2.391(2)
Mo(1)-S(1)	2.396(2)
Mo(1)-Mo(2)	2.8176(9)
Mo(2)-O(2)	1.691(5)
Mo(2)-S(3)	2.318(2)
Mo(2)-S(4)	2.335(2)
Mo(2)-S(6)	2.395(2)
Mo(2)-S(5)	2.404(2)
S(1)-S(2)	2.103(3)
S(5)-S(6)	2.064(3)
N(1)-C(5B)	1.43(2)
N(1)-C(1A)	1.481(12)
N(1)-C(3A)	1.499(13)
N(1)-C(7B)	1.522(19)
N(1)-C(5A)	1.524(12)
N(1)-C(3B)	1.54(2)
N(1)-C(1B)	1.556(19)
N(1)-C(7A)	1.557(12)
N(2)-C(11)	1.484(14)
N(2)-C(9)	1.498(10)
N(2)-C(13)	1.539(11)
N(2)-C(15)	1.552(14)
C(1A)-C(2)	1.516(14)
C(1B)-C(2)	1.40(2)
C(3A)-C(4)	1.495(13)
C(3B)-C(4)	1.44(2)
C(5A)-C(6)	1.412(14)
C(5B)-C(6)	1.51(2)
C(7A)-C(8)	1.479(13)
C(7B)-C(8)	1.551(19)
C(9)-C(10)	1.494(12)
C(11)-C(12)	1.493(19)
C(13)-C(14)	1.508(13)
C(15)-C(16)	1.495(18)

Table S3. Bond angles (deg.) for $[Et_4N]_2[(S_2)Mo(O)(\mu\text{-}S)_2Mo(O)(S_2)]$. Symmetry transformations used to generate equivalent atoms:

O(1)-Mo(1)-S(4)	109.53(18)	C(2)-C(1B)-N(1)	119.3(13)
O(1)-Mo(1)-S(3)	107.31(19)	C(4)-C(3A)-N(1)	116.7(8)
S(4)-Mo(1)-S(3)	102.55(7)	C(4)-C(3B)-N(1)	117.4(13)
O(1)-Mo(1)-S(2)	109.49(19)	C(6)-C(5A)-N(1)	120.8(9)
S(4)-Mo(1)-S(2)	133.37(8)	N(1)-C(5B)-C(6)	120.4(14)
S(3)-Mo(1)-S(2)	89.19(8)	C(8)-C(7A)-N(1)	115.1(8)
O(1)-Mo(1)-S(1)	109.6(2)	N(1)-C(7B)-C(8)	113.0(12)
S(4)-Mo(1)-S(1)	90.98(8)	C(10)-C(9)-N(2)	115.7(7)
S(3)-Mo(1)-S(1)	133.38(9)	N(2)-C(11)-C(12)	116.5(11)
S(2)-Mo(1)-S(1)	52.13(9)	C(14)-C(13)-N(2)	115.3(8)
O(1)-Mo(1)-Mo(2)	105.76(19)	C(16)-C(15)-N(2)	115.3(8)
S(4)-Mo(1)-Mo(2)	53.01(5)		
S(3)-Mo(1)-Mo(2)	52.46(5)		
S(2)-Mo(1)-Mo(2)	134.24(6)		
S(1)-Mo(1)-Mo(2)	136.42(6)		
O(2)-Mo(2)-S(3)	110.5(2)		
O(2)-Mo(2)-S(4)	106.6(2)		
S(3)-Mo(2)-S(4)	102.44(7)		
O(2)-Mo(2)-S(6)	111.2(2)		
S(3)-Mo(2)-S(6)	130.08(8)		
S(4)-Mo(2)-S(6)	90.64(8)		
O(2)-Mo(2)-S(5)	107.9(2)		
S(3)-Mo(2)-S(5)	90.77(8)		
S(4)-Mo(2)-S(5)	135.56(8)		
S(6)-Mo(2)-S(5)	50.94(8)		
O(2)-Mo(2)-Mo(1)	106.03(18)		
S(3)-Mo(2)-Mo(1)	52.95(5)		
S(4)-Mo(2)-Mo(1)	52.41(5)		
S(6)-Mo(2)-Mo(1)	133.82(6)		
S(5)-Mo(2)-Mo(1)	137.28(6)		
S(2)-S(1)-Mo(1)	63.82(9)		
S(1)-S(2)-Mo(1)	64.05(9)		
Mo(2)-S(3)-Mo(1)	74.59(6)		
Mo(1)-S(4)-Mo(2)	74.58(6)		
S(6)-S(5)-Mo(2)	64.30(8)		
S(5)-S(6)-Mo(2)	64.77(8)		
C(11)-N(2)-C(9)	111.3(8)		
C(11)-N(2)-C(13)	110.9(8)		
C(9)-N(2)-C(13)	107.1(6)		
C(11)-N(2)-C(15)	108.9(9)		
C(9)-N(2)-C(15)	109.8(7)		
C(13)-N(2)-C(15)	108.9(7)		
N(1)-C(1A)-C(2)	116.8(8)		

Table S4. Anisotropic displacement parameters (Å^2 x 10^3) for $[Et_4N]_2[(S_2)Mo(O)(\mu\text{-}S)_2Mo(O)(S_2)]$. The anisotropic displacement factor exponent takes the form: $-2\pi^2[h^2a^{*2}U^{11} + ... + 2hka^*b^*U^{12}]$.

Atom	U^{11}	U^{22}	U^{33}	U^{23}	U^{13}	U^{12}
Mo(1)	24(1)	24(1)	40(1)	4(1)	5(1)	-1(1)
Mo(2)	38(1)	26(1)	35(1)	-1(1)	5(1)	-3(1)
S(1)	78(2)	45(1)	63(2)	3(1)	35(1)	18(1)
S(2)	59(1)	59(2)	51(1)	-14(1)	2(1)	-14(1)
S(3)	27(1)	50(1)	38(1)	2(1)	1(1)	10(1)
S(4)	30(1)	46(1)	43(1)	10(1)	-4(1)	3(1)
S(5)	45(1)	49(1)	51(1)	9(1)	16(1)	2(1)
S(6)	58(1)	50(1)	37(1)	7(1)	4(1)	1(1)
O(1)	38(3)	37(3)	52(3)	8(3)	1(2)	-9(2)
O(2)	63(4)	45(3)	55(4)	-13(3)	20(3)	-14(3)
N(1)	20(3)	28(3)	23(3)	1(2)	3(2)	1(2)
N(2)	40(4)	33(4)	96(6)	25(4)	14(4)	-2(3)
C(1A)	31(5)	34(6)	31(5)	-1(4)	6(4)	1(4)
C(1B)	31(5)	34(6)	31(5)	-1(4)	6(4)	1(4)
C(3A)	38(6)	28(6)	33(6)	-3(4)	2(4)	6(4)
C(3B)	38(6)	28(6)	33(6)	-3(4)	2(4)	6(4)
C(5A)	28(6)	46(6)	32(6)	-1(5)	0(4)	2(5)
C(5B)	28(6)	46(6)	32(6)	-1(5)	0(4)	2(5)
C(7A)	29(5)	36(6)	26(5)	1(4)	3(4)	1(4)
C(7B)	29(5)	36(6)	26(5)	1(4)	3(4)	1(4)
C(2)	43(5)	60(6)	43(5)	-5(4)	14(4)	4(4)
C(4)	41(5)	40(5)	44(5)	3(4)	10(4)	-11(4)
C(6)	33(5)	85(7)	56(5)	5(5)	7(4)	15(5)
C(8)	37(4)	57(5)	35(4)	9(4)	4(3)	-4(4)
C(9)	52(5)	32(5)	70(6)	4(4)	-1(4)	-5(4)
C(10)	57(6)	55(6)	95(8)	-10(5)	-10(5)	14(5)
C(11)	88(9)	88(9)	153(13)	77(10)	73(9)	45(7)
C(12)	94(10)	175(16)	93(10)	78(11)	46(8)	62(10)
C(13)	38(5)	78(7)	63(6)	22(5)	4(4)	-7(5)
C(14)	51(6)	103(9)	93(8)	43(7)	19(5)	34(6)
C(15)	44(6)	34(6)	203(15)	-24(8)	16(8)	-12(5)
C(16)	82(9)	101(10)	126(12)	-56(9)	-22(8)	-1(7)

Table S5. Hydrogen coordinates (x 10^4) and isotropic displacement parameters ($Å^2$ x 10^3) for $[Et_4N]_2[(S_2)Mo(O)(\mu\text{-}S)_2Mo(O)(S_2)]$.

H atom	x	y	z	U(eq)
H(1A1)	518	2989	7979	38
H(1A2)	1944	3262	8051	38
H(1B1)	2201	2296	9572	38
H(1B2)	3356	2680	9411	38
H(3A1)	1904	1832	7477	40
H(3A2)	1886	2012	8946	40
H(3B1)	34	2732	7611	40
H(3B2)	329	2438	6350	40
H(5A1)	3979	2861	7804	43
H(5A2)	3839	2493	8957	43
H(5B1)	2544	2112	6309	43
H(5B2)	2635	1880	7729	43
H(7A1)	2042	2324	5725	37
H(7A2)	716	2626	5932	37
H(7B1)	3254	3160	7511	37
H(7B2)	1652	3273	7334	37
H(2A)	1232	3243	10122	72
H(2B)	1188	2671	10088	72
H(2C)	2619	2945	10160	72
H(4A)	-228	1704	8110	62
H(4B)	-376	2263	8404	62
H(4C)	-359	2082	6931	62
H(6A)	5380	2244	7727	87
H(6B)	4124	1878	7606	87
H(6C)	4265	2248	6445	87
H(8A)	2036	3046	4639	65
H(8B)	1983	3329	5984	65
H(8C)	3312	3026	5776	65
H(9A)	2254	273	3352	63
H(9B)	1889	181	1814	63
H(10A)	-20	454	2672	106
H(10B)	-292	-79	2131	106
H(10C)	74	14	3674	106
H(11A)	2426	-965	4213	125
H(11B)	1070	-653	4181	125
H(12A)	2487	-530	6132	176
H(12B)	3691	-354	5350	176
H(12C)	2330	-41	5318	176
H(13A)	3927	-271	1874	72
H(13B)	4258	-179	3416	72

Table S5. Hydrogen coordinates (x 10^4) and isotropic displacement parameters (Å^2 x 10^3) for $[Et_4N]_2[(S_2)Mo(O)(\mu\text{-}S)_2Mo(O)(S_2)]$.

H atom	x	y	z	U(eq)
H(14A)	5545	-821	2813	122
H(14B)	4512	-1007	3775	122
H(14C)	4181	-1099	2229	122
H(15A)	1941	-1091	1913	112
H(15B)	590	-772	1830	112
H(16A)	1277	-843	-230	159
H(16B)	1377	-294	221	159
H(16C)	2731	-614	304	159

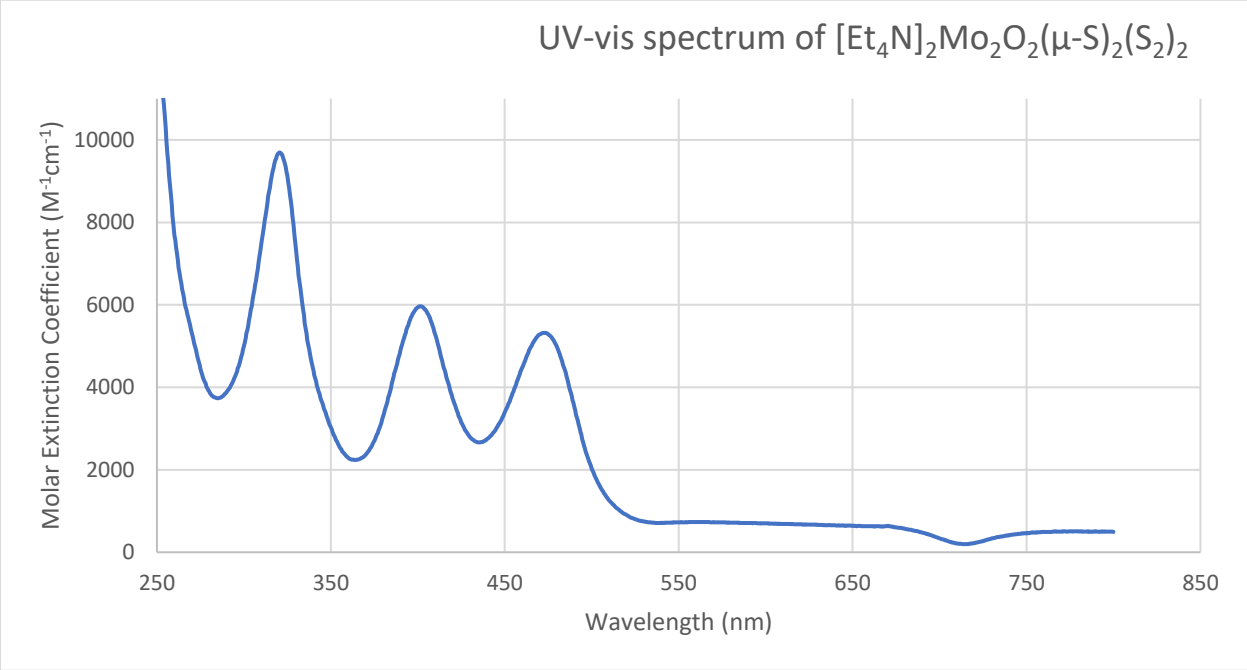

Structure Determination Summary

Tulane University

Full Atom Labeling for [(^{i}Bu$_2$NCS$_2$)Mo(O)(μ-S)$_2$Mo(O)(S$_2$CN^{i}Bu$_2$)]

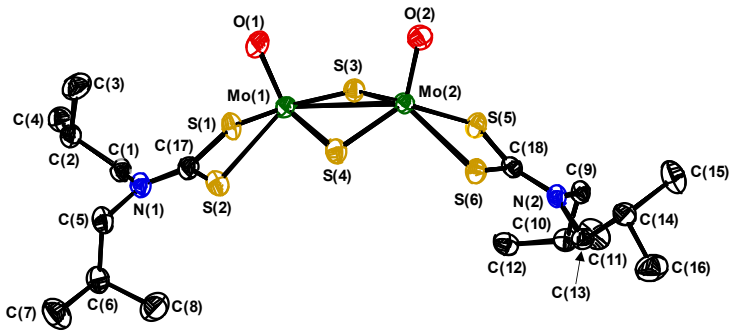

The thermal ellipsoid plot is drawn at the 50% level. All H atoms are omitted for clarity.

Crystal Data and Structure Refinement for [(^{i}Bu$_2$NCS$_2$)Mo(O)(μ-S)$_2$Mo(O)(S$_2$CN^{i}Bu$_2$)]

Identification code	JPD1399_0m_M_a	
Empirical formula	$C_{18}H_{36}Mo_2N_2O_2S_6$	
Formula weight	696.73	
Temperature	150(2) K	
Wavelength	1.54178 Å	
Crystal system	Monoclinic	
Space group	$P2_1/c$	
Unit cell dimensions	a = 18.7186(5) Å	α = 90°
	b = 9.6217(2) Å	β = 111.6280(10)°
	c = 16.9453(4) Å	γ = 90°
Volume	2837.06(12) Å^3	
Z	4	
Density (calculated)	1.631 g/cm^3	
Absorption coefficient	11.507 mm^{-1}	
F(000)	1416	
Crystal size	0.178 x 0.145 x 0.071 mm^3	
θ range for data collection	2.54 to 72.31°	
Index ranges	$-23 \le h \le 23$, $-11 \le k \le 11$, $-20 \le l \le 20$	
Reflections collected	67808	
Independent reflections	5576 [R(int) = 0.0394]	

Completeness to θ = 72.30°	99.5 %
Absorption correction	Semi-empirical from equivalents
Max. and min. transmission	0.49 and 0.32
Refinement method	Full-matrix least-squares on F^2
Data / restraints / parameters	5576 / 0 / 279
Goodness-of-fit on F^2	1.053
Final R indices [I>2σ(I)]	R1 = 0.0190, wR2 = 0.0478
R indices (all data)	R1 = 0.0199, wR2 = 0.0485
Extinction coefficient	n/a
Largest diff. peak and hole	0.391 and -0.658 e·Å^{-3}

Table S1. Atomic coordinates (x 10^4) and equivalent isotropic displacement parameters (Å^2 x 10^3) for [(^{i}Bu$_2$NCS$_2$)Mo(O)(μ-S)$_2$Mo(O)(S$_2$CN^{i}Bu$_2$)]. U(eq) is defined as one third of the trace of the orthogonalized U^{ij} tensor.

Atom	x	y	z	U(eq)
Mo(1)	1731(1)	6499(1)	4440(1)	26(1)
Mo(2)	2821(1)	4400(1)	5221(1)	24(1)
S(1)	1543(1)	8898(1)	4835(1)	35(1)
S(2)	1675(1)	8060(1)	3283(1)	32(1)
S(3)	2440(1)	6231(1)	5879(1)	30(1)
S(4)	2419(1)	5161(1)	3827(1)	30(1)
S(5)	3958(1)	4485(1)	6528(1)	28(1)
S(6)	3939(1)	3489(1)	4934(1)	27(1)
O(1)	854(1)	5759(2)	4187(1)	40(1)
O(2)	2323(1)	2972(2)	5269(1)	35(1)
N(1)	1079(1)	10555(2)	3444(1)	30(1)
N(2)	5236(1)	3509(2)	6329(1)	23(1)
C(1)	825(1)	11625(2)	3909(1)	31(1)
C(2)	-43(1)	11846(2)	3554(1)	34(1)
C(3)	-480(1)	10485(3)	3460(2)	49(1)
C(4)	-252(1)	12852(2)	4129(2)	42(1)
C(5)	949(1)	10853(2)	2546(1)	33(1)
C(6)	1468(1)	11987(2)	2423(1)	35(1)
C(7)	1252(2)	12182(3)	1469(2)	49(1)
C(8)	2314(1)	11630(3)	2865(2)	51(1)
C(9)	5692(1)	3820(2)	7230(1)	26(1)
C(10)	6162(1)	5163(2)	7352(1)	29(1)
C(11)	6662(2)	5302(3)	8288(2)	55(1)
C(12)	5652(1)	6433(2)	7041(1)	36(1)
C(13)	5664(1)	3035(2)	5797(1)	26(1)
C(14)	5598(1)	1485(2)	5590(1)	27(1)
C(15)	5844(2)	589(2)	6380(1)	42(1)
C(16)	6084(1)	1186(2)	5057(2)	42(1)
C(17)	1380(1)	9378(2)	3795(1)	30(1)
C(18)	4494(1)	3753(2)	5993(1)	23(1)

Table S2. Bond lengths (Å) for [(^{i}Bu$_2$NCS$_2$)Mo(O)(μ-S)$_2$Mo(O)(S$_2$CN^{i}Bu$_2$)]. Symmetry transformations used to generate equivalent atoms:

Mo(1)-O(1)	1.6925(14)	C(8)-H(8B)	0.9800
Mo(1)-S(4)	2.3191(5)	C(8)-H(8C)	0.9800
Mo(1)-S(3)	2.3203(5)	C(9)-C(10)	1.533(2)
Mo(1)-S(2)	2.4413(5)	C(9)-H(9A)	0.9900
Mo(1)-S(1)	2.4643(5)	C(9)-H(9B)	0.9900
Mo(1)-Mo(2)	2.8290(2)	C(10)-C(12)	1.519(3)
Mo(2)-O(2)	1.6800(14)	C(10)-C(11)	1.523(3)
Mo(2)-S(4)	2.3172(5)	C(10)-H(10)	1.0000
Mo(2)-S(3)	2.3324(5)	C(11)-H(11A)	0.9800
Mo(2)-S(5)	2.4428(5)	C(11)-H(11B)	0.9800
Mo(2)-S(6)	2.4769(5)	C(11)-H(11C)	0.9800
S(1)-C(17)	1.736(2)	C(12)-H(12A)	0.9800
S(2)-C(17)	1.739(2)	C(12)-H(12B)	0.9800
S(5)-C(18)	1.7314(18)	C(12)-H(12C)	0.9800
S(6)-C(18)	1.7285(18)	C(13)-C(14)	1.527(2)
N(1)-C(17)	1.307(3)	C(13)-H(13A)	0.9900
N(1)-C(1)	1.478(3)	C(13)-H(13B)	0.9900
N(1)-C(5)	1.478(3)	C(14)-C(15)	1.515(3)
N(2)-C(18)	1.313(2)	C(14)-C(16)	1.527(3)
N(2)-C(9)	1.480(2)	C(14)-H(14)	1.0000
N(2)-C(13)	1.481(2)	C(15)-H(15A)	0.9800
C(1)-C(2)	1.526(3)	C(15)-H(15B)	0.9800
C(1)-H(1A)	0.9900	C(15)-H(15C)	0.9800
C(1)-H(1B)	0.9900	C(16)-H(16A)	0.9800
C(2)-C(3)	1.521(3)	C(16)-H(16B)	0.9800
C(2)-C(4)	1.523(3)	C(16)-H(16C)	0.9800
C(2)-H(2)	1.0000		
C(3)-H(3A)	0.9800		
C(3)-H(3B)	0.9800		
C(3)-H(3C)	0.9800		
C(4)-H(4A)	0.9800		
C(4)-H(4B)	0.9800		
C(4)-H(4C)	0.9800		
C(5)-C(6)	1.525(3)		
C(5)-H(5A)	0.9900		
C(5)-H(5B)	0.9900		
C(6)-C(8)	1.521(3)		
C(6)-C(7)	1.526(3)		
C(6)-H(6)	1.0000		
C(7)-H(7A)	0.9800		
C(7)-H(7B)	0.9800		
C(7)-H(7C)	0.9800		
C(8)-H(8A)	0.9800		

Table S3. Bond angles (Å) for [(^{i}Bu$_2$NCS$_2$)Mo(O)(μ-S)$_2$Mo(O)(S$_2$CN^{i}Bu$_2$)]. Symmetry transformations used to generate equivalent atoms:

O(1)-Mo(1)-S(4)	107.42(6)	N(1)-C(1)-H(1A)	109.0
O(1)-Mo(1)-S(3)	110.20(6)	C(2)-C(1)-H(1A)	109.0
S(4)-Mo(1)-S(3)	102.221(17)	N(1)-C(1)-H(1B)	109.0
O(1)-Mo(1)-S(2)	107.75(5)	C(2)-C(1)-H(1B)	109.0
S(4)-Mo(1)-S(2)	81.251(17)	H(1A)-C(1)-H(1B)	107.8
S(3)-Mo(1)-S(2)	138.641(18)	C(3)-C(2)-C(4)	111.06(19)
O(1)-Mo(1)-S(1)	103.94(6)	C(3)-C(2)-C(1)	111.97(18)
S(4)-Mo(1)-S(1)	143.103(18)	C(4)-C(2)-C(1)	108.87(17)
S(3)-Mo(1)-S(1)	84.413(17)	C(3)-C(2)-H(2)	108.3
S(2)-Mo(1)-S(1)	70.965(17)	C(4)-C(2)-H(2)	108.3
O(1)-Mo(1)-Mo(2)	106.44(5)	C(1)-C(2)-H(2)	108.3
S(4)-Mo(1)-Mo(2)	52.367(12)	C(2)-C(3)-H(3A)	109.5
S(3)-Mo(1)-Mo(2)	52.749(12)	C(2)-C(3)-H(3B)	109.5
S(2)-Mo(1)-Mo(2)	128.642(13)	H(3A)-C(3)-H(3B)	109.5
S(1)-Mo(1)-Mo(2)	133.813(13)	C(2)-C(3)-H(3C)	109.5
O(2)-Mo(2)-S(4)	109.27(5)	H(3A)-C(3)-H(3C)	109.5
O(2)-Mo(2)-S(3)	108.77(5)	H(3B)-C(3)-H(3C)	109.5
S(4)-Mo(2)-S(3)	101.908(17)	C(2)-C(4)-H(4A)	109.5
O(2)-Mo(2)-S(5)	107.28(5)	C(2)-C(4)-H(4B)	109.5
S(4)-Mo(2)-S(5)	139.566(17)	H(4A)-C(4)-H(4B)	109.5
S(3)-Mo(2)-S(5)	81.892(16)	C(2)-C(4)-H(4C)	109.5
O(2)-Mo(2)-S(6)	104.15(5)	H(4A)-C(4)-H(4C)	109.5
S(4)-Mo(2)-S(6)	83.870(16)	H(4B)-C(4)-H(4C)	109.5
S(3)-Mo(2)-S(6)	142.213(17)	N(1)-C(5)-C(6)	114.08(16)
S(5)-Mo(2)-S(6)	70.909(15)	N(1)-C(5)-H(5A)	108.7
O(2)-Mo(2)-Mo(1)	106.79(5)	C(6)-C(5)-H(5A)	108.7
S(4)-Mo(2)-Mo(1)	52.428(12)	N(1)-C(5)-H(5B)	108.7
S(3)-Mo(2)-Mo(1)	52.358(12)	C(6)-C(5)-H(5B)	108.7
S(5)-Mo(2)-Mo(1)	129.592(12)	H(5A)-C(5)-H(5B)	107.6
S(6)-Mo(2)-Mo(1)	132.631(12)	C(8)-C(6)-C(5)	111.80(17)
C(17)-S(1)-Mo(1)	87.88(7)	C(8)-C(6)-C(7)	111.7(2)
C(17)-S(2)-Mo(1)	88.55(7)	C(5)-C(6)-C(7)	107.41(19)
Mo(1)-S(3)-Mo(2)	74.894(15)	C(8)-C(6)-H(6)	108.6
Mo(2)-S(4)-Mo(1)	75.205(15)	C(5)-C(6)-H(6)	108.6
C(18)-S(5)-Mo(2)	89.48(6)	C(7)-C(6)-H(6)	108.6
C(18)-S(6)-Mo(2)	88.43(6)	C(6)-C(7)-H(7A)	109.5
C(17)-N(1)-C(1)	121.99(17)	C(6)-C(7)-H(7B)	109.5
C(17)-N(1)-C(5)	121.17(17)	H(7A)-C(7)-H(7B)	109.5
C(1)-N(1)-C(5)	116.80(15)	C(6)-C(7)-H(7C)	109.5
C(18)-N(2)-C(9)	121.81(15)	H(7A)-C(7)-H(7C)	109.5
C(18)-N(2)-C(13)	120.96(15)	H(7B)-C(7)-H(7C)	109.5
C(9)-N(2)-C(13)	116.99(14)	C(6)-C(8)-H(8A)	109.5
N(1)-C(1)-C(2)	113.08(16)	C(6)-C(8)-H(8B)	109.5

Table S3. Bond angles (Å) for [(^{i}Bu$_2$NCS$_2$)Mo(O)(μ-S)$_2$Mo(O)(S$_2$CN^{i}Bu$_2$)]. Symmetry transformations used to generate equivalent atoms:

H(8A)-C(8)-H(8B)	109.5	C(14)-C(15)-H(15C)	109.5
C(6)-C(8)-H(8C)	109.5	H(15A)-C(15)-H(15C)	109.5
H(8A)-C(8)-H(8C)	109.5	H(15B)-C(15)-H(15C)	109.5
H(8B)-C(8)-H(8C)	109.5	C(14)-C(16)-H(16A)	109.5
N(2)-C(9)-C(10)	113.12(15)	C(14)-C(16)-H(16B)	109.5
N(2)-C(9)-H(9A)	109.0	H(16A)-C(16)-H(16B)	109.5
C(10)-C(9)-H(9A)	109.0	C(14)-C(16)-H(16C)	109.5
N(2)-C(9)-H(9B)	109.0	H(16A)-C(16)-H(16C)	109.5
C(10)-C(9)-H(9B)	109.0	H(16B)-C(16)-H(16C)	109.5
H(9A)-C(9)-H(9B)	107.8	N(1)-C(17)-S(1)	125.33(16)
C(12)-C(10)-C(11)	110.93(19)	N(1)-C(17)-S(2)	124.58(16)
C(12)-C(10)-C(9)	112.10(16)	S(1)-C(17)-S(2)	110.08(11)
C(11)-C(10)-C(9)	108.40(17)	N(2)-C(18)-S(6)	123.94(14)
C(12)-C(10)-H(10)	108.4	N(2)-C(18)-S(5)	124.78(14)
C(11)-C(10)-H(10)	108.4	S(6)-C(18)-S(5)	111.15(10)
C(9)-C(10)-H(10)	108.4		
C(10)-C(11)-H(11A)	109.5		
C(10)-C(11)-H(11B)	109.5		
H(11A)-C(11)-H(11B)	109.5		
C(10)-C(11)-H(11C)	109.5		
H(11A)-C(11)-H(11C)	109.5		
H(11B)-C(11)-H(11C)	109.5		
C(10)-C(12)-H(12A)	109.5		
C(10)-C(12)-H(12B)	109.5		
H(12A)-C(12)-H(12B)	109.5		
C(10)-C(12)-H(12C)	109.5		
H(12A)-C(12)-H(12C)	109.5		
H(12B)-C(12)-H(12C)	109.5		
N(2)-C(13)-C(14)	115.22(15)		
N(2)-C(13)-H(13A)	108.5		
C(14)-C(13)-H(13A)	108.5		
N(2)-C(13)-H(13B)	108.5		
C(14)-C(13)-H(13B)	108.5		
H(13A)-C(13)-H(13B)	107.5		
C(15)-C(14)-C(16)	111.32(18)		
C(15)-C(14)-C(13)	112.29(16)		
C(16)-C(14)-C(13)	107.82(16)		
C(15)-C(14)-H(14)	108.4		
C(16)-C(14)-H(14)	108.4		
C(13)-C(14)-H(14)	108.4		
C(14)-C(15)-H(15A)	109.5		
C(14)-C(15)-H(15B)	109.5		
H(15A)-C(15)-H(15B)	109.5		

Table S4. Anisotropic displacement parameters (Å^2 x 10^3) for [(^{i}Bu$_2$NCS$_2$)Mo(O)(μ-S)$_2$Mo(O)(S$_2$CN^{i}Bu$_2$)]. The anisotropic displacement factor exponent takes the form: $-2\pi^2[h^2 a^{*2}U^{11} + ... + 2hka^*b^*U^{12}]$.

Atom	U^{11}	U^{22}	U^{33}	U^{23}	U^{13}	U^{12}
Mo(1)	19(1)	28(1)	28(1)	4(1)	5(1)	-1(1)
Mo(2)	21(1)	23(1)	24(1)	3(1)	5(1)	-1(1)
S(1)	39(1)	34(1)	27(1)	5(1)	7(1)	7(1)
S(2)	36(1)	29(1)	27(1)	3(1)	6(1)	2(1)
S(3)	28(1)	34(1)	27(1)	4(1)	10(1)	6(1)
S(4)	29(1)	31(1)	26(1)	1(1)	5(1)	2(1)
S(5)	24(1)	33(1)	23(1)	-2(1)	6(1)	4(1)
S(6)	26(1)	30(1)	22(1)	-1(1)	5(1)	3(1)
O(1)	23(1)	42(1)	48(1)	6(1)	5(1)	-3(1)
O(2)	27(1)	35(1)	38(1)	5(1)	5(1)	-7(1)
N(1)	26(1)	28(1)	28(1)	1(1)	1(1)	-1(1)
N(2)	24(1)	20(1)	25(1)	-1(1)	7(1)	-1(1)
C(1)	27(1)	28(1)	31(1)	0(1)	2(1)	-2(1)
C(2)	27(1)	33(1)	36(1)	6(1)	4(1)	-1(1)
C(3)	33(1)	42(1)	66(2)	-4(1)	11(1)	-11(1)
C(4)	37(1)	37(1)	50(1)	6(1)	15(1)	3(1)
C(5)	31(1)	31(1)	27(1)	5(1)	1(1)	3(1)
C(6)	37(1)	27(1)	42(1)	5(1)	15(1)	6(1)
C(7)	66(2)	41(1)	49(1)	13(1)	30(1)	15(1)
C(8)	36(1)	46(1)	71(2)	5(1)	19(1)	1(1)
C(9)	25(1)	25(1)	23(1)	1(1)	2(1)	-1(1)
C(10)	30(1)	30(1)	27(1)	-5(1)	9(1)	-7(1)
C(11)	56(2)	51(1)	38(1)	-1(1)	-4(1)	-21(1)
C(12)	46(1)	24(1)	41(1)	-4(1)	19(1)	-6(1)
C(13)	24(1)	24(1)	30(1)	-1(1)	11(1)	-2(1)
C(14)	28(1)	25(1)	30(1)	-2(1)	10(1)	-1(1)
C(15)	59(1)	27(1)	38(1)	4(1)	16(1)	9(1)
C(16)	45(1)	38(1)	51(1)	-10(1)	28(1)	-3(1)
C(17)	23(1)	31(1)	29(1)	2(1)	1(1)	-3(1)
C(18)	26(1)	19(1)	24(1)	2(1)	7(1)	-1(1)

Table S5. Hydrogen coordinates (x 10^4) and isotropic displacement parameters (Å^2 x 10^3) for [(^{i}Bu$_2$NCS$_2$)Mo(O)(μ-S)$_2$Mo(O)(S$_2$CN^{i}Bu$_2$)].

H atom	x	y	z	U(eq)
H(1A)	1081	12515	3885	38
H(1B)	989	11347	4512	38
H(2)	-191	12281	2979	41
H(3A)	-1034	10670	3227	74
H(3B)	-341	10041	4017	74
H(3C)	-347	9867	3076	74
H(4A)	52	13704	4198	63
H(4B)	-142	12420	4685	63
H(4C)	-800	13080	3873	63
H(5A)	406	11136	2251	39
H(5B)	1031	9989	2274	39
H(6)	1361	12873	2668	42
H(7A)	1374	11333	1225	74
H(7B)	1543	12962	1368	74
H(7C)	701	12375	1203	74
H(8A)	2428	10769	2624	77
H(8B)	2430	11502	3473	77
H(8C)	2629	12387	2781	77
H(9A)	6047	3035	7478	31
H(9B)	5341	3898	7544	31
H(10)	6505	5086	7020	35
H(11A)	6993	4482	8471	82
H(11B)	6334	5377	8623	82
H(11C)	6982	6137	8374	82
H(12A)	5331	6315	6440	54
H(12B)	5974	7262	7110	54
H(12C)	5323	6542	7372	54
H(13A)	6214	3266	6094	31
H(13B)	5477	3562	5258	31
H(14)	5050	1270	5240	33
H(15A)	5823	-392	6219	63
H(15B)	5497	750	6686	63
H(15C)	6370	831	6748	63
H(16A)	6033	204	4892	63
H(16B)	6624	1393	5390	63
H(16C)	5908	1768	4546	63

Appendix B: Chapter 3 Supplemental Information:

Computational Details:

Density Functional Theory calculations though the WebMO program or on Tulane Cypress Computing Core using Gaussian09. Structures were generated *de novo* on the WebMo Graphical interface or loaded from pre-existing SC-XRD coordinates. All calculations were carried out in the gas phase. Initial geometry was run at the “loose” level with Cu, Mo, Si using the LANL2dz basis set and all lighter atoms using 6-311++G(2d,2p) basis. Once convergence was achieved at this level, the limits were tightened one step at a time until convergence was achieved under “tight" parameters. A vibrational calculation was then run to check for imaginary vibrational frequencies and necessary structural changes were made to eliminate them if they appeared. At this point the minimized structure was used to calculate any number of the following employing the appropriate keywords: Molecular Orbitals, Natural Bonding Orbitals, or Excitation States.

Computational Minimized Coordinates:

$[Cu(Me_4phen)(^tBu_3P)(MeCN)]^+$

Cu	0.35506	0.03864	0.60243
P	2.48516	0.00852	-0.43277
C	3.68568	-1.28406	0.48687
C	2.84113	-2.54581	0.82525
H	3.46193	-3.23749	1.41262
H	1.96539	-2.28032	1.43088
H	2.50114	-3.08302	-0.0627
C	4.1377	-0.68513	1.84619
H	4.63704	-1.47604	2.4236
H	3.28563	-0.32696	2.43557
H	4.85511	0.13175	1.73039
C	4.94336	-1.70301	-0.31612
H	5.55268	-2.37397	0.30702
H	4.69502	-2.25023	-1.23061
H	5.57076	-0.84876	-0.58764
C	2.29035	-0.53502	-2.33542
C	1.03463	0.1864	-2.90289
H	0.83673	-0.19704	-3.91409

H	0.151	-0.01146	-2.28463
H	1.16039	1.26801	-2.98103
C	1.9874	-2.05645	-2.40115
H	1.71297	-2.3086	-3.43494
H	2.85046	-2.6733	-2.13577
H	1.14269	-2.32995	-1.75787
C	3.51652	-0.23078	-3.23191
H	3.32315	-0.62271	-4.24113
H	4.43125	-0.70505	-2.86456
H	3.70351	0.84247	-3.33397
C	3.32153	1.81241	-0.36438
C	3.05088	2.39702	1.05104
H	3.38951	3.44293	1.07159
H	3.58145	1.86375	1.84219
H	1.98043	2.3779	1.29163
C	4.84254	1.84286	-0.65627
H	5.18541	2.88776	-0.63915
H	5.42363	1.30063	0.0955
H	5.08756	1.43386	-1.64102
C	2.60082	2.74522	-1.3747
H	2.9334	3.77684	-1.19207
H	2.84157	2.50697	-2.41425
H	1.51133	2.71697	-1.25418
N	-1.19955	-1.35986	0.234
C	-2.38618	-0.74304	-0.0757
C	-2.40984	0.70715	-0.09308
N	-1.24425	1.37046	0.20203
C	-1.26112	2.71281	0.20904
C	-2.40903	3.50127	-0.07912

C	-3.6113	2.83923	-0.39517
C	-3.6147	1.40327	-0.39993
C	-4.79319	0.62235	-0.69822
C	-4.77066	-0.7522	-0.68146
C	-3.56724	-1.48621	-0.36457
C	-3.51588	-2.92076	-0.32428
C	-2.29213	-3.53441	0.00688
C	-1.17082	-2.70141	0.27347
H	-0.21725	-3.15588	0.52645
C	-2.11351	-5.03793	0.09101
H	-2.77578	-5.48404	0.84394
H	-2.33116	-5.52788	-0.86663
H	-1.08435	-5.29291	0.36521
C	-4.75855	-3.73165	-0.62987
H	-5.56904	-3.49471	0.07218
H	-5.132	-3.51844	-1.64017
H	-4.57205	-4.80486	-0.56759
H	-5.67889	-1.30044	-0.9087
H	-5.71879	1.13487	-0.93845
C	-4.88017	3.60016	-0.72095
H	-5.68345	3.35194	-0.01454
H	-4.73074	4.68031	-0.68343
H	-5.24403	3.35085	-1.72647
C	-2.28098	5.0115	-0.03324
H	-2.95939	5.45425	0.70717
H	-1.26146	5.30804	0.2351
H	-2.51321	5.46868	-1.00355
H	-0.32454	3.20635	0.45303
N	0.39134	0.08175	2.76819

C	0.33544	0.12083	3.93968
C	0.26214	0.17081	5.40216
H	0.71909	1.09414	5.77524
H	0.79243	-0.68218	5.84002
H	-0.78207	0.13964	5.73234

$[Cu(Me_4phen)(^tBu_3P)]^+$

P	-2.61734	-0.00308	-0.01152
Cu	-0.29836	-0.00605	-0.06155
N	1.27853	-1.35967	-0.04087
C	2.4954	-0.7232	-0.03408
C	2.49399	0.72553	-0.03431
N	1.27581	1.35959	-0.04166
C	1.25634	2.70299	-0.02891
C	2.42258	3.51634	-0.01295
C	3.6811	2.88329	-0.01058
C	3.71985	1.44711	-0.02013
C	4.95156	0.69125	-0.01237
C	4.9528	-0.68451	-0.01251
C	3.72245	-1.44258	-0.02016
C	3.68609	-2.87887	-0.01113
C	2.42868	-3.51408	-0.01315
C	1.26069	-2.70316	-0.02829
H	0.28385	-3.17524	-0.0301
C	2.26267	-5.02066	-2.7E-4
H	2.72866	-5.48527	-0.87843
H	2.72257	-5.46955	0.88915
H	1.20277	-5.29492	-0.0016
C	4.97799	-3.66726	0.00297
H	5.59457	-3.42884	-0.87343

H	5.5751	-3.42857	0.89287
H	4.79942	-4.74331	0.00126
H	5.89908	-1.21437	-0.00451
H	5.89688	1.22282	-0.00419
C	4.97155	3.67402	0.00487
H	5.58896	3.43756	-0.87147
H	4.79101	4.74974	0.00412
H	5.56862	3.43554	0.89483
C	2.25378	5.02257	0.00121
H	2.71965	5.4889	-0.87608
H	1.19341	5.29501	-6.3E-4
H	2.71218	5.47131	0.89149
H	0.27896	3.17477	-0.02964
C	-3.37908	-1.33088	-1.27741
C	-2.48725	-2.60274	-1.22627
H	-2.87888	-3.33144	-1.95021
H	-1.45525	-2.36707	-1.51275
H	-2.47511	-3.08297	-0.2462
C	-3.27403	-0.78635	-2.72746
H	-3.52386	-1.60453	-3.41734
H	-2.25677	-0.45149	-2.96462
H	-3.97159	0.03158	-2.92702
C	-4.8524	-1.71477	-0.9878
H	-5.19606	-2.40073	-1.77569
H	-4.96776	-2.23469	-0.03183
H	-5.51917	-0.84762	-0.99102
C	-3.15752	-0.4701	1.84166
C	-2.19754	0.27452	2.81293
H	-2.43184	-0.03817	3.84063

H	-1.14964	0.01352	2.6146
H	-2.29406	1.36051	2.76641
C	-2.92628	-1.98672	2.077
H	-3.0788	-2.19327	3.14557
H	-3.6248	-2.61768	1.52064
H	-1.90099	-2.28414	1.82521
C	-4.62561	-0.12071	2.19059
H	-4.83249	-0.46156	3.21539
H	-5.34112	-0.61449	1.5267
H	-4.81483	0.95655	2.16166
C	-3.31852	1.79884	-0.46722
C	-2.52822	2.31356	-1.70387
H	-2.81281	3.35907	-1.88912
H	-2.73951	1.74785	-2.61275
H	-1.44595	2.28403	-1.5289
C	-4.83833	1.8477	-0.76906
H	-5.12018	2.8918	-0.96917
H	-5.10789	1.2641	-1.65426
H	-5.44481	1.49797	0.07197
C	-3.00858	2.7777	0.69745
H	-3.2316	3.79808	0.35606
H	-3.62083	2.59026	1.584
H	-1.95182	2.74803	0.98927

[Cu(Me_4phen)($^tBu_3$P)]Cl

Cu	0	0	0
P	-2.15013	-0.01368	1.049
C	-3.34236	-1.28947	0.09208
C	-2.48568	-2.54191	-0.25349
H	-3.106	-3.23725	-0.83908

H	-1.627	-2.25507	-0.87176
H	-2.13261	-3.07895	0.63136
C	-3.7586	-0.67171	-1.2712
H	-4.23929	-1.46038	-1.86945
H	-2.88676	-0.31361	-1.83054
H	-4.48568	0.1392	-1.16155
C	-4.61542	-1.71788	0.86492
H	-5.21361	-2.37549	0.21578
H	-4.38768	-2.28206	1.77565
H	-5.2456	-0.86494	1.13796
C	-2.04208	-0.56515	2.96132
C	-0.80238	0.14369	3.57894
H	-0.62631	-0.26309	4.58641
H	0.09297	-0.03526	2.97266
H	-0.93408	1.22341	3.67687
C	-1.74181	-2.08743	3.02696
H	-1.5061	-2.35183	4.06856
H	-2.59153	-2.70196	2.71666
H	-0.87375	-2.34931	2.41107
C	-3.29144	-0.26498	3.82697
H	-3.12947	-0.66381	4.84062
H	-4.19752	-0.73139	3.42828
H	-3.47603	0.80944	3.92763
C	-2.98701	1.79201	0.97464
C	-2.69168	2.3804	-0.43498
H	-2.98255	3.44231	-0.4404
H	-3.2464	1.8782	-1.22867
H	-1.63044	2.30326	-0.69565
C	-4.51264	1.83352	1.24022

H	-4.85075	2.88077	1.20412
H	-5.07719	1.28442	0.4809
H	-4.77876	1.43337	2.22382
C	-2.27818	2.71595	2.00164
H	-2.59369	3.75284	1.81365
H	-2.5417	2.4773	3.0367
H	-1.18726	2.67169	1.90084
N	1.53476	-1.38064	0.54178
C	2.73097	-0.76431	0.80717
C	2.75138	0.68359	0.80215
N	1.57398	1.33286	0.52697
C	1.59078	2.67287	0.4661
C	2.74856	3.46993	0.68283
C	3.96095	2.82175	0.98603
C	3.96704	1.38845	1.04085
C	5.15691	0.61387	1.30946
C	5.13797	-0.76166	1.31074
C	3.92659	-1.50301	1.0453
C	3.87892	-2.93572	0.99402
C	2.64739	-3.54974	0.6965
C	1.51162	-2.72044	0.48448
H	0.55366	-3.17265	0.24435
C	2.47401	-5.05295	0.58524
H	3.10914	-5.47646	-0.20387
H	2.72769	-5.56582	1.52262
H	1.43622	-5.3031	0.34041
C	5.13799	-3.74503	1.23786
H	5.90933	-3.51099	0.49143
H	5.5655	-3.52821	2.22613

H	4.94676	-4.8188	1.18884
H	6.05769	-1.30488	1.50462
H	6.09114	1.13193	1.50285
C	5.24213	3.59473	1.23262
H	6.00829	3.33797	0.48829
H	5.08244	4.67362	1.18259
H	5.66061	3.36606	2.22205
C	2.61875	4.9773	0.56941
H	3.26923	5.38173	-0.21717
H	1.58962	5.25712	0.32015
H	2.88301	5.48315	1.50766
H	0.64841	3.15358	0.21901
Cl	-0.18449	-0.05296	-2.36279

[Cu(Me_4phen)(^{t}Bu_3P)]Br

Cu	0.31659	0.03531	0.56633
P	2.46243	0.01661	-0.49536
C	3.66963	-1.26459	0.43504
C	2.82013	-2.52036	0.78528
H	3.44683	-3.21502	1.36457
H	1.96391	-2.24042	1.41014
H	2.46213	-3.05642	-0.09807
C	4.10914	-0.65376	1.79387
H	4.59857	-1.44492	2.3813
H	3.2495	-0.29523	2.37111
H	4.83451	0.15743	1.67602
C	4.93134	-1.68866	-0.3589
H	5.5386	-2.34999	0.2778
H	4.6904	-2.24767	-1.26928
H	5.55758	-0.83428	-0.63602

C	2.32236	-0.5286	-2.40816
C	1.07484	0.1838	-3.00544
H	0.88657	-0.21709	-4.01305
H	0.18677	9.4E-4	-2.38992
H	1.20487	1.26408	-3.09877
C	2.02049	-2.05046	-2.47536
H	1.76771	-2.30985	-3.51415
H	2.87531	-2.66642	-2.1824
H	1.16265	-2.31551	-1.84679
C	3.55935	-0.22636	-3.29055
H	3.3826	-0.62293	-4.30254
H	4.47063	-0.69409	-2.90584
H	3.74273	0.84816	-3.39147
C	3.30333	1.82127	-0.42929
C	3.03238	2.40607	0.98643
H	3.32356	3.46783	0.99044
H	3.60083	1.90233	1.76957
H	1.97564	2.32926	1.26551
C	4.82447	1.8612	-0.71987
H	5.16406	2.90798	-0.68655
H	5.40102	1.30993	0.02875
H	5.0744	1.46372	-1.70873
C	2.57938	2.74896	-1.44221
H	2.89895	3.78482	-1.25589
H	2.82646	2.51336	-2.48199
H	1.49022	2.70571	-1.32459
N	-1.21851	-1.35007	0.03301
C	-2.41824	-0.73573	-0.2207
C	-2.44111	0.71241	-0.22144

N	-1.26194	1.36565	0.035
C	-1.28081	2.70558	0.09186
C	-2.44323	3.49945	-0.11074
C	-3.65817	2.8474	-0.39408
C	-3.66171	1.41389	-0.44455
C	-4.85382	0.63649	-0.69357
C	-4.8323	-0.73886	-0.69075
C	-3.61602	-1.47697	-0.43967
C	-3.56597	-2.90944	-0.38367
C	-2.32986	-3.52113	-0.10142
C	-1.19281	-2.68961	0.09344
H	-0.23174	-3.1402	0.32376
C	-2.15308	-5.02369	0.01257
H	-2.77589	-5.44475	0.81271
H	-2.42016	-5.54031	-0.91899
H	-1.11153	-5.27191	0.24299
C	-4.82745	-3.72107	-0.60602
H	-5.58807	-3.48452	0.15051
H	-5.26944	-3.50904	-1.58894
H	-4.63433	-4.79439	-0.55501
H	-5.75361	-1.28443	-0.86974
H	-5.79165	1.15227	-0.87511
C	-4.94478	3.61662	-0.62339
H	-5.69875	3.36	0.1333
H	-4.78697	4.696	-0.57858
H	-5.37771	3.38427	-1.60571
C	-2.31541	5.00735	-0.00316
H	-2.95414	5.41172	0.79298
H	-1.28318	5.29037	0.22906

H	-2.59604	5.51036	-0.93817
H	-0.33666	3.1893	0.32559
Br	0.39446	0.01943	3.09165

[Cu(Me$_4$phen)(^{t}Bu$_3$P)]I

Cu	0.31629	0.03718	0.38219
P	2.45589	0.01137	-0.70295
C	3.67929	-1.27523	0.1983
C	2.83629	-2.53211	0.55898
H	3.47144	-3.22767	1.12769
H	1.98808	-2.25596	1.19631
H	2.46573	-3.06641	-0.32008
C	4.14792	-0.67062	1.5499
H	4.64982	-1.4637	2.12376
H	3.30226	-0.31407	2.14819
H	4.86957	0.14205	1.421
C	4.92543	-1.69815	-0.62082
H	5.5435	-2.36238	0.0022
H	4.66669	-2.25386	-1.52817
H	5.54735	-0.84368	-0.90673
C	2.27646	-0.53111	-2.6142
C	1.02012	0.18599	-3.18659
H	0.81319	-0.21131	-4.19193
H	0.14262	0.00301	-2.55637
H	1.15068	1.26626	-3.27905
C	1.97027	-2.05219	-2.6796
H	1.69889	-2.30795	-3.71457
H	2.82917	-2.67051	-2.40404
H	1.12305	-2.31805	-2.03732
C	3.49782	-0.23072	-3.51858

H	3.30017	-0.62399	-4.52795
H	4.414	-0.7035	-3.15237
H	3.68371	0.84319	-3.6203
C	3.30442	1.81322	-0.65216
C	3.06175	2.39894	0.76787
H	3.36598	3.45692	0.76968
H	3.63445	1.88746	1.54295
H	2.00783	2.33621	1.0607
C	4.8202	1.84766	-0.9706
H	5.16313	2.89352	-0.94529
H	5.4091	1.29634	-0.23176
H	5.05129	1.44834	-1.96324
C	2.56627	2.74447	-1.65149
H	2.89342	3.77875	-1.46992
H	2.79404	2.50879	-2.69559
H	1.47929	2.70599	-1.5149
N	-1.21475	-1.35401	-0.15538
C	-2.41559	-0.7426	-0.41083
C	-2.44105	0.70549	-0.42061
N	-1.26311	1.36322	-0.17024
C	-1.28453	2.70354	-0.1244
C	-2.44852	3.49363	-0.33114
C	-3.66299	2.8369	-0.60537
C	-3.66371	1.40311	-0.64517
C	-4.85522	0.62219	-0.88516
C	-4.83123	-0.75294	-0.87379
C	-3.6128	-1.48714	-0.62233
C	-3.56043	-2.91917	-0.55906
C	-2.32224	-3.52773	-0.2792

C	-1.18647	-2.69342	-0.0909
H	-0.22438	-3.1417	0.13945
C	-2.14252	-5.02944	-0.1593
H	-2.76031	-5.44739	0.64632
H	-2.41393	-5.55093	-1.08688
H	-1.09942	-5.27509	0.06681
C	-4.82161	-3.73386	-0.77128
H	-5.579	-3.49405	-0.01256
H	-5.26846	-3.52817	-1.75334
H	-4.62665	-4.80655	-0.7149
H	-5.75208	-1.30132	-1.04624
H	-5.79451	1.13524	-1.06672
C	-4.95199	3.60175	-0.83569
H	-5.702	3.35002	-0.07347
H	-4.7961	4.68176	-0.80056
H	-5.3888	3.3603	-1.81407
C	-2.32336	5.00252	-0.23597
H	-2.95948	5.41146	0.5599
H	-1.29079	5.28957	-0.01029
H	-2.60917	5.49769	-1.17357
H	-0.34153	3.19106	0.10566
I	0.28284	0.04666	3.0841

[Cu(Me_4phen)($^tBu_3$P)]CN

Cu	0.32847	0.02304	1.0406
P	2.41345	0.01565	-0.29507
C	3.67844	-1.25467	0.57699
C	2.85514	-2.5169	0.9645
H	3.50853	-3.20475	1.5217
H	2.02112	-2.24231	1.62031

H	2.46731	-3.0583	0.09718
C	4.18162	-0.64584	1.91496
H	4.71781	-1.43244	2.46657
H	3.35438	-0.30747	2.5466
H	4.88495	0.17946	1.76576
C	4.90495	-1.67286	-0.27408
H	5.54482	-2.33045	0.33393
H	4.6256	-2.23345	-1.17231
H	5.5123	-0.81484	-0.57998
C	2.19643	-0.53577	-2.20063
C	0.91993	0.17101	-2.74048
H	0.68536	-0.23219	-3.73752
H	0.06258	-0.01388	-2.08357
H	1.04198	1.25156	-2.84219
C	1.89966	-2.05948	-2.25435
H	1.60337	-2.32039	-3.28135
H	2.7706	-2.67009	-1.99999
H	1.07235	-2.3319	-1.58918
C	3.39043	-0.23154	-3.13949
H	3.16569	-0.62433	-4.14361
H	4.31719	-0.70321	-2.79918
H	3.57198	0.84271	-3.24517
C	3.25185	1.82322	-0.27475
C	3.02962	2.41524	1.14634
H	3.36145	3.46492	1.147
H	3.58749	1.88804	1.92134
H	1.97435	2.3803	1.43874
C	4.76173	1.86609	-0.62
H	5.09883	2.91425	-0.6093

H	5.36736	1.32378	0.1116
H	4.97687	1.46026	-1.61371
C	2.49446	2.74841	-1.26581
H	2.82455	3.78394	-1.09565
H	2.70432	2.50728	-2.31241
H	1.41	2.71157	-1.11102
N	-1.17561	-1.34914	0.38117
C	-2.35691	-0.73302	0.05263
C	-2.37576	0.71428	0.05201
N	-1.21172	1.36181	0.38304
C	-1.2283	2.7029	0.43297
C	-2.37083	3.50113	0.15219
C	-3.56974	2.85384	-0.20444
C	-3.57674	1.42054	-0.25054
C	-4.75343	0.64624	-0.57317
C	-4.73573	-0.72926	-0.57095
C	-3.53914	-1.47161	-0.24665
C	-3.494	-2.90406	-0.19649
C	-2.27717	-3.51878	0.15773
C	-1.15495	-2.69027	0.43191
H	-0.20948	-3.14301	0.7165
C	-2.10847	-5.02242	0.26939
H	-2.77946	-5.45003	1.02594
H	-2.31843	-5.53044	-0.68128
H	-1.08317	-5.27413	0.56065
C	-4.73966	-3.71287	-0.5027
H	-5.54519	-3.48251	0.20797
H	-5.12075	-3.49168	-1.50874
H	-4.55051	-4.78679	-0.44963

H	-5.64549	-1.27214	-0.80791
H	-5.67681	1.16476	-0.812
C	-4.83546	3.62855	-0.51659
H	-5.63617	3.38033	0.19352
H	-4.67469	4.70732	-0.46791
H	-5.20844	3.39305	-1.52239
C	-2.24218	5.00894	0.26064
H	-2.92805	5.42085	1.01251
H	-1.2253	5.28834	0.55617
H	-2.46051	5.5085	-0.69263
H	-0.29831	3.18287	0.72413
C	0.68844	0.02775	2.95881
N	0.96374	0.03317	4.1214

$[Cu(Me_2bpy)(^tBu_3P)(thiourea)]^+$

Cu	-0.03022	-0.4715	-0.3828
P	-2.17941	0.3074	0.33444
C	-3.3729	-1.23633	0.72838
C	-2.51453	-2.32379	1.43577
H	-3.14598	-3.2057	1.61528
H	-1.67783	-2.63887	0.80039
H	-2.12089	-1.99997	2.40188
C	-3.87283	-1.86814	-0.5994
H	-4.37904	-2.81321	-0.35736
H	-3.05107	-2.10342	-1.28434
H	-4.59904	-1.23874	-1.12152
C	-4.60434	-0.89517	1.60588
H	-5.21587	-1.80218	1.71793
H	-4.32744	-0.56662	2.61182
H	-5.23889	-0.12675	1.15471

C	-1.97761	1.39014	1.99258
C	-0.73325	2.30467	1.8132
H	-0.55657	2.84409	2.75494
H	0.16057	1.71134	1.59039
H	-0.85667	3.05043	1.02562
C	-1.65378	0.44833	3.18405
H	-1.38	1.06815	4.04966
H	-2.50507	-0.1682	3.4842
H	-0.803	-0.20701	2.96291
C	-3.20509	2.26147	2.36342
H	-3.00323	2.76651	3.31947
H	-4.11728	1.67162	2.49041
H	-3.402	3.04229	1.62249
C	-3.03951	1.43844	-1.05819
C	-2.78957	0.75298	-2.43105
H	-3.1663	1.4106	-3.22774
H	-3.29779	-0.20775	-2.52722
H	-1.72071	0.5787	-2.60555
C	-4.56055	1.67163	-0.86888
H	-4.91376	2.34696	-1.66196
H	-5.13921	0.74701	-0.95356
H	-4.79929	2.1399	0.09067
C	-2.3306	2.81905	-1.10931
H	-2.6841	3.35546	-2.0013
H	-2.56087	3.44542	-0.24285
H	-1.24155	2.7204	-1.18868
N	1.54503	-0.89484	0.96337
C	2.61848	-0.05094	0.90028
C	2.5406	1.01836	-0.13533

N	1.53532	0.88183	-1.05756
C	1.4251	1.81327	-2.0437
C	2.28515	2.91271	-2.14859
C	3.31752	3.08564	-1.1956
C	3.43018	2.11129	-0.18376
H	4.20168	2.21896	0.57098
C	4.25157	4.27287	-1.26394
H	5.01584	4.23556	-0.48141
H	4.76127	4.31715	-2.23493
H	3.69691	5.2133	-1.14914
H	2.15012	3.6255	-2.95693
H	0.62545	1.65784	-2.76076
C	3.7301	-0.21733	1.75204
C	3.7567	-1.26216	2.6978
C	2.63927	-2.12854	2.73441
C	1.5667	-1.91401	1.85892
H	0.70091	-2.56751	1.86368
H	2.60364	-2.95882	3.43367
C	4.926	-1.45246	3.63825
H	5.77206	-0.81133	3.37062
H	4.63676	-1.21123	4.67005
H	5.27227	-2.49318	3.63578
H	4.58189	0.45015	1.67726
S	-0.28804	-2.46527	-1.88066
C	1.23827	-2.75911	-2.70109
N	1.40767	-3.89041	-3.43736
H	0.64448	-4.55236	-3.48837
H	2.25567	-4.09467	-3.95292
N	2.26768	-1.87512	-2.63242

H	3.15494	-2.02562	-3.09796
H	2.12873	-1.02481	-2.09414

[Cu(Me2bpy)(^{t}Bu$_3$P)(tetrahydrothiophene)]$^{+}$

Cu	0	0	0
S	0	0	2.51083
C	1.73044	0	3.18662
H	1.75605	-0.71382	4.00636
H	2.41127	-0.32937	2.40774
C	2.00481	1.42629	3.66639
H	2.34309	2.04057	2.8302
H	2.79408	1.43278	4.41844
C	0.68767	1.97889	4.2168
H	0.43555	1.47907	5.15316
H	0.74733	3.04833	4.42117
C	-0.38694	1.69039	3.16916
H	-0.3482	2.40347	2.34947
H	-1.39214	1.67078	3.58014
P	-1.84491	-1.03854	-0.99599
C	-2.25042	-2.70824	-0.09025
C	-0.91188	-3.4042	0.24025
H	-0.28297	-2.7682	0.86283
H	-0.34729	-3.69607	-0.63887
H	-1.12356	-4.31276	0.80782
C	-2.91931	-2.42198	1.26897
H	-2.98411	-3.36327	1.81853
H	-3.93155	-2.04089	1.17354
H	-2.33699	-1.73347	1.8783
C	-3.14567	-3.68372	-0.87432
H	-2.67846	-4.04256	-1.7873

H	-4.10925	-3.25232	-1.13233
H	-3.33915	-4.5589	-0.24974
C	-3.40261	0.11498	-0.90421
C	-4.75461	-0.57201	-1.16601
H	-4.99856	-1.31848	-0.4154
H	-4.80127	-1.04488	-2.14334
H	-5.54363	0.18305	-1.13287
C	-3.42806	0.76456	0.49624
H	-4.26307	1.46711	0.53989
H	-2.51241	1.32413	0.68728
H	-3.55982	0.05219	1.30297
C	-3.24926	1.27618	-1.906
H	-4.03111	2.01035	-1.70111
H	-3.3683	0.96436	-2.93933
H	-2.2899	1.78183	-1.80648
C	-1.45329	-1.41393	-2.8614
C	-2.67161	-1.74564	-3.74076
H	-3.35953	-0.90966	-3.83424
H	-3.22927	-2.6059	-3.38088
H	-2.32173	-1.98343	-4.74811
C	-0.72134	-0.19047	-3.45523
H	-0.41473	-0.43391	-4.4748
H	0.17528	0.04992	-2.88628
H	-1.33816	0.69959	-3.50848
C	-0.45316	-2.58333	-2.95119
H	-0.88773	-3.54005	-2.67775
H	0.43129	-2.41082	-2.3398
H	-0.11988	-2.66753	-3.98747
N	0.831	1.94002	-0.54732

C	0.18134	3.10933	-0.54616
H	-0.85708	3.07805	-0.24503
C	0.76614	4.31004	-0.90737
H	0.18248	5.21974	-0.88313
C	2.10494	4.32508	-1.30217
C	2.77593	3.10588	-1.2987
H	3.81309	3.08403	-1.59441
C	2.12439	1.93063	-0.919
C	2.81222	0.60781	-0.89555
N	2.07828	-0.44107	-0.48117
C	2.66232	-1.64391	-0.42995
C	3.98039	-1.86814	-0.785
C	4.7594	-0.79805	-1.22918
C	4.14673	0.45056	-1.27569
H	4.72227	1.29839	-1.61264
C	6.19083	-0.9925	-1.64251
H	6.25154	-1.63136	-2.52509
H	6.76038	-1.48227	-0.8522
H	6.67416	-0.0466	-1.87673
H	4.39122	-2.86593	-0.71857
H	2.04049	-2.46077	-0.08966
C	2.78264	5.59961	-1.71939
H	3.84896	5.45484	-1.8784
H	2.65012	6.37616	-0.96577
H	2.3508	5.97618	-2.6482

$[Cu(Me_4phen)(^tBu_3P)(thiourea)]^+$

Cu	-0.42633	-0.03222	-0.67025
P	-2.46165	0.04626	0.59642
C	-3.71733	-1.36776	-0.02746

C	-2.86976	-2.6355	-0.33324
H	-3.53363	-3.41261	-0.73837
H	-2.10631	-2.41938	-1.09072
H	-2.3807	-3.04783	0.55214
C	-4.36525	-0.9416	-1.37288
H	-4.9098 -	1.80608	-1.77832
H	-3.61882	-0.64603	-2.11812
H	-5.08902	-0.13042	-1.25731
C	-4.84478	-1.72318	0.97492
H	-5.50277	-2.47253	0.51119
H	-4.46179	-2.1599	1.90195
H	-5.4646	-0.85897	1.23255
C	-2.0534	-0.27315	2.51874
C	-0.77427	0.53868	2.86931
H	-0.48929	0.31252	3.90701
H	0.06136	0.25649	2.21925
H	-0.91682	1.61823	2.79431
C	-1.68569	-1.76784	2.72431
H	-1.29345	-1.88901	3.74414
H	-2.54519	-2.4366	2.62677
H	-0.90402	-2.09183	2.02696
C	-3.18634	0.10417	3.50697
H	-2.86678	-0.15699	4.52667
H	-4.11666	-0.43536	3.30738
H	-3.4041	1.17667	3.50301
C	-3.36047	1.81328	0.42557
C	-3.274	2.23405	-1.0682
H	-3.66552	3.25667	-1.16993
H	-3.85704	1.59062	-1.72892

H	-2.23821	2.22452	-1.42844
C	-4.83947	1.84312	0.8875
H	-5.2175	2.87162	0.79218
H	-5.48232	1.2062	0.27312
H	-4.95977	1.54553	1.93336
C	-2.56802	2.8768	1.23309
H	-2.96041	3.86985	0.97185
H	-2.68036	2.75929	2.31462
H	-1.49906	2.8652	0.98875
N	1.15492	-1.37478	-0.17907
C	2.27486	-0.73812	0.29528
C	2.29342	0.71044	0.24788
N	1.20805	1.34391	-0.31394
C	1.21603	2.68878	-0.36734
C	2.26849	3.5033	0.13206
C	3.38905	2.8703	0.70856
C	3.40794	1.4352	0.76055
C	4.51341	0.6806	1.30547
C	4.50827	-0.69468	1.3231
C	3.39079	-1.45616	0.81344
C	3.355	-2.89173	0.81226
C	2.21074	-3.5281	0.29102
C	1.14261	-2.71713	-0.1839
H	0.24679	-3.18759	-0.57797
C	2.05951	-5.03517	0.22226
H	2.85168	-5.49565	-0.38171
H	2.10017	-5.4938	1.2186
H	1.10014	-5.30992	-0.2284
C	4.52738	-3.67927	1.36058

H	5.45114	-3.45133	0.81227
H	4.70845	-3.43647	2.41615
H	4.36297	-4.75583	1.29478
H	5.36225	-1.22303	1.7339
H	5.36952	1.2134	1.70559
C	4.55503	3.66237	1.26304
H	5.48728	3.41893	0.7359
H	4.39808	4.73838	1.17492
H	4.71617	3.43703	2.32548
C	2.13563	5.00948	0.01785
H	2.95528	5.44847	-0.56501
H	1.1969	5.28176	-0.47581
H	2.14178	5.49196	1.00364
H	0.35065	3.15451	-0.83031
S	-0.95517	-0.31942	-3.10195
C	0.49981	-0.04741	-4.04741
N	0.50845	-0.32507	-5.37968
H	-0.33246	-0.69791	-5.80034
H	1.30993	-0.15631	-5.97605
N	1.63418	0.45027	-3.48833
H	2.48527	0.60838	-4.01468
H	1.61722	0.67357	-2.49876

[Cu(Me_4phen)($^tBu_3$P)(benzenethiolate)]

Cu	-0.54223	-0.15616	0.40702
P	-2.86905	-0.06001	-0.20966
C	-3.97044	0.46605	1.36312
C	-3.18937	1.5832	2.11339
H	-3.7373	1.8376	3.0331
H	-2.19251	1.22882	2.40198

H	-3.08528	2.50015	1.52703
C	-4.061	-0.72975	2.35012
H	-4.49388	-0.36317	3.29276
H	-3.07514	-1.14642	2.58155
H	-4.71268	-1.52943	1.98495
C	-5.40502	0.95427	1.03778
H	-5.92822	1.16356	1.98328
H	-5.41198	1.87896	0.45195
H	-5.98923	0.20207	0.49775
C	-3.19629	1.26074	-1.67072
C	-2.03711	1.10615	-2.69686
H	-2.10836	1.91715	-3.4377
H	-1.06314	1.17712	-2.19984
H	-2.07192	0.15894	-3.23959
C	-3.07156	2.69744	-1.09486
H	-3.08569	3.40976	-1.93333
H	-3.89593	2.96289	-0.42706
H	-2.12541	2.83408	-0.55975
C	-4.5552	1.1372	-2.40425
H	-4.63151	1.94223	-3.15181
H	-5.40682	1.23544	-1.72405
H	-4.6527	0.18798	-2.94051
C	-3.50173	-1.84147	-0.83784
C	-2.88633	-2.91253	0.1076
H	-3.05115	-3.90768	-0.33363
H	-3.33861	-2.91193	1.10076
H	-1.81053	-2.76207	0.25115
C	-5.0391	-2.02783	-0.89043
H	-5.26053	-3.03473	-1.27693

H	-5.49614	-1.95321	0.10058
H	-5.52971	-1.30514	-1.54972
C	-2.91933	-2.10976	-2.25227
H	-3.10513	-3.1627	-2.5108
H	-3.38933	-1.49701	-3.02759
H	-1.83643	-1.9418	-2.28335
N	0.66386	1.59919	0.14932
C	1.80141	1.3541	-0.57922
C	1.961	0.02986	-1.14086
N	0.95759	-0.87853	-0.91438
C	1.12489	-2.12996	-1.36921
C	2.26533	-2.57307	-2.09182
C	3.29215	-1.64674	-2.35853
C	3.14128	-0.30985	-1.86422
C	4.14163	0.7169	-2.04518
C	3.98729	1.97786	-1.51778
C	2.81732	2.34015	-0.75129
C	2.64587	3.62716	-0.14339
C	1.48058	3.85493	0.61566
C	0.52889	2.80513	0.72431
H	-0.36845	2.95327	1.31852
C	1.19761	5.16377	1.32919
H	1.97429	5.39876	2.06876
H	1.14335	6.00859	0.6296
H	0.24189	5.11297	1.86182
C	3.71214	4.69245	-0.30934
H	4.66717	4.36791	0.12635
H	3.89647	4.90939	-1.3701
H	3.43032	5.62933	0.17538

H	4.76951	2.71555	-1.66851
H	5.04417	0.48202	-2.60101
C	4.54273	-2.0371	-3.12192
H	5.43751	-1.92904	-2.49367
H	4.50336	-3.07339	-3.4633
H	4.68587	-1.40093	-4.00572
C	2.32316	-4.02425	-2.52977
H	3.18827	-4.54217	-2.09541
H	1.42416	-4.55981	-2.20651
H	2.39421	-4.12181	-3.62141
H	0.32857	-2.83237	-1.14039
S	-0.25924	-1.19233	2.54516
C	1.53325	-1.53586	2.70536
C	1.98461	-2.85924	2.94534
H	1.24931	-3.65763	3.01171
C	3.35385	-3.1428	3.10943
C	4.3133	-2.11224	3.03287
C	3.87755	-0.79252	2.79467
C	2.5083	-0.50851	2.63344
H	2.1799	0.51541	2.47358
H	4.60284	0.0187	2.74256
H	5.37121	-2.33066	3.16437
H	3.6695	-4.16753	3.30112

$[Cu(Me_4phen(^tBu_3P)(Ph_3P=S)]^+$

Cu	1.11606	-0.39704	-0.0364
P	2.91275	-1.99112	-0.01232
C	2.70573	-3.3875	-1.41794
C	2.14424	-2.689	-2.68938
H	1.96899	-3.45366	-3.46014

H	1.18477	-2.2016	-2.47747
H	2.82949	-1.9493	-3.10998
C	1.634	-4.41927	-0.97506
H	1.41062	-5.06899	-1.83335
H	0.69586	-3.94028	-0.67399
H	1.9797	-5.06501	-0.16306
C	4.0075	-4.15074	-1.7714
H	3.76705	-4.93239	-2.50677
H	4.76544	-3.50423	-2.22303
H	4.45055	-4.64378	-0.90096
C	4.61655	-1.00962	-0.34746
C	4.56612	0.32098	0.45616
H	5.45099	0.92014	0.19592
H	3.67415	0.90436	0.20213
H	4.57836	0.17085	1.53744
C	4.68588	-0.6096	-1.84612
H	5.53734	0.07238	-1.98226
H	4.84739	-1.46463	-2.50792
H	3.78178	-0.07945	-2.16628
C	5.90765	-1.78303	0.02196
H	6.77746	-1.17195	-0.26129
H	5.98986	-2.73692	-0.50615
H	5.98678	-1.97627	1.09624
C	3.04881	-2.89225	1.75634
C	1.60905	-3.27606	2.2001
H	1.65606	-3.69797	3.21501
H	1.14291	-4.02033	1.55231
H	0.95134	-2.39843	2.22162
C	3.9507	-4.15286	1.78774

H	3.99977	-4.52568	2.82146
H	3.55504	-4.96528	1.17115
H	4.9749	-3.94478	1.46476
C	3.57793	-1.87704	2.80525
H	3.45598	-2.31761	3.80511
H	4.64068	-1.65223	2.67853
H	3.01569	-0.93624	2.7822
N	1.17709	1.31435	-1.30619
C	1.15131	2.48849	-0.5968
C	0.99834	2.40159	0.84221
N	0.89135	1.15101	1.39815
C	0.72092	1.05966	2.72629
C	0.6591	2.17632	3.60464
C	0.78695	3.46672	3.05487
C	0.95666	3.58496	1.63445
C	1.08912	4.85662	0.96143
C	1.23456	4.93882	-0.40357
C	1.26129	3.75764	-1.23486
C	1.39233	3.80898	-2.66364
C	1.39574	2.59385	-3.37638
C	1.2874	1.38027	-2.64202
H	1.29541	0.43161	-3.17156
C	1.52163	2.51677	-4.88595
H	0.70744	3.05139	-5.39194
H	2.46569	2.95254	-5.23751
H	1.49257	1.47593	-5.22505
C	1.52522	5.14628	-3.36411
H	0.65889	5.79057	-3.16289
H	2.4163	5.68636	-3.01726

H	1.60891	5.03486	-4.44641
H	1.33193	5.91434	-0.86896
H	1.07364	5.76878	1.54915
C	0.75011	4.71042	3.91975
H	-0.07213	5.37617	3.62509
H	0.61743	4.47018	4.97588
H	1.68118	5.28489	3.82555
C	0.46709	1.92122	5.08733
H	-0.44595	2.39724	5.46752
H	0.38811	0.84787	5.28999
H	1.30703	2.30772	5.6788
H	0.6286	0.05616	3.13222
S	-0.96926	-1.74973	-0.38136
P	-2.93627	-0.84911	-0.18053
C	-4.04036	-1.35837	-1.60255
C	-3.79197	-2.58307	-2.25318
C	-4.6435	-3.00814	-3.28907
C	-5.73812	-2.21194	-3.67795
C	-5.97918	-0.98449	-3.03115
C	-5.13347	-0.55499	-1.99192
H	-5.32039	0.40121	-1.50965
H	-6.81904	-0.36425	-3.33293
H	-6.39391	-2.54182	-4.47958
H	-4.45172	-3.9534	-3.78962
H	-2.93625	-3.18673	-1.96236
C	-3.77318	-1.4144	1.39725
C	-3.01104	-2.04587	2.39832
C	-3.63449	-2.47987	3.58371
C	-5.01617	-2.28545	3.7682

C	-5.77814	-1.65867	2.7621
C	-5.16063	-1.22356	1.57583
H	-5.76427	-0.75825	0.80136
H	-6.84728	-1.51728	2.89557
H	-5.49809	-2.62744	4.68052
H	-3.04649	-2.97599	4.35135
H	-1.94958	-2.21551	2.23702
C	-2.93931	1.0161	-0.16256
C	-2.60566	1.70901	-1.34629
C	-2.59913	3.11383	-1.35695
C	-2.91625	3.83269	-0.18689
C	-3.23682	3.14029	0.99524
C	-3.24722	1.73233	1.01085
H	-3.50479	1.20662	1.92577
H	-3.48721	3.68889	1.89955
H	-2.918	4.91969	-0.19916
H	-2.35508	3.64377	-2.27396
H	-2.35947	1.16053	-2.25227

$[Cu(Me_2bpy)(^tBu_3P)(Ph_3P{=}S)]^+$

Cu	1.17983	-0.11082	-0.0741
P	3.09799	-1.46965	-0.09278
C	3.00846	-2.79101	-1.51365
C	2.40608	-2.10689	-2.7607
H	2.29819	-2.8567	-3.54753
H	1.41488	-1.70595	-2.55275
H	3.02669	-1.31031	-3.15746
C	2.02194	-3.91142	-1.12824
H	1.86056	-4.53615	-2.00924
H	1.05137	-3.52455	-0.82458

H	2.40258	-4.56024	-0.34484
C	4.34927	-3.44303	-1.89538
H	4.16289	-4.19789	-2.66294
H	5.05866	-2.73432	-2.31375
H	4.82472	-3.94597	-1.05731
C	4.67367	-0.36411	-0.37243
C	4.51863	0.92165	0.46869
H	5.35897	1.58271	0.24507
H	3.60233	1.45142	0.2162
H	4.52406	0.74373	1.53815
C	4.72054	0.10181	-1.84108
H	5.50808	0.85238	-1.93539
H	4.95739	-0.69775	-2.53635
H	3.78736	0.57011	-2.14938
C	6.01978	-1.02547	-0.028
H	6.82468	-0.32848	-0.27387
H	6.19856	-1.9372	-0.59122
H	6.11314	-1.25576	1.02997
C	3.28636	-2.39349	1.60457
C	1.89044	-2.90174	2.02368
H	1.96633	-3.34227	3.02042
H	1.48695	-3.65947	1.36175
H	1.17027	-2.08581	2.0684
C	4.27452	-3.5731	1.61862
H	4.32325	-3.97655	2.63304
H	3.96438	-4.38659	0.9688
H	5.28286	-3.28021	1.33897
C	3.71597	-1.38952	2.69225
H	3.6253	-1.87872	3.66437

H	4.74912	-1.07037	2.59177
H	3.08052	-0.50535	2.70888
N	1.04183	1.71079	-1.27536
C	0.94629	2.85554	-0.57849
C	0.80354	2.71643	0.89889
N	0.80292	1.4615	1.38367
C	0.64432	1.291	2.69999
C	0.49391	2.33646	3.59371
C	0.50985	3.64817	3.11719
C	0.66343	3.8182	1.74501
H	0.66866	4.81906	1.34239
C	0.37806	4.82047	4.04876
H	0.22478	5.75038	3.50512
H	-0.45579	4.68235	4.73699
H	1.27972	4.9307	4.65409
H	0.36892	2.12813	4.6472
H	0.63843	0.26802	3.05057
C	0.96797	4.09616	-1.21898
C	1.0774	4.17878	-2.60359
C	1.14838	2.9749	-3.30651
C	1.12937	1.78086	-2.60674
H	1.18723	0.83563	-3.12949
H	1.22307	2.96386	-4.38511
C	1.12912	5.503	-3.3134
H	0.85871	6.32403	-2.65256
H	2.13532	5.69478	-3.69084
H	0.45709	5.5153	-4.17137
H	0.89856	5.00846	-0.64722
S	-0.85108	-1.45184	-0.59108

P	-2.71576	-0.81775	-0.17723
C	-3.93079	-1.61607	-1.28625
C	-3.70007	-2.92672	-1.71202
C	-4.63652	-3.57642	-2.50572
C	-5.80642	-2.92438	-2.88448
C	-6.0382	-1.6182	-2.46824
C	-5.1052	-0.96336	-1.6711
H	-5.29367	0.05534	-1.36469
H	-6.94166	-1.10471	-2.76613
H	-6.53179	-3.43097	-3.50572
H	-4.45025	-4.58997	-2.83211
H	-2.7854	-3.42921	-1.43226
C	-3.24709	-1.23793	1.52452
C	-2.30505	-1.64878	2.46656
C	-2.70428	-1.98202	3.75687
C	-4.04618	-1.90937	4.11297
C	-4.99243	-1.50779	3.174
C	-4.5977	-1.17626	1.88416
H	-5.34645	-0.88473	1.16163
H	-6.03861	-1.46236	3.44222
H	-4.35713	-2.17543	5.11365
H	-1.96897	-2.30943	4.47877
H	-1.26796	-1.72801	2.17561
C	-2.95034	0.98159	-0.38626
C	-2.76509	1.53358	-1.65868
C	-2.94724	2.89388	-1.86267
C	-3.30449	3.71916	-0.79827
C	-3.47264	3.17893	0.47067
C	-3.29743	1.81323	0.6787

H	-3.44049	1.40284	1.6671
H	-3.75152	3.8143	1.29976
H	-3.45635	4.77731	-0.96123
H	-2.81792	3.30945	-2.85223
H	-2.4861	0.89921	-2.48849

Syn-[[Cu(Me_4phen)(^{t}Bu_3P)]$_2$$N_3$]$BF_4$

Cu	-3.08942	-0.4974	-0.03074
P	-4.00113	-2.89511	-0.20546
C	-2.93975	-4.04031	0.99282
C	-2.71369	-3.25995	2.31432
H	-2.08378	-3.85912	2.96592
H	-2.19998	-2.32578	2.12545
H	-3.6267	-3.05292	2.85006
C	-1.52779	-4.25757	0.39485
H	-0.91003	-4.72936	1.1535
H	-1.0595	-3.32155	0.1234
H	-1.53371	-4.91425	-0.46262
C	-3.55186	-5.42168	1.31542
H	-2.85097	-5.97769	1.93232
H	-4.47612	-5.34719	1.87036
H	-3.73924	-6.0087	0.4273
C	-5.89676	-2.99767	0.31571
C	-6.62811	-1.78025	-0.30842
H	-7.65312	-1.76938	0.0511
H	-6.16042	-0.84959	-0.01313
H	-6.66508	-1.81054	-1.38518
C	-6.02738	-2.82045	1.84829
H	-7.08006	-2.71039	2.0897
H	-5.65904	-3.66937	2.40405

H	-5.51844	-1.92936	2.19406
C	-6.63827	-4.29263	-0.08468
H	-7.6528	-4.24914	0.30229
H	-6.17265	-5.17925	0.32186
H	-6.71106	-4.41212	-1.15603
C	-3.81071	-3.55191	-2.05096
C	-2.44507	-3.0559	-2.59435
H	-2.37338	-3.32451	-3.64487
H	-1.60048	-3.49178	-2.08788
H	-2.35233	-1.98028	-2.51304
C	-3.89773	-5.08392	-2.23226
H	-3.82999	-5.31517	-3.29206
H	-3.08872	-5.60336	-1.73971
H	-4.83029	-5.49225	-1.86945
C	-4.88718	-2.8986	-2.95183
H	-4.64897	-3.12485	-3.98667
H	-5.8801	-3.27777	-2.76305
H	-4.90423	-1.82087	-2.84555
N	-3.94183	0.9552	1.45708
C	-4.48171	2.06503	0.89985
C	-4.46586	2.18836	-0.54602
N	-3.9097	1.1891	-1.27167
C	-3.86215	1.29771	-2.58241
C	-4.37319	2.40043	-3.30492
C	-4.9591	3.43188	-2.58509
C	-5.00443	3.32735	-1.16238
C	-5.57843	4.35292	-0.32359
C	-5.59199	4.23843	1.02428
C	-5.03373	3.08467	1.68904

C	-5.01745	2.94649	3.10953
C	-4.44634	1.80599	3.65613
C	-3.9212	0.83931	2.76794
H	-3.47328	-0.0501	3.16164
C	-4.35781	1.54473	5.1458
H	-3.78891	2.31429	5.65442
H	-5.33877	1.50175	5.60466
H	-3.86784	0.59898	5.33631
C	-5.61218	4.03652	3.97626
H	-5.10315	4.98024	3.81606
H	-6.66106	4.18533	3.74644
H	-5.53899	3.80042	5.02506
H	-6.02409	5.02221	1.61011
H	-6.00016	5.22498	-0.7773
C	-5.53964	4.6531	-3.26673
H	-5.0363	5.55581	-2.93941
H	-5.4453	4.59755	-4.33869
H	-6.5932	4.76166	-3.03584
C	-4.25372	2.39501	-4.81517
H	-3.67715	3.2394	-5.1745
H	-3.75701	1.495	-5.15297
H	-5.22509	2.43048	-5.29458
H	-3.40154	0.48948	-3.11275
N	-0.96262	-0.51034	0.00733
N	0.07735	0.0316	0.01566
N	1.11742	0.57366	0.0253
Cu	3.24144	0.56737	-0.00163
P	4.12696	2.97976	-0.13479
C	5.92543	3.1635	0.53911

C	6.74181	1.87629	0.29059
H	7.69372	1.94424	0.80891
H	6.95227	1.7292	-0.76172
H	6.22216	0.99938	0.65272
C	6.75896	4.39979	0.14065
H	7.66415	4.41894	0.74039
H	7.06549	4.36456	-0.89625
H	6.23971	5.33186	0.30553
H	5.75734	3.22538	1.60859
C	4.04162	3.63621	-1.96573
C	2.69309	3.17952	-2.57658
H	2.55044	2.11065	-2.47895
H	1.84322	3.66335	-2.11977
H	2.68606	3.42897	-3.63415
C	5.16417	2.92918	-2.76496
H	5.03793	3.1529	-3.81997
H	6.15143	3.26245	-2.47955
H	5.123	1.85258	-2.64598
C	4.17653	5.1627	-2.15086
H	5.10678	5.5483	-1.75922
H	4.14833	5.39258	-3.2127
H	3.36261	5.70096	-1.68381
C	3.0747	4.08634	1.07692
C	2.93874	3.26912	2.38672
H	2.38688	3.85558	3.11561
H	2.39461	2.34914	2.21513
H	3.90064	3.02789	2.82661
C	3.69511	5.45821	1.42038
H	3.0145	5.99575	2.07489

H	4.63537	5.35911	1.9476
H	3.8585	6.07265	0.54586
C	1.65061	4.30029	0.51641
H	1.03416	4.74291	1.29392
H	1.642	4.9807	-0.3252
H	1.19228	3.36651	0.21952
N	4.07432	-1.10298	-1.24855
C	4.64478	-2.09835	-0.52859
C	4.66972	-1.97774	0.91738
N	4.12224	-0.8747	1.48076
C	4.11582	-0.75823	2.79172
C	4.66134	-1.71915	3.67398
C	5.23764	-2.85396	3.1211
C	5.2407	-2.99161	1.70041
C	5.805	-4.13881	1.0295
C	5.78122	-4.25172	-0.31836
C	5.19046	-3.23065	-1.15099
C	5.13658	-3.33277	-2.57357
C	4.53606	-2.30554	-3.28739
C	4.01926	-1.2093	-2.55923
H	3.54764	-0.40428	-3.08482
C	4.40667	-2.29813	-4.79682
H	5.37519	-2.32349	-5.28261
H	3.8357	-3.14715	-5.15416
H	3.89938	-1.40211	-5.12944
C	5.72442	-4.54688	-3.26163
H	6.78071	-4.6451	-3.0387
H	5.23271	-5.45521	-2.93219
H	5.62158	-4.49049	-4.33276

H	6.20801	-5.11883	-0.77679
H	6.2502	-4.91877	1.61059
C	5.8525	-3.93809	3.98114
H	6.90074	-4.07517	3.74129
H	5.78657	-3.70375	5.03081
H	5.35236	-4.88719	3.82485
C	4.58746	-1.45832	5.16452
H	4.09166	-0.5167	5.36041
H	4.03086	-2.23255	5.67965
H	5.57313	-1.40694	5.61226
H	3.66371	0.12677	3.19028

[Cu(Me_4phen)(^{t}Bu_3P)](μ-S)[MoO_2(OSiPh_2^{t}Bu)]

Cu	2.32251	-0.17939	0.14182
P	3.86175	-1.95336	-0.28112
C	3.01966	-3.40917	-1.34432
C	2.13056	-2.74111	-2.43065
H	1.58578	-3.5294	-2.96977
H	1.38101	-2.08172	-1.98222
H	2.70433	-2.17206	-3.16623
C	2.05825	-4.21322	-0.42751
H	1.4431	-4.86563	-1.06231
H	1.37144	-3.55942	0.12006
H	2.59051	-4.85466	0.28247
C	4.01565	-4.38618	-2.01896
H	3.44054	-5.1841	-2.51166
H	4.62246	-3.90006	-2.79061
H	4.6896	-4.8625	-1.29992
C	5.41752	-1.24103	-1.30262
C	5.78527	0.14307	-0.69615

H	6.56346	0.60648	-1.32135
H	4.91491	0.80924	-0.68301
H	6.17534	0.07538	0.3215
C	4.98057	-0.96572	-2.76707
H	5.78406	-0.40701	-3.26938
H	4.81253	-1.88246	-3.33913
H	4.07259	-0.35298	-2.80931
C	6.67495	-2.14721	-1.32187
H	7.44271	-1.6757	-1.9545
H	6.46914	-3.13898	-1.73597
H	7.11097	-2.27582	-0.32606
C	4.54199	-2.72782	1.42207
C	3.32873	-2.86773	2.38412
H	3.69821	-3.17504	3.37443
H	2.60445	-3.61265	2.05247
H	2.78678	-1.92166	2.49345
C	5.25402	-4.09842	1.29298
H	5.62685	-4.39682	2.28487
H	4.57398	-4.88529	0.95354
H	6.11142	-4.06612	0.61351
C	5.51945	-1.72132	2.08595
H	5.73125	-2.06749	3.10821
H	6.47658	-1.64871	1.56106
H	5.08321	-0.71787	2.15437
N	1.80353	1.34572	-1.2049
C	1.88684	2.59991	-0.65259
C	2.38156	2.70457	0.70486
N	2.71972	1.54148	1.35027
C	3.13039	1.61816	2.62386

C	3.25703	2.83357	3.35233
C	2.93072	4.03837	2.70262
C	2.47319	3.97571	1.34379
C	2.07853	5.14265	0.59039
C	1.60045	5.04058	-0.69566
C	1.47172	3.76387	-1.35861
C	0.92598	3.61669	-2.67948
C	0.81108	2.32081	-3.21041
C	1.27723	1.22294	-2.43218
H	1.18405	0.21694	-2.82059
C	0.19904	2.02398	-4.56512
H	-0.8242	2.41445	-4.63674
H	0.78093	2.46573	-5.38571
H	0.14424	0.94366	-4.72903
C	0.46778	4.83978	-3.44908
H	-0.3686	5.33716	-2.93864
H	1.27635	5.57666	-3.54445
H	0.13409	4.58275	-4.45621
H	1.29868	5.94051	-1.22246
H	2.14873	6.12082	1.05555
C	3.03243	5.37813	3.40481
H	2.04989	5.86527	3.46799
H	3.4169	5.27762	4.42164
H	3.69935	6.06157	2.86238
C	3.7292	2.76723	4.79263
H	2.97931	3.17241	5.48455
H	3.9218	1.7302	5.08794
H	4.6575	3.33351	4.94525
H	3.36393	0.67664	3.11256

S	0.15043	-0.96079	1.11584
Mo	-1.447	-1.37471	-0.4601
O	-3.11068	-0.69846	0.10681
Si	-4.63469	-0.13357	0.60707
C	-5.7334	-1.66328	0.83501
C	-5.17505	-2.95655	0.67846
C	-5.96248	-4.11203	0.845
C	-7.32706	-3.99931	1.17169
C	-7.90055	-2.72242	1.32658
C	-7.11032	-1.56992	1.15796
H	-7.58462	-0.59747	1.27771
H	-8.95546	-2.62398	1.57432
H	-7.93578	-4.89198	1.30003
H	-5.50974	-5.09261	0.71636
H	-4.12562	-3.06666	0.41739
C	-4.34549	0.82148	2.25961
C	-5.67753	1.37751	2.83346
H	-5.47442	1.91605	3.77196
H	-6.15782	2.08798	2.14698
H	-6.39198	0.57648	3.06576
C	-3.37149	2.00427	2.00011
H	-3.19765	2.55369	2.93876
H	-2.39966	1.6497	1.635
H	-3.77664	2.71346	1.26542
C	-3.7089	-0.14693	3.29523
H	-3.5268	0.38842	4.24027
H	-4.36621	-0.99926	3.5139
H	-2.74742	-0.53914	2.94183
C	-5.26049	1.00202	-0.7809

C	-4.42385	1.27884	-1.89114
C	-4.85785	2.11657	-2.93667
C	-6.13888	2.69888	-2.89492
C	-6.98518	2.43333	-1.80123
C	-6.54866	1.59266	-0.75995
H	-7.23056	1.39812	0.06561
H	-7.97997	2.87221	-1.76144
H	-6.47574	3.34404	-3.70385
H	-4.20005	2.30629	-3.78245
H	-3.43426	0.83197	-1.9458
O	-1.55298	-3.10373	-0.69383
O	-0.96939	-0.63842	-1.98056

Characterization:

[Cu(Me$_4$phen)(^{i}Pr$_3$P)]PF6

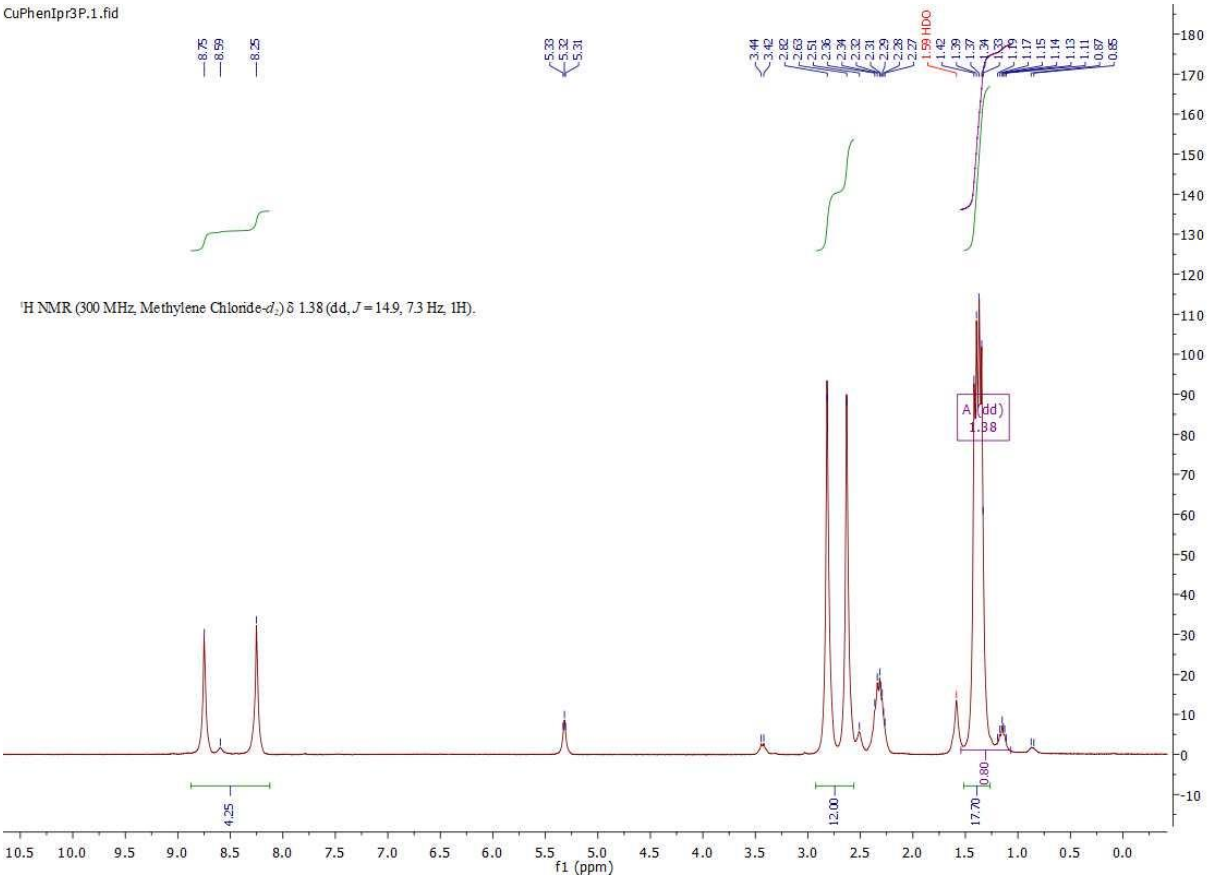

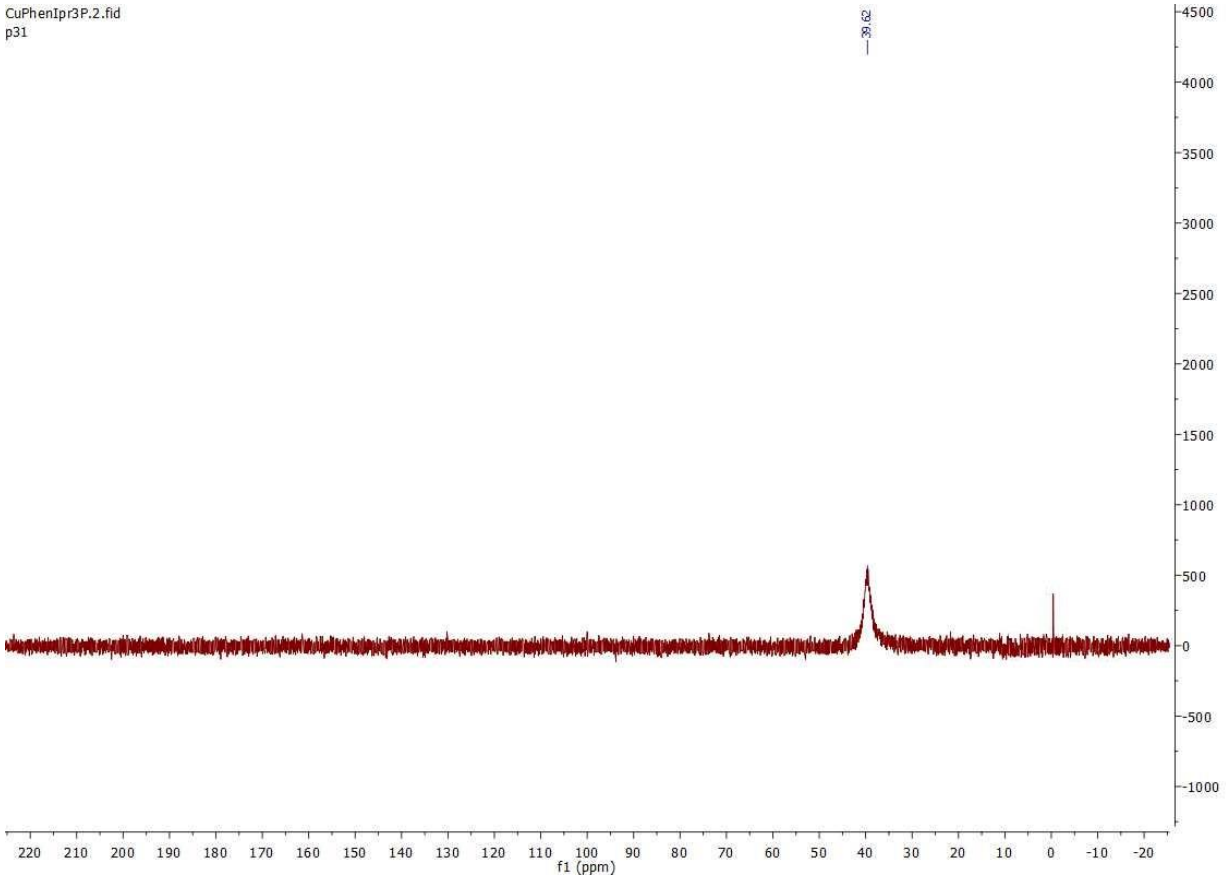

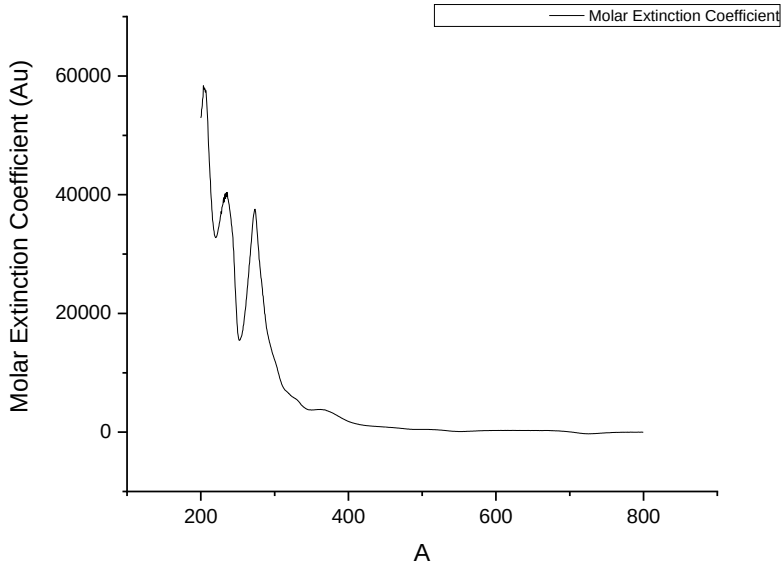

[Cu(Me$_4$phen)(^{t}Bu$_3$P)(MeCN)]PF$_6$

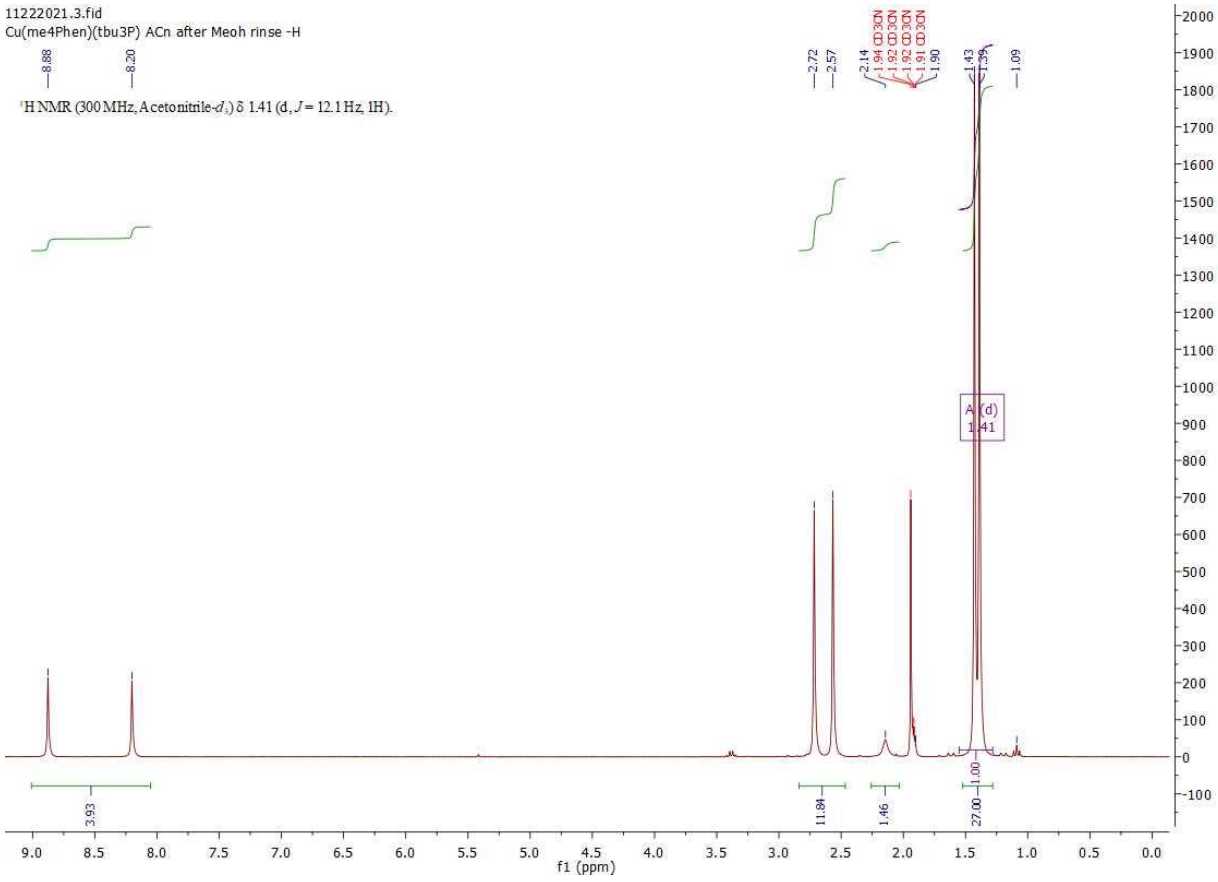
11222021.3.fid
Cu(me4Phen)(tbu3P) ACn after Meoh rinse -H
^{1}H NMR (300 MHz, Acetonitrile-d_3) δ 1.41 (d, J = 12.1 Hz, 1H).
8.88
8.20
2.72
2.57
2.14
1.94 CD3CN
1.92 CD3CN
1.91 CD3CN
1.90
1.43
1.39
1.09
A (d)
1.41
3.93
11.84
1.46
27.00
1.00
f1 (ppm)

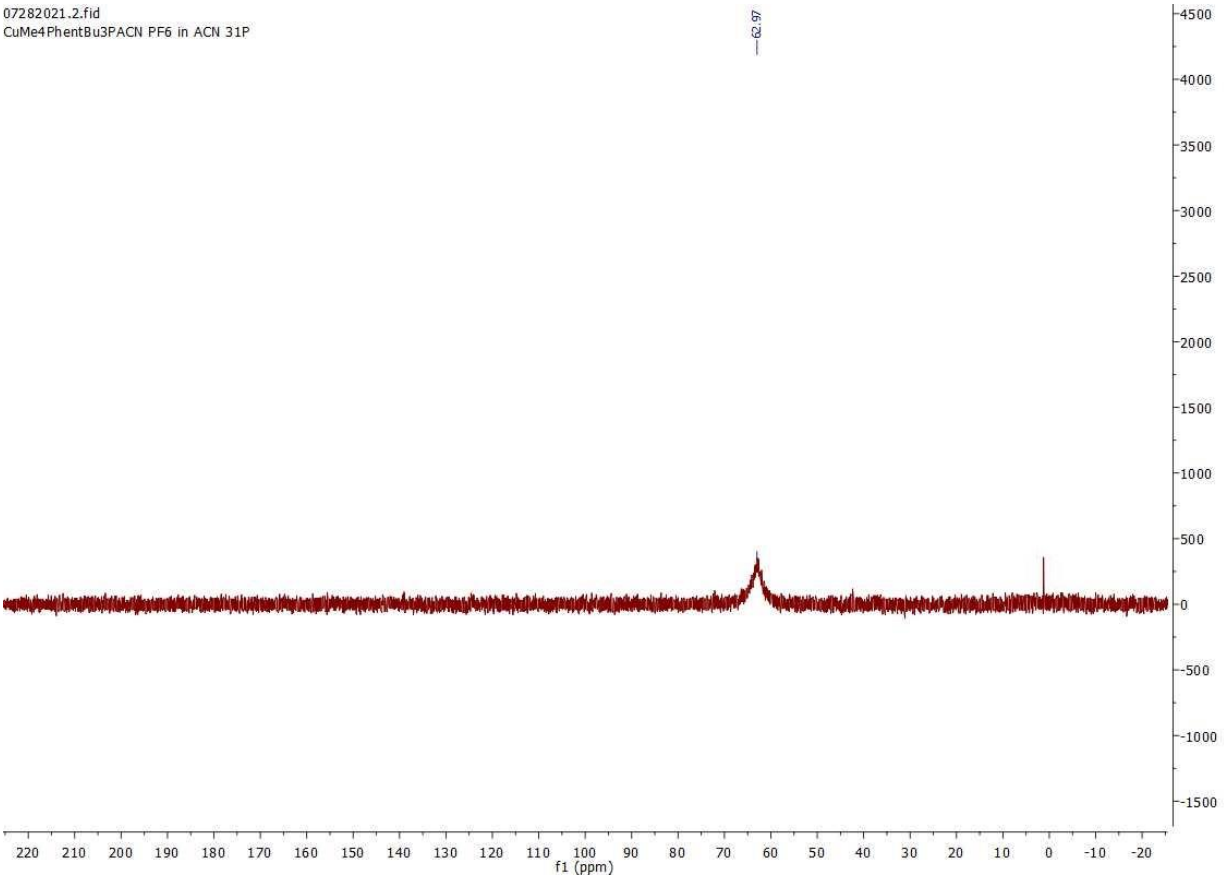

$[Cu(Me_2bpy)(^tBu_3P)(MeCN)]PF_6$

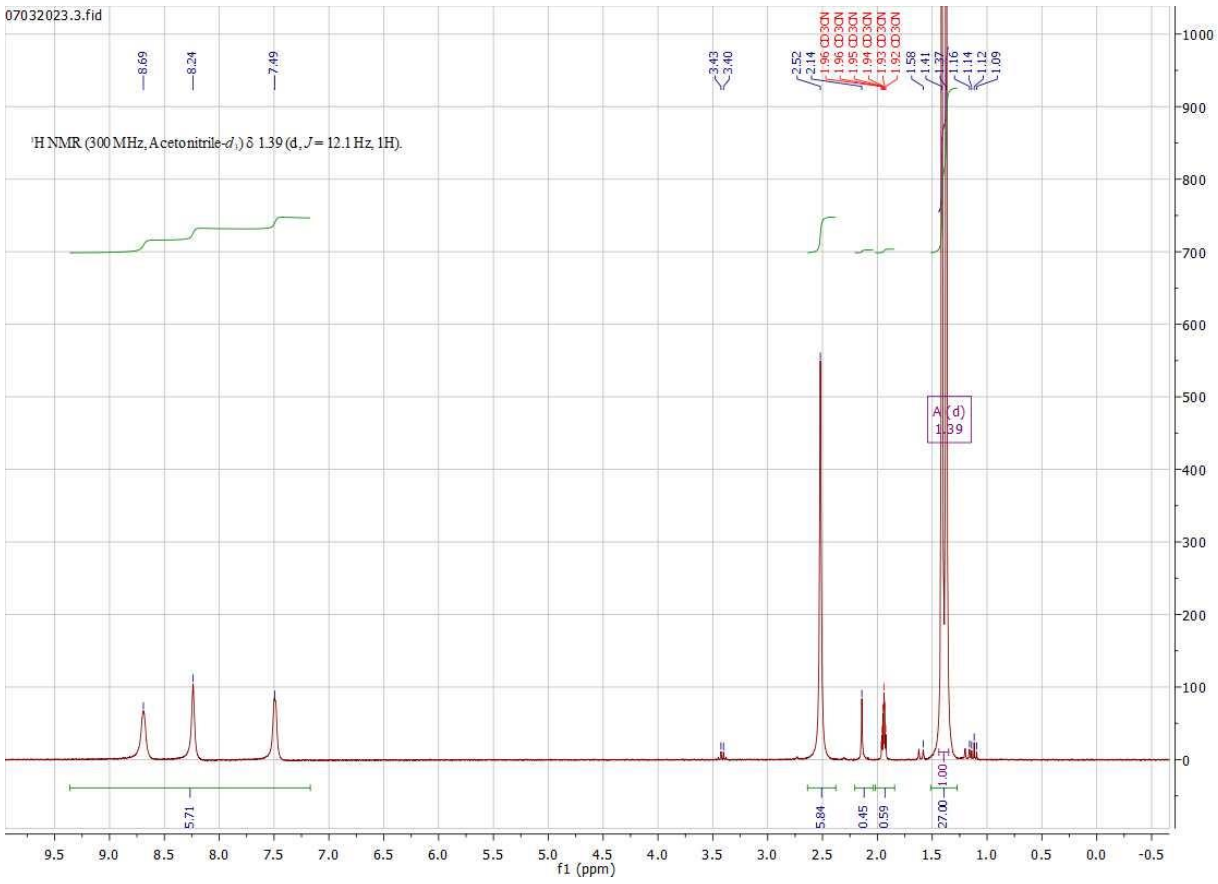
07032023.3.fid
^{1}H NMR (300 MHz, Acetonitrile-d_3) δ 1.39 (d, J = 12.1 Hz, 1H).
8.69
8.24
7.49
3.43
3.40
2.52
2.14
1.96 CD3CN
1.96 CD3CN
1.95 CD3CN
1.94 CD3CN
1.93 CD3CN
1.92 CD3CN
1.58
1.41
1.37
1.16
1.14
1.12
1.09
A (d)
1.39
5.71
5.84
0.45
0.59
1.00
27.00
f1 (ppm)

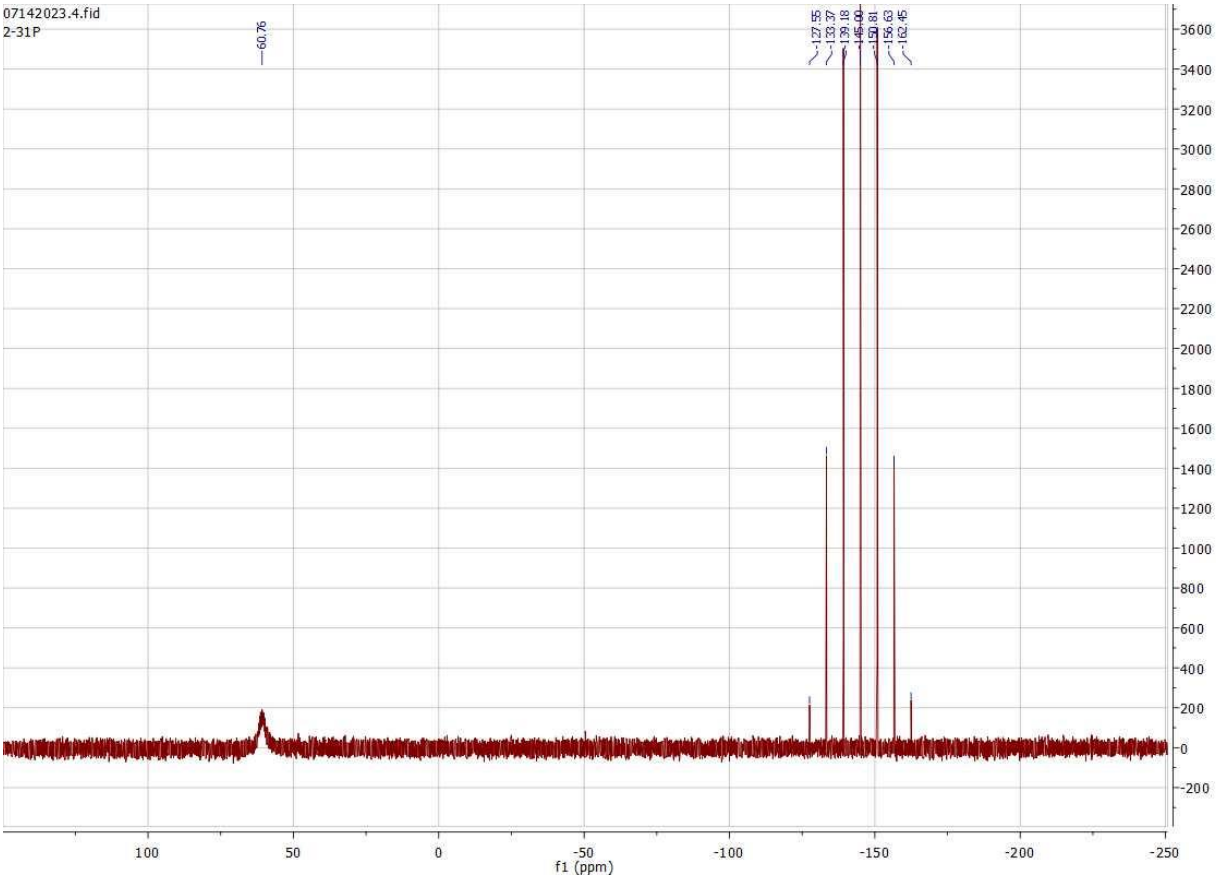

[Cu(Me$_4$phen)(^{t}Bu$_3$P)]PF$_6$

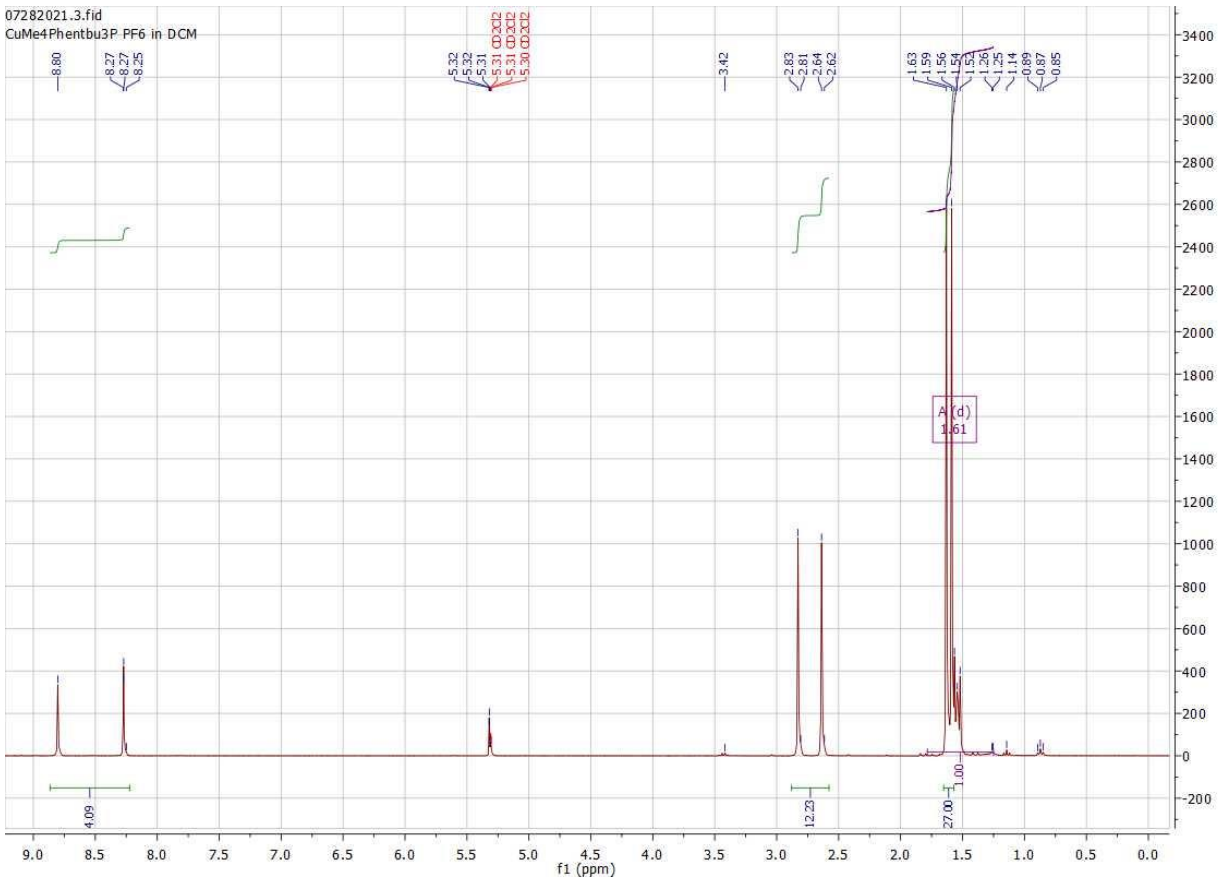
07282021.3.fid
CuMe4Phentbu3P PF6 in DCM
8.80
8.27
8.27
8.25
5.32
5.32
5.31
5.31
5.31
5.30
3.42
2.83
2.81
2.64
2.62
1.63
1.59
1.56
1.54
1.54
1.26
1.25
1.14
0.89
0.87
0.85
A (d)
1.61
4.09
12.23
27.00
1.00
f1 (ppm)

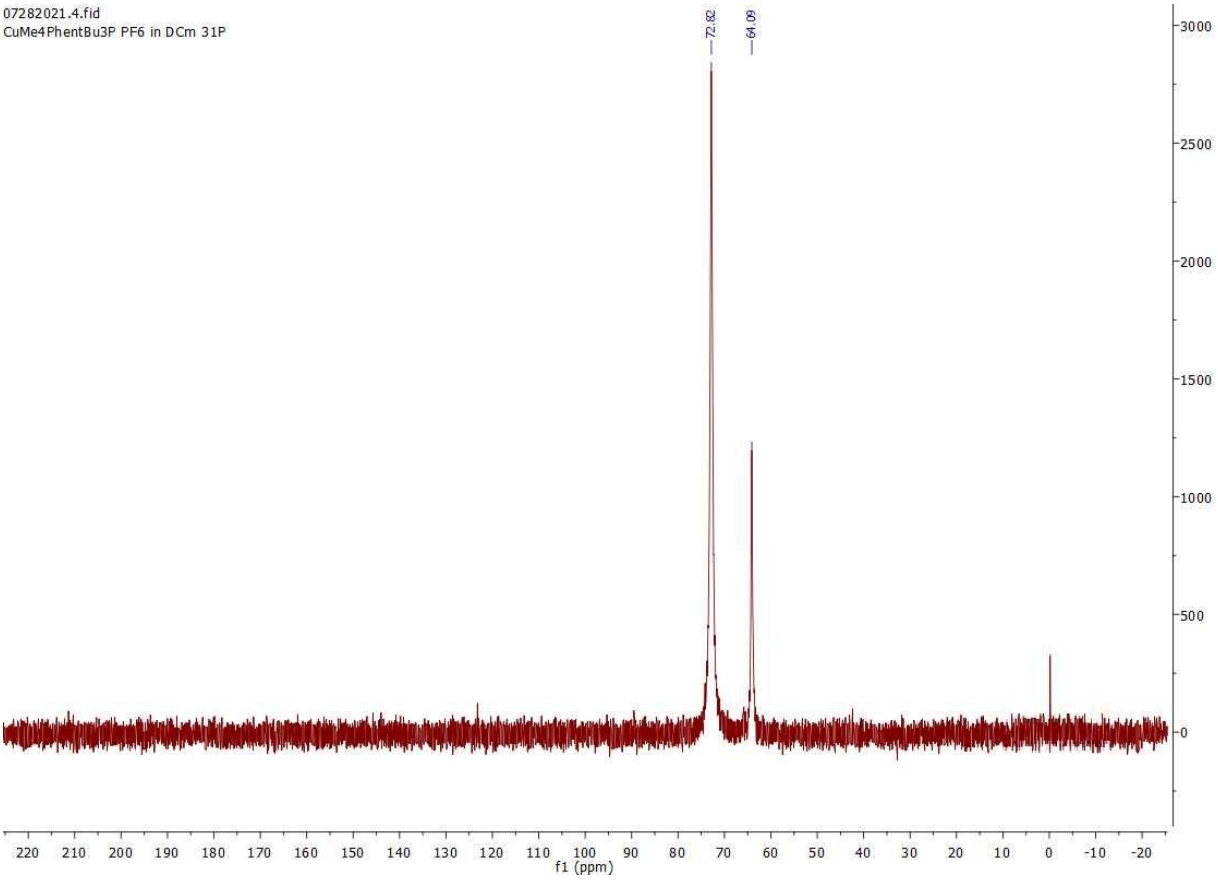

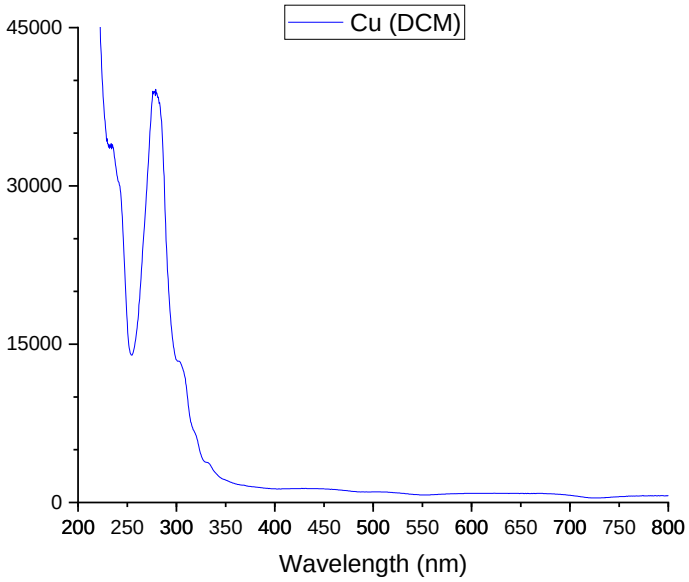

[Cu(Me$_2$bpy)(^{t}Bu$_3$P)]PF$_6$

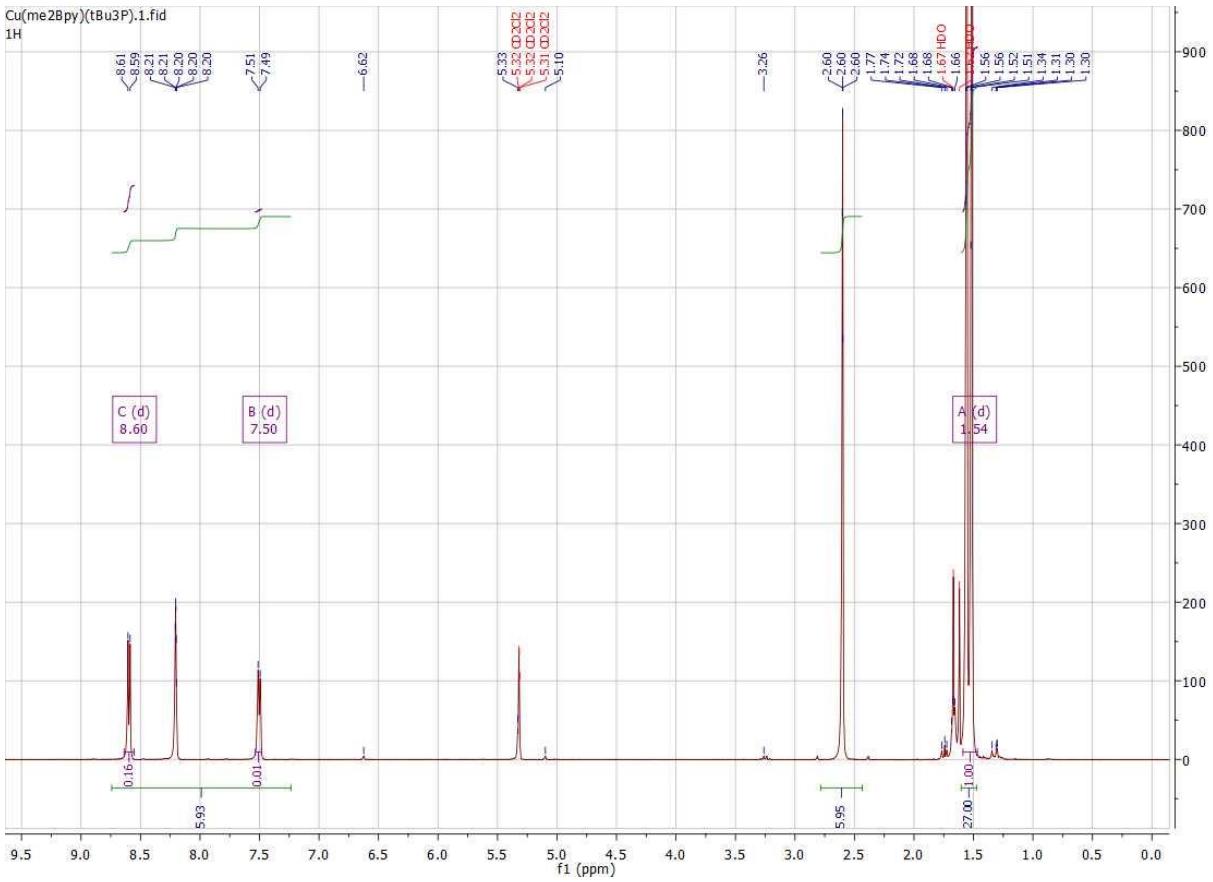
Cu(me2Bpy)(tBu3P).1.fid
1H
C (d)
8.60
B (d)
7.50
A (d)
1.54
HDO
f1 (ppm)

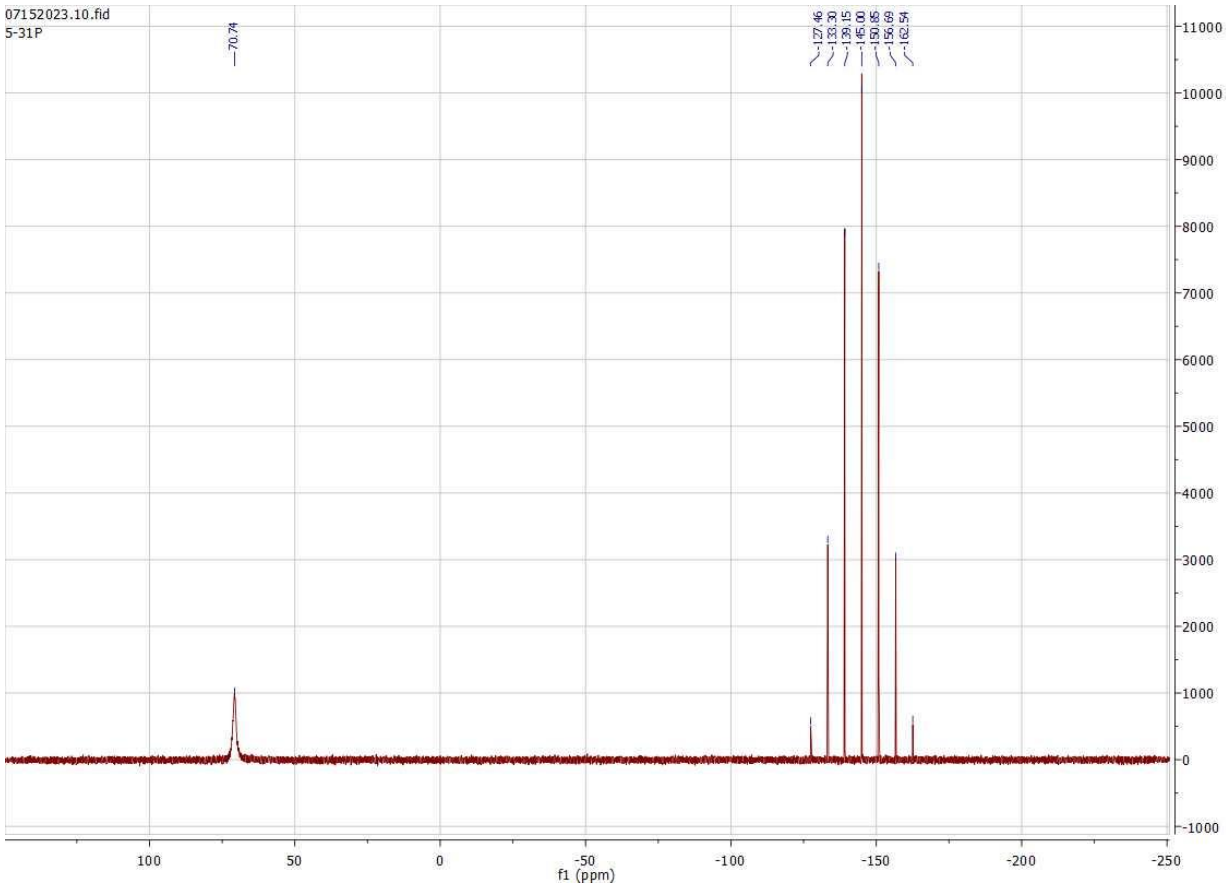
07152023.10.fid
5-31P
70.74
-127.46
-133.30
-139.15
-145.00
-150.85
-156.69
-162.54
11000
10000
9000
8000
7000
6000
5000
4000
3000
2000
1000
0
-1000
100
50
0
-50
-100
-150
-200
-250
f1 (ppm)

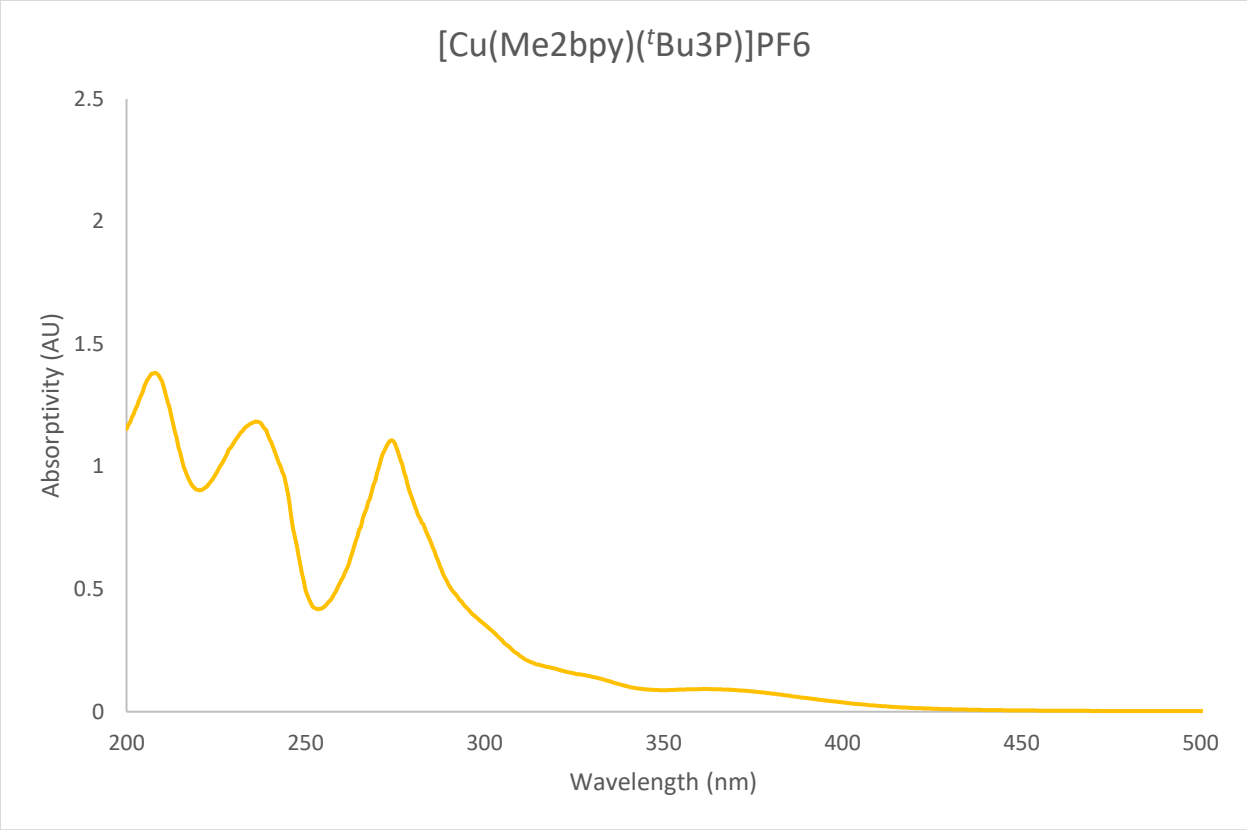

[Cu(Me$_4$phen)(^{t}Bu$_3$P)]Cl

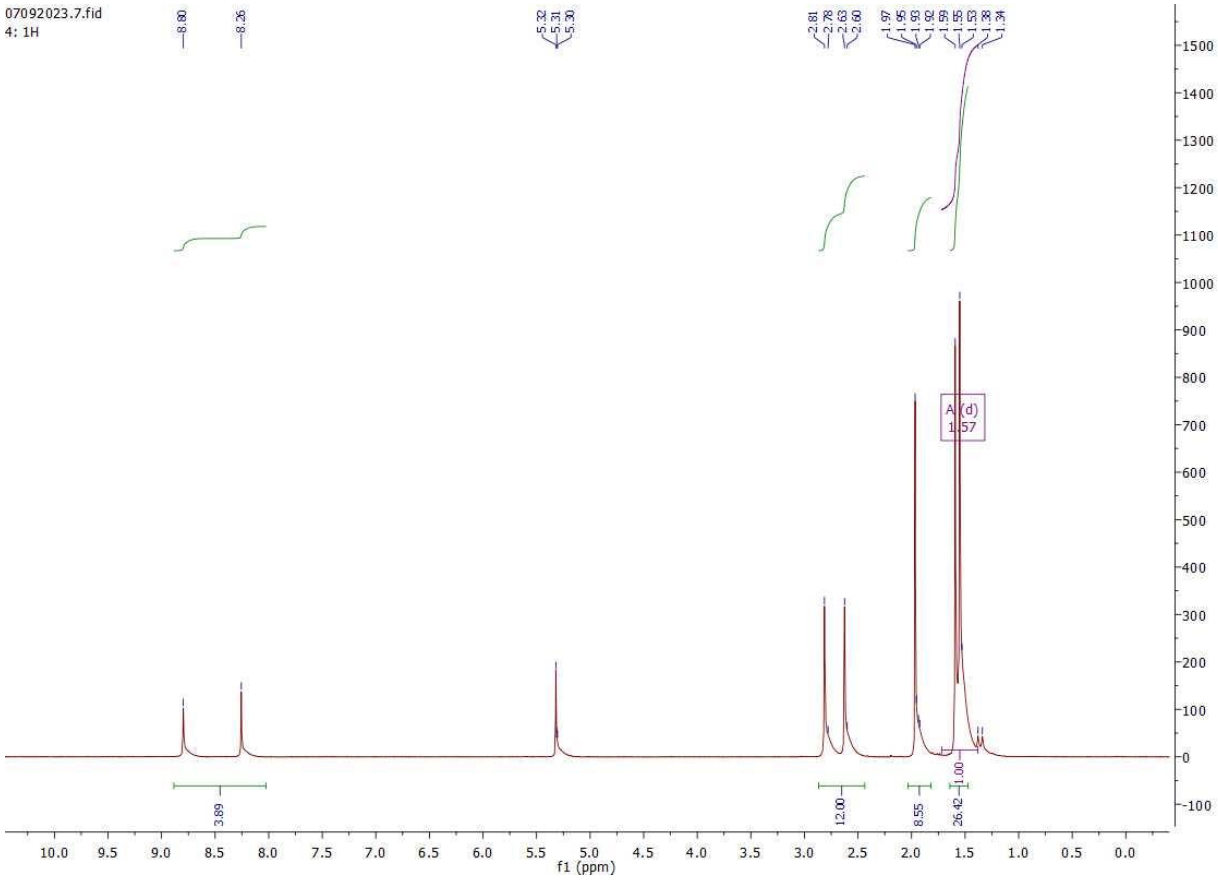
07092023.7.fid
4: 1H
8.80
8.26
5.32
5.31
5.30
2.81
2.78
2.63
2.60
1.97
1.95
1.93
1.92
1.59
1.55
1.53
1.38
1.34
A (d)
1.57
3.89
12.00
8.55
1.00
26.42
f1 (ppm)

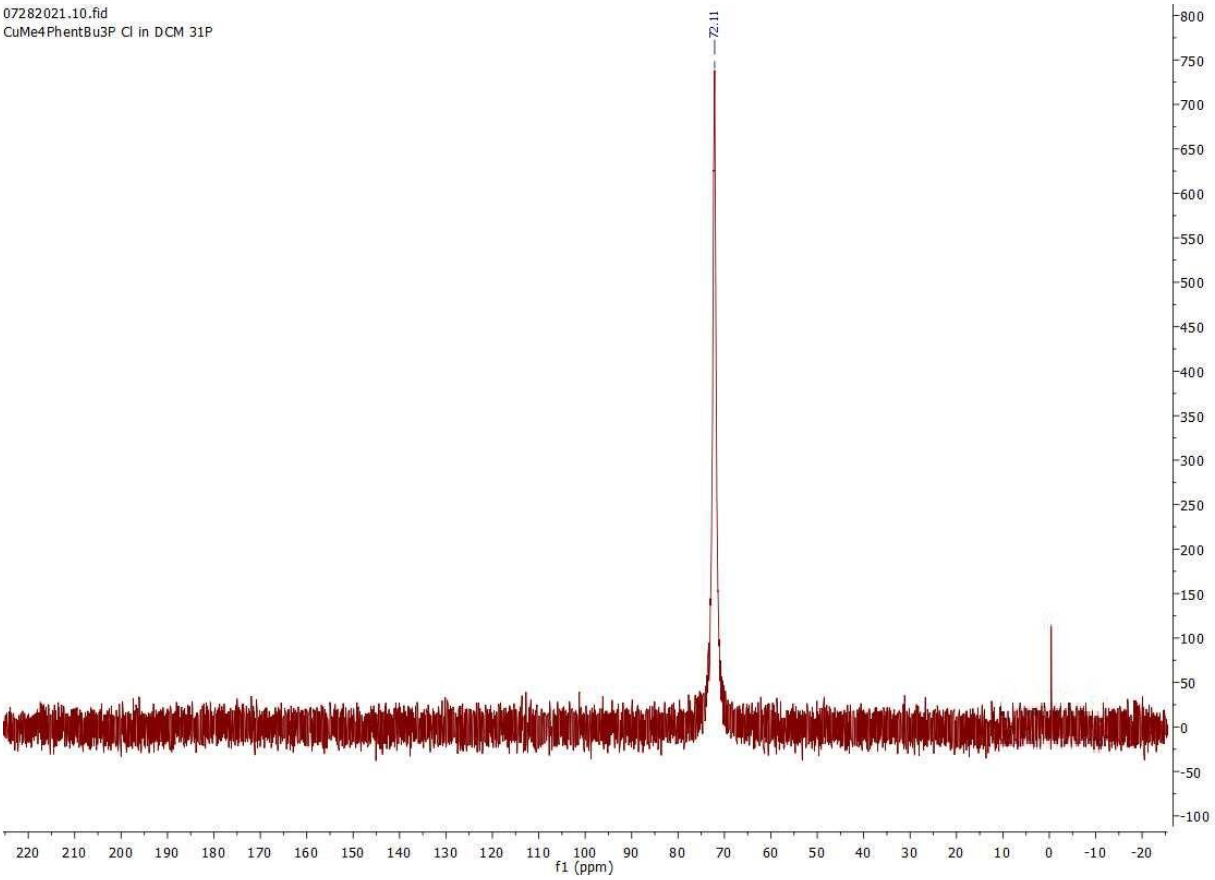
07282021.10.fid
CuMe4PhentBu3P Cl in DCM 31P
72.11
f1 (ppm)

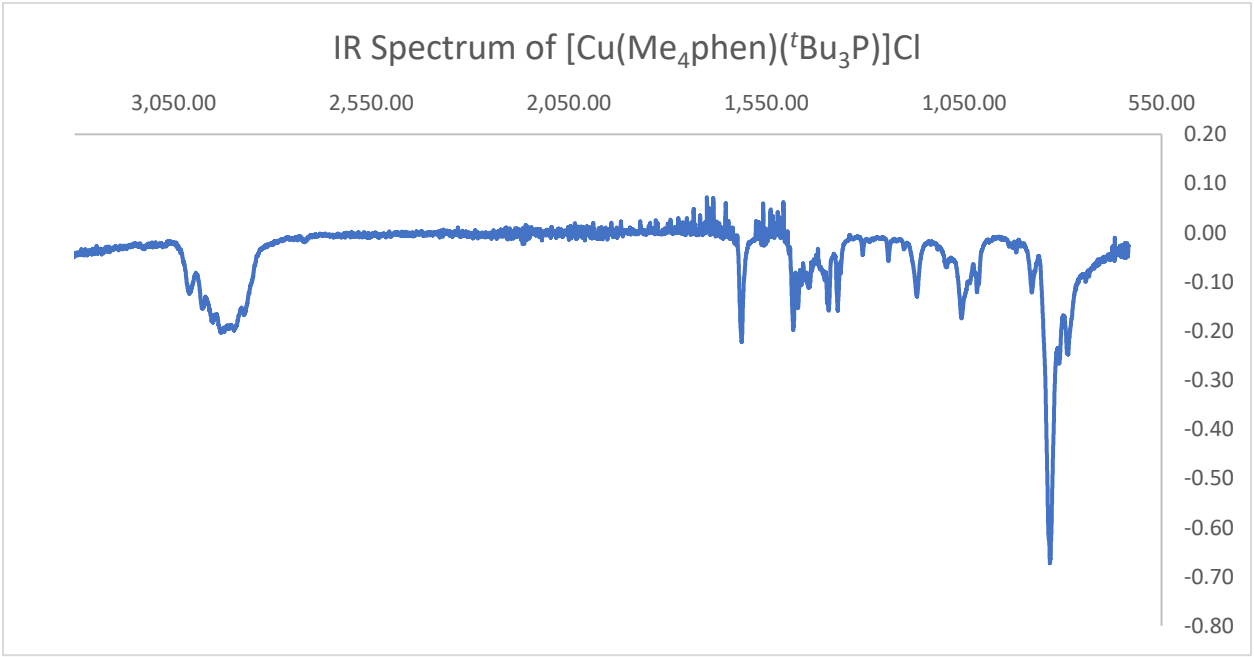
IR Spectrum of [Cu(Me4phen)(tBu3P)]Cl
3,050.00
2,550.00
2,050.00
1,550.00
1,050.00
550.00
0.20
0.10
0.00
-0.10
-0.20
-0.30
-0.40
-0.50
-0.60
-0.70
-0.80

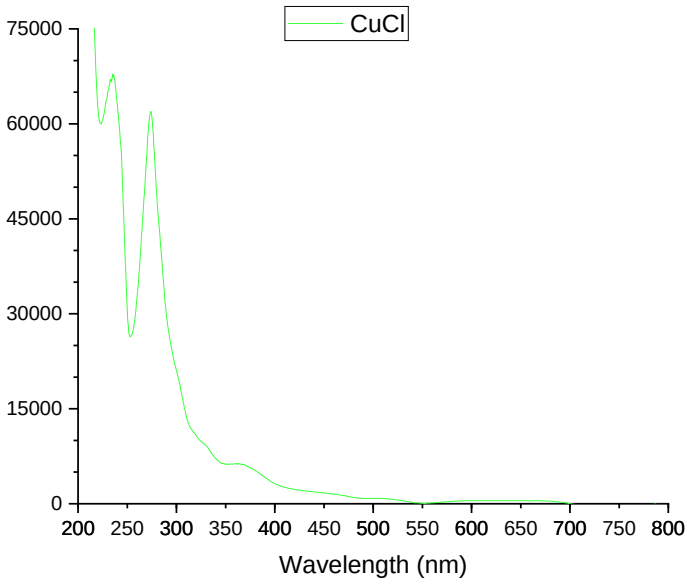

[Cu(Me$_2$bpy)(^{t}Bu$_3$P)]Cl

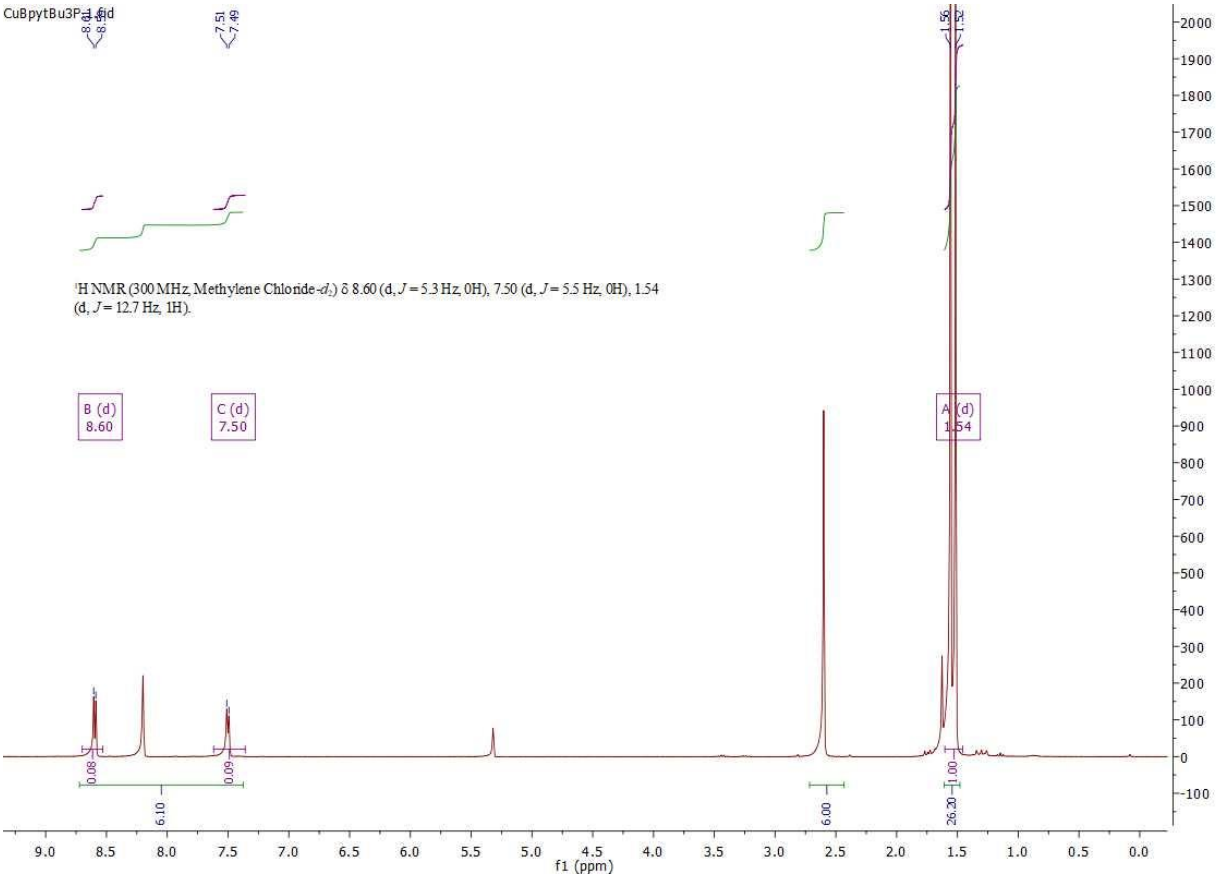

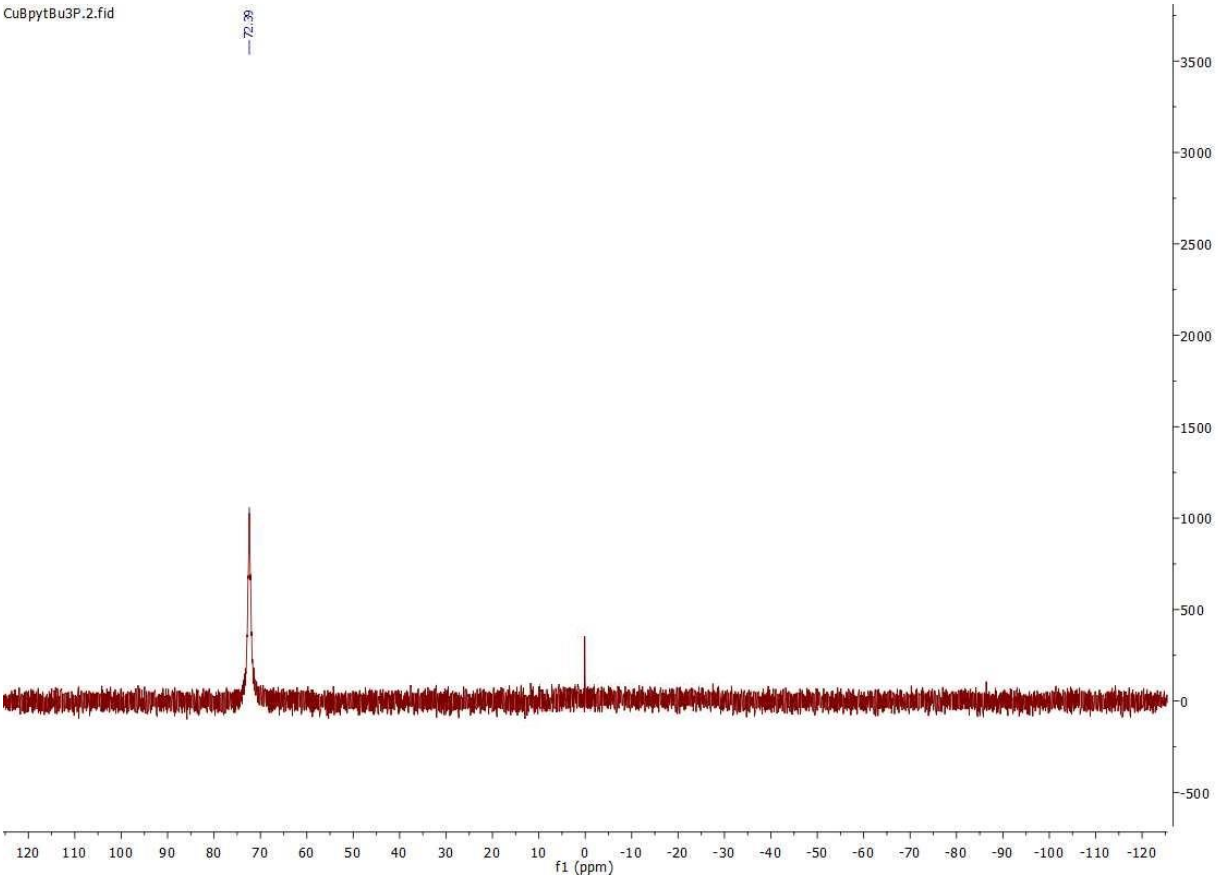
CuBpytBu3P.2.fid
72.39
3500
3000
2500
2000
1500
1000
500
0
-500
120 110 100 90 80 70 60 50 40 30 20 10 0 -10 -20 -30 -40 -50 -60 -70 -80 -90 -100 -110 -120
f1 (ppm)

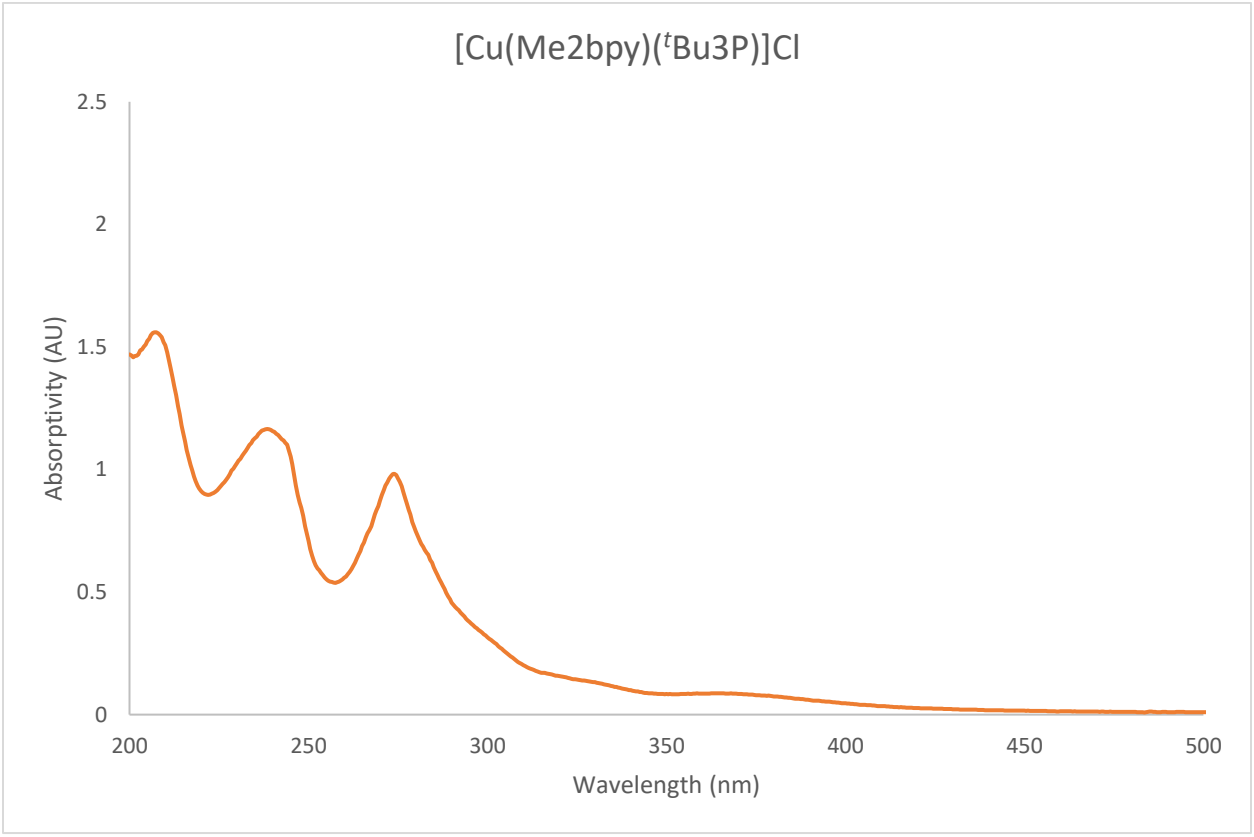
[Cu(Me2bpy)(tBu3P)]Cl
Absorptivity (AU)
2.5
2
1.5
1
0.5
0
200 250 300 350 400 450 500
Wavelength (nm)

[Cu(Me$_4$phen)(^{t}Bu$_3$P)]Br

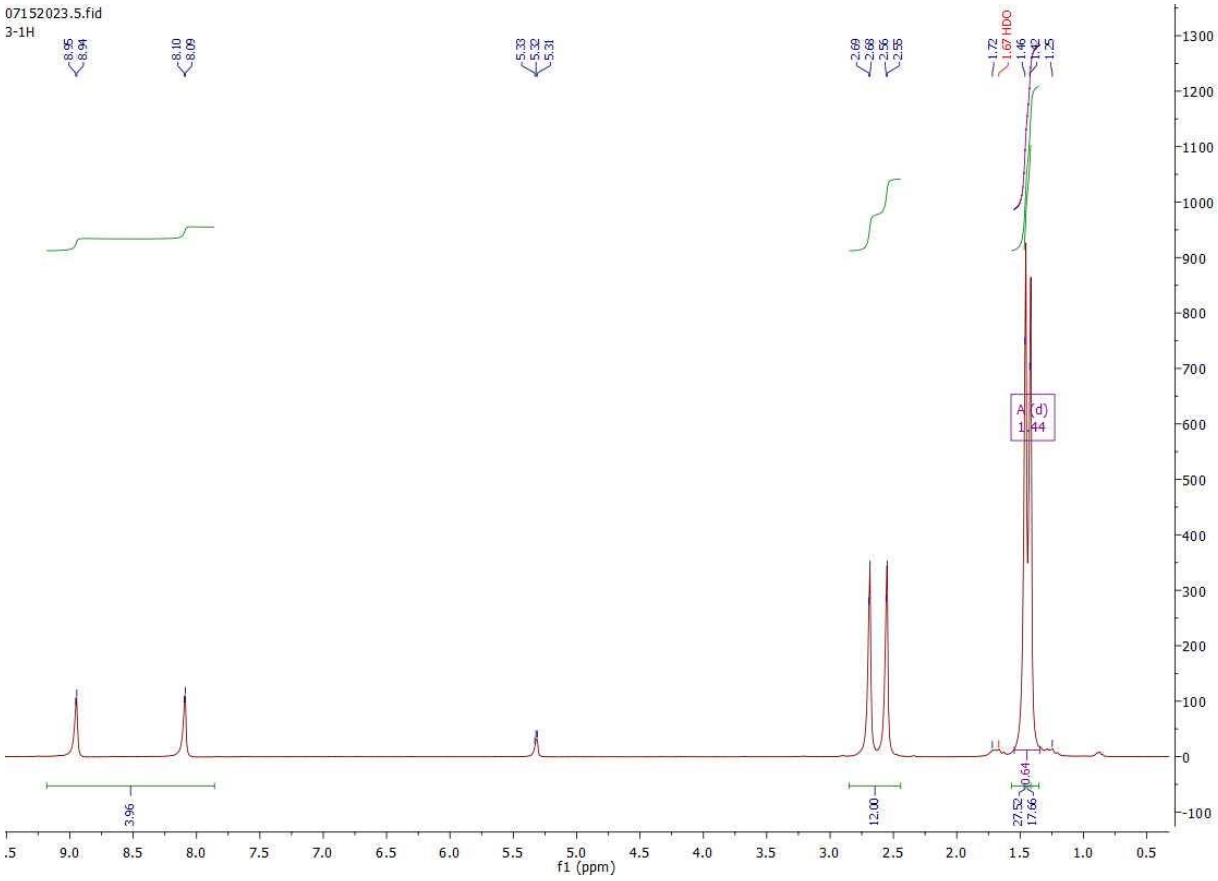

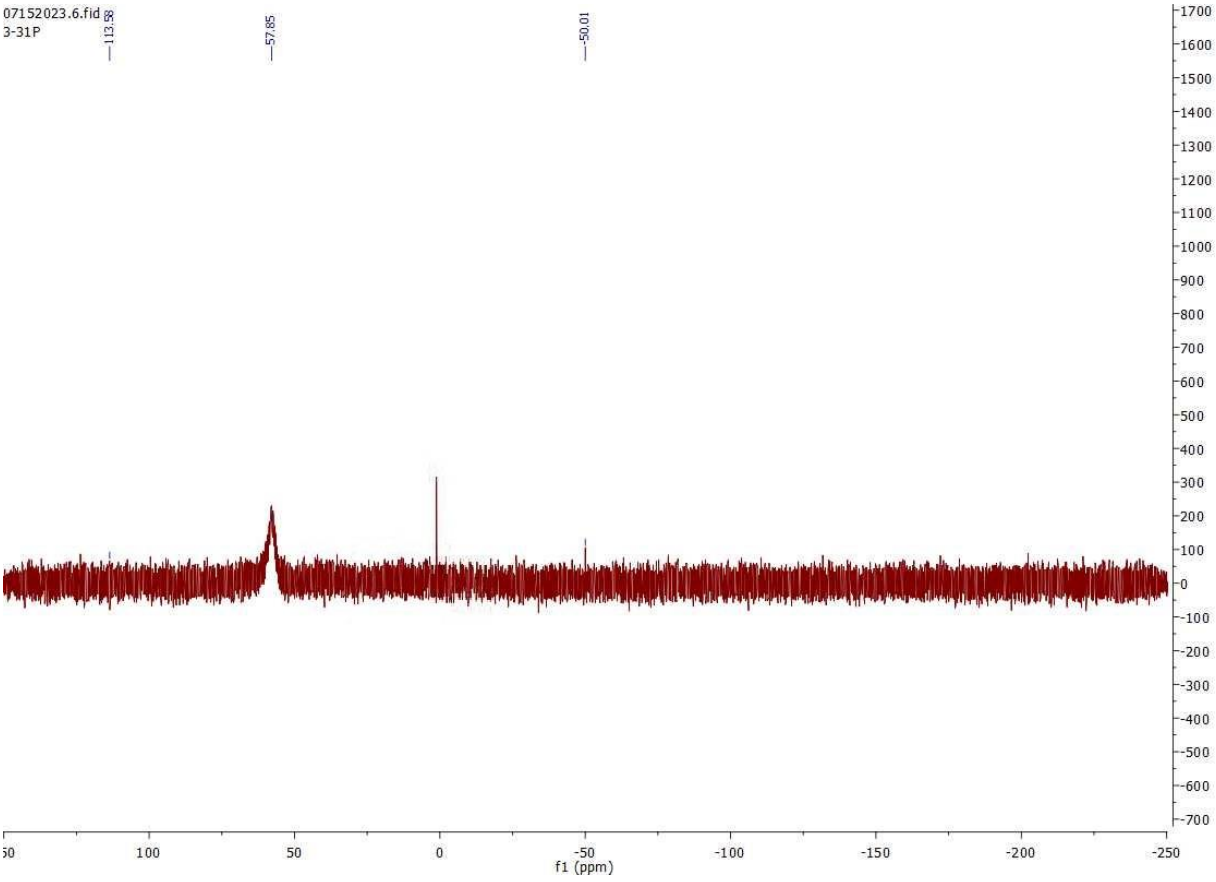

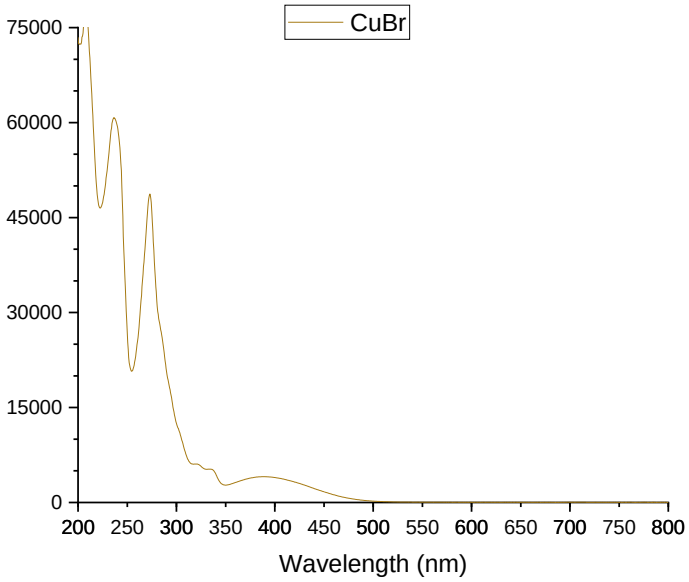

[Cu(Me$_2$bpy)(^{t}Bu$_3$P)]Br

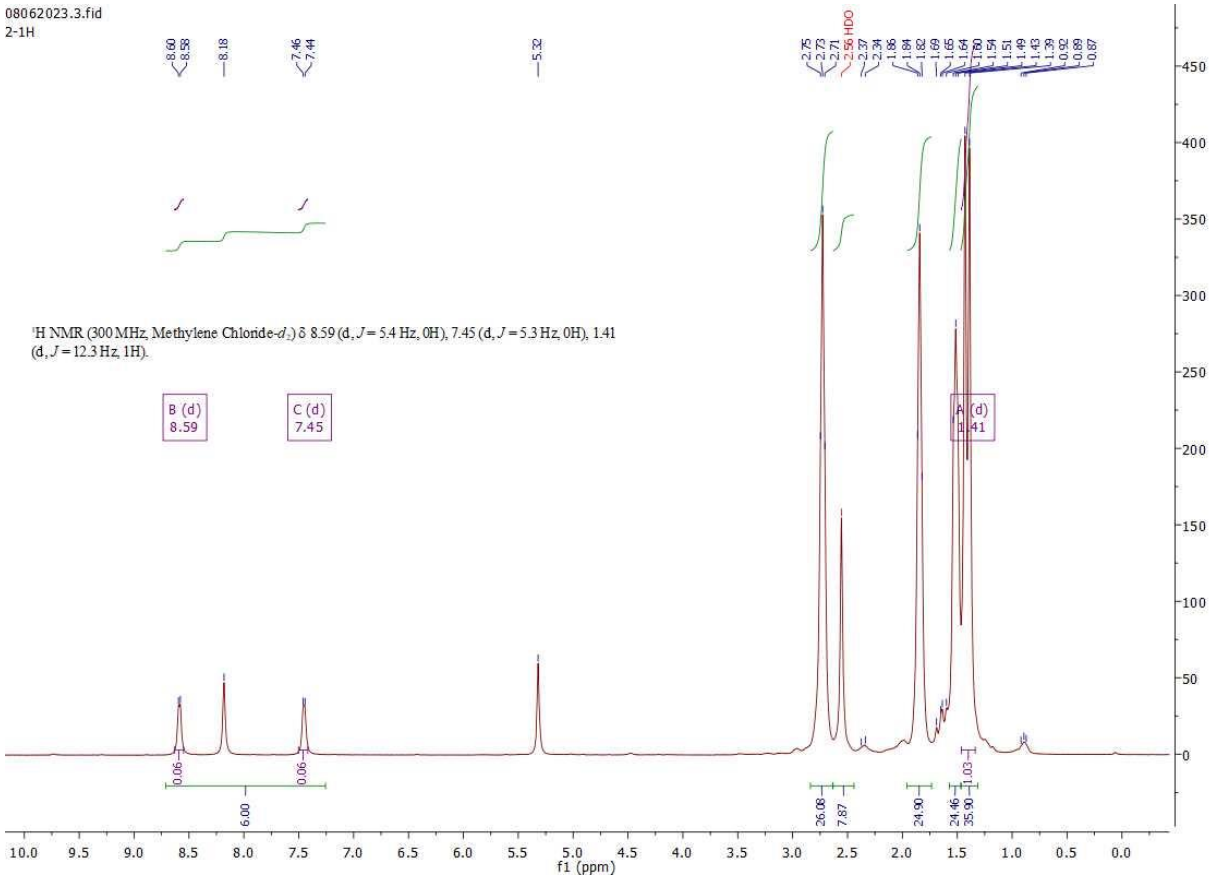
08062023.3.fid
2-1H
8.60
8.59
8.18
7.46
7.44
5.32
2.75
2.73
2.71
2.56 HDO
2.37
2.34
1.86
1.84
1.82
1.69
1.65
1.64
1.60
1.54
1.51
1.49
1.43
1.39
0.92
0.89
0.87
^{1}H NMR (300 MHz, Methylene Chloride-d_2) δ 8.59 (d, J = 5.4 Hz, 0H), 7.45 (d, J = 5.3 Hz, 0H), 1.41 (d, J = 12.3 Hz, 1H).
B (d)
8.59
C (d)
7.45
A (d)
1.41
0.06
6.00
0.06
26.08
7.87
24.90
24.46
35.90
1.03
f1 (ppm)

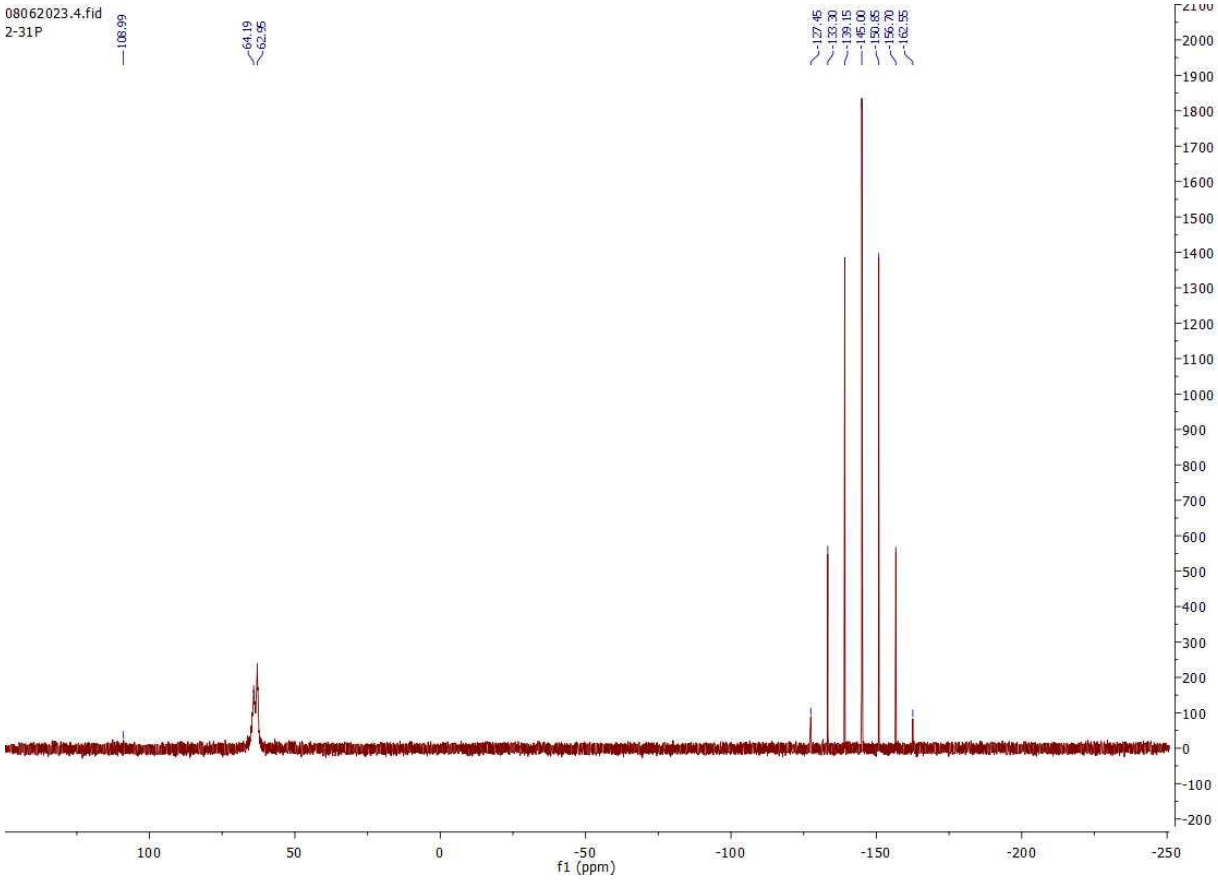
08062023.4.fid
2-31P
108.99
64.19
62.95
-127.45
-133.30
-139.15
-145.00
-150.85
-156.70
-162.55
f1 (ppm)

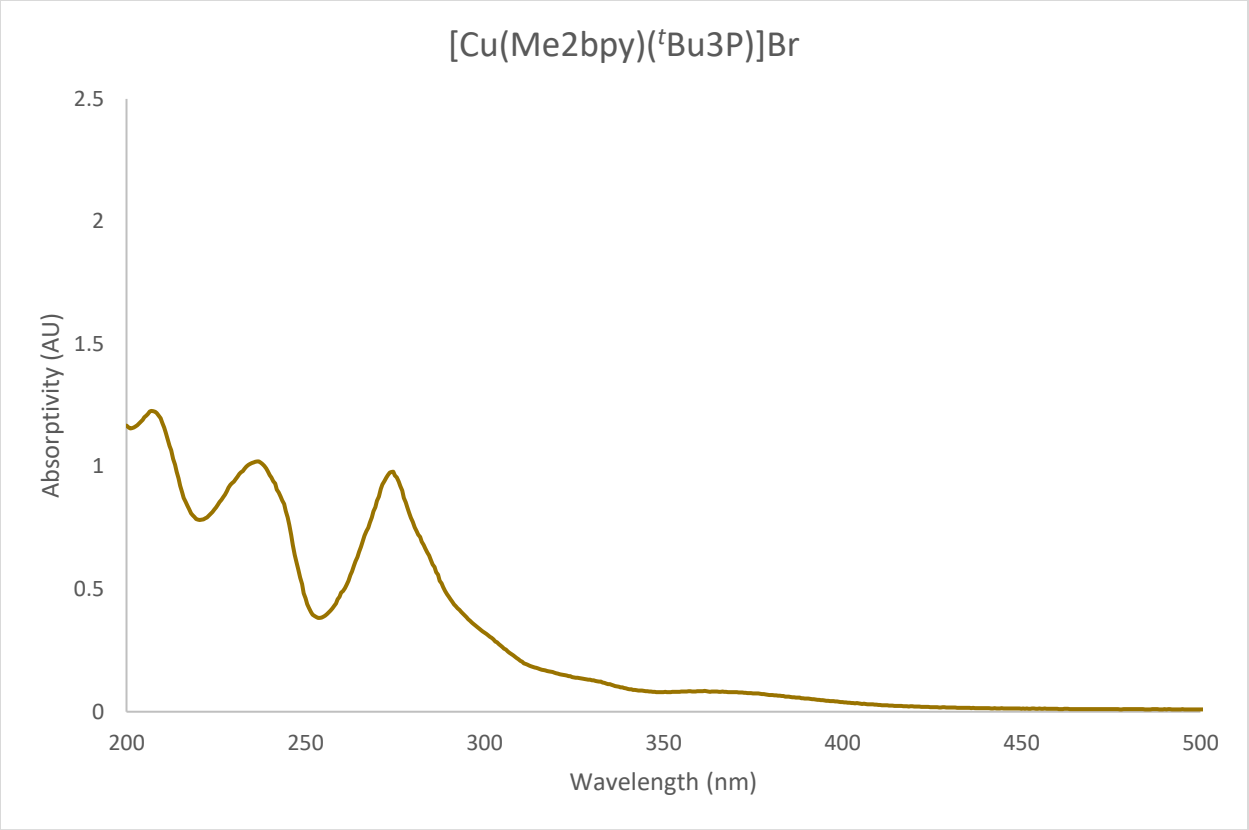

[Cu(Me$_4$phen)(^{t}Bu$_3$P)]I

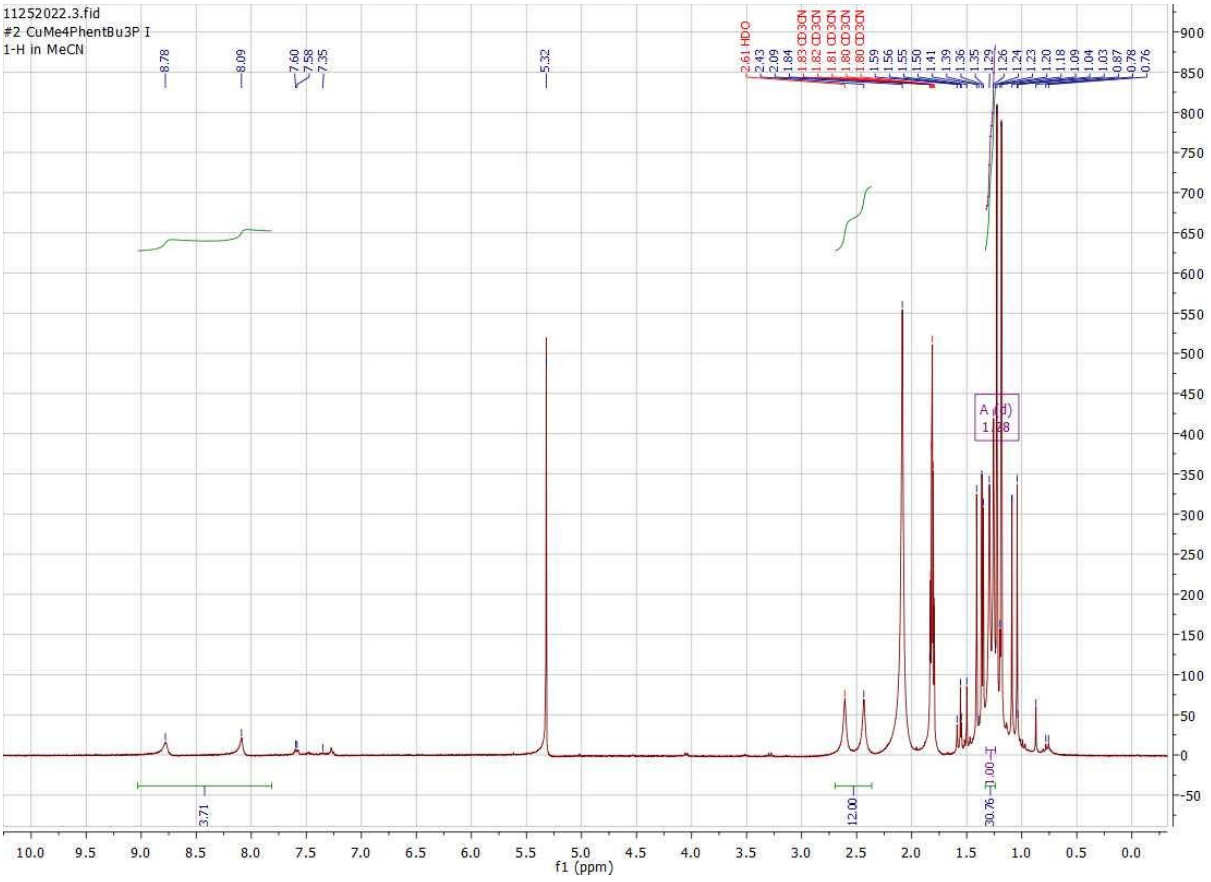

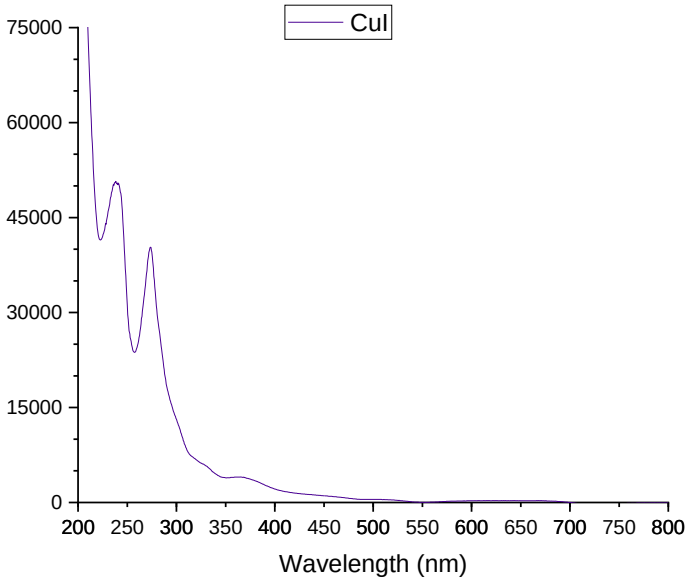

[Cu(Me$_2$bpy)(^{t}Bu$_3$P)]I

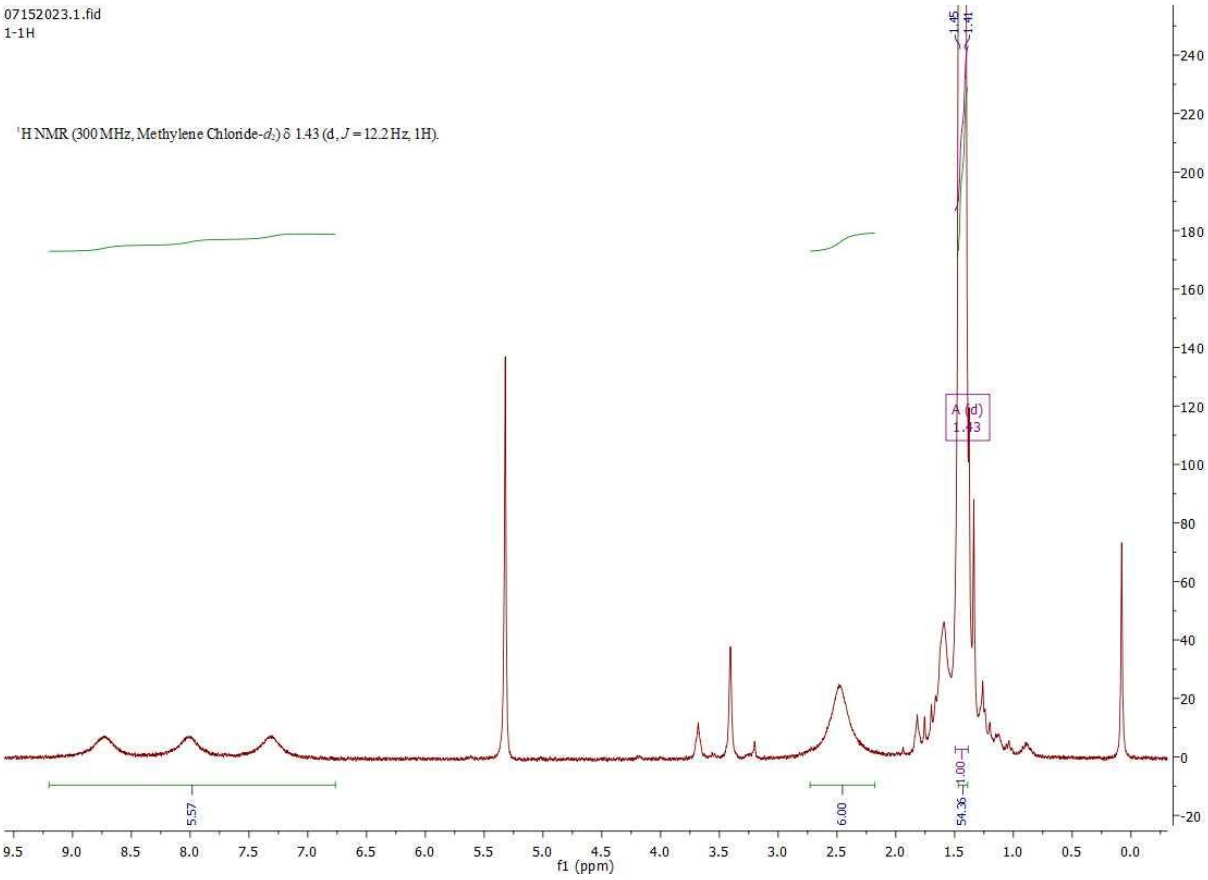
07152023.1.fid
1-1H
^{1}H NMR (300 MHz, Methylene Chloride-d_2) δ 1.43 (d, J = 12.2 Hz, 1H).
1.45
1.41
A (d)
1.43
5.57
6.00
1.00
54.36
f1 (ppm)

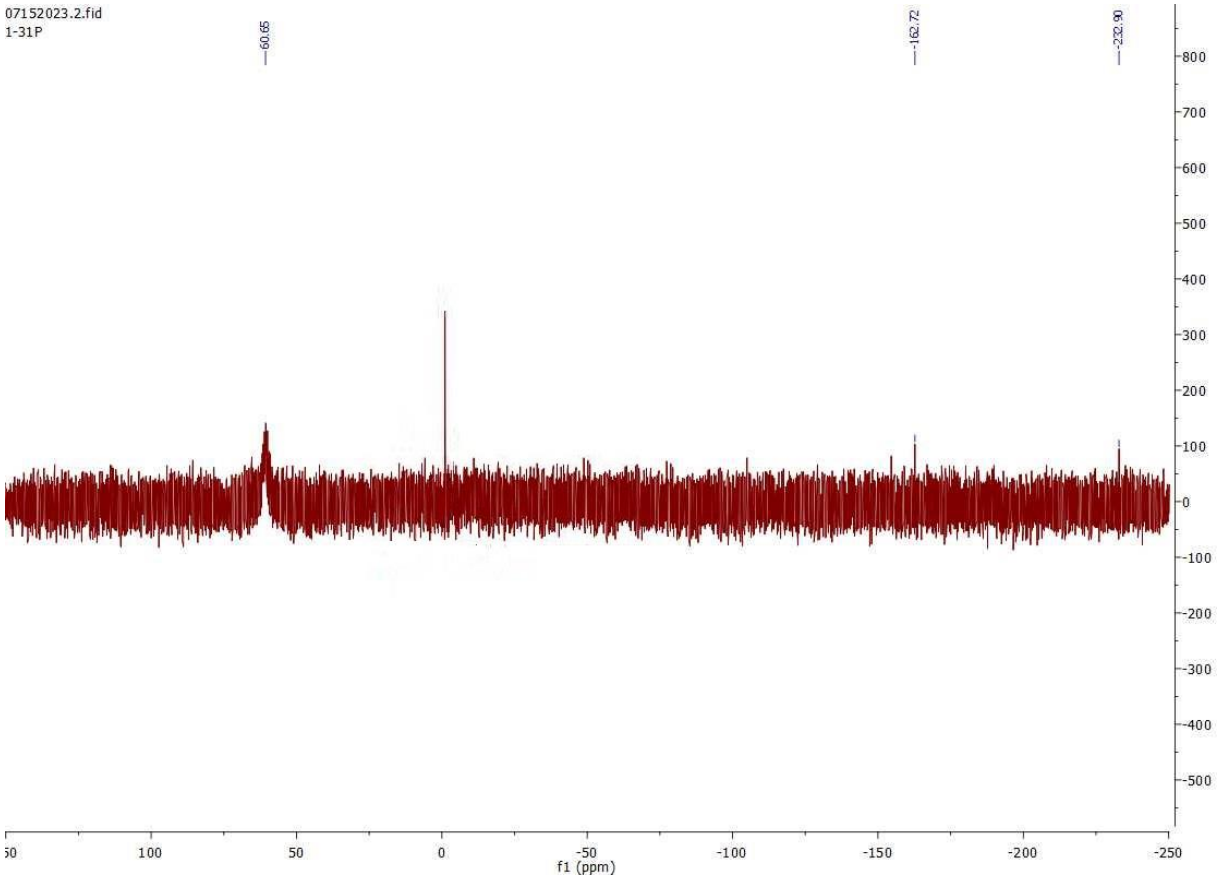
07152023.2.fid
1-31P
60.65
-162.72
-232.90
800
700
600
500
400
300
200
100
0
-100
-200
-300
-400
-500
100
50
0
-50
-100
-150
-200
-250
f1 (ppm)

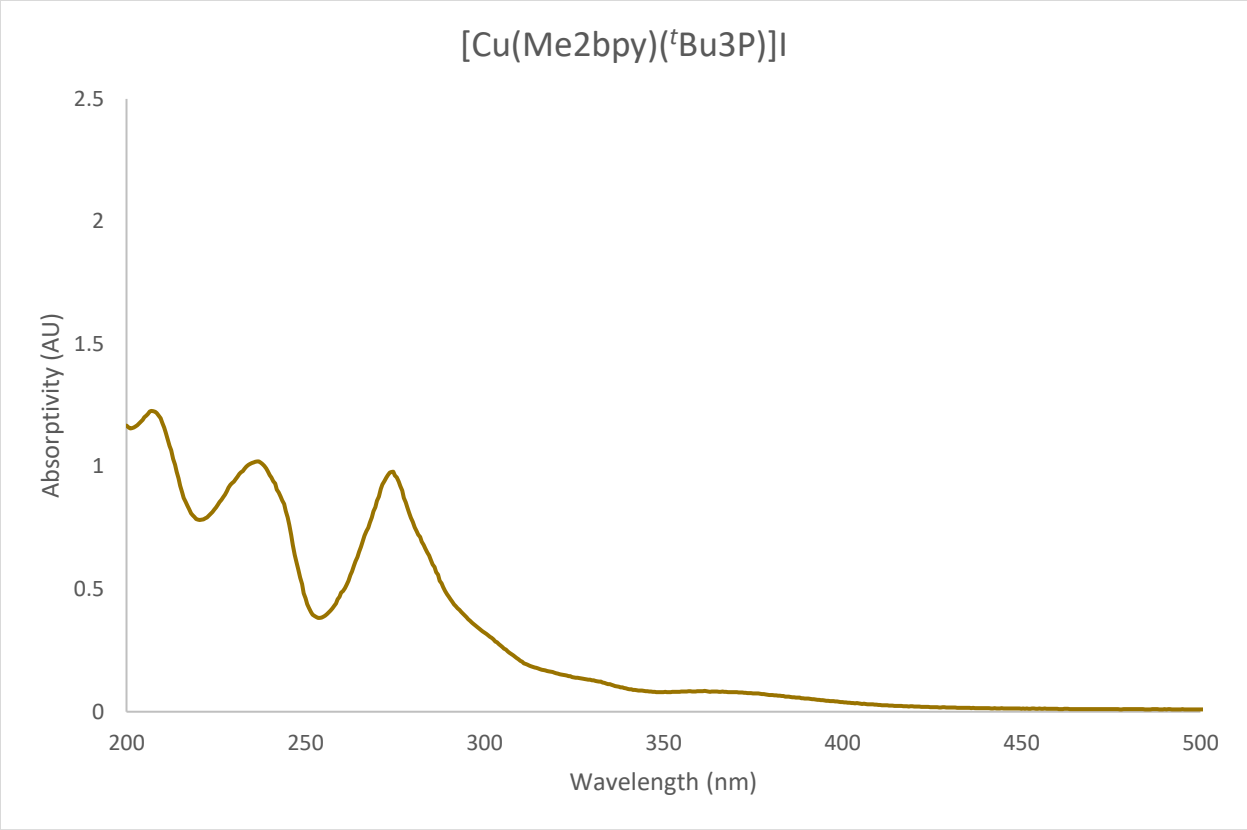

[Cu(Me$_4$phen)(^{t}Bu$_3$P)]CN

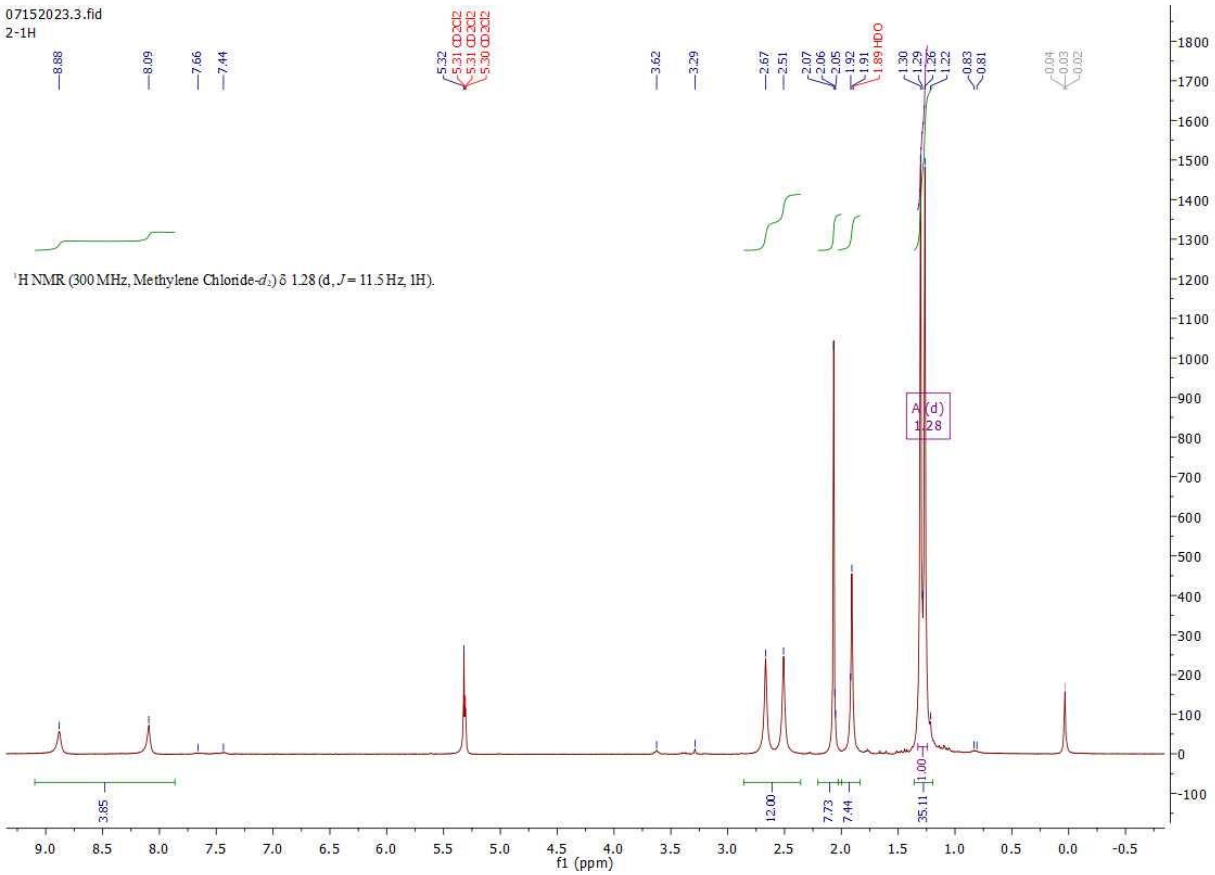

^{1}H NMR (300 MHz, Methylene Chloride-d_2) δ 1.28 (d, J = 11.5 Hz, 1H).

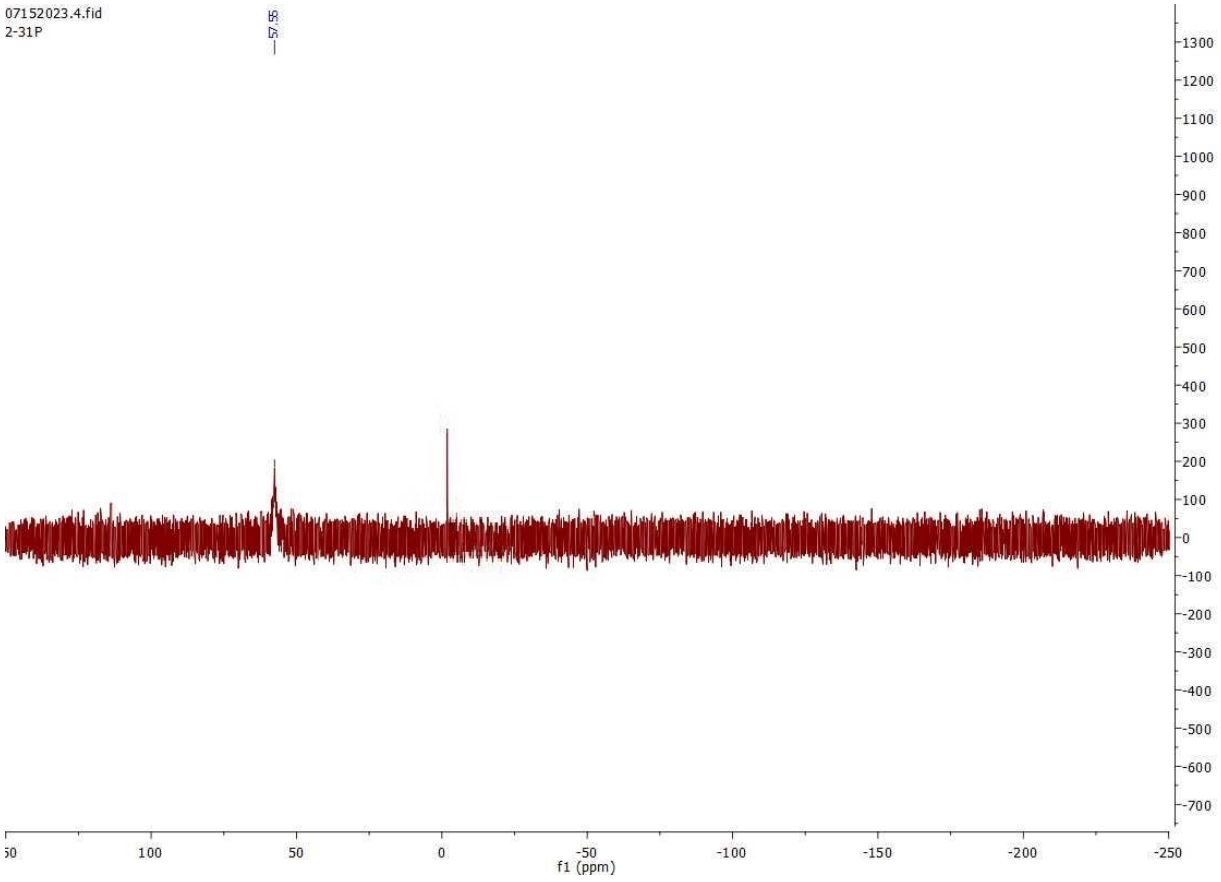

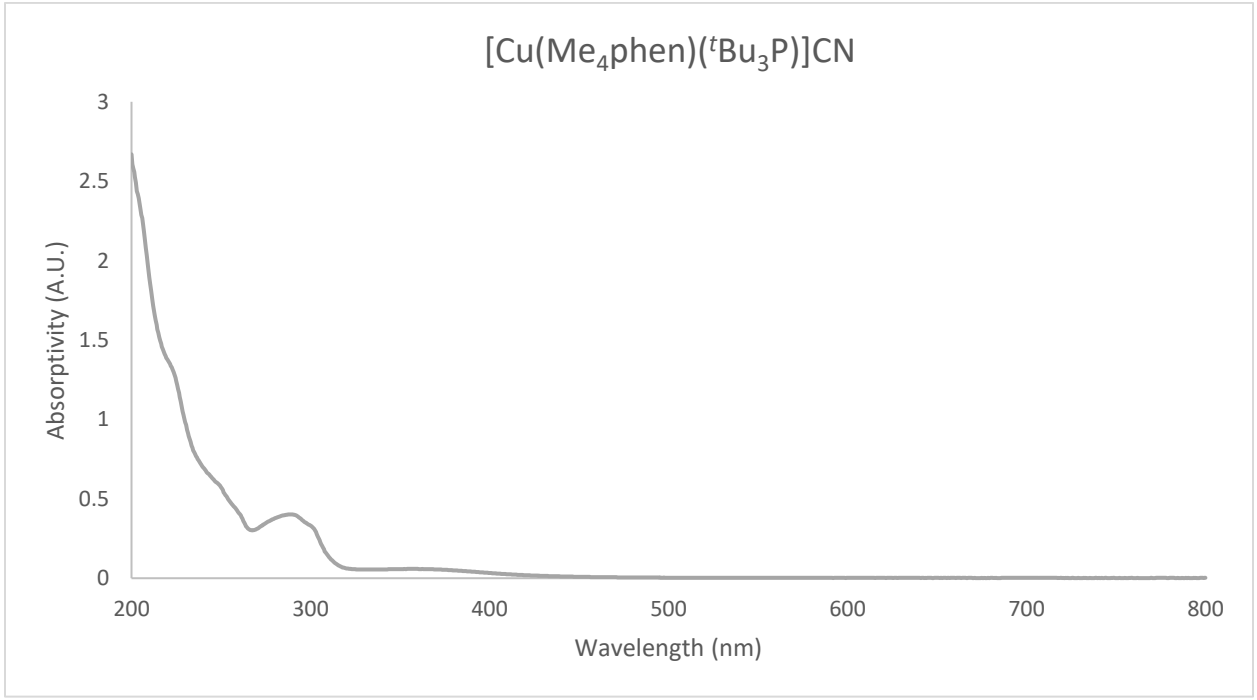

[Cu(Me$_2$bpy)(^{t}Bu$_3$P)]CN

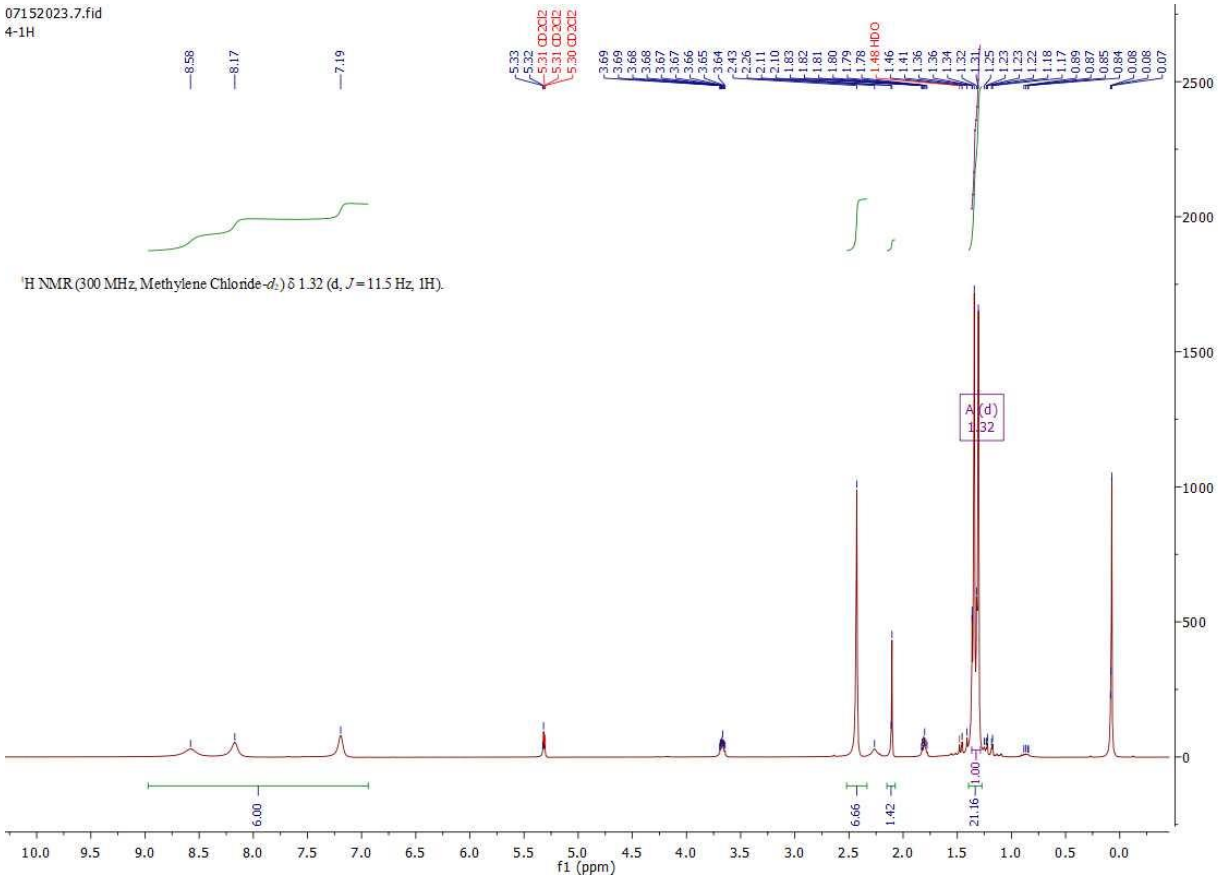

^{1}H NMR (300 MHz, Methylene Chloride-d_2) δ 1.32 (d, J = 11.5 Hz, 1H).

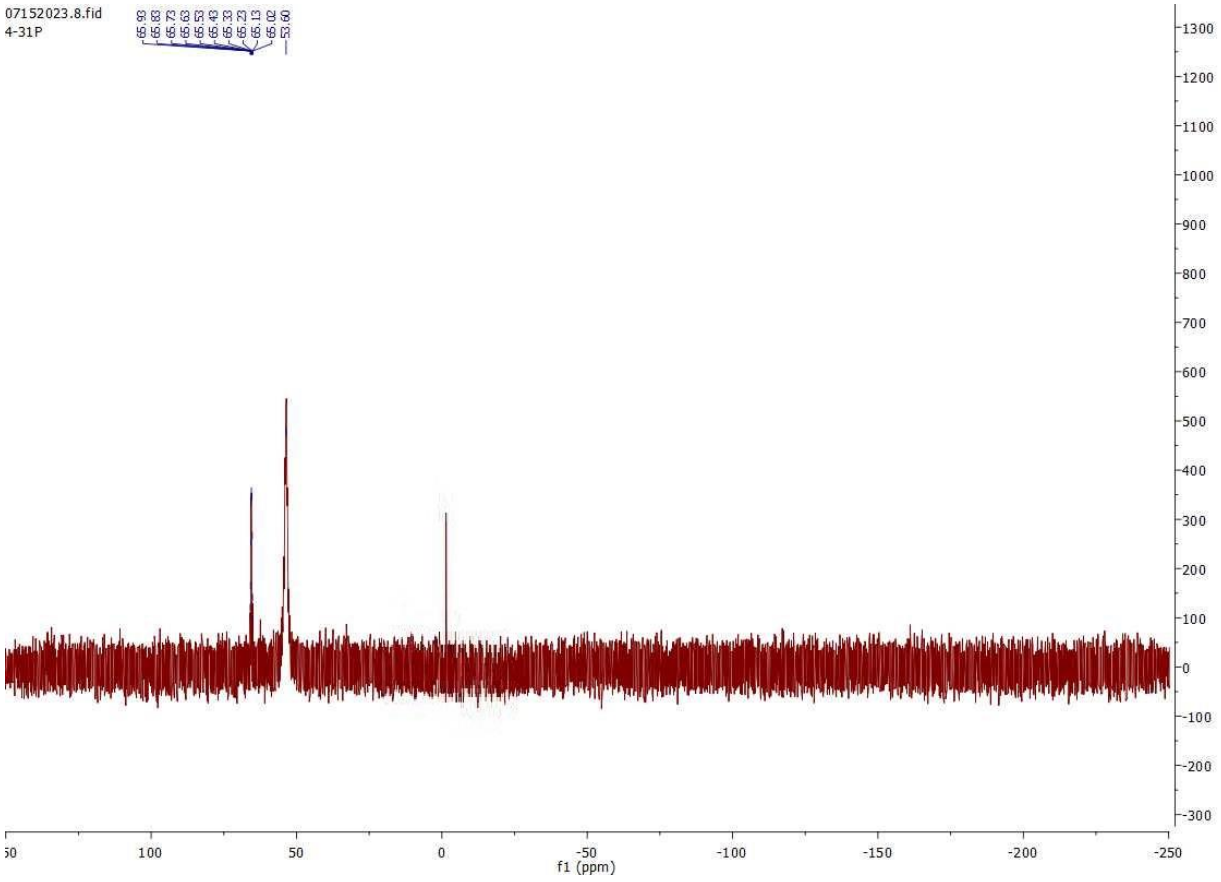

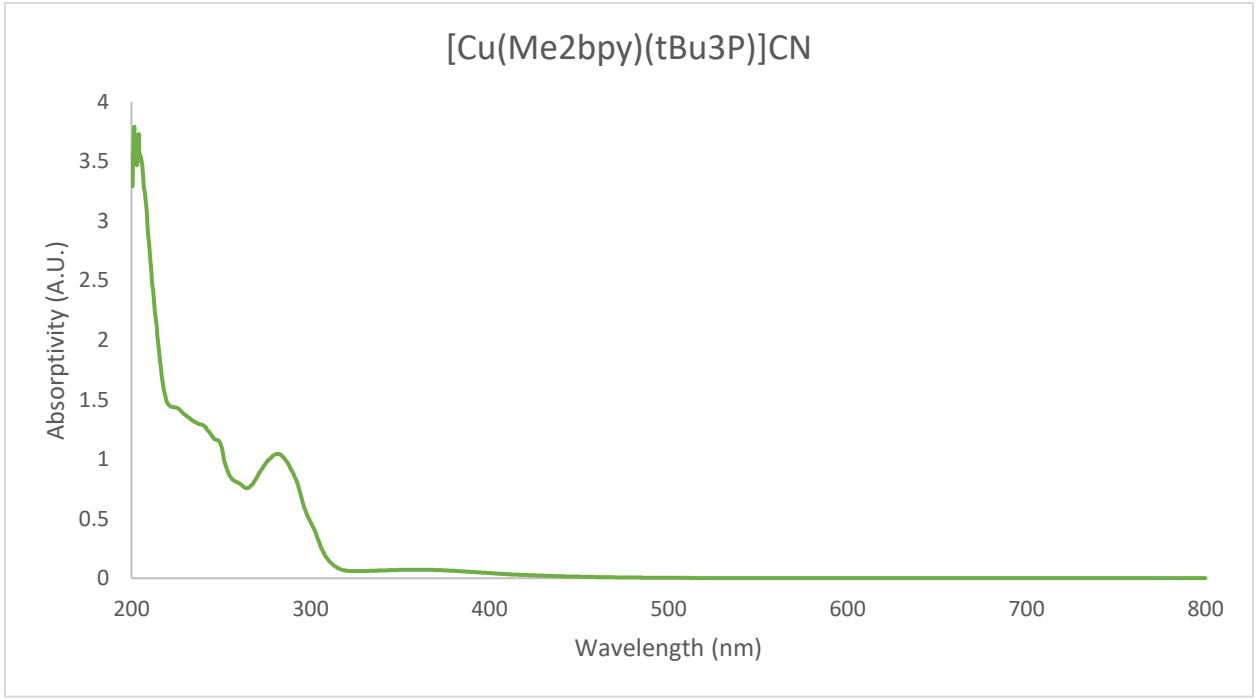

[Cu(Me$_4$phen)(^{t}Bu$_3$P)]NCS

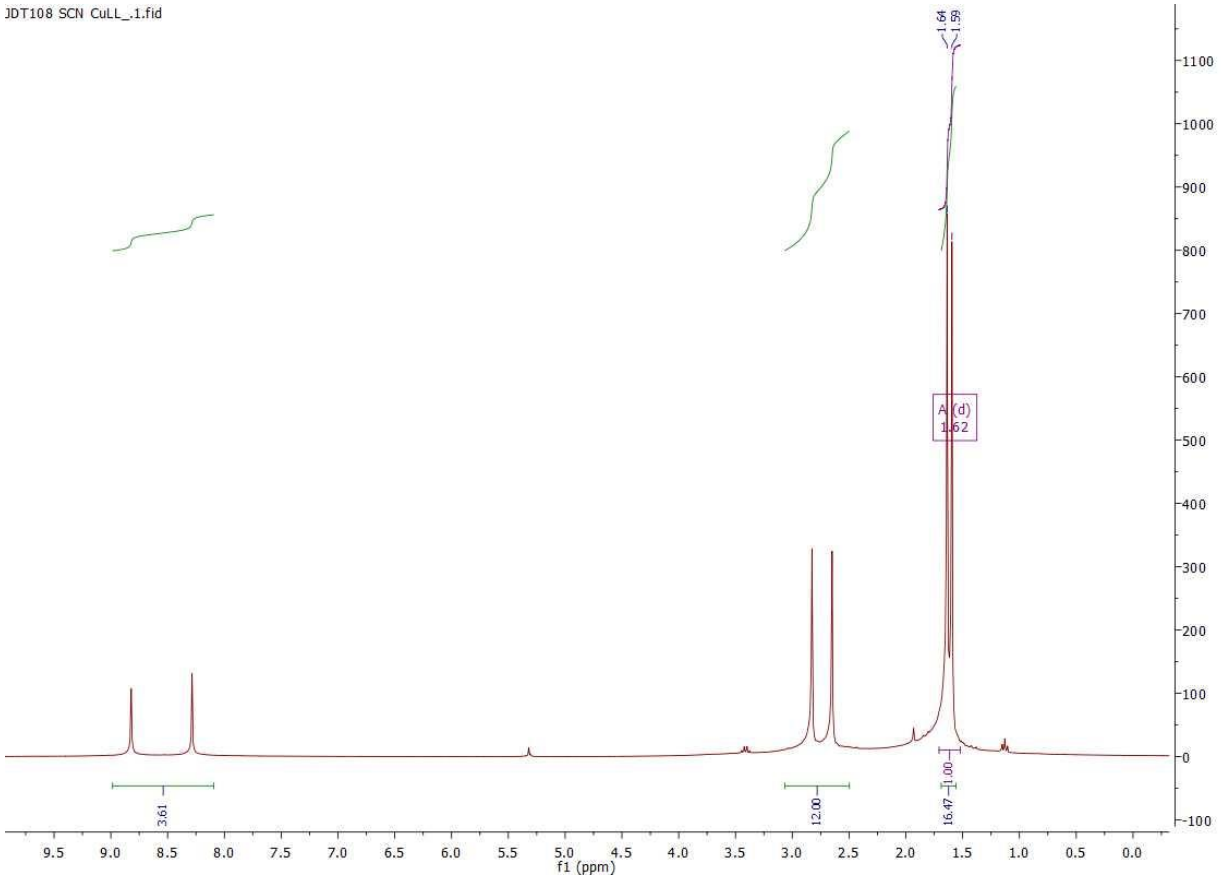
JDT108 SCN CuLL_.1.fid
1.64
1.59
A (d)
1.62
3.61
12.00
1.00
16.47
f1 (ppm)

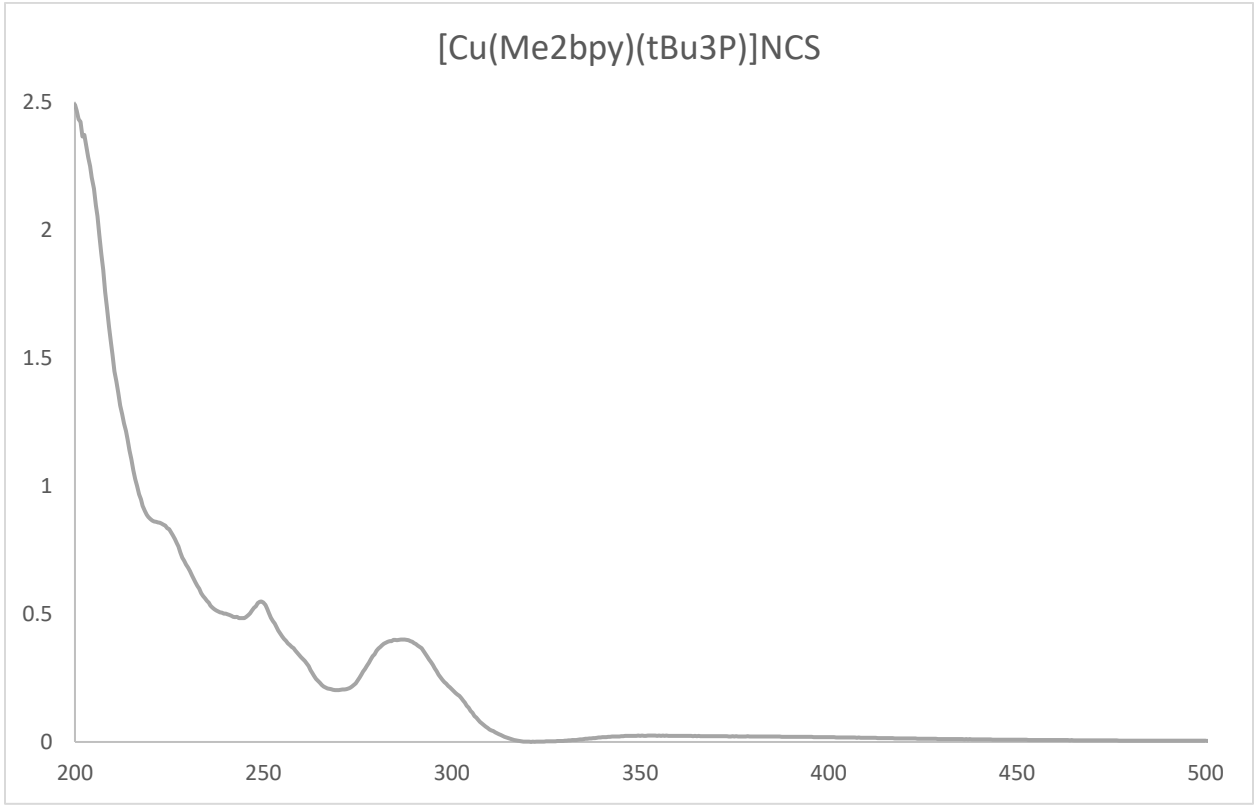
[Cu(Me2bpy)(tBu3P)]NCS

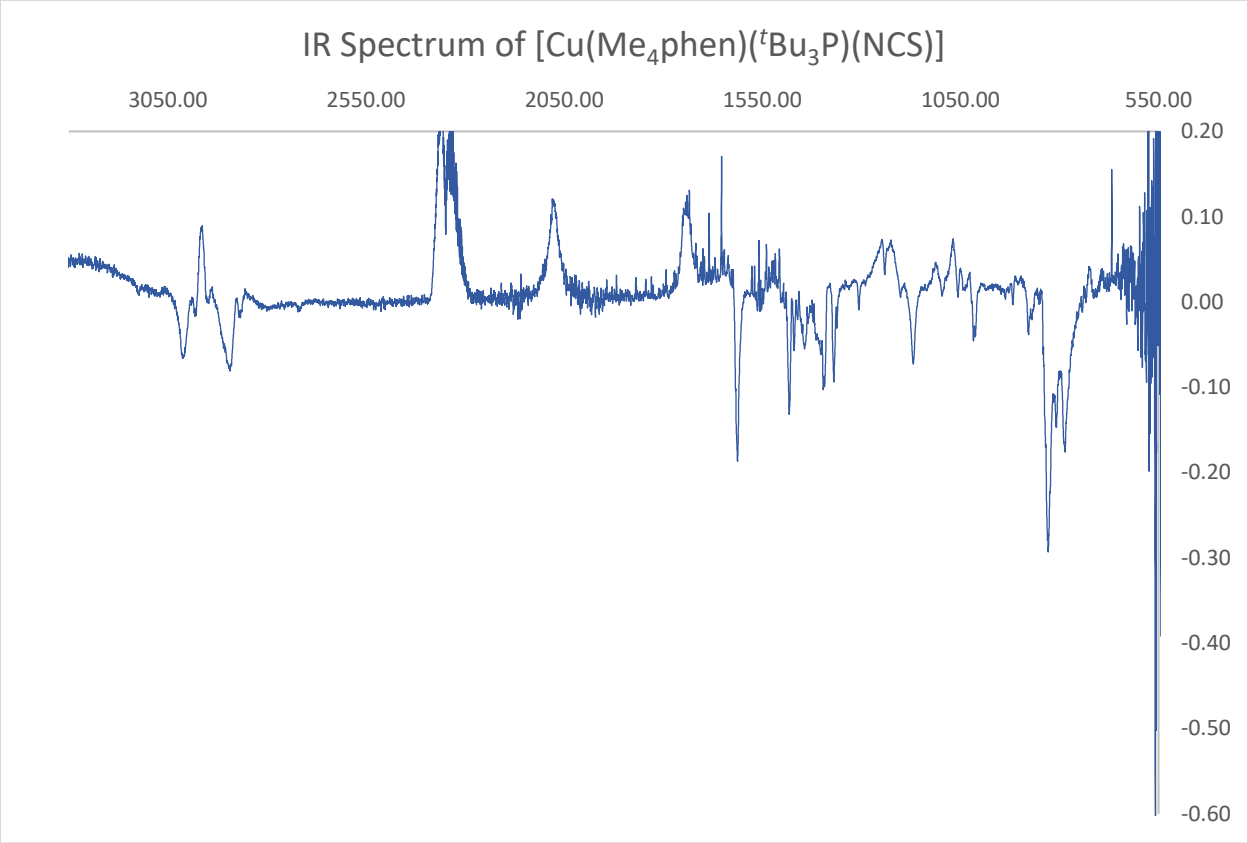

[$Cu(Me_2bpy)(^tBu_3P)$]NCS

[$Cu(Me_2bpy)(^tBu_3P)$]SeCN

[$Cu(Me_2bpy)(^tBu_3P)$(thiourea)]BF_4

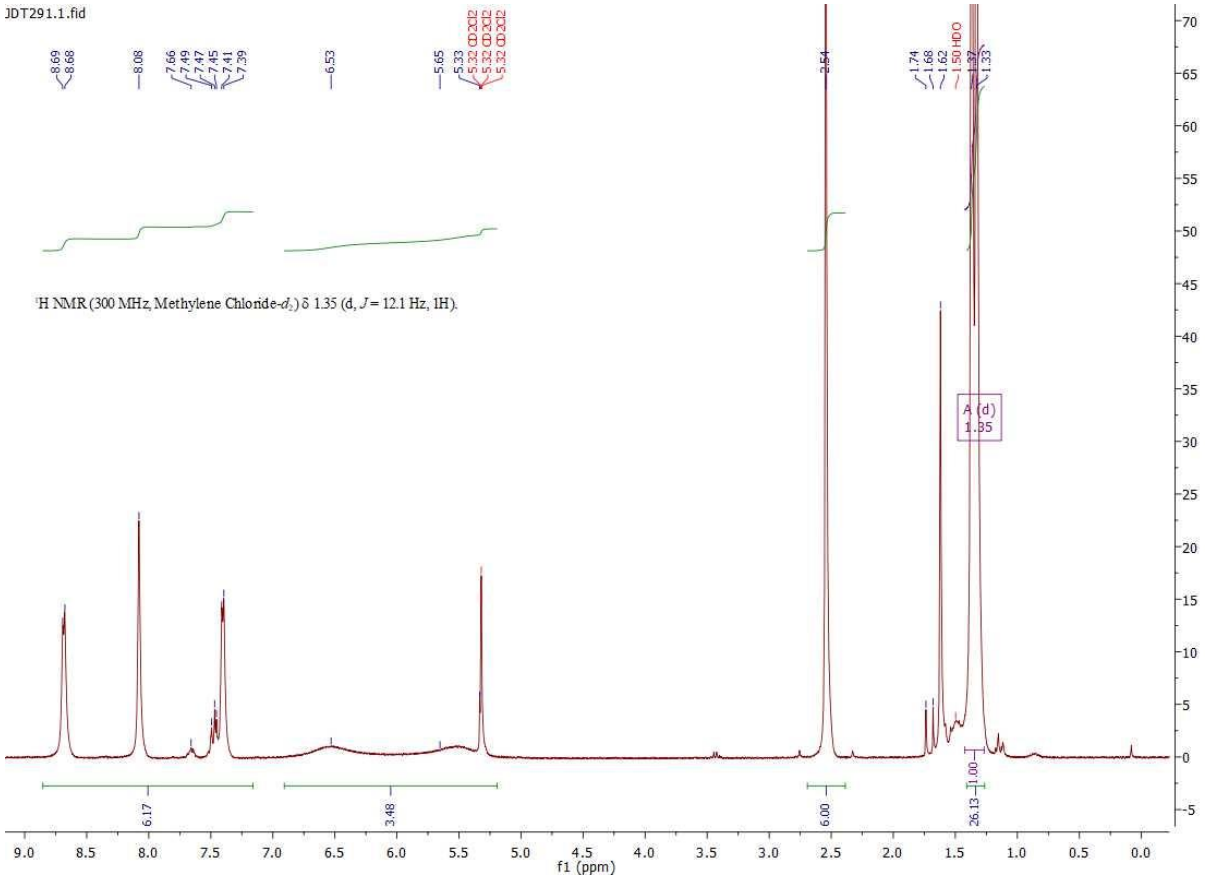

^{1}H NMR (300 MHz, Methylene Chloride-d_2) δ 1.35 (d, J = 12.1 Hz, 1H).

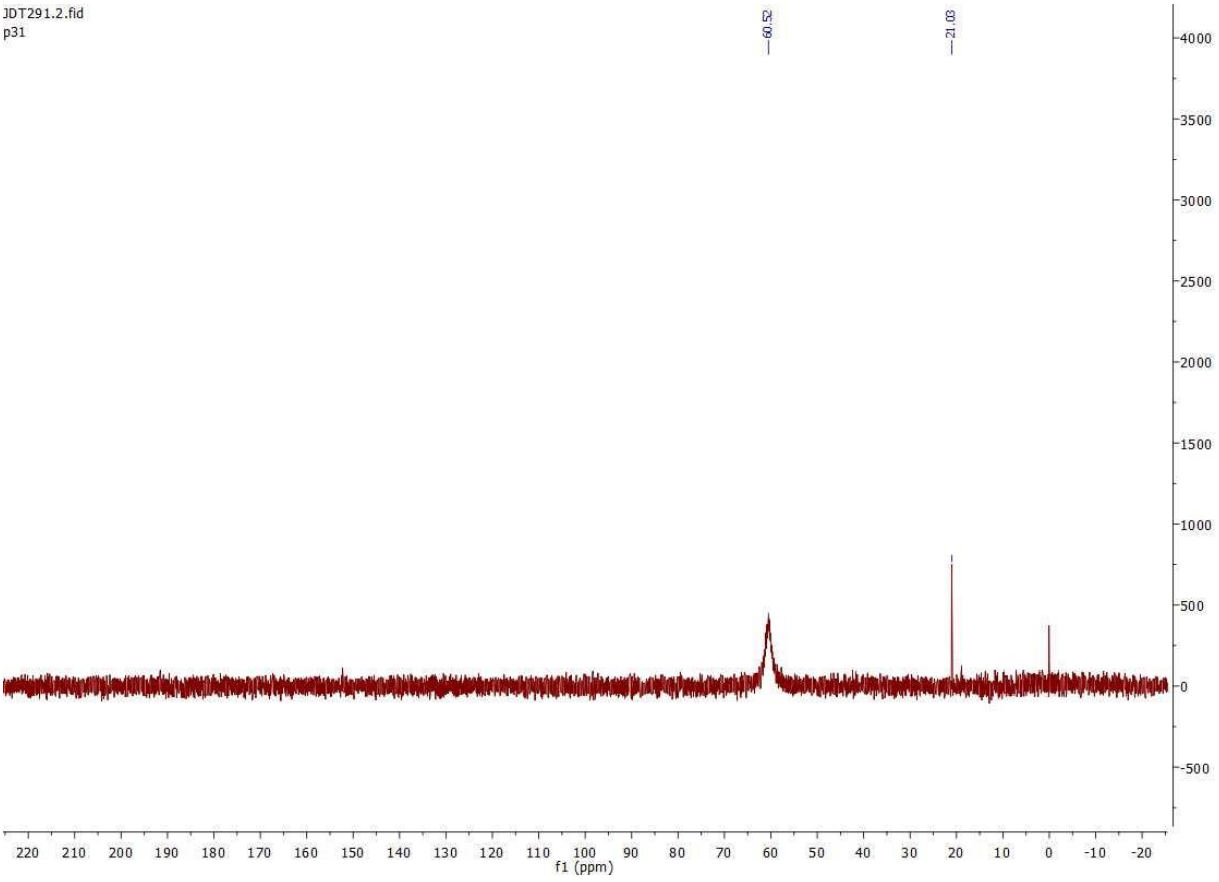

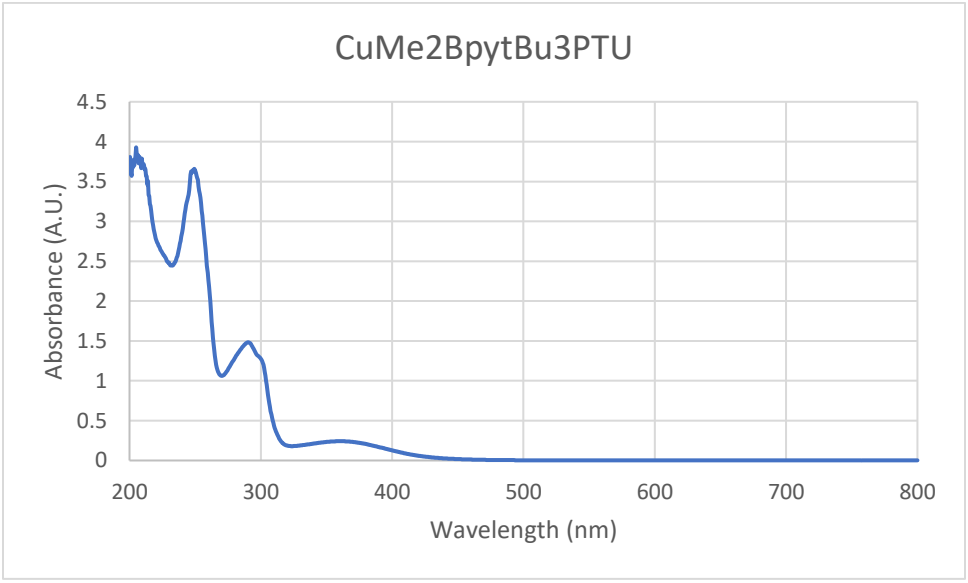

[Cu(Me$_2$bpy)(^{t}Bu$_3$P)(tetrahydrothiophene)]PF$_6$

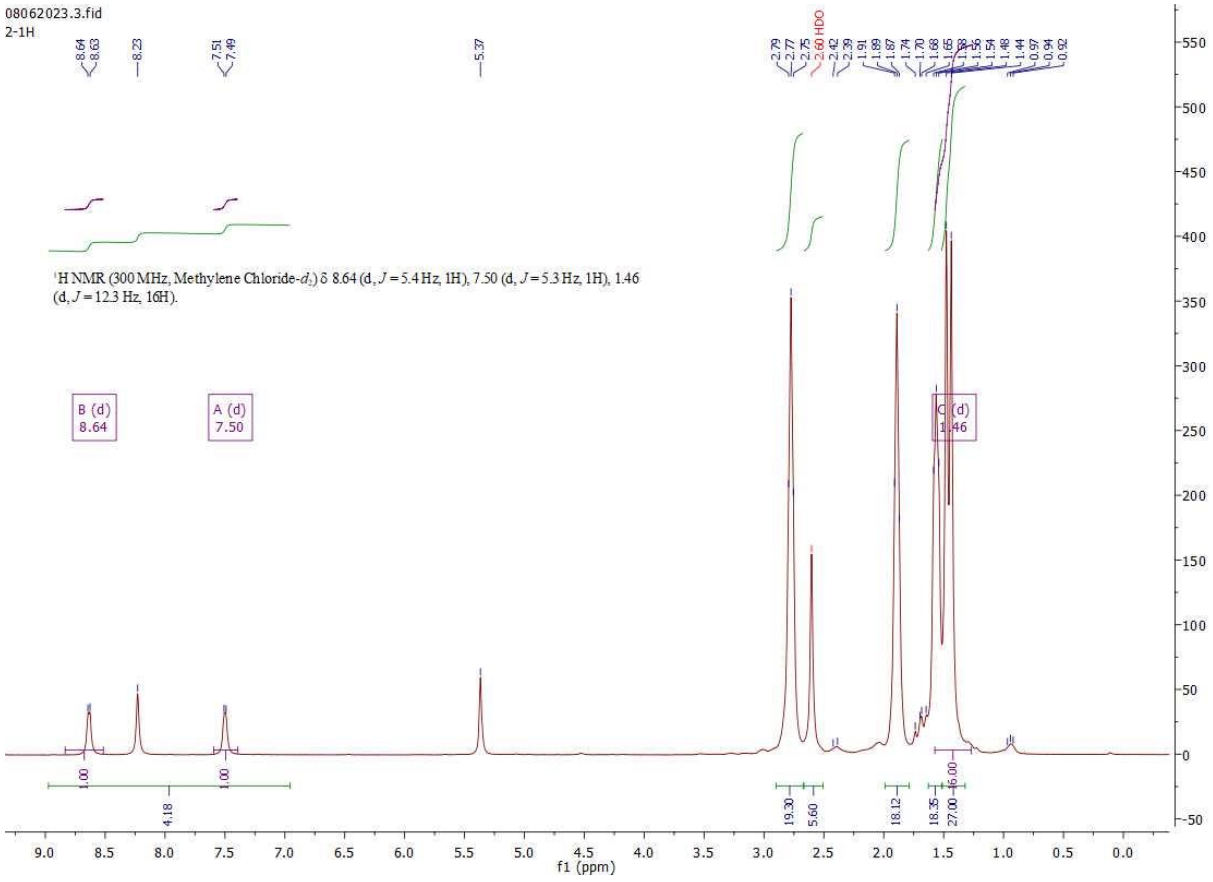
08062023.3.fid
2-1H
8.64
8.63
8.23
7.51
7.49
5.37
2.79
2.77
2.75
2.60 HDO
2.42
2.39
1.91
1.89
1.87
1.74
1.70
1.68
1.65
1.54
1.48
1.44
0.97
0.94
0.92
¹H NMR (300 MHz, Methylene Chloride-d_2) δ 8.64 (d, J = 5.4 Hz, 1H), 7.50 (d, J = 5.3 Hz, 1H), 1.46 (d, J = 12.3 Hz, 16H).
B (d)
8.64
A (d)
7.50
C (d)
1.46
1.00
4.18
1.00
19.30
5.60
18.12
18.35
16.00
27.00
f1 (ppm)

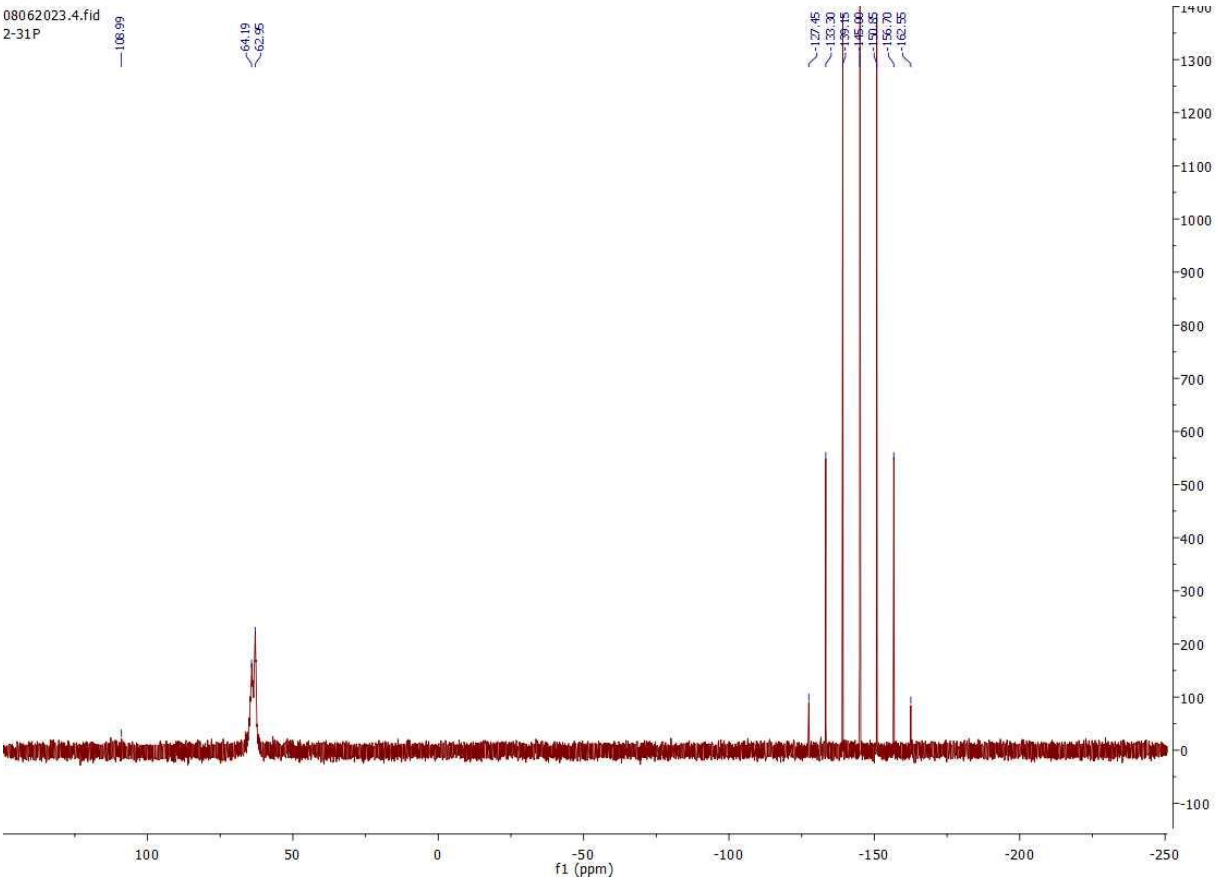

[Cu(Me$_4$phen)(^{t}Bu$_3$P)(tetrahydrothiophene)]PF$_6$

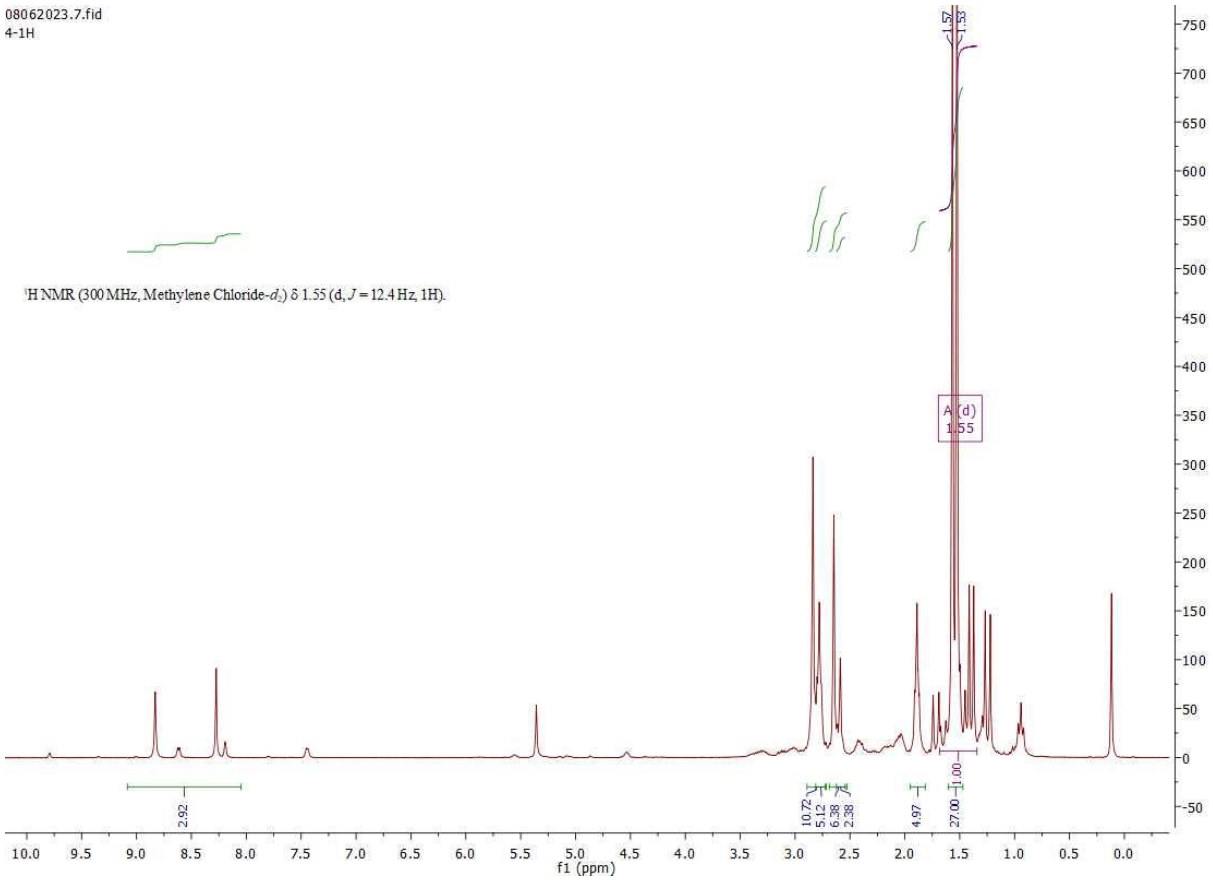
08062023.7.fid
4-1H
¹H NMR (300 MHz, Methylene Chloride-d_2) δ 1.55 (d, J = 12.4 Hz, 1H).
A (d)
1.55
1.57
1.53
2.92
10.72
5.12
5.38
2.38
4.97
27.00
1.00
f1 (ppm)

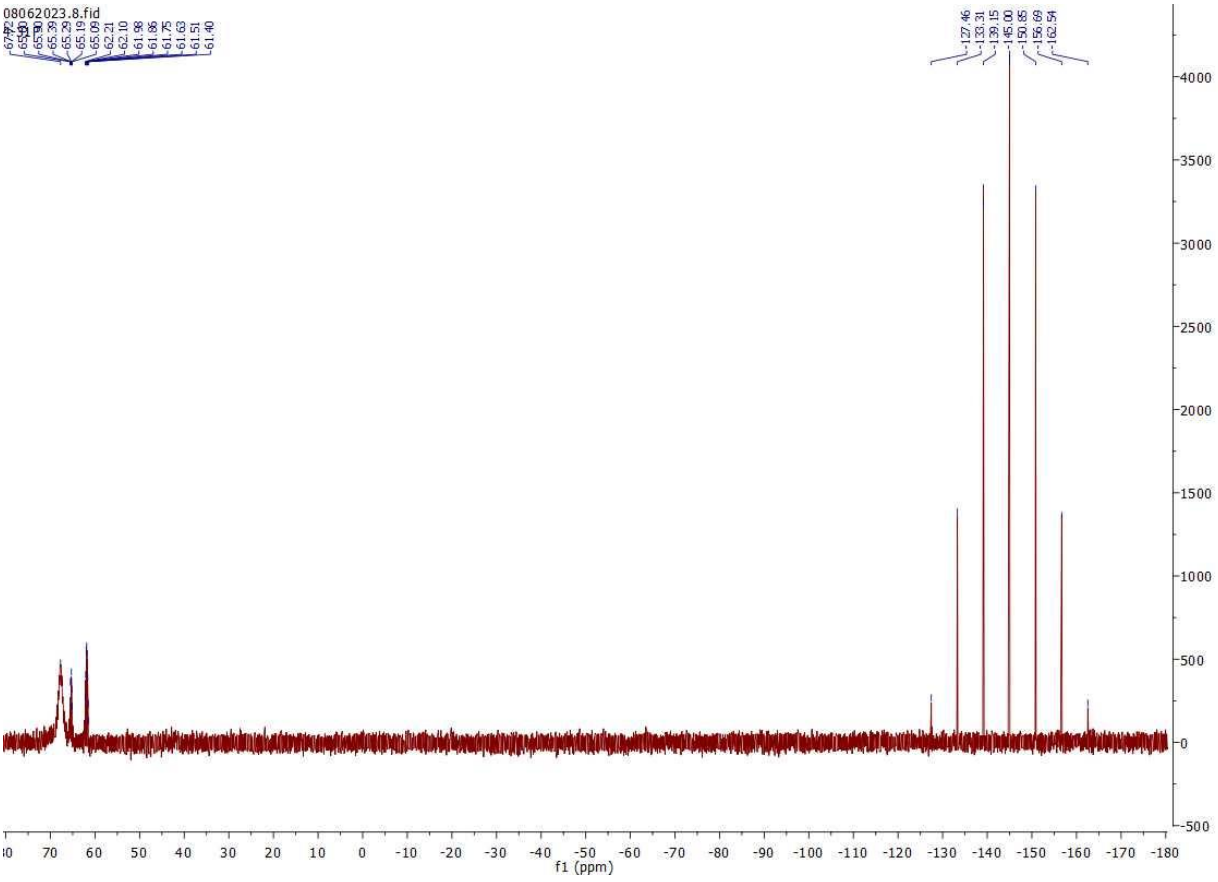

$[[Cu(Me_4phen)(^tBu_3P)]_2N_3]BF_4$

$[Cu(Me_4phen)(^tBu_3P)Ph_3PS]PF_6$

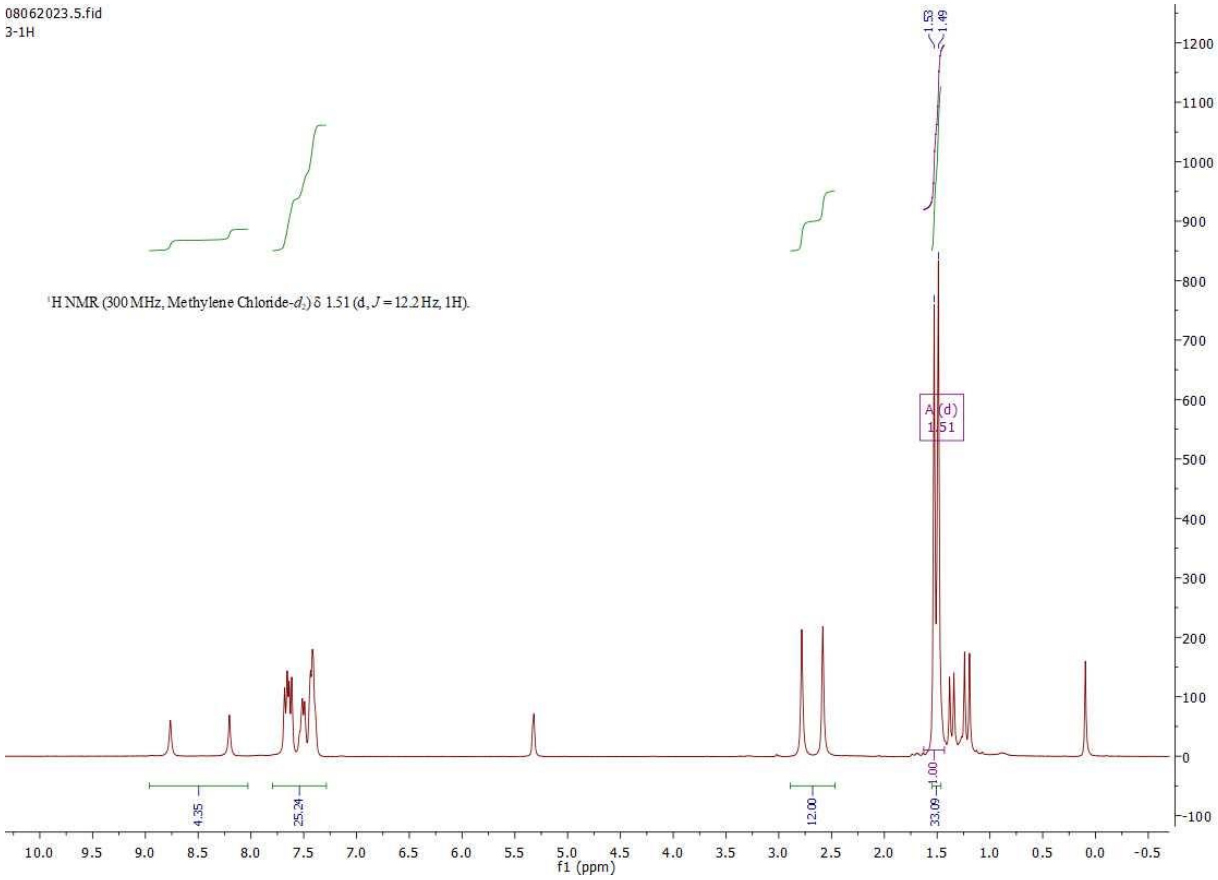
08062023.5.fid
3-1H
¹H NMR (300 MHz, Methylene Chloride-d_2) δ 1.51 (d, J = 12.2 Hz, 1H).
1.53
1.49
A (d)
1.51
4.35
25.24
12.00
33.09
1.00
f1 (ppm)

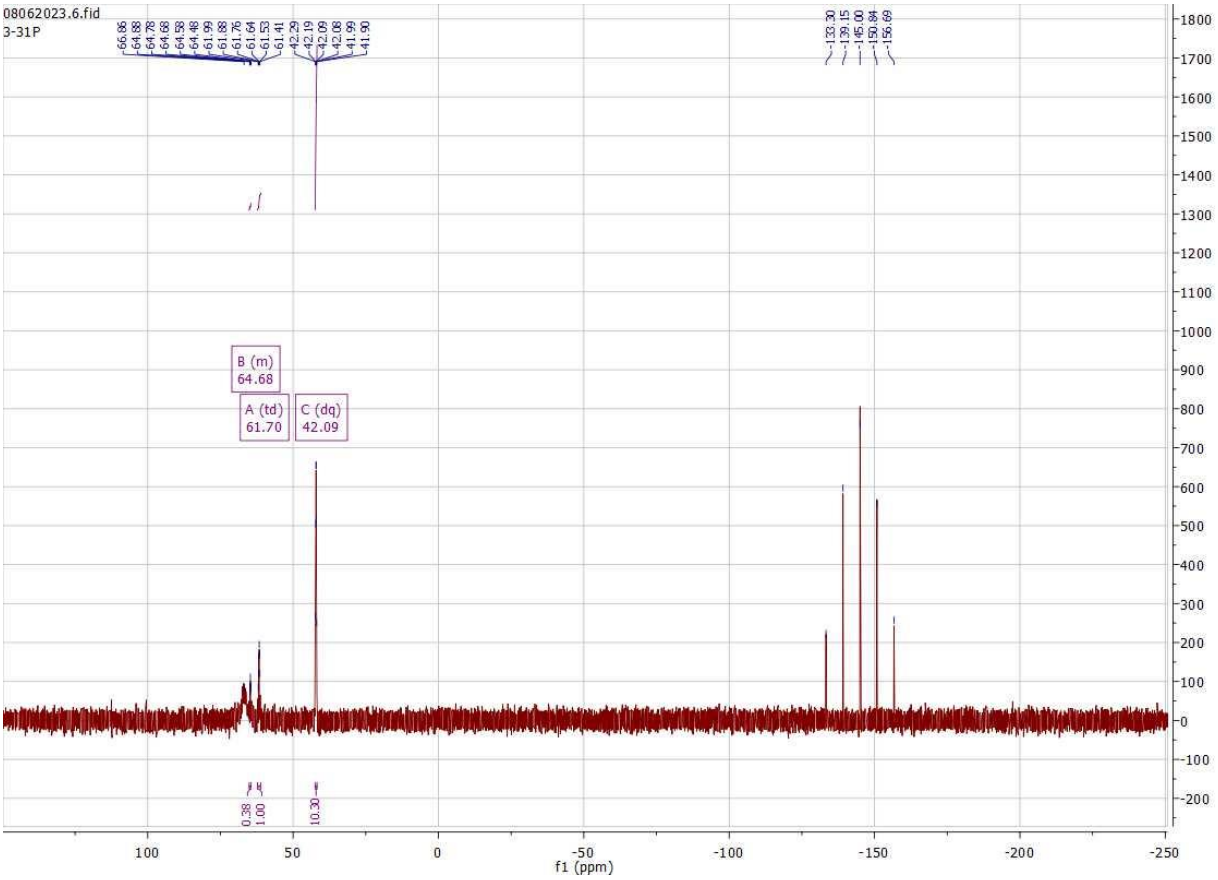

XRD Details:

Crystal Structure Report for [Cu(Me$_4$phen)(^{i}Pr$_3$P)]BF$_4$

A specimen of C21H33CuF6N2P2, approximate dimensions 0.107 mm x 0.185 mm x 0.304 mm, was used for the X-ray crystallographic analysis. The X-ray intensity data were measured on a Bruker Smart APEX CCD system equipped with a fine-focus sealed tube (Mo-Kα, λ = 0.71073 Å) and a graphite monochromator. The frames were integrated with the Bruker SAINT software package using a narrow-frame algorithm. The integration of the data using a triclinic unit cell yielded a total of 23335 reflections to a maximum θ angle of 28.85° (0.74 Å resolution), of which 6369 were independent (average redundancy 3.664, completeness = 98.8%, Rint = 3.36%, Rsig = 3.82%) and 4983 (78.24%) were greater than 2σ(F2). The final cell constants of a = 9.0724(12) Å, b = 9.1353(12) Å, c = 15.618(2) Å, α = 74.169(2)°, β = 81.003(2)°, γ = 83.846(2)°, volume = 1227.1(3) Å3, are based upon the refinement of the XYZ-centroids of reflections above 20 σ(I). Data were corrected for absorption effects using the multi-scan method (SADABS). The calculated minimum and maximum transmission coefficients (based on crystal size) are 0.7350 and 0.8930. The structure was solved and refined using the Bruker SHELXTL Software Package, using the space group P -1, with Z = 2 for the formula unit, C21H33CuF6N2P2. The final anisotropic full-matrix least-squares refinement on F2 with 297 variables converged at R1 = 3.75%, for the observed data and wR2 = 10.13% for all data. The goodness-of-fit was 1.025. The largest peak in the final difference electron density synthesis was 0.822 e-/Å3 and the largest hole was -0.363 e/Å3 with

an RMS deviation of 0.083 e-/Å3. On the basis of the final model, the calculated density was 1.497 g/cm3 and F(000), 572 e-.

Table 1. Sample and crystal data for JPD1051.

Identification code	JPD1051	
Chemical formula	C21H33CuF6N2P2	
Formula weight	552.97 g/mol	
Temperature	150(2) K	
Wavelength	0.71073 Å	
Crystal size	0.107 x 0.185 x 0.304 mm	
Crystal system	triclinic	
Space group	P -1	
Unit cell dimensions	a = 9.0724(12) Å	α = 74.169(2)°
	b = 9.1353(12) Å	β = 81.003(2)°
	c = 15.618(2) Å	γ = 83.846(2)°
Volume	1227.1(3) Å3	
Z	2	
Density (calculated)	1.497 g/cm3	
Absorption coefficient	1.077 mm-1	
F(000)	572	

Table 2. Data collection and structure refinement for JPD1051.

Diffractometer	Bruker Smart APEX CCD
Radiation source	fine-focus sealed tube (Mo-Kα, λ = 0.71073 Å)
Theta range for data collection	2.28 to 28.85°

Index ranges	-12<=h<=12, -12<=k<=12, -21<=l<=21
Reflections collected	23335
Independent reflections	6369 [R(int) = 0.0336]
Absorption correction	multi-scan
Max. and min. transmission	0.8930 and 0.7350
Structure solution technique	direct methods
Structure solution program	SHELXT (Sheldrick, 2015a)
Refinement method	Full-matrix least-squares on F2
Refinement program	SHELXL-2018/1 (Sheldrick, 2015b)
Function minimized	Σ w(Fo2 - Fc2)2
Data / restraints / parameters	6369 / 0 / 297
Goodness-of-fit on F2	1.025
Δ/σmax	0.001
Final R indices	4983 data; I>2σ(I) R1 = 0.0375, wR2 = 0.0979
	all data R1 = 0.0482, wR2 = 0.1013
Weighting scheme	w=1/[σ2(Fo2)+(0.0630P)2] where P=(Fo2+2Fc2)/3
Largest diff. peak and hole	0.822 and -0.363 eÅ-3
R.M.S. deviation from mean	0.083 eÅ-3

Table 3. Atomic coordinates and equivalent isotropic atomic displacement parameters (Å2) for JPD1051.

U(eq) is defined as one third of the trace of the orthogonalized Uij tensor.

	x/a	y/b	z/c	U(eq)
Cu1	0.70223(2)	0.13227(2)	0.30373(2)	0.02286(8)
P1	0.69824(5)	0.19629(5)	0.15962(3)	0.01948(11)
N1	0.79934(17)	0.98949(17)	0.40595(10)	0.0218(3)
N2	0.58599(17)	0.20857(16)	0.40790(10)	0.0219(3)
C1	0.9075(2)	0.8789(2)	0.40050(13)	0.0265(4)
C2	0.9662(2)	0.7864(2)	0.47418(14)	0.0288(4)
C3	0.9155(2)	0.8071(2)	0.55861(13)	0.0265(4)
C4	0.8050(2)	0.9236(2)	0.56431(12)	0.0236(4)
C5	0.7475(2)	0.01147(19)	0.48776(12)	0.0206(4)
C6	0.6260(2)	0.13385(19)	0.48943(12)	0.0201(4)
C7	0.5556(2)	0.1683(2)	0.56737(12)	0.0238(4)
C8	0.4388(2)	0.2826(2)	0.56353(13)	0.0240(4)
C9	0.3999(2)	0.3587(2)	0.47943(13)	0.0250(4)
C10	0.4753(2)	0.3192(2)	0.40399(13)	0.0244(4)
C11	0.9742(2)	0.7073(2)	0.64143(15)	0.0378(5)
C12	0.3590(2)	0.3205(2)	0.64696(14)	0.0333(5)
C13	0.5236(2)	0.1420(2)	0.13308(13)	0.0245(4)
C14	0.3885(2)	0.2048(2)	0.18758(14)	0.0317(4)
C15	0.5055(2)	0.1851(3)	0.03377(14)	0.0352(5)
C16	0.7032(2)	0.4061(2)	0.11008(13)	0.0270(4)
C17	0.7788(3)	0.4802(2)	0.16743(16)	0.0436(6)
C18	0.7721(3)	0.4549(2)	0.01143(14)	0.0349(5)
C19	0.8521(2)	0.1056(2)	0.09527(12)	0.0241(4)
C20	0.0019(2)	0.1372(2)	0.11725(14)	0.0301(4)

	x/a	y/b	z/c	U(eq)
C21	0.8365(2)	0.9338(2)	0.11728(14)	0.0304(4)
P2	0.24345(6)	0.71410(6)	0.23503(4)	0.03075(13)
F1	0.2756(2)	0.55632(17)	0.20961(11)	0.0703(5)
F2	0.41586(17)	0.7472(2)	0.20434(11)	0.0693(5)
F3	0.20812(16)	0.79812(16)	0.13603(9)	0.0496(4)
F4	0.21483(17)	0.87171(14)	0.26274(9)	0.0487(4)
F5	0.07142(15)	0.68276(16)	0.26602(10)	0.0464(3)
F6	0.27784(18)	0.63042(17)	0.33513(9)	0.0568(4)

Table 4. Bond lengths (Å) for JPD1051.

Cu1-N1	2.0208(15)	Cu1-N2	2.0419(15)
Cu1-P1	2.1707(6)	P1-C19	1.8474(19)
P1-C13	1.8478(19)	P1-C16	1.8633(19)
N1-C1	1.342(2)	N1-C5	1.351(2)
N2-C10	1.342(2)	N2-C6	1.355(2)
C1-C2	1.373(3)	C1-H1	0.95
C2-C3	1.383(3)	C2-H2	0.95
C3-C4	1.393(3)	C3-C11	1.502(3)
C4-C5	1.388(2)	C4-H4	0.95
C5-C6	1.486(2)	C6-C7	1.383(2)
C7-C8	1.401(3)	C7-H7	0.95
C8-C9	1.388(3)	C8-C12	1.496(3)
C9-C10	1.383(3)	C9-H9	0.95

C10-H10	0.95	C11-H11A	0.98
C11-H11B	0.98	C11-H11C	0.98
C12-H12A	0.98	C12-H12B	0.98
C12-H12C	0.98	C13-C15	1.523(3)
C13-C14	1.532(3)	C13-H13	1.0
C14-H14A	0.98	C14-H14B	0.98
C14-H14C	0.98	C15-H15A	0.98
C15-H15B	0.98	C15-H15C	0.98
C16-C18	1.532(3)	C16-C17	1.534(3)
C16-H16	1.0	C17-H17A	0.98
C17-H17B	0.98	C17-H17C	0.98
C18-H18A	0.98	C18-H18B	0.98
C18-H18C	0.98	C19-C20	1.527(3)
C19-C21	1.529(3)	C19-H19	1.0
C20-H20A	0.98	C20-H20B	0.98
C20-H20C	0.98	C21-H21A	0.98
C21-H21B	0.98	C21-H21C	0.98
P2-F1	1.5831(15)	P2-F5	1.5924(14)
P2-F3	1.5929(14)	P2-F4	1.5975(14)
P2-F2	1.5988(16)	P2-F6	1.6047(14)

Table 5. Bond angles (°) for JPD1051.

N1-Cu1-N2	80.82(6)	N1-Cu1-P1	144.96(5)
N2-Cu1-P1	134.22(5)	C19-P1-C13	105.80(9)

C19-P1-C16	106.75(9)	C13-P1-C16	106.05(9)
C19-P1-Cu1	114.77(6)	C13-P1-Cu1	110.45(6)
C16-P1-Cu1	112.45(7)	C1-N1-C5	118.16(16)
C1-N1-Cu1	127.16(13)	C5-N1-Cu1	114.68(12)
C10-N2-C6	118.24(16)	C10-N2-Cu1	127.44(13)
C6-N2-Cu1	114.30(12)	N1-C1-C2	123.02(18)
N1-C1-H1	118.5	C2-C1-H1	118.5
C1-C2-C3	119.91(18)	C1-C2-H2	120.0
C3-C2-H2	120.0	C2-C3-C4	117.21(18)
C2-C3-C11	121.96(19)	C4-C3-C11	120.82(19)
C5-C4-C3	120.35(18)	C5-C4-H4	119.8
C3-C4-H4	119.8	N1-C5-C4	121.32(16)
N1-C5-C6	115.51(15)	C4-C5-C6	123.16(16)
N2-C6-C7	121.76(16)	N2-C6-C5	114.67(15)
C7-C6-C5	123.55(16)	C6-C7-C8	120.09(17)
C6-C7-H7	120.0	C8-C7-H7	120.0
C9-C8-C7	117.39(17)	C9-C8-C12	121.41(17)
C7-C8-C12	121.20(17)	C10-C9-C8	119.68(17)
C10-C9-H9	120.2	C8-C9-H9	120.2
N2-C10-C9	122.84(17)	N2-C10-H10	118.6
C9-C10-H10	118.6	C3-C11-H11A	109.5
C3-C11-H11B	109.5	H11A-C11-H11B	109.5
C3-C11-H11C	109.5	H11A-C11-H11C	109.5
H11B-C11-H11C	109.5	C8-C12-H12A	109.5
C8-C12-H12B	109.5	H12A-C12-H12B	109.5

C8-C12-H12C	109.5	H12A-C12-H12C	109.5
H12B-C12-H12C	109.5	C15-C13-C14	110.86(16)
C15-C13-P1	115.45(13)	C14-C13-P1	109.85(13)
C15-C13-H13	106.7	C14-C13-H13	106.7
P1-C13-H13	106.7	C13-C14-H14A	109.5
C13-C14-H14B	109.5	H14A-C14-H14B	109.5
C13-C14-H14C	109.5	H14A-C14-H14C	109.5
H14B-C14-H14C	109.5	C13-C15-H15A	109.5
C13-C15-H15B	109.5	H15A-C15-H15B	109.5
C13-C15-H15C	109.5	H15A-C15-H15C	109.5
H15B-C15-H15C	109.5	C18-C16-C17	110.51(17)
C18-C16-P1	115.29(13)	C17-C16-P1	111.09(14)
C18-C16-H16	106.5	C17-C16-H16	106.5
P1-C16-H16	106.5	C16-C17-H17A	109.5
C16-C17-H17B	109.5	H17A-C17-H17B	109.5
C16-C17-H17C	109.5	H17A-C17-H17C	109.5
H17B-C17-H17C	109.5	C16-C18-H18A	109.5
C16-C18-H18B	109.5	H18A-C18-H18B	109.5
C16-C18-H18C	109.5	H18A-C18-H18C	109.5
H18B-C18-H18C	109.5	C20-C19-C21	110.44(16)
C20-C19-P1	109.44(13)	C21-C19-P1	110.41(13)
C20-C19-H19	108.8	C21-C19-H19	108.8
P1-C19-H19	108.8	C19-C20-H20A	109.5
C19-C20-H20B	109.5	H20A-C20-H20B	109.5
C19-C20-H20C	109.5	H20A-C20-H20C	109.5

H20B-C20-H20C	109.5	C19-C21-H21A	109.5
C19-C21-H21B	109.5	H21A-C21-H21B	109.5
C19-C21-H21C	109.5	H21A-C21-H21C	109.5
H21B-C21-H21C	109.5	F1-P2-F5	90.98(9)
F1-P2-F3	90.87(9)	F5-P2-F3	90.26(8)
F1-P2-F4	178.22(10)	F5-P2-F4	89.99(8)
F3-P2-F4	90.61(8)	F1-P2-F2	89.66(10)
F5-P2-F2	179.36(10)	F3-P2-F2	89.81(8)
F4-P2-F2	89.37(9)	F1-P2-F6	89.54(9)
F5-P2-F6	89.42(8)	F3-P2-F6	179.48(9)
F4-P2-F6	88.98(8)	F2-P2-F6	90.51(9)

Table 6. Torsion angles (°) for JPD1051.

C5-N1-C1-C2	0.8(3)	Cu1-N1-C1-C2	-179.55(13)
N1-C1-C2-C3	-1.1(3)	C1-C2-C3-C4	0.0(3)
C1-C2-C3-C11	178.94(17)	C2-C3-C4-C5	1.3(3)
C11-C3-C4-C5	-177.58(16)	C1-N1-C5-C4	0.6(2)
Cu1-N1-C5-C4	-179.06(12)	C1-N1-C5-C6	-178.98(15)
Cu1-N1-C5-C6	1.34(18)	C3-C4-C5-N1	-1.7(3)
C3-C4-C5-C6	177.85(16)	C10-N2-C6-C7	0.4(2)
Cu1-N2-C6-C7	-178.18(13)	C10-N2-C6-C5	179.00(15)
Cu1-N2-C6-C5	0.46(18)	N1-C5-C6-N2	-1.2(2)
C4-C5-C6-N2	179.22(16)	N1-C5-C6-C7	177.42(16)
C4-C5-C6-C7	-2.2(3)	N2-C6-C7-C8	0.4(3)

C5-C6-C7-C8	-178.12(16)	C6-C7-C8-C9	-0.8(2)
C6-C7-C8-C12	179.02(17)	C7-C8-C9-C10	0.5(3)
C12-C8-C9-C10	-179.33(17)	C6-N2-C10-C9	-0.7(3)
Cu1-N2-C10-C9	177.63(13)	C8-C9-C10-N2	0.3(3)
C19-P1-C13-C15	-56.88(16)	C16-P1-C13-C15	56.26(16)
Cu1-P1-C13-C15	178.36(13)	C19-P1-C13-C14	176.88(13)
C16-P1-C13-C14	-69.97(15)	Cu1-P1-C13-C14	52.12(14)
C19-P1-C16-C18	26.00(18)	C13-P1-C16-C18	-86.49(16)
Cu1-P1-C16-C18	152.70(14)	C19-P1-C16-C17	-100.69(16)
C13-P1-C16-C17	146.82(16)	Cu1-P1-C16-C17	26.01(17)
C13-P1-C19-C20	-176.89(13)	C16-P1-C19-C20	70.45(15)
Cu1-P1-C19-C20	-54.86(14)	C13-P1-C19-C21	-55.12(15)
C16-P1-C19-C21	-167.78(13)	Cu1-P1-C19-C21	66.91(14)

Table 7. Anisotropic atomic displacement parameters (Å2) for JPD1051.

The anisotropic atomic displacement factor exponent takes the form: -2π2[h2 a*2 U11 + ... + 2 h k a* b* U12]

	U11	U22	U33	U23	U13	U12
Cu1	0.02601(14)	0.02612(13)	0.01597(12)	-0.00544(9)	-0.00196(9)	-0.00098(9)
P1	0.0213(2)	0.0197(2)	0.0164(2)	-0.00431(17)	-0.00216(17)	0.00171(16)
N1	0.0204(8)	0.0244(7)	0.0206(8)	-0.0066(6)	-0.0025(6)	0.0000(6)
N2	0.0251(8)	0.0215(7)	0.0182(7)	-0.0043(6)	-0.0025(6)	-0.0012(6)
C1	0.0234(10)	0.0312(10)	0.0260(10)	-0.0112(8)	-0.0012(8)	0.0001(7)
C2	0.0219(10)	0.0248(9)	0.0386(12)	-0.0069(8)	-0.0052(8)	0.0013(7)

	U11	U22	U33	U23	U13	U12
C3	0.0239(10)	0.0232(9)	0.0294(10)	0.0007(7)	-0.0062(8)	-0.0049(7)
C4	0.0245(10)	0.0243(9)	0.0212(9)	-0.0027(7)	-0.0037(7)	-0.0056(7)
C5	0.0217(9)	0.0191(8)	0.0216(9)	-0.0059(7)	-0.0013(7)	-0.0048(6)
C6	0.0228(9)	0.0196(8)	0.0187(9)	-0.0046(7)	-0.0036(7)	-0.0050(6)
C7	0.0303(10)	0.0221(9)	0.0195(9)	-0.0049(7)	-0.0031(7)	-0.0061(7)
C8	0.0262(10)	0.0231(9)	0.0248(10)	-0.0104(7)	0.0014(8)	-0.0060(7)
C9	0.0257(10)	0.0204(8)	0.0291(10)	-0.0082(7)	-0.0015(8)	-0.0007(7)
C10	0.0277(10)	0.0217(9)	0.0232(9)	-0.0045(7)	-0.0051(8)	-0.0005(7)
C11	0.0361(12)	0.0328(11)	0.0393(13)	0.0029(9)	-0.0127(10)	-0.0002(9)
C12	0.0383(12)	0.0345(11)	0.0281(11)	-0.0143(9)	0.0036(9)	-0.0031(9)
C13	0.0216(9)	0.0263(9)	0.0258(10)	-0.0079(7)	-0.0028(7)	0.0001(7)
C14	0.0232(10)	0.0385(11)	0.0321(11)	-0.0105(9)	0.0015(8)	-0.0007(8)
C15	0.0277(11)	0.0525(13)	0.0303(11)	-0.0173(10)	-0.0089(9)	0.0003(9)
C16	0.0302(10)	0.0198(8)	0.0285(10)	-0.0043(7)	-0.0023(8)	0.0018(7)
C17	0.0650(16)	0.0262(10)	0.0430(14)	-0.0110(9)	-0.0079(12)	-0.0114(10)
C18	0.0422(13)	0.0263(10)	0.0295(11)	0.0046(8)	-0.0057(9)	-0.0025(8)
C19	0.0247(10)	0.0266(9)	0.0189(9)	-0.0056(7)	-0.0013(7)	0.0034(7)
C20	0.0239(10)	0.0341(11)	0.0297(10)	-0.0056(8)	-0.0030(8)	0.0019(8)
C21	0.0322(11)	0.0273(10)	0.0321(11)	-0.0113(8)	-0.0039(9)	0.0052(8)
P2	0.0335(3)	0.0286(3)	0.0259(3)	-0.0042(2)	-0.0040(2)	0.0090(2)
F1	0.0991(14)	0.0422(8)	0.0647(11)	-0.0256(8)	0.0040(10)	0.0257(8)
F2	0.0353(8)	0.0955(13)	0.0598(10)	0.0030(9)	-0.0010(7)	0.0034(8)
F3	0.0538(9)	0.0581(9)	0.0300(7)	-0.0046(6)	-0.0102(6)	0.0152(7)
F4	0.0681(10)	0.0321(7)	0.0477(8)	-0.0120(6)	-0.0089(7)	-0.0051(6)

	U11	U22	U33	U23	U13	U12
F5	0.0378(8)	0.0483(8)	0.0538(9)	-0.0190(7)	0.0013(6)	-0.0024(6)
F6	0.0714(10)	0.0534(9)	0.0332(8)	0.0059(6)	-0.0139(7)	0.0158(7)

Table 8. Hydrogen atomic coordinates and isotropic atomic displacement parameters (Å2) for JPD1051.

	x/a	y/b	z/c	U(eq)
H1	0.9452	-0.1362	0.3430	0.032
H2	1.0415	-0.2918	0.4672	0.035
H4	0.7687	-0.0570	0.6209	0.028
H7	0.5864	0.1145	0.6236	0.029
H9	0.3219	0.4375	0.4737	0.03
H10	0.4475	0.3727	0.3469	0.029
H11A	1.0738	-0.3379	0.6248	0.057
H11B	0.9065	-0.3739	0.6704	0.057
H11C	0.9806	-0.2313	0.6831	0.057
H12A	0.4265	0.3698	0.6720	0.05
H12B	0.3274	0.2267	0.6911	0.05
H12C	0.2710	0.3899	0.6324	0.05
H13	0.5245	0.0283	0.1542	0.029
H14A	0.3774	0.3160	0.1649	0.048
H14B	0.4036	0.1780	0.2509	0.048
H14C	0.2979	0.1606	0.1817	0.048
H15A	0.4958	0.2964	0.0114	0.053

	x/a	y/b	z/c	U(eq)
H15B	0.4157	0.1421	0.0258	0.053
H15C	0.5934	0.1446	0.0002	0.053
H16	0.5968	0.4485	0.1126	0.032
H17A	0.8866	0.4525	0.1607	0.065
H17B	0.7367	0.4442	0.2306	0.065
H17C	0.7614	0.5913	0.1476	0.065
H18A	0.7195	0.4105	-0.0247	0.052
H18B	0.8781	0.4191	0.0058	0.052
H18C	0.7629	0.5664	-0.0100	0.052
H19	0.8475	0.1506	0.0297	0.029
H20A	1.0836	0.0908	0.0823	0.045
H20B	1.0074	0.0937	0.1815	0.045
H20C	1.0107	0.2476	0.1021	0.045
H21A	0.7437	-0.0848	0.0984	0.046
H21B	0.8340	-0.1104	0.1821	0.046
H21C	0.9219	-0.1136	0.0854	0.046

Table 9. Hydrogen bond distances (Å) and angles (°) for JPD1051.

	Donor-H	Acceptor-H	Donor-Acceptor	Angle
C1-H1...F5#1	0.95	2.40	3.215(2)	144.2
C9-H9...F6	0.95	2.45	3.099(2)	125.7

Symmetry transformations used to generate equivalent atoms:

#1 x+1, y-1, z

Crystal Structure Report for $[Cu(Me_2bpy)(^tBu_3P)]BF_4$

A specimen of C24H39BCuF4N2P, approximate dimensions 0.197 mm x 0.244 mm x 0.425 mm, was used for the X-ray crystallographic analysis. The X-ray intensity data were measured on a Bruker Smart APEX CCD system equipped with a fine-focus sealed tube (Mo-Kα, λ = 0.71073 Å) and a graphite monochromator. The frames were integrated with the Bruker SAINT software package using a narrow-frame algorithm. The integration of the data using a monoclinic unit cell yielded a total of 49101 reflections to a maximum θ angle of 29.22° (0.73 Å resolution), of which 6920 were independent (average redundancy 7.096, completeness = 99.5%, Rint = 4.61%, Rsig = 3.85%) and 5567 (80.45%) were greater than 2σ(F2). The final cell constants of a = 9.2758(15) Å, b = 16.212(3) Å, c = 17.041(3) Å, β = 92.112(3)°, volume = 2560.9(7) Å3, are based upon the refinement of the XYZ-centroids of reflections above 20 σ(I). Data were corrected for absorption effects using the multi-scan method (SADABS). The calculated minimum and maximum transmission coefficients (based on crystal size) are 0.6860 and 0.8340. The structure was solved and refined using the Bruker SHELXTL Software Package, using the space group P 1 21/n 1, with Z = 4 for the formula unit, C24H39BCuF4N2P. The final anisotropic full-matrix least-squares refinement on F2 with 309 variables converged at R1 = 4.08%, for the observed data and wR2 = 11.23% for all data. The goodness-of-fit was 1.030. The largest peak in the final difference electron density synthesis was 1.215 e-/Å3 and the largest hole was -0.381 e-/Å3 with an RMS deviation of 0.089 e-/Å3. On the basis of the final model, the calculated density was 1.393 g/cm3 and F(000), 1128 e-.

Table 1. Sample and crystal data for JPD1050.

Identification code	JPD1050
Chemical formula	C24H39BCuF4N2P
Formula weight	536.89 g/mol
Temperature	150(2) K
Wavelength	0.71073 Å
Crystal size	0.197 x 0.244 x 0.425 mm
Crystal system	monoclinic
Space group	P 1 21/n 1
Unit cell dimensions	a = 9.2758(15) Å α = 90°
	b = 16.212(3) Å β = 92.112(3)°
	c = 17.041(3) Å γ = 90°
Volume	2560.9(7) Å3

Z	4
Density (calculated)	1.393 g/cm3
Absorption coefficient	0.959 mm-1
F(000)	1128

Table 2. Data collection and structure refinement for JPD1050.

Diffractometer	Bruker Smart APEX CCD
Radiation source	fine-focus sealed tube (Mo-Kα, λ = 0.71073 Å)
Theta range for data collection	1.73 to 29.22°
Index ranges	-12<=h<=12, -22<=k<=22, -23<=l<=23
Reflections collected	49101
Independent reflections	6920 [R(int) = 0.0461]
Absorption correction	multi-scan
Max. and min. transmission	0.8340 and 0.6860
Structure solution technique	direct methods
Structure solution program	SHELXT (Sheldrick, 2015a)
Refinement method	Full-matrix least-squares on F2
Refinement program	SHELXL-2018/1 (Sheldrick, 2015b)
Function minimized	Σ w(Fo2 - Fc2)2
Data / restraints / parameters	6920 / 0 / 309
Goodness-of-fit on F2	1.030
Δ/σmax	0.001
Final R indices	5567 data; I>2σ(I) R1 = 0.0408, wR2 = 0.1074
all data	R1 = 0.0516, wR2 = 0.1123
Weighting scheme	w=1/[σ2(Fo2)+(0.0710P)2+0.4945P]
where P=(Fo2+2Fc2)/3	
Largest diff. peak and hole	1.215 and -0.381 eÅ-3
R.M.S. deviation from mean	0.089 eÅ-3

Table 3. Atomic coordinates and equivalent isotropic atomic displacement parameters (Å2) for JPD1050. U(eq) is defined as one third of the trace of the orthogonalized Uij tensor.

x/a	y/b	z/c	U(eq)
Cu1	0.66643(2)	0.53128(2)	0.68510(2)	0.01870(8)
P1	0.65280(5)	0.59126(3)	0.79970(2)	0.01678(10)
N1	0.56879(15)	0.43384(9)	0.62722(8)	0.0185(3)
N2	0.76394(16)	0.54088(8)	0.58072(8)	0.0188(3)
C1	0.47553(19)	0.37927(11)	0.65534(10)	0.0209(3)
C2	0.41593(18)	0.31540(10)	0.61040(10)	0.0207(3)
C3	0.45431(18)	0.30632(10)	0.53322(10)	0.0199(3)
C4	0.55233(18)	0.36292(10)	0.50383(10)	0.0190(3)
C5	0.60731(17)	0.42557(10)	0.55174(9)	0.0165(3)
C6	0.71429(18)	0.48712(10)	0.52490(10)	0.0168(3)
C7	0.76129(19)	0.48942(10)	0.44899(10)	0.0190(3)
C8	0.86271(19)	0.54808(11)	0.42720(10)	0.0207(3)
C9	0.91370(19)	0.60225(11)	0.48481(11)	0.0228(4)
C10	0.86345(19)	0.59639(11)	0.56018(11)	0.0224(3)
C11	0.3956(2)	0.23658(11)	0.48297(11)	0.0269(4)
C12	0.9125(2)	0.55189(13)	0.34446(11)	0.0286(4)
C13	0.4763(2)	0.56201(11)	0.84573(10)	0.0233(4)
C14	0.4309(2)	0.61600(13)	0.91472(11)	0.0297(4)
C15	0.4850(2)	0.47173(12)	0.87305(12)	0.0295(4)
C16	0.3558(2)	0.56442(13)	0.78087(12)	0.0300(4)
C17	0.8106(2)	0.55361(11)	0.86531(10)	0.0234(4)
C18	0.7956(2)	0.56811(13)	0.95369(11)	0.0306(4)
C19	0.8323(2)	0.46106(12)	0.84953(13)	0.0317(4)
C20	0.9508(2)	0.59587(13)	0.84010(12)	0.0296(4)
C21	0.66067(19)	0.70763(10)	0.78999(10)	0.0220(3)

C22	0.5173(2)	0.73868(12)	0.75263(12)	0.0304(4)
C23	0.7761(2)	0.73063(12)	0.73158(12)	0.0295(4)
C24	0.6914(2)	0.75407(11)	0.86771(11)	0.0261(4)
F1	0.33518(18)	0.29285(11)	0.79408(9)	0.0615(5)
F2	0.3354(2)	0.17071(10)	0.85364(12)	0.0868(7)
F3	0.47006(16)	0.27374(9)	0.90499(10)	0.0541(4)
F4	0.2281(2)	0.27929(16)	0.90696(11)	0.0968(8)
B1	0.3432(3)	0.25444(14)	0.86466(13)	0.0300(5)

Table 4. Bond lengths (Å) for JPD1050.

Cu1-N2	2.0309(15)	Cu1-N1	2.0550(14)
Cu1-P1	2.1895(5)	P1-C21	1.8954(18)
P1-C13	1.9014(19)	P1-C17	1.9091(18)
N1-C1	1.338(2)	N1-C5	1.354(2)
N2-C10	1.345(2)	N2-C6	1.358(2)
C1-C2	1.390(2)	C1-H1	0.95
C2-C3	1.383(2)	C2-H2	0.95
C3-C4	1.397(2)	C3-C11	1.508(2)
C4-C5	1.388(2)	C4-H4	0.95
C5-C6	1.491(2)	C6-C7	1.381(2)
C7-C8	1.398(2)	C7-H7	0.95
C8-C9	1.387(2)	C8-C12	1.501(2)
C9-C10	1.386(2)	C9-H9	0.95
C10-H10	0.95	C11-H11A	0.98
C11-H11B	0.98	C11-H11C	0.98
C12-H12A	0.98	C12-H12B	0.98
C12-H12C	0.98	C13-C15	1.537(3)
C13-C14	1.537(2)	C13-C16	1.543(3)
C14-H14A	0.98	C14-H14B	0.98

C14-H14C	0.98	C15-H15A	0.98
C15-H15B	0.98	C15-H15C	0.98
C16-H16A	0.98	C16-H16B	0.98
C16-H16C	0.98	C17-C18	1.536(2)
C17-C19	1.539(2)	C17-C20	1.545(3)
C18-H18A	0.98	C18-H18B	0.98
C18-H18C	0.98	C19-H19A	0.98
C19-H19B	0.98	C19-H19C	0.98
C20-H20A	0.98	C20-H20B	0.98
C20-H20C	0.98	C21-C23	1.535(3)
C21-C22	1.538(3)	C21-C24	1.541(2)
C22-H22A	0.98	C22-H22B	0.98
C22-H22C	0.98	C23-H23A	0.98
C23-H23B	0.98	C23-H23C	0.98
C24-H24A	0.98	C24-H24B	0.98
C24-H24C	0.98	F1-B1	1.354(3)
F2-B1	1.372(3)	F3-B1	1.377(3)
F4-B1	1.370(3)		

Table 5. Bond angles (°) for JPD1050.

N2-Cu1-N1	80.86(6)	N2-Cu1-P1	142.13(4)
N1-Cu1-P1	136.94(4)	C21-P1-C13	108.71(8)
C21-P1-C17	109.77(8)	C13-P1-C17	109.38(8)
C21-P1-Cu1	111.13(6)	C13-P1-Cu1	109.64(6)
C17-P1-Cu1	108.19(6)	C1-N1-C5	118.12(14)
C1-N1-Cu1	127.99(12)	C5-N1-Cu1	113.88(11)
C10-N2-C6	117.74(15)	C10-N2-Cu1	127.69(12)
C6-N2-Cu1	114.45(11)	N1-C1-C2	122.97(16)
N1-C1-H1	118.5	C2-C1-H1	118.5

C3-C2-C1	119.48(16)	C3-C2-H2	120.3
C1-C2-H2	120.3	C2-C3-C4	117.68(15)
C2-C3-C11	121.30(16)	C4-C3-C11	121.00(16)
C5-C4-C3	119.97(15)	C5-C4-H4	120.0
C3-C4-H4	120.0	N1-C5-C4	121.79(15)
N1-C5-C6	115.28(14)	C4-C5-C6	122.92(15)
N2-C6-C7	121.89(15)	N2-C6-C5	115.27(14)
C7-C6-C5	122.83(15)	C6-C7-C8	120.41(16)
C6-C7-H7	119.8	C8-C7-H7	119.8
C9-C8-C7	117.26(16)	C9-C8-C12	122.00(16)
C7-C8-C12	120.74(16)	C10-C9-C8	119.67(16)
C10-C9-H9	120.2	C8-C9-H9	120.2
N2-C10-C9	123.00(16)	N2-C10-H10	118.5
C9-C10-H10	118.5	C3-C11-H11A	109.5
C3-C11-H11B	109.5	H11A-C11-H11B	109.5
C3-C11-H11C	109.5	H11A-C11-H11C	109.5
H11B-C11-H11C	109.5	C8-C12-H12A	109.5
C8-C12-H12B	109.5	H12A-C12-H12B	109.5
C8-C12-H12C	109.5	H12A-C12-H12C	109.5
H12B-C12-H12C	109.5	C15-C13-C14	108.86(15)
C15-C13-C16	105.65(16)	C14-C13-C16	108.77(16)
C15-C13-P1	109.03(13)	C14-C13-P1	115.98(13)
C16-C13-P1	108.06(12)	C13-C14-H14A	109.5
C13-C14-H14B	109.5	H14A-C14-H14B	109.5
C13-C14-H14C	109.5	H14A-C14-H14C	109.5
H14B-C14-H14C	109.5	C13-C15-H15A	109.5
C13-C15-H15B	109.5	H15A-C15-H15B	109.5
C13-C15-H15C	109.5	H15A-C15-H15C	109.5
H15B-C15-H15C	109.5	C13-C16-H16A	109.5

C13-C16-H16B	109.5	H16A-C16-H16B	109.5
C13-C16-H16C	109.5	H16A-C16-H16C	109.5
H16B-C16-H16C	109.5	C18-C17-C19	109.75(16)
C18-C17-C20	108.21(16)	C19-C17-C20	105.48(15)
C18-C17-P1	115.48(13)	C19-C17-P1	108.16(13)
C20-C17-P1	109.30(13)	C17-C18-H18A	109.5
C17-C18-H18B	109.5	H18A-C18-H18B	109.5
C17-C18-H18C	109.5	H18A-C18-H18C	109.5
H18B-C18-H18C	109.5	C17-C19-H19A	109.5
C17-C19-H19B	109.5	H19A-C19-H19B	109.5
C17-C19-H19C	109.5	H19A-C19-H19C	109.5
H19B-C19-H19C	109.5	C17-C20-H20A	109.5
C17-C20-H20B	109.5	H20A-C20-H20B	109.5
C17-C20-H20C	109.5	H20A-C20-H20C	109.5
H20B-C20-H20C	109.5	C23-C21-C22	105.39(15)
C23-C21-C24	109.10(15)	C22-C21-C24	109.01(15)
C23-C21-P1	109.18(12)	C22-C21-P1	109.06(12)
C24-C21-P1	114.70(13)	C21-C22-H22A	109.5
C21-C22-H22B	109.5	H22A-C22-H22B	109.5
C21-C22-H22C	109.5	H22A-C22-H22C	109.5
H22B-C22-H22C	109.5	C21-C23-H23A	109.5
C21-C23-H23B	109.5	H23A-C23-H23B	109.5
C21-C23-H23C	109.5	H23A-C23-H23C	109.5
H23B-C23-H23C	109.5	C21-C24-H24A	109.5
C21-C24-H24B	109.5	H24A-C24-H24B	109.5
C21-C24-H24C	109.5	H24A-C24-H24C	109.5
H24B-C24-H24C	109.5	F1-B1-F4	108.3(2)
F1-B1-F2	109.4(2)	F4-B1-F2	109.0(2)
F1-B1-F3	110.89(18)	F4-B1-F3	109.79(19)

F2-B1-F3 109.45(19)

Table 6. Torsion angles (°) for JPD1050.

C5-N1-C1-C2	-0.6(2)	Cu1-N1-C1-C2	179.98(13)
N1-C1-C2-C3	0.6(3)	C1-C2-C3-C4	-0.2(2)
C1-C2-C3-C11	178.29(16)	C2-C3-C4-C5	-0.1(2)
C11-C3-C4-C5	-178.62(15)	C1-N1-C5-C4	0.3(2)
Cu1-N1-C5-C4	179.76(12)	C1-N1-C5-C6	-178.51(14)
Cu1-N1-C5-C6	0.96(17)	C3-C4-C5-N1	0.1(2)
C3-C4-C5-C6	178.79(15)	C10-N2-C6-C7	-1.1(2)
Cu1-N2-C6-C7	175.14(12)	C10-N2-C6-C5	178.35(14)
Cu1-N2-C6-C5	-5.40(18)	N1-C5-C6-N2	2.9(2)
C4-C5-C6-N2	-175.84(15)	N1-C5-C6-C7	-177.61(15)
C4-C5-C6-C7	3.6(2)	N2-C6-C7-C8	-0.1(2)
C5-C6-C7-C8	-179.47(15)	C6-C7-C8-C9	0.6(2)
C6-C7-C8-C12	-178.99(16)	C7-C8-C9-C10	0.0(3)
C12-C8-C9-C10	179.59(17)	C6-N2-C10-C9	1.8(3)
Cu1-N2-C10-C9	-173.92(13)	C8-C9-C10-N2	-1.2(3)
C13-P1-C21-C23	-162.86(12)	C17-P1-C21-C23	77.54(14)
Cu1-P1-C21-C23	-42.11(14)	C13-P1-C21-C22	-48.19(14)
C17-P1-C21-C22	-167.80(12)	Cu1-P1-C21-C22	72.56(13)
C13-P1-C21-C24	74.37(14)	C17-P1-C21-C24	-45.23(15)
Cu1-P1-C21-C24	-164.88(11)		

Table 7. Anisotropic atomic displacement parameters (Å2) for JPD1050.

The anisotropic atomic displacement factor exponent takes the form: -2π2[h2 a*2 U11 + ... + 2 h k a* b* U12]

	U11	U22	U33	U23	U13	U12
Cu1	0.02302(13)	0.02020(12)	0.01295(12)	-0.00274(7)	0.00166(8)	0.00012(7)

P1	0.0199(2)	0.0176(2)	0.0128(2)	-0.00167(14)	0.00146(16)	0.00004(15)
N1	0.0207(7)	0.0191(7)	0.0160(7)	-0.0013(5)	0.0023(5)	0.0002(5)
N2	0.0205(7)	0.0207(7)	0.0152(7)	-0.0013(5)	0.0015(5)	-0.0012(5)
C1	0.0227(8)	0.0241(8)	0.0161(8)	0.0007(6)	0.0042(6)	-0.0002(6)
C2	0.0211(8)	0.0198(8)	0.0213(8)	0.0026(6)	0.0021(7)	-0.0009(6)
C3	0.0213(8)	0.0170(7)	0.0212(8)	-0.0002(6)	-0.0034(7)	0.0019(6)
C4	0.0244(8)	0.0187(8)	0.0140(7)	-0.0012(6)	0.0003(6)	0.0018(6)
C5	0.0174(8)	0.0171(7)	0.0150(7)	0.0004(6)	0.0005(6)	0.0020(6)
C6	0.0176(8)	0.0167(7)	0.0160(8)	0.0001(6)	0.0000(6)	0.0025(6)
C7	0.0206(8)	0.0206(8)	0.0159(8)	-0.0010(6)	0.0013(6)	0.0017(6)
C8	0.0205(8)	0.0232(8)	0.0185(8)	0.0015(6)	0.0030(7)	0.0026(6)
C9	0.0217(9)	0.0224(8)	0.0245(9)	0.0001(7)	0.0038(7)	-0.0031(6)
C10	0.0214(8)	0.0237(8)	0.0224(9)	-0.0026(7)	0.0020(7)	-0.0020(6)
C11	0.0354(10)	0.0228(9)	0.0223(9)	-0.0032(7)	-0.0013(8)	-0.0053(7)
C12	0.0289(10)	0.0358(10)	0.0217(9)	-0.0003(7)	0.0076(8)	-0.0038(8)
C13	0.0243(9)	0.0275(9)	0.0182(8)	-0.0025(7)	0.0042(7)	-0.0029(7)
C14	0.0311(10)	0.0361(10)	0.0225(9)	-0.0071(8)	0.0108(8)	-0.0024(8)
C15	0.0370(11)	0.0298(10)	0.0222(9)	-0.0010(7)	0.0068(8)	-0.0071(8)
C16	0.0210(9)	0.0410(11)	0.0279(10)	-0.0051(8)	0.0009(7)	-0.0040(8)
C17	0.0261(9)	0.0257(9)	0.0183(8)	-0.0013(7)	-0.0018(7)	0.0054(7)
C18	0.0346(11)	0.0386(11)	0.0180(9)	0.0001(8)	-0.0049(8)	0.0049(8)
C19	0.0390(12)	0.0252(9)	0.0305(11)	-0.0002(7)	-0.0034(9)	0.0101(8)
C20	0.0251(9)	0.0347(10)	0.0288(10)	-0.0058(8)	-0.0007(8)	0.0042(8)
C21	0.0258(9)	0.0183(8)	0.0220(9)	-0.0029(6)	0.0004(7)	0.0005(6)
C22	0.0334(10)	0.0249(9)	0.0327(10)	0.0018(8)	-0.0026(8)	0.0056(7)
C23	0.0381(11)	0.0224(9)	0.0283(10)	0.0007(7)	0.0073(8)	-0.0026(7)
C24	0.0281(9)	0.0234(8)	0.0268(9)	-0.0093(7)	0.0014(7)	-0.0004(7)
F1	0.0744(11)	0.0691(11)	0.0407(8)	0.0270(7)	-0.0028(7)	-0.0257(8)
F2	0.1267(17)	0.0295(8)	0.0997(15)	0.0060(8)	-0.0574(13)	-0.0196(9)

F3	0.0488(8)	0.0401(7)	0.0713(10)	-0.0070(7)	-0.0250(7)	-0.0010(6)
F4	0.0551(11)	0.173(2)	0.0648(12)	-0.0302(14)	0.0295(9)	-0.0082(13)
B1	0.0352(12)	0.0279(11)	0.0268(11)	0.0043(8)	0.0027(9)	-0.0069(9)

Table 8. Hydrogen atomic coordinates and isotropic atomic displacement parameters (Å2) for JPD1050.

x/a	y/b	z/c	U(eq)
H1	0.4488	0.3844	0.7084	0.025
H2	0.3494	0.2783	0.6325	0.025
H4	0.5813	0.3585	0.4511	0.023
H7	0.7244	0.4509	0.4113	0.023
H9	0.9827	0.6432	0.4726	0.027
H10	0.9010	0.6333	0.5991	0.027
H11A	0.2980	0.2504	0.4632	0.04
H11B	0.3924	0.1861	0.5144	0.04
H11C	0.4581	0.2280	0.4386	0.04
H12A	0.9097	0.4965	0.3215	0.043
H12B	1.0115	0.5731	0.3446	0.043
H12C	0.8489	0.5886	0.3133	0.043
H14A	0.4110	0.6722	0.8960	0.044
H14B	0.5089	0.6173	0.9551	0.044
H14C	0.3438	0.5929	0.9371	0.044
H15A	0.3888	0.4527	0.8866	0.044
H15B	0.5507	0.4675	0.9192	0.044
H15C	0.5210	0.4374	0.8307	0.044
H16A	0.3339	0.6219	0.7671	0.045
H16B	0.2690	0.5377	0.7999	0.045
H16C	0.3880	0.5352	0.7343	0.045
H18A	0.7847	0.6273	0.9637	0.046
H18B	0.8819	0.5476	0.9823	0.046

H18C	0.7105	0.5387	0.9716	0.046
H19A	0.8372	0.4518	0.7929	0.048
H19B	0.7511	0.4299	0.8698	0.048
H19C	0.9223	0.4425	0.8758	0.048
H20A	0.9579	0.5917	0.7830	0.044
H20B	1.0341	0.5686	0.8659	0.044
H20C	0.9494	0.6541	0.8554	0.044
H22A	0.5273	0.7968	0.7378	0.046
H22B	0.4409	0.7332	0.7905	0.046
H22C	0.4925	0.7058	0.7058	0.046
H23A	0.7555	0.7026	0.6815	0.044
H23B	0.8712	0.7136	0.7527	0.044
H23C	0.7755	0.7904	0.7233	0.044
H24A	0.6861	0.8136	0.8582	0.039
H24B	0.7881	0.7397	0.8886	0.039
H24C	0.6196	0.7384	0.9058	0.039

Table 9. Hydrogen bond distances (Å) and angles (°) for JPD1050.

Donor-H	Acceptor-H		Donor-Acceptor	Angle
C1-H1...F1	0.95	2.36	3.078(2)	132.2
C7-H7...F2#1	0.95	2.45	3.152(2)	130.9

Symmetry transformations used to generate equivalent atoms:

#1 x+1/2, -y+1/2, z-1/2

Crystal Structure Report for JPD1049

A yellow-orange plate-like specimen of C58H90BCl4Cu2F4N7P2, approximate dimensions 0.064 mm x 0.189 mm x 0.366 mm, was used for the X-ray crystallographic analysis. The X-ray intensity data were measured on a Bruker D8 VENTURE PHOTON 100 CMOS system equipped with a INCOATEC IμS micro--focus source (Cu-Kα, λ = 1.54178 Å) and a mirror monochromator.

Table 1: Data collection details for JPD1049.

Axis	dx/mm	2θ/°	ω/°	ϕ/°	χ/°	Width/°	Frames	Time/s	Wavelength/Å	Voltage/kV	
	Current/mA		Temperature/K								
Omega	40.074	85.20	-87.30	71.17	54.74	0.50	330	20.00	1.54184	50	1.0
	n/a										
Omega	40.074	104.95	-66.55	-160.00	54.74	0.50	326	20.00	1.54184	50	1.0
	n/a										
Omega	40.074	104.95	-66.55	-40.00	54.74	0.50	326	20.00	1.54184	50	1.0
	n/a										
Omega	40.074	4.97	-166.53	0.00	54.74	0.50	326	10.00	1.54184	50	1.0
	n/a										
Omega	40.074	104.95	-66.55	-80.00	54.74	0.50	326	20.00	1.54184	50	1.0
	n/a										
Omega	40.074	104.95	-66.55	160.00	54.74	0.50	326	20.00	1.54184	50	1.0
	n/a										

A total of 1960 frames were collected. The total exposure time was 9.98 hours. The frames were integrated with the Bruker SAINT software package using a narrow-frame algorithm. The integration of the data using a triclinic unit cell yielded a total of 36011 reflections to a maximum θ angle of 70.47° (0.82 Å resolution), of which 36011 were independent (average redundancy 1.000, completeness = 90.2%, Rsig = 6.88%) and 28263 (78.48%) were greater than 2σ(F2). The final cell constants of a = 13.2481(5) Å, b = 13.6667(5) Å, c = 18.5159(6) Å, α = 78.779(2)°, β = 78.930(2)°, γ = 81.571(2)°, volume = 3206.3(2) Å3, are based upon the refinement of the XYZ-centroids of 9866 reflections above 20 σ(I) with 6.636° < 2θ < 140.9°. Data were corrected for absorption effects using the multi-scan method (SADABS). The calculated minimum and maximum transmission coefficients (based on crystal size) are 0.3820 and 0.8190. The final anisotropic full-matrix least-squares refinement on F2 with 730 variables converged at R1 = 5.62%, for the observed data and wR2 = 15.02% for all data. The goodness-of-fit was 1.023. The largest peak in the final difference electron density synthesis was 0.884 e-/Å3 and the largest hole was -0.971 e-/Å3 with an RMS deviation of 0.090 e-/Å3. On the basis of the final model, the calculated density was 1.350 g/cm3 and F(000), 1368 e-.

Table 2. Sample and crystal data for JPD1049.

Identification code	JPD1049
Chemical formula	C58H90BCl4Cu2F4N7P2
Formula weight	1302.99 g/mol
Temperature	150(2) K
Wavelength	1.54178 Å
Crystal size	0.064 x 0.189 x 0.366 mm

Crystal habit	yellow-orange plate
Crystal system	triclinic
Space group	P -1
Unit cell dimensions	a = 13.2481(5) Å α = 78.779(2)°
	b = 13.6667(5) Å β = 78.930(2)°
	c = 18.5159(6) Å γ = 81.571(2)°
Volume	3206.3(2) Å3
Z	2
Density (calculated)	1.350 g/cm3
Absorption coefficient	3.255 mm-1
F(000)	1368

Table 3. Data collection and structure refinement for JPD1049.

Diffractometer	Bruker D8 VENTURE PHOTON 100 CMOS
Radiation source	INCOATEC IμS micro--focus source (Cu-Kα, λ = 1.54178 Å)
Theta range for data collection	3.32 to 70.47°
Index ranges	-16<=h<=16, -16<=k<=16, -22<=l<=22
Reflections collected	36011
Coverage of independent reflections	90.2%
Absorption correction	multi-scan
Max. and min. transmission	0.8190 and 0.3820
Refinement method	Full-matrix least-squares on F2
Refinement program	SHELXL-2018/3 (Sheldrick, 2018)
Function minimized	Σ w(Fo2 - Fc2)2
Data / restraints / parameters	36011 / 0 / 730
Goodness-of-fit on F2	1.023
Δ/σmax	0.001
Final R indices	28263 data; I>2σ(I) R1 = 0.0562, wR2 = 0.1378
all data	R1 = 0.0744, wR2 = 0.1502

Weighting scheme	w=1/[σ2(Fo2)+(0.0628P)2+2.7406P]
where P=(Fo2+2Fc2)/3	
Largest diff. peak and hole	0.884 and -0.971 eÅ-3
R.M.S. deviation from mean	0.090 eÅ-3

Table 4. Atomic coordinates and equivalent isotropic atomic displacement parameters (Å2) for JPD1049. U(eq) is defined as one third of the trace of the orthogonalized Uij tensor.

x/a	y/b	z/c	U(eq)
Cu1	0.56966(4)	0.66399(4)	0.69198(3)	0.02345(15)
Cu2	0.82552(5)	0.24444(4)	0.72013(3)	0.02615(16)
P1	0.47193(8)	0.67440(7)	0.80141(5)	0.0218(2)
P2	0.86885(8)	0.17086(7)	0.82916(5)	0.0248(2)
N1	0.6648(2)	0.7687(2)	0.62326(18)	0.0215(7)
N2	0.5238(2)	0.6722(2)	0.58769(17)	0.0208(7)
N3	0.9220(3)	0.2843(2)	0.61761(19)	0.0242(7)
N4	0.7605(3)	0.1764(2)	0.64842(18)	0.0247(7)
N5	0.6835(3)	0.5429(3)	0.6817(3)	0.0446(11)
N6	0.7021(3)	0.4572(3)	0.70160(19)	0.0269(7)
N7	0.7192(3)	0.3709(3)	0.7212(2)	0.0435(10)
C1	0.7336(3)	0.8172(3)	0.6412(2)	0.0243(8)
C2	0.8070(3)	0.8702(3)	0.5896(2)	0.0239(8)
C3	0.8096(3)	0.8724(3)	0.5145(2)	0.0248(8)
C4	0.7364(3)	0.8218(3)	0.4930(2)	0.0225(8)
C5	0.7330(3)	0.8167(3)	0.4170(2)	0.0276(9)
C6	0.6625(3)	0.7670(3)	0.3989(2)	0.0261(9)
C7	0.5865(3)	0.7178(3)	0.4550(2)	0.0219(8)
C8	0.5099(3)	0.6684(3)	0.4374(2)	0.0240(8)
C9	0.4409(3)	0.6232(3)	0.4962(2)	0.0237(8)
C10	0.4521(3)	0.6274(3)	0.5697(2)	0.0234(8)

C11	0.5898(3)	0.7191(3)	0.5302(2)	0.0199(8)
C12	0.6655(3)	0.7712(3)	0.5495(2)	0.0196(8)
C13	0.8805(3)	0.9208(3)	0.6191(3)	0.0340(10)
C14	0.8882(3)	0.9265(3)	0.4560(3)	0.0336(10)
C15	0.5057(4)	0.6634(3)	0.3576(2)	0.0355(10)
C16	0.3543(3)	0.5705(3)	0.4855(2)	0.0290(9)
C17	0.5393(4)	0.7348(3)	0.8609(2)	0.0332(10)
C18	0.6540(4)	0.6927(4)	0.8517(3)	0.0422(12)
C19	0.4943(4)	0.7234(4)	0.9445(3)	0.0447(12)
C20	0.5364(5)	0.8473(4)	0.8288(3)	0.0472(13)
C21	0.4477(3)	0.5431(3)	0.8523(2)	0.0278(9)
C22	0.5471(4)	0.4904(4)	0.8807(3)	0.0374(11)
C23	0.4325(4)	0.4830(3)	0.7939(3)	0.0361(10)
C24	0.3570(4)	0.5343(4)	0.9179(3)	0.0380(11)
C25	0.3420(3)	0.7513(3)	0.7906(2)	0.0299(9)
C26	0.2764(4)	0.7849(4)	0.8617(3)	0.0413(11)
C27	0.3599(4)	0.8443(4)	0.7307(3)	0.0439(12)
C28	0.2771(4)	0.6896(4)	0.7595(3)	0.0401(11)
C29	0.0027(3)	0.3369(3)	0.6023(2)	0.0262(8)
C30	0.0553(3)	0.3700(3)	0.5302(2)	0.0263(9)
C31	0.0209(3)	0.3483(3)	0.4693(2)	0.0254(8)
C32	0.9336(3)	0.2935(3)	0.4837(2)	0.0232(8)
C33	0.8881(3)	0.2696(3)	0.4259(2)	0.0272(9)
C34	0.8074(3)	0.2146(3)	0.4415(2)	0.0268(9)
C35	0.7618(3)	0.1777(3)	0.5167(2)	0.0228(8)
C36	0.6768(3)	0.1196(3)	0.5356(2)	0.0244(8)
C37	0.6357(3)	0.0927(3)	0.6105(2)	0.0250(8)
C38	0.6801(3)	0.1237(3)	0.6640(2)	0.0252(8)
C39	0.8014(3)	0.2035(3)	0.5750(2)	0.0212(8)

C40	0.8884(3)	0.2618(3)	0.5585(2)	0.0223(8)
C41	0.1458(3)	0.4288(3)	0.5214(3)	0.0317(9)
C42	0.0726(3)	0.3830(3)	0.3909(2)	0.0321(10)
C43	0.6307(3)	0.0898(3)	0.4762(2)	0.0309(9)
C44	0.5439(3)	0.0335(3)	0.6366(3)	0.0321(9)
C45	0.9929(4)	0.0809(3)	0.8165(2)	0.0359(11)
C46	0.9873(5)	0.0220(4)	0.7546(3)	0.0489(14)
C47	0.0848(4)	0.1419(4)	0.7866(3)	0.0465(12)
C48	0.0161(5)	0.0055(4)	0.8867(3)	0.0506(14)
C49	0.8904(4)	0.2701(3)	0.8825(2)	0.0316(9)
C50	0.9491(4)	0.3495(4)	0.8263(3)	0.0443(12)
C51	0.9479(4)	0.2325(4)	0.9487(3)	0.0448(12)
C52	0.7855(4)	0.3263(4)	0.9105(3)	0.0421(12)
C53	0.7609(4)	0.0971(3)	0.8876(2)	0.0363(10)
C54	0.7619(5)	0.0003(4)	0.8576(3)	0.0536(14)
C55	0.6573(4)	0.1594(4)	0.8771(3)	0.0449(12)
C56	0.7645(4)	0.0678(4)	0.9725(3)	0.0481(13)
Cl1	0.03876(16)	0.25355(12)	0.20939(13)	0.0879(6)
Cl2	0.0819(2)	0.39860(18)	0.07196(13)	0.1126(8)
C57	0.0419(7)	0.3790(5)	0.1689(4)	0.084(2)
F1	0.8161(3)	0.5382(3)	0.20293(16)	0.0614(9)
F2	0.9080(2)	0.5068(3)	0.29618(19)	0.0654(9)
F3	0.7343(2)	0.5061(3)	0.32438(16)	0.0537(8)
F4	0.8044(3)	0.6510(2)	0.2782(2)	0.0735(11)
B1	0.8154(4)	0.5502(4)	0.2753(3)	0.0313(10)
Cl3	0.62889(19)	0.89207(16)	0.17477(14)	0.0987(7)
Cl4	0.7241(3)	0.7812(2)	0.05419(15)	0.1309(10)
C58	0.6706(9)	0.7782(6)	0.1485(5)	0.102(3)

Table 5. Bond lengths (Å) for JPD1049.

Cu1-N5	2.081(4)	Cu1-N2	2.111(3)
Cu1-N1	2.112(3)	Cu1-P1	2.2030(11)
Cu2-N7	2.064(4)	Cu2-N3	2.099(3)
Cu2-N4	2.127(3)	Cu2-P2	2.2140(11)
P1-C21	1.899(4)	P1-C25	1.904(4)
P1-C17	1.908(4)	P2-C53	1.906(5)
P2-C49	1.907(4)	P2-C45	1.908(5)
N1-C1	1.325(5)	N1-C12	1.358(5)
N2-C10	1.325(5)	N2-C11	1.360(5)
N3-C29	1.330(5)	N3-C40	1.359(5)
N4-C38	1.328(5)	N4-C39	1.363(5)
N5-N6	1.162(5)	N6-N7	1.166(5)
C1-C2	1.402(5)	C1-H1	0.95
C2-C3	1.379(6)	C2-C13	1.508(6)
C3-C4	1.424(6)	C3-C14	1.512(5)
C4-C12	1.409(5)	C4-C5	1.432(6)
C5-C6	1.357(6)	C5-H5	0.95
C6-C7	1.438(5)	C6-H6	0.95
C7-C11	1.405(5)	C7-C8	1.417(6)
C8-C9	1.387(6)	C8-C15	1.503(6)
C9-C10	1.412(6)	C9-C16	1.503(6)
C10-H10	0.95	C11-C12	1.446(5)
C13-H13A	0.98	C13-H13B	0.98
C13-H13C	0.98	C14-H14A	0.98
C14-H14B	0.98	C14-H14C	0.98
C15-H15A	0.98	C15-H15B	0.98
C15-H15C	0.98	C16-H16A	0.98
C16-H16B	0.98	C16-H16C	0.98

C17-C18	1.533(7)	C17-C20	1.534(7)
C17-C19	1.534(6)	C18-H18A	0.98
C18-H18B	0.98	C18-H18C	0.98
C19-H19A	0.98	C19-H19B	0.98
C19-H19C	0.98	C20-H20A	0.98
C20-H20B	0.98	C20-H20C	0.98
C21-C24	1.535(6)	C21-C23	1.537(6)
C21-C22	1.539(6)	C22-H22A	0.98
C22-H22B	0.98	C22-H22C	0.98
C23-H23A	0.98	C23-H23B	0.98
C23-H23C	0.98	C24-H24A	0.98
C24-H24B	0.98	C24-H24C	0.98
C25-C27	1.531(6)	C25-C28	1.541(6)
C25-C26	1.541(6)	C26-H26A	0.98
C26-H26B	0.98	C26-H26C	0.98
C27-H27A	0.98	C27-H27B	0.98
C27-H27C	0.98	C28-H28A	0.98
C28-H28B	0.98	C28-H28C	0.98
C29-C30	1.404(6)	C29-H29	0.95
C30-C31	1.391(6)	C30-C41	1.506(6)
C31-C32	1.425(6)	C31-C42	1.500(6)
C32-C40	1.410(6)	C32-C33	1.434(6)
C33-C34	1.350(6)	C33-H33	0.95
C34-C35	1.432(6)	C34-H34	0.95
C35-C39	1.410(5)	C35-C36	1.422(6)
C36-C37	1.387(6)	C36-C43	1.501(5)
C37-C38	1.403(6)	C37-C44	1.510(6)
C38-H38	0.95	C39-C40	1.448(6)
C41-H41A	0.98	C41-H41B	0.98

C41-H41C	0.98	C42-H42A	0.98		
C42-H42B	0.98	C42-H42C	0.98		
C43-H43A	0.98	C43-H43B	0.98		
C43-H43C	0.98	C44-H44A	0.98		
C44-H44B	0.98	C44-H44C	0.98		
C45-C47	1.530(7)	C45-C46	1.541(6)		
C45-C48	1.545(6)	C46-H46A	0.98		
C46-H46B	0.98	C46-H46C	0.98		
C47-H47A	0.98	C47-H47B	0.98		
C47-H47C	0.98	C48-H48A	0.98		
C48-H48B	0.98	C48-H48C	0.98		
C49-C51	1.533(7)	C49-C52	1.534(6)		
C49-C50	1.537(6)	C50-H50A	0.98		
C50-H50B	0.98	C50-H50C	0.98		
C51-H51A	0.98	C51-H51B	0.98		
C51-H51C	0.98	C52-H52A	0.98		
C52-H52B	0.98	C52-H52C	0.98		
C53-C54	1.529(7)	C53-C55	1.530(7)		
C53-C56	1.553(6)	C54-H54A	0.98		
C54-H54B	0.98	C54-H54C	0.98		
C55-H55A	0.98	C55-H55B	0.98		
C55-H55C	0.98	C56-H56A	0.98		
C56-H56B	0.98	C56-H56C	0.98		
Cl1-C57	1.736(7)	Cl2-C57	1.749(8)		
C57-H57A	0.99	C57-H57B	0.99		
F1-B1	1.379(6)	F2-B1	1.374(6)		
F3-B1	1.394(6)	F4-B1	1.375(6)		
Cl3-C58	1.705(9)	Cl4-C58	1.748(9)		
C58-H58A	0.99	C58-H58B	0.99		

Table 6. Bond angles (°) for JPD1049.

N5-Cu1-N2	96.27(16)	N5-Cu1-N1	93.56(13)
N2-Cu1-N1	78.90(12)	N5-Cu1-P1	119.43(12)
N2-Cu1-P1	128.72(9)	N1-Cu1-P1	128.81(9)
N7-Cu2-N3	100.68(15)	N7-Cu2-N4	97.04(15)
N3-Cu2-N4	78.90(13)	N7-Cu2-P2	116.28(13)
N3-Cu2-P2	128.89(10)	N4-Cu2-P2	126.14(9)
C21-P1-C25	108.62(19)	C21-P1-C17	108.38(19)
C25-P1-C17	108.7(2)	C21-P1-Cu1	109.02(13)
C25-P1-Cu1	111.35(13)	C17-P1-Cu1	110.72(14)
C53-P2-C49	108.48(19)	C53-P2-C45	108.6(2)
C49-P2-C45	108.5(2)	C53-P2-Cu2	110.25(15)
C49-P2-Cu2	109.71(14)	C45-P2-Cu2	111.30(14)
C1-N1-C12	117.4(3)	C1-N1-Cu1	129.3(3)
C12-N1-Cu1	112.2(2)	C10-N2-C11	116.8(3)
C10-N2-Cu1	130.1(3)	C11-N2-Cu1	112.3(3)
C29-N3-C40	116.9(3)	C29-N3-Cu2	129.1(3)
C40-N3-Cu2	113.5(3)	C38-N4-C39	117.4(3)
C38-N4-Cu2	129.6(3)	C39-N4-Cu2	112.5(3)
N6-N5-Cu1	143.5(3)	N5-N6-N7	178.7(5)
N6-N7-Cu2	147.4(4)	N1-C1-C2	124.7(4)
N1-C1-H1	117.7	C2-C1-H1	117.7
C3-C2-C1	118.6(4)	C3-C2-C13	123.1(4)
C1-C2-C13	118.2(4)	C2-C3-C4	118.3(3)
C2-C3-C14	121.3(4)	C4-C3-C14	120.4(4)
C12-C4-C3	118.5(4)	C12-C4-C5	118.0(4)
C3-C4-C5	123.5(4)	C6-C5-C4	121.7(4)
C6-C5-H5	119.1	C4-C5-H5	119.1

C5-C6-C7	121.7(4)	C5-C6-H6	119.1
C7-C6-H6	119.1	C11-C7-C8	119.3(4)
C11-C7-C6	117.9(4)	C8-C7-C6	122.8(3)
C9-C8-C7	117.7(4)	C9-C8-C15	121.5(4)
C7-C8-C15	120.8(4)	C8-C9-C10	118.4(4)
C8-C9-C16	123.3(4)	C10-C9-C16	118.3(4)
N2-C10-C9	125.1(4)	N2-C10-H10	117.5
C9-C10-H10	117.5	N2-C11-C7	122.7(4)
N2-C11-C12	117.0(3)	C7-C11-C12	120.3(3)
N1-C12-C4	122.5(4)	N1-C12-C11	117.2(3)
C4-C12-C11	120.3(3)	C2-C13-H13A	109.5
C2-C13-H13B	109.5	H13A-C13-H13B	109.5
C2-C13-H13C	109.5	H13A-C13-H13C	109.5
H13B-C13-H13C	109.5	C3-C14-H14A	109.5
C3-C14-H14B	109.5	H14A-C14-H14B	109.5
C3-C14-H14C	109.5	H14A-C14-H14C	109.5
H14B-C14-H14C	109.5	C8-C15-H15A	109.5
C8-C15-H15B	109.5	H15A-C15-H15B	109.5
C8-C15-H15C	109.5	H15A-C15-H15C	109.5
H15B-C15-H15C	109.5	C9-C16-H16A	109.5
C9-C16-H16B	109.5	H16A-C16-H16B	109.5
C9-C16-H16C	109.5	H16A-C16-H16C	109.5
H16B-C16-H16C	109.5	C18-C17-C20	106.1(4)
C18-C17-C19	108.9(4)	C20-C17-C19	108.2(4)
C18-C17-P1	108.8(3)	C20-C17-P1	107.9(3)
C19-C17-P1	116.5(3)	C17-C18-H18A	109.5
C17-C18-H18B	109.5	H18A-C18-H18B	109.5
C17-C18-H18C	109.5	H18A-C18-H18C	109.5
H18B-C18-H18C	109.5	C17-C19-H19A	109.5

C17-C19-H19B	109.5	H19A-C19-H19B	109.5
C17-C19-H19C	109.5	H19A-C19-H19C	109.5
H19B-C19-H19C	109.5	C17-C20-H20A	109.5
C17-C20-H20B	109.5	H20A-C20-H20B	109.5
C17-C20-H20C	109.5	H20A-C20-H20C	109.5
H20B-C20-H20C	109.5	C24-C21-C23	109.5(4)
C24-C21-C22	108.5(4)	C23-C21-C22	104.9(4)
C24-C21-P1	117.1(3)	C23-C21-P1	107.3(3)
C22-C21-P1	108.8(3)	C21-C22-H22A	109.5
C21-C22-H22B	109.5	H22A-C22-H22B	109.5
C21-C22-H22C	109.5	H22A-C22-H22C	109.5
H22B-C22-H22C	109.5	C21-C23-H23A	109.5
C21-C23-H23B	109.5	H23A-C23-H23B	109.5
C21-C23-H23C	109.5	H23A-C23-H23C	109.5
H23B-C23-H23C	109.5	C21-C24-H24A	109.5
C21-C24-H24B	109.5	H24A-C24-H24B	109.5
C21-C24-H24C	109.5	H24A-C24-H24C	109.5
H24B-C24-H24C	109.5	C27-C25-C28	105.4(4)
C27-C25-C26	108.7(4)	C28-C25-C26	108.1(4)
C27-C25-P1	109.0(3)	C28-C25-P1	108.4(3)
C26-C25-P1	116.7(3)	C25-C26-H26A	109.5
C25-C26-H26B	109.5	H26A-C26-H26B	109.5
C25-C26-H26C	109.5	H26A-C26-H26C	109.5
H26B-C26-H26C	109.5	C25-C27-H27A	109.5
C25-C27-H27B	109.5	H27A-C27-H27B	109.5
C25-C27-H27C	109.5	H27A-C27-H27C	109.5
H27B-C27-H27C	109.5	C25-C28-H28A	109.5
C25-C28-H28B	109.5	H28A-C28-H28B	109.5
C25-C28-H28C	109.5	H28A-C28-H28C	109.5

H28B-C28-H28C	109.5	N3-C29-C30	124.9(4)
N3-C29-H29	117.6	C30-C29-H29	117.6
C31-C30-C29	118.7(4)	C31-C30-C41	122.3(4)
C29-C30-C41	119.0(4)	C30-C31-C32	117.8(4)
C30-C31-C42	121.3(4)	C32-C31-C42	120.9(4)
C40-C32-C31	118.6(4)	C40-C32-C33	118.0(4)
C31-C32-C33	123.4(4)	C34-C33-C32	121.8(4)
C34-C33-H33	119.1	C32-C33-H33	119.1
C33-C34-C35	121.9(4)	C33-C34-H34	119.0
C35-C34-H34	119.0	C39-C35-C36	118.4(4)
C39-C35-C34	117.8(4)	C36-C35-C34	123.8(4)
C37-C36-C35	118.4(4)	C37-C36-C43	120.4(4)
C35-C36-C43	121.1(4)	C36-C37-C38	118.5(4)
C36-C37-C44	122.8(4)	C38-C37-C44	118.7(4)
N4-C38-C37	124.7(4)	N4-C38-H38	117.7
C37-C38-H38	117.7	N4-C39-C35	122.6(4)
N4-C39-C40	117.0(3)	C35-C39-C40	120.4(3)
N3-C40-C32	123.0(4)	N3-C40-C39	117.1(3)
C32-C40-C39	119.9(4)	C30-C41-H41A	109.5
C30-C41-H41B	109.5	H41A-C41-H41B	109.5
C30-C41-H41C	109.5	H41A-C41-H41C	109.5
H41B-C41-H41C	109.5	C31-C42-H42A	109.5
C31-C42-H42B	109.5	H42A-C42-H42B	109.5
C31-C42-H42C	109.5	H42A-C42-H42C	109.5
H42B-C42-H42C	109.5	C36-C43-H43A	109.5
C36-C43-H43B	109.5	H43A-C43-H43B	109.5
C36-C43-H43C	109.5	H43A-C43-H43C	109.5
H43B-C43-H43C	109.5	C37-C44-H44A	109.5
C37-C44-H44B	109.5	H44A-C44-H44B	109.5

C37-C44-H44C 109.5 H44A-C44-H44C109.5

H44B-C44-H44C109.5 C47-C45-C46 105.7(4)

C47-C45-C48 108.7(4) C46-C45-C48 108.8(4)

C47-C45-P2 109.1(3) C46-C45-P2 108.0(3)

C48-C45-P2 116.1(3) C45-C46-H46A 109.5

C45-C46-H46B 109.5 H46A-C46-H46B 109.5

C45-C46-H46C 109.5 H46A-C46-H46C109.5

H46B-C46-H46C109.5 C45-C47-H47A 109.5

C45-C47-H47B 109.5 H47A-C47-H47B 109.5

C45-C47-H47C 109.5 H47A-C47-H47C109.5

H47B-C47-H47C109.5 C45-C48-H48A 109.5

C45-C48-H48B 109.5 H48A-C48-H48B 109.5

C45-C48-H48C 109.5 H48A-C48-H48C109.5

H48B-C48-H48C109.5 C51-C49-C52 108.5(4)

C51-C49-C50 109.5(4) C52-C49-C50 105.0(4)

C51-C49-P2 116.4(3) C52-C49-P2 109.2(3)

C50-C49-P2 107.7(3) C49-C50-H50A 109.5

C49-C50-H50B 109.5 H50A-C50-H50B 109.5

C49-C50-H50C 109.5 H50A-C50-H50C109.5

H50B-C50-H50C109.5 C49-C51-H51A 109.5

C49-C51-H51B 109.5 H51A-C51-H51B 109.5

C49-C51-H51C 109.5 H51A-C51-H51C109.5

H51B-C51-H51C109.5 C49-C52-H52A 109.5

C49-C52-H52B 109.5 H52A-C52-H52B 109.5

C49-C52-H52C 109.5 H52A-C52-H52C109.5

H52B-C52-H52C109.5 C54-C53-C55 106.5(4)

C54-C53-C56 107.6(4) C55-C53-C56 108.8(4)

C54-C53-P2 109.5(4) C55-C53-P2 108.1(3)

C56-C53-P2 116.0(3) C53-C54-H54A 109.5

C53-C54-H54B	109.5	H54A-C54-H54B	109.5
C53-C54-H54C	109.5	H54A-C54-H54C	109.5
H54B-C54-H54C	109.5	C53-C55-H55A	109.5
C53-C55-H55B	109.5	H55A-C55-H55B	109.5
C53-C55-H55C	109.5	H55A-C55-H55C	109.5
H55B-C55-H55C	109.5	C53-C56-H56A	109.5
C53-C56-H56B	109.5	H56A-C56-H56B	109.5
C53-C56-H56C	109.5	H56A-C56-H56C	109.5
H56B-C56-H56C	109.5	Cl1-C57-Cl2	114.0(4)
Cl1-C57-H57A	108.8	Cl2-C57-H57A	108.8
Cl1-C57-H57B	108.8	Cl2-C57-H57B	108.8
H57A-C57-H57B	107.7	F2-B1-F4	109.0(4)
F2-B1-F1	108.9(4)	F4-B1-F1	109.0(4)
F2-B1-F3	109.5(4)	F4-B1-F3	109.1(4)
F1-B1-F3	111.3(4)	Cl3-C58-Cl4	115.7(4)
Cl3-C58-H58A	108.4	Cl4-C58-H58A	108.4
Cl3-C58-H58B	108.4	Cl4-C58-H58B	108.4
H58A-C58-H58B	107.4		

Table 7. Torsion angles (°) for JPD1049.

C12-N1-C1-C2	-0.3(5)	Cu1-N1-C1-C2	167.1(3)
N1-C1-C2-C3	-0.5(6)	N1-C1-C2-C13	-179.5(4)
C1-C2-C3-C4	0.9(5)	C13-C2-C3-C4	179.8(3)
C1-C2-C3-C14	-178.7(4)	C13-C2-C3-C14	0.2(6)
C2-C3-C4-C12	-0.5(5)	C14-C3-C4-C12	179.1(3)
C2-C3-C4-C5	-178.5(3)	C14-C3-C4-C5	1.2(6)
C12-C4-C5-C6	1.6(6)	C3-C4-C5-C6	179.5(4)
C4-C5-C6-C7	0.8(6)	C5-C6-C7-C11	-2.5(5)

C5-C6-C7-C8	177.8(4)	C11-C7-C8-C9	0.1(5)
C6-C7-C8-C9	179.7(3)	C11-C7-C8-C15	-178.5(3)
C6-C7-C8-C15	1.2(6)	C7-C8-C9-C10	-1.1(5)
C15-C8-C9-C10	177.4(3)	C7-C8-C9-C16	178.4(3)
C15-C8-C9-C16	-3.0(6)	C11-N2-C10-C9	1.4(5)
Cu1-N2-C10-C9	-167.4(3)	C8-C9-C10-N2	0.5(6)
C16-C9-C10-N2	-179.2(3)	C10-N2-C11-C7	-2.5(5)
Cu1-N2-C11-C7	168.2(3)	C10-N2-C11-C12	177.7(3)
Cu1-N2-C11-C12	-11.5(4)	C8-C7-C11-N2	1.8(5)
C6-C7-C11-N2	-177.8(3)	C8-C7-C11-C12	-178.4(3)
C6-C7-C11-C12	1.9(5)	C1-N1-C12-C4	0.7(5)
Cu1-N1-C12-C4	-168.7(3)	C1-N1-C12-C11	-179.4(3)
Cu1-N1-C12-C11	11.1(4)	C3-C4-C12-N1	-0.3(5)
C5-C4-C12-N1	177.8(3)	C3-C4-C12-C11	179.8(3)
C5-C4-C12-C11	-2.1(5)	N2-C11-C12-N1	0.3(5)
C7-C11-C12-N1	-179.5(3)	N2-C11-C12-C4	-179.9(3)
C7-C11-C12-C4	0.4(5)	C25-P1-C21-C24	-40.7(4)
C17-P1-C21-C24	77.2(4)	Cu1-P1-C21-C24	-162.3(3)
C25-P1-C21-C23	82.8(3)	C17-P1-C21-C23	-159.2(3)
Cu1-P1-C21-C23	-38.7(3)	C25-P1-C21-C22	-164.2(3)
C17-P1-C21-C22	-46.3(3)	Cu1-P1-C21-C22	74.3(3)
C40-N3-C29-C30	-0.2(5)	Cu2-N3-C29-C30	-172.0(3)
N3-C29-C30-C31	0.9(6)	N3-C29-C30-C41	-179.9(4)
C29-C30-C31-C32	0.2(5)	C41-C30-C31-C32	-179.0(3)
C29-C30-C31-C42	179.0(4)	C41-C30-C31-C42	-0.2(6)
C30-C31-C32-C40	-1.7(5)	C42-C31-C32-C40	179.5(3)
C30-C31-C32-C33	177.6(3)	C42-C31-C32-C33	-1.3(6)
C40-C32-C33-C34	-3.0(5)	C31-C32-C33-C34	177.7(4)
C32-C33-C34-C35	0.6(6)	C33-C34-C35-C39	2.2(6)

C33-C34-C35-C36	179.9(4)	C39-C35-C36-C37	1.1(5)
C34-C35-C36-C37	-176.6(3)	C39-C35-C36-C43	179.8(3)
C34-C35-C36-C43	2.1(6)	C35-C36-C37-C38	-0.2(5)
C43-C36-C37-C38	-178.9(3)	C35-C36-C37-C44	178.5(3)
C43-C36-C37-C44	-0.3(6)	C39-N4-C38-C37	1.1(6)
Cu2-N4-C38-C37	171.6(3)	C36-C37-C38-N4	-1.0(6)
C44-C37-C38-N4	-179.7(4)	C38-N4-C39-C35	0.0(5)
Cu2-N4-C39-C35	-172.1(3)	C38-N4-C39-C40	179.4(3)
Cu2-N4-C39-C40	7.2(4)	C36-C35-C39-N4	-1.1(5)
C34-C35-C39-N4	176.8(3)	C36-C35-C39-C40	179.6(3)
C34-C35-C39-C40	-2.6(5)	C29-N3-C40-C32	-1.5(5)
Cu2-N3-C40-C32	171.6(3)	C29-N3-C40-C39	179.2(3)
Cu2-N3-C40-C39	-7.7(4)	C31-C32-C40-N3	2.5(5)
C33-C32-C40-N3	-176.8(3)	C31-C32-C40-C39	-178.2(3)
C33-C32-C40-C39	2.5(5)	N4-C39-C40-N3	0.2(5)
C35-C39-C40-N3	179.6(3)	N4-C39-C40-C32	-179.1(3)
C35-C39-C40-C32	0.3(5)		

Table 8. Anisotropic atomic displacement parameters (Å2) for JPD1049.

The anisotropic atomic displacement factor exponent takes the form: -2π2[h2 a*2 U11 + ... + 2 h k a* b* U12]

U11	U22	U33	U23	U13	U12
Cu1	0.0263(3)	0.0233(3)	0.0182(3)	-0.0019(2)	0.0003(2)	-0.0020(2)
Cu2	0.0326(3)	0.0226(3)	0.0221(3)	-0.0035(2)	-0.0051(2)	0.0009(2)
P1	0.0254(5)	0.0231(5)	0.0160(5)	-0.0023(4)	-0.0021(4)	-0.0026(4)
P2	0.0326(6)	0.0220(5)	0.0196(5)	-0.0056(4)	-0.0039(4)	-0.0006(4)
N1	0.0214(17)	0.0168(15)	0.0252(18)	-0.0047(12)	-0.0024(13)	0.0011(12)
N2	0.0215(17)	0.0170(15)	0.0215(17)	-0.0046(12)	0.0026(12)	-0.0005(12)
N3	0.0249(18)	0.0187(15)	0.0284(18)	-0.0038(13)	-0.0074(13)	0.0027(13)
N4	0.0258(18)	0.0214(16)	0.0255(18)	-0.0023(13)	-0.0045(13)	-0.0005(13)

N5	0.035(2)	0.0216(19)	0.062(3)	0.0061(18)	0.0102(19)	0.0051(16)
N6	0.0233(17)	0.030(2)	0.0252(19)	-0.0049(14)	-0.0023(13)	0.0025(14)
N7	0.046(2)	0.026(2)	0.053(3)	-0.0036(17)	-0.0063(19)	0.0090(17)
C1	0.027(2)	0.0199(18)	0.026(2)	-0.0059(15)	-0.0028(16)	-0.0003(16)
C2	0.022(2)	0.0145(17)	0.033(2)	-0.0051(15)	-0.0015(16)	-0.0002(15)
C3	0.022(2)	0.0152(17)	0.031(2)	-0.0009(15)	0.0027(16)	0.0025(15)
C4	0.024(2)	0.0148(16)	0.024(2)	-0.0011(14)	0.0010(15)	0.0031(14)
C5	0.030(2)	0.0227(19)	0.024(2)	0.0008(16)	0.0037(16)	0.0014(16)
C6	0.031(2)	0.027(2)	0.0159(19)	-0.0022(15)	0.0007(15)	0.0032(17)
C7	0.026(2)	0.0172(17)	0.020(2)	-0.0035(14)	-0.0047(15)	0.0057(15)
C8	0.025(2)	0.0206(18)	0.025(2)	-0.0068(15)	-0.0056(15)	0.0084(15)
C9	0.023(2)	0.0169(18)	0.032(2)	-0.0100(16)	-0.0072(16)	0.0060(15)
C10	0.023(2)	0.0198(18)	0.025(2)	-0.0066(15)	-0.0005(15)	0.0013(15)
C11	0.0204(19)	0.0147(17)	0.021(2)	-0.0032(14)	0.0006(14)	0.0044(14)
C12	0.021(2)	0.0134(16)	0.021(2)	-0.0026(14)	-0.0002(14)	0.0058(14)
C13	0.029(2)	0.027(2)	0.046(3)	-0.0071(19)	-0.0064(19)	-0.0038(18)
C14	0.028(2)	0.027(2)	0.039(3)	0.0008(18)	0.0061(18)	-0.0064(17)
C15	0.042(3)	0.039(2)	0.028(2)	-0.0125(19)	-0.0100(19)	0.002(2)
C16	0.025(2)	0.027(2)	0.037(2)	-0.0115(18)	-0.0074(17)	0.0006(17)
C17	0.039(3)	0.038(2)	0.026(2)	-0.0084(18)	-0.0039(18)	-0.011(2)
C18	0.037(3)	0.058(3)	0.035(3)	-0.004(2)	-0.008(2)	-0.019(2)
C19	0.051(3)	0.062(3)	0.027(3)	-0.015(2)	-0.006(2)	-0.014(3)
C20	0.060(4)	0.039(3)	0.047(3)	-0.012(2)	-0.003(2)	-0.021(2)
C21	0.030(2)	0.029(2)	0.022(2)	-0.0017(17)	0.0016(16)	-0.0044(17)
C22	0.042(3)	0.036(2)	0.028(2)	0.0031(19)	-0.0035(19)	0.000(2)
C23	0.042(3)	0.030(2)	0.036(3)	-0.0098(19)	0.001(2)	-0.010(2)
C24	0.041(3)	0.038(2)	0.028(2)	0.0018(19)	0.0058(19)	-0.009(2)
C25	0.032(2)	0.035(2)	0.021(2)	-0.0077(17)	-0.0018(16)	0.0044(18)
C26	0.039(3)	0.051(3)	0.029(3)	-0.013(2)	0.0005(19)	0.011(2)

C27	0.050(3)	0.041(3)	0.031(3)	0.002(2)	-0.004(2)	0.013(2)
C28	0.026(2)	0.057(3)	0.037(3)	-0.014(2)	-0.0089(19)	0.005(2)
C29	0.025(2)	0.0220(19)	0.032(2)	-0.0047(16)	-0.0072(16)	-0.0006(16)
C30	0.022(2)	0.0172(18)	0.037(2)	-0.0025(16)	-0.0057(16)	0.0050(15)
C31	0.021(2)	0.0194(18)	0.031(2)	-0.0015(16)	0.0004(16)	0.0040(15)
C32	0.022(2)	0.0149(17)	0.029(2)	-0.0024(15)	-0.0006(15)	0.0048(14)
C33	0.032(2)	0.0243(19)	0.022(2)	-0.0016(16)	-0.0036(16)	0.0027(17)
C34	0.032(2)	0.0249(19)	0.023(2)	-0.0040(16)	-0.0071(16)	0.0023(17)
C35	0.024(2)	0.0156(17)	0.027(2)	-0.0036(15)	-0.0068(15)	0.0049(15)
C36	0.026(2)	0.0172(18)	0.029(2)	-0.0044(15)	-0.0085(16)	0.0055(15)
C37	0.025(2)	0.0191(18)	0.029(2)	-0.0015(15)	-0.0052(16)	0.0011(15)
C38	0.029(2)	0.0194(18)	0.025(2)	-0.0003(15)	-0.0037(16)	-0.0010(16)
C39	0.024(2)	0.0152(17)	0.022(2)	-0.0032(14)	-0.0040(15)	0.0041(14)
C40	0.023(2)	0.0178(17)	0.025(2)	-0.0038(15)	-0.0043(15)	0.0037(15)
C41	0.026(2)	0.024(2)	0.042(3)	-0.0034(18)	-0.0027(18)	-0.0018(17)
C42	0.031(2)	0.028(2)	0.030(2)	0.0007(17)	0.0024(17)	-0.0005(18)
C43	0.033(2)	0.029(2)	0.034(2)	-0.0079(18)	-0.0126(18)	-0.0001(18)
C44	0.032(2)	0.027(2)	0.037(3)	-0.0018(18)	-0.0062(18)	-0.0055(18)
C45	0.046(3)	0.032(2)	0.026(2)	-0.0063(18)	-0.0070(19)	0.011(2)
C46	0.074(4)	0.035(3)	0.035(3)	-0.014(2)	-0.014(3)	0.016(2)
C47	0.034(3)	0.059(3)	0.040(3)	-0.008(2)	-0.002(2)	0.011(2)
C48	0.061(4)	0.047(3)	0.038(3)	-0.005(2)	-0.017(2)	0.020(3)
C49	0.037(2)	0.031(2)	0.029(2)	-0.0110(18)	-0.0022(18)	-0.0070(18)
C50	0.049(3)	0.039(3)	0.047(3)	-0.015(2)	0.003(2)	-0.015(2)
C51	0.048(3)	0.057(3)	0.037(3)	-0.021(2)	-0.010(2)	-0.010(2)
C52	0.048(3)	0.040(3)	0.037(3)	-0.019(2)	0.005(2)	0.001(2)
C53	0.047(3)	0.036(2)	0.027(2)	-0.0037(19)	-0.0068(19)	-0.014(2)
C54	0.082(4)	0.038(3)	0.048(3)	-0.003(2)	-0.022(3)	-0.023(3)
C55	0.039(3)	0.059(3)	0.039(3)	-0.009(2)	-0.002(2)	-0.017(2)

C56	0.061(3)	0.056(3)	0.027(3)	0.003(2)	-0.003(2)	-0.024(3)
Cl1	0.0901(13)	0.0419(8)	0.1156(16)	-0.0012(9)	0.0021(11)	0.0027(8)
Cl2	0.164(2)	0.1010(16)	0.0726(13)	-0.0173(12)	-0.0207(14)	-0.0119(16)
C57	0.104(6)	0.052(4)	0.081(5)	-0.013(3)	0.011(4)	0.009(4)
F1	0.0541(19)	0.100(3)	0.0360(17)	-0.0166(17)	0.0001(13)	-0.0318(18)
F2	0.0429(18)	0.086(2)	0.061(2)	0.0007(18)	-0.0176(15)	0.0079(17)
F3	0.0479(18)	0.079(2)	0.0379(16)	-0.0063(15)	0.0001(13)	-0.0336(16)
F4	0.085(3)	0.0406(17)	0.078(2)	-0.0121(16)	0.026(2)	-0.0007(17)
B1	0.028(3)	0.036(3)	0.031(3)	-0.006(2)	-0.007(2)	-0.003(2)
Cl3	0.0995(16)	0.0805(13)	0.1112(17)	-0.0195(12)	-0.0125(12)	0.0026(11)
Cl4	0.202(3)	0.0987(17)	0.0955(17)	-0.0245(13)	-0.0407(18)	0.0035(18)
C58	0.165(10)	0.062(5)	0.084(6)	0.008(4)	-0.036(6)	-0.040(5)

Table 9. Hydrogen atomic coordinates and isotropic atomic displacement parameters (Å2) for JPD1049.

x/a	y/b	z/c	U(eq)
H1	0.7331	0.8158	0.6928	0.029
H5	0.7814	0.8489	0.3783	0.033
H6	0.6633	0.7647	0.3479	0.031
H10	0.4047	0.5957	0.6095	0.028
H13A	0.9518	0.8927	0.6028	0.051
H13B	0.8651	0.9095	0.6738	0.051
H13C	0.8724	0.9931	0.5998	0.051
H14A	0.8523	0.9760	0.4209	0.05
H14B	0.9343	0.8778	0.4289	0.05
H14C	0.9290	0.9606	0.4802	0.05
H15A	0.5077	0.7307	0.3276	0.053
H15B	0.4415	0.6374	0.3553	0.053
H15C	0.5652	0.6187	0.3381	0.053
H16A	0.3083	0.6178	0.4561	0.043
H16B	0.3151	0.5448	0.5343	0.043

H16C	0.3831	0.5145	0.4590	0.043
H18A	0.6801	0.6883	0.7990	0.063
H18B	0.6617	0.6257	0.8821	0.063
H18C	0.6935	0.7373	0.8680	0.063
H19A	0.4206	0.7490	0.9510	0.067
H19B	0.5311	0.7615	0.9687	0.067
H19C	0.5023	0.6523	0.9673	0.067
H20A	0.5545	0.8565	0.7743	0.071
H20B	0.5862	0.8765	0.8488	0.071
H20C	0.4666	0.8808	0.8429	0.071
H22A	0.6065	0.4995	0.8404	0.056
H22B	0.5409	0.4186	0.8971	0.056
H22C	0.5571	0.5196	0.9228	0.056
H23A	0.3684	0.5109	0.7747	0.054
H23B	0.4280	0.4126	0.8172	0.054
H23C	0.4913	0.4873	0.7527	0.054
H24A	0.2918	0.5577	0.8992	0.057
H24B	0.3649	0.5755	0.9538	0.057
H24C	0.3566	0.4640	0.9425	0.057
H26A	0.3113	0.8333	0.8778	0.062
H26B	0.2677	0.7264	0.9014	0.062
H26C	0.2083	0.8165	0.8509	0.062
H27A	0.4055	0.8244	0.6864	0.066
H27B	0.3921	0.8916	0.7501	0.066
H27C	0.2934	0.8765	0.7171	0.066
H28A	0.2154	0.7322	0.7453	0.06
H28B	0.2561	0.6326	0.7978	0.06
H28C	0.3186	0.6648	0.7155	0.06
H29	1.0266	0.3532	0.6433	0.031

H33	0.9155	0.2931	0.3752	0.033
H34	0.7801	0.1999	0.4015	0.032
H38	0.6505	0.1057	0.7150	0.03
H41A	1.2084	0.3923	0.4973	0.048
H41B	1.1558	0.4379	0.5707	0.048
H41C	1.1321	0.4947	0.4905	0.048
H42A	1.0697	0.3335	0.3598	0.048
H42B	1.1451	0.3906	0.3908	0.048
H42C	1.0369	0.4477	0.3709	0.048
H43A	0.5860	0.1471	0.4543	0.046
H43B	0.5896	0.0339	0.4984	0.046
H43C	0.6862	0.0689	0.4372	0.046
H44A	0.4851	0.0689	0.6135	0.048
H44B	0.5252	0.0261	0.6911	0.048
H44C	0.5618	-0.0331	0.6223	0.048
H46A	0.9645	0.0686	0.7119	0.073
H46B	0.9378	-0.0275	0.7739	0.073
H46C	1.0558	-0.0125	0.7387	0.073
H47A	1.1473	0.0965	0.7733	0.07
H47B	1.0952	0.1777	0.8251	0.07
H47C	1.0707	0.1904	0.7422	0.07
H48A	0.9646	-0.0426	0.9007	0.076
H48B	1.0130	0.0417	0.9280	0.076
H48C	1.0854	-0.0307	0.8760	0.076
H50A	1.0165	0.3181	0.8046	0.066
H50B	0.9592	0.4027	0.8519	0.066
H50C	0.9088	0.3783	0.7864	0.066
H51A	1.0195	0.2071	0.9305	0.067
H51B	0.9134	0.1785	0.9828	0.067

H51C	0.9478	0.2880	0.9753	0.067
H52A	0.7480	0.3512	0.8686	0.063
H52B	0.7968	0.3830	0.9321	0.063
H52C	0.7449	0.2805	0.9487	0.063
H54A	0.7660	0.0158	0.8032	0.08
H54B	0.6983	-0.0302	0.8803	0.08
H54C	0.8220	-0.0465	0.8700	0.08
H55A	0.6557	0.1814	0.8237	0.067
H55B	0.6491	0.2183	0.9015	0.067
H55C	0.6007	0.1185	0.8995	0.067
H56A	0.8282	0.0235	0.9800	0.072
H56B	0.7045	0.0328	0.9975	0.072
H56C	0.7631	0.1285	0.9936	0.072
H57A	1.0894	0.4084	0.1918	0.101
H57B	0.9719	0.4151	0.1803	0.101
H58A	0.6114	0.7379	0.1604	0.122
H58B	0.7231	0.7429	0.1789	0.122

Crystal Structure Report for [Cu(Me_2bpy)(^{i}Pr_3P)]PF_6

A yellow column-like specimen of C25H37CuF6N2P2, approximate dimensions 0.170 mm x 0.243 mm x 0.403 mm, was used for the X-ray crystallographic analysis. The X-ray intensity data were measured on a Bruker Smart APEX CCD system equipped with a fine-focus sealed tube (Mo-Kα, λ = 0.71073 Å) and a graphite monochromator. The total exposure time was 11.66 hours. The frames were integrated with the Bruker SAINT software package using a narrow-frame algorithm. The integration of the data using a monoclinic unit cell yielded a total of 53065 reflections to a maximum θ angle of 29.51° (0.72 Å resolution), of which 7563 were independent (average redundancy 7.016, completeness = 98.7%, Rint = 3.17%, Rsig = 2.34%) and 6236 (82.45%) were greater than 2σ(F2). The final cell constants of a = 8.9575(5) Å, b = 17.6041(9) Å, c = 17.4749(9) Å, β = 96.3330(10)°, volume = 2738.8(3) Å3, are based upon the refinement of the XYZ-centroids of 9906 reflections above 20 σ(I) with 5.127° < 2θ < 58.84°. Data were corrected for absorption effects using the multi-scan method (SADABS). The ratio of minimum to maximum apparent transmission was 0.883. The calculated minimum and maximum transmission coefficients (based on crystal size) are 0.6950 and 0.8520. The structure was solved and refined using the Bruker SHELXTL Software Package, using the space group P 1 21/c 1, with Z = 4 for the formula unit, C25H37CuF6N2P2. The final anisotropic full-matrix least-squares refinement on F2 with 335 variables converged at R1 = 3.90%, for the observed data and wR2 = 11.93% for all data. The

goodness-of-fit was 1.114. The largest peak in the final difference electron density synthesis was 0.886 e-/Å3 and the largest hole was -0.488 e-/Å3 with an RMS deviation of 0.079 e-/Å3. On the basis of the final model, the calculated density was 1.467 g/cm3 and F(000), 1256 e-.

Table 1. Sample and crystal data for JPD1052.

Identification code	JPD1052
Chemical formula	C25H37CuF6N2P2
Formula weight	605.04 g/mol
Temperature	150(2) K
Wavelength	0.71073 Å
Crystal size	0.170 x 0.243 x 0.403 mm
Crystal habit	yellow column
Crystal system	monoclinic
Space group	P 1 21/c 1
Unit cell dimensions	a = 8.9575(5) Å α = 90°
	b = 17.6041(9) Å β = 96.3330(10)°
	c = 17.4749(9) Å γ = 90°
Volume	2738.8(3) Å3
Z	4
Density (calculated)	1.467 g/cm3
Absorption coefficient	0.973 mm-1
F(000)	1256

Table 2. Data collection and structure refinement for JPD1052.

Diffractometer	Bruker Smart APEX CCD
Radiation source	fine-focus sealed tube (Mo-Kα, λ = 0.71073 Å)
Theta range for data collection	1.65 to 29.51°
Index ranges	-12<=h<=12, -24<=k<=24, -24<=l<=23
Reflections collected	53065
Independent reflections	7563 [R(int) = 0.0317]
Coverage of independent reflections	98.7%

Absorption correction	multi-scan
Max. and min. transmission	0.8520 and 0.6950
Structure solution technique	direct methods
Structure solution program	SHELXT (Sheldrick, 2015a)
Refinement method	Full-matrix least-squares on F2
Refinement program	SHELXL-2018/1 (Sheldrick, 2015b)
Function minimized	Σ w(Fo2 - Fc2)2
Data / restraints / parameters	7563 / 0 / 335
Goodness-of-fit on F2	1.114
Δ/σmax	0.001
Final R indices	6236 data; I>2σ(I) R1 = 0.0390, wR2 = 0.1154
all data	R1 = 0.0471, wR2 = 0.1193
Weighting scheme	w=1/[σ2(Fo2)+(0.0748P)2+0.4451P]
where P=(Fo2+2Fc2)/3	
Largest diff. peak and hole	0.886 and -0.488 eÅ-3
R.M.S. deviation from mean	0.079 eÅ-3

Table 3. Atomic coordinates and equivalent isotropic atomic displacement parameters (Å2) for JPD1052. U(eq) is defined as one third of the trace of the orthogonalized Uij tensor.

x/a	y/b	z/c	U(eq)
Cu1	0.31872(2)	0.32362(2)	0.47592(2)	0.02434(8)
P1	0.29351(5)	0.20325(2)	0.44974(2)	0.02327(10)
N1	0.22646(15)	0.42811(8)	0.45331(8)	0.0226(3)
N2	0.43475(15)	0.38125(7)	0.56488(8)	0.0229(3)
C1	0.11823(18)	0.45018(9)	0.39966(9)	0.0248(3)
C2	0.05745(18)	0.52428(9)	0.39420(10)	0.0257(3)
C3	0.11192(18)	0.57774(9)	0.44822(10)	0.0256(3)
C4	0.22675(18)	0.55547(9)	0.50661(9)	0.0237(3)
C5	0.2891(2)	0.60537(9)	0.56708(11)	0.0296(4)

C6	0.3976(2)	0.58240(10)	0.62178(10)	0.0291(4)
C7	0.45427(18)	0.50594(9)	0.62386(9)	0.0239(3)
C8	0.56425(18)	0.47869(10)	0.68216(9)	0.0262(3)
C9	0.60361(18)	0.40263(10)	0.68056(9)	0.0266(3)
C10	0.53597(18)	0.35666(10)	0.62051(10)	0.0260(3)
C11	0.39406(17)	0.45555(8)	0.56637(9)	0.0212(3)
C12	0.28032(17)	0.48051(8)	0.50668(9)	0.0209(3)
C13	0.9350(2)	0.54079(11)	0.32998(11)	0.0346(4)
C14	0.0526(2)	0.65766(10)	0.44590(13)	0.0377(4)
C15	0.6335(2)	0.53115(12)	0.74422(11)	0.0351(4)
C16	0.7165(2)	0.36637(13)	0.73949(11)	0.0372(4)
C17	0.1984(3)	0.18359(11)	0.35288(12)	0.0410(5)
C18	0.2866(4)	0.21965(16)	0.29213(13)	0.0645(8)
C19	0.0381(3)	0.21418(16)	0.34701(18)	0.0664(8)
C20	0.1741(2)	0.16032(11)	0.51843(11)	0.0320(4)
C21	0.1433(3)	0.07534(12)	0.50741(17)	0.0536(6)
C22	0.2394(3)	0.17802(12)	0.60068(13)	0.0427(5)
C23	0.47061(19)	0.14730(10)	0.46103(10)	0.0280(3)
C24	0.4696(3)	0.07508(11)	0.41230(14)	0.0420(5)
C25	0.6051(2)	0.19767(12)	0.44885(12)	0.0365(4)
P2	0.79237(6)	0.37276(4)	0.17655(3)	0.04249(14)
F1	0.7785(3)	0.40409(13)	0.09122(11)	0.1074(8)
F2	0.71362(16)	0.44772(8)	0.20411(9)	0.0553(4)
F3	0.95187(19)	0.41267(14)	0.19217(15)	0.1088(9)
F4	0.6337(2)	0.33328(11)	0.15933(14)	0.0850(6)
F5	0.8078(3)	0.34325(12)	0.26170(9)	0.0941(7)
F6	0.8687(2)	0.29726(11)	0.15050(12)	0.0846(6)

Table 4. Bond lengths (Å) for JPD1052.

Cu1-N1	2.0374(14)	Cu1-N2	2.0420(13)

Cu1-P1	2.1743(4)	P1-C17	1.8419(19)
P1-C20	1.8548(19)	P1-C23	1.8593(18)
N1-C1	1.330(2)	N1-C12	1.362(2)
N2-C10	1.327(2)	N2-C11	1.359(2)
C1-C2	1.413(2)	C1-H1	0.95
C2-C3	1.383(2)	C2-C13	1.508(2)
C3-C4	1.422(2)	C3-C14	1.503(2)
C4-C12	1.404(2)	C4-C5	1.439(2)
C5-C6	1.348(3)	C5-H5	0.95
C6-C7	1.438(2)	C6-H6	0.95
C7-C11	1.403(2)	C7-C8	1.420(2)
C8-C9	1.386(3)	C8-C15	1.505(2)
C9-C10	1.408(2)	C9-C16	1.503(2)
C10-H10	0.95	C11-C12	1.444(2)
C13-H13A	0.98	C13-H13B	0.98
C13-H13C	0.98	C14-H14A	0.98
C14-H14B	0.98	C14-H14C	0.98
C15-H15A	0.98	C15-H15B	0.98
C15-H15C	0.98	C16-H16A	0.98
C16-H16B	0.98	C16-H16C	0.98
C17-C19	1.526(4)	C17-C18	1.529(4)
C17-H17	1.0	C18-H18A	0.98
C18-H18B	0.98	C18-H18C	0.98
C19-H19A	0.98	C19-H19B	0.98
C19-H19C	0.98	C20-C22	1.523(3)
C20-C21	1.530(3)	C20-H20	1.0
C21-H21A	0.98	C21-H21B	0.98
C21-H21C	0.98	C22-H22A	0.98
C22-H22B	0.98	C22-H22C	0.98

C23-C25	1.529(3)	C23-C24	1.530(3)
C23-H23	1.0	C24-H24A	0.98
C24-H24B	0.98	C24-H24C	0.98
C25-H25A	0.98	C25-H25B	0.98
C25-H25C	0.98	P2-F5	1.5678(18)
P2-F4	1.5809(18)	P2-F1	1.582(2)
P2-F6	1.5841(17)	P2-F3	1.5885(18)
P2-F2	1.5956(15)		

Table 5. Bond angles (°) for JPD1052.

N1-Cu1-N2	81.98(5)	N1-Cu1-P1	143.96(4)
N2-Cu1-P1	132.59(4)	C17-P1-C20	106.07(10)
C17-P1-C23	107.50(9)	C20-P1-C23	105.17(8)
C17-P1-Cu1	113.78(6)	C20-P1-Cu1	108.35(6)
C23-P1-Cu1	115.24(6)	C1-N1-C12	117.42(14)
C1-N1-Cu1	130.46(11)	C12-N1-Cu1	111.92(10)
C10-N2-C11	117.59(14)	C10-N2-Cu1	130.17(11)
C11-N2-Cu1	112.19(10)	N1-C1-C2	124.25(15)
N1-C1-H1	117.9	C2-C1-H1	117.9
C3-C2-C1	118.54(15)	C3-C2-C13	123.33(16)
C1-C2-C13	118.13(16)	C2-C3-C4	118.36(15)
C2-C3-C14	121.43(16)	C4-C3-C14	120.21(16)
C12-C4-C3	118.68(15)	C12-C4-C5	117.92(15)
C3-C4-C5	123.38(15)	C6-C5-C4	121.93(15)
C6-C5-H5	119.0	C4-C5-H5	119.0
C5-C6-C7	121.58(15)	C5-C6-H6	119.2
C7-C6-H6	119.2	C11-C7-C8	118.79(15)
C11-C7-C6	117.85(15)	C8-C7-C6	123.33(15)
C9-C8-C7	118.02(15)	C9-C8-C15	121.47(16)
C7-C8-C15	120.50(16)	C8-C9-C10	118.74(15)

C8-C9-C16	123.35(16)	C10-C9-C16	117.90(16)
N2-C10-C9	124.17(16)	N2-C10-H10	117.9
C9-C10-H10	117.9	N2-C11-C7	122.66(15)
N2-C11-C12	116.64(13)	C7-C11-C12	120.66(14)
N1-C12-C4	122.74(15)	N1-C12-C11	117.20(13)
C4-C12-C11	120.03(14)	C2-C13-H13A	109.5
C2-C13-H13B	109.5	H13A-C13-H13B	109.5
C2-C13-H13C	109.5	H13A-C13-H13C	109.5
H13B-C13-H13C	109.5	C3-C14-H14A	109.5
C3-C14-H14B	109.5	H14A-C14-H14B	109.5
C3-C14-H14C	109.5	H14A-C14-H14C	109.5
H14B-C14-H14C	109.5	C8-C15-H15A	109.5
C8-C15-H15B	109.5	H15A-C15-H15B	109.5
C8-C15-H15C	109.5	H15A-C15-H15C	109.5
H15B-C15-H15C	109.5	C9-C16-H16A	109.5
C9-C16-H16B	109.5	H16A-C16-H16B	109.5
C9-C16-H16C	109.5	H16A-C16-H16C	109.5
H16B-C16-H16C	109.5	C19-C17-C18	111.2(2)
C19-C17-P1	109.38(17)	C18-C17-P1	109.75(15)
C19-C17-H17	108.8	C18-C17-H17	108.8
P1-C17-H17	108.8	C17-C18-H18A	109.5
C17-C18-H18B	109.5	H18A-C18-H18B	109.5
C17-C18-H18C	109.5	H18A-C18-H18C	109.5
H18B-C18-H18C	109.5	C17-C19-H19A	109.5
C17-C19-H19B	109.5	H19A-C19-H19B	109.5
C17-C19-H19C	109.5	H19A-C19-H19C	109.5
H19B-C19-H19C	109.5	C22-C20-C21	111.35(19)
C22-C20-P1	109.77(13)	C21-C20-P1	115.20(14)
C22-C20-H20	106.7	C21-C20-H20	106.7

P1-C20-H20	106.7	C20-C21-H21A	109.5
C20-C21-H21B	109.5	H21A-C21-H21B	109.5
C20-C21-H21C	109.5	H21A-C21-H21C	109.5
H21B-C21-H21C	109.5	C20-C22-H22A	109.5
C20-C22-H22B	109.5	H22A-C22-H22B	109.5
C20-C22-H22C	109.5	H22A-C22-H22C	109.5
H22B-C22-H22C	109.5	C25-C23-C24	111.16(16)
C25-C23-P1	110.72(13)	C24-C23-P1	115.37(14)
C25-C23-H23	106.3	C24-C23-H23	106.3
P1-C23-H23	106.3	C23-C24-H24A	109.5
C23-C24-H24B	109.5	H24A-C24-H24B	109.5
C23-C24-H24C	109.5	H24A-C24-H24C	109.5
H24B-C24-H24C	109.5	C23-C25-H25A	109.5
C23-C25-H25B	109.5	H25A-C25-H25B	109.5
C23-C25-H25C	109.5	H25A-C25-H25C	109.5
H25B-C25-H25C	109.5	F5-P2-F4	91.04(14)
F5-P2-F1	178.83(13)	F4-P2-F1	89.90(13)
F5-P2-F6	89.95(11)	F4-P2-F6	89.07(11)
F1-P2-F6	90.76(13)	F5-P2-F3	90.01(15)
F4-P2-F3	178.93(14)	F1-P2-F3	89.06(14)
F6-P2-F3	90.69(11)	F5-P2-F2	89.03(9)
F4-P2-F2	90.17(10)	F1-P2-F2	90.27(11)
F6-P2-F2	178.72(11)	F3-P2-F2	90.08(9)

Table 6. Torsion angles (°) for JPD1052.

C12-N1-C1-C2	0.7(2)	Cu1-N1-C1-C2	175.15(12)
N1-C1-C2-C3	-0.7(2)	N1-C1-C2-C13	179.94(16)
C1-C2-C3-C4	0.1(2)	C13-C2-C3-C4	179.46(15)
C1-C2-C3-C14	179.95(16)	C13-C2-C3-C14	-0.7(3)
C2-C3-C4-C12	0.3(2)	C14-C3-C4-C12	-179.52(15)

C2-C3-C4-C5	-178.18(15)	C14-C3-C4-C5	2.0(2)
C12-C4-C5-C6	1.2(2)	C3-C4-C5-C6	179.76(16)
C4-C5-C6-C7	-1.7(3)	C5-C6-C7-C11	0.6(2)
C5-C6-C7-C8	-177.49(16)	C11-C7-C8-C9	-1.9(2)
C6-C7-C8-C9	176.26(15)	C11-C7-C8-C15	179.06(15)
C6-C7-C8-C15	-2.8(2)	C7-C8-C9-C10	1.6(2)
C15-C8-C9-C10	-179.35(16)	C7-C8-C9-C16	-179.00(16)
C15-C8-C9-C16	0.1(3)	C11-N2-C10-C9	-0.1(2)
Cu1-N2-C10-C9	-177.43(12)	C8-C9-C10-N2	-0.6(3)
C16-C9-C10-N2	179.93(16)	C10-N2-C11-C7	-0.2(2)
Cu1-N2-C11-C7	177.59(12)	C10-N2-C11-C12	-178.11(14)
Cu1-N2-C11-C12	-0.34(17)	C8-C7-C11-N2	1.2(2)
C6-C7-C11-N2	-177.03(15)	C8-C7-C11-C12	179.03(14)
C6-C7-C11-C12	0.8(2)	C1-N1-C12-C4	-0.3(2)
Cu1-N1-C12-C4	-175.67(12)	C1-N1-C12-C11	177.89(14)
Cu1-N1-C12-C11	2.47(17)	C3-C4-C12-N1	-0.3(2)
C5-C4-C12-N1	178.33(14)	C3-C4-C12-C11	-178.37(14)
C5-C4-C12-C11	0.2(2)	N2-C11-C12-N1	-1.5(2)
C7-C11-C12-N1	-179.44(14)	N2-C11-C12-C4	176.73(14)
C7-C11-C12-C4	-1.2(2)	C20-P1-C17-C19	55.75(18)
C23-P1-C17-C19	167.86(16)	Cu1-P1-C17-C19	-63.27(18)
C20-P1-C17-C18	177.96(17)	C23-P1-C17-C18	-69.93(18)
Cu1-P1-C17-C18	58.94(19)	C17-P1-C20-C22	-176.56(14)
C23-P1-C20-C22	69.71(15)	Cu1-P1-C20-C22	-54.03(14)
C17-P1-C20-C21	56.80(19)	C23-P1-C20-C21	-56.93(19)
Cu1-P1-C20-C21	179.33(16)	C17-P1-C23-C25	100.73(14)
C20-P1-C23-C25	-146.54(13)	Cu1-P1-C23-C25	-27.30(15)
C17-P1-C23-C24	-26.60(17)	C20-P1-C23-C24	86.12(16)
Cu1-P1-C23-C24	-154.64(12)		

Table 7. Anisotropic atomic displacement parameters (Å2) for JPD1052.

The anisotropic atomic displacement factor exponent takes the form: -2π2[h2 a*2 U11 + ... + 2 h k a* b* U12]

U11	U22	U33	U23	U13	U12
Cu1	0.02769(12)	0.01674(11)	0.02830(13)	-0.00387(7)	0.00185(8)	-0.00150(7)
P1	0.0266(2)	0.01665(19)	0.0254(2)	-0.00286(14)	-0.00267(16)	-0.00146(15)
N1	0.0233(6)	0.0202(6)	0.0246(6)	-0.0010(5)	0.0041(5)	-0.0013(5)
N2	0.0226(6)	0.0204(6)	0.0257(6)	-0.0026(5)	0.0028(5)	-0.0012(5)
C1	0.0245(7)	0.0244(8)	0.0257(7)	0.0003(6)	0.0033(6)	-0.0029(6)
C2	0.0221(7)	0.0264(8)	0.0298(8)	0.0071(6)	0.0085(6)	-0.0014(6)
C3	0.0240(7)	0.0212(7)	0.0336(8)	0.0054(6)	0.0117(6)	-0.0003(6)
C4	0.0262(7)	0.0178(7)	0.0288(8)	0.0008(6)	0.0104(6)	-0.0027(6)
C5	0.0364(9)	0.0178(7)	0.0365(9)	-0.0040(6)	0.0125(7)	-0.0029(6)
C6	0.0339(9)	0.0223(8)	0.0323(8)	-0.0087(6)	0.0095(7)	-0.0078(7)
C7	0.0243(7)	0.0235(7)	0.0255(7)	-0.0038(6)	0.0102(6)	-0.0062(6)
C8	0.0240(7)	0.0325(8)	0.0231(7)	-0.0048(6)	0.0071(6)	-0.0090(6)
C9	0.0207(7)	0.0350(9)	0.0246(8)	-0.0011(6)	0.0048(6)	-0.0048(6)
C10	0.0248(8)	0.0262(8)	0.0271(8)	-0.0009(6)	0.0030(6)	-0.0002(6)
C11	0.0200(7)	0.0199(7)	0.0250(7)	-0.0020(6)	0.0078(6)	-0.0035(5)
C12	0.0207(7)	0.0185(7)	0.0244(7)	0.0004(6)	0.0069(6)	-0.0026(5)
C13	0.0303(9)	0.0363(10)	0.0368(9)	0.0097(8)	0.0015(7)	0.0022(7)
C14	0.0383(10)	0.0235(8)	0.0520(12)	0.0060(8)	0.0082(9)	0.0040(7)
C15	0.0332(9)	0.0407(10)	0.0309(9)	-0.0098(7)	0.0017(7)	-0.0100(8)
C16	0.0311(9)	0.0503(12)	0.0292(9)	0.0032(8)	-0.0011(7)	-0.0023(8)
C17	0.0560(13)	0.0292(9)	0.0330(10)	-0.0052(7)	-0.0167(9)	-0.0045(8)
C18	0.109(2)	0.0515(14)	0.0281(10)	0.0039(9)	-0.0138(12)	-0.0139(14)
C19	0.0604(16)	0.0535(15)	0.0740(18)	-0.0056(13)	-0.0430(14)	0.0006(12)
C20	0.0264(8)	0.0258(8)	0.0451(11)	-0.0025(7)	0.0090(8)	-0.0030(6)
C21	0.0615(14)	0.0285(10)	0.0763(16)	-0.0050(10)	0.0323(13)	-0.0144(10)

C22	0.0442(12)	0.0495(13)	0.0367(11)	0.0039(8)	0.0147(9)	-0.0034(9)
C23	0.0280(8)	0.0242(8)	0.0322(8)	0.0005(7)	0.0056(7)	0.0026(6)
C24	0.0484(12)	0.0254(9)	0.0548(12)	-0.0077(8)	0.0163(10)	0.0051(8)
C25	0.0308(9)	0.0371(10)	0.0427(11)	-0.0029(8)	0.0098(8)	-0.0037(8)
P2	0.0415(3)	0.0465(3)	0.0388(3)	-0.0109(2)	0.0013(2)	0.0005(2)
F1	0.181(2)	0.0922(15)	0.0517(10)	0.0013(10)	0.0241(13)	-0.0324(15)
F2	0.0467(7)	0.0480(8)	0.0698(9)	-0.0025(7)	0.0005(7)	0.0115(6)
F3	0.0460(9)	0.1236(17)	0.160(2)	-0.0940(16)	0.0266(11)	-0.0163(10)
F4	0.0600(10)	0.0708(11)	0.1220(17)	-0.0107(11)	0.0010(11)	-0.0246(8)
F5	0.1416(19)	0.0991(14)	0.0411(8)	0.0059(9)	0.0072(10)	0.0740(14)
F6	0.0943(13)	0.0708(11)	0.0935(14)	-0.0441(10)	0.0314(11)	0.0116(10)

Table 8. Hydrogen atomic coordinates and isotropic atomic displacement parameters (Å2) for JPD1052.

x/a	y/b	z/c	U(eq)
H1	0.0793	0.4137	0.3626	0.03
H5	0.2527	0.6560	0.5685	0.035
H6	0.4376	0.6176	0.6599	0.035
H10	0.5646	0.3047	0.6198	0.031
H13A	-0.1544	0.5594	0.3518	0.052
H13B	-0.0900	0.4942	0.3006	0.052
H13C	-0.0302	0.5795	0.2958	0.052
H14A	0.1343	0.6932	0.4390	0.057
H14B	0.0114	0.6690	0.4943	0.057
H14C	-0.0267	0.6629	0.4029	0.057
H15A	0.7200	0.5062	0.7729	0.053
H15B	0.5590	0.5435	0.7794	0.053
H15C	0.6665	0.5779	0.7207	0.053
H16A	0.6840	0.3728	0.7909	0.056
H16B	0.8146	0.3906	0.7379	0.056
H16C	0.7244	0.3121	0.7281	0.056

H17	0.1946	0.1274	0.3447	0.049
H18A	0.3896	0.2000	0.2980	0.097
H18B	0.2886	0.2749	0.2988	0.097
H18C	0.2381	0.2071	0.2406	0.097
H19A	0.0399	0.2676	0.3629	0.1
H19B	-0.0204	0.1846	0.3807	0.1
H19C	-0.0082	0.2100	0.2937	0.1
H20	0.0745	0.1865	0.5101	0.038
H21A	0.0681	0.0593	0.5408	0.08
H21B	0.2365	0.0469	0.5209	0.08
H21C	0.1056	0.0654	0.4535	0.08
H22A	0.1665	0.1642	0.6362	0.064
H22B	0.2617	0.2324	0.6054	0.064
H22C	0.3320	0.1489	0.6133	0.064
H23	0.4856	0.1305	0.5160	0.034
H24A	0.3888	0.0415	0.4252	0.063
H24B	0.5663	0.0490	0.4229	0.063
H24C	0.4529	0.0885	0.3576	0.063
H25A	0.6974	0.1675	0.4563	0.055
H25B	0.6115	0.2396	0.4860	0.055
H25C	0.5924	0.2183	0.3964	0.055

Structure Determination Summary

Crystal Data and Structure Refinement for [(Me_4phen)Cu(N≡C–S)(P^tBu_3)]

Identification code	JPD1134_0m_a	
Empirical formula	$C_{29}H_{43}CuN_3PS$	
Formula weight	560.23	
Temperature	150(2) K	
Wavelength	0.71073 Å	
Crystal system	monoclinic	
Space group	$P2_1$	
Unit cell dimensions	a = 8.5199(8) Å	α = 90°

	b = 19.8526(17) Å β = 91.544(3)°
	c = 33.916(3) Å γ = 90°
Volume	5734.6(9) Å^3
Z	8
Density (calculated)	1.298 g/cm^3
Absorption coefficient	0.913 mm^{-1}
F(000)	2384
Crystal size	0.286 x 0.284 x 0.110 mm^3
θ range for data collection	0.601 to 29.398°
Index ranges	$-11 \leq h \leq 11$, $-27 \leq k - 27$, $-46 \leq l \leq 46$
Reflections collected	249830
Independent reflections	31145 [R(int) = 0.0485]
Completeness to θ = 28.000°	99.8 %
Absorption correction	Numerical
Max. and min. transmission	0.91 and 0.80
Refinement method	Full-matrix least-squares on F^2
Data / restraints / parameters	31145 / 700 / 1314
Goodness-of-fit on F^2	1.042
Final R indices [I>2σ(I)]	R1 = 0.0723, wR2 = 0.2082
R indices (all data)	R1 = 0.0924, wR2 = 0.2254
Absolute structure parameter	0.484(17)
Extinction coefficient	n/a
Largest diff. peak and hole	1.677 and -1.126 e·Å^{-3}

Table S1. Atomic coordinates (x 10^4) and equivalent isotropic displacement parameters (Å^2 x 10^3) for [(Me_4phen)Cu(N≡C–S)(P^tBu_3)]. U(eq) is defined as one third of the trace of the orthogonalized U^{ij} tensor.

Atom	x	y	z	U(eq)
Cu(1)	8477(1)	5264(1)	3669(1)	27(1)
S(5)	11696(4)	5602(2)	2582(1)	61(1)
P(1)	7198(2)	4300(1)	3764(1)	20(1)
N(1)	9216(7)	5954(3)	4115(2)	26(1)
N(2)	7368(7)	6154(3)	3475(2)	28(1)
N(3)	10296(11)	5282(4)	3290(2)	53(2)
C(1)	10172(9)	5871(4)	4430(2)	35(2)
C(2)	10663(9)	6366(5)	4695(2)	36(2)
C(3)	10132(9)	7014(5)	4622(3)	38(2)
C(4)	9167(10)	7138(5)	4287(3)	39(2)
C(5)	8617(12)	7804(5)	4179(3)	46(2)
C(6)	7708(12)	7903(5)	3855(3)	47(2)
C(7)	7233(10)	7353(4)	3604(3)	41(2)
C(8)	6220(10)	7449(5)	3261(3)	44(2)
C(9)	5843(11)	6898(5)	3040(3)	47(2)
C(10)	6477(11)	6254(5)	3159(3)	44(2)
C(11)	8728(9)	6598(4)	4039(2)	27(1)
C(12)	7768(8)	6704(4)	3694(2)	26(1)
C(13)	11709(12)	6158(7)	5039(3)	54(3)
C(14)	10572(12)	7593(6)	4899(3)	60(3)
C(15)	5537(14)	8122(6)	3140(4)	69(4)
C(16)	4839(13)	6935(7)	2672(3)	64(3)
C(17)	5944(9)	4309(4)	4214(2)	33(2)
C(18)	4639(10)	3775(4)	4238(3)	42(2)
C(19)	7079(12)	4256(5)	4603(2)	51(2)
C(20)	5257(10)	5006(4)	4254(3)	40(2)
C(21)	8701(10)	3566(4)	3829(3)	40(2)
C(22)	10047(10)	3808(5)	4073(3)	50(2)
C(23)	8021(11)	2912(4)	3993(3)	43(2)
C(24)	9383(15)	3426(7)	3408(4)	77(4)
C(25)	5924(13)	4082(5)	3316(3)	51(2)
C(26)	5219(13)	3399(5)	3276(3)	46(2)
C(27)	6689(16)	4308(6)	2952(3)	68(3)
C(28)	4390(12)	4616(6)	3359(4)	71(3)
C(29)	10827(10)	5412(4)	2983(3)	38(2)
Cu(2)	8258(1)	4622(1)	6146(1)	25(1)
S(6)	11944(3)	4321(2)	5122(1)	51(1)
P(2)	6910(2)	5561(1)	6244(1)	18(1)
N(4)	9146(7)	3965(4)	6602(2)	29(1)

Table S1. Atomic coordinates (x 10^4) and equivalent isotropic displacement parameters (Å^2 x 10^3) for [(Me$_4$phen)Cu(N≡C–S)(P^{t}Bu$_3$)]. U(eq) is defined as one third of the trace of the orthogonalized U^{ij} tensor.

Atom	x	y	z	U(eq)
N(5)	7191(7)	3696(3)	5988(2)	23(1)
N(6)	9967(8)	4615(4)	5743(2)	35(1)
C(30)	10085(9)	4123(4)	6917(2)	32(2)
C(31)	10608(10)	3628(5)	7195(2)	38(2)
C(32)	10123(10)	2969(5)	7150(2)	39(2)
C(33)	9162(9)	2803(4)	6816(2)	30(2)
C(34)	8646(11)	2140(5)	6730(3)	41(2)
C(35)	7719(10)	1990(4)	6417(3)	36(2)
C(36)	7161(9)	2505(4)	6145(2)	27(1)
C(37)	6158(9)	2375(4)	5817(2)	30(2)
C(38)	5724(9)	2905(4)	5583(2)	30(2)
C(39)	6258(8)	3563(3)	5678(2)	25(1)
C(40)	8696(8)	3324(4)	6555(2)	25(1)
C(41)	7665(8)	3175(3)	6225(2)	25(1)
C(42)	11675(11)	3830(7)	7523(3)	52(3)
C(43)	10577(13)	2420(7)	7442(3)	61(3)
C(44)	5641(11)	1673(4)	5739(3)	43(2)
C(45)	4679(11)	2832(5)	5212(3)	43(2)
C(46)	4911(8)	5392(4)	6466(2)	35(2)
C(47)	3862(11)	5048(6)	6125(3)	60(3)
C(48)	5048(12)	4835(5)	6784(3)	56(3)
C(49)	4037(11)	5990(5)	6632(3)	43(2)
C(50)	8035(9)	6148(4)	6588(2)	35(2)
C(51)	7867(11)	5855(5)	7024(2)	45(2)
C(52)	7518(11)	6887(4)	6592(3)	43(2)
C(53)	9736(10)	6098(5)	6507(3)	49(2)
C(54)	6564(9)	6013(4)	5754(2)	31(2)
C(55)	6204(11)	5501(5)	5435(2)	43(2)
C(56)	8156(11)	6335(4)	5637(3)	44(2)
C(57)	5361(13)	6585(5)	5746(3)	45(2)
C(58)	10766(8)	4495(4)	5487(2)	28(1)
Cu(3)	8324(2)	4718(1)	1099(1)	46(1)
S(7)	11836(3)	4395(2)	58(1)	59(1)
P(3)	7065(3)	5678(1)	1203(1)	38(1)
N(7)	7199(9)	3830(4)	900(2)	39(2)
N(8)	9082(9)	4007(4)	1526(2)	41(2)
N(9)	10139(11)	4723(5)	709(3)	62(3)
C(59)	6269(11)	3717(5)	580(2)	45(2)
C(60)	5693(11)	3104(5)	453(3)	44(2)

Table S1. Atomic coordinates (x 10^4) and equivalent isotropic displacement parameters (Å^2 x 10^3) for [(Me_4phen)Cu(N≡C–S)(P^tBu_3)]. U(eq) is defined as one third of the trace of the orthogonalized U^{ij} tensor.

Atom	x	y	z	U(eq)
C(61)	6009(10)	2550(5)	680(3)	42(2)
C(62)	6990(9)	2619(4)	1026(2)	34(2)
C(63)	7396(10)	2059(5)	1272(3)	40(2)
C(64)	8349(11)	2161(5)	1598(3)	42(2)
C(65)	8930(9)	2817(5)	1705(2)	36(2)
C(66)	9880(11)	2915(6)	2045(3)	45(2)
C(67)	10415(11)	3570(6)	2120(3)	46(2)
C(68)	9958(11)	4114(5)	1858(3)	43(2)
C(69)	7552(10)	3270(4)	1119(2)	33(2)
C(70)	8551(9)	3376(4)	1459(2)	34(2)
C(71)	4650(14)	3065(7)	84(3)	63(3)
C(72)	5379(13)	1862(6)	577(4)	62(3)
C(73)	10305(13)	2349(7)	2318(3)	61(3)
C(74)	11458(13)	3753(7)	2475(3)	56(3)
C(75)	5937(12)	5938(4)	752(3)	65(3)
C(77)	6883(16)	5753(7)	383(3)	82(4)
C(76)	4500(17)	5461(9)	786(6)	132(7)
C(78)	5336(17)	6670(5)	694(4)	72(4)
C(79)	8520(12)	6370(6)	1337(3)	59(3)
C(80)	7864(14)	7045(6)	1476(4)	65(3)
C(81)	9385(17)	6558(7)	907(4)	90(4)
C(82)	9925(18)	6108(9)	1596(5)	97(5)
C(83)	5648(18)	5603(8)	1603(5)	94(4)
C(84)	7030(20)	5691(10)	2023(4)	116(6)
C(85)	4447(16)	6199(6)	1657(4)	80(4)
C(86)	4900(20)	4934(10)	1649(6)	113(6)
C(87)	10796(10)	4572(5)	444(3)	41(2)
Cu(4)	1901(1)	388(1)	1422(1)	29(1)
S(8)	-1968(3)	671(2)	2401(1)	49(1)
P(4)	3198(2)	-562(1)	1312(1)	21(1)
N(10)	3005(8)	1312(3)	1601(2)	28(1)
N(11)	1084(8)	1058(4)	967(2)	34(2)
N(12)	185(8)	401(4)	1808(2)	36(2)
C(88)	3918(10)	1430(4)	1912(2)	34(2)
C(89)	4463(9)	2072(4)	2026(2)	34(2)
C(90)	4068(10)	2620(4)	1800(3)	37(2)
C(91)	3101(11)	2515(4)	1458(3)	40(2)
C(92)	2571(12)	3036(5)	1188(3)	47(2)
C(93)	1674(11)	2913(5)	870(3)	47(2)

Table S1. Atomic coordinates (x 10^4) and equivalent isotropic displacement parameters (Å^2 x 10^3) for [(Me_4phen)Cu(N≡C–S)(P^tBu_3)]. U(eq) is defined as one third of the trace of the orthogonalized U^{ij} tensor.

Atom	x	y	z	U(eq)
C(94)	1119(10)	2258(5)	777(3)	41(2)
C(95)	137(11)	2084(6)	442(3)	44(2)
C(96)	-338(10)	1458(6)	388(2)	43(2)
C(97)	136(11)	963(5)	662(3)	41(2)
C(98)	2579(9)	1851(4)	1373(2)	29(2)
C(99)	1579(9)	1715(4)	1036(2)	33(2)
C(100)	5418(12)	2132(5)	2391(3)	52(2)
C(101)	4659(12)	3323(5)	1882(3)	52(2)
C(102)	-322(12)	2640(7)	148(3)	63(3)
C(103)	-1348(13)	1211(8)	42(3)	64(3)
C(104)	2090(9)	-1105(4)	942(3)	43(2)
C(105)	2520(13)	-1865(5)	939(4)	60(3)
C(106)	321(11)	-1079(6)	1032(4)	65(3)
C(107)	2242(12)	-813(6)	519(3)	61(3)
C(108)	3533(10)	-1021(4)	1798(2)	32(2)
C(109)	3965(12)	-526(5)	2116(2)	48(2)
C(110)	4779(13)	-1592(5)	1786(3)	48(2)
C(111)	1891(15)	-1334(6)	1911(4)	76(4)
C(112)	5221(8)	-409(4)	1097(2)	32(1)
C(113)	6039(9)	-1013(5)	921(3)	41(2)
C(114)	4953(13)	112(6)	763(3)	64(3)
C(115)	6339(9)	-114(5)	1432(3)	52(2)
C(116)	-706(9)	505(5)	2061(2)	33(2)

Table S2. Bond lengths (Å) for [(Me_4phen)Cu(N≡C–S)(P^tBu_3)]. Symmetry transformations used to generate equivalent atoms:

Cu(1)-N(3)	2.040(7)	C(16)-H(16B)	0.9800
Cu(1)-N(2)	2.102(6)	C(16)-H(16C)	0.9800
Cu(1)-N(1)	2.124(6)	C(17)-C(20)	1.509(10)
Cu(1)-P(1)	2.2297(19)	C(17)-C(18)	1.541(11)
S(5)-C(29)	1.611(9)	C(17)-C(19)	1.617(12)
P(1)-C(17)	1.886(7)	C(18)-H(18A)	0.9800
P(1)-C(25)	1.893(9)	C(18)-H(18B)	0.9800
P(1)-C(21)	1.949(8)	C(18)-H(18C)	0.9800
N(1)-C(1)	1.335(10)	C(19)-H(19A)	0.9800
N(1)-C(11)	1.367(10)	C(19)-H(19B)	0.9800
N(2)-C(10)	1.311(10)	C(19)-H(19C)	0.9800
N(2)-C(12)	1.358(10)	C(20)-H(20A)	0.9800
N(3)-C(29)	1.176(11)	C(20)-H(20B)	0.9800
C(1)-C(2)	1.389(11)	C(20)-H(20C)	0.9800
C(1)-H(1)	0.9500	C(21)-C(22)	1.475(13)
C(2)-C(3)	1.382(14)	C(21)-C(23)	1.534(12)
C(2)-C(13)	1.508(13)	C(21)-C(24)	1.582(14)
C(3)-C(4)	1.407(13)	C(22)-H(22A)	0.9800
C(3)-C(14)	1.525(12)	C(22)-H(22B)	0.9800
C(4)-C(11)	1.407(11)	C(22)-H(22C)	0.9800
C(4)-C(5)	1.446(14)	C(23)-H(23A)	0.9800
C(5)-C(6)	1.342(15)	C(23)-H(23B)	0.9800
C(5)-H(5)	0.9500	C(23)-H(23C)	0.9800
C(6)-C(7)	1.436(14)	C(24)-H(24A)	0.9800
C(6)-H(6)	0.9500	C(24)-H(24B)	0.9800
C(7)-C(12)	1.397(11)	C(24)-H(24C)	0.9800
C(7)-C(8)	1.441(14)	C(25)-C(27)	1.481(14)
C(8)-C(9)	1.359(15)	C(25)-C(26)	1.487(12)
C(8)-C(15)	1.510(13)	C(25)-C(28)	1.693(16)
C(9)-C(10)	1.442(13)	C(26)-H(26A)	0.9800
C(9)-C(16)	1.497(14)	C(26)-H(26B)	0.9800
C(10)-H(10)	0.9500	C(26)-H(26C)	0.9800
C(11)-C(12)	1.428(11)	C(27)-H(27A)	0.9800
C(13)-H(13A)	0.9800	C(27)-H(27B)	0.9800
C(13)-H(13B)	0.9800	C(27)-H(27C)	0.9800
C(13)-H(13C)	0.9800	C(28)-H(28A)	0.9800
C(14)-H(14A)	0.9800	C(28)-H(28B)	0.9800
C(14)-H(14B)	0.9800	C(28)-H(28C)	0.9800
C(14)-H(14C)	0.9800	Cu(2)-N(6)	2.025(7)
C(15)-H(15A)	0.9800	Cu(2)-N(5)	2.113(6)
C(15)-H(15B)	0.9800	Cu(2)-N(4)	2.144(6)
C(15)-H(15C)	0.9800	Cu(2)-P(2)	2.2204(18)
C(16)-H(16A)	0.9800	S(6)-C(58)	1.650(8)

Table S2. Bond lengths (Å) for [(Me_4phen)Cu(N≡C–S)(P^tBu_3)]. Symmetry transformations used to generate equivalent atoms:

P(2)-C(50)	1.891(8)	C(47)-H(47A)	0.9800
P(2)-C(54)	1.906(7)	C(47)-H(47B)	0.9800
P(2)-C(46)	1.909(8)	C(47)-H(47C)	0.9800
N(4)-C(40)	1.338(10)	C(48)-H(48A)	0.9800
N(4)-C(30)	1.353(10)	C(48)-H(48B)	0.9800
N(5)-C(39)	1.327(9)	C(48)-H(48C)	0.9800
N(5)-C(41)	1.363(9)	C(49)-H(49A)	0.9800
N(6)-C(58)	1.142(10)	C(49)-H(49B)	0.9800
C(30)-C(31)	1.424(12)	C(49)-H(49C)	0.9800
C(30)-H(30)	0.9500	C(50)-C(53)	1.486(12)
C(31)-C(32)	1.379(15)	C(50)-C(52)	1.533(11)
C(31)-C(42)	1.475(13)	C(50)-C(51)	1.596(12)
C(32)-C(33)	1.420(12)	C(51)-H(51A)	0.9800
C(32)-C(43)	1.517(12)	C(51)-H(51B)	0.9800
C(33)-C(40)	1.412(10)	C(51)-H(51C)	0.9800
C(33)-C(34)	1.415(13)	C(52)-H(52A)	0.9800
C(34)-C(35)	1.339(14)	C(52)-H(52B)	0.9800
C(34)-H(34)	0.9500	C(52)-H(52C)	0.9800
C(35)-C(36)	1.448(10)	C(53)-H(53A)	0.9800
C(35)-H(35)	0.9500	C(53)-H(53B)	0.9800
C(36)-C(37)	1.409(11)	C(53)-H(53C)	0.9800
C(36)-C(41)	1.422(10)	C(54)-C(55)	1.510(11)
C(37)-C(38)	1.364(11)	C(54)-C(57)	1.530(11)
C(37)-C(44)	1.484(11)	C(54)-C(56)	1.559(12)
C(38)-C(39)	1.418(10)	C(55)-H(55A)	0.9800
C(38)-C(45)	1.528(11)	C(55)-H(55B)	0.9800
C(39)-H(39)	0.9500	C(55)-H(55C)	0.9800
C(40)-C(41)	1.435(10)	C(56)-H(56A)	0.9800
C(42)-H(42A)	0.9800	C(56)-H(56B)	0.9800
C(42)-H(42B)	0.9800	C(56)-H(56C)	0.9800
C(42)-H(42C)	0.9800	C(57)-H(57A)	0.9800
C(43)-H(43A)	0.9800	C(57)-H(57B)	0.9800
C(43)-H(43B)	0.9800	C(57)-H(57C)	0.9800
C(43)-H(43C)	0.9800	Cu(3)-N(9)	2.063(8)
C(44)-H(44A)	0.9800	Cu(3)-N(7)	2.109(8)
C(44)-H(44B)	0.9800	Cu(3)-N(8)	2.112(7)
C(44)-H(44C)	0.9800	Cu(3)-P(3)	2.219(2)
C(45)-H(45A)	0.9800	S(7)-C(87)	1.640(10)
C(45)-H(45B)	0.9800	P(3)-C(83)	1.847(13)
C(45)-H(45C)	0.9800	P(3)-C(75)	1.859(10)
C(46)-C(49)	1.518(12)	P(3)-C(79)	1.898(11)
C(46)-C(48)	1.548(12)	N(7)-C(59)	1.345(12)
C(46)-C(47)	1.594(12)	N(7)-C(69)	1.367(9)

Table S2. Bond lengths (Å) for [(Me_4phen)Cu(N≡C–S)(P^tBu_3)]. Symmetry transformations used to generate equivalent atoms:

N(8)-C(70)	1.349(13)	C(76)-H(76C)	0.9800
N(8)-C(68)	1.351(11)	C(78)-H(78A)	0.9800
N(9)-C(87)	1.111(12)	C(78)-H(78B)	0.9800
C(59)-C(60)	1.378(14)	C(78)-H(78C)	0.9800
C(59)-H(59)	0.9500	C(79)-C(80)	1.532(15)
C(60)-C(61)	1.365(13)	C(79)-C(82)	1.554(17)
C(60)-C(71)	1.518(14)	C(79)-C(81)	1.694(16)
C(61)-C(62)	1.429(13)	C(80)-H(80A)	0.9800
C(61)-C(72)	1.505(15)	C(80)-H(80B)	0.9800
C(62)-C(69)	1.412(12)	C(80)-H(80C)	0.9800
C(62)-C(63)	1.427(11)	C(81)-H(81A)	0.9800
C(63)-C(64)	1.368(13)	C(81)-H(81B)	0.9800
C(63)-H(63)	0.9500	C(81)-H(81C)	0.9800
C(64)-C(65)	1.438(14)	C(82)-H(82A)	0.9800
C(64)-H(64)	0.9500	C(82)-H(82B)	0.9800
C(65)-C(66)	1.404(13)	C(82)-H(82C)	0.9800
C(65)-C(70)	1.420(11)	C(83)-C(86)	1.48(2)
C(66)-C(67)	1.399(16)	C(83)-C(85)	1.578(18)
C(66)-C(73)	1.494(13)	C(83)-C(84)	1.83(2)
C(67)-C(68)	1.444(14)	C(84)-H(84A)	0.9800
C(67)-C(74)	1.522(14)	C(84)-H(84B)	0.9800
C(68)-H(68)	0.9500	C(84)-H(84C)	0.9800
C(69)-C(70)	1.429(12)	C(85)-H(85A)	0.9800
C(71)-H(71A)	0.9800	C(85)-H(85B)	0.9800
C(71)-H(71B)	0.9800	C(85)-H(85C)	0.9800
C(71)-H(71C)	0.9800	C(86)-H(86A)	0.9800
C(72)-H(72A)	0.9800	C(86)-H(86B)	0.9800
C(72)-H(72B)	0.9800	C(86)-H(86C)	0.9800
C(72)-H(72C)	0.9800	Cu(4)-N(12)	1.988(6)
C(73)-H(73A)	0.9800	Cu(4)-N(11)	2.139(7)
C(73)-H(73B)	0.9800	Cu(4)-N(10)	2.142(6)
C(73)-H(73C)	0.9800	Cu(4)-P(4)	2.2226(19)
C(74)-H(74A)	0.9800	S(8)-C(116)	1.630(9)
C(74)-H(74B)	0.9800	P(4)-C(104)	1.888(8)
C(74)-H(74C)	0.9800	P(4)-C(108)	1.897(7)
C(75)-C(77)	1.549(3)	P(4)-C(112)	1.915(7)
C(75)-C(78)	1.551(3)	N(10)-C(88)	1.315(10)
C(75)-C(76)	1.555(3)	N(10)-C(98)	1.363(9)
C(77)-H(77A)	0.9800	N(11)-C(97)	1.311(11)
C(77)-H(77B)	0.9800	N(11)-C(99)	1.388(12)
C(77)-H(77C)	0.9800	N(12)-C(116)	1.180(10)
C(76)-H(76A)	0.9800	C(88)-C(89)	1.407(11)
C(76)-H(76B)	0.9800	C(88)-H(88)	0.9500

Table S2. Bond lengths (Å) for [(Me_4phen)Cu(N≡C–S)(P^tBu_3)]. Symmetry transformations used to generate equivalent atoms:

C(89)-C(90)	1.367(12)	C(108)-C(110)	1.555(11)
C(89)-C(100)	1.469(13)	C(108)-C(111)	1.588(14)
C(90)-C(91)	1.420(13)	C(109)-H(10V)	0.9800
C(90)-C(101)	1.506(12)	C(109)-H(10W)	0.9800
C(91)-C(98)	1.418(12)	C(109)-H(10X)	0.9800
C(91)-C(92)	1.447(12)	C(110)-H(11A)	0.9800
C(92)-C(93)	1.327(15)	C(110)-H(11B)	0.9800
C(92)-H(92)	0.9500	C(110)-H(11C)	0.9800
C(93)-C(94)	1.417(15)	C(111)-H(11D)	0.9800
C(93)-H(93)	0.9500	C(111)-H(11E)	0.9800
C(94)-C(95)	1.436(14)	C(111)-H(11F)	0.9800
C(94)-C(99)	1.438(11)	C(112)-C(113)	1.516(11)
C(95)-C(96)	1.319(16)	C(112)-C(114)	1.546(12)
C(95)-C(102)	1.531(13)	C(112)-C(115)	1.575(12)
C(96)-C(97)	1.403(13)	C(113)-H(11G)	0.9800
C(96)-C(103)	1.518(14)	C(113)-H(11H)	0.9800
C(97)-H(97)	0.9500	C(113)-H(11I)	0.9800
C(98)-C(99)	1.433(12)	C(114)-H(11J)	0.9800
C(100)-H(10A)	0.9800	C(114)-H(11K)	0.9800
C(100)-H(10B)	0.9800	C(114)-H(11L)	0.9800
C(100)-H(10C)	0.9800	C(115)-H(11M)	0.9800
C(101)-H(10D)	0.9800	C(115)-H(11N)	0.9800
C(101)-H(10E)	0.9800	C(115)-H(11O)	0.9800
C(101)-H(10F)	0.9800		
C(102)-H(10G)	0.9800		
C(102)-H(10H)	0.9800		
C(102)-H(10I)	0.9800		
C(103)-H(10J)	0.9800		
C(103)-H(10K)	0.9800		
C(103)-H(10L)	0.9800		
C(104)-C(106)	1.547(13)		
C(104)-C(105)	1.553(13)		
C(104)-C(107)	1.557(15)		
C(105)-H(10M)	0.9800		
C(105)-H(10N)	0.9800		
C(105)-H(10O)	0.9800		
C(106)-H(10P)	0.9800		
C(106)-H(10Q)	0.9800		
C(106)-H(10R)	0.9800		
C(107)-H(10S)	0.9800		
C(107)-H(10T)	0.9800		
C(107)-H(10U)	0.9800		
C(108)-C(109)	1.498(12)		

Table S3. Bond angles (deg.) for [(Me_4phen)Cu(N≡C–S)(P^tBu_3)]. Symmetry transformations used to generate equivalent atoms:

N(3)-Cu(1)-N(2)	97.4(3)	C(8)-C(9)-C(10)	118.5(9)
N(3)-Cu(1)-N(1)	102.8(3)	C(8)-C(9)-C(16)	122.9(9)
N(2)-Cu(1)-N(1)	78.6(2)	C(10)-C(9)-C(16)	118.6(10)
N(3)-Cu(1)-P(1)	119.3(2)	N(2)-C(10)-C(9)	124.6(10)
N(2)-Cu(1)-P(1)	123.36(18)	N(2)-C(10)-H(10)	117.7
N(1)-Cu(1)-P(1)	125.97(18)	C(9)-C(10)-H(10)	117.7
C(17)-P(1)-C(25)	109.1(4)	N(1)-C(11)-C(4)	121.8(8)
C(17)-P(1)-C(21)	107.5(3)	N(1)-C(11)-C(12)	117.2(6)
C(25)-P(1)-C(21)	106.3(4)	C(4)-C(11)-C(12)	121.0(8)
C(17)-P(1)-Cu(1)	113.4(2)	N(2)-C(12)-C(7)	123.1(8)
C(25)-P(1)-Cu(1)	110.6(3)	N(2)-C(12)-C(11)	117.4(6)
C(21)-P(1)-Cu(1)	109.6(3)	C(7)-C(12)-C(11)	119.5(8)
C(1)-N(1)-C(11)	116.2(7)	C(2)-C(13)-H(13A)	109.5
C(1)-N(1)-Cu(1)	130.8(5)	C(2)-C(13)-H(13B)	109.5
C(11)-N(1)-Cu(1)	112.7(5)	H(13A)-C(13)-H(13B)	109.5
C(10)-N(2)-C(12)	117.1(7)	C(2)-C(13)-H(13C)	109.5
C(10)-N(2)-Cu(1)	129.0(6)	H(13A)-C(13)-H(13C)	109.5
C(12)-N(2)-Cu(1)	113.6(5)	H(13B)-C(13)-H(13C)	109.5
C(29)-N(3)-Cu(1)	151.6(9)	C(3)-C(14)-H(14A)	109.5
N(1)-C(1)-C(2)	126.6(8)	C(3)-C(14)-H(14B)	109.5
N(1)-C(1)-H(1)	116.7	H(14A)-C(14)-H(14B)	109.5
C(2)-C(1)-H(1)	116.7	C(3)-C(14)-H(14C)	109.5
C(3)-C(2)-C(1)	116.8(8)	H(14A)-C(14)-H(14C)	109.5
C(3)-C(2)-C(13)	125.3(8)	H(14B)-C(14)-H(14C)	109.5
C(1)-C(2)-C(13)	117.9(9)	C(8)-C(15)-H(15A)	109.5
C(2)-C(3)-C(4)	119.3(8)	C(8)-C(15)-H(15B)	109.5
C(2)-C(3)-C(14)	121.1(9)	H(15A)-C(15)-H(15B)	109.5
C(4)-C(3)-C(14)	119.6(9)	C(8)-C(15)-H(15C)	109.5
C(11)-C(4)-C(3)	119.2(8)	H(15A)-C(15)-H(15C)	109.5
C(11)-C(4)-C(5)	117.9(9)	H(15B)-C(15)-H(15C)	109.5
C(3)-C(4)-C(5)	122.9(8)	C(9)-C(16)-H(16A)	109.5
C(6)-C(5)-C(4)	121.1(9)	C(9)-C(16)-H(16B)	109.5
C(6)-C(5)-H(5)	119.5	H(16A)-C(16)-H(16B)	109.5
C(4)-C(5)-H(5)	119.5	C(9)-C(16)-H(16C)	109.5
C(5)-C(6)-C(7)	121.5(9)	H(16A)-C(16)-H(16C)	109.5
C(5)-C(6)-H(6)	119.2	H(16B)-C(16)-H(16C)	109.5
C(7)-C(6)-H(6)	119.2	C(20)-C(17)-C(18)	110.1(7)
C(12)-C(7)-C(6)	119.1(9)	C(20)-C(17)-C(19)	102.3(7)
C(12)-C(7)-C(8)	118.9(8)	C(18)-C(17)-C(19)	109.2(7)
C(6)-C(7)-C(8)	122.1(8)	C(20)-C(17)-P(1)	108.1(5)
C(9)-C(8)-C(7)	117.8(8)	C(18)-C(17)-P(1)	117.4(5)
C(9)-C(8)-C(15)	118.6(10)	C(19)-C(17)-P(1)	108.6(5)
C(7)-C(8)-C(15)	123.7(10)	C(17)-C(18)-H(18A)	109.5

Table S3. Bond angles (deg.) for [(Me_4phen)Cu(N≡C–S)(P^tBu_3)]. Symmetry transformations used to generate equivalent atoms:

C(17)-C(18)-H(18B)	109.5	C(26)-C(25)-C(28)	105.6(9)
H(18A)-C(18)-H(18B)	109.5	C(27)-C(25)-P(1)	110.1(7)
C(17)-C(18)-H(18C)	109.5	C(26)-C(25)-P(1)	120.2(7)
H(18A)-C(18)-H(18C)	109.5	C(28)-C(25)-P(1)	102.5(7)
H(18B)-C(18)-H(18C)	109.5	C(25)-C(26)-H(26A)	109.5
C(17)-C(19)-H(19A)	109.5	C(25)-C(26)-H(26B)	109.5
C(17)-C(19)-H(19B)	109.5	H(26A)-C(26)-H(26B)	109.5
H(19A)-C(19)-H(19B)	109.5	C(25)-C(26)-H(26C)	109.5
C(17)-C(19)-H(19C)	109.5	H(26A)-C(26)-H(26C)	109.5
H(19A)-C(19)-H(19C)	109.5	H(26B)-C(26)-H(26C)	109.5
H(19B)-C(19)-H(19C)	109.5	C(25)-C(27)-H(27A)	109.5
C(17)-C(20)-H(20A)	109.5	C(25)-C(27)-H(27B)	109.5
C(17)-C(20)-H(20B)	109.5	H(27A)-C(27)-H(27B)	109.5
H(20A)-C(20)-H(20B)	109.5	C(25)-C(27)-H(27C)	109.5
C(17)-C(20)-H(20C)	109.5	H(27A)-C(27)-H(27C)	109.5
H(20A)-C(20)-H(20C)	109.5	H(27B)-C(27)-H(27C)	109.5
H(20B)-C(20)-H(20C)	109.5	C(25)-C(28)-H(28A)	109.5
C(22)-C(21)-C(23)	111.6(8)	C(25)-C(28)-H(28B)	109.5
C(22)-C(21)-C(24)	105.3(9)	H(28A)-C(28)-H(28B)	109.5
C(23)-C(21)-C(24)	109.4(8)	C(25)-C(28)-H(28C)	109.5
C(22)-C(21)-P(1)	108.6(6)	H(28A)-C(28)-H(28C)	109.5
C(23)-C(21)-P(1)	114.9(6)	H(28B)-C(28)-H(28C)	109.5
C(24)-C(21)-P(1)	106.6(6)	N(3)-C(29)-S(5)	175.1(9)
C(21)-C(22)-H(22A)	109.5	N(6)-Cu(2)-N(5)	97.8(3)
C(21)-C(22)-H(22B)	109.5	N(6)-Cu(2)-N(4)	103.7(3)
H(22A)-C(22)-H(22B)	109.5	N(5)-Cu(2)-N(4)	78.2(3)
C(21)-C(22)-H(22C)	109.5	N(6)-Cu(2)-P(2)	119.4(2)
H(22A)-C(22)-H(22C)	109.5	N(5)-Cu(2)-P(2)	123.20(17)
H(22B)-C(22)-H(22C)	109.5	N(4)-Cu(2)-P(2)	125.19(19)
C(21)-C(23)-H(23A)	109.5	C(50)-P(2)-C(54)	108.2(4)
C(21)-C(23)-H(23B)	109.5	C(50)-P(2)-C(46)	108.0(4)
H(23A)-C(23)-H(23B)	109.5	C(54)-P(2)-C(46)	107.9(4)
C(21)-C(23)-H(23C)	109.5	C(50)-P(2)-Cu(2)	110.8(2)
H(23A)-C(23)-H(23C)	109.5	C(54)-P(2)-Cu(2)	109.5(2)
H(23B)-C(23)-H(23C)	109.5	C(46)-P(2)-Cu(2)	112.4(3)
C(21)-C(24)-H(24A)	109.5	C(40)-N(4)-C(30)	118.4(7)
C(21)-C(24)-H(24B)	109.5	C(40)-N(4)-Cu(2)	113.4(5)
H(24A)-C(24)-H(24B)	109.5	C(30)-N(4)-Cu(2)	128.1(6)
C(21)-C(24)-H(24C)	109.5	C(39)-N(5)-C(41)	118.5(6)
H(24A)-C(24)-H(24C)	109.5	C(39)-N(5)-Cu(2)	128.2(5)
H(24B)-C(24)-H(24C)	109.5	C(41)-N(5)-Cu(2)	113.1(5)
C(27)-C(25)-C(26)	112.7(9)	C(58)-N(6)-Cu(2)	165.7(7)
C(27)-C(25)-C(28)	103.8(9)	N(4)-C(30)-C(31)	122.0(8)

Table S3. Bond angles (deg.) for [(Me_4phen)Cu(N≡C–S)(P^tBu_3)]. Symmetry transformations used to generate equivalent atoms:

N(4)-C(30)-H(30)	119.0	H(43A)-C(43)-H(43B)	109.5
C(31)-C(30)-H(30)	119.0	C(32)-C(43)-H(43C)	109.5
C(32)-C(31)-C(30)	119.7(8)	H(43A)-C(43)-H(43C)	109.5
C(32)-C(31)-C(42)	121.2(9)	H(43B)-C(43)-H(43C)	109.5
C(30)-C(31)-C(42)	119.1(9)	C(37)-C(44)-H(44A)	109.5
C(31)-C(32)-C(33)	118.2(7)	C(37)-C(44)-H(44B)	109.5
C(31)-C(32)-C(43)	122.7(9)	H(44A)-C(44)-H(44B)	109.5
C(33)-C(32)-C(43)	119.1(10)	C(37)-C(44)-H(44C)	109.5
C(40)-C(33)-C(34)	118.2(8)	H(44A)-C(44)-H(44C)	109.5
C(40)-C(33)-C(32)	118.5(8)	H(44B)-C(44)-H(44C)	109.5
C(34)-C(33)-C(32)	123.3(8)	C(38)-C(45)-H(45A)	109.5
C(35)-C(34)-C(33)	122.8(7)	C(38)-C(45)-H(45B)	109.5
C(35)-C(34)-H(34)	118.6	H(45A)-C(45)-H(45B)	109.5
C(33)-C(34)-H(34)	118.6	C(38)-C(45)-H(45C)	109.5
C(34)-C(35)-C(36)	121.7(8)	H(45A)-C(45)-H(45C)	109.5
C(34)-C(35)-H(35)	119.2	H(45B)-C(45)-H(45C)	109.5
C(36)-C(35)-H(35)	119.2	C(49)-C(46)-C(48)	109.1(7)
C(37)-C(36)-C(41)	119.6(7)	C(49)-C(46)-C(47)	109.5(7)
C(37)-C(36)-C(35)	123.8(7)	C(48)-C(46)-C(47)	103.2(8)
C(41)-C(36)-C(35)	116.6(7)	C(49)-C(46)-P(2)	117.4(6)
C(38)-C(37)-C(36)	117.9(7)	C(48)-C(46)-P(2)	110.4(6)
C(38)-C(37)-C(44)	123.2(8)	C(47)-C(46)-P(2)	106.2(5)
C(36)-C(37)-C(44)	118.9(7)	C(46)-C(47)-H(47A)	109.5
C(37)-C(38)-C(39)	119.8(7)	C(46)-C(47)-H(47B)	109.5
C(37)-C(38)-C(45)	123.3(7)	H(47A)-C(47)-H(47B)	109.5
C(39)-C(38)-C(45)	116.9(7)	C(46)-C(47)-H(47C)	109.5
N(5)-C(39)-C(38)	123.1(7)	H(47A)-C(47)-H(47C)	109.5
N(5)-C(39)-H(39)	118.4	H(47B)-C(47)-H(47C)	109.5
C(38)-C(39)-H(39)	118.4	C(46)-C(48)-H(48A)	109.5
N(4)-C(40)-C(33)	123.2(7)	C(46)-C(48)-H(48B)	109.5
N(4)-C(40)-C(41)	117.2(6)	H(48A)-C(48)-H(48B)	109.5
C(33)-C(40)-C(41)	119.6(7)	C(46)-C(48)-H(48C)	109.5
N(5)-C(41)-C(36)	121.1(7)	H(48A)-C(48)-H(48C)	109.5
N(5)-C(41)-C(40)	118.0(6)	H(48B)-C(48)-H(48C)	109.5
C(36)-C(41)-C(40)	121.0(6)	C(46)-C(49)-H(49A)	109.5
C(31)-C(42)-H(42A)	109.5	C(46)-C(49)-H(49B)	109.5
C(31)-C(42)-H(42B)	109.5	H(49A)-C(49)-H(49B)	109.5
H(42A)-C(42)-H(42B)	109.5	C(46)-C(49)-H(49C)	109.5
C(31)-C(42)-H(42C)	109.5	H(49A)-C(49)-H(49C)	109.5
H(42A)-C(42)-H(42C)	109.5	H(49B)-C(49)-H(49C)	109.5
H(42B)-C(42)-H(42C)	109.5	C(53)-C(50)-C(52)	110.4(8)
C(32)-C(43)-H(43A)	109.5	C(53)-C(50)-C(51)	105.1(7)
C(32)-C(43)-H(43B)	109.5	C(52)-C(50)-C(51)	107.9(7)

Table S3. Bond angles (deg.) for [(Me$_4$phen)Cu(N≡C–S)(P^{t}Bu$_3$)]. Symmetry transformations used to generate equivalent atoms:

C(53)-C(50)-P(2)	108.9(6)	H(57A)-C(57)-H(57C)	109.5
C(52)-C(50)-P(2)	117.0(5)	H(57B)-C(57)-H(57C)	109.5
C(51)-C(50)-P(2)	106.8(6)	N(6)-C(58)-S(6)	179.1(7)
C(50)-C(51)-H(51A)	109.5	N(9)-Cu(3)-N(7)	98.1(4)
C(50)-C(51)-H(51B)	109.5	N(9)-Cu(3)-N(8)	102.9(3)
H(51A)-C(51)-H(51B)	109.5	N(7)-Cu(3)-N(8)	77.8(3)
C(50)-C(51)-H(51C)	109.5	N(9)-Cu(3)-P(3)	118.1(3)
H(51A)-C(51)-H(51C)	109.5	N(7)-Cu(3)-P(3)	123.4(2)
H(51B)-C(51)-H(51C)	109.5	N(8)-Cu(3)-P(3)	127.2(2)
C(50)-C(52)-H(52A)	109.5	C(83)-P(3)-C(75)	107.1(6)
C(50)-C(52)-H(52B)	109.5	C(83)-P(3)-C(79)	108.5(7)
H(52A)-C(52)-H(52B)	109.5	C(75)-P(3)-C(79)	108.4(5)
C(50)-C(52)-H(52C)	109.5	C(83)-P(3)-Cu(3)	112.1(5)
H(52A)-C(52)-H(52C)	109.5	C(75)-P(3)-Cu(3)	110.5(3)
H(52B)-C(52)-H(52C)	109.5	C(79)-P(3)-Cu(3)	110.1(3)
C(50)-C(53)-H(53A)	109.5	C(59)-N(7)-C(69)	114.9(8)
C(50)-C(53)-H(53B)	109.5	C(59)-N(7)-Cu(3)	130.5(6)
H(53A)-C(53)-H(53B)	109.5	C(69)-N(7)-Cu(3)	114.5(6)
C(50)-C(53)-H(53C)	109.5	C(70)-N(8)-C(68)	117.6(8)
H(53A)-C(53)-H(53C)	109.5	C(70)-N(8)-Cu(3)	114.2(5)
H(53B)-C(53)-H(53C)	109.5	C(68)-N(8)-Cu(3)	128.2(7)
C(55)-C(54)-C(57)	111.3(7)	C(87)-N(9)-Cu(3)	156.9(10)
C(55)-C(54)-C(56)	104.8(7)	N(7)-C(59)-C(60)	126.6(8)
C(57)-C(54)-C(56)	106.2(7)	N(7)-C(59)-H(59)	116.7
C(55)-C(54)-P(2)	109.3(6)	C(60)-C(59)-H(59)	116.7
C(57)-C(54)-P(2)	117.0(5)	C(61)-C(60)-C(59)	118.2(9)
C(56)-C(54)-P(2)	107.4(5)	C(61)-C(60)-C(71)	121.8(10)
C(54)-C(55)-H(55A)	109.5	C(59)-C(60)-C(71)	119.9(9)
C(54)-C(55)-H(55B)	109.5	C(60)-C(61)-C(62)	119.3(9)
H(55A)-C(55)-H(55B)	109.5	C(60)-C(61)-C(72)	122.5(9)
C(54)-C(55)-H(55C)	109.5	C(62)-C(61)-C(72)	118.2(9)
H(55A)-C(55)-H(55C)	109.5	C(69)-C(62)-C(63)	120.4(8)
H(55B)-C(55)-H(55C)	109.5	C(69)-C(62)-C(61)	117.3(7)
C(54)-C(56)-H(56A)	109.5	C(63)-C(62)-C(61)	122.3(8)
C(54)-C(56)-H(56B)	109.5	C(64)-C(63)-C(62)	119.1(9)
H(56A)-C(56)-H(56B)	109.5	C(64)-C(63)-H(63)	120.4
C(54)-C(56)-H(56C)	109.5	C(62)-C(63)-H(63)	120.4
H(56A)-C(56)-H(56C)	109.5	C(63)-C(64)-C(65)	122.1(8)
H(56B)-C(56)-H(56C)	109.5	C(63)-C(64)-H(64)	119.0
C(54)-C(57)-H(57A)	109.5	C(65)-C(64)-H(64)	119.0
C(54)-C(57)-H(57B)	109.5	C(66)-C(65)-C(70)	119.5(9)
H(57A)-C(57)-H(57B)	109.5	C(66)-C(65)-C(64)	121.4(8)
C(54)-C(57)-H(57C)	109.5	C(70)-C(65)-C(64)	119.2(8)

Table S3. Bond angles (deg.) for [(Me_4phen)Cu(N≡C–S)(P^tBu_3)]. Symmetry transformations used to generate equivalent atoms:

C(67)-C(66)-C(65)	117.1(8)	C(78)-C(75)-P(3)	121.7(7)
C(67)-C(66)-C(73)	121.0(10)	C(76)-C(75)-P(3)	99.1(9)
C(65)-C(66)-C(73)	121.9(10)	C(75)-C(77)-H(77A)	109.5
C(66)-C(67)-C(68)	120.2(9)	C(75)-C(77)-H(77B)	109.5
C(66)-C(67)-C(74)	123.0(9)	H(77A)-C(77)-H(77B)	109.5
C(68)-C(67)-C(74)	116.8(10)	C(75)-C(77)-H(77C)	109.5
N(8)-C(68)-C(67)	121.8(10)	H(77A)-C(77)-H(77C)	109.5
N(8)-C(68)-H(68)	119.1	H(77B)-C(77)-H(77C)	109.5
C(67)-C(68)-H(68)	119.1	C(75)-C(76)-H(76A)	109.5
N(7)-C(69)-C(62)	123.7(8)	C(75)-C(76)-H(76B)	109.5
N(7)-C(69)-C(70)	115.9(8)	H(76A)-C(76)-H(76B)	109.5
C(62)-C(69)-C(70)	120.4(7)	C(75)-C(76)-H(76C)	109.5
N(8)-C(70)-C(65)	123.7(8)	H(76A)-C(76)-H(76C)	109.5
N(8)-C(70)-C(69)	117.5(7)	H(76B)-C(76)-H(76C)	109.5
C(65)-C(70)-C(69)	118.7(8)	C(75)-C(78)-H(78A)	109.5
C(60)-C(71)-H(71A)	109.5	C(75)-C(78)-H(78B)	109.5
C(60)-C(71)-H(71B)	109.5	H(78A)-C(78)-H(78B)	109.5
H(71A)-C(71)-H(71B)	109.5	C(75)-C(78)-H(78C)	109.5
C(60)-C(71)-H(71C)	109.5	H(78A)-C(78)-H(78C)	109.5
H(71A)-C(71)-H(71C)	109.5	H(78B)-C(78)-H(78C)	109.5
H(71B)-C(71)-H(71C)	109.5	C(80)-C(79)-C(82)	113.5(10)
C(61)-C(72)-H(72A)	109.5	C(80)-C(79)-C(81)	104.1(10)
C(61)-C(72)-H(72B)	109.5	C(82)-C(79)-C(81)	102.3(11)
H(72A)-C(72)-H(72B)	109.5	C(80)-C(79)-P(3)	117.8(8)
C(61)-C(72)-H(72C)	109.5	C(82)-C(79)-P(3)	112.4(10)
H(72A)-C(72)-H(72C)	109.5	C(81)-C(79)-P(3)	104.5(7)
H(72B)-C(72)-H(72C)	109.5	C(79)-C(80)-H(80A)	109.5
C(66)-C(73)-H(73A)	109.5	C(79)-C(80)-H(80B)	109.5
C(66)-C(73)-H(73B)	109.5	H(80A)-C(80)-H(80B)	109.5
H(73A)-C(73)-H(73B)	109.5	C(79)-C(80)-H(80C)	109.5
C(66)-C(73)-H(73C)	109.5	H(80A)-C(80)-H(80C)	109.5
H(73A)-C(73)-H(73C)	109.5	H(80B)-C(80)-H(80C)	109.5
H(73B)-C(73)-H(73C)	109.5	C(79)-C(81)-H(81A)	109.5
C(67)-C(74)-H(74A)	109.5	C(79)-C(81)-H(81B)	109.5
C(67)-C(74)-H(74B)	109.5	H(81A)-C(81)-H(81B)	109.5
H(74A)-C(74)-H(74B)	109.5	C(79)-C(81)-H(81C)	109.5
C(67)-C(74)-H(74C)	109.5	H(81A)-C(81)-H(81C)	109.5
H(74A)-C(74)-H(74C)	109.5	H(81B)-C(81)-H(81C)	109.5
H(74B)-C(74)-H(74C)	109.5	C(79)-C(82)-H(82A)	109.5
C(77)-C(75)-C(78)	107.4(9)	C(79)-C(82)-H(82B)	109.5
C(77)-C(75)-C(76)	110.1(11)	H(82A)-C(82)-H(82B)	109.5
C(78)-C(75)-C(76)	108.8(11)	C(79)-C(82)-H(82C)	109.5
C(77)-C(75)-P(3)	109.2(6)	H(82A)-C(82)-H(82C)	109.5

Table S3. Bond angles (deg.) for [(Me_4phen)Cu(N≡C–S)(P^tBu_3)]. Symmetry transformations used to generate equivalent atoms:

H(82B)-C(82)-H(82C)	109.5	C(99)-N(11)-Cu(4)	111.8(5)
C(86)-C(83)-C(85)	112.2(12)	C(116)-N(12)-Cu(4)	168.7(7)
C(86)-C(83)-C(84)	105.8(14)	N(10)-C(88)-C(89)	124.4(8)
C(85)-C(83)-C(84)	104.1(13)	N(10)-C(88)-H(88)	117.8
C(86)-C(83)-P(3)	116.1(12)	C(89)-C(88)-H(88)	117.8
C(85)-C(83)-P(3)	117.6(10)	C(90)-C(89)-C(88)	119.6(8)
C(84)-C(83)-P(3)	98.4(9)	C(90)-C(89)-C(100)	122.0(8)
C(83)-C(84)-H(84A)	109.5	C(88)-C(89)-C(100)	118.4(8)
C(83)-C(84)-H(84B)	109.5	C(89)-C(90)-C(91)	117.9(8)
H(84A)-C(84)-H(84B)	109.5	C(89)-C(90)-C(101)	124.0(9)
C(83)-C(84)-H(84C)	109.5	C(91)-C(90)-C(101)	118.1(9)
H(84A)-C(84)-H(84C)	109.5	C(98)-C(91)-C(90)	118.4(8)
H(84B)-C(84)-H(84C)	109.5	C(98)-C(91)-C(92)	116.4(9)
C(83)-C(85)-H(85A)	109.5	C(90)-C(91)-C(92)	125.2(9)
C(83)-C(85)-H(85B)	109.5	C(93)-C(92)-C(91)	123.2(9)
H(85A)-C(85)-H(85B)	109.5	C(93)-C(92)-H(92)	118.4
C(83)-C(85)-H(85C)	109.5	C(91)-C(92)-H(92)	118.4
H(85A)-C(85)-H(85C)	109.5	C(92)-C(93)-C(94)	122.0(8)
H(85B)-C(85)-H(85C)	109.5	C(92)-C(93)-H(93)	119.0
C(83)-C(86)-H(86A)	109.5	C(94)-C(93)-H(93)	119.0
C(83)-C(86)-H(86B)	109.5	C(93)-C(94)-C(95)	125.5(8)
H(86A)-C(86)-H(86B)	109.5	C(93)-C(94)-C(99)	118.0(9)
C(83)-C(86)-H(86C)	109.5	C(95)-C(94)-C(99)	116.5(9)
H(86A)-C(86)-H(86C)	109.5	C(96)-C(95)-C(94)	120.4(8)
H(86B)-C(86)-H(86C)	109.5	C(96)-C(95)-C(102)	121.2(10)
N(9)-C(87)-S(7)	176.2(11)	C(94)-C(95)-C(102)	118.4(10)
N(12)-Cu(4)-N(11)	103.6(3)	C(95)-C(96)-C(97)	119.2(9)
N(12)-Cu(4)-N(10)	97.3(3)	C(95)-C(96)-C(103)	125.2(9)
N(11)-Cu(4)-N(10)	78.7(3)	C(97)-C(96)-C(103)	115.6(11)
N(12)-Cu(4)-P(4)	120.0(2)	N(11)-C(97)-C(96)	125.5(10)
N(11)-Cu(4)-P(4)	124.11(19)	N(11)-C(97)-H(97)	117.2
N(10)-Cu(4)-P(4)	123.89(18)	C(96)-C(97)-H(97)	117.2
C(104)-P(4)-C(108)	111.4(4)	N(10)-C(98)-C(91)	122.4(8)
C(104)-P(4)-C(112)	106.0(4)	N(10)-C(98)-C(99)	116.6(7)
C(108)-P(4)-C(112)	106.9(3)	C(91)-C(98)-C(99)	121.0(7)
C(104)-P(4)-Cu(4)	110.7(3)	N(11)-C(99)-C(98)	118.9(7)
C(108)-P(4)-Cu(4)	109.0(2)	N(11)-C(99)-C(94)	121.7(8)
C(112)-P(4)-Cu(4)	112.7(2)	C(98)-C(99)-C(94)	119.4(8)
C(88)-N(10)-C(98)	117.3(7)	C(89)-C(100)-H(10A)	109.5
C(88)-N(10)-Cu(4)	128.7(5)	C(89)-C(100)-H(10B)	109.5
C(98)-N(10)-Cu(4)	113.8(5)	H(10A)-C(100)-H(10B)	109.5
C(97)-N(11)-C(99)	116.6(7)	C(89)-C(100)-H(10C)	109.5
C(97)-N(11)-Cu(4)	131.4(7)	H(10A)-C(100)-H(10C)	109.5

Table S3. Bond angles (deg.) for [(Me$_4$phen)Cu(N≡C–S)(P^{t}Bu$_3$)]. Symmetry transformations used to generate equivalent atoms:

H(10B)-C(100)-H(10C)	109.5	C(109)-C(108)-C(110)	110.0(8)
C(90)-C(101)-H(10D)	109.5	C(109)-C(108)-C(111)	106.5(8)
C(90)-C(101)-H(10E)	109.5	C(110)-C(108)-C(111)	109.1(8)
H(10D)-C(101)-H(10E)	109.5	C(109)-C(108)-P(4)	109.9(6)
C(90)-C(101)-H(10F)	109.5	C(110)-C(108)-P(4)	114.5(6)
H(10D)-C(101)-H(10F)	109.5	C(111)-C(108)-P(4)	106.5(7)
H(10E)-C(101)-H(10F)	109.5	C(108)-C(109)-H(10V)	109.5
C(95)-C(102)-H(10G)	109.5	C(108)-C(109)-H(10W)	109.5
C(95)-C(102)-H(10H)	109.5	H(10V)-C(109)-H(10W)	109.5
H(10G)-C(102)-H(10H)	109.5	C(108)-C(109)-H(10X)	109.5
C(95)-C(102)-H(10I)	109.5	H(10V)-C(109)-H(10X)	109.5
H(10G)-C(102)-H(10I)	109.5	H(10W)-C(109)-H(10X)	109.5
H(10H)-C(102)-H(10I)	109.5	C(108)-C(110)-H(11A)	109.5
C(96)-C(103)-H(10J)	109.5	C(108)-C(110)-H(11B)	109.5
C(96)-C(103)-H(10K)	109.5	H(11A)-C(110)-H(11B)	109.5
H(10J)-C(103)-H(10K)	109.5	C(108)-C(110)-H(11C)	109.5
C(96)-C(103)-H(10L)	109.5	H(11A)-C(110)-H(11C)	109.5
H(10J)-C(103)-H(10L)	109.5	H(11B)-C(110)-H(11C)	109.5
H(10K)-C(103)-H(10L)	109.5	C(108)-C(111)-H(11D)	109.5
C(106)-C(104)-C(105)	105.4(8)	C(108)-C(111)-H(11E)	109.5
C(106)-C(104)-C(107)	106.0(8)	H(11D)-C(111)-H(11E)	109.5
C(105)-C(104)-C(107)	109.4(9)	C(108)-C(111)-H(11F)	109.5
C(106)-C(104)-P(4)	108.7(7)	H(11D)-C(111)-H(11F)	109.5
C(105)-C(104)-P(4)	116.4(6)	H(11E)-C(111)-H(11F)	109.5
C(107)-C(104)-P(4)	110.4(7)	C(113)-C(112)-C(114)	107.5(7)
C(104)-C(105)-H(10M)	109.5	C(113)-C(112)-C(115)	107.6(6)
C(104)-C(105)-H(10N)	109.5	C(114)-C(112)-C(115)	110.7(9)
H(10M)-C(105)-H(10N)	109.5	C(113)-C(112)-P(4)	116.9(6)
C(104)-C(105)-H(10O)	109.5	C(114)-C(112)-P(4)	105.6(5)
H(10M)-C(105)-H(10O)	109.5	C(115)-C(112)-P(4)	108.5(5)
H(10N)-C(105)-H(10O)	109.5	C(112)-C(113)-H(11G)	109.5
C(104)-C(106)-H(10P)	109.5	C(112)-C(113)-H(11H)	109.5
C(104)-C(106)-H(10Q)	109.5	H(11G)-C(113)-H(11H)	109.5
H(10P)-C(106)-H(10Q)	109.5	C(112)-C(113)-H(11I)	109.5
C(104)-C(106)-H(10R)	109.5	H(11G)-C(113)-H(11I)	109.5
H(10P)-C(106)-H(10R)	109.5	H(11H)-C(113)-H(11I)	109.5
H(10Q)-C(106)-H(10R)	109.5	C(112)-C(114)-H(11J)	109.5
C(104)-C(107)-H(10S)	109.5	C(112)-C(114)-H(11K)	109.5
C(104)-C(107)-H(10T)	109.5	H(11J)-C(114)-H(11K)	109.5
H(10S)-C(107)-H(10T)	109.5	C(112)-C(114)-H(11L)	109.5
C(104)-C(107)-H(10U)	109.5	H(11J)-C(114)-H(11L)	109.5
H(10S)-C(107)-H(10U)	109.5	H(11K)-C(114)-H(11L)	109.5
H(10T)-C(107)-H(10U)	109.5	C(112)-C(115)-H(11M)	109.5

Table S3. Bond angles (deg.) for [(Me_4phen)Cu(N≡C–S)(P^tBu_3)]. Symmetry transformations used to generate equivalent atoms:

C(112)-C(115)-H(11N)	109.5
H(11M)-C(115)-H(11N)	109.5
C(112)-C(115)-H(11O)	109.5
H(11M)-C(115)-H(11O)	109.5
H(11N)-C(115)-H(11O)	109.5
N(12)-C(116)-S(8)	177.8(8)

Table S4. Anisotropic displacement parameters (Å^2 x 10^3) for [(Me$_4$phen)Cu(N≡C–S)(P^{t}Bu$_3$)]. The anisotropic displacement factor exponent takes the form: $-2\pi^2[h^2a^{*2}U^{11} + ... + 2hka^*b^*U^{12}]$.

Atom	U^{11}	U^{22}	U^{33}	U^{23}	U^{13}	U^{12}
Cu(1)	28(1)	19(1)	33(1)	1(1)	1(1)	-1(1)
S(5)	91(2)	49(2)	44(1)	1(1)	16(1)	-18(1)
P(1)	24(1)	16(1)	19(1)	-2(1)	1(1)	1(1)
N(1)	26(3)	19(3)	33(3)	-1(2)	1(2)	-6(2)
N(2)	28(3)	24(3)	33(3)	4(2)	3(2)	-2(2)
N(3)	92(6)	27(3)	42(4)	-7(3)	44(4)	-20(4)
C(1)	31(3)	35(3)	38(4)	-2(3)	-4(3)	-10(3)
C(2)	27(3)	46(4)	34(3)	-4(3)	3(3)	-18(3)
C(3)	29(3)	44(4)	42(4)	-14(3)	16(3)	-18(3)
C(4)	37(4)	36(4)	44(4)	-12(3)	19(3)	-8(3)
C(5)	52(4)	34(4)	56(4)	-7(3)	32(4)	-3(3)
C(6)	52(4)	28(4)	62(5)	5(3)	30(4)	8(3)
C(7)	35(4)	34(4)	56(4)	7(3)	24(3)	5(3)
C(8)	35(4)	40(4)	60(4)	20(3)	26(3)	13(3)
C(9)	41(4)	54(5)	45(4)	21(4)	10(3)	5(4)
C(10)	42(4)	46(4)	42(4)	18(3)	-5(3)	3(3)
C(11)	28(3)	22(3)	32(3)	-3(2)	11(3)	-8(2)
C(12)	18(3)	24(3)	35(3)	4(2)	13(2)	-2(2)
C(13)	44(5)	84(7)	34(4)	0(5)	-1(4)	-21(5)
C(14)	44(5)	68(6)	68(6)	-40(5)	20(4)	-25(4)
C(15)	59(6)	60(6)	89(7)	38(6)	38(5)	21(5)
C(16)	51(5)	81(7)	60(6)	36(5)	0(5)	9(5)
C(17)	37(3)	24(3)	38(3)	-6(3)	13(3)	5(3)
C(18)	41(4)	29(4)	56(5)	-1(3)	22(4)	-12(3)
C(19)	73(6)	53(5)	29(4)	-7(4)	11(4)	-8(5)
C(20)	43(4)	19(3)	58(5)	-3(3)	28(4)	14(3)
C(21)	41(4)	35(3)	44(4)	7(3)	3(3)	20(3)
C(22)	32(4)	43(5)	76(6)	5(4)	3(4)	15(4)
C(23)	50(5)	25(4)	54(5)	11(3)	4(4)	9(3)
C(24)	82(7)	63(6)	88(8)	6(6)	41(6)	29(6)
C(25)	67(5)	42(4)	45(4)	8(3)	-20(4)	-18(4)
C(26)	71(6)	34(4)	34(4)	-7(3)	-14(4)	-17(4)
C(27)	118(9)	65(6)	21(4)	3(4)	-2(5)	-20(6)
C(28)	56(5)	65(6)	89(7)	34(6)	-35(5)	-10(5)
C(29)	41(4)	27(3)	44(4)	2(3)	2(3)	-1(3)
Cu(2)	25(1)	18(1)	32(1)	2(1)	3(1)	4(1)
S(6)	58(1)	57(2)	39(1)	0(1)	24(1)	9(1)
P(2)	21(1)	16(1)	18(1)	3(1)	1(1)	3(1)
N(4)	23(3)	31(3)	32(3)	5(3)	-2(2)	12(2)

Table S4. Anisotropic displacement parameters (Å^2 x 10^3) for [(Me$_4$phen)Cu(N≡C–S)(P^{t}Bu$_3$)].

The anisotropic displacement factor exponent takes the form: $-2\pi^2[h^2a^{*2}U^{11} + ... + 2hka^*b^*U^{12}]$.

Atom	U^{11}	U^{22}	U^{33}	U^{23}	U^{13}	U^{12}
N(5)	24(3)	20(3)	25(3)	1(2)	5(2)	-1(2)
N(6)	29(3)	31(3)	45(4)	-3(3)	9(3)	3(3)
C(30)	24(3)	38(4)	33(3)	-4(3)	4(3)	10(3)
C(31)	29(3)	54(4)	30(3)	1(3)	6(3)	15(3)
C(32)	33(4)	56(4)	27(3)	12(3)	11(3)	19(3)
C(33)	27(3)	33(3)	32(3)	10(3)	12(3)	12(3)
C(34)	45(4)	34(4)	45(4)	17(3)	15(3)	14(3)
C(35)	46(4)	19(3)	45(4)	13(3)	21(3)	8(3)
C(36)	27(3)	18(3)	36(3)	2(2)	19(3)	3(2)
C(37)	30(3)	23(3)	38(3)	-4(3)	16(3)	-2(2)
C(38)	24(3)	31(3)	35(3)	-10(3)	4(3)	-2(3)
C(39)	28(3)	19(3)	29(3)	-1(2)	7(2)	3(2)
C(40)	19(3)	24(3)	31(3)	7(2)	9(2)	6(2)
C(41)	24(3)	18(3)	32(3)	3(2)	8(2)	4(2)
C(42)	32(4)	87(7)	36(4)	10(4)	-5(3)	20(4)
C(43)	63(6)	78(7)	43(5)	30(5)	6(4)	29(5)
C(44)	40(4)	30(4)	60(5)	-9(4)	20(4)	-7(3)
C(45)	39(4)	45(5)	43(4)	-15(4)	4(3)	-6(4)
C(46)	27(3)	42(4)	37(3)	3(3)	5(3)	2(3)
C(47)	32(4)	66(6)	82(7)	-4(5)	-2(4)	-17(4)
C(48)	56(5)	48(5)	65(6)	30(4)	29(5)	-8(4)
C(49)	40(4)	49(5)	40(4)	-1(4)	12(3)	9(4)
C(50)	30(3)	34(3)	41(4)	-10(3)	-13(3)	7(3)
C(51)	47(5)	61(5)	27(3)	-7(3)	-11(3)	19(4)
C(52)	48(5)	28(4)	52(5)	-18(3)	-14(4)	1(3)
C(53)	24(4)	48(5)	76(6)	-18(4)	-5(4)	-6(3)
C(54)	41(4)	33(3)	19(3)	3(2)	0(3)	8(3)
C(55)	61(5)	43(4)	25(3)	-4(3)	-13(3)	10(4)
C(56)	54(5)	35(4)	42(4)	13(3)	21(4)	-5(4)
C(57)	64(6)	38(4)	30(4)	8(3)	-8(4)	20(4)
C(58)	24(3)	28(3)	31(3)	4(3)	0(2)	1(3)
Cu(3)	61(1)	35(1)	43(1)	11(1)	19(1)	26(1)
S(7)	42(1)	89(2)	46(1)	-18(1)	11(1)	-6(1)
P(3)	48(1)	28(1)	38(1)	11(1)	18(1)	17(1)
N(7)	59(4)	37(4)	22(3)	10(3)	10(3)	24(3)
N(8)	43(4)	53(5)	27(3)	0(3)	3(3)	22(3)
N(9)	75(6)	49(5)	66(5)	16(4)	49(5)	18(4)
C(59)	53(4)	49(4)	32(4)	3(3)	6(3)	23(4)
C(60)	43(4)	54(4)	34(4)	-2(3)	10(3)	10(3)

Table S4. Anisotropic displacement parameters ($Å^2$ x 10^3) for [(Me_4phen)Cu(N≡C–S)(P^tBu_3)]. The anisotropic displacement factor exponent takes the form: $-2\pi^2[h^2a^{*2}U^{11} + ... + 2hka^*b^*U^{12}]$.

Atom	U^{11}	U^{22}	U^{33}	U^{23}	U^{13}	U^{12}
C(61)	36(4)	50(4)	42(4)	-4(3)	16(3)	4(3)
C(62)	34(3)	34(3)	34(3)	7(3)	20(3)	12(3)
C(63)	36(4)	38(4)	48(4)	12(3)	17(3)	9(3)
C(64)	41(4)	39(4)	46(4)	19(3)	15(3)	11(3)
C(65)	29(3)	42(4)	39(4)	13(3)	17(3)	10(3)
C(66)	39(4)	56(5)	41(4)	19(4)	13(3)	19(3)
C(67)	41(4)	64(5)	35(4)	0(4)	9(3)	18(4)
C(68)	40(4)	52(4)	38(4)	-2(3)	6(3)	16(3)
C(69)	37(4)	34(3)	28(3)	8(3)	8(3)	14(3)
C(70)	30(3)	36(4)	35(3)	6(3)	10(3)	14(3)
C(71)	61(6)	91(8)	37(5)	-4(5)	3(4)	19(6)
C(72)	45(5)	69(7)	75(7)	1(5)	32(5)	-12(5)
C(73)	51(5)	71(7)	59(6)	37(5)	-6(4)	9(5)
C(74)	63(6)	75(7)	32(4)	1(4)	9(4)	12(5)
C(75)	69(5)	54(5)	71(5)	-18(4)	-29(4)	12(4)
C(77)	127(9)	75(7)	44(5)	-3(5)	-13(6)	39(7)
C(76)	126(8)	127(8)	142(8)	-9(5)	-9(5)	4(5)
C(78)	106(9)	48(6)	62(6)	10(5)	-5(6)	38(6)
C(79)	52(5)	61(5)	62(5)	-18(4)	-15(4)	10(4)
C(80)	59(6)	52(6)	85(7)	-26(5)	2(5)	5(5)
C(81)	96(8)	73(7)	102(9)	-23(7)	59(7)	-34(7)
C(82)	81(8)	98(10)	110(10)	-23(8)	-33(7)	20(7)
C(83)	95(6)	85(6)	105(7)	24(5)	51(5)	17(5)
C(84)	156(12)	127(11)	65(7)	22(8)	-14(8)	56(9)
C(85)	85(8)	62(6)	96(8)	16(6)	60(7)	31(6)
C(86)	117(7)	102(7)	122(7)	-4(5)	22(5)	-2(5)
C(87)	37(4)	44(4)	43(4)	4(3)	-1(3)	8(3)
Cu(4)	28(1)	27(1)	31(1)	1(1)	4(1)	10(1)
S(8)	40(1)	71(2)	37(1)	-13(1)	7(1)	5(1)
P(4)	15(1)	24(1)	24(1)	-2(1)	-1(1)	2(1)
N(10)	36(3)	17(3)	30(3)	1(2)	7(2)	8(2)
N(11)	29(3)	41(4)	30(3)	3(3)	8(3)	18(3)
N(12)	31(3)	37(4)	42(4)	-1(3)	14(3)	5(3)
C(88)	37(4)	36(4)	29(3)	-3(3)	2(3)	2(3)
C(89)	34(3)	29(3)	40(4)	-8(3)	17(3)	0(3)
C(90)	35(4)	30(3)	47(4)	-6(3)	24(3)	3(3)
C(91)	40(4)	30(3)	51(4)	8(3)	23(3)	9(3)
C(92)	51(4)	32(4)	60(5)	12(3)	21(4)	9(3)
C(93)	43(4)	42(4)	56(4)	23(4)	19(4)	17(3)

Table S4. Anisotropic displacement parameters ($Å^2$ x 10^3) for [(Me_4phen)Cu(N≡C–S)(P^{t}Bu$_3$)]. The anisotropic displacement factor exponent takes the form: $-2\pi^2[h^2a^{*2}U^{11} + ... + 2hka^*b^*U^{12}]$.

Atom	U^{11}	U^{22}	U^{33}	U^{23}	U^{13}	U^{12}
C(94)	35(4)	47(4)	40(4)	16(3)	16(3)	19(3)
C(95)	35(4)	60(5)	37(4)	15(3)	12(3)	23(4)
C(96)	33(4)	69(5)	29(3)	9(3)	7(3)	22(4)
C(97)	43(4)	41(4)	39(4)	-3(3)	8(3)	12(3)
C(98)	28(3)	27(3)	33(3)	5(3)	15(3)	12(3)
C(99)	30(3)	33(3)	37(3)	8(3)	17(3)	15(3)
C(100)	54(5)	47(5)	54(5)	-16(4)	7(4)	-2(4)
C(101)	45(5)	35(4)	78(6)	-11(4)	20(5)	-8(4)
C(102)	44(5)	83(7)	61(6)	42(5)	18(4)	25(5)
C(103)	49(5)	109(9)	34(4)	6(5)	0(4)	27(6)
C(104)	28(3)	41(4)	59(4)	-16(3)	-13(3)	4(3)
C(105)	52(5)	43(5)	85(7)	-27(5)	-18(5)	4(4)
C(106)	26(4)	69(7)	98(8)	-19(6)	-19(5)	7(4)
C(107)	54(5)	71(6)	56(5)	-16(5)	-24(4)	22(5)
C(108)	44(4)	23(3)	31(3)	8(3)	10(3)	5(3)
C(109)	68(6)	53(5)	23(3)	0(3)	0(3)	15(4)
C(110)	67(6)	36(4)	40(4)	10(4)	-1(4)	19(4)
C(111)	88(8)	63(7)	78(7)	20(6)	41(6)	-3(6)
C(112)	25(3)	34(3)	37(3)	4(3)	13(2)	5(3)
C(113)	22(3)	59(5)	42(4)	-5(4)	10(3)	13(3)
C(114)	66(6)	69(6)	60(6)	25(5)	45(5)	31(5)
C(115)	26(4)	53(5)	79(6)	-29(5)	7(4)	-7(4)
C(116)	31(3)	37(4)	31(3)	-3(3)	-4(3)	7(3)

Table S5. Hydrogen coordinates (x 10^4) and isotropic displacement parameters (Å^2 x 10^3) for [(Me$_4$phen)Cu(N≡C–S)(P^{t}Bu$_3$)].

H atom	x	y	z	U(eq)
H(1)	10556	5428	4478	42
H(5)	8904	8178	4340	56
H(6)	7370	8346	3790	56
H(10)	6232	5876	2998	52
H(13A)	11847	5668	5036	81
H(13B)	11225	6292	5286	81
H(13C)	12734	6377	5019	81
H(14A)	11286	7901	4767	90
H(14B)	11092	7413	5138	90
H(14C)	9620	7836	4971	90
H(15A)	6222	8337	2950	103
H(15B)	5454	8410	3373	103
H(15C)	4492	8055	3019	103
H(16A)	5404	7177	2468	96
H(16B)	3862	7174	2727	96
H(16C)	4594	6478	2580	96
H(18A)	3841	3858	4031	63
H(18B)	4156	3800	4497	63
H(18C)	5092	3326	4202	63
H(19A)	7784	3869	4577	77
H(19B)	6440	4197	4836	77
H(19C)	7701	4669	4631	77
H(20A)	6093	5342	4234	59
H(20B)	4764	5047	4511	59
H(20C)	4467	5080	4043	59
H(22A)	10556	4183	3938	75
H(22B)	10802	3441	4113	75
H(22C)	9676	3962	4329	75
H(23A)	7271	2719	3800	64
H(23B)	7484	3008	4239	64
H(23C)	8873	2589	4046	64
H(24A)	8532	3448	3208	115
H(24B)	9864	2978	3405	115
H(24C)	10177	3767	3350	115
H(26A)	4285	3422	3102	70
H(26B)	4923	3235	3536	70
H(26C)	5986	3091	3164	70
H(27A)	7500	3982	2882	102
H(27B)	7172	4750	2998	102
H(27C)	5902	4340	2737	102

Table S5. Hydrogen coordinates (x 10^4) and isotropic displacement parameters (Å^2 x 10^3) for [(Me$_4$phen)Cu(N≡C–S)(P^{t}Bu$_3$)].

H atom	x	y	z	U(eq)
H(28A)	3656	4554	3134	106
H(28B)	4774	5081	3362	106
H(28C)	3851	4522	3604	106
H(30)	10405	4577	6954	38
H(34)	8972	1785	6902	49
H(35)	7421	1535	6372	43
H(39)	5934	3926	5512	30
H(42A)	11084	3861	7766	78
H(42B)	12138	4270	7465	78
H(42C)	12511	3495	7556	78
H(43A)	11667	2487	7534	92
H(43B)	10477	1979	7314	92
H(43C)	9883	2438	7668	92
H(44A)	6561	1377	5732	64
H(44B)	5069	1652	5485	64
H(44C)	4951	1524	5949	64
H(45A)	3838	2509	5262	64
H(45B)	5309	2670	4994	64
H(45C)	4220	3270	5143	64
H(47A)	4408	4651	6025	90
H(47B)	3681	5370	5910	90
H(47C)	2853	4910	6232	90
H(48A)	5662	5004	7011	84
H(48B)	5572	4440	6674	84
H(48C)	3996	4707	6867	84
H(49A)	3008	5842	6721	64
H(49B)	3896	6334	6427	64
H(49C)	4644	6179	6855	64
H(51A)	8570	6101	7206	68
H(51B)	8146	5376	7026	68
H(51C)	6780	5908	7106	68
H(52A)	8114	7130	6798	65
H(52B)	6395	6913	6645	65
H(52C)	7714	7092	6335	65
H(53A)	10349	6293	6727	74
H(53B)	9957	6344	6264	74
H(53C)	10024	5623	6475	74
H(55A)	7083	5185	5418	65
H(55B)	6046	5732	5182	65
H(55C)	5249	5253	5499	65

Table S5. Hydrogen coordinates (x 10^4) and isotropic displacement parameters (Å^2 x 10^3) for [(Me$_4$phen)Cu(N≡C–S)(P^{t}Bu$_3$)].

H atom	x	y	z	U(eq)
H(56A)	8464	6679	5832	66
H(56B)	8037	6543	5376	66
H(56C)	8966	5985	5631	66
H(57A)	4365	6421	5848	67
H(57B)	5194	6742	5474	67
H(57C)	5751	6958	5910	67
H(59)	5980	4100	426	53
H(63)	7009	1622	1211	49
H(64)	8636	1785	1758	50
H(68)	10283	4560	1921	52
H(71A)	5203	2824	-123	95
H(71B)	4393	3522	-7	95
H(71C)	3680	2824	143	95
H(72A)	4854	1876	317	94
H(72B)	4626	1723	775	94
H(72C)	6247	1539	573	94
H(73A)	10485	1940	2164	91
H(73B)	9446	2272	2499	91
H(73C)	11263	2465	2469	91
H(74A)	12239	3397	2521	85
H(74B)	10813	3799	2709	85
H(74C)	11995	4180	2425	85
H(77A)	6156	5652	162	123
H(77B)	7536	5357	442	123
H(77C)	7556	6132	313	123
H(76A)	3535	5710	720	198
H(76B)	4454	5290	1057	198
H(76C)	4606	5083	603	198
H(78A)	6232	6973	661	108
H(78B)	4754	6808	926	108
H(78C)	4644	6692	459	108
H(80A)	8718	7375	1499	98
H(80B)	7390	6986	1734	98
H(80C)	7067	7206	1285	98
H(81A)	10089	6190	835	134
H(81B)	9990	6975	938	134
H(81C)	8577	6617	699	134
H(82A)	10791	6432	1587	146
H(82B)	10273	5672	1495	146
H(82C)	9595	6056	1869	146

Table S5. Hydrogen coordinates (x 10^4) and isotropic displacement parameters (Å^2 x 10^3) for [(Me$_4$phen)Cu(N≡C–S)(P^{t}Bu$_3$)].

H atom	x	y	z	U(eq)
H(84A)	7848	5347	2007	175
H(84B)	6464	5632	2269	175
H(84C)	7505	6139	2019	175
H(85A)	5020	6609	1733	120
H(85B)	3713	6082	1864	120
H(85C)	3862	6276	1409	120
H(86A)	4268	4829	1411	170
H(86B)	4224	4941	1878	170
H(86C)	5715	4590	1688	170
H(88)	4230	1056	2071	41
H(92)	2880	3487	1241	57
H(93)	1396	3276	700	56
H(97)	-265	520	622	49
H(10A)	5518	1688	2517	77
H(10B)	4911	2445	2571	77
H(10C)	6463	2302	2329	77
H(10D)	5689	3382	1765	78
H(10E)	4752	3394	2168	78
H(10F)	3919	3651	1767	78
H(10G)	590	2927	102	94
H(10H)	-1169	2913	255	94
H(10I)	-682	2436	-102	94
H(10J)	-714	1192	-195	96
H(10K)	-2228	1522	-3	96
H(10L)	-1752	761	100	96
H(10M)	1950	-2089	721	91
H(10N)	2228	-2070	1190	91
H(10O)	3652	-1916	905	91
H(10P)	-286	-1283	814	97
H(10Q)	-4	-609	1064	97
H(10R)	131	-1327	1276	97
H(10S)	1507	-1046	338	92
H(10T)	3317	-879	430	92
H(10U)	1997	-331	521	92
H(10V)	4980	-320	2060	72
H(10W)	4040	-760	2371	72
H(10X)	3159	-175	2127	72
H(11A)	4547	-1887	1561	71
H(11B)	4751	-1854	2031	71
H(11C)	5825	-1394	1760	71

Table S5. Hydrogen coordinates (x 10^4) and isotropic displacement parameters ($Å^2$ x 10^3) for [(Me$_4$phen)Cu(N≡C–S)(P^{t}Bu$_3$)].

H atom	x	y	z	U(eq)
H(11D)	1107	-974	1927	113
H(11E)	1996	-1560	2167	113
H(11F)	1555	-1661	1709	113
H(11G)	5339	-1227	724	61
H(11H)	6305	-1337	1130	61
H(11I)	7001	-865	795	61
H(11J)	5961	224	646	96
H(11K)	4487	521	872	96
H(11L)	4243	-77	560	96
H(11M)	7397	-57	1330	79
H(11N)	6378	-425	1656	79
H(11O)	5937	323	1517	79

Structure Determination Summary

Crystal Data and Structure Refinement for [(4,4'-Me$_2$-bipy)Cu(S(CH$_2$)$_4$)(P^{t}Bu$_3$)][PF$_6$]

Identification code	jpd1162_4_a_sq	
Empirical formula	$C_{28}H_{47}CuF_6N_2P_2S$	
Formula weight	683.21	
Temperature	150(2) K	
Wavelength	0.71073 Å	
Crystal system	trigonal	
Space group	*R*32	
Unit cell dimensions	a = 18.9515(8) Å	α = 90°
	b = 18.9515(8) Å	β = 90°
	c = 50.949(3) Å	γ = 120°
Volume	15847.1(16) $Å^3$	
Z	18	
Density (calculated)	1.289 g/cm^3	
Absorption coefficient	0.821 mm^{-1}	
F(000)	6444	
Crystal size	0.280 x 0.269 x 0.194 mm^3	
θ range for data collection	1.476 to 26.425°	
Index ranges	$-23 \le h \le 23$, $-23 \le k \le 23$, $-63 \le l \le 63$	
Reflections collected	14442	
Independent reflections	7241 [R(int) = 0.0144]	
Completeness to θ = 25.242°	99.8 %	
Absorption correction	Semi-empirical from equivalents	
Max. and min. transmission	0.86 and 0.76	

Refinement method	Full-matrix least-squares on F^2
Data / restraints / parameters	7241 / 38 / 359
Goodness-of-fit on F^2	1.053
Final R indices [I>2σ(I)]	R1 = 0.0620, wR2 = 0.1833
R indices (all data)	R1 = 0.0656, wR2 = 0.1870
Absolute structure parameter	0.03(2)
Extinction coefficient	n/a
Largest diff. peak and hole	2.077 and -1.074 e·Å^{-3}

Table S1. Atomic coordinates (x 10^4) and equivalent isotropic displacement parameters (Å^2 x 10^3) for [(4,4'-Me_2-bipy)Cu(S(CH_2)$_4$)(P^tBu_3)][PF_6]. U(eq) is defined as one third of the trace of the orthogonalized U^{ij} tensor.

Atom	x	y	z	U(eq)
Cu(1)	6780(1)	7123(1)	4165(1)	33(1)
S(1)	7470(2)	7271(2)	4568(1)	64(1)
P(1)	6224(1)	7907(1)	4107(1)	28(1)
N(1)	7505(3)	6994(3)	3880(1)	35(1)
N(2)	6135(3)	5861(3)	4107(1)	34(1)
C(1)	8175(4)	7587(4)	3770(1)	37(1)
C(2)	8579(3)	7461(4)	3566(1)	34(1)
C(3)	8271(4)	6668(4)	3469(1)	34(1)
C(4)	7570(4)	6055(4)	3585(1)	34(1)
C(5)	7204(4)	6229(3)	3791(1)	30(1)
C(6)	6468(3)	5586(3)	3931(1)	31(1)
C(7)	6162(4)	4765(4)	3884(1)	37(1)
C(8)	5469(4)	4193(4)	4026(1)	40(1)
C(9)	5148(4)	4490(4)	4209(1)	39(1)
C(10)	5491(4)	5322(4)	4243(1)	39(1)
C(11)	8689(5)	6501(5)	3245(2)	54(2)
C(12)	5103(6)	3294(4)	3972(2)	66(3)
C(13)	5638(4)	7892(5)	4414(1)	39(1)
C(14)	5208(5)	7010(5)	4520(2)	49(2)
C(15)	6240(6)	8414(6)	4633(2)	54(2)
C(16)	5015(5)	8173(6)	4378(2)	53(2)
C(17)	7031(4)	9015(4)	4030(1)	37(1)
C(18)	6775(5)	9649(4)	4066(2)	49(2)
C(19)	7761(4)	9215(4)	4212(2)	49(2)
C(20)	7356(4)	9071(4)	3749(1)	43(2)
C(21)	5481(4)	7510(4)	3820(1)	31(1)
C(22)	5243(4)	8111(5)	3705(1)	43(2)
C(23)	5863(4)	7247(4)	3602(1)	41(1)
C(24)	4694(4)	6722(5)	3900(1)	46(2)
C(25A)	7273(9)	6261(8)	4677(4)	72(4)
C(26A)	8122(10)	6354(9)	4614(4)	71(3)
C(27A)	8825(9)	7275(10)	4655(4)	88(5)
C(28A)	8574(8)	7904(9)	4568(5)	98(6)
C(25B)	7001(12)	6336(10)	4750(4)	72(4)
C(26B)	7521(13)	5979(11)	4637(5)	71(3)
C(27B)	8428(13)	6653(15)	4571(6)	88(5)
C(28B)	8505(10)	7470(14)	4477(7)	98(6)
P(2)	10000	10000	3667(1)	46(1)
F(1)	9785(4)	9232(3)	3846(1)	79(2)

Table S1. Atomic coordinates (x 10^4) and equivalent isotropic displacement parameters (Å^2 x 10^3) for [(4,4'-Me_2-bipy)Cu(S(CH_2)$_4$)(P^tBu_3)][PF_6]. U(eq) is defined as one third of the trace of the orthogonalized U^{ij} tensor.

Atom	x	y	z	U(eq)
F(2)	10201(4)	10766(4)	3490(1)	89(2)
P(3)	4528(2)	4528(2)	5000	72(1)
F(3)	4070(5)	4450(6)	4733(1)	102(4)
F(4)	4655(5)	3797(4)	4915(2)	109(5)
F(5)	5366(3)	5150(5)	4867(2)	157(8)
F(6)	4986(5)	4604(6)	5267(1)	157(8)
F(7)	3691(3)	3905(5)	5133(2)	143(7)
F(8)	4401(6)	5258(4)	5085(2)	220(13)
P(4)	6667	3333	3333	33(1)
F(9)	6667	3333	3023(1)	44(2)
F(10)	7501(1)	4168(1)	3333	158(9)
F(11)	6188(1)	3819(2)	3332(1)	77(4)

Table S2. Bond lengths (Å) for [(4,4'-Me_2-bipy)Cu($S(CH_2)_4$)(P^tBu_3)][PF_6]. Symmetry transformations used to generate equivalent atoms: #1 -y+2, x-y+1, z; #2 -x+y+1, -x+2, z; #3 y, x, -z+1; #4 -x+y+1, -x+1, z; #5 -y+1, x-y, z; #6 y+⅓, x-⅓,-z+⅔; #7 x-y+⅓,-y+⅔,-z+⅔; #8 -x+1⅓, -x+y+⅔, -z+⅔.

Cu(1)-N(2)	2.091(5)	C(14)-H(14A)	0.9800
Cu(1)-N(1)	2.095(5)	C(14)-H(14B)	0.9800
Cu(1)-P(1)	2.2314(16)	C(14)-H(14C)	0.9800
Cu(1)-S(1)	2.373(2)	C(15)-H(15A)	0.9800
S(1)-C(25B)	1.793(12)	C(15)-H(15B)	0.9800
S(1)-C(28A)	1.819(12)	C(15)-H(15C)	0.9800
S(1)-C(25A)	1.843(11)	C(16)-H(16A)	0.9800
S(1)-C(28B)	1.862(13)	C(16)-H(16B)	0.9800
P(1)-C(21)	1.903(6)	C(16)-H(16C)	0.9800
P(1)-C(13)	1.912(6)	C(17)-C(18)	1.514(10)
P(1)-C(17)	1.921(7)	C(17)-C(20)	1.543(10)
N(1)-C(1)	1.326(8)	C(17)-C(19)	1.544(9)
N(1)-C(5)	1.344(8)	C(18)-H(18A)	0.9800
N(2)-C(10)	1.329(8)	C(18)-H(18B)	0.9800
N(2)-C(6)	1.345(8)	C(18)-H(18C)	0.9800
C(1)-C(2)	1.381(9)	C(19)-H(19A)	0.9800
C(1)-H(1)	0.9500	C(19)-H(19B)	0.9800
C(2)-C(3)	1.403(9)	C(19)-H(19C)	0.9800
C(2)-H(2)	0.9500	C(20)-H(20A)	0.9800
C(3)-C(4)	1.387(8)	C(20)-H(20B)	0.9800
C(3)-C(11)	1.512(9)	C(20)-H(20C)	0.9800
C(4)-C(5)	1.386(8)	C(21)-C(22)	1.537(9)
C(4)-H(4)	0.9500	C(21)-C(24)	1.546(9)
C(5)-C(6)	1.496(8)	C(21)-C(23)	1.541(9)
C(6)-C(7)	1.383(8)	C(22)-H(22A)	0.9800
C(7)-C(8)	1.415(9)	C(22)-H(22B)	0.9800
C(7)-H(7)	0.9500	C(22)-H(22C)	0.9800
C(8)-C(9)	1.376(10)	C(23)-H(23A)	0.9800
C(8)-C(12)	1.510(10)	C(23)-H(23B)	0.9800
C(9)-C(10)	1.383(9)	C(23)-H(23C)	0.9800
C(9)-H(9)	0.9500	C(24)-H(24A)	0.9800
C(10)-H(10)	0.9500	C(24)-H(24B)	0.9800
C(11)-H(11A)	0.9800	C(24)-H(24C)	0.9800
C(11)-H(11B)	0.9800	C(25A)-C(26A)	1.562(12)
C(11)-H(11C)	0.9800	C(25A)-H(25A)	0.9900
C(12)-H(12A)	0.9800	C(25A)-H(25B)	0.9900
C(12)-H(12B)	0.9800	C(26A)-C(27A)	1.594(12)
C(12)-H(12C)	0.9800	C(26A)-H(26A)	0.9900
C(13)-C(16)	1.529(9)	C(26A)-H(26B)	0.9900
C(13)-C(15)	1.547(10)	C(27A)-C(28A)	1.554(13)
C(13)-C(14)	1.546(11)	C(27A)-H(27A)	0.9900

Table S2. Bond lengths (Å) for [(4,4'-Me_2-bipy)Cu($S(CH_2)_4$)(P^tBu_3)][PF_6]. Symmetry transformations used to generate equivalent atoms: #1 -y+2, x-y+1, z; #2 -x+y+1, -x+2, z; #3 y, x, -z+1; #4 -x+y+1, -x+1, z; #5 -y+1, x-y, z; #6 y+⅓, x-⅓,-z+⅔; #7 x-y+⅓,-y+⅔,-z+⅔; #8 -x+1⅓, -x+y+⅔, -z+⅔.

C(27A)-H(27B)	0.9900	P(4)-F(10)	1.5814(12)
C(28A)-H(28A)	0.9900	P(4)-F(10)#5	1.5814(12)
C(28A)-H(28B)	0.9900	P(4)-F(9)	1.5818(12)
C(25B)-C(26B)	1.558(13)	P(4)-F(9)#6	1.5816(12)
C(25B)-H(25C)	0.9900	P(4)-F(11)#4	1.5829(14)
C(25B)-H(25D)	0.9900	P(4)-F(11)#5	1.5829(14)
C(26B)-C(27B)	1.583(12)	P(4)-F(11)#6	1.5830(14)
C(26B)-H(26C)	0.9900	P(4)-F(11)#7	1.5829(14)
C(26B)-H(26D)	0.9900	P(4)-F(11)#8	1.5829(14)
C(27B)-C(28B)	1.556(13)	P(4)-F(11)	1.5829(14)
C(27B)-H(27C)	0.9900	F(10)-F(11)#8	0.825(3)
C(27B)-H(27D)	0.9900	F(10)-F(11)#4	0.825(3)
C(28B)-H(28C)	0.9900	F(11)-F(11)#8	1.573(4)
C(28B)-H(28D)	0.9900	F(11)-F(11)#7	1.593(6)
P(2)-F(2)	1.587(6)		
P(2)-F(2)#1	1.587(6)		
P(2)-F(2)#2	1.587(6)		
P(2)-F(1)#1	1.588(6)		
P(2)-F(1)#2	1.588(6)		
P(2)-F(1)	1.589(6)		
P(3)-F(7)#3	1.5798(12)		
P(3)-F(7)	1.5798(12)		
P(3)-F(8)	1.5797(12)		
P(3)-F(8)#3	1.5797(12)		
P(3)-F(3)	1.5801(12)		
P(3)-F(3)#3	1.5802(12)		
P(3)-F(6)#3	1.5807(12)		
P(3)-F(6)	1.5807(12)		
P(3)-F(5)	1.5810(12)		
P(3)-F(5)#3	1.5811(12)		
P(3)-F(4)#3	1.5815(12)		
P(3)-F(4)	1.5815(12)		
F(3)-F(6)#3	1.014(16)		
F(3)-F(7)#3	1.479(13)		
F(4)-F(8)#3	1.144(16)		
F(4)-F(7)#3	1.355(14)		
F(5)-F(8)#3	1.351(14)		
F(5)-F(6)#3	1.482(13)		
F(5)-F(5)#3	1.530(16)		
F(7)-F(7)#3	1.528(16)		
P(4)-F(10)#4	1.5814(12)		

Table S3. Bond angles (deg.) for [(4,4'-Me_2-bipy)Cu($S(CH_2)_4$)(P^tBu_3)][PF_6]. Symmetry transformations used to generate equivalent atoms: #1 -y+2, x-y+1, z; #2 -x+y+1, -x+2, z; #3 y, x, -z+1; #4 -x+y+1, -x+1, z; #5 -y+1, x-y, z; #6 y+⅓, x-⅓,-z+⅔; #7 x-y+⅓,-y+⅔,-z+⅔; #8 -x+1⅓, -x+y+⅔, -z+⅔.

N(2)-Cu(1)-N(1)	79.2(2)	C(7)-C(6)-C(5)	122.1(5)
N(2)-Cu(1)-P(1)	122.80(16)	C(6)-C(7)-C(8)	118.7(6)
N(1)-Cu(1)-P(1)	122.77(17)	C(6)-C(7)-H(7)	120.7
N(2)-Cu(1)-S(1)	103.29(16)	C(8)-C(7)-H(7)	120.7
N(1)-Cu(1)-S(1)	105.02(17)	C(9)-C(8)-C(7)	117.6(6)
P(1)-Cu(1)-S(1)	116.84(7)	C(9)-C(8)-C(12)	122.6(6)
C(28A)-S(1)-C(25A)	104.7(7)	C(7)-C(8)-C(12)	119.8(6)
C(25B)-S(1)-C(28B)	106.3(9)	C(8)-C(9)-C(10)	120.0(6)
C(25B)-S(1)-Cu(1)	111.0(8)	C(8)-C(9)-H(9)	120.0
C(28A)-S(1)-Cu(1)	117.6(8)	C(10)-C(9)-H(9)	120.0
C(25A)-S(1)-Cu(1)	108.8(6)	N(2)-C(10)-C(9)	122.6(6)
C(28B)-S(1)-Cu(1)	105.6(11)	N(2)-C(10)-H(10)	118.7
C(21)-P(1)-C(13)	108.3(3)	C(9)-C(10)-H(10)	118.7
C(21)-P(1)-C(17)	107.7(3)	C(3)-C(11)-H(11A)	109.5
C(13)-P(1)-C(17)	108.8(3)	C(3)-C(11)-H(11B)	109.5
C(21)-P(1)-Cu(1)	109.9(2)	H(11A)-C(11)-H(11B)	109.5
C(13)-P(1)-Cu(1)	110.2(2)	C(3)-C(11)-H(11C)	109.5
C(17)-P(1)-Cu(1)	111.8(2)	H(11A)-C(11)-H(11C)	109.5
C(1)-N(1)-C(5)	118.8(5)	H(11B)-C(11)-H(11C)	109.5
C(1)-N(1)-Cu(1)	126.8(4)	C(8)-C(12)-H(12A)	109.5
C(5)-N(1)-Cu(1)	114.1(4)	C(8)-C(12)-H(12B)	109.5
C(10)-N(2)-C(6)	118.5(5)	H(12A)-C(12)-H(12B)	109.5
C(10)-N(2)-Cu(1)	126.4(4)	C(8)-C(12)-H(12C)	109.5
C(6)-N(2)-Cu(1)	114.7(4)	H(12A)-C(12)-H(12C)	109.5
N(1)-C(1)-C(2)	123.4(6)	H(12B)-C(12)-H(12C)	109.5
N(1)-C(1)-H(1)	118.3	C(16)-C(13)-C(15)	108.3(6)
C(2)-C(1)-H(1)	118.3	C(16)-C(13)-C(14)	109.7(6)
C(1)-C(2)-C(3)	118.7(5)	C(15)-C(13)-C(14)	105.2(6)
C(1)-C(2)-H(2)	120.6	C(16)-C(13)-P(1)	116.1(5)
C(3)-C(2)-H(2)	120.6	C(15)-C(13)-P(1)	110.1(5)
C(4)-C(3)-C(2)	117.4(5)	C(14)-C(13)-P(1)	106.8(4)
C(4)-C(3)-C(11)	121.9(6)	C(13)-C(14)-H(14A)	109.5
C(2)-C(3)-C(11)	120.7(6)	C(13)-C(14)-H(14B)	109.5
C(5)-C(4)-C(3)	120.4(6)	H(14A)-C(14)-H(14B)	109.5
C(5)-C(4)-H(4)	119.8	C(13)-C(14)-H(14C)	109.5
C(3)-C(4)-H(4)	119.8	H(14A)-C(14)-H(14C)	109.5
N(1)-C(5)-C(4)	121.3(6)	H(14B)-C(14)-H(14C)	109.5
N(1)-C(5)-C(6)	116.1(5)	C(13)-C(15)-H(15A)	109.5
C(4)-C(5)-C(6)	122.6(5)	C(13)-C(15)-H(15B)	109.5
N(2)-C(6)-C(7)	122.6(5)	H(15A)-C(15)-H(15B)	109.5
N(2)-C(6)-C(5)	115.3(5)	C(13)-C(15)-H(15C)	109.5

Table S3. Bond angles (deg.) for [(4,4'-Me_2-bipy)Cu($S(CH_2)_4$)(P^tBu_3)][PF_6]. Symmetry transformations used to generate equivalent atoms: #1 -y+2, x-y+1, z; #2 -x+y+1, -x+2, z; #3 y, x, -z+1; #4 -x+y+1, -x+1, z; #5 -y+1, x-y, z; #6 y+⅓, x-⅓,-z+⅔; #7 x-y+⅓,-y+⅔,-z+⅔; #8 -x+1⅓, -x+y+⅔, -z+⅔.

H(15A)-C(15)-H(15C)	109.5	C(21)-C(22)-H(22C)	109.5
H(15B)-C(15)-H(15C)	109.5	H(22A)-C(22)-H(22C)	109.5
C(13)-C(16)-H(16A)	109.5	H(22B)-C(22)-H(22C)	109.5
C(13)-C(16)-H(16B)	109.5	C(21)-C(23)-H(23A)	109.5
H(16A)-C(16)-H(16B)	109.5	C(21)-C(23)-H(23B)	109.5
C(13)-C(16)-H(16C)	109.5	H(23A)-C(23)-H(23B)	109.5
H(16A)-C(16)-H(16C)	109.5	C(21)-C(23)-H(23C)	109.5
H(16B)-C(16)-H(16C)	109.5	H(23A)-C(23)-H(23C)	109.5
C(18)-C(17)-C(20)	109.3(6)	H(23B)-C(23)-H(23C)	109.5
C(18)-C(17)-C(19)	109.7(6)	C(21)-C(24)-H(24A)	109.5
C(20)-C(17)-C(19)	105.1(6)	C(21)-C(24)-H(24B)	109.5
C(18)-C(17)-P(1)	116.6(5)	H(24A)-C(24)-H(24B)	109.5
C(20)-C(17)-P(1)	109.6(4)	C(21)-C(24)-H(24C)	109.5
C(19)-C(17)-P(1)	105.9(5)	H(24A)-C(24)-H(24C)	109.5
C(17)-C(18)-H(18A)	109.5	H(24B)-C(24)-H(24C)	109.5
C(17)-C(18)-H(18B)	109.5	C(26A)-C(25A)-S(1)	99.2(8)
H(18A)-C(18)-H(18B)	109.5	C(26A)-C(25A)-H(25A)	111.9
C(17)-C(18)-H(18C)	109.5	S(1)-C(25A)-H(25A)	111.9
H(18A)-C(18)-H(18C)	109.5	C(26A)-C(25A)-H(25B)	111.9
H(18B)-C(18)-H(18C)	109.5	S(1)-C(25A)-H(25B)	111.9
C(17)-C(19)-H(19A)	109.5	H(25A)-C(25A)-H(25B)	109.6
C(17)-C(19)-H(19B)	109.5	C(25A)-C(26A)-C(27A)	110.3(9)
H(19A)-C(19)-H(19B)	109.5	C(25A)-C(26A)-H(26A)	109.6
C(17)-C(19)-H(19C)	109.5	C(27A)-C(26A)-H(26A)	109.6
H(19A)-C(19)-H(19C)	109.5	C(25A)-C(26A)-H(26B)	109.6
H(19B)-C(19)-H(19C)	109.5	C(27A)-C(26A)-H(26B)	109.6
C(17)-C(20)-H(20A)	109.5	H(26A)-C(26A)-H(26B)	108.1
C(17)-C(20)-H(20B)	109.5	C(28A)-C(27A)-C(26A)	113.2(10)
H(20A)-C(20)-H(20B)	109.5	C(28A)-C(27A)-H(27A)	108.9
C(17)-C(20)-H(20C)	109.5	C(26A)-C(27A)-H(27A)	108.9
H(20A)-C(20)-H(20C)	109.5	C(28A)-C(27A)-H(27B)	108.9
H(20B)-C(20)-H(20C)	109.5	C(26A)-C(27A)-H(27B)	108.9
C(22)-C(21)-C(24)	108.5(6)	H(27A)-C(27A)-H(27B)	107.8
C(22)-C(21)-C(23)	108.8(5)	C(27A)-C(28A)-S(1)	100.8(9)
C(24)-C(21)-C(23)	105.1(5)	C(27A)-C(28A)-H(28A)	111.6
C(22)-C(21)-P(1)	115.7(4)	S(1)-C(28A)-H(28A)	111.6
C(24)-C(21)-P(1)	110.2(4)	C(27A)-C(28A)-H(28B)	111.6
C(23)-C(21)-P(1)	108.0(4)	S(1)-C(28A)-H(28B)	111.6
C(21)-C(22)-H(22A)	109.5	H(28A)-C(28A)-H(28B)	109.4
C(21)-C(22)-H(22B)	109.5	C(26B)-C(25B)-S(1)	97.5(10)
H(22A)-C(22)-H(22B)	109.5	C(26B)-C(25B)-H(25C)	112.3

Table S3. Bond angles (deg.) for [(4,4'-Me_2-bipy)Cu($S(CH_2)_4$)(P^tBu_3)][PF_6]. Symmetry transformations used to generate equivalent atoms: #1 -y+2, x-y+1, z; #2 -x+y+1, -x+2, z; #3 y, x, -z+1; #4 -x+y+1, -x+1, z; #5 -y+1, x-y, z; #6 y+⅓, x-⅓,-z+⅔; #7 x-y+⅓,-y+⅔,-z+⅔; #8 -x+1⅓, -x+y+⅔, -z+⅔.

S(1)-C(25B)-H(25C)	112.3	F(7)-P(3)-F(8)#3	129.3(6)
C(26B)-C(25B)-H(25D)	112.3	F(8)-P(3)-F(8)#3	137.5(7)
S(1)-C(25B)-H(25D)	112.3	F(7)#3-P(3)-F(3)	55.8(5)
H(25C)-C(25B)-H(25D)	109.9	F(7)-P(3)-F(3)	90.06(8)
C(25B)-C(26B)-C(27B)	113.3(10)	F(8)-P(3)-F(3)	90.07(8)
C(25B)-C(26B)-H(26C)	108.9	F(8)#3-P(3)-F(3)	103.4(3)
C(27B)-C(26B)-H(26C)	108.9	F(7)#3-P(3)-F(3)#3	90.06(8)
C(25B)-C(26B)-H(26D)	108.9	F(7)-P(3)-F(3)#3	55.8(5)
C(27B)-C(26B)-H(26D)	108.9	F(8)-P(3)-F(3)#3	103.4(3)
H(26C)-C(26B)-H(26D)	107.7	F(8)#3-P(3)-F(3)#3	90.07(8)
C(28B)-C(27B)-C(26B)	113.1(11)	F(3)-P(3)-F(3)#3	142.6(6)
C(28B)-C(27B)-H(27C)	109.0	F(7)#3-P(3)-F(6)#3	90.01(8)
C(26B)-C(27B)-H(27C)	109.0	F(7)-P(3)-F(6)#3	124.2(5)
C(28B)-C(27B)-H(27D)	109.0	F(8)-P(3)-F(6)#3	76.5(3)
C(26B)-C(27B)-H(27D)	109.0	F(8)#3-P(3)-F(6)#3	90.03(8)
H(27C)-C(27B)-H(27D)	107.8	F(3)-P(3)-F(6)#3	37.4(6)
C(27B)-C(28B)-S(1)	99.0(10)	F(3)#3-P(3)-F(6)#3	179.88(11)
C(27B)-C(28B)-H(28C)	112.0	F(7)#3-P(3)-F(6)	124.2(5)
S(1)-C(28B)-H(28C)	112.0	F(7)-P(3)-F(6)	90.01(8)
C(27B)-C(28B)-H(28D)	112.0	F(8)-P(3)-F(6)	90.03(8)
S(1)-C(28B)-H(28D)	112.0	F(8)#3-P(3)-F(6)	76.5(3)
H(28C)-C(28B)-H(28D)	109.6	F(3)-P(3)-F(6)	179.88(11)
F(2)-P(2)-F(2)#1	90.6(4)	F(3)#3-P(3)-F(6)	37.4(6)
F(2)-P(2)-F(2)#2	90.7(4)	F(6)#3-P(3)-F(6)	142.6(6)
F(2)#1-P(2)-F(2)#2	90.6(4)	F(7)#3-P(3)-F(5)	122.1(7)
F(2)-P(2)-F(1)#1	90.2(4)	F(7)-P(3)-F(5)	179.92(13)
F(2)#1-P(2)-F(1)#1	179.0(4)	F(8)-P(3)-F(5)	90.02(8)
F(2)#2-P(2)-F(1)#1	88.9(3)	F(8)#3-P(3)-F(5)	50.6(6)
F(2)-P(2)-F(1)#2	88.9(3)	F(3)-P(3)-F(5)	89.98(8)
F(2)#1-P(2)-F(1)#2	90.2(4)	F(3)#3-P(3)-F(5)	124.1(6)
F(2)#2-P(2)-F(1)#2	179.0(4)	F(6)#3-P(3)-F(5)	55.9(6)
F(1)#1-P(2)-F(1)#2	90.3(4)	F(6)-P(3)-F(5)	89.95(8)
F(2)-P(2)-F(1)	179.0(4)	F(7)#3-P(3)-F(5)#3	179.92(13)
F(2)#1-P(2)-F(1)	88.9(3)	F(7)-P(3)-F(5)#3	122.1(7)
F(2)#2-P(2)-F(1)	90.2(4)	F(8)-P(3)-F(5)#3	50.6(6)
F(1)#1-P(2)-F(1)	90.3(4)	F(8)#3-P(3)-F(5)#3	90.02(8)
F(1)#2-P(2)-F(1)	90.3(4)	F(3)-P(3)-F(5)#3	124.1(5)
F(7)#3-P(3)-F(7)	57.8(7)	F(3)#3-P(3)-F(5)#3	89.97(8)
F(7)#3-P(3)-F(8)	129.3(6)	F(6)#3-P(3)-F(5)#3	89.96(8)
F(7)-P(3)-F(8)	90.05(8)	F(6)-P(3)-F(5)#3	55.9(6)
F(7)#3-P(3)-F(8)#3	90.05(8)	F(5)-P(3)-F(5)#3	57.9(7)

Table S3. Bond angles (deg.) for [(4,4'-Me_2-bipy)Cu($S(CH_2)_4$)(P^tBu_3)][PF_6]. Symmetry transformations used to generate equivalent atoms: #1 -y+2, x-y+1, z; #2 -x+y+1, -x+2, z; #3 y, x, -z+1; #4 -x+y+1, -x+1, z; #5 -y+1, x-y, z; #6 y+⅓, x-⅓,-z+⅔; #7 x-y+⅓,-y+⅔,-z+⅔; #8 -x+1⅓, -x+y+⅔, -z+⅔.

F(7)#3-P(3)-F(4)#3	90.00(8)	F(7)#3-F(7)-P(3)	61.1(3)
F(7)-P(3)-F(4)#3	50.8(6)	F(4)#3-F(8)-F(5)#3	127.0(3)
F(8)-P(3)-F(4)#3	42.4(6)	F(4)#3-F(8)-P(3)	68.9(3)
F(8)#3-P(3)-F(4)#3	179.94(14)	F(5)#3-F(8)-P(3)	64.7(3)
F(3)-P(3)-F(4)#3	76.6(3)	F(10)#4-P(4)-F(10)	120.0
F(3)#3-P(3)-F(4)#3	89.97(8)	F(10)#4-P(4)-F(10)#5	120.000(1)
F(6)#3-P(3)-F(4)#3	89.94(8)	F(10)-P(4)-F(10)#5	120.001(1)
F(6)-P(3)-F(4)#3	103.5(3)	F(10)#4-P(4)-F(9)	90.0
F(5)-P(3)-F(4)#3	129.3(6)	F(10)-P(4)-F(9)	90.0
F(5)#3-P(3)-F(4)#3	89.93(8)	F(10)#5-P(4)-F(9)	90.0
F(7)#3-P(3)-F(4)	50.7(6)	F(10)#4-P(4)-F(9)#6	90.0
F(7)-P(3)-F(4)	90.00(8)	F(10)-P(4)-F(9)#6	90.000(1)
F(8)-P(3)-F(4)	179.94(14)	F(10)#5-P(4)-F(9)#6	90.004(1)
F(8)#3-P(3)-F(4)	42.4(6)	F(9)-P(4)-F(9)#6	180.0
F(3)-P(3)-F(4)	89.96(8)	F(10)#4-P(4)-F(11)#4	89.78(10)
F(3)#3-P(3)-F(4)	76.6(3)	F(10)-P(4)-F(11)#4	30.21(10)
F(6)#3-P(3)-F(4)	103.5(3)	F(10)#5-P(4)-F(11)#4	150.22(10)
F(6)-P(3)-F(4)	89.94(8)	F(9)-P(4)-F(11)#4	89.84(10)
F(5)-P(3)-F(4)	89.93(8)	F(9)#6-P(4)-F(11)#4	90.16(10)
F(5)#3-P(3)-F(4)	129.3(6)	F(10)#4-P(4)-F(11)#5	30.22(10)
F(4)#3-P(3)-F(4)	137.6(7)	F(10)-P(4)-F(11)#5	150.21(10)
F(6)#3-F(3)-F(7)#3	126.5(3)	F(10)#5-P(4)-F(11)#5	89.78(10)
F(6)#3-F(3)-P(3)	71.3(3)	F(9)-P(4)-F(11)#5	89.84(10)
F(7)#3-F(3)-P(3)	62.1(3)	F(9)#6-P(4)-F(11)#5	90.16(10)
F(8)#3-F(4)-F(7)#3	126.7(3)	F(11)#4-P(4)-F(11)#5	119.999(1)
F(8)#3-F(4)-P(3)	68.7(3)	F(10)#4-P(4)-F(11)#6	30.21(10)
F(7)#3-F(4)-P(3)	64.6(3)	F(10)-P(4)-F(11)#6	89.79(10)
F(8)#3-F(5)-F(6)#3	104.1(8)	F(10)#5-P(4)-F(11)#6	150.21(10)
F(8)#3-F(5)-F(5)#3	101.6(7)	F(9)-P(4)-F(11)#6	90.15(10)
F(6)#3-F(5)-F(5)#3	95.8(6)	F(9)#6-P(4)-F(11)#6	89.85(10)
F(8)#3-F(5)-P(3)	64.6(3)	F(11)#4-P(4)-F(11)#6	59.6(2)
F(6)#3-F(5)-P(3)	62.0(3)	F(11)#5-P(4)-F(11)#6	60.4(2)
F(5)#3-F(5)-P(3)	61.1(3)	F(10)#4-P(4)-F(11)#7	89.78(10)
F(3)#3-F(6)-F(5)#3	126.2(3)	F(10)-P(4)-F(11)#7	150.22(10)
F(3)#3-F(6)-P(3)	71.3(3)	F(10)#5-P(4)-F(11)#7	30.22(10)
F(5)#3-F(6)-P(3)	62.1(3)	F(9)-P(4)-F(11)#7	90.15(10)
F(4)#3-F(7)-F(3)#3	104.1(8)	F(9)#6-P(4)-F(11)#7	89.85(10)
F(4)#3-F(7)-F(7)#3	101.5(7)	F(11)#4-P(4)-F(11)#7	179.6(2)
F(3)#3-F(7)-F(7)#3	96.1(6)	F(11)#5-P(4)-F(11)#7	59.6(2)
F(4)#3-F(7)-P(3)	64.7(3)	F(11)#6-P(4)-F(11)#7	119.997(1)
F(3)#3-F(7)-P(3)	62.1(3)	F(10)#4-P(4)-F(11)#8	150.21(10)

Table S3. Bond angles (deg.) for [(4,4'-Me_2-bipy)Cu($S(CH_2)_4$)(P^tBu_3)][PF_6]. Symmetry transformations used to generate equivalent atoms: #1 -y+2, x-y+1, z; #2 -x+y+1, -x+2, z; #3 y, x, -z+1; #4 -x+y+1, -x+1, z; #5 -y+1, x-y, z; #6 y+⅓, x-⅓,-z+⅔; #7 x-y+⅓,-y+⅔,-z+⅔; #8 -x+1⅓, -x+y+⅔, -z+⅔.

F(10)-P(4)-F(11)#8	30.21(10)
F(10)#5-P(4)-F(11)#8	89.79(10)
F(9)-P(4)-F(11)#8	90.15(10)
F(9)#6-P(4)-F(11)#8	89.85(10)
F(11)#4-P(4)-F(11)#8	60.4(2)
F(11)#5-P(4)-F(11)#8	179.6(2)
F(11)#6-P(4)-F(11)#8	119.997(2)
F(11)#7-P(4)-F(11)#8	120.005(1)
F(10)#4-P(4)-F(11)	150.21(10)
F(10)-P(4)-F(11)	89.79(10)
F(10)#5-P(4)-F(11)	30.21(10)
F(9)-P(4)-F(11)	89.84(10)
F(9)#6-P(4)-F(11)	90.16(10)
F(11)#4-P(4)-F(11)	120.001(3)
F(11)#5-P(4)-F(11)	119.998(2)
F(11)#6-P(4)-F(11)	179.6(2)
F(11)#7-P(4)-F(11)	60.4(2)
F(11)#8-P(4)-F(11)	59.6(2)
F(11)#8-F(10)-F(11)#4	150.0(3)
F(11)#8-F(10)-P(4)	74.99(13)
F(11)#4-F(10)-P(4)	74.99(13)
F(10)#5-F(11)-F(11)#8	135.00(13)
F(10)#5-F(11)-P(4)	74.79(14)
F(11)#8-F(11)-P(4)	60.21(10)
F(10)#5-F(11)-F(11)#7	15.01(13)
F(11)#8-F(11)-F(11)#7	119.994(5)
P(4)-F(11)-F(11)#7	59.78(10)

Table S4. Anisotropic displacement parameters ($Å^2$ x 10^3) for [(4,4'-Me_2-bipy)Cu($S(CH_2)_4$)(P^tBu_3)][PF_6]. The anisotropic displacement factor exponent takes the form: $-2\pi^2[h^2a^{*2}U^{11} + ... + 2hka^*b^*U^{12}]$.

Atom	U^{11}	U^{22}	U^{33}	U^{23}	U^{13}	U^{12}
Cu(1)	28(1)	27(1)	45(1)	-2(1)	3(1)	15(1)
S(1)	70(1)	69(1)	69(1)	-10(1)	-26(1)	48(1)
P(1)	24(1)	27(1)	32(1)	-5(1)	-1(1)	14(1)
N(1)	23(2)	27(2)	57(3)	-5(2)	3(2)	13(2)
N(2)	32(3)	24(2)	43(3)	0(2)	6(2)	13(2)
C(1)	29(3)	25(3)	56(4)	-4(3)	3(3)	12(2)
C(2)	22(2)	28(3)	48(3)	4(2)	4(2)	10(2)
C(3)	26(3)	33(3)	43(3)	0(2)	4(2)	14(2)
C(4)	28(3)	26(3)	49(3)	2(2)	7(2)	13(2)
C(5)	25(3)	20(2)	45(3)	3(2)	3(2)	13(2)
C(6)	17(2)	24(3)	49(3)	2(2)	1(2)	9(2)
C(7)	31(3)	27(3)	52(4)	3(2)	7(3)	16(3)
C(8)	32(3)	28(3)	60(4)	8(3)	9(3)	14(3)
C(9)	28(3)	28(3)	55(4)	11(3)	10(3)	9(3)
C(10)	37(3)	37(3)	42(3)	-4(3)	7(3)	18(3)
C(11)	43(4)	41(4)	66(5)	-12(3)	22(3)	12(3)
C(12)	60(5)	25(3)	105(7)	7(4)	32(5)	15(3)
C(13)	38(3)	56(4)	38(3)	-7(3)	2(3)	35(3)
C(14)	44(4)	64(5)	41(3)	7(3)	12(3)	29(4)
C(15)	68(5)	77(6)	38(3)	-22(4)	-15(3)	51(5)
C(16)	54(4)	81(6)	51(4)	-7(4)	3(3)	54(4)
C(17)	30(3)	29(3)	50(4)	-7(3)	-7(3)	13(3)
C(18)	44(4)	36(4)	70(5)	-4(3)	-10(3)	22(3)
C(19)	36(4)	35(3)	70(5)	-16(3)	-16(3)	14(3)
C(20)	28(3)	33(3)	59(4)	14(3)	8(3)	8(3)
C(21)	25(3)	31(3)	33(3)	-3(2)	-3(2)	10(2)
C(22)	38(3)	54(4)	42(3)	1(3)	-8(3)	26(3)
C(23)	41(3)	39(3)	33(3)	-5(2)	3(3)	12(3)
C(24)	29(3)	44(4)	45(4)	-4(3)	-3(3)	3(3)
P(2)	28(1)	28(1)	82(2)	0	0	14(1)
F(1)	70(4)	45(3)	120(5)	8(3)	-30(3)	28(3)
F(2)	94(5)	57(3)	116(5)	36(3)	48(4)	39(3)

Table S5. Hydrogen coordinates (x 10^4) and isotropic displacement parameters (Å^2 x 10^3) for [(4,4'-Me_2-bipy)Cu(S(CH_2)$_4$)(P^{t}Bu$_3$)][PF_6].

H atom	x	y	z	U(eq)
H(1)	8388	8125	3836	45
H(2)	9056	7904	3493	41
H(4)	7338	5511	3523	41
H(7)	6412	4588	3759	44
H(9)	4690	4124	4311	47
H(10)	5257	5515	4369	47
H(11A)	8448	5911	3223	81
H(11B)	9271	6744	3284	81
H(11C)	8618	6738	3083	81
H(12A)	4882	3174	3794	99
H(12B)	4665	2982	4098	99
H(12C)	5525	3142	3990	99
H(14A)	5618	6865	4571	73
H(14B)	4857	6636	4383	73
H(14C)	4876	6968	4673	73
H(15A)	5939	8347	4796	82
H(15B)	6521	8989	4581	82
H(15C)	6640	8238	4661	82
H(16A)	4554	7767	4275	80
H(16B)	5271	8697	4287	80
H(16C)	4820	8233	4550	80
H(18A)	6565	9613	4244	74
H(18B)	6348	9551	3938	74
H(18C)	7246	10193	4037	74
H(19A)	8202	9771	4176	73
H(19B)	7952	8830	4178	73
H(19C)	7590	9172	4395	73
H(20A)	7817	9620	3719	64
H(20B)	6922	8957	3623	64
H(20C)	7536	8671	3727	64
H(22A)	5732	8597	3641	65
H(22B)	4983	8268	3841	65
H(22C)	4862	7852	3559	65
H(23A)	5497	7053	3450	62
H(23B)	5948	6808	3666	62
H(23C)	6388	7713	3550	62
H(24A)	4364	6861	4014	69
H(24B)	4837	6361	3995	69
H(24C)	4382	6446	3742	69
H(25A)	7142	6172	4866	87

Table S5. Hydrogen coordinates (x 10^4) and isotropic displacement parameters (Å^2 x 10^3) for [(4,4'-Me_2-bipy)Cu(S(CH_2)$_4$)(P^{t}Bu$_3$)][PF_6].

H atom	x	y	z	U(eq)
H(25B)	6831	5815	4574	87
H(26A)	8130	6187	4431	86
H(26B)	8218	5993	4731	86
H(27A)	8978	7362	4843	105
H(27B)	9312	7371	4554	105
H(28A)	8786	8125	4392	118
H(28B)	8761	8359	4695	118
H(25C)	7074	6429	4942	87
H(25D)	6415	5992	4708	87
H(26C)	7257	5668	4476	86
H(26D)	7531	5594	4767	86
H(27C)	8769	6758	4729	105
H(27D)	8641	6444	4432	105
H(28C)	8602	7551	4285	118
H(28D)	8939	7944	4572	118

Structure Determination Summary

Crystal Data and Structure Refinement for [(4,4′-Me_2-bipy)Cu(S=C(NH_2)$_2$)(P^{t}Bu$_3$)][BF_4].

Identification code	JPD1053_0m_a	
Empirical formula	$C_{25}H_{43}BCuF_4N_4PS$	
Formula weight	613.01	
Temperature	150(2) K	
Wavelength	0.71073 Å	
Crystal system	Monoclinic	
Space group	$P2_1/n$	
Unit cell dimensions	a = 8.513(2) Å	α = 90°
	b = 21.959(5) Å	β = 103.105(4)°
	c = 16.595(4) Å	γ = 90°
Volume	3021.2(13) Å^3	
Z	4	
Density (calculated)	1.348 g/cm^3	
Absorption coefficient	0.891 mm^{-1}	
F(000)	1288	
Crystal size	0.373 x 0.214 x 0.201 mm^3	
θ range for data collection	1.564 to 29.586°	
Index ranges	$-11 \le h \le 11$, $-30 \le k \le 30$, $-22 \le l \le 23$	
Reflections collected	58481	
Independent reflections	8379 [R(int) = 0.0409]	

Completeness to θ = 25.242°	100.0 %
Absorption correction	Semi-empirical from equivalents
Refinement method	Full-matrix least-squares on F^2
Data / restraints / parameters	8379 / 36 / 315
Goodness-of-fit on F^2	1.049
Final R indices [I>2σ(I)]	R1 = 0.0575, wR2 = 0.1463
R indices (all data)	R1 = 0.0693, wR2 = 0.1560
Extinction coefficient	n/a
Largest diff. peak and hole	1.332 and -1.183 e·Å^{-3}

Table S1. Atomic coordinates (x 10^4) and equivalent isotropic displacement parameters ($Å^2$ x 10^3) for [(4,4′-Me_2-bipy)Cu(S=C(NH_2)$_2$)(P^{t}Bu$_3$)][BF_4]. U(eq) is defined as one third of the trace of the orthogonalized U^{ij} tensor.

Atom	x	y	z	U(eq)
Cu(1)	2804(1)	4580(1)	7087(1)	21(1)
P(1)	1942(1)	5426(1)	7606(1)	22(1)
S(1)	3864(1)	4716(1)	5948(1)	34(1)
F(1)	5246(2)	2336(1)	5721(1)	37(1)
F(2)	5397(3)	1745(1)	4614(1)	43(1)
F(3)	7673(3)	2092(1)	5468(2)	63(1)
F(4)	6016(3)	2750(1)	4621(1)	55(1)
N(1)	4161(3)	3935(1)	7888(1)	25(1)
N(2)	1235(3)	3799(1)	6938(1)	24(1)
N(3)	3942(3)	3509(1)	5916(2)	32(1)
N(4)	5143(3)	3993(1)	4998(2)	35(1)
C(1)	5711(3)	3983(1)	8287(2)	34(1)
C(2)	6459(4)	3580(2)	8893(2)	37(1)
C(3)	5577(4)	3098(1)	9111(2)	32(1)
C(4)	3969(3)	3043(1)	8692(2)	27(1)
C(5)	3304(3)	3463(1)	8080(2)	22(1)
C(6)	1616(3)	3416(1)	7588(2)	20(1)
C(7)	505(3)	3006(1)	7777(2)	23(1)
C(8)	-1049(3)	2975(1)	7286(2)	25(1)
C(9)	-1411(3)	3357(1)	6600(2)	31(1)
C(10)	-254(3)	3756(1)	6451(2)	31(1)
C(11)	6312(5)	2641(2)	9764(2)	47(1)
C(12)	-2265(4)	2541(2)	7487(2)	34(1)
C(13A)	861(2)	5257(1)	8506(1)	29(1)
C(14A)	-765(2)	4987(1)	8070(2)	47(1)
C(15A)	1933(3)	4782(1)	9041(2)	43(1)
C(16A)	650(4)	5824(1)	9007(2)	36(1)
C(13B)	1297(2)	5247(1)	8664(2)	29(1)
C(14B)	362(3)	4647(1)	8527(3)	47(1)
C(15B)	2874(2)	5182(2)	9317(3)	43(1)
C(16B)	260(3)	5766(1)	8873(3)	36(1)
C(17A)	3814(2)	5978(1)	8054(1)	34(1)
C(18A)	4665(4)	5720(1)	8896(1)	52(1)
C(19A)	4887(3)	5944(2)	7431(1)	51(1)
C(20A)	3204(4)	6626(1)	8131(2)	44(1)
C(17B)	3621(3)	6030(1)	7791(1)	34(1)
C(18B)	5121(3)	5647(1)	8140(2)	52(1)
C(19B)	3597(6)	6257(2)	6917(1)	51(1)
C(20B)	3449(5)	6556(1)	8370(1)	44(1)

Table S1. Atomic coordinates (x 10^4) and equivalent isotropic displacement parameters (Å^2 x 10^3) for [(4,4′-Me_2-bipy)Cu(S=C(NH_2)$_2$)(P^tBu_3)][BF_4]. U(eq) is defined as one third of the trace of the orthogonalized U^{ij} tensor.

Atom	x	y	z	U(eq)
C(21A)	453(2)	5863(1)	6696(1)	39(1)
C(22A)	-571(3)	5349(1)	6224(2)	54(1)
C(23A)	1503(3)	6165(1)	6174(2)	53(1)
C(24A)	-586(3)	6330(1)	7020(2)	51(1)
C(21B)	51(2)	5703(2)	6826(3)	39(1)
C(22B)	-1445(2)	5344(1)	6904(2)	54(1)
C(23B)	332(4)	5676(2)	5953(2)	53(1)
C(24B)	-303(6)	6411(1)	7008(2)	51(1)
C(25)	4348(3)	4023(1)	5595(2)	24(1)
B(1)	6094(4)	2217(2)	5105(2)	31(1)

Table S2. Bond lengths (Å) for [(4,4′-Me_2-bipy)Cu(S=C(NH_2)$_2$)(P^tBu_3)][BF_4]. Symmetry transformations used to generate equivalent atoms:

Cu(1)-N(1)	2.098(2)	C(11)-H(11B)	0.9800
Cu(1)-N(2)	2.153(2)	C(11)-H(11C)	0.9800
Cu(1)-P(1)	2.2412(8)	C(12)-H(12A)	0.9800
Cu(1)-S(1)	2.2918(9)	C(12)-H(12B)	0.9800
P(1)-C(17B)	1.923(2)	C(12)-H(12C)	0.9800
P(1)-C(21B)	1.922(4)	C(13A)-C(15A)	1.5291(3)
P(1)-C(13A)	1.960(2)	C(13A)-C(14A)	1.5290(3)
P(1)-C(21A)	1.9851(17)	C(13A)-C(16A)	1.5290(3)
P(1)-C(13B)	1.994(3)	C(14A)-H(14A)	0.9800
P(1)-C(17A)	2.0058(19)	C(14A)-H(14B)	0.9800
S(1)-C(25)	1.714(3)	C(14A)-H(14C)	0.9800
F(1)-B(1)	1.402(4)	C(15A)-H(15A)	0.9800
F(2)-B(1)	1.368(4)	C(15A)-H(15B)	0.9800
F(3)-B(1)	1.370(4)	C(15A)-H(15C)	0.9800
F(4)-B(1)	1.413(4)	C(16A)-H(16A)	0.9800
N(1)-C(1)	1.339(4)	C(16A)-H(16B)	0.9800
N(1)-C(5)	1.347(3)	C(16A)-H(16C)	0.9800
N(2)-C(10)	1.343(3)	C(13B)-C(15B)	1.5290(3)
N(2)-C(6)	1.347(3)	C(13B)-C(14B)	1.5290(3)
N(3)-C(25)	1.327(3)	C(13B)-C(16B)	1.5290(3)
N(3)-H(3A)	0.8800	C(14B)-H(14D)	0.9800
N(3)-H(3B)	0.8800	C(14B)-H(14E)	0.9800
N(4)-C(25)	1.323(3)	C(14B)-H(14F)	0.9800
N(4)-H(4A)	0.8800	C(15B)-H(15D)	0.9800
N(4)-H(4B)	0.8800	C(15B)-H(15E)	0.9800
C(1)-C(2)	1.382(5)	C(15B)-H(15F)	0.9800
C(1)-H(1)	0.9500	C(16B)-H(16D)	0.9800
C(2)-C(3)	1.392(5)	C(16B)-H(16E)	0.9800
C(2)-H(2)	0.9500	C(16B)-H(16F)	0.9800
C(3)-C(4)	1.392(4)	C(17A)-C(20A)	1.5290(3)
C(3)-C(11)	1.506(4)	C(17A)-C(18A)	1.5290(3)
C(4)-C(5)	1.393(4)	C(17A)-C(19A)	1.5290(3)
C(4)-H(4)	0.9500	C(18A)-H(18A)	0.9800
C(5)-C(6)	1.487(3)	C(18A)-H(18B)	0.9800
C(6)-C(7)	1.393(3)	C(18A)-H(18C)	0.9800
C(7)-C(8)	1.389(4)	C(19A)-H(19A)	0.9800
C(7)-H(7)	0.9500	C(19A)-H(19B)	0.9800
C(8)-C(9)	1.390(4)	C(19A)-H(19C)	0.9800
C(8)-C(12)	1.500(4)	C(20A)-H(20A)	0.9800
C(9)-C(10)	1.382(4)	C(20A)-H(20B)	0.9800
C(9)-H(9)	0.9500	C(20A)-H(20C)	0.9800
C(10)-H(10)	0.9500	C(17B)-C(18B)	1.5290(3)
C(11)-H(11A)	0.9800	C(17B)-C(20B)	1.5290(3)

Table S2. Bond lengths (Å) for [(4,4′-Me_2-bipy)Cu(S=C(NH_2)$_2$)(P^tBu_3)][BF_4]. Symmetry transformations used to generate equivalent atoms:

C(17B)-C(19B)	1.5290(4)
C(18B)-H(18D)	0.9800
C(18B)-H(18E)	0.9800
C(18B)-H(18F)	0.9800
C(19B)-H(19D)	0.9800
C(19B)-H(19E)	0.9800
C(19B)-H(19F)	0.9800
C(20B)-H(20D)	0.9800
C(20B)-H(20E)	0.9800
C(20B)-H(20F)	0.9800
C(21A)-C(23A)	1.5290(3)
C(21A)-C(22A)	1.5290(3)
C(21A)-C(24A)	1.5290(3)
C(22A)-H(22A)	0.9800
C(22A)-H(22B)	0.9800
C(22A)-H(22C)	0.9800
C(23A)-H(23A)	0.9800
C(23A)-H(23B)	0.9800
C(23A)-H(23C)	0.9800
C(24A)-H(24A)	0.9800
C(24A)-H(24B)	0.9800
C(24A)-H(24C)	0.9800
C(21B)-C(23B)	1.522(5)
C(21B)-C(22B)	1.5290(3)
C(21B)-C(24B)	1.625(5)
C(22B)-H(22D)	0.9800
C(22B)-H(22E)	0.9800
C(22B)-H(22F)	0.9800
C(23B)-H(23D)	0.9800
C(23B)-H(23E)	0.9800
C(23B)-H(23F)	0.9800
C(24B)-H(24D)	0.9800
C(24B)-H(24E)	0.9800
C(24B)-H(24F)	0.9800

Table S3. Bond angles (deg.) for [(4,4′-Me_2-bipy)Cu(S=C(NH_2)$_2$)(P^tBu_3)][BF_4]. Symmetry transformations used to generate equivalent atoms:

N(1)-Cu(1)-N(2)	76.95(9)	N(1)-C(5)-C(4)	122.0(2)
N(1)-Cu(1)-P(1)	119.83(7)	N(1)-C(5)-C(6)	115.5(2)
N(2)-Cu(1)-P(1)	117.11(7)	C(4)-C(5)-C(6)	122.5(2)
N(1)-Cu(1)-S(1)	110.33(7)	N(2)-C(6)-C(7)	122.1(2)
N(2)-Cu(1)-S(1)	111.07(6)	N(2)-C(6)-C(5)	115.1(2)
P(1)-Cu(1)-S(1)	115.64(3)	C(7)-C(6)-C(5)	122.8(2)
C(17B)-P(1)-C(21B)	111.60(10)	C(8)-C(7)-C(6)	120.3(2)
C(13A)-P(1)-C(21A)	110.03(8)	C(8)-C(7)-H(7)	119.8
C(17B)-P(1)-C(13B)	109.76(9)	C(6)-C(7)-H(7)	119.8
C(21B)-P(1)-C(13B)	107.43(14)	C(7)-C(8)-C(9)	117.1(2)
C(13A)-P(1)-C(17A)	107.62(8)	C(7)-C(8)-C(12)	121.0(3)
C(21A)-P(1)-C(17A)	107.87(8)	C(9)-C(8)-C(12)	121.9(3)
C(17B)-P(1)-Cu(1)	109.73(7)	C(10)-C(9)-C(8)	119.6(2)
C(21B)-P(1)-Cu(1)	107.54(15)	C(10)-C(9)-H(9)	120.2
C(13A)-P(1)-Cu(1)	112.74(6)	C(8)-C(9)-H(9)	120.2
C(21A)-P(1)-Cu(1)	108.51(6)	N(2)-C(10)-C(9)	123.4(3)
C(13B)-P(1)-Cu(1)	110.74(6)	N(2)-C(10)-H(10)	118.3
C(17A)-P(1)-Cu(1)	109.98(6)	C(9)-C(10)-H(10)	118.3
C(25)-S(1)-Cu(1)	109.62(9)	C(3)-C(11)-H(11A)	109.5
C(1)-N(1)-C(5)	117.9(2)	C(3)-C(11)-H(11B)	109.5
C(1)-N(1)-Cu(1)	126.9(2)	H(11A)-C(11)-H(11B)	109.5
C(5)-N(1)-Cu(1)	114.77(17)	C(3)-C(11)-H(11C)	109.5
C(10)-N(2)-C(6)	117.5(2)	H(11A)-C(11)-H(11C)	109.5
C(10)-N(2)-Cu(1)	127.00(19)	H(11B)-C(11)-H(11C)	109.5
C(6)-N(2)-Cu(1)	111.97(16)	C(8)-C(12)-H(12A)	109.5
C(25)-N(3)-H(3A)	120.0	C(8)-C(12)-H(12B)	109.5
C(25)-N(3)-H(3B)	120.0	H(12A)-C(12)-H(12B)	109.5
H(3A)-N(3)-H(3B)	120.0	C(8)-C(12)-H(12C)	109.5
C(25)-N(4)-H(4A)	120.0	H(12A)-C(12)-H(12C)	109.5
C(25)-N(4)-H(4B)	120.0	H(12B)-C(12)-H(12C)	109.5
H(4A)-N(4)-H(4B)	120.0	C(15A)-C(13A)-C(14A)	111.578(18)
N(1)-C(1)-C(2)	123.4(3)	C(15A)-C(13A)-C(16A)	111.578(19)
N(1)-C(1)-H(1)	118.3	C(14A)-C(13A)-C(16A)	111.579(16)
C(2)-C(1)-H(1)	118.3	C(15A)-C(13A)-P(1)	104.48(15)
C(1)-C(2)-C(3)	119.3(3)	C(14A)-C(13A)-P(1)	104.10(15)
C(1)-C(2)-H(2)	120.4	C(16A)-C(13A)-P(1)	113.11(15)
C(3)-C(2)-H(2)	120.4	C(13A)-C(14A)-H(14A)	109.5
C(2)-C(3)-C(4)	117.6(3)	C(13A)-C(14A)-H(14B)	109.5
C(2)-C(3)-C(11)	122.2(3)	H(14A)-C(14A)-H(14B)	109.5
C(4)-C(3)-C(11)	120.2(3)	C(13A)-C(14A)-H(14C)	109.5
C(3)-C(4)-C(5)	119.8(3)	H(14A)-C(14A)-H(14C)	109.5
C(3)-C(4)-H(4)	120.1	H(14B)-C(14A)-H(14C)	109.5
C(5)-C(4)-H(4)	120.1	C(13A)-C(15A)-H(15A)	109.5

Table S3. Bond angles (deg.) for [(4,4′-Me_2-bipy)Cu(S=C(NH_2)$_2$)(P^tBu_3)][BF_4]. Symmetry transformations used to generate equivalent atoms:

C(13A)-C(15A)-H(15B)	109.5	H(18A)-C(18A)-H(18B)	109.5
H(15A)-C(15A)-H(15B)	109.5	C(17A)-C(18A)-H(18C)	109.5
C(13A)-C(15A)-H(15C)	109.5	H(18A)-C(18A)-H(18C)	109.5
H(15A)-C(15A)-H(15C)	109.5	H(18B)-C(18A)-H(18C)	109.5
H(15B)-C(15A)-H(15C)	109.5	C(17A)-C(19A)-H(19A)	109.5
C(13A)-C(16A)-H(16A)	109.5	C(17A)-C(19A)-H(19B)	109.5
C(13A)-C(16A)-H(16B)	109.5	H(19A)-C(19A)-H(19B)	109.5
H(16A)-C(16A)-H(16B)	109.5	C(17A)-C(19A)-H(19C)	109.5
C(13A)-C(16A)-H(16C)	109.5	H(19A)-C(19A)-H(19C)	109.5
H(16A)-C(16A)-H(16C)	109.5	H(19B)-C(19A)-H(19C)	109.5
H(16B)-C(16A)-H(16C)	109.5	C(17A)-C(20A)-H(20A)	109.5
C(15B)-C(13B)-C(14B)	111.583(14)	C(17A)-C(20A)-H(20B)	109.5
C(15B)-C(13B)-C(16B)	111.584(16)	H(20A)-C(20A)-H(20B)	109.5
C(14B)-C(13B)-C(16B)	111.58(2)	C(17A)-C(20A)-H(20C)	109.5
C(15B)-C(13B)-P(1)	105.7(2)	H(20A)-C(20A)-H(20C)	109.5
C(14B)-C(13B)-P(1)	106.1(2)	H(20B)-C(20A)-H(20C)	109.5
C(16B)-C(13B)-P(1)	110.0(2)	C(18B)-C(17B)-C(20B)	111.581(15)
C(13B)-C(14B)-H(14D)	109.5	C(18B)-C(17B)-C(19B)	111.582(13)
C(13B)-C(14B)-H(14E)	109.5	C(20B)-C(17B)-C(19B)	111.582(19)
H(14D)-C(14B)-H(14E)	109.5	C(18B)-C(17B)-P(1)	101.99(15)
C(13B)-C(14B)-H(14F)	109.5	C(20B)-C(17B)-P(1)	116.60(17)
H(14D)-C(14B)-H(14F)	109.5	C(19B)-C(17B)-P(1)	102.90(19)
H(14E)-C(14B)-H(14F)	109.5	C(17B)-C(18B)-H(18D)	109.5
C(13B)-C(15B)-H(15D)	109.5	C(17B)-C(18B)-H(18E)	109.5
C(13B)-C(15B)-H(15E)	109.5	H(18D)-C(18B)-H(18E)	109.5
H(15D)-C(15B)-H(15E)	109.5	C(17B)-C(18B)-H(18F)	109.5
C(13B)-C(15B)-H(15F)	109.5	H(18D)-C(18B)-H(18F)	109.5
H(15D)-C(15B)-H(15F)	109.5	H(18E)-C(18B)-H(18F)	109.5
H(15E)-C(15B)-H(15F)	109.5	C(17B)-C(19B)-H(19D)	109.5
C(13B)-C(16B)-H(16D)	109.5	C(17B)-C(19B)-H(19E)	109.5
C(13B)-C(16B)-H(16E)	109.5	H(19D)-C(19B)-H(19E)	109.5
H(16D)-C(16B)-H(16E)	109.5	C(17B)-C(19B)-H(19F)	109.5
C(13B)-C(16B)-H(16F)	109.5	H(19D)-C(19B)-H(19F)	109.5
H(16D)-C(16B)-H(16F)	109.5	H(19E)-C(19B)-H(19F)	109.5
H(16E)-C(16B)-H(16F)	109.5	C(17B)-C(20B)-H(20D)	109.5
C(20A)-C(17A)-C(18A)	111.582(14)	C(17B)-C(20B)-H(20E)	109.5
C(20A)-C(17A)-C(19A)	111.581(12)	H(20D)-C(20B)-H(20E)	109.5
C(18A)-C(17A)-C(19A)	111.581(19)	C(17B)-C(20B)-H(20F)	109.5
C(20A)-C(17A)-P(1)	109.67(13)	H(20D)-C(20B)-H(20F)	109.5
C(18A)-C(17A)-P(1)	106.70(14)	H(20E)-C(20B)-H(20F)	109.5
C(19A)-C(17A)-P(1)	105.41(13)	C(23A)-C(21A)-C(22A)	111.581(18)
C(17A)-C(18A)-H(18A)	109.5	C(23A)-C(21A)-C(24A)	111.582(19)
C(17A)-C(18A)-H(18B)	109.5	C(22A)-C(21A)-C(24A)	111.58(2)

Table S3. Bond angles (deg.) for [(4,4′-Me_2-bipy)Cu(S=C(NH_2)$_2$)(P^tBu_3)][BF_4]. Symmetry transformations used to generate equivalent atoms:

C(23A)-C(21A)-P(1)	106.59(13)	H(24D)-C(24B)-H(24F)	109.5
C(22A)-C(21A)-P(1)	102.94(14)	H(24E)-C(24B)-H(24F)	109.5
C(24A)-C(21A)-P(1)	112.16(13)	N(4)-C(25)-N(3)	118.8(2)
C(21A)-C(22A)-H(22A)	109.5	N(4)-C(25)-S(1)	120.3(2)
C(21A)-C(22A)-H(22B)	109.5	N(3)-C(25)-S(1)	120.9(2)
H(22A)-C(22A)-H(22B)	109.5	F(2)-B(1)-F(3)	111.1(3)
C(21A)-C(22A)-H(22C)	109.5	F(2)-B(1)-F(1)	110.5(3)
H(22A)-C(22A)-H(22C)	109.5	F(3)-B(1)-F(1)	109.4(3)
H(22B)-C(22A)-H(22C)	109.5	F(2)-B(1)-F(4)	109.3(3)
C(21A)-C(23A)-H(23A)	109.5	F(3)-B(1)-F(4)	109.3(3)
C(21A)-C(23A)-H(23B)	109.5	F(1)-B(1)-F(4)	107.1(2)
H(23A)-C(23A)-H(23B)	109.5		
C(21A)-C(23A)-H(23C)	109.5		
H(23A)-C(23A)-H(23C)	109.5		
H(23B)-C(23A)-H(23C)	109.5		
C(21A)-C(24A)-H(24A)	109.5		
C(21A)-C(24A)-H(24B)	109.5		
H(24A)-C(24A)-H(24B)	109.5		
C(21A)-C(24A)-H(24C)	109.5		
H(24A)-C(24A)-H(24C)	109.5		
H(24B)-C(24A)-H(24C)	109.5		
C(23B)-C(21B)-C(22B)	112.0(3)		
C(23B)-C(21B)-C(24B)	106.9(2)		
C(22B)-C(21B)-C(24B)	106.6(2)		
C(23B)-C(21B)-P(1)	109.9(2)		
C(22B)-C(21B)-P(1)	111.4(2)		
C(24B)-C(21B)-P(1)	109.9(3)		
C(21B)-C(22B)-H(22D)	109.5		
C(21B)-C(22B)-H(22E)	109.5		
H(22D)-C(22B)-H(22E)	109.5		
C(21B)-C(22B)-H(22F)	109.5		
H(22D)-C(22B)-H(22F)	109.5		
H(22E)-C(22B)-H(22F)	109.5		
C(21B)-C(23B)-H(23D)	109.5		
C(21B)-C(23B)-H(23E)	109.5		
H(23D)-C(23B)-H(23E)	109.5		
C(21B)-C(23B)-H(23F)	109.5		
H(23D)-C(23B)-H(23F)	109.5		
H(23E)-C(23B)-H(23F)	109.5		
C(21B)-C(24B)-H(24D)	109.5		
C(21B)-C(24B)-H(24E)	109.5		
H(24D)-C(24B)-H(24E)	109.5		
C(21B)-C(24B)-H(24F)	109.5		

Table S4. Anisotropic displacement parameters ($Å^2$ x 10^3) for [(4,4′-Me_2-bipy)Cu(S=C(NH_2)$_2$)(P^tBu_3)][BF_4]. The anisotropic displacement factor exponent takes the form: $-2\pi^2[h^2\, a^{*2}U^{11} + ... + 2hka^*b^*U^{12}]$.

Atom	U^{11}	U^{22}	U^{33}	U^{23}	U^{13}	U^{12}
Cu(1)	23(1)	17(1)	24(1)	-1(1)	10(1)	0(1)
P(1)	27(1)	19(1)	25(1)	-1(1)	14(1)	2(1)
S(1)	53(1)	18(1)	39(1)	1(1)	32(1)	3(1)
F(1)	42(1)	39(1)	33(1)	-4(1)	13(1)	9(1)
F(2)	62(1)	32(1)	37(1)	-10(1)	15(1)	-11(1)
F(3)	36(1)	88(2)	63(1)	-20(1)	8(1)	14(1)
F(4)	100(2)	25(1)	49(1)	-2(1)	34(1)	1(1)
N(1)	21(1)	23(1)	31(1)	-1(1)	4(1)	0(1)
N(2)	24(1)	24(1)	24(1)	4(1)	3(1)	-5(1)
N(3)	44(1)	19(1)	40(1)	-6(1)	25(1)	-3(1)
N(4)	55(2)	23(1)	36(1)	1(1)	29(1)	6(1)
C(1)	22(1)	29(1)	51(2)	-3(1)	4(1)	-2(1)
C(2)	23(1)	37(2)	45(2)	-9(1)	-4(1)	4(1)
C(3)	33(1)	31(1)	27(1)	-5(1)	-2(1)	8(1)
C(4)	30(1)	25(1)	26(1)	0(1)	4(1)	2(1)
C(5)	21(1)	21(1)	24(1)	-2(1)	4(1)	1(1)
C(6)	21(1)	20(1)	21(1)	-1(1)	5(1)	0(1)
C(7)	27(1)	20(1)	21(1)	1(1)	6(1)	-4(1)
C(8)	24(1)	23(1)	29(1)	-4(1)	9(1)	-6(1)
C(9)	25(1)	31(1)	32(1)	0(1)	-1(1)	-7(1)
C(10)	31(1)	31(1)	26(1)	7(1)	-2(1)	-5(1)
C(11)	47(2)	47(2)	37(2)	1(1)	-11(1)	14(2)
C(12)	30(1)	36(2)	39(2)	-1(1)	12(1)	-12(1)
C(25)	29(1)	22(1)	25(1)	-1(1)	11(1)	2(1)
B(1)	35(2)	26(2)	31(2)	-5(1)	9(1)	0(1)

Table S5. Hydrogen coordinates (x 10^4) and isotropic displacement parameters (Å^2 x 10^3) for [(4,4′-Me_2-bipy)Cu(S=C(NH_2)$_2$)(P^tBu_3)][BF_4].

H atom	x	y	z	U(eq)
H(3A)	4202	3156	5731	38
H(3B)	3413	3521	6314	38
H(4A)	5393	3636	4820	42
H(4B)	5421	4329	4778	42
H(1)	6327	4310	8147	41
H(2)	7564	3631	9158	44
H(4)	3327	2720	8823	33
H(7)	810	2747	8245	27
H(9)	-2448	3343	6237	37
H(10)	-526	4012	5979	37
H(11A)	6587	2270	9498	70
H(11B)	5537	2542	10100	70
H(11C)	7290	2813	10119	70
H(12A)	-2443	2207	7085	52
H(12B)	-3284	2756	7462	52
H(12C)	-1864	2377	8045	52
H(14A)	-1421	5302	7734	71
H(14B)	-590	4650	7713	71
H(14C)	-1328	4835	8484	71
H(15A)	2963	4970	9311	64
H(15B)	1393	4629	9463	64
H(15C)	2131	4444	8692	64
H(16A)	-41	6118	8647	54
H(16B)	150	5709	9461	54
H(16C)	1707	6008	9233	54
H(14D)	-639	4705	8106	71
H(14E)	1022	4335	8341	71
H(14F)	105	4517	9047	71
H(15D)	3441	5574	9389	64
H(15E)	2637	5057	9843	64
H(15F)	3555	4874	9137	64
H(16D)	-738	5795	8444	54
H(16E)	-2	5685	9409	54
H(16F)	856	6150	8902	54
H(18A)	5040	5306	8825	79
H(18B)	5591	5978	9140	79
H(18C)	3911	5711	9263	79
H(19A)	5256	5524	7397	77
H(19B)	4271	6074	6886	77
H(19C)	5822	6212	7611	77

Table S5. Hydrogen coordinates (x 10^4) and isotropic displacement parameters (Å^2 x 10^3) for [(4,4′-Me_2-bipy)Cu(S=C(NH_2)$_2$)(P^tBu_3)][BF_4].

H atom	x	y	z	U(eq)
H(20A)	2667	6777	7582	66
H(20B)	2438	6624	8491	66
H(20C)	4118	6891	8368	66
H(18D)	5194	5316	7755	79
H(18E)	6084	5904	8213	79
H(18F)	5046	5476	8675	79
H(19D)	2623	6500	6713	77
H(19E)	4553	6508	6928	77
H(19F)	3601	5907	6550	77
H(20D)	2479	6791	8129	66
H(20E)	3360	6392	8907	66
H(20F)	4398	6820	8445	66
H(22A)	-1227	5166	6575	81
H(22B)	-1278	5513	5721	81
H(22C)	137	5038	6073	81
H(23A)	2141	6491	6494	79
H(23B)	2228	5860	6022	79
H(23C)	812	6335	5671	79
H(24A)	-1241	6123	7351	76
H(24B)	113	6630	7364	76
H(24C)	-1294	6537	6552	76
H(22D)	-1584	5373	7473	81
H(22E)	-2397	5512	6524	81
H(22F)	-1312	4916	6766	81
H(23D)	1298	5911	5928	79
H(23E)	482	5251	5805	79
H(23F)	-603	5847	5563	79
H(24D)	-492	6449	7567	76
H(24E)	628	6661	6963	76
H(24F)	-1260	6552	6603	76

Structure Determination Summary

Crystal Data and Structure Refinement for [(Me_4phen)CuCl(P^tBu_3)]·CH_2Cl_2

Identification code	JPD1153_0m_b
Empirical formula	$C_{29}H_{45}Cl_3CuN_2P$
Formula weight	622.53
Temperature	150(2) K
Wavelength	0.71073 Å

Crystal system	orthorhombic	
Space group	*Pbca*	
Unit cell dimensions	a = 17.5756(9) Å	α = 90°
	b = 14.4820(8) Å	β = 90°
	c = 24.3504(13) Å	γ = 90°
Volume	6197.9(6) Å^3	
Z	8	
Density (calculated)	1.334 g/cm^3	
Absorption coefficient	1.036 mm^{-1}	
F(000)	2624	
Crystal size	0.274 x 0.250 x 0.160 mm^3	
θ range for data collection	1.673 to 30.540°	
Index ranges	$-25 \leq h \leq 25$, $-20 \leq k \leq 20$, $-34 \leq l \leq 34$	
Reflections collected	211726	
Independent reflections	9479 [R(int) = 0.0436]	
Completeness to θ = 25.242°	99.8%	
Absorption correction	Semi-empirical from equivalents	
Max. and min. transmission	0.85 and 0.76	
Refinement method	Full-matrix least-squares on F^2	
Data / restraints / parameters	9479 / 18 / 446	
Goodness-of-fit on F^2	1.127	
Final R indices [I>2σ(I)]	R1 = 0.0822, wR2 = 0.2220	
R indices (all data)	R1 = 0.0991, wR2 = 0.2334	
Extinction coefficient	n/a	
Largest diff. peak and hole	0.889 and -1.747 e·Å^{-3}	

Table S1. Atomic coordinates (x 10^4) and equivalent isotropic displacement parameters ($Å^2$ x 10^3) for [(Me_4phen)CuCl(P^tBu_3)]·CH_2Cl_2. U(eq) is defined as one third of the trace of the orthogonalized U^{ij} tensor.

Atom	x	y	z	U(eq)
Cu(1)	4136(1)	6518(1)	3541(1)	36(1)
Cl(1)	3313(1)	7111(1)	4210(1)	49(1)
P(1)	3792(1)	6797(1)	2685(1)	32(1)
N(1)	4420(2)	5223(3)	3879(1)	36(1)
N(2)	5235(2)	6788(3)	3852(1)	36(1)
C(1)	3999(2)	4458(4)	3914(2)	42(1)
C(2)	4238(2)	3640(3)	4179(2)	39(1)
C(3)	4949(2)	3609(3)	4420(2)	39(1)
C(4)	5402(2)	4418(3)	4394(2)	37(1)
C(5)	6146(2)	4482(4)	4642(2)	43(1)
C(6)	6562(2)	5262(4)	4608(2)	45(1)
C(7)	6291(2)	6074(3)	4337(2)	37(1)
C(8)	6704(2)	6912(4)	4314(2)	42(1)
C(9)	6354(2)	7685(3)	4084(2)	41(1)
C(10)	5622(3)	7572(3)	3857(2)	41(1)
C(11)	5555(2)	6045(3)	4098(1)	34(1)
C(12)	5120(2)	5204(3)	4119(2)	34(1)
C(13)	3693(3)	2826(4)	4188(2)	52(1)
C(14)	5233(3)	2758(4)	4708(2)	49(1)
C(15)	7506(3)	6982(4)	4530(2)	55(1)
C(16)	6723(3)	8622(4)	4074(2)	56(1)
C(17A)	2720(4)	6657(5)	2603(3)	42(2)
C(18A)	2515(11)	5850(11)	2987(7)	40(3)
C(19A)	2406(11)	6496(12)	2020(4)	57(4)
C(20A)	2311(6)	7512(6)	2837(4)	50(2)
C(21A)	4068(4)	7998(6)	2425(3)	48(2)
C(22A)	3664(7)	8374(8)	1910(4)	61(3)
C(23A)	4934(5)	8056(9)	2335(6)	58(3)
C(24A)	3909(15)	8607(17)	2930(9)	62(6)
C(25A)	4280(5)	5928(6)	2199(3)	54(2)
C(26A)	3935(8)	4961(6)	2283(6)	67(3)
C(27A)	4263(9)	6140(10)	1581(3)	67(3)
C(28A)	5110(9)	5848(16)	2395(14)	80(9)
C(17B)	3059(6)	5934(7)	2453(4)	47(3)
C(18B)	2452(15)	5734(19)	2892(10)	56(8)
C(19B)	2596(14)	6163(15)	1935(7)	63(5)
C(20B)	3464(9)	5009(7)	2341(5)	58(4)
C(21B)	3341(5)	8003(7)	2667(4)	44(2)
C(22B)	2529(6)	7986(11)	2904(6)	55(3)

Table S1. Atomic coordinates (x 10^4) and equivalent isotropic displacement parameters (Å^2 x 10^3) for [(Me$_4$phen)CuCl(P^{t}Bu$_3$)]·CH$_2$Cl$_2$. U(eq) is defined as one third of the trace of the orthogonalized U^{ij} tensor.

Atom	x	y	z	U(eq)
C(23B)	3285(9)	8464(9)	2098(4)	55(3)
C(24B)	3796(17)	8690(20)	3019(14)	58(6)
C(25B)	4637(6)	6795(6)	2212(3)	41(2)
C(26B)	5140(12)	5955(13)	2347(13)	45(5)
C(27B)	4448(8)	6743(11)	1595(3)	57(3)
C(28B)	5127(8)	7659(7)	2317(7)	48(3)
Cl(2)	6833(1)	5193(2)	608(1)	87(1)
Cl(3A)	5273(3)	4925(5)	807(3)	85(2)
Cl(3B)	5187(3)	4581(6)	627(3)	102(2)
C(29)	6102(5)	4418(6)	437(4)	84(2)

Table S2. Bond lengths (Å) for [(Me$_4$phen)CuCl(P^{t}Bu$_3$)]·CH$_2$Cl$_2$. Symmetry transformations used to generate equivalent atoms:

Cu(1)-N(1)	2.108(4)	C(16)-H(16A)	0.9800
Cu(1)-N(2)	2.111(3)	C(16)-H(16B)	0.9800
Cu(1)-P(1)	2.2071(11)	C(16)-H(16C)	0.9800
Cu(1)-Cl(1)	2.3405(12)	C(17A)-C(18A)	1.540(5)
P(1)-C(25B)	1.881(10)	C(17A)-C(19A)	1.540(5)
P(1)-C(17B)	1.881(10)	C(17A)-C(20A)	1.541(5)
P(1)-C(17A)	1.906(7)	C(18A)-H(18A)	0.9800
P(1)-C(21A)	1.915(8)	C(18A)-H(18B)	0.9800
P(1)-C(21B)	1.918(10)	C(18A)-H(18C)	0.9800
P(1)-C(25A)	1.930(9)	C(19A)-H(19A)	0.9800
N(1)-C(1)	1.336(6)	C(19A)-H(19B)	0.9800
N(1)-C(12)	1.364(5)	C(19A)-H(19C)	0.9800
N(2)-C(10)	1.324(6)	C(20A)-H(20A)	0.9800
N(2)-C(11)	1.355(5)	C(20A)-H(20B)	0.9800
C(1)-C(2)	1.413(6)	C(20A)-H(20C)	0.9800
C(1)-H(1)	0.9500	C(21A)-C(23A)	1.540(5)
C(2)-C(3)	1.381(6)	C(21A)-C(24A)	1.539(5)
C(2)-C(13)	1.519(7)	C(21A)-C(22A)	1.541(5)
C(3)-C(4)	1.419(7)	C(22A)-H(22A)	0.9800
C(3)-C(14)	1.503(6)	C(22A)-H(22B)	0.9800
C(4)-C(12)	1.410(6)	C(22A)-H(22C)	0.9800
C(4)-C(5)	1.444(6)	C(23A)-H(23A)	0.9800
C(5)-C(6)	1.349(7)	C(23A)-H(23B)	0.9800
C(5)-H(5)	0.9500	C(23A)-H(23C)	0.9800
C(6)-C(7)	1.430(7)	C(24A)-H(24A)	0.9800
C(6)-H(6)	0.9500	C(24A)-H(24B)	0.9800
C(7)-C(8)	1.415(7)	C(24A)-H(24C)	0.9800
C(7)-C(11)	1.418(5)	C(25A)-C(27A)	1.537(5)
C(8)-C(9)	1.394(7)	C(25A)-C(26A)	1.539(5)
C(8)-C(15)	1.509(6)	C(25A)-C(28A)	1.539(5)
C(9)-C(10)	1.410(6)	C(26A)-H(26A)	0.9800
C(9)-C(16)	1.505(7)	C(26A)-H(26B)	0.9800
C(10)-H(10)	0.9500	C(26A)-H(26C)	0.9800
C(11)-C(12)	1.438(6)	C(27A)-H(27A)	0.9800
C(13)-H(13A)	0.9800	C(27A)-H(27B)	0.9800
C(13)-H(13B)	0.9800	C(27A)-H(27C)	0.9800
C(13)-H(13C)	0.9800	C(28A)-H(28A)	0.9800
C(14)-H(14A)	0.9800	C(28A)-H(28B)	0.9800
C(14)-H(14B)	0.9800	C(28A)-H(28C)	0.9800
C(14)-H(14C)	0.9800	C(17B)-C(18B)	1.539(5)
C(15)-H(15A)	0.9800	C(17B)-C(19B)	1.539(5)
C(15)-H(15B)	0.9800	C(17B)-C(20B)	1.541(5)
C(15)-H(15C)	0.9800	C(18B)-H(18D)	0.9800

Table S2. Bond lengths (Å) for [(Me$_4$phen)CuCl(P^{t}Bu$_3$)]·CH$_2$Cl$_2$. Symmetry transformations used to generate equivalent atoms:

C(18B)-H(18E)	0.9800
C(18B)-H(18F)	0.9800
C(19B)-H(19D)	0.9800
C(19B)-H(19E)	0.9800
C(19B)-H(19F)	0.9800
C(20B)-H(20D)	0.9800
C(20B)-H(20E)	0.9800
C(20B)-H(20F)	0.9800
C(21B)-C(22B)	1.538(5)
C(21B)-C(24B)	1.539(5)
C(21B)-C(23B)	1.541(5)
C(22B)-H(22D)	0.9800
C(22B)-H(22E)	0.9800
C(22B)-H(22F)	0.9800
C(23B)-H(23D)	0.9800
C(23B)-H(23E)	0.9800
C(23B)-H(23F)	0.9800
C(24B)-H(24D)	0.9800
C(24B)-H(24E)	0.9800
C(24B)-H(24F)	0.9800
C(25B)-C(27B)	1.539(5)
C(25B)-C(26B)	1.540(5)
C(25B)-C(28B)	1.540(5)
C(26B)-H(26D)	0.9800
C(26B)-H(26E)	0.9800
C(26B)-H(26F)	0.9800
C(27B)-H(27D)	0.9800
C(27B)-H(27E)	0.9800
C(27B)-H(27F)	0.9800
C(28B)-H(28D)	0.9800
C(28B)-H(28E)	0.9800
C(28B)-H(28F)	0.9800
Cl(2)-C(29)	1.756(8)
Cl(3A)-C(29)	1.864(10)
Cl(3B)-C(29)	1.690(10)
C(29)-H(29A)	0.9900
C(29)-H(29B)	0.9900

Table S3. Bond angles (deg.) for [(Me$_4$phen)CuCl(P^{t}Bu$_3$)]·CH$_2$Cl$_2$. Symmetry transformations used to generate equivalent atoms:

N(1)-Cu(1)-N(2)	78.93(14)	C(8)-C(7)-C(6)	123.5(4)
N(1)-Cu(1)-P(1)	126.56(10)	C(11)-C(7)-C(6)	118.0(4)
N(2)-Cu(1)-P(1)	123.74(10)	C(9)-C(8)-C(7)	118.6(4)
N(1)-Cu(1)-Cl(1)	101.64(10)	C(9)-C(8)-C(15)	119.8(5)
N(2)-Cu(1)-Cl(1)	104.39(10)	C(7)-C(8)-C(15)	121.6(5)
P(1)-Cu(1)-Cl(1)	114.85(4)	C(8)-C(9)-C(10)	117.8(4)
C(25B)-P(1)-C(17B)	110.8(4)	C(8)-C(9)-C(16)	122.8(4)
C(17A)-P(1)-C(21A)	108.2(3)	C(10)-C(9)-C(16)	119.3(5)
C(25B)-P(1)-C(21B)	108.3(4)	N(2)-C(10)-C(9)	124.8(4)
C(17B)-P(1)-C(21B)	108.4(4)	N(2)-C(10)-H(10)	117.6
C(17A)-P(1)-C(25A)	107.8(3)	C(9)-C(10)-H(10)	117.6
C(21A)-P(1)-C(25A)	106.1(3)	N(2)-C(11)-C(7)	122.4(4)
C(25B)-P(1)-Cu(1)	111.2(3)	N(2)-C(11)-C(12)	117.9(3)
C(17B)-P(1)-Cu(1)	110.5(3)	C(7)-C(11)-C(12)	119.7(4)
C(17A)-P(1)-Cu(1)	110.6(2)	N(1)-C(12)-C(4)	122.5(4)
C(21A)-P(1)-Cu(1)	114.2(2)	N(1)-C(12)-C(11)	116.6(4)
C(21B)-P(1)-Cu(1)	107.5(3)	C(4)-C(12)-C(11)	120.9(4)
C(25A)-P(1)-Cu(1)	109.8(3)	C(2)-C(13)-H(13A)	109.5
C(1)-N(1)-C(12)	117.1(4)	C(2)-C(13)-H(13B)	109.5
C(1)-N(1)-Cu(1)	129.2(3)	H(13A)-C(13)-H(13B)	109.5
C(12)-N(1)-Cu(1)	113.6(3)	C(2)-C(13)-H(13C)	109.5
C(10)-N(2)-C(11)	117.6(4)	H(13A)-C(13)-H(13C)	109.5
C(10)-N(2)-Cu(1)	129.2(3)	H(13B)-C(13)-H(13C)	109.5
C(11)-N(2)-Cu(1)	113.1(3)	C(3)-C(14)-H(14A)	109.5
N(1)-C(1)-C(2)	124.1(4)	C(3)-C(14)-H(14B)	109.5
N(1)-C(1)-H(1)	117.9	H(14A)-C(14)-H(14B)	109.5
C(2)-C(1)-H(1)	117.9	C(3)-C(14)-H(14C)	109.5
C(3)-C(2)-C(1)	119.4(4)	H(14A)-C(14)-H(14C)	109.5
C(3)-C(2)-C(13)	122.6(4)	H(14B)-C(14)-H(14C)	109.5
C(1)-C(2)-C(13)	118.0(4)	C(8)-C(15)-H(15A)	109.5
C(2)-C(3)-C(4)	117.5(4)	C(8)-C(15)-H(15B)	109.5
C(2)-C(3)-C(14)	121.7(4)	H(15A)-C(15)-H(15B)	109.5
C(4)-C(3)-C(14)	120.7(4)	C(8)-C(15)-H(15C)	109.5
C(12)-C(4)-C(3)	119.4(4)	H(15A)-C(15)-H(15C)	109.5
C(12)-C(4)-C(5)	117.7(4)	H(15B)-C(15)-H(15C)	109.5
C(3)-C(4)-C(5)	122.9(4)	C(9)-C(16)-H(16A)	109.5
C(6)-C(5)-C(4)	121.3(4)	C(9)-C(16)-H(16B)	109.5
C(6)-C(5)-H(5)	119.4	H(16A)-C(16)-H(16B)	109.5
C(4)-C(5)-H(5)	119.4	C(9)-C(16)-H(16C)	109.5
C(5)-C(6)-C(7)	122.4(4)	H(16A)-C(16)-H(16C)	109.5
C(5)-C(6)-H(6)	118.8	H(16B)-C(16)-H(16C)	109.5
C(7)-C(6)-H(6)	118.8	C(18A)-C(17A)-C(19A)	111.2(12)
C(8)-C(7)-C(11)	118.5(4)	C(18A)-C(17A)-C(20A)	106.0(10)

Table S3. Bond angles (deg.) for [(Me$_4$phen)CuCl(P^{t}Bu$_3$)]·CH$_2$Cl$_2$. Symmetry transformations used to generate equivalent atoms:

C(19A)-C(17A)-C(20A)	107.3(8)	C(21A)-C(24A)-H(24C)	109.5
C(18A)-C(17A)-P(1)	104.3(8)	H(24A)-C(24A)-H(24C)	109.5
C(19A)-C(17A)-P(1)	117.8(9)	H(24B)-C(24A)-H(24C)	109.5
C(20A)-C(17A)-P(1)	109.6(6)	C(27A)-C(25A)-C(26A)	107.7(9)
C(17A)-C(18A)-H(18A)	109.5	C(27A)-C(25A)-C(28A)	109.7(15)
C(17A)-C(18A)-H(18B)	109.5	C(26A)-C(25A)-C(28A)	105.3(13)
H(18A)-C(18A)-H(18B)	109.5	C(27A)-C(25A)-P(1)	117.5(7)
C(17A)-C(18A)-H(18C)	109.5	C(26A)-C(25A)-P(1)	109.6(7)
H(18A)-C(18A)-H(18C)	109.5	C(28A)-C(25A)-P(1)	106.3(12)
H(18B)-C(18A)-H(18C)	109.5	C(25A)-C(26A)-H(26A)	109.5
C(17A)-C(19A)-H(19A)	109.5	C(25A)-C(26A)-H(26B)	109.5
C(17A)-C(19A)-H(19B)	109.5	H(26A)-C(26A)-H(26B)	109.5
H(19A)-C(19A)-H(19B)	109.5	C(25A)-C(26A)-H(26C)	109.5
C(17A)-C(19A)-H(19C)	109.5	H(26A)-C(26A)-H(26C)	109.5
H(19A)-C(19A)-H(19C)	109.5	H(26B)-C(26A)-H(26C)	109.5
H(19B)-C(19A)-H(19C)	109.5	C(25A)-C(27A)-H(27A)	109.5
C(17A)-C(20A)-H(20A)	109.5	C(25A)-C(27A)-H(27B)	109.5
C(17A)-C(20A)-H(20B)	109.5	H(27A)-C(27A)-H(27B)	109.5
H(20A)-C(20A)-H(20B)	109.5	C(25A)-C(27A)-H(27C)	109.5
C(17A)-C(20A)-H(20C)	109.5	H(27A)-C(27A)-H(27C)	109.5
H(20A)-C(20A)-H(20C)	109.5	H(27B)-C(27A)-H(27C)	109.5
H(20B)-C(20A)-H(20C)	109.5	C(25A)-C(28A)-H(28A)	109.5
C(23A)-C(21A)-C(24A)	105.2(12)	C(25A)-C(28A)-H(28B)	109.5
C(23A)-C(21A)-C(22A)	108.7(9)	H(28A)-C(28A)-H(28B)	109.5
C(24A)-C(21A)-C(22A)	111.4(15)	C(25A)-C(28A)-H(28C)	109.5
C(23A)-C(21A)-P(1)	110.3(7)	H(28A)-C(28A)-H(28C)	109.5
C(24A)-C(21A)-P(1)	102.1(11)	H(28B)-C(28A)-H(28C)	109.5
C(22A)-C(21A)-P(1)	118.3(7)	C(18B)-C(17B)-C(19B)	104.1(17)
C(21A)-C(22A)-H(22A)	109.5	C(18B)-C(17B)-C(20B)	106.2(14)
C(21A)-C(22A)-H(22B)	109.5	C(19B)-C(17B)-C(20B)	106.6(11)
H(22A)-C(22A)-H(22B)	109.5	C(18B)-C(17B)-P(1)	113.0(12)
C(21A)-C(22A)-H(22C)	109.5	C(19B)-C(17B)-P(1)	117.7(11)
H(22A)-C(22A)-H(22C)	109.5	C(20B)-C(17B)-P(1)	108.4(8)
H(22B)-C(22A)-H(22C)	109.5	C(17B)-C(18B)-H(18D)	109.5
C(21A)-C(23A)-H(23A)	109.5	C(17B)-C(18B)-H(18E)	109.5
C(21A)-C(23A)-H(23B)	109.5	H(18D)-C(18B)-H(18E)	109.5
H(23A)-C(23A)-H(23B)	109.5	C(17B)-C(18B)-H(18F)	109.5
C(21A)-C(23A)-H(23C)	109.5	H(18D)-C(18B)-H(18F)	109.5
H(23A)-C(23A)-H(23C)	109.5	H(18E)-C(18B)-H(18F)	109.5
H(23B)-C(23A)-H(23C)	109.5	C(17B)-C(19B)-H(19D)	109.5
C(21A)-C(24A)-H(24A)	109.5	C(17B)-C(19B)-H(19E)	109.5
C(21A)-C(24A)-H(24B)	109.5	H(19D)-C(19B)-H(19E)	109.5
H(24A)-C(24A)-H(24B)	109.5	C(17B)-C(19B)-H(19F)	109.5

Table S3. Bond angles (deg.) for [(Me$_4$phen)CuCl(P^{t}Bu$_3$)]·CH$_2$Cl$_2$. Symmetry transformations used to generate equivalent atoms:

H(19D)-C(19B)-H(19F)	109.5	H(26E)-C(26B)-H(26F)	109.5
H(19E)-C(19B)-H(19F)	109.5	C(25B)-C(27B)-H(27D)	109.5
C(17B)-C(20B)-H(20D)	109.5	C(25B)-C(27B)-H(27E)	109.5
C(17B)-C(20B)-H(20E)	109.5	H(27D)-C(27B)-H(27E)	109.5
H(20D)-C(20B)-H(20E)	109.5	C(25B)-C(27B)-H(27F)	109.5
C(17B)-C(20B)-H(20F)	109.5	H(27D)-C(27B)-H(27F)	109.5
H(20D)-C(20B)-H(20F)	109.5	H(27E)-C(27B)-H(27F)	109.5
H(20E)-C(20B)-H(20F)	109.5	C(25B)-C(28B)-H(28D)	109.5
C(22B)-C(21B)-C(24B)	106.4(16)	C(25B)-C(28B)-H(28E)	109.5
C(22B)-C(21B)-C(23B)	106.5(10)	H(28D)-C(28B)-H(28E)	109.5
C(24B)-C(21B)-C(23B)	104.6(18)	C(25B)-C(28B)-H(28F)	109.5
C(22B)-C(21B)-P(1)	111.1(7)	H(28D)-C(28B)-H(28F)	109.5
C(24B)-C(21B)-P(1)	111.2(16)	H(28E)-C(28B)-H(28F)	109.5
C(23B)-C(21B)-P(1)	116.3(7)	Cl(3B)-C(29)-Cl(2)	122.9(6)
C(21B)-C(22B)-H(22D)	109.5	Cl(2)-C(29)-Cl(3A)	101.9(5)
C(21B)-C(22B)-H(22E)	109.5	Cl(2)-C(29)-H(29A)	111.4
H(22D)-C(22B)-H(22E)	109.5	Cl(3A)-C(29)-H(29A)	111.4
C(21B)-C(22B)-H(22F)	109.5	Cl(2)-C(29)-H(29B)	111.4
H(22D)-C(22B)-H(22F)	109.5	Cl(3A)-C(29)-H(29B)	111.4
H(22E)-C(22B)-H(22F)	109.5	H(29A)-C(29)-H(29B)	109.3
C(21B)-C(23B)-H(23D)	109.5		
C(21B)-C(23B)-H(23E)	109.5		
H(23D)-C(23B)-H(23E)	109.5		
C(21B)-C(23B)-H(23F)	109.5		
H(23D)-C(23B)-H(23F)	109.5		
H(23E)-C(23B)-H(23F)	109.5		
C(21B)-C(24B)-H(24D)	109.5		
C(21B)-C(24B)-H(24E)	109.5		
H(24D)-C(24B)-H(24E)	109.5		
C(21B)-C(24B)-H(24F)	109.5		
H(24D)-C(24B)-H(24F)	109.5		
H(24E)-C(24B)-H(24F)	109.5		
C(27B)-C(25B)-C(26B)	107.1(13)		
C(27B)-C(25B)-C(28B)	108.8(11)		
C(26B)-C(25B)-C(28B)	106.5(13)		
C(27B)-C(25B)-P(1)	115.3(7)		
C(26B)-C(25B)-P(1)	108.9(13)		
C(28B)-C(25B)-P(1)	109.8(8)		
C(25B)-C(26B)-H(26D)	109.5		
C(25B)-C(26B)-H(26E)	109.5		
H(26D)-C(26B)-H(26E)	109.5		
C(25B)-C(26B)-H(26F)	109.5		
H(26D)-C(26B)-H(26F)	109.5		

Table S4. Anisotropic displacement parameters (Å^2 x 10^3) for [(Me$_4$phen)CuCl(P^{t}Bu$_3$)]·CH$_2$Cl$_2$. The anisotropic displacement factor exponent takes the form: $-2\pi^2[h^2 a^{*2}U^{11} + ... + 2hka^*b^*U^{12}]$.

Atom	U^{11}	U^{22}	U^{33}	U^{23}	U^{13}	U^{12}
Cu(1)	29(1)	49(1)	30(1)	0(1)	-4(1)	4(1)
Cl(1)	38(1)	75(1)	34(1)	-8(1)	0(1)	12(1)
P(1)	31(1)	36(1)	29(1)	3(1)	-2(1)	1(1)
N(1)	27(1)	51(2)	28(1)	3(1)	-1(1)	2(1)
N(2)	28(2)	50(2)	30(2)	-3(1)	-4(1)	2(1)
C(1)	31(2)	64(3)	30(2)	4(2)	-2(2)	-1(2)
C(2)	37(2)	53(2)	27(2)	2(2)	3(2)	0(2)
C(3)	40(2)	54(2)	22(2)	2(2)	3(1)	6(2)
C(4)	32(2)	56(2)	22(2)	-3(2)	1(1)	8(2)
C(5)	36(2)	59(3)	33(2)	-1(2)	-7(2)	12(2)
C(6)	31(2)	69(3)	36(2)	-5(2)	-8(2)	6(2)
C(7)	29(2)	59(3)	25(2)	-6(2)	-1(1)	4(2)
C(8)	30(2)	68(3)	26(2)	-9(2)	0(1)	-2(2)
C(9)	36(2)	58(3)	28(2)	-6(2)	2(2)	-5(2)
C(10)	39(2)	53(3)	30(2)	0(2)	-1(2)	0(2)
C(11)	28(2)	53(2)	22(2)	-3(2)	-1(1)	4(2)
C(12)	28(2)	53(2)	23(2)	-2(2)	0(1)	8(2)
C(13)	47(2)	67(3)	41(2)	9(2)	-2(2)	-13(2)
C(14)	50(3)	58(3)	39(2)	3(2)	-4(2)	9(2)
C(15)	34(2)	85(4)	45(2)	-9(3)	-8(2)	-8(2)
C(16)	50(3)	68(3)	50(3)	-4(2)	0(2)	-18(2)
C(17A)	36(4)	56(5)	35(4)	12(3)	-13(3)	-8(3)
C(18A)	34(5)	48(6)	39(6)	11(5)	-17(5)	-21(5)
C(19A)	56(7)	72(10)	44(6)	8(5)	-21(5)	-10(6)
C(20A)	37(4)	59(6)	56(5)	18(5)	3(4)	11(4)
C(21A)	49(5)	52(5)	43(4)	14(4)	8(4)	-3(4)
C(22A)	60(6)	72(8)	50(6)	24(5)	4(5)	1(5)
C(23A)	53(6)	60(7)	61(6)	0(6)	9(5)	-14(5)
C(24A)	52(7)	25(6)	110(16)	-4(7)	5(8)	5(6)
C(25A)	56(5)	64(6)	41(4)	-11(4)	10(4)	3(4)
C(26A)	74(7)	50(6)	76(8)	-23(5)	-12(7)	6(6)
C(27A)	92(9)	73(8)	35(4)	-7(5)	8(5)	-4(7)
C(28A)	65(13)	81(14)	93(19)	-11(11)	37(11)	17(11)
C(17B)	50(6)	58(6)	32(4)	9(4)	-11(4)	-15(5)
C(18B)	42(9)	78(14)	47(10)	8(8)	-24(7)	-26(8)
C(19B)	66(13)	69(13)	53(8)	11(7)	-31(8)	-20(9)
C(20B)	91(11)	44(7)	40(6)	-2(5)	-8(7)	-17(7)
C(21B)	42(5)	46(6)	44(5)	12(4)	4(4)	16(4)
C(22B)	40(6)	62(8)	63(7)	19(7)	15(6)	21(6)

Table S4. Anisotropic displacement parameters (Å^2 x 10^3) for [(Me$_4$phen)CuCl(P^{t}Bu$_3$)]·CH$_2$Cl$_2$.

The anisotropic displacement factor exponent takes the form: $-2\pi^2[h^2 a^{*2}U^{11} + ... + 2hka^*b^*U^{12}]$.

Atom	U^{11}	U^{22}	U^{33}	U^{23}	U^{13}	U^{12}
C(23B)	60(8)	48(7)	56(7)	18(6)	-3(6)	14(6)
C(24B)	65(14)	36(10)	72(10)	-21(7)	-7(10)	16(8)
C(25B)	47(5)	42(5)	34(4)	1(4)	5(4)	-4(4)
C(26B)	44(10)	52(10)	38(7)	-1(7)	7(7)	14(8)
C(27B)	69(8)	72(9)	30(5)	3(5)	17(5)	13(7)
C(28B)	45(6)	43(7)	56(7)	8(6)	8(6)	-9(5)

Table S5. Hydrogen coordinates (x 10^4) and isotropic displacement parameters (Å^2 x 10^3) for [(Me$_4$phen)CuCl(P^{t}Bu$_3$)]·CH$_2$Cl$_2$.

H atom	x	y	z	U(eq)
H(1)	3507	4464	3752	50
H(5)	6347	3964	4833	51
H(6)	7054	5273	4770	54
H(10)	5390	8098	3694	49
H(13A)	3871	2352	3931	77
H(13B)	3184	3034	4080	77
H(13C)	3673	2567	4560	77
H(14A)	4827	2294	4720	74
H(14B)	5387	2917	5083	74
H(14C)	5671	2507	4508	74
H(15A)	7744	7546	4388	82
H(15B)	7799	6444	4409	82
H(15C)	7496	7002	4932	82
H(16A)	6864	8803	4448	84
H(16B)	6364	9075	3923	84
H(16C)	7179	8601	3843	84
H(18A)	2720	5969	3354	61
H(18B)	2733	5276	2842	61
H(18C)	1960	5789	3009	61
H(19A)	2562	5883	1891	86
H(19B)	2608	6968	1771	86
H(19C)	1850	6533	2026	86
H(20A)	1772	7369	2894	76
H(20B)	2358	8027	2578	76
H(20C)	2543	7684	3188	76
H(22A)	3813	9019	1850	91
H(22B)	3112	8339	1961	91
H(22C)	3810	8005	1589	91
H(23A)	5071	8684	2222	87
H(23B)	5085	7618	2048	87
H(23C)	5198	7903	2678	87
H(24A)	4296	8491	3211	93
H(24B)	3405	8458	3079	93
H(24C)	3923	9259	2823	93
H(26A)	3415	4950	2138	100
H(26B)	3926	4815	2676	100
H(26C)	4245	4502	2090	100
H(27A)	4575	6687	1506	100
H(27B)	3738	6257	1465	100
H(27C)	4467	5612	1377	100

Table S5. Hydrogen coordinates (x 10^4) and isotropic displacement parameters (Å^2 x 10^3) for [(Me$_4$phen)CuCl(P^{t}Bu$_3$)]·CH$_2$Cl$_2$.

H atom	x	y	z	U(eq)
H(28A)	5350	5312	2222	120
H(28B)	5120	5774	2795	120
H(28C)	5389	6409	2294	120
H(18D)	2180	5165	2798	83
H(18E)	2091	6249	2908	83
H(18F)	2698	5660	3251	83
H(19D)	2937	6187	1616	94
H(19E)	2346	6762	1981	94
H(19F)	2210	5684	1876	94
H(20D)	3788	4850	2655	87
H(20E)	3778	5065	2011	87
H(20F)	3083	4523	2287	87
H(22D)	2510	7563	3217	82
H(22E)	2173	7777	2620	82
H(22F)	2388	8609	3024	82
H(23D)	3077	8022	1833	82
H(23E)	3792	8662	1979	82
H(23F)	2948	9003	2121	82
H(24D)	3471	9216	3116	87
H(24E)	4237	8912	2810	87
H(24F)	3970	8384	3355	87
H(26D)	4852	5386	2284	67
H(26E)	5298	5985	2733	67
H(26F)	5591	5960	2110	67
H(27D)	4921	6730	1382	86
H(27E)	4147	7285	1490	86
H(27F)	4154	6181	1521	86
H(28D)	5304	7656	2698	72
H(28E)	4821	8214	2251	72
H(28F)	5566	7655	2069	72
H(29A)	6216	3787	570	101
H(29B)	6014	4401	36	101

Structure Determination Summary

Crystal Data and Structure Refinement for [(Me$_4$phen)CuI(P^{t}Bu$_3$)]·CH$_2$Cl$_2$

Identification code	JPD1152_0m_a
Empirical formula	$C_{29}H_{45}Cl_2CuIN_2P$

Formula weight	713.98	
Temperature	150(2) K	
Wavelength	0.71073 Å	
Crystal system	monoclinic	
Space group	$P2_1/c$	
Unit cell dimensions	a = 12.8280(7) Å	α = 90°
	b = 14.5770(8) Å	β = 103.598(2)°
	c = 17.5423(10) Å	γ = 90°
Volume	3188.4(3) A^3	
Z	4	
Density (calculated)	1.487 g/cm^3	
Absorption coefficient	1.891 mm^{-1}	
F(000)	1456	
Crystal size	0.255 x 0.156 x 0.115 mm^3	
θ range for data collection	2.265 to 34.422°	
Index ranges	$-20 \le h \le 20$, $-23 \le k \le 23$, $-27 \le l \le 27$	
Reflections collected	160862	
Independent reflections	13386 [R(int) = 0.0342]	
Completeness to θ = 34.000°	99.9 %	
Absorption correction	Numerical	
Max. and min. transmission	0.81 and 0.70	
Refinement method	Full-matrix least-squares on F^2	
Data / restraints / parameters	13386 / 0 / 338	
Goodness-of-fit on F^2	1.061	
Final R indices [I>2σ(I)]	R1 = 0.0285, wR2 = 0.0656	
R indices (all data)	R1 = 0.0395, wR2 = 0.0716	
Extinction coefficient	n/a	
Largest diff. peak and hole	1.116 and -0.867 $e \cdot Å^{-3}$	

Table S1. Atomic coordinates (x 10^4) and equivalent isotropic displacement parameters (Å^2 x 10^3) for [(Me_4phen)CuI(P^tBu_3)]·CH_2Cl_2. U(eq) is defined as one third of the trace of the orthogonalized U^{ij} tensor.

Atom	x	y	z	U(eq)
I(1)	8876(1)	1733(1)	4067(1)	26(1)
Cu(1)	7362(1)	3003(1)	3828(1)	19(1)
P(1)	5649(1)	2573(1)	3540(1)	17(1)
N(1)	7929(1)	4051(1)	3199(1)	21(1)
N(2)	7961(1)	3934(1)	4729(1)	20(1)
C(1)	7979(1)	4090(1)	2451(1)	24(1)
C(2)	8302(1)	4864(1)	2086(1)	25(1)
C(3)	8571(1)	5657(1)	2524(1)	24(1)
C(4)	8604(1)	5616(1)	3340(1)	21(1)
C(5)	9001(1)	6351(1)	3875(1)	26(1)
C(6)	9063(1)	6278(1)	4653(1)	25(1)
C(7)	8711(1)	5465(1)	4984(1)	20(1)
C(8)	8762(1)	5362(1)	5798(1)	21(1)
C(9)	8419(1)	4538(1)	6052(1)	22(1)
C(10)	8031(1)	3854(1)	5491(1)	22(1)
C(11)	8308(1)	4734(1)	4474(1)	19(1)
C(12)	8272(1)	4803(1)	3648(1)	19(1)
C(13)	8349(2)	4801(1)	1235(1)	34(1)
C(14)	8820(2)	6532(1)	2147(1)	32(1)
C(15)	9179(1)	6132(1)	6361(1)	29(1)
C(16)	8441(1)	4343(1)	6898(1)	29(1)
C(17)	4780(1)	3513(1)	3836(1)	24(1)
C(18)	5196(1)	4449(1)	3620(1)	32(1)
C(19)	4944(2)	3536(1)	4733(1)	35(1)
C(20)	3570(1)	3453(1)	3473(1)	35(1)
C(21)	5445(1)	1476(1)	4080(1)	26(1)
C(22)	6151(2)	1544(1)	4922(1)	34(1)
C(23)	4286(1)	1260(1)	4118(1)	39(1)
C(24)	5882(2)	654(1)	3705(1)	35(1)
C(25)	5147(1)	2361(1)	2438(1)	24(1)
C(26)	4087(1)	1828(1)	2167(1)	33(1)
C(27)	6046(1)	1845(1)	2165(1)	31(1)
C(28)	5029(2)	3287(1)	2005(1)	32(1)
Cl(1)	1297(1)	3854(1)	1601(1)	66(1)
Cl(2)	2431(1)	3438(1)	390(1)	51(1)
C(29)	1386(2)	4075(1)	632(1)	37(1)

Table S2. Bond lengths (Å) for [(Me$_4$phen)CuI(P^{t}Bu$_3$)]·CH$_2$Cl$_2$. Symmetry transformations used to generate equivalent atoms:

I(1)-Cu(1)	2.6449(2)	C(17)-C(20)	1.535(2)
Cu(1)-N(2)	2.0877(12)	C(17)-C(19)	1.538(2)
Cu(1)-N(1)	2.1115(12)	C(17)-C(18)	1.544(2)
Cu(1)-P(1)	2.2257(4)	C(18)-H(18A)	0.9800
P(1)-C(21)	1.9079(15)	C(18)-H(18B)	0.9800
P(1)-C(25)	1.9125(15)	C(18)-H(18C)	0.9800
P(1)-C(17)	1.9137(15)	C(19)-H(19A)	0.9800
N(1)-C(1)	1.3303(19)	C(19)-H(19B)	0.9800
N(1)-C(12)	1.3607(18)	C(19)-H(19C)	0.9800
N(2)-C(10)	1.3253(19)	C(20)-H(20A)	0.9800
N(2)-C(11)	1.3601(17)	C(20)-H(20B)	0.9800
C(1)-C(2)	1.406(2)	C(20)-H(20C)	0.9800
C(1)-H(1)	0.9500	C(21)-C(23)	1.537(2)
C(2)-C(3)	1.386(2)	C(21)-C(24)	1.537(2)
C(2)-C(13)	1.511(2)	C(21)-C(22)	1.543(2)
C(3)-C(4)	1.423(2)	C(22)-H(22A)	0.9800
C(3)-C(14)	1.506(2)	C(22)-H(22B)	0.9800
C(4)-C(12)	1.4095(19)	C(22)-H(22C)	0.9800
C(4)-C(5)	1.437(2)	C(23)-H(23A)	0.9800
C(5)-C(6)	1.353(2)	C(23)-H(23B)	0.9800
C(5)-H(5)	0.9500	C(23)-H(23C)	0.9800
C(6)-C(7)	1.438(2)	C(24)-H(24A)	0.9800
C(6)-H(6)	0.9500	C(24)-H(24B)	0.9800
C(7)-C(11)	1.4084(19)	C(24)-H(24C)	0.9800
C(7)-C(8)	1.422(2)	C(25)-C(28)	1.539(2)
C(8)-C(9)	1.389(2)	C(25)-C(26)	1.542(2)
C(8)-C(15)	1.508(2)	C(25)-C(27)	1.544(2)
C(9)-C(10)	1.407(2)	C(26)-H(26A)	0.9800
C(9)-C(16)	1.504(2)	C(26)-H(26B)	0.9800
C(10)-H(10)	0.9500	C(26)-H(26C)	0.9800
C(11)-C(12)	1.4430(19)	C(27)-H(27A)	0.9800
C(13)-H(13A)	0.9800	C(27)-H(27B)	0.9800
C(13)-H(13B)	0.9800	C(27)-H(27C)	0.9800
C(13)-H(13C)	0.9800	C(28)-H(28A)	0.9800
C(14)-H(14A)	0.9800	C(28)-H(28B)	0.9800
C(14)-H(14B)	0.9800	C(28)-H(28C)	0.9800
C(14)-H(14C)	0.9800	Cl(1)-C(29)	1.760(2)
C(15)-H(15A)	0.9800	Cl(2)-C(29)	1.763(2)
C(15)-H(15B)	0.9800	C(29)-H(29A)	0.9900
C(15)-H(15C)	0.9800	C(29)-H(29B)	0.9900
C(16)-H(16A)	0.9800		
C(16)-H(16B)	0.9800		
C(16)-H(16C)	0.9800		

Table S3. Bond angles (deg.) for [(Me$_4$phen)CuI(P^{t}Bu$_3$)]·CH$_2$Cl$_2$. Symmetry transformations used to generate equivalent atoms:

N(2)-Cu(1)-N(1)	79.28(5)	C(8)-C(9)-C(16)	123.07(13)
N(2)-Cu(1)-P(1)	121.57(4)	C(10)-C(9)-C(16)	118.52(13)
N(1)-Cu(1)-P(1)	121.91(3)	N(2)-C(10)-C(9)	124.88(13)
N(2)-Cu(1)-I(1)	102.06(3)	N(2)-C(10)-H(10)	117.6
N(1)-Cu(1)-I(1)	105.01(3)	C(9)-C(10)-H(10)	117.6
P(1)-Cu(1)-I(1)	119.172(12)	N(2)-C(11)-C(7)	122.65(13)
C(21)-P(1)-C(25)	108.30(7)	N(2)-C(11)-C(12)	116.94(12)
C(21)-P(1)-C(17)	107.94(7)	C(7)-C(11)-C(12)	120.39(12)
C(25)-P(1)-C(17)	108.08(7)	N(1)-C(12)-C(4)	122.76(13)
C(21)-P(1)-Cu(1)	111.53(5)	N(1)-C(12)-C(11)	117.08(12)
C(25)-P(1)-Cu(1)	110.77(5)	C(4)-C(12)-C(11)	120.14(13)
C(17)-P(1)-Cu(1)	110.10(5)	C(2)-C(13)-H(13A)	109.5
C(1)-N(1)-C(12)	116.93(12)	C(2)-C(13)-H(13B)	109.5
C(1)-N(1)-Cu(1)	130.44(10)	H(13A)-C(13)-H(13B)	109.5
C(12)-N(1)-Cu(1)	112.61(9)	C(2)-C(13)-H(13C)	109.5
C(10)-N(2)-C(11)	117.23(12)	H(13A)-C(13)-H(13C)	109.5
C(10)-N(2)-Cu(1)	129.19(10)	H(13B)-C(13)-H(13C)	109.5
C(11)-N(2)-Cu(1)	113.58(9)	C(3)-C(14)-H(14A)	109.5
N(1)-C(1)-C(2)	124.78(14)	C(3)-C(14)-H(14B)	109.5
N(1)-C(1)-H(1)	117.6	H(14A)-C(14)-H(14B)	109.5
C(2)-C(1)-H(1)	117.6	C(3)-C(14)-H(14C)	109.5
C(3)-C(2)-C(1)	118.57(14)	H(14A)-C(14)-H(14C)	109.5
C(3)-C(2)-C(13)	122.39(14)	H(14B)-C(14)-H(14C)	109.5
C(1)-C(2)-C(13)	119.04(15)	C(8)-C(15)-H(15A)	109.5
C(2)-C(3)-C(4)	117.89(13)	C(8)-C(15)-H(15B)	109.5
C(2)-C(3)-C(14)	120.96(14)	H(15A)-C(15)-H(15B)	109.5
C(4)-C(3)-C(14)	121.16(15)	C(8)-C(15)-H(15C)	109.5
C(12)-C(4)-C(3)	118.69(13)	H(15A)-C(15)-H(15C)	109.5
C(12)-C(4)-C(5)	117.99(13)	H(15B)-C(15)-H(15C)	109.5
C(3)-C(4)-C(5)	123.27(13)	C(9)-C(16)-H(16A)	109.5
C(6)-C(5)-C(4)	121.89(13)	C(9)-C(16)-H(16B)	109.5
C(6)-C(5)-H(5)	119.1	H(16A)-C(16)-H(16B)	109.5
C(4)-C(5)-H(5)	119.1	C(9)-C(16)-H(16C)	109.5
C(5)-C(6)-C(7)	121.52(14)	H(16A)-C(16)-H(16C)	109.5
C(5)-C(6)-H(6)	119.2	H(16B)-C(16)-H(16C)	109.5
C(7)-C(6)-H(6)	119.2	C(20)-C(17)-C(19)	107.90(14)
C(11)-C(7)-C(8)	118.79(12)	C(20)-C(17)-C(18)	108.78(14)
C(11)-C(7)-C(6)	118.03(13)	C(19)-C(17)-C(18)	105.03(14)
C(8)-C(7)-C(6)	123.17(13)	C(20)-C(17)-P(1)	116.36(11)
C(9)-C(8)-C(7)	118.03(13)	C(19)-C(17)-P(1)	110.18(11)
C(9)-C(8)-C(15)	121.61(14)	C(18)-C(17)-P(1)	107.99(10)
C(7)-C(8)-C(15)	120.36(13)	C(17)-C(18)-H(18A)	109.5
C(8)-C(9)-C(10)	118.41(13)	C(17)-C(18)-H(18B)	109.5

Table S3. Bond angles (deg.) for [(Me$_4$phen)CuI(P^{t}Bu$_3$)]·CH$_2$Cl$_2$. Symmetry transformations used to generate equivalent atoms:

H(18A)-C(18)-H(18B)	109.5	C(28)-C(25)-P(1)	109.17(11)
C(17)-C(18)-H(18C)	109.5	C(26)-C(25)-P(1)	117.14(12)
H(18A)-C(18)-H(18C)	109.5	C(27)-C(25)-P(1)	107.07(10)
H(18B)-C(18)-H(18C)	109.5	C(25)-C(26)-H(26A)	109.5
C(17)-C(19)-H(19A)	109.5	C(25)-C(26)-H(26B)	109.5
C(17)-C(19)-H(19B)	109.5	H(26A)-C(26)-H(26B)	109.5
H(19A)-C(19)-H(19B)	109.5	C(25)-C(26)-H(26C)	109.5
C(17)-C(19)-H(19C)	109.5	H(26A)-C(26)-H(26C)	109.5
H(19A)-C(19)-H(19C)	109.5	H(26B)-C(26)-H(26C)	109.5
H(19B)-C(19)-H(19C)	109.5	C(25)-C(27)-H(27A)	109.5
C(17)-C(20)-H(20A)	109.5	C(25)-C(27)-H(27B)	109.5
C(17)-C(20)-H(20B)	109.5	H(27A)-C(27)-H(27B)	109.5
H(20A)-C(20)-H(20B)	109.5	C(25)-C(27)-H(27C)	109.5
C(17)-C(20)-H(20C)	109.5	H(27A)-C(27)-H(27C)	109.5
H(20A)-C(20)-H(20C)	109.5	H(27B)-C(27)-H(27C)	109.5
H(20B)-C(20)-H(20C)	109.5	C(25)-C(28)-H(28A)	109.5
C(23)-C(21)-C(24)	108.21(14)	C(25)-C(28)-H(28B)	109.5
C(23)-C(21)-C(22)	109.17(14)	H(28A)-C(28)-H(28B)	109.5
C(24)-C(21)-C(22)	105.57(14)	C(25)-C(28)-H(28C)	109.5
C(23)-C(21)-P(1)	116.17(12)	H(28A)-C(28)-H(28C)	109.5
C(24)-C(21)-P(1)	109.51(12)	H(28B)-C(28)-H(28C)	109.5
C(22)-C(21)-P(1)	107.69(11)	Cl(1)-C(29)-Cl(2)	111.19(11)
C(21)-C(22)-H(22A)	109.5	Cl(1)-C(29)-H(29A)	109.4
C(21)-C(22)-H(22B)	109.5	Cl(2)-C(29)-H(29A)	109.4
H(22A)-C(22)-H(22B)	109.5	Cl(1)-C(29)-H(29B)	109.4
C(21)-C(22)-H(22C)	109.5	Cl(2)-C(29)-H(29B)	109.4
H(22A)-C(22)-H(22C)	109.5	H(29A)-C(29)-H(29B)	108.0
H(22B)-C(22)-H(22C)	109.5		
C(21)-C(23)-H(23A)	109.5		
C(21)-C(23)-H(23B)	109.5		
H(23A)-C(23)-H(23B)	109.5		
C(21)-C(23)-H(23C)	109.5		
H(23A)-C(23)-H(23C)	109.5		
H(23B)-C(23)-H(23C)	109.5		
C(21)-C(24)-H(24A)	109.5		
C(21)-C(24)-H(24B)	109.5		
H(24A)-C(24)-H(24B)	109.5		
C(21)-C(24)-H(24C)	109.5		
H(24A)-C(24)-H(24C)	109.5		
H(24B)-C(24)-H(24C)	109.5		
C(28)-C(25)-C(26)	108.20(13)		
C(28)-C(25)-C(27)	105.54(14)		
C(26)-C(25)-C(27)	109.12(13)		

Table S4. Anisotropic displacement parameters ($Å^2$ x 10^3) for [(Me_4phen)CuI(P^tBu_3)]·CH_2Cl_2. The anisotropic displacement factor exponent takes the form: $-2\pi^2[h^2 a^{*2}U^{11} + ... + 2hka^*b^*U^{12}]$.

Atom	U^{11}	U^{22}	U^{33}	U^{23}	U^{13}	U^{12}
I(1)	20(1)	23(1)	35(1)	-1(1)	4(1)	2(1)
Cu(1)	18(1)	17(1)	22(1)	-1(1)	3(1)	-4(1)
P(1)	15(1)	15(1)	20(1)	0(1)	3(1)	-1(1)
N(1)	19(1)	21(1)	21(1)	1(1)	4(1)	-3(1)
N(2)	20(1)	18(1)	21(1)	0(1)	3(1)	-3(1)
C(1)	23(1)	26(1)	23(1)	0(1)	5(1)	-4(1)
C(2)	20(1)	31(1)	23(1)	4(1)	6(1)	0(1)
C(3)	20(1)	24(1)	28(1)	7(1)	8(1)	1(1)
C(4)	19(1)	18(1)	28(1)	3(1)	8(1)	0(1)
C(5)	28(1)	16(1)	36(1)	2(1)	10(1)	-3(1)
C(6)	26(1)	16(1)	34(1)	-3(1)	10(1)	-3(1)
C(7)	17(1)	17(1)	26(1)	-2(1)	5(1)	-1(1)
C(8)	16(1)	21(1)	26(1)	-5(1)	5(1)	-1(1)
C(9)	18(1)	24(1)	22(1)	-2(1)	3(1)	-2(1)
C(10)	22(1)	21(1)	22(1)	1(1)	4(1)	-4(1)
C(11)	16(1)	17(1)	23(1)	0(1)	4(1)	-1(1)
C(12)	16(1)	18(1)	23(1)	1(1)	5(1)	-1(1)
C(13)	34(1)	43(1)	25(1)	4(1)	9(1)	-4(1)
C(14)	33(1)	29(1)	37(1)	12(1)	14(1)	0(1)
C(15)	27(1)	28(1)	33(1)	-12(1)	8(1)	-5(1)
C(16)	30(1)	33(1)	23(1)	-2(1)	5(1)	-4(1)
C(17)	21(1)	22(1)	30(1)	-3(1)	6(1)	4(1)
C(18)	34(1)	19(1)	39(1)	-2(1)	5(1)	4(1)
C(19)	35(1)	41(1)	31(1)	-7(1)	12(1)	3(1)
C(20)	20(1)	36(1)	47(1)	-4(1)	5(1)	7(1)
C(21)	22(1)	21(1)	35(1)	6(1)	6(1)	-4(1)
C(22)	32(1)	36(1)	31(1)	14(1)	5(1)	-1(1)
C(23)	27(1)	37(1)	53(1)	14(1)	11(1)	-8(1)
C(24)	32(1)	18(1)	52(1)	2(1)	3(1)	-1(1)
C(25)	22(1)	26(1)	22(1)	-4(1)	1(1)	-1(1)
C(26)	24(1)	36(1)	34(1)	-8(1)	-3(1)	-4(1)
C(27)	29(1)	35(1)	29(1)	-11(1)	7(1)	-1(1)
C(28)	33(1)	35(1)	24(1)	5(1)	2(1)	1(1)
Cl(1)	125(1)	39(1)	35(1)	-3(1)	23(1)	6(1)
Cl(2)	42(1)	47(1)	67(1)	11(1)	17(1)	2(1)
C(29)	42(1)	35(1)	30(1)	1(1)	-1(1)	2(1)

Table S5. Hydrogen coordinates (x 10^4) and isotropic displacement parameters (Å^2 x 10^3) for [(Me$_4$phen)CuI(P^{t}Bu$_3$)]·CH$_2$Cl$_2$.

H atom	x	y	z	U(eq)
H(1)	7782	3556	2140	29
H(5)	9227	6905	3677	31
H(6)	9346	6775	4989	30
H(10)	7803	3292	5673	27
H(13A)	8271	4159	1065	50
H(13B)	9040	5037	1174	50
H(13C)	7767	5166	913	50
H(14A)	9587	6554	2160	48
H(14B)	8629	7059	2435	48
H(14C)	8405	6554	1602	48
H(15A)	9213	5928	6899	44
H(15B)	8697	6661	6239	44
H(15C)	9898	6308	6313	44
H(16A)	9139	4523	7227	44
H(16B)	8325	3687	6964	44
H(16C)	7873	4694	7053	44
H(18A)	5956	4513	3880	47
H(18B)	4786	4943	3791	47
H(18C)	5108	4484	3050	47
H(19A)	5712	3579	4979	52
H(19B)	4652	2974	4909	52
H(19C)	4573	4070	4883	52
H(20A)	3202	3952	3678	53
H(20B)	3296	2862	3608	53
H(20C)	3438	3508	2901	53
H(22A)	6103	969	5202	50
H(22B)	5900	2053	5198	50
H(22C)	6897	1652	4901	50
H(23A)	4010	1757	4392	58
H(23B)	4270	682	4402	58
H(23C)	3837	1201	3585	58
H(24A)	5902	112	4039	52
H(24B)	6609	792	3650	52
H(24C)	5416	532	3186	52
H(26A)	3514	2151	2340	49
H(26B)	4170	1211	2395	49
H(26C)	3902	1782	1594	49
H(27A)	6127	1229	2396	46
H(27B)	6722	2182	2335	46
H(27C)	5859	1797	1592	46

Table S5. Hydrogen coordinates (x 10^4) and isotropic displacement parameters (Å^2 x 10^3) for [(Me_4phen)CuI(P^tBu_3)]·CH_2Cl_2.

H atom	x	y	z	U(eq)
H(28A)	5679	3653	2194	47
H(28B)	4409	3617	2104	47
H(28C)	4924	3179	1440	47
H(29A)	1515	4737	572	45
H(29B)	697	3913	266	45